



NATIONAL & KAPODISTRIAN UNIVERSITY OF ATHENS

SCHOOL OF SCIENCES

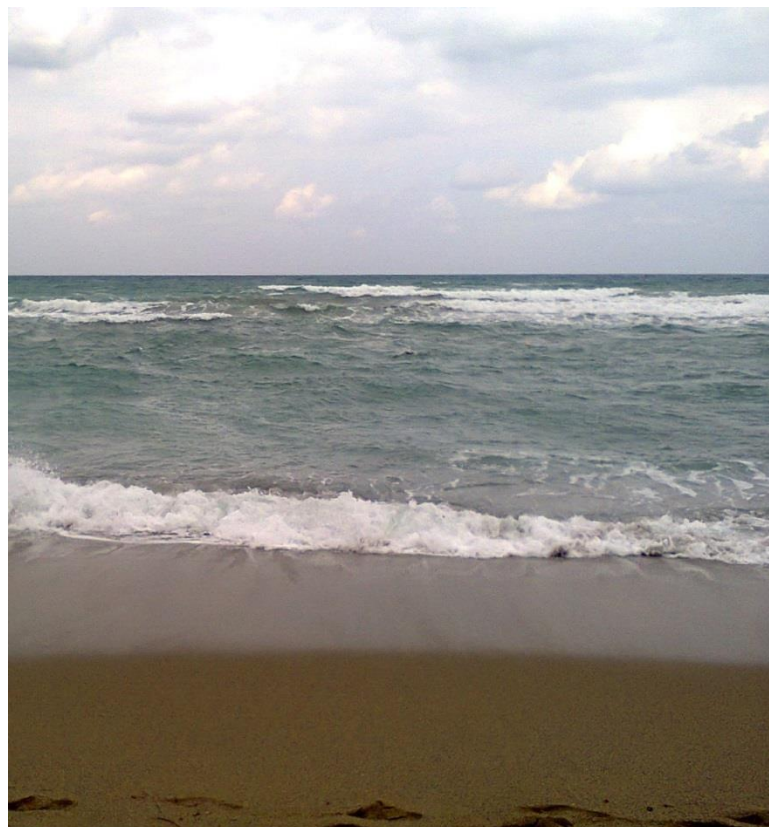
FACULTY OF GEOLOGY & GEOENVIRONMENT

DEPARTMENT OF GEOGRAPHY & CLIMATOLOGY

**Study of the wave characteristics of the Greek Seas in
relation to the present and future atmospheric
conditions and their impact on the coastal zone**

PhD Thesis

SIFNIOTI DAFNI



ATHENS, 2015



NATIONAL & KAPODISTRIAN UNIVERSITY OF ATHENS

SCHOOL OF NATURAL SCIENCES

FACULTY OF GEOLOGY & GEOENVIRONMENT

*STUDY OF THE WAVE CHARACTERISTICS OF THE GREEK SEAS IN RELATION TO THE PRESENT AND
FUTURE ATMOSPHERIC CONDITIONS AND THEIR IMPACT ON THE COASTAL ZONE*

PhD Thesis

SIFNIOTI DAFNI

ID: 145

SUPERVISOR: SERAFEIM POULOS, Associate Professor (NKUA)

ADVISORY COMMITTEE:

Serafeim Poulos, Associate Professor (NKUA)

Panagiotis Nastos, Professor (NKUA)

Takvor Soukissian, Researcher B' (HCMR)

EXAMINATION COMMITTEE

Theofanis Karampas, Professor (AUTH)

Vasileios Zervakis, Associate Professor (University of Aegean)

Helena Flocas, Associate Professor (NKUA)

Maria Hatzaki, Lecturer (NKUA)

ATHENS, 2015

Dedicated to my loving family...

*“Live in the sunshine, swim the sea,
drink the cold air”*

R.V. Emerson

© Dafni Sifnioti, © National & Kapodistrian University of Athens – Faculty of Geology & Geoenvironment

All rights reserved

Cover Photograph: Ammoudara Beach, Heraklion, Crete, Personal Collection

PREFACE

This thesis would not have been feasible without the endless support (in all manners) of my loving family to whom I owe my greatest gratitude and love. I would like to extend my honest thanks to my supervisor Assist. Professor Serafeim Poulos for providing me, of what I think was the greatest lesson, to always remember to see beyond the numbers and have a broader scientific thinking, by constantly reminding me that I am a geologist after all. I would also like to thank him for believing in me these past few years and trusting me with the management of the THALIS-DAPHNE project; helping me in this way to improve my organizational skills and working as part of a team. I would also like to thank HCMR's Researcher Dr. Takvor Soukissian, for his endless persistence and patience in teaching me almost everything about waves (at least as much as my geological brain could tolerate!) and for spending so much of his time in discussing the results of this Thesis, as well as further analyses, it has sincerely been a privilege. To Professor Panagiotis Nastos, I extend my thanks for helping me improve my interest and knowledge in Meteorology – Climatology as well as for discussing any issues that might have risen during this study. I would also like to thank him for offering me an office, in the Laboratory of Climatology, NKUA. To Dr. George Ghionis, thank you for always being there to offer advice on any subject, from waves to project management, but most of all thank you for teaching me about scientific instruments and how to do proper research and fieldwork; it has been a tremendous experience working with you at the field and for any scientific work in general. To Lecturer Maria Hatzaki, thank you for your support and input throughout the progress of this work and for all your suggestions (scientific or not). To Professor T. Karampas, Assoc. Professor H. Flocas and Assoc. Professor V. Zervakis thank you very much for reviewing my PhD and for offering your input and ideas.

To all my friends who have always been there for me during my PhD studies, I would not have been able to do this without your support and occasional laughter or advice (you know who you are)!! To my colleagues with whom we have shared countless lunches and hours of fieldtrips and discussions you have made this even easier for me with your companionship and I have gained something from all of you; hopefully, I have given something back to you in return!

Finally, I would like to acknowledge the scientific teams of ECMWF and Poseidon HCMR; without their work this thesis would not have been possible; as well as the representative of DHI in Greece, Elias Moussoulis for providing the license for MIKE and any information when needed!

Thank you!

ABSTRACT

The present study has as main goal the description of wave and selected meteorological characteristics from *in-situ* data (Poseidon System - HCMR) of the Greek Seas and their sub-regions, so that new details can be added to already known information and to enhance existing knowledge. In addition, as the *in-situ* measurements do not spatially cover the total area of Greek waters, the reanalysis database ERA-Interim (ECMWF) has been used, after statistically compared with the database of Poseidon System (buoys).

The measurements analysed include parameters given directly from the buoys or from the ERA-Interim database such as height, period and wave direction, wind speed and direction, air temperature and atmospheric pressure, as well as measurements of sea surface elevation. The latter was analysed to obtain the spectral and statistical characteristics of the wave. For the collocation of the two databases, three different methods were used: (i) nearest intersect; (ii) weighted distance average from the buoy; and (iii) weighted distance average of the 4 grid boxes closest to the buoy.

For selected points at the Greek Seas, the possibility of having trends in monthly and annual values and mean monthly anomalies has been investigated for the following parameters: wave height and period, wind speed and temperature at 2 m.

The ERA-Interim database is also used as initial input of the study of wave propagation from offshore to the nearshore zone of Pinios River (Thessaly) with the use of the mathematical model (MIKE 21 PMS). Additionally, the impact of sea level rise (as presented in the 5th Report of IPCC) on wave propagation is examined for the aforementioned area.

The most important findings of the present research are: (i) the analysis of sea surface elevation can provide more characteristics for the wave state than the direct data obtained by the buoys and it is, therefore, suggested to be preferred than the direct buoy measurements; (ii) the effect of the complex coastline and the presence of the islands to wave propagation is evident; (iii) the database of ERA-Interim can be considered representative for the wave and meteorological state of the Greek Seas, but for offshore locations; (iv) the empirical equations, suggested in literature, for the ratios of spectral / statistical wave characteristics, as well as those used for wave propagation from the offshore to the nearshore zone differ for the Greek Seas and should be used carefully; (v) sea level rise has an impact on the nearshore hydrodynamic conditions (i.e. moving the wave breaking zone closer to the coastline).

Keywords: Wave characteristics, Poseidon System, ERA-Interim, sea level rise, nearshore hydrodynamics, Greek Seas

ΠΕΡΙΛΗΨΗ

Τίτλος: Μελέτη των κυματικών χαρακτηριστικών των Ελληνικών Θαλασσών σε σχέση με τις παρούσες και μελλοντικές ατμοσφαιρικές συνθήκες και οι επιπτώσεις τους στη παράκτια ζώνη

Η παρούσα μελέτη έχει ως πρωταρχικό στόχο την περιγραφή των κυματικών και μετεωρολογικών χαρακτηριστικών από επιτόπιες μετρήσεις (Σύστημα Ποσειδών – ΕΛΚΕΘΕ) στις Ελληνικές Θάλασσες και τις υπο-περιοχές τους, ώστε νέα στοιχεία να προστεθούν στις ήδη υπάρχουσες πληροφορίες και να ενισχυθεί η υπάρχουσα γνώση. Επιπροσθέτως, καθώς οι επιτόπιες μετρήσεις είναι διάσπαρτες χρονικά και χωρικά και δεν καλύπτουν χωρικά τα ελληνικά νερά, στα πλαίσια της εργασίας αυτής, αξιοποιείται μια ακόμα βάση δεδομένων (ERA-Interim, ECMWF), η οποία και συγκρίνεται με τη βάση δεδομένων του Συστήματος Ποσειδών (πλωτοί μετρητικοί σταθμοί).

Οι μετρήσεις που αναλύονται περιλαμβάνουν χαρακτηριστικά που δίνονται είτε αυτούσια από τους πλωτούς ωκεανογραφικούς μετρητικούς σταθμούς (ΠΩΜΣ), είτε από τη βάση Reanalysis δεδομένων ERA-Interim και αφορούν ύψος, περίοδο, διεύθυνση κύματος, ταχύτητα και διεύθυνση ανέμου, θερμοκρασία αέρα και ατμοσφαιρική πίεση, καθώς και μετρήσεις της διακύμανσης της στάθμης της θάλασσας από όπου προέκυψαν μετά από επεξεργασία, τα φασματικά και στατιστικά χαρακτηριστικά του κύματος. Για τη σύγκριση των δύο βάσεων, χρησιμοποιήθηκαν τρεις διαφορετικές μέθοδοι χωρικής τοποθέτησης ΠΩΜΣ - (ERA-Interim, 0.125x0.125) καννάβου: (i) του κοντινότερου σημείου, (ii) του σταθμικού μέσου (με βάρος την απόσταση από τη σηματοδούρα), (iii) των σταθμικών μέσων των 4 κοντινότερων κουτιά του καννάβου στη σηματοδούρα.

Σε επιλεγμένα σημεία των Ελληνικών Θαλασσών, διερευνάται η πιθανότητα να υπάρχουν τάσεις αλλαγής στις μηνιαίες και ετήσιες τιμές, καθώς και στις μηνιαίες ανωμαλίες, των παρακάτω παραμέτρων: ύψος και περίοδος κύματος, ταχύτητα του ανέμου και θερμοκρασία της ατμόσφαιρας.

Η βάση δεδομένων ERA-Interim χρησιμοποιείται ως αρχική πληροφορία για τη μελέτη της διάδοσης του κύματος από τα ανοιχτά νερά στην παράλια ζώνη του Πηνειού Ποταμού (Θεσσαλίας) με χρήση του μαθηματικού μοντέλου (MIKE 21 PMS). Ακόμα, ερευνάται η επίδραση της αύξησης της στάθμης της θάλασσας, όπως αυτή ορίζεται από την 5η Έκθεση του IPCC, στη διάδοση του κύματος στην προαναφερθείσα περιοχή.

Τα σημαντικότερα ευρήματα της παρούσας μελέτης είναι ότι: (i) η επεξεργασία των δεδομένων της διακύμανσης της στάθμης της θάλασσας μπορεί να προσφέρει περισσότερα χαρακτηριστικά για το κυματικό καθεστώς και προτείνεται να προτιμάται αντί των απευθείας μετρήσεων από τους ΠΩΜΣ, (ii) είναι εμφανής η επίδραση της περίπλοκης Ελληνικής ακτογραμμής και της παρουσίας των νησιών στη διάδοση των κυμάτων, (iii) τα δεδομένα της βάσης ERA-Interim μπορούν να θεωρηθούν αντιπροσωπευτικά για την κυματική και μετεωρολογική κατάσταση που επικρατεί στις Ελληνικές Θάλασσες, ως καταστάσεις ανοικτής θάλασσας, (iv) οι εμπειρικές εξισώσεις για τους λόγους των φασματικών / στατιστικών κυματικών χαρακτηριστικών, καθώς και αυτές που χρησιμοποιούνται για τη διάδοση του κύματος από τα ανοιχτά νερά στην παράλια ζώνη, διαφέρουν στις Ελληνικές Θάλασσες και θα πρέπει να εφαρμόζονται με προσοχή, (v) η άνοδος της στάθμης της θάλασσας επιδρά στις παράκτιες υδροδυναμικές συνθήκες (π.χ. μετατοπίζοντας τη ζώνη θραύσης των κυμάτων πιο κοντά στην ακτογραμμή).

Λέξεις κλειδιά: Κυματικά χαρακτηριστικά, Σύστημα Ποσειδών, ERA-INTERIM, άνοδος στάθμης θάλασσας, Παράκτια υδροδυναμική, Ελληνικές Θάλασσες

CONTENTS

| | |
|---------------------------------------------------------------------------------|----|
| PREFACE | iv |
| ABSTRACT | v |
| ΠΕΡΙΛΗΨΗ | vi |
| 1 Introduction..... | 3 |
| 1.1 Significance of this Study | 3 |
| 1.2 Thesis Outline | 4 |
| 2 Theory..... | 8 |
| 2.1 Coastal System..... | 8 |
| 2.2 Waves..... | 9 |
| 2.2.1 Wind and Waves..... | 10 |
| 2.2.2 Sea and Swell waves | 11 |
| 2.3 Wave Theories | 12 |
| 2.3.1 Time Series Analysis..... | 13 |
| 2.3.2 Spectral – Frequency Analysis | 15 |
| 2.3.3 Statistics..... | 18 |
| 2.4 Deep Water Waves | 19 |
| 2.5 Nearshore Processes..... | 22 |
| 2.5.1 Shoaling | 23 |
| 2.5.2 Refraction | 24 |
| 2.5.3 Diffraction..... | 26 |
| 2.5.4 Refraction & Diffraction..... | 26 |
| 2.5.5 Reflection..... | 26 |
| 2.5.6 Breaking..... | 27 |
| 2.6 Sources of Wave Data..... | 29 |
| 2.7 Climate Change & Sea Level Rise | 30 |
| 2.7.1 Sea Level Rise (SLR) in Europe | 30 |
| 2.7.2 Representative Concentration Pathway (RCPs) and Future SLR in Europe..... | 32 |
| 3 The Case Study Areas | 38 |
| 3.1 Mediterranean..... | 38 |
| 3.1.1 Geomorphological Characteristics..... | 38 |
| 3.1.2 Wave and Weather Characteristics | 40 |
| 3.1.3 Tides..... | 52 |
| 3.1.4 Storm Surge | 53 |
| 3.2 Pinios Case Study | 54 |
| 3.2.1 Geomorphological Characteristics..... | 54 |

| | | |
|--------|---------------------------------------------------|-----|
| 3.2.2 | Climatic Conditions | 55 |
| 3.2.3 | Coastal Oceanography and Sedimentology | 56 |
| 4 | Data Collection & Methodology | 66 |
| 4.1 | Poseidon..... | 66 |
| 4.1.1 | Poseidon System Description | 66 |
| 4.1.2 | Poseidon Data & Methodology of Data Analysis..... | 69 |
| 4.2 | ERA-Interim..... | 77 |
| 4.2.1 | Data Assimilation | 77 |
| 4.2.2 | Data Sources | 79 |
| 4.2.3 | Data Quality and Selection | 81 |
| 4.2.4 | Data Accumulation | 82 |
| 4.2.5 | Buoy - Interim Data analysis | 84 |
| 4.3 | Pinios Methodology | 89 |
| 4.3.1 | Background Information..... | 89 |
| 4.3.2 | Meteorological and Oceanographic Data..... | 89 |
| 4.3.3 | Site Investigations..... | 90 |
| 4.3.4 | MIKE 21 PMS..... | 93 |
| 4.3.5 | Scenarios..... | 98 |
| 5 | Results | 101 |
| 5.1 | POSEIDON Buoys..... | 102 |
| 5.1.1 | ATHOS | 102 |
| 5.1.2 | AVGO..... | 112 |
| 5.1.3 | DIA | 118 |
| 5.1.4 | E1M3A..... | 121 |
| 5.1.5 | KALAMATA..... | 127 |
| 5.1.6 | KATERINI | 137 |
| 5.1.7 | LESVOS | 144 |
| 5.1.8 | MYKONOS | 151 |
| 5.1.9 | PETROKARAVO..... | 160 |
| 5.1.10 | PYLOS | 167 |
| 5.1.11 | SANTORINI | 178 |
| 5.1.12 | SKYROS..... | 187 |
| 5.1.13 | ZAKYNTHOS..... | 197 |
| 5.1.14 | Seasonal Synoptics..... | 207 |
| 5.2 | ERA-Interim | 210 |
| 5.2.1 | Buoy - Interim Correlation | 210 |
| 5.2.2 | 35 years analysis | 234 |
| 5.3 | Case Study: Pinios | 259 |

| | | |
|-------|----------------------------------------------------------------------------------------------------------------------------------|-----|
| 5.3.1 | Wave and Weather Climate in Offshore Conditions | 259 |
| 5.3.2 | Wave propagation to the Nearshore Zone (MIKE 21 PMS)..... | 264 |
| 6 | Discussion..... | 286 |
| 6.1 | Poseidon Buoys..... | 286 |
| 6.1.1 | North Aegean Sea..... | 286 |
| 6.1.2 | Central Aegean Sea..... | 290 |
| 6.1.3 | South Aegean Sea..... | 294 |
| 6.1.4 | Northeast Ionian Sea..... | 297 |
| 6.1.5 | Southeast Ionian Sea..... | 299 |
| 6.1.6 | Remarks for the Greek Seas / Observations..... | 302 |
| 6.2 | ERA-INTERIM..... | 304 |
| 6.2.1 | North Aegean..... | 304 |
| 6.2.2 | Central Aegean..... | 307 |
| 6.2.3 | South Aegean..... | 308 |
| 6.2.4 | North Ionian..... | 311 |
| 6.2.5 | South Ionian..... | 311 |
| 6.2.6 | Remarks for ERA-Interim analysis | 313 |
| 6.3 | Pinios..... | 314 |
| 6.3.1 | Wind and Wave Characteristics from ERA-Interim | 314 |
| 6.3.2 | MIKE 21 PMS..... | 314 |
| 7 | Synopsis, Conclusions & Future Work..... | 320 |
| 7.1 | Synopsis of the Results | 320 |
| 7.2 | Wave and Weather State of the Greek Seas | 323 |
| 7.3 | Concluding remarks on the correlation of ERA-I and buoys..... | 324 |
| 7.4 | Trends of wave and atmospheric parameters from ERA-Interim long-term analysis | 325 |
| 7.5 | Wave propagation of offshore generated waves to the nearshore zone: present characteristics and the effect of potential SLR..... | 327 |
| 7.6 | Future Work..... | 328 |
| | Bibliography..... | 331 |
| | ACRONYMS..... | 339 |
| | List of Figures..... | 341 |
| | List of Tables..... | 347 |
| | APPENDIX | 352 |

Chapter 1 - Introduction

1 Introduction

1.1 Significance of this Study

The accurate representation of the wave and weather state of any coastal area is of great importance for uses such as marine planning, maritime transport, coastal adaptation to climate change, offshore wave and wind energy etc. In many studies, this has been achieved from the use of *in-situ* data, considered valid only for localized areas and from model - simulation runs that have as boundary-input conditions atmospheric characteristics (usually from land meteorological stations). The lack of detailed measurements leads to the use of reanalysis gridded datasets such as that of ERA-Interim (ECMWF); as another source of wave and meteorological data for the Greek Seas. These datasets have to be evaluated with *in-situ* data whilst taking into consideration the uncertainty of using them close to the coastline. Furthermore, the analysis of onshore wave propagation, as in the case of the deltaic coast of the outer Thermaikos Gulf (R. Pinios), can provide information on wave characteristics transformation in intermediate and shallow water conditions, as well as how a potential sea level rise (due to climate change) will alter them along their course of propagation.

The motivation of this research is based on the need of describing the wave and meteorological state of the Greek Seas in a more analytical way and in a smaller spatial scale. Information on the wave and meteorological state of the Greek Seas from *in-situ* data are shown in the form of Atlases (Athanasoulis and Skarsoulis, 1992; Soukissian et al., 2007) but there are also studies for their relation to other parameters such as wave and wind energy (T. Soukissian et al., 2012; Bagiorgas et al., 2012), weather systems (Poulos et al., 1997; Kotroni et al., 2001) and climate change and its impacts at the Eastern Mediterranean (Lionello, Malanotte-Rizzoli, Boscolo, Tsimplis, et al., 2006; Lelieveld et al., 2012; Galiatsatou and Prinos, 2014). The importance of the aforementioned analyses has been linked to the coastal zone evolution and the processes of erosion or progradation in a variety of studies (Alexandrakis et al., 2011; Poulos et al., 2014; Monioudi et al., 2014). Several questions have, therefore, risen and throughout the progress of this research are needed to be answered:

- Do we really know the characteristics of the Greek Seas? How different are the wave and meteorological state for each sub-region?
- What is the difference in using sea surface elevation (SSE) measurements in relation to direct records of wave characteristics from offshore buoys? Does the analysis of these records provide more details about the wave state and how different are the results from spectral and statistical analysis of heave records?
- Can ERA-Interim be used for the representation of the marine characteristics of the Greek Seas? How well are they correlated to the *in-situ* data? Can they provide information about long term changes in the marine state?
- Will a potential sea level rise have an impact on wave propagation from the offshore to the nearshore zone?

- How much do the results provided by the empirical equations for onshore wave propagation differ from those of numerical simulations (e.g. MIKE21 PMS)?

The implementation of the thesis includes numerical and empirical analyses. The numerical analyses are conducted by WAFO toolbox for the analysis of sea surface elevation and MIKE 21 PMS for the simulation of the propagation of waves from offshore to nearshore conditions. Additionally, the probability distribution of the apparent wave height is studied with EasyFit software, while the trends - statistical analyses are conducted using STATISTICA software. Furthermore, scripts in MatLab have been written to examine the relation between data from the Poseidon buoys and data from the ERA-Interim reanalysis dataset. These scripts include three different methods for the collocation of the *in-situ* and reanalysis data, as those established in (Mooney et al., 2011; Stopa et al., 2013; Chawla et al., 2013; Shanas and Sanil Kumar, 2014).

The empirical equations discussed in this thesis, can be found in a variety of sources such as (CERC, 1984; WMO, 1998; Komar, 2009).

On the basis of the above, **the innovative objectives of the thesis** could be:

- The description of the Wave and Meteorological Characteristics of the Greek Seas from both *in-situ* (i.e. Poseidon Buoys) and reanalysis (i.e. ERA-Interim) dataset and to establish the correlation among the 2 datasets (ERA-Interim - Poseidon Buoys)
- The importance of using sea surface elevation data instead of already-analysed buoy records and present the relation of statistical and spectral wave characteristics (e.g. $H_{1/3}$ and H_{m_0})
- The identification of potential trends of wave and meteorological characteristics for the Greek Seas, by analysing the long-term ERA-Interim database
- The investigation of the use of ERA-Interim as offshore input for wave propagation to the nearshore zone, under different wave conditions: mean conditions, mean upper 2% according to wave height, mean upper 2% for different sea level rises (i.e., 0.3 m and 0.63 m as given by the IPCC AR5 for RCP 8.5) and to evaluate potential differences.

1.2 Thesis Outline

Chapter 1: Introduction (as described above).

Chapter 2: Theory. It summarizes wave theory whilst emphasizing on the characteristics of waves in deep waters and the processes related to wave propagation within the nearshore zone. It also provides information about climate change and sea level rise for Europe as estimated under the RCP's scenarios as described in the Fifth Assessment Report (AR5) of IPCC.

Chapter 3: The Case Study areas. It presents existing information for the wave and atmospheric conditions of the Mediterranean Sea and the case study area (i.e. deltaic coast of Pinios River (outer Thermaikos Gulf)). Basic wave data sources of the Greek Seas are also discussed in this chapter.

Chapter 4: Data collection and Methodology. It describes in detail the methodology of the analyses performed for this research. Chapter 4 includes 3 subchapters (SC): **SC4.1** describes the data obtained from the Poseidon Buoys as well as the methodology of their analysis; **SC4.2** provides information about the reanalysis dataset ERA-Interim and how they are analyzed and collocated - correlated with *in-situ* data as well as how any potential trends are commented; and **SC4.3** describes the MIKE21 PMS model and its set up for the case study of the eastern deltaic coast of the Pinios River.

Chapter 5: Results. It is divided in 3 sub-chapters: **SC5.1** presents the results of the analysis of the *in-situ* data (Poseidon System buoys), according to wave (direct buoy records and Sea Surface Elevation statistical and spectral analysis), atmospheric and wind – wave data. **SC5.2** includes the results of the correlation and collocation of the buoys and the reanalysis dataset, for wave and atmospheric data, as well as the results of the long - term analysis and trends of wave and weather characteristics of chosen locations at the Greek Seas. **SC5.3** presents the results of the long term statistical analysis of a point considered representative for wave and weather characteristics of the case study of Pinios east deltaic coast, as well as the results of MIKE21 PMS simulations for the different offshore wave scenarios and their comparison with the results from empirical equations (CERC, 1984).

Chapter 6: Discussion. It includes 3 sub-chapters: **SC6.1** presents a discussion of the results of SC5.1 and new information about the wave and wind state of the Greek Seas from the Poseidon Dataset. **SC6.2** discusses the correlation and collocation of the buoys and the ERA-Interim reanalysis, in relation to other studies, as well as the trends presented from the analysis in SC5.2. Finally, **SC6.3** reviews the results of the runs of MIKE 21 PMS, for different wave scenarios and the propagation of the waves from the offshore to the nearshore zone of the R. Pinios east deltaic coast.

Chapter 7: Synopsis, Conclusions & Future Work. Provides a synopsis of the thesis' outcomes, presents the conclusions and suggests future research, based on the achievements of this work. **SC7.1** gives the synopsis of the results as given by the analysis of Poseidon Buoys and ERA-Interim. **SC7.2** presents the basic characteristics of the wave and weather state of the Greek Seas, **SC7.3** shows the concluding remarks on the correlation of ERA-Interim and Buoys, **SC7.4** presents the trends of wave and atmospheric parameters from ERA-Interim long-term analysis, **SC7.5** provides the conclusions on wave propagation of offshore generated waves to the nearshore zone: present characteristics and the effect of potential SLR and **SC7.6** suggests future work.

Finally, the cited references are shown in Bibliography and the MatLab scripts written for the basic analyses of this research are presented in the Appendix.

Chapter 2 - Theory

2 Theory

2.1 Coastal System

A simple coastal subsystem along with the processes controlling its evolution is shown in Figure 2.1.1. As shore or beach, is considered a zone consisted by loose sediments such as sand, pebbles, breccia, and extends spatially to the depth where it is possible to move the bottom sediments due to hydrodynamic causes (closure depth) and landwards to a characteristic physiographic point, which may be a field of coastal dunes or a vigorous vegetation zone. It can be divided into two main parts: (1) marine, and (2) the land.

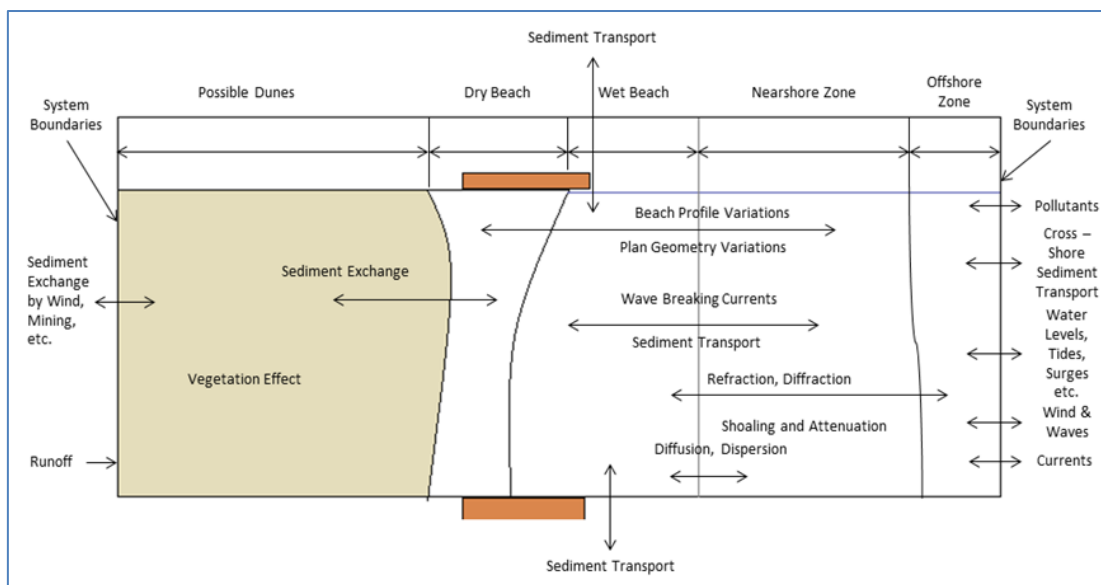


Figure 2.1.1: A coastal subsystem and controlling processes (from (Kamphuis, 2000))

The marine area (foreshore) can be temporarily covered by sea, either because of the wave, or because of the tide, including the front of the beach (beach - face) and the areas of the open sea (offshore), is relatively smooth and starts from the zone where the waves "break" (breaking zone) and extends seawards to the edge of the continental shelf and the area near the coast (nearshore zone) extending from the coastline to the open sea up to the maximum depth of closure depth. According to the wave regime this zone is divided in (Figure 2.1.2):

- Swash zone: the nearshore region in which the beach is affected by wave swash and backwash.
- Surf zone: the nearshore part in which waves propagate after they have broken in the breaker zone.
- Breaker zone: starts at the point where propagating waves break and become unstable.

The land area of the beach (backshore) extends from the upper point of the sea elevation to the depth where land morphology changes significantly. This part of the beach can be temporarily affected by waves, during events of intense storms.

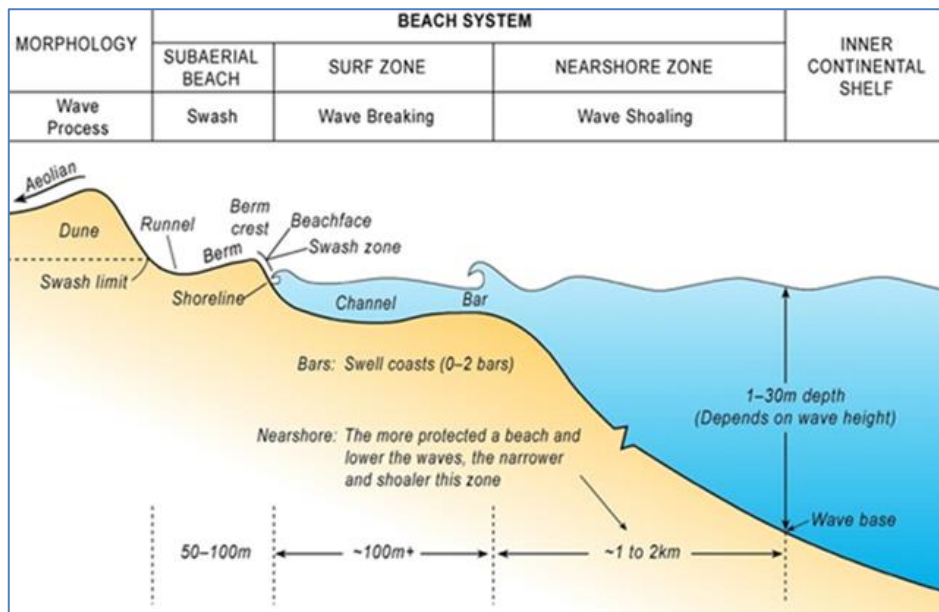


Figure 2.1.2: Shore zone physiographic characteristics (Short, 2012)

2.2 Waves

Water waves are one of the types of water level variation, along with currents, accelerations and flow – pressure fluctuations. One of the simplest forms is that of the sinusoidal wave described by high water levels (wave crests) and low water levels (wave troughs). The basic parameters of a wave are height, period, frequency, length and velocity. Wave height H is considered the vertical distance between the crest (highest point) and the trough (lowest) of a wave. Period T is the time interval between one zero crossing to the successive one, whilst frequency f is the inverse of the period. Length L is the horizontal distance that a wave repeats itself and velocity C is how fast the wave is propagating (Figure 2.2.1).

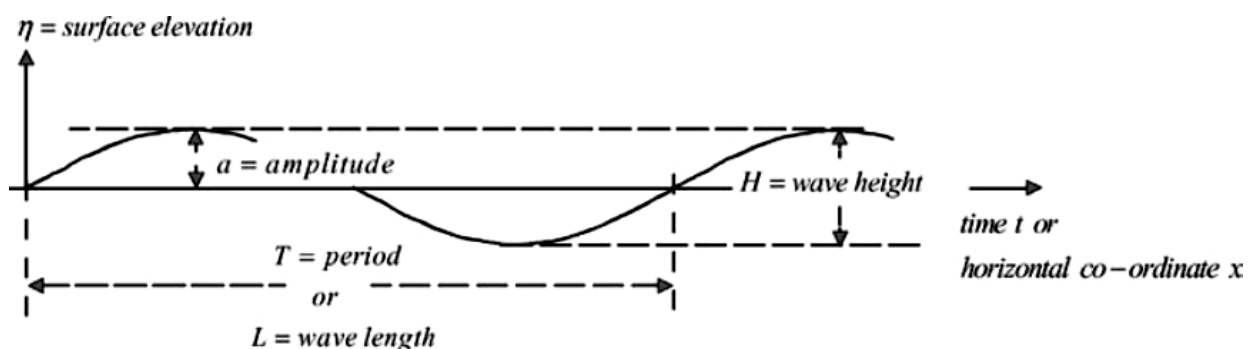


Figure 2.2.1: Basic Wave Parameters (Holthuijsen, 2007)

According to their period and wave length, waves can be classified as (Figure 2.2.2):

- Trans-tidal: Generated by low-frequency fluctuations in the Earth's crust and atmosphere. These are the longest waves.
- Tides: Slightly shorter waves, generated by the interaction between the Sun and the Moon with the oceans. Their period can be from a few hours to a day and their wavelengths range from a few hundred to a few thousand kilometers.
- Storm surges: their periods are shorter than the tides, and they represent the large scale elevation of the sea surface during an intense storm. They are generated by low atmospheric pressure and high wind speeds in the storm whilst their period and wavelength depend on the duration and the intensity of the storm.
- Tsunamis: Caused by underwater landslides or earthquakes and are mostly unpredictable and dangerous in coastal regions.
- Seiches: Standing waves with frequency that of the basin in which they are formed. Can be created by waves from the open sea (generated by storms).
- Infra-gravity waves: created by grouped wind-generated waves with periods of few minutes.
- Wind-generated waves: waves with periods smaller than 30 sec. If they are dominated by gravity (period greater than 1/4 sec) then they are called surface gravity waves. If they are created by local wind with irregular and short crests then they are called wind sea. Finally, if the generation area is far from where they are observed and they are described by regular and long crests then they are called swell.
- Capillary waves: waves with periods less than 1/4 sec and wave lengths of about 10cm. They are created by surface tension.

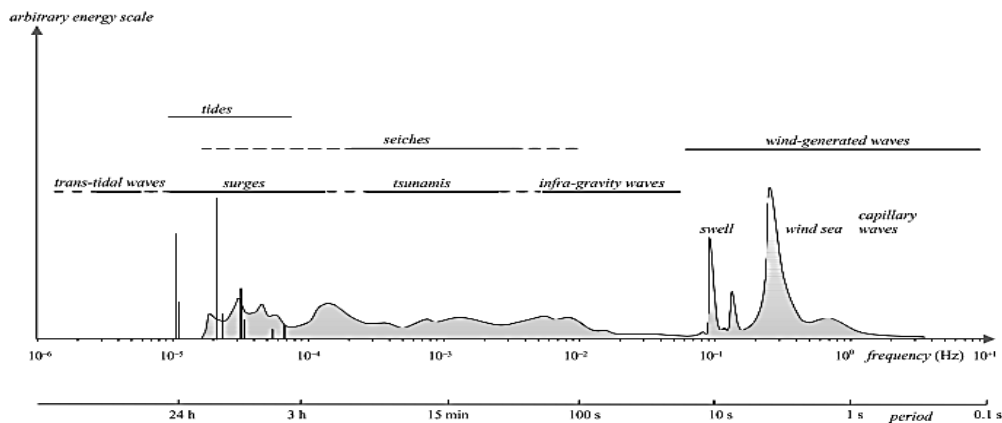


Figure 2.2.2: Classifying waves according to their period and height (Holthuijsen, 2007)

2.2.1 Wind and Waves

In general, wind and wave states are closely linked and this is supported in a variety of studies such as Dingemans, (1983) and Dean and Dalrymple (1984). However, variables such as depth, storm duration and fetch should also be considered for wave generation.

When only wind speed is affecting the water level then the resulting waves are called fully developed sea and are generated in deep, open sea; otherwise, the conditions are named as fetch or duration limited. One of the most common ways to empirically relate wind speed and wave formation is with the Beaufort scale as shown in Table 2.2.1.

Table 2.2.1: Beaufort Wind Scale

| Beaufort wind scale | Mean Wind Speed | | Limits of wind speed | | Wind descriptive terms | Probable wave height * | Probable maximum wave height | Sea-state | Sea descriptive terms |
|---------------------|-----------------|------------------|----------------------|------------------|------------------------|------------------------|------------------------------|-----------|-----------------------|
| | Knots | ms ⁻¹ | Knots | ms ⁻¹ | | | | | |
| 0 | 0 | 0 | <1 | <1 | Calm | - | - | 0 | Calm (glassy) |
| 1 | 2 | 1 | 1-3 | 1-2 | Light air | 0.1 | 0.1 | 1 | Calm (rippled) |
| 2 | 5 | 3 | 4-6 | 2-3 | Light breeze | 0.2 | 0.3 | 2 | Smooth (wavelets) |
| 3 | 9 | 5 | 7-10 | 4-5 | Gentle breeze | 0.6 | 1.0 | 3 | Slight |
| 4 | 13 | 7 | 11-16 | 6-8 | Moderate breeze | 1.0 | 1.5 | 3-4 | Slight - Moderate |
| 5 | 19 | 10 | 17-21 | 9-11 | Fresh breeze | 2.0 | 2.5 | 4 | Moderate |
| 6 | 24 | 12 | 22-27 | 11-14 | Strong breeze | 3.0 | 4.0 | 5 | Rough |
| 7 | 30 | 15 | 28-33 | 14-17 | Near gale | 4.0 | 5.5 | 5-6 | Rough-Very rough |
| 8 | 37 | 19 | 34-40 | 17-21 | Gale | 5.5 | 7.5 | 6-7 | Very rough - High |
| 9 | 44 | 23 | 41-47 | 21-24 | Strong gale* | 7.0 | 10.0 | 7 | High |
| 10 | 52 | 27 | 48-55 | 25-28 | Storm | 9.0 | 12.5 | 8 | Very High |
| 11 | 60 | 31 | 56-63 | 29-32 | Violent storm | 11.5 | 16.0 | 8 | Very High |
| 12 | - | | 64+ | 33+ | Hurricane | 14+ | - | 9 | Phenomenal |

2.2.2 Sea and Swell waves

Sea is defined as the type of waves locally generated by wind (or storm events) and may be consisted of various waves with different characteristics (heights and periods) that most likely will propagate in the same direction with the wind generating them. In larger areas, where waves may travel beyond the area of generation, their energy slowly dissipates by internal friction and is transferred from higher to lower frequencies. Waves that have been generated in a faraway area and have propagated elsewhere are called swell. In enclosed water bodies, such as lakes, swells might be blocked and might not arrive at that area, thus the region might be only described by locally generated sea (Kamphuis, 2000).

2.3 Wave Theories

One of the most common wave theories is that of Stokes Wave Theory, based on the equations of motion and continuity of a frictionless fluid, on specific boundary conditions. Assuming that the wave height is significantly smaller in comparison to wavelength and depth, then the result is the Small Amplitude Wave Theory, presented in Airy (1845); i.e. the first approximation of Stokes Theory. Stokes wave theory is applicable in deep water; the small wave amplitude theory is more suitable in deep water for small waves, whilst higher approximations can be used for higher waves. In shallow water, the Cnoidal theory should be applied as it describes the changes of wave shape due to bottom interference. At the point where the waves break, solitary theory should be used. These three theories are continuous throughout wave propagation from offshore to nearshore conditions. Under different wave state conditions (deep, coastal waters or the breaking zone) different theories apply (Figure 2.3.1).

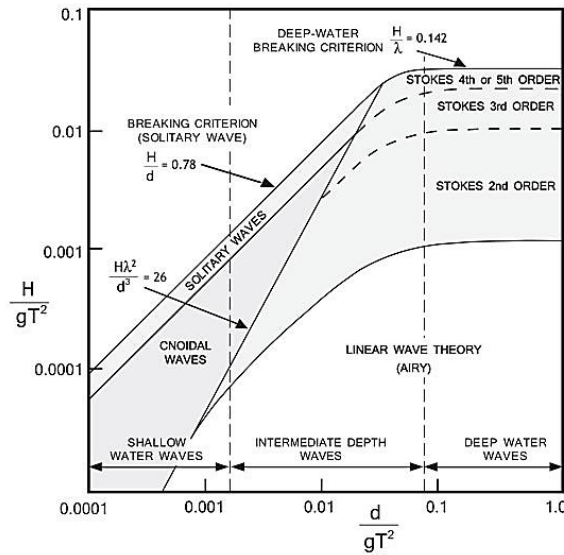


Figure 2.3.1: Wave theories applications in relation to water depth (from Le Mehaute, 1976)

To describe the dynamics of a free harmonic wave, atmospheric pressure at the water surface should be considered as constant and equal to 0 (Holthuijsen, 2007). Thus, if a wave is propagating in x - direction (variations in the y -axis are considered negligible) with the water level at 0 m, then the water level can be described as:

$$\eta(x,t) = \alpha \cos(kx - \omega t) = \frac{H}{2} \cos\left(\frac{2\pi x}{L} - \frac{2\pi t}{T}\right) \quad (2.1)$$

with α the amplitude of the wave, x the distance of wave propagation, t is time, k is wavenumber $k = \frac{2\pi}{L}$, the angular wave frequency $\omega = \frac{2\pi}{T}$ and T, L are the wave period and wave length respectively.

Furthermore, the maximum vertical distance between a crest and a trough is the wave height and is equal to $H = 2\alpha$. As steepness S is described the ratio of H/L and the velocity of propagation is $C = L/T$. Deep water conditions are applied when $d/L > 0.5$ while shallow water when $d/L < 0.05$ and the zone between these depths is considered as transitional. In CERC (1984), the empirical equations for estimating wave parameters in different zones of a coastal system are presented (Table 2.3.1).

Table 2.3.1: Empirical Equations for Wave Parameters (CERC, 1984)

| Parameter | Transitional Zone | Deep Water ($d/L > 0.5$) | Shallow Water ($d/L < 0.05$) |
|------------------------------------|--------------------------------------------------------------------------------------------------------|---------------------------------------------|--------------------------------------------|
| Water Surface (m) | $\eta = \frac{H}{2} \cos(kx - \omega t)$ | | |
| Velocity of Propagation (m/s) | $C = \frac{L}{T} = \frac{\omega}{k} = \frac{gT}{2\pi} \tanh kd$ $= \sqrt{\frac{gL}{2\pi} \tanh kd}$ | $C_o = \frac{gT}{2\pi}$ | $C = \sqrt{gd}$ |
| Wave Length (m) | $L = CT = \frac{gT^2}{2\pi} \tanh kd$ | $L_o = \frac{gT^2}{2\pi}$ | |
| Energy Density (j/m ²) | $E = \frac{1}{8} \rho g H^2; KE = PE = \frac{E}{2}$ | | |
| Wave Power (w/m) | $P = EC_g$ | $P_o = \frac{EC_o}{2}$ | $P = EC$ |
| Group Velocity (m/s) | $C_g = nC$ | $(C_G)_o = \frac{C_o}{2}$ | $C_G = C$ |
| Group Velocity Parameter | $n = \frac{1}{2} \left[1 + \frac{2kd}{\sinh 2kd} \right]$ | $n_o = \frac{1}{2}$ | $n = 1$ |
| Wave Breaking Criterion | $\left(\frac{H}{L} \right)_{\max} = 0.142 \tanh kd$ | $\left(\frac{H}{L} \right)_{\max} = 0.142$ | $\left(\frac{H}{d} \right)_{\max} = 0.78$ |

2.3.1 Time Series Analysis

As stated in Holthuijsen (2007), a wave is considered as the profile of the surface elevation between two successive downward or upward zero-crossings of the elevation (Figure 2.3.2).

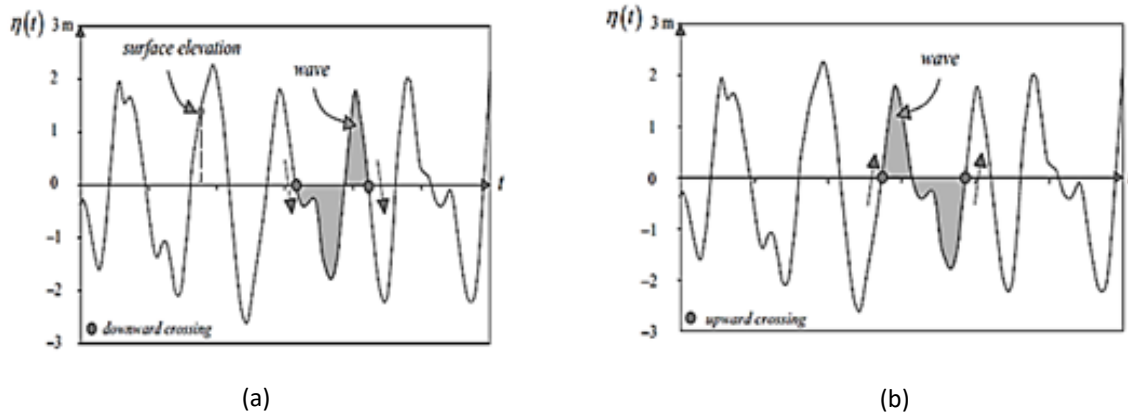


Figure 2.3.2: Definition of surface elevation and wave, a) zero-down crossing waves and b) zero-up crossing waves. (Holthuijsen, 2007)

Each wave is represented by one apparent height. Thus, in a wave records with N waves, the average wave height \bar{H} is defined as follows:

$$\bar{H} = \frac{1}{N} \sum_{i=1}^N H_i \quad (2.2)$$

where, i the number of the wave in the record.

Another common estimation of wave height is that of the quadratically weighted average value of mean-square wave height H_{rms} calculated as:

$$H_{rms} = \left(\frac{1}{N} \sum_{i=1}^N H_i^2 \right)^{1/2} \quad (2.3)$$

The significant wave height should be rather used and is estimated as follows:

$$H_s = H_{1/3} = \frac{1}{N/3} \sum_{j=1}^{N/3} H_j \quad (2.4)$$

where, j is the rank number of the wave depending on wave height.

The mean of the highest one-tenth of waves, is:

$$H_{1/10} = \frac{1}{N/10} \sum_{j=1}^{N/10} H_j \quad (2.5)$$

The visually observed wave height H_v is estimated in relation to the significant wave height as:

$$H_{1/3} = 1.67 H_v^{0.77} \quad (2.6)$$

If the reference level is zero then the period is named zero-crossing period T_0 and the average of this wave period is estimated by:

$$\bar{T}_0 = \frac{1}{N} \sum_{i=1}^N T_{0,i} \quad (2.7)$$

where, i the number of the wave in the record.

Significant wave period is estimated as follows:

$$T_s = T_{1/3} = \frac{1}{N/3} \sum_{j=1}^{N/3} T_j \quad (2.8)$$

where j is the rank number of the wave depending on wave height.

Finally, the mean period of the highest one-tenth of waves:

$$T_{1/10} = \frac{1}{N/10} \sum_{j=1}^{N/10} T_j \quad (2.9)$$

The significant wave period is related to the visually observed T_v as follows:

$$T_{1/3} = 2.83T_v^{0.44} \quad (2.10)$$

2.3.2 Spectral – Frequency Analysis

Sea surface elevation can be expressed as a superposition of an infinite number of waves, i.e. a random record of sea surface elevation $\eta(t)$ at a specified location in a specific moment of time, with duration (D) is expressed as:

$$\underline{\eta}(t) = \sum_{i=1}^N \underline{a}_i \cos(2\pi f_i t + \underline{\alpha}_i) \quad (2.11)$$

where, \underline{a}_i the random amplitude, $\underline{\alpha}_i$ the random phase of frequency $f_i = i/D$, and frequency interval $\Delta f = 1/D$ and N the number of frequencies; the phases are between 0 and 2π (Holthuijsen, 2007).

By applying a Fourier analysis, one can determine the exact values of amplitude and phases per frequency, thus getting the amplitude and phase spectrum of the record.

For the application of this model, the following assumptions are made: (i) sea state is a stationary (Gaussian) process and to achieve this, the wave record should be split in 15-30 min nominal sub-records; and (ii) the model is a combination of wave components with discrete frequencies. Instead of the amplitude spectrum, the variance density spectrum $E^*(f_i)$ is used.

This is done as noted in Holthuijsen (2007), 'by distributing the variance $E\left\{\frac{1}{2}\alpha_i^2\right\}$ over the frequency interval Δf_i at frequency f_i ', as shown below:

$$E^*(f_i) = \frac{1}{\Delta f_i} E\left\{\frac{1}{2}\alpha_i^2\right\} \text{ OR } E(f) = \lim_{\Delta f \rightarrow 0} \frac{1}{\Delta f} E\left\{\frac{1}{2}\alpha^2\right\} \quad (2.12)$$

To calculate wave spectrum parameters, spectral moments are used i.e.:

$$m_n = \int_0^\infty f^n E(f) df \quad (2.13)$$

for $n = \dots, -3, -2, -1, 0, 1, 2, 3, \dots$

The variance of the sea surface elevation $\overline{\eta^2}$ is equal to the zeroth order moment m_0 :

$$E\{\overline{\eta^2}\} = \int_0^\infty E(f) df = m_0 = \sigma_f^2 \quad (2.14)$$

The significant wave height H_{m_0} is defined as:

$$H_{m_0} \approx 4\sqrt{m_0} \quad (2.15)$$

The mean wave height \bar{H} is:

$$\bar{H} = \sqrt{\frac{\pi}{8}} H_{m_0} \quad (2.16)$$

and the root mean square H_{rms} :

$$H_{rms} = \frac{1}{2}\sqrt{2}H_{m_0} \quad (2.17)$$

The average time interval \bar{T}_η between crossings of a reference level η can be calculated from the spectrum as:

$$\bar{T}_\eta = \sqrt{\frac{m_0}{m_2}} / \exp\left(-\frac{\eta^2}{2m_0}\right) \quad (2.18)$$

with m_0 and m_2 the zeroth and the second order spectral moments respectively.

The mean frequency is:

$$\bar{f}_\eta = \sqrt{\frac{m_2}{m_0}} \exp\left(-\frac{\eta^2}{2m_0}\right) \quad (2.19)$$

The mean zero crossing period with the reference level being $\eta = 0$ is:

$$\bar{T}_0 = \bar{T}_{m_{02}} = \sqrt{\frac{m_0}{m_2}} \quad (2.20)$$

The mean zero crossing frequency is equal to:

$$\bar{f}_0 = \bar{T}_0^{-1} = \sqrt{\frac{m_2}{m_0}} \quad (2.21)$$

The higher the order of moments the more uncertain the results are due to sensitivity of noise in the higher frequencies of the spectrum. To avoid use of the second order moment, mean $T_{m_{01}}$ is estimated as:

$$T_{m_{01}} = f_{mean}^{-1} = \left(\frac{m_1}{m_0} \right)^{-1} \quad (2.22)$$

It is often stated that in deep waters observations can be described – estimated satisfyingly by probability density functions. However, this does not apply in conditions close to the coast as wave crests are sharper and troughs are shallower due to the nonlinear processes (Holthuijsen, 2007). Different spectra according to wave types are shown in Figure 2.3.3.

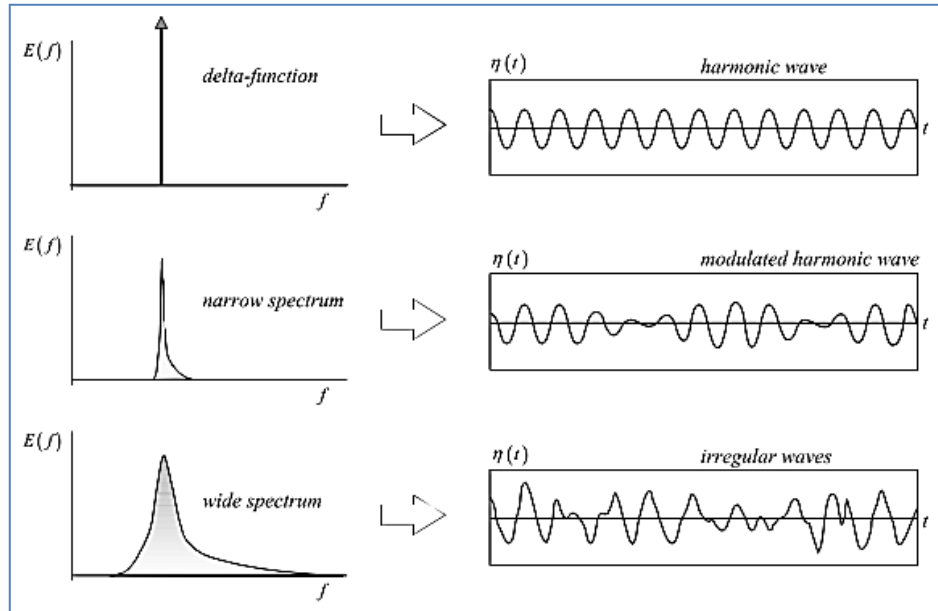


Figure 2.3.3: Wave spectrums and how they describe ocean waves. (Holthuijsen, 2007)

For swell conditions:

$$T_{1/3} \approx T_{peak} \quad (2.23)$$

with T_{peak} the peak period of the spectrum.

If a wind-sea spectrum is unimodal, then as shown in Goda (1978), the period of the higher- waves is:

$$\bar{T}_H \approx 0.95T_{peak} \text{ and } H \geq 1.5\bar{H} \quad (2.24)$$

with \bar{H} the mean wave height and the significant wave period is:

$$T_{1/3} \approx 0.95T_{peak} \quad (2.25)$$

To estimate the maximum value of wave height H_{max} in relation to the significant wave height, the following relationship can be used (Holthuijsen, 2007):

$$H_{max} \approx 2H_s \quad (2.26)$$

The spectral width parameter ε can be defined as (Cartwright and Longuet-Higgins, 1956):

$$\varepsilon = \left(1 - \frac{m_2^2}{m_0 m_4} \right)^{1/2} \quad (2.27)$$

For $\varepsilon \rightarrow 0$ (i.e. narrow spectrum), the probability distributions of sea surface elevation and wave height are of Rayleigh type, while for $\varepsilon \rightarrow 1$ (wide spectrum) by Gaussian type. Moreover, ε depends on the shape of the spectrum, the high-frequency cut-off and alterations of the spectrum in high frequencies. Another parameter of spectral width is the broadness factor ν (Longuet-Higgins, 1975) and is estimated as:

$$\nu = \left(\frac{m_0 m_2}{m_1^2} - 1 \right)^{1/2} = \left(\frac{T_{m_{02}}^2}{T_{m_{01}}^2} - 1 \right)^{1/2} \quad (2.28)$$

2.3.3 Statistics

Short – term wave analysis usually applies for wave records of a specific period or during a storm. Long-term covers analysis for periods of years usually in terms of distributional patterns (Kamphuis, 2000).

The probability density function (PDF) of the random process sea surface elevation η , $p(\eta)$ can be described as follows:

$$p(\eta) = \frac{1}{\sigma\sqrt{2\pi}} \exp\left[\frac{-\eta^2}{2\sigma^2}\right] \quad (2.29)$$

where, σ is the standard deviation of the process $\eta(t)$ and is the square root of variance of η (Kamphuis, 2000):

$$\sigma^2 = \frac{1}{N} \sum_{j=1}^N \eta_j^2 \quad (2.30)$$

For narrow spectra, the PDF of the maximum sea surface elevation is:

$$p(\eta_{\max}) = \frac{\eta_{\max}}{\sigma^2} \exp\left(\frac{-\eta_{\max}^2}{2\sigma^2}\right) \quad (2.31)$$

and if $H = 2\eta_{\max}$ then the pdf is:

$$p(H) = \frac{1}{4} \frac{H}{\sigma^2} \exp\left(\frac{-H^2}{8\sigma^2}\right) \quad (2.32)$$

The equations (2.31) and (2.32) are the Rayleigh Distribution for wave height (Forristall, 1978; Tayfun and Fedele, 2007; Casas-Prat and Holthuijsen, 2010).

The Cumulative Distribution Function (CDF) of wave heights for any individual wave height H' is not higher than a specified value of wave height H is:

$$P(H' < H) = 1 - \exp\left[\frac{-H^2}{8\sigma^2}\right] \quad (2.33)$$

Whilst the probability of a wave height H' will exceed a specific value of wave height H is:

$$Q(H' > H) = \exp\left[\frac{-H^2}{8\sigma^2}\right] \quad (2.34)$$

2.4 Deep Water Waves

When wave observations are not available (present or past), waves can be forecasted or hindcasted by using wind data depending on the complexity of the case. Waves are basically the result of pressure variations at the sea surface (not of wind friction) due to wave induced fluctuations at the wind above the waves. The newly generated waves will form in an angle to the wind direction in order to achieve a propagating speed similar to that of the wind (Phillips, 1957; Miles, 1957). When the first waves are formed, wind energy is transferred from the wind to the high frequency waves.

The energy is afterwards distributed to the lower frequencies via the slower moving water particles (i.e. from wind-wave to swells) with white-capping the only wave to dissipate energy. For an idealized wind state (constant in space and time and perpendicular to a straight coastline), an ideal wave state can be described by significant wave height and a significant wave period or a universal 1D or 2D spectrum. In these conditions, the wave generation depends only on wind speed, the distance towards the nearest shore (according to the wind direction that is blowing) or the duration of the wind-blowing. For a given location P , that has a distance F from the coast, a wave has direction θ and arrives at P within time t and has travelled a distance $c_g t$ from that direction since the wind started blowing (Figure 2.4.1). To describe accurately the wave state, wind speed U_{10} , fetch F , duration t and gravitational acceleration g are needed.

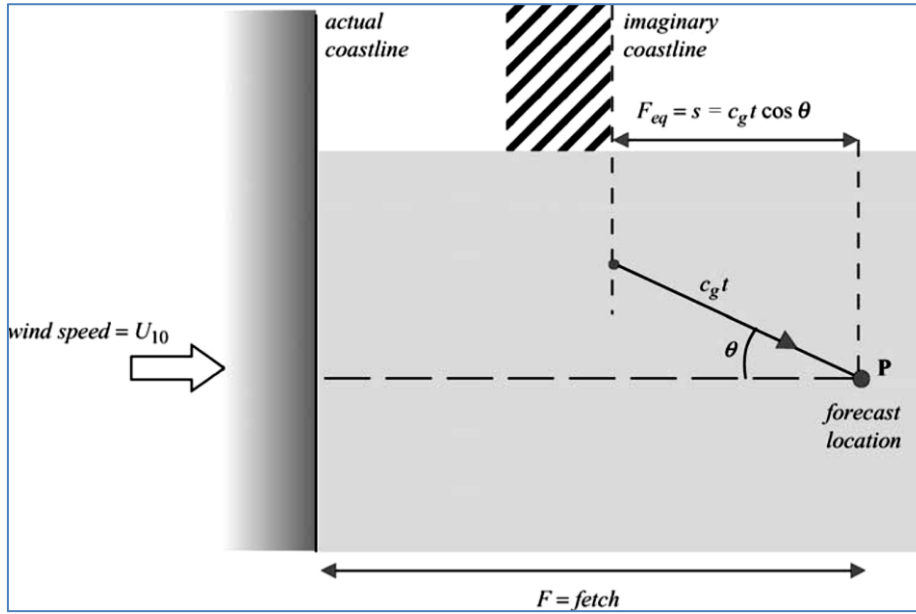


Figure 2.4.1: Equivalent fetch (F_{eq}) for the generation of a wind wave (Holthuijsen, 2007).

These four parameters can be decreased to three, in the form of an equivalent fetch F_{eq} used in terms of t . Equivalent fetch represents the distance between the point and the imaginary coast line if the wind was blowing with an infinite duration. Thus:

$$F_{eq} = s = c_g t \cos \theta \quad (2.35)$$

If the actual fetch is smaller than the equivalent fetch, then fetch is the limiting factor and the conditions are fetch-limited. If it is longer, the condition is then duration-limited.

As wind speed varies vertically above water surface, the height that is most commonly used for these equations is that of 10 m. For different heights, the logarithmic velocity profile is used for the estimation of wind speed:

$$\frac{U_{10}}{U_z} = \left(\frac{10}{z} \right)^{1/7} \quad (2.36)$$

with z the anemometer height. For this theory to apply, the atmospheric conditions in the vertical dimension are considered to be neutral and stable. Caution should be given when wind parameters (speed or direction) from land stations are used for these calculations, especially due to the complexity of friction and turbulence above land (Kamphuis, 2000).

The following dimensionless parameter of dimensionless fetch is given:

$$\tilde{F} = \frac{gF}{U_{10}^2} \quad (2.37)$$

To calculate the dimensionless significant wave height and significant wave period by using fetch, wind speed and gravitational acceleration the following equations apply:

$$\begin{aligned}\tilde{H}_{1/3} &= \frac{gH_{1/3}}{U_{10}^2} \\ \tilde{H}_{m_0} &= \frac{gH_{m_0}}{U_{10}^2}\end{aligned}\tag{2.38}$$

and

$$\begin{aligned}\tilde{T}_{1/3} &= \frac{gT_{1/3}}{U_{10}} \\ \tilde{T}_{peak} &= \frac{gT_{peak}}{U_{10}}\end{aligned}\tag{2.39}$$

For young sea states, waves grow rather fast but their growth slowly decays until it stops. In that stage, the waves are said to be fully developed. In such states, fetch does not affect the wave characteristics, as it approaches infinite, and depth is considered negligible.

A fully developed sea spectrum in deep water, as proven by (Pierson and Moskowitz, 1964) is estimated by:

$$E_{PM}(f) = a_{PM} g^2 (2\pi)^{-4} f^{-5} \exp\left[-\frac{5}{4}\left(\frac{f}{f_{PM}}\right)^{-4}\right]\tag{2.40}$$

with $a_{PM} = 0.0081$ and f_{PM} the energy scale and peak frequency.

For developing sea states the Joint North Sea Wave Project (JONSWAP) spectrum was suggested by (Hasselmann et al., 1973). JONSWAP results showed that the spectra had sharper peaks than that of the PM spectrum (Figure 2.4.2).

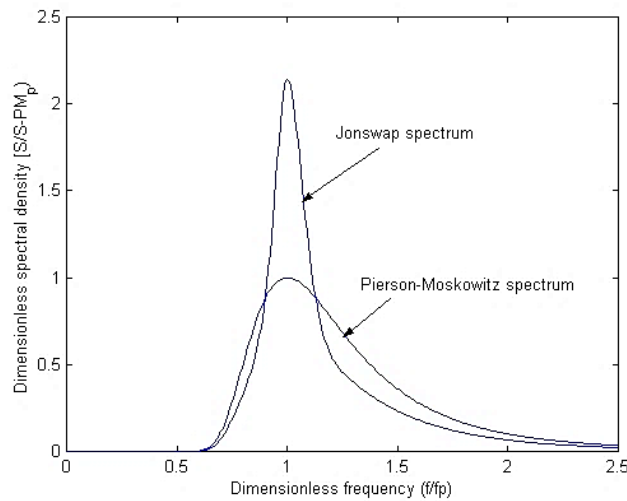


Figure 2.4.2 Comparison of a PM and a Jonswap Spectrum (Kamphuis, 2000)

The scientists of JONSWAP project decided to add a peak-enhancement function in order to parameterize the difference between the 2 spectra. Thus:

$$E_{JONSWAP}(f) = ag^2(2\pi)^{-4} f^{-5} \exp\left[-\frac{5}{4}\left(\frac{f}{f_{peak}}\right)^{-4}\right] \gamma \exp\left[\frac{1}{2}\left(\frac{f/f_{peak}-1}{\sigma}\right)^2\right] \quad (2.41)$$

with γ and σ the peak-enhancement factor and peak-width parameter, respectively.

The coefficient α can be described according to generating conditions of the wave state such as fetch length F and wind intensity U :

$$\alpha_j = 0.076 \left(\frac{gF}{U^2}\right)^{-0.22} \quad (2.42)$$

A schematic of wave spectra in relation to fetch is presented in Figure 2.4.3.

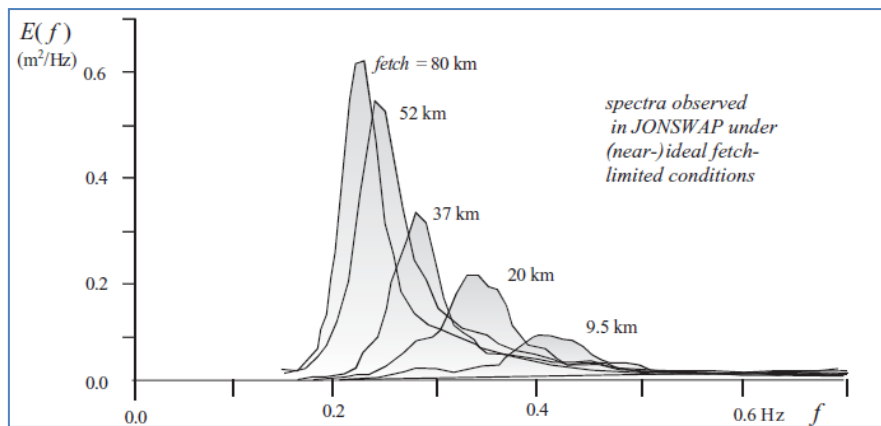


Figure 2.4.3: Wave Spectra according to fetch as given by JONSWAP (Hasselmann et al., 1973; Holthuijsen, 2007)

2.5 Nearshore Processes

During wave propagation from offshore to nearshore conditions, water depth has an effect on wave height and direction. If the waves change in their direction of propagation due to the variation of group velocity in the same direction then the phenomenon is called shoaling and leads to increasing wave height close to the shore. When waves' direction changes due to depth limitations in the phase speed along the waves' crest the phenomenon is called refraction. This leads to changing the directionality of waves towards shallower water and increasing or decreasing wave height, depending on the changes in wave direction. If the waves propagate in areas with obstacles such as islands, reefs, breakwaters etc. the variation in amplitude might "generate" areas with smaller amplitude. This phenomenon is called diffraction and can also lead to the generation of currents and set-up or set-down of the water surface especially close to the surf zone. In areas of small steepness and not too shallow water this phenomena can be described by the linear wave theory but in other cases, high resolution models (e.g. Boussinesq) that can represent non-linear effects should be used (Holthuijsen, 2007).

2.5.1 Shoaling

When a harmonic wave propagates in a perpendicular direction towards a straight shoreline, over gentle sloped topography with no currents, it will retain its frequency but its wave length and phase will decrease, with decreasing depths:

$$c = \sqrt{\frac{g}{k} \tanh(kd)} \quad (2.43)$$

The group velocity will increase slightly and then decrease:

$$c_g = nc$$

with

$$n = \frac{1}{2} \left(1 + \frac{2kd}{\sinh(2kd)} \right) \quad (2.44)$$

The effect of shoaling can be described as the slow decrease of wave amplitude and then an increase close to the shore. In theory, without including currents and other phenomena (e.g. refraction, wave breaking) as the group velocity approaches 0 m depth, the amplitude should go to infinity (Figure 2.5.1).

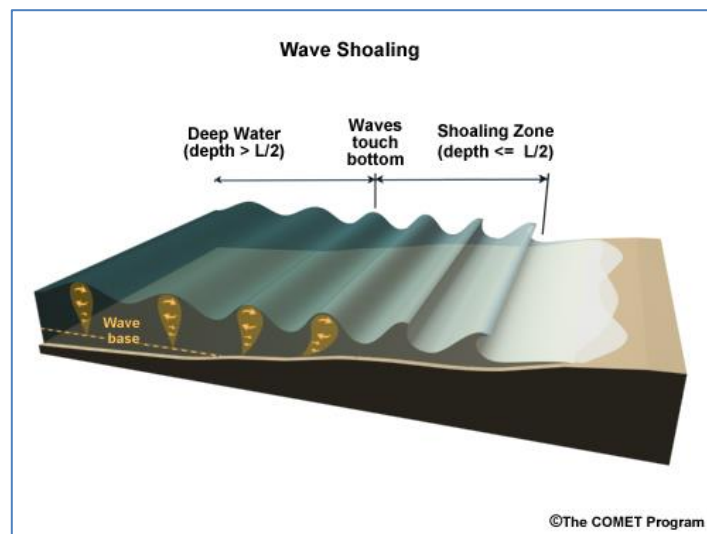


Figure 2.5.1: Wave Shoaling (NOAA, 2012)

To relate the wave height offshore H_0 to the wave height nearshore H , only under shoaling conditions, the shoaling coefficient can be used:

$$K_s = \frac{H}{H_0} \quad (2.45)$$

In deep water, the coefficient is approximately equal to 1, decreases in relation to depth to 0.91 and, then, approaches infinity as water depth reaches 0.

2.5.2 Refraction

When waves approach the coastline in an angle, then the phenomenon of refraction applies. The wave crests become more aligned with the bottom contours and the wave direction turns to shallower water (see wave rays in Figure 2.5.2). Wave refraction can result in wave energy spreading or converging but can be examined by looking carefully at the wave rays and at the direction that the wave is advancing and propagating.

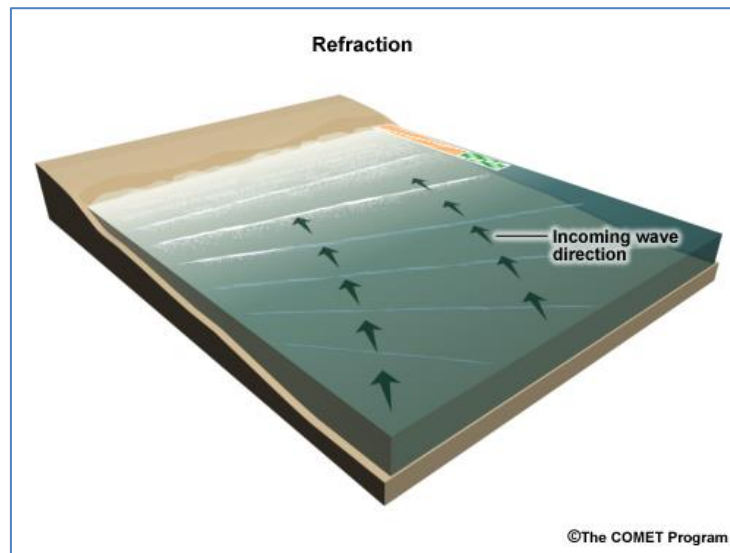


Figure 2.5.2: Wave Refraction (1) (NOAA, 2012)

If energy flux remains constant at the wave rays, then:

$$nCEb = \text{const.} \quad (2.46)$$

with n as given in Eq. 2.44, C the velocity of propagation, $E = \frac{1}{8}\rho gH^2$ the wave energy and b the distance among wave rays.

Offshore wave height H_0 can be related to the wave height at a location with the refraction coefficient K_r :

$$\frac{H}{H_0} = K_s K_r \quad (2.47)$$

With $K_r = \sqrt{\frac{b_0}{b}}$ and K_s as given in Eq. 2.45.

If the bottom contours and the shoreline are parallel and straight then Snell's Law can be applied (Kamphuis, 2000) to estimate the direction that the waves are propagating to.

Therefore, in Cartesian coordinates:

$$\frac{\partial}{\partial x}(k \sin \alpha) + \frac{\partial}{\partial y}(k \cos \alpha) = 0 \quad (2.48)$$

with x the cross-shore direction, y the alongshore direction and α the angle of the x -axis and a wave ray (Figure 2.5.3).

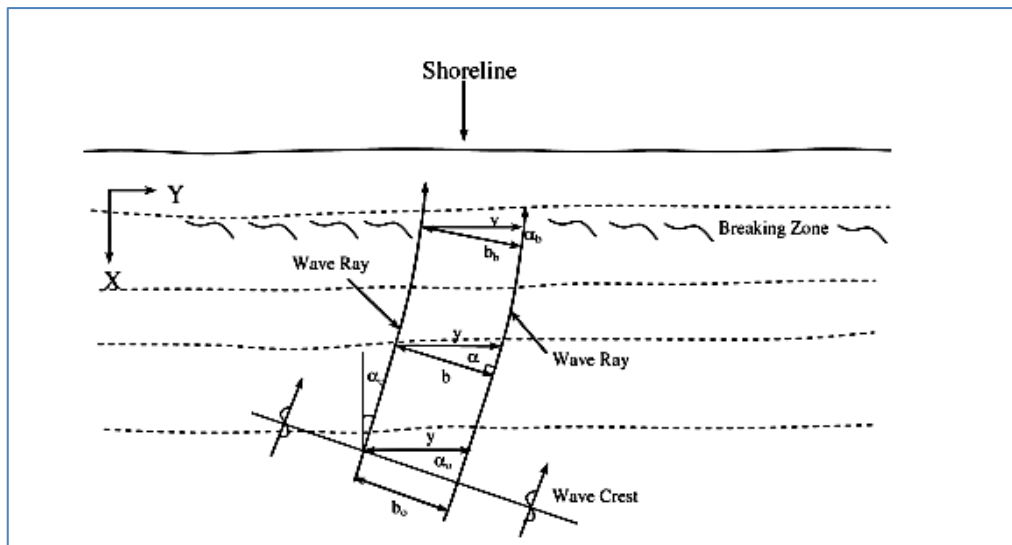


Figure 2.5.3: Wave Refraction (2) (Kamphuis, 2000)

If there is no refraction, then:

$$k \sin \alpha = \text{const.} \quad \text{and} \quad \frac{C}{\sin \alpha} = \text{const.} \quad (2.49)$$

Wave angles can be estimated as:

$$\frac{\sin \alpha_2}{\sin \alpha_1} = \frac{C_2}{C_1} \quad \text{and} \quad \frac{\sin \alpha}{\sin \alpha_0} = \frac{C}{C_0} = \tanh \frac{2\pi d}{L} \quad (2.50)$$

Additionally, if the distance of the wave rays parallel to the shore is constant then:

$$\frac{b}{\cos \alpha} = \text{const.} \quad \text{and} \quad K_r = \sqrt{\frac{\cos \alpha_0}{\cos \alpha}} \quad (2.51)$$

2.5.3 Diffraction

A harmonic, long crested wave that propagates in constant depths and under no refraction (horizontal bottom) towards an obstacle (barrier, breakwater, island etc.), will reach the shadow of the obstacle in circular pattern of crests with decreasing amplitudes (Figure 2.5.4a). The large variations in amplitude will be across the geometric shadow line of the headland. If there is no diffraction and the depth is constant, the waves will travel along straight wave rays and no energy will cross the shadow line thus, no waves will penetrate the shadow area behind the headland (Figure 2.5.4b).

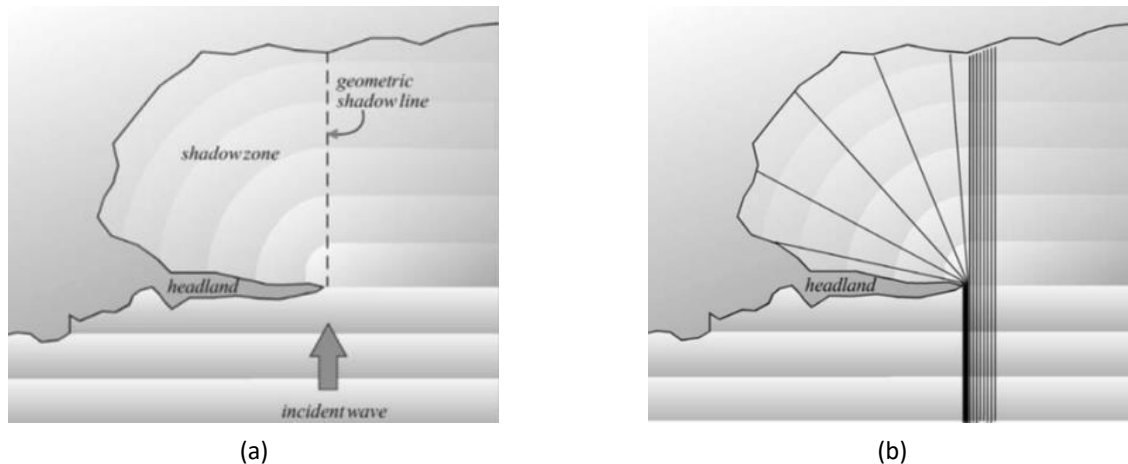


Figure 2.5.4: Wave diffraction in the lee of the barrier (Holthuijsen, 2007)

2.5.4 Refraction & Diffraction

In shallow waters with non - horizontal bottom, with wave propagation characterized by spatial variations in wave amplitude, refraction and diffraction phenomena should be included as nearshore processes. To numerically represent these variations, approaches such as the parabolic approximation of the mild-slope equation can be used (see Ch. 4.3). For this case, wave characteristics are computed line-by-line, in forward direction, towards a non-reflecting coast, in a directional sector of 60° – 90° of the main wave direction that remains constant over the computational region. For more analytical and advanced results where the waves can be random, short-crested and nonlinear the Boussinesq models are suggested (Holthuijsen, 2007).

2.5.5 Reflection

The coast where the waves propagate to will very probably reflect waves to some degree. Computing the effect of such reflection on the wave field is generally complicated as at each point in front of the reflecting coast, the wave motion would be the sum of the incoming wave and one or more reflected waves. The mechanisms involved in the reflection off a structure or coast are usually so complex that the reflection coefficient cannot be determined theoretically.

2.5.6 Breaking

As it has already been mentioned, in theory during wave shoaling conditions, the amplitude of the waves goes to infinity at the waterline. However, waves are described by their steepness and at when this is greater than the physical limit, the waves tend to break. When waves propagate from offshore to nearshore, the phenomena of shoaling, refraction and diffraction apply until their breaking point and after that their height decreases significantly until the waterline due to energy dissipation. At the breaking limit, the following parameters are defined H_b (wave height at breaking), d_b (breaking depth) and x_b (distance from shore) (Kamphuis, 2000).

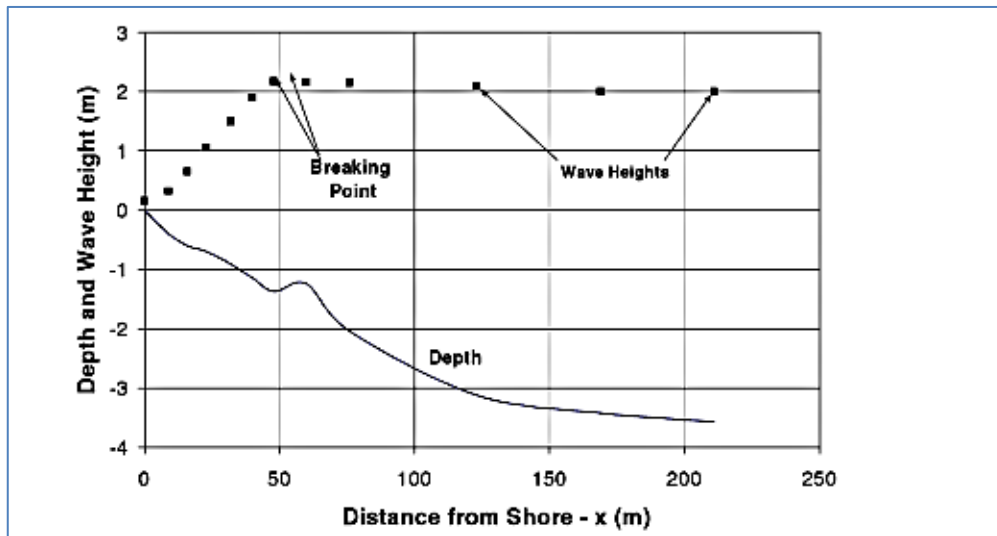


Figure 2.5.5: Wave Breaking Parameters (Kamphuis, 2000)

For a shore with small slope α , waves can be categorized according to their shape at the breaking zone via the Iribarren number or surf similarity parameter ξ_{br} (Iribarren and Nogales, 1949; Battjes, 1974):

$$\xi_{br} = \frac{\tan \alpha}{\sqrt{H_b/L_0}} \quad (2.52)$$

As shown in Table 2.5.1, spilling breakers occur when parts of wave crests break gently at flat beaches (steep waves or both). Plunger breakers are formed in steeper beaches (and/or flatter waves) with wave crests propagating faster and therefore plunging forward abruptly. Collapsing breakers form when a wave front explodes forward; for example a swell breaking at a beach with coarse material. Surging breakers are generated at very steep beaches, with the waves surging up and down the beach with little or no breaking.

Table 2.5.1: Types of waves according to the surf similarity parameter (Battjes, 1974)

| | |
|-----------------------|------------------------|
| Spilling | $\xi_{br} < 0.4$ |
| Plunging | $0.4 < \xi_{br} < 2.0$ |
| Collapsing or surging | $\xi_{br} > 2.0$ |

A schematic of the types of breaking waves according to Galvin (1968) is given in Figure 2.5.6.

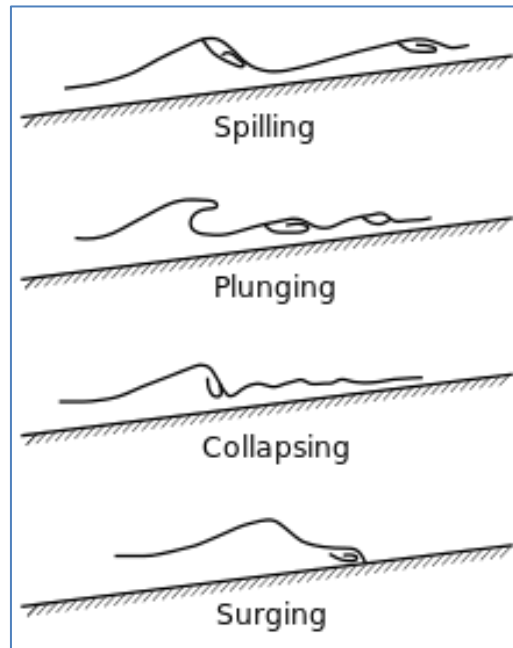


Figure 2.5.6: Types of Breaking Waves (Galvin, 1968)

A variety of criteria has been suggested to find the limiting depth according to wave height at the breaking point for regular waves (Kamphuis, 2000).

When the limiting wave steepness is exceeded, wave breaking can be estimated as shown in (Miche, 1944):

$$\frac{H_b}{L_b} = 0.14 \tanh\left(\frac{2\pi d_b}{L_b}\right) \quad (2.53)$$

When depth limits wave height, the solitary wave theory criterion (McCowan, 1894; Munk, 1949) can be applied:

$$\frac{H_b}{d_b} = 0.78 \quad (2.54)$$

In (CERC, 1984) the beach slope m is included in the relationship through c_1 and c_2 coefficients:

$$\frac{H_b}{d_b} = \left(c_1 - c_2 \frac{H_b}{gT^2} \right) \quad (2.55)$$

with $c_1 = 43.75 [1 - e^{-19m}]$ and $c_2 = \frac{1.56}{[1 + e^{-19.5m}]}$.

Furthermore, Goda (1970) suggested the following relationship:

$$\frac{H_b}{d_b} = 0.17 \frac{L_0}{d_b} \left[1 - e^{-\left\{ \frac{1.5\pi d_b (1+15m^{4/3})}{L_0} \right\}} \right] \quad (2.56)$$

For the case of irregular waves, two criteria are proposed using H_s as the wave height at breaking (Kamphuis, 1991):

$$H_{sb} = 0.095e^{4.0m} L_{bp} \tanh\left(\frac{2\pi d_b}{L_{bp}}\right) \quad (2.57)$$

as the steepness criterion and

$$\frac{H_{sb}}{d_b} = 0.56e^{3.5m} \quad (2.58)$$

as the depth limited criterion.

2.6 Sources of Wave Data

Wave data are needed for a variety of applications such as tourism, coastal engineering, maritime transport, renewable energy, leisure activities and more. Some of the most common sources of wave data are:

- **Visual observations:** Obtained from trained observers on board of vessels, structures etc. For a visual characterization of a wave, the observer should focus on the highest wave of the wave field (Holthuijsen, 2007). The World Meteorological Organisation in its guidelines states that wave height and period of a wave are “the average height and period of 15 to 20 well defined, higher waves of a number of wave groups” (WMO, 1998). Visual observations of waves are often used but can be relatively biased due to the lack of objectivity i.e. not experienced - qualified observers or ships avoiding sometimes severe atmospheric conditions.
- **In situ data:** Instruments are usually preferred as they are more objective and less biased. Some of these instruments are: wave buoys, wave poles, pressure transducers, current meters and echo-sounders. Instruments can sometimes be erroneous mostly due to hazards of the marine environment (i.e. corrosion etc.) or to limitations of the basic principles of the instrument, such as the swerving or capsizing of a buoy.
- **Altimetry:** provides information mostly about sea level and wave height as well as wind velocity vectors. It can be distinguished in laser, radar (i.e. wave scatterometers) and acoustic.

- **Imaging techniques:** obtaining data from stereo-photography data. To describe the sea state from cameras, more than one are needed to be installed e.g. two airplanes flying in formation.
- **Wave atlases - hindcasts:** The atlases are consisted by long term wave statistics from observational datasets gathered by institutions or government agencies. Hindcasts are data provided by computer simulations that are based mostly on archived wind fields from meteorological stations (Holthuijsen, 2007).

2.7 Climate Change & Sea Level Rise

2.7.1 Sea Level Rise (SLR) in Europe

Global atmospheric temperature and sea level rise are of the most common indicators of climate change (past and future). Moreover, sea level rise can be associated to many impacts on settlements, natural systems and can last for longer temporal scales. SLR can be a result of a variety of processes such as thermal expansion of the ocean from warming ocean water, additional water masses to the ocean from the melting of glaciers and ice caps as well as from changes in land-water storage (natural reservoirs such as groundwater or man-made). It should be mentioned, that sea level rise is not globally uniform due to changes in water density that vary spatially (large ocean circulation variability), changes in the gravity field and finally, the vertical land movement in either direction that can affect a location (tectonism) (IPCC, 2013). Most vulnerable to sea level rise are low-lying and small tidal coastlines with high population and especially with low adaptation policies mostly due to economical restraints. Some of the potential impacts of SLR in Europe are: flooding, coastal erosion, loss of flat coastal regions and salt-water intrusion into low-lying aquifers. Extreme events such as storm surges can cause significant damage especially in cases where positive storm surge is added to the tidal level, therefore increasing the coastal flooding by reaching extreme water levels. Storm surge parameters are related to atmospheric parameters such as the frequency, track and storm intensity. It should be mentioned though, that the shape of the coastline can also affect the height of the surge. Most of the studies of trends in extreme coastal sea level and storm surges include trends from hourly tide gauge records at least for the period since 1970 and even earlier in some locations (EEA, 2014). Past changes of sea level rise in Europe in relation to the level of 1990, as estimated from data of tide gauges and satellite altimetry are presented in Figure 2.7.1. It is evident that since 1880 there has been an increase in sea level but it is more significant after the 1990, where it is higher than the reference level of 1990; this is supported from the data of the tide gauges as well as those from the satellites.

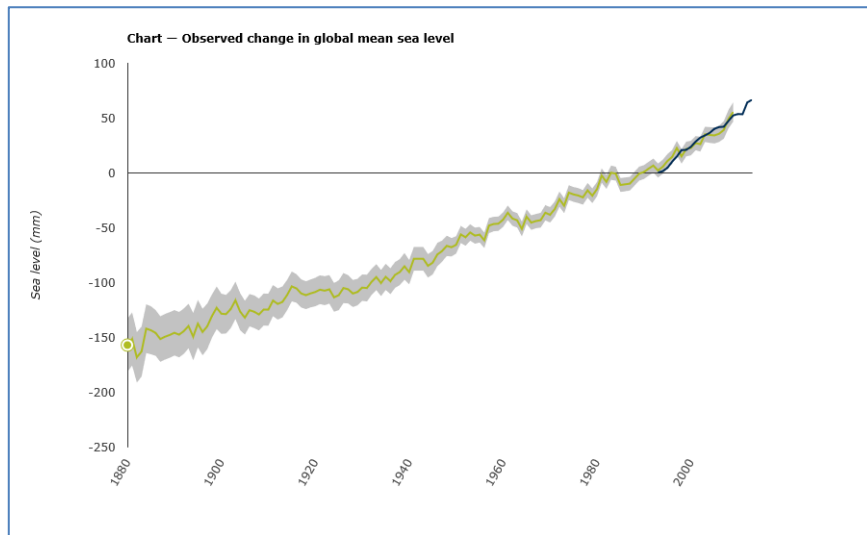


Figure 2.7.1: Global mean sea level from 1880 to 2013 relative to the level of 1990 according to tide gauge and satellite altimetry data. Uncertainty level is shown in grey and dark blue line is time series of satellite altimetry data for the period 1993-2013 (Church and White, 2011; Masters et al., 2012)

Trends of relative sea level from tide gauges in selected locations over Europe are shown in Figure 2.7.2. It should be noted that these trends have not been corrected for local movement and as tide gauges have longer temporal cover than the satellites, there might be additional differences. Decrease in sea level is shown in the Scandinavian countries and in the Central Aegean, whilst the rest of the European countries show increasing trends. The data are available at www.psmsl.org.

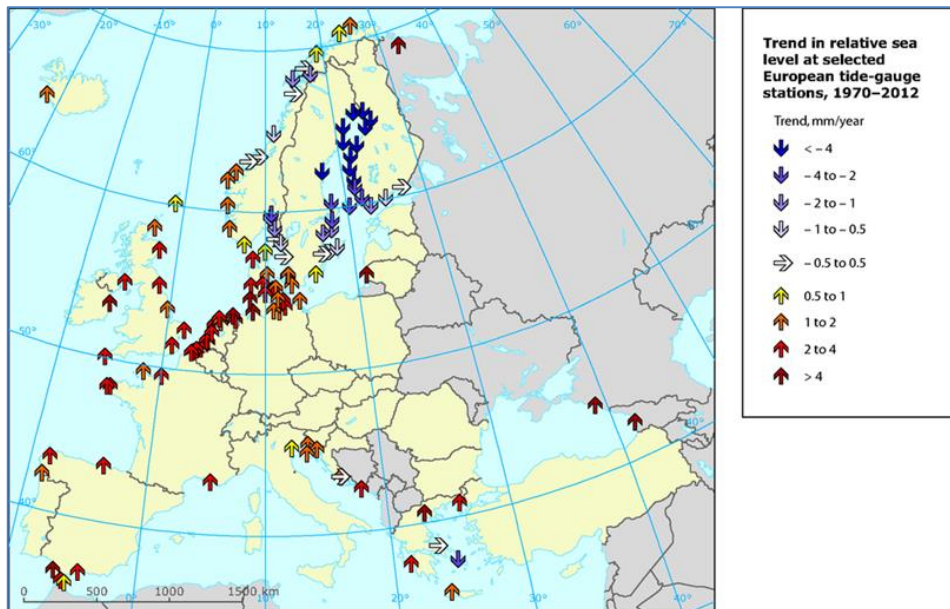


Figure 2.7.2: Sea level trends as estimated by several European tide gauges (from EEA, 2014; Woodworth and Blackman, 2004)

Regional mean sea level data from the satellite altimetry missions of Envisat, ERS-1, ERS-2, Geosat-FollowOn can be found at www.myocean.eu. Global mean sea level in Europe, is estimated to have risen by 0.19 mm from 1901 to 2013 with an average rate of 1.77 mm/year (EEA, 2014). From data of satellite altimetry, it is estimated that for the past 2 decades, sea level rise has presented a rate higher than 3.2 mm/year. Trends for the period 1992-2013, as estimated by satellite altimetry data, are presented in Figure 2.7.3. In the Mediterranean Sea there are areas that present increasing rates of 6 mm/year (South East Ionian Sea) whilst others decrease around 4 mm/year (Carpathian Sea). The variability of SLR among a region can be due to physical processes as mentioned in Holgate et al. (2013).

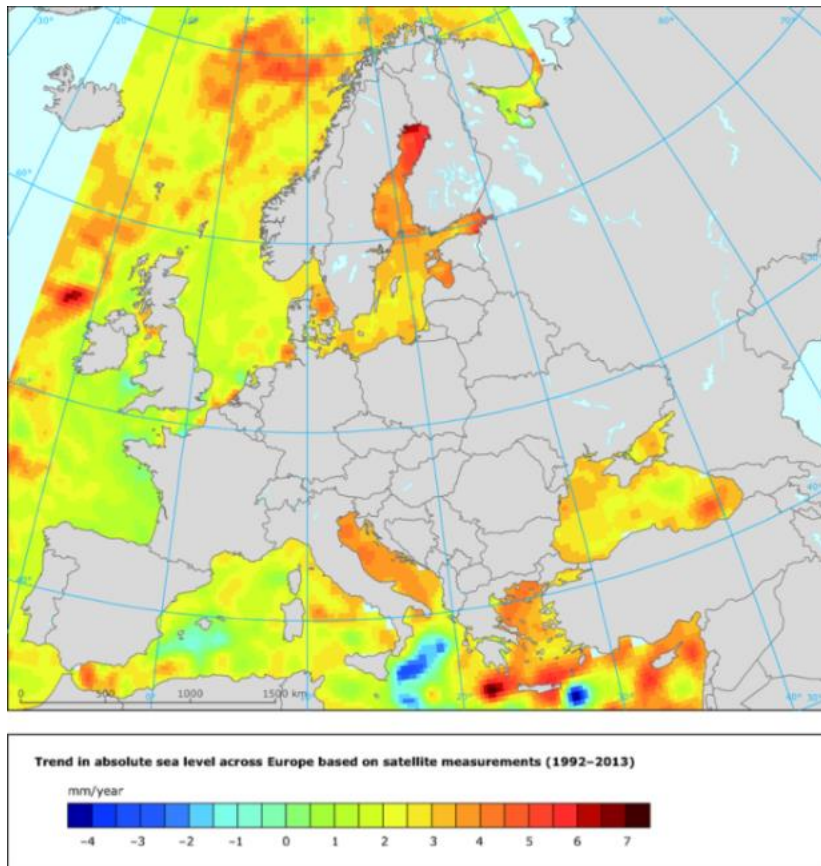


Figure 2.7.3: Trend of absolute sea level in Europe from satellite altimetry data for the period 1992-2013 (Holgate et al., 2013; European Environmental Agency, 2014)

2.7.2 Representative Concentration Pathway (RCPs) and Future SLR in Europe

2.7.2.1 RCPs definition

For climate change research, several scenarios have been established over time, to provide different research groups a common ground to combine conditions, historical data and future projections. The Intergovernmental Panel on Climate Change (IPCC) presented in the Fifth Assessment Report (AR5), the Representative Concentration Pathways (RCPs); RCP8.5, RCP6, RCP4.5 and RCP 2.6.

These scenarios are named as pathways in order to provide time dependent projections of the atmospheric greenhouse gases (GHG) concentrations and to present the path of the greenhouse that was needed to achieve a specific level (IPCC Expert Meeting Report, 2008). Many driving forces are included in these scenarios such as processes (physical, ecological, socioeconomic) and responses from climate change policy applications. Every RCP is characterized by starting values of emissions and estimates for up to 2100, based on a variety of assumptions about economy, energy sources, population etc. To process them, the emissions and socioeconomic scenarios are developed in a parallel way, via different paths of radiative forcings over time. They are not associated with any socioeconomic or emission scenarios but they depend on different economic, technological factors. In Moss et al. 2010 and van Vuuren et al. 2011, the criteria used in designing the RCPs are mentioned:

- The RCPs should be created from different modelling groups that will incorporate details from literature about emissions and concentrations
- The RCPs should describe all types of radiative forcing used as input for climate modelling and provide information about emissions of greenhouse gases, air pollutants and land use; available in a geographically explicit way
- The RCPs should have base year assumptions for emissions and land use and provide temporal smoothness among historical and future periods
- The RCPs’ time period should cover up to 2100, but information about the centuries afterwards should also be available

The basic difference with the previous Special Report Emission Scenarios (SRES) is that the SRES were distinguished according to the socio - economic circumstances but were not flexible in including potential changes in emissions and radiative forcings. On the other hand, the RCPs are able to include the emissions trajectory and the warming but also allow the socio economic options to change at will. Every RCP was developed and implemented by a different Integrated Assessment Modelling (IAM) group (Table 2.7.1).

Table 2.7.1: Representative Concentration Pathways (RCPs) publications and models (T.F. Stocker et al., 2013)

| RCP | Publications | Model |
|---------|------------------------------------------------------------------|---------|
| RCP 2.6 | (van Vuuren et al., 2006; Van Vuuren et al., 2007) | IMAGE |
| RCP 4.5 | (Clarke et al., 2007; Smith and Wigley, 2006; Wise et al., 2009) | GCAM |
| RCP6 | (Fujino et al., 2006; Hijioka et al., 2008) | AIM |
| RCP8.5 | (Riahi et al., 2007) | MESSAGE |

The MESSAGE model was developed and implemented by the International Institute for Applied Systems Analysis (IIASA), Austria with RCP8.5 based on increasing over time GHGs in accordance to levels leading to high GHGs amounts as described by literature (Riahi et al., 2007). The National Institute for Environmental Studies (NIES) in Japan, established RCP6, which is a stable scenario with total radiative forcing becoming more stable after 2100 due to application of technologies and policies, i.e. leading to reduction of GHGs emissions (Fujino et al., 2006; Hijioka et al., 2008). The Pacific Northwest National Laboratory’s Joint Global Change Research Institute (JGCRI) in the United States, established RCP 4.5 scenario in which total radiative forcing is stabilized after 2100, without exceeding the long-run radiative forcing target level (Clarke et al., 2007; Smith and Wigley, 2006; Wise et al., 2009). Finally, the RCP2.6 scenario was set by the PBL Netherlands Environmental Assessment Agency and the IMAGE modelling team. In this scenario, the GHGs levels remain low and it can be ultimately described by a radiative

forcing level of around 3.1 W/m^2 by mid-century, and a 2.6 W/m^2 by 2100. To reach these radiative forcing levels, GHGs emissions are reduced significantly, over time (Van Vuuren et al., 2007). The RCPs along with the SRES temperature equivalent are presented in Table 2.7.2.

Table 2.7.2: Representative Concentration Pathways (RCPs) (Moss et al., 2010; Riahi et al., 2007)

| RCP | Radiative Forcing | Concentration (ppm) | Temperature Anomaly ($^{\circ}\text{C}$) | Pathway | SRES Temperature Equivalent |
|--------|-----------------------------------------------------------------|-----------------------------------------------------------------------------|--------------------------------------------|--------------------------|-----------------------------|
| RCP8.5 | $>8.5 \text{ W m}^{-2}$ in 2100 | $>1370 \text{ CO}_2\text{-equiv.}$ in 2100 | 4.9 | Rising | A1F1 |
| RCP6.0 | $\sim 6 \text{ W m}^{-2}$ stable after 2100 | $\sim 850 \text{ CO}_2\text{-equiv.}$ (at stabilization after 2100) | 3.0 | Stable without overshoot | B2 |
| RCP4.5 | $\sim 4.5 \text{ W m}^{-2}$ stable after 2100 | $\sim 650 \text{ CO}_2\text{-equiv.}$ (at stabilization after 2100) | 2.4 | Stable without overshoot | B1 |
| RCP2.6 | Peak at $\sim 3 \text{ W m}^{-2}$ before 2100 and then declines | Peak at $\sim 490 \text{ CO}_2\text{-equiv.}$ before 2100 and then declines | 1.5 | Peak and decline | - |

2.7.2.1.1 Future Sea Level Rise in Europe

The projected changes in global mean sea level rise for the mid and late 21st century in relation to the period of 1986-2005 are presented in Table 2.7.3. GMSL rise during the 21st century will very likely occur at a higher rate than during 1971–2010. Process-based models estimate the rise in GMSL for the period 2081–2100, compared to 1986–2005, to be likely in the range 0.26–0.54 m for RCP2.6, 0.32–0.62 m for RCP4.5, 0.33–0.62 m for RCP6.0, and 0.45–0.81 m for RCP8.5. If the rate of SLR for the period 2081–2100 is 7-15 mm/year, then for RCP8.5 the rise is estimated to be by 2100, 0.53–0.97 m (T. Stocker et al., 2013).

Table 2.7.3: GMSLR estimates according to the RCPs for the periods 2046-2065 and 2081-2100 in relation to the reference period 1986-2005 (IPCC, 2013)

| | Scenario | 2046-2065 | | 2081-2100 | |
|--------------------------------|----------|-----------|--------------|-----------|--------------|
| | | Mean | Likely Range | Mean | Likely Range |
| Global Mean Sea Level Rise (m) | RCP2.6 | 0.24 | 0.17-0.32 | 0.40 | 0.26-0.55 |
| | RCP4.5 | 0.26 | 0.19-0.33 | 0.47 | 0.32-0.63 |
| | RCP6.0 | 0.25 | 0.18-0.32 | 0.48 | 0.33-0.63 |
| | RCP8.5 | 0.30 | 0.22-0.38 | 0.63 | 0.45-0.82 |

The contributions to global mean sea level rise according to the RCPs and A1B of the SRES are presented in Figure 2.7.4. In the worst case scenario (RCP8.5), thermal expansion is considered as the most significant contributor in sea level rise.

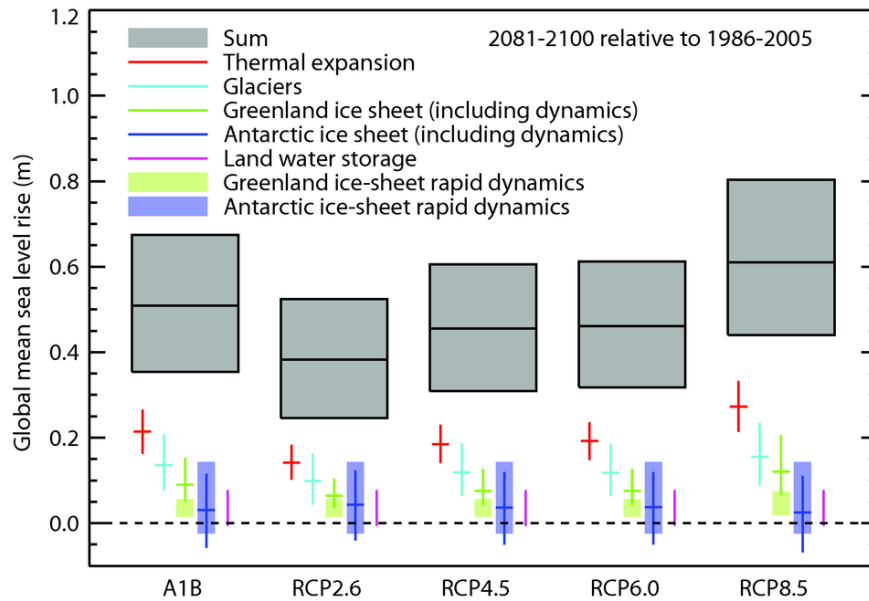


Figure 2.7.4: Projections of GMSLR and its contributors (IPCC, 2013)

Projected sea level change in 2081-2100 for Europe is shown in Figure 2.7.5, as estimated in relation to the period 1986-2005 for the RCP4.5 scenario based on CMIP5 climate model. For the Eastern Mediterranean it is presented that relative sea level rise will range from 0.3 m to 0.5 m (Church and White, 2011).

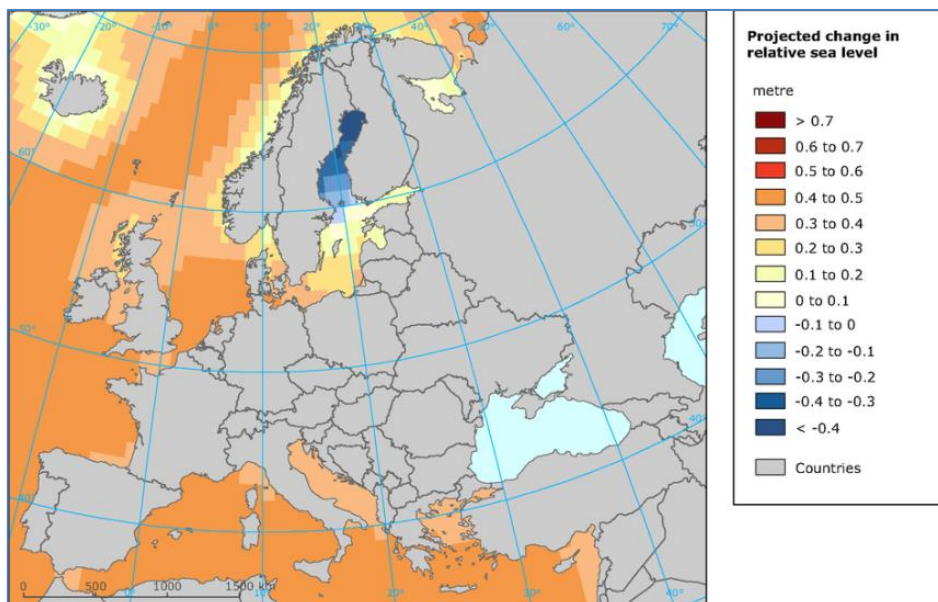


Figure 2.7.5: Projections for relative sea level (Church and White, 2011; IPCC, 2013)

Chapter 3 - The Case Study Areas

3 The Case Study Areas

3.1 Mediterranean

3.1.1 Geomorphological Characteristics

The Mediterranean Sea covers an area of about 2.5 million km² with distance from north to south of 900 km and 3800 km from east to west. Its' geographical limits are: at the west the Strait of Gibraltar (320 m deep and 14 km wide; the only connection to the Atlantic), at the northeast the Bosphorus and the Dardanelles Channel (maximum depth is 70 m and connects the Mediterranean with the Black Sea), the Suez Canal (163 km length, 300 m width, depth of 13 m, connection to the Red Sea). The Eastern Mediterranean can be divided in 4 sub - basins: Adriatic, Ionian, Levantine and the Aegean (along with its sub-basins) as shown in Figure 3.1.1. The Adriatic is an almost rectangular semi-enclosed sub basin with 800km length and 200km width that is connected to the Eastern Mediterranean via the Otranto Straits (75 km width and 800 m depth). The Ionian basin is located at the south of Italy and Greece and extends to the Libyan coast. It is characterized by the deepest point of the Mediterranean at the Hellenic Trough at the west of the ridge among western Crete and Libya, separating the Ionian and the Levantine (Zenetos, 2005; Mertens, 2006).

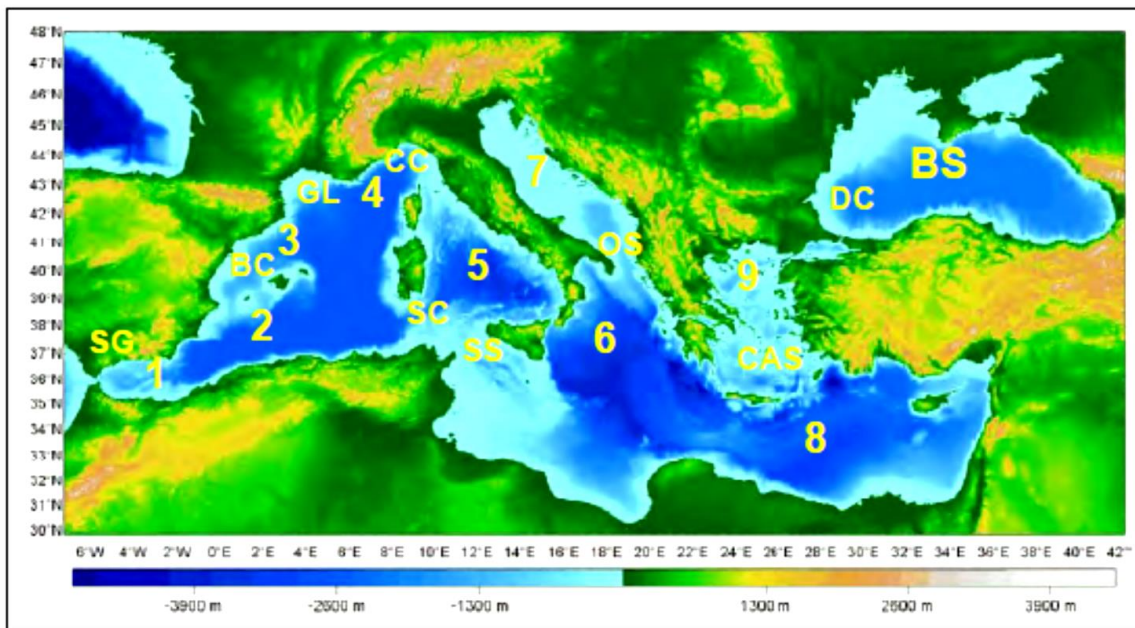


Figure 3.1.1: The sub-basins of the Mediterranean: 1) Alboran Sea, 2) Algerian, 3) Balearic, 4) Liguro- Provençal, 5) Tyrrhenian, 6) Ionian Sea, 7) Adriatic Sea, 8) Levantine and 9) Aegean Sea. SG: Strait of Gibraltar, BC: Balearic Channels, CC: Corsica Channel, SC: Sardinia Channel, SS: Strait of Sicily, OS: Otranto Strait, CAS: Cretan Arc Straits, DC: Dardanelles Channel, GL: Gulf of Lions; BS: Black Sea. (Mertens, 2006)

3.1.1.1 The Greek Seas

The Aegean Sea is located among the Greek Peninsula and the Asian Minor and is characterized by its complexity of physical and geographical aspects (Figure 3.1.2). In the northeast, it is connected with the Black Sea via the Dardanelles, the sea of Marmaras and Bosphorus. At the south, its border is the Island of Crete while at the southeast is also connected with the Levantine, at the southeast of Kassos (depth 700m, width 67km), Karpathos (depth 550m, width 43km) and Rhodes (depth 350m, width 17km). The morphology of the sea floor at the north part is characterized by an extensive shelf, while the southern part is more complex especially due to the high tectonic activity of the region. Moreover, the Aegean Sea is divided in 3 sub-regions: northern, central and southern. The North Aegean is characterized by the North Aegean Trough (which accommodates the Sporades Basin (1500 m maximum depth) and the Mount Athos Basin (1000 m maximum depth)) and the North Aegean Shelf. The Central Aegean is characterized by Chios Basin with depths of up to 1200 m (Sylaios 2011). The Southern Aegean is characterized by basins that are distributed from the volcanic arc to the island arc to the south and some of them are distinguished due to their big depths (Figure 3.1.2). The Cretan basin has the largest and deepest depression within the region, with water depths exceeding 2000 m in the northeast of Crete. The Ionian Sea is connected with the Aegean in 3 locations: Antikithira (depth 700 m, width 32 km), Kithira (depth 60 m, width 33 km) and at Elafonissos (depth 180 m, width 11 km). Furthermore, the deepest point of the Ionian Sea is located outside of Pylos (Southwest Peloponnese) and is estimated around 4.5 km.



Figure 3.1.2: Major morphological features of the Greek Seas. Adopted by (Zenetos, 2005)

The Hellenic coastline covers more than 18000 km with cliffs, beaches etc. Factors such as geology, geomorphology and geodynamics as well as climatic-meteorological factors contribute significantly to the evolution of the coastal zone.

A spatial classification according to sediment characteristics is presented in (Figure 3.1.3). The majority of the Hellenic coastline (75-80%) is described by cliffs and rocky shores, 5% by cliffs with beaches while 15% are depositional coasts (Zenetos, 2005).

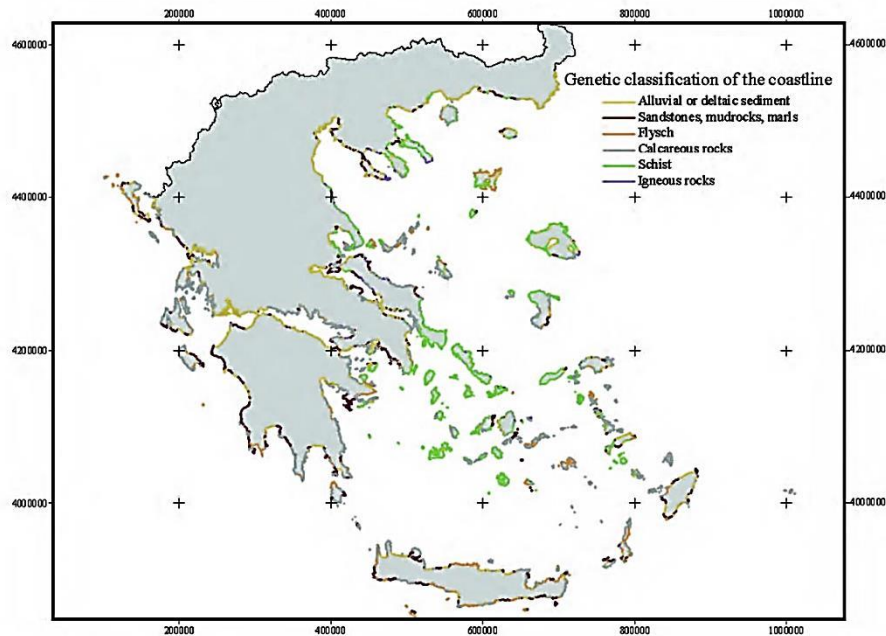


Figure 3.1.3: Sedimentary Classification of the Greek Coastline (Zenetos, 2005)

3.1.2 Wave and Weather Characteristics

The Mediterranean climate can be characterized by mild and rainy winters with warm and dry summers. The complex topography of Greece in combination with the passing through weather systems can produce intense climatic variability, in a way that in small spatial scales climate can change from Mediterranean to Alpine. In general, there are 4 climatic types in Greece:

- Maritime Mediterranean: with characteristics of temperate climate in the west coastal areas of Greece and the Ionian Islands
- Land Mediterranean: mostly in SE Greece, part of Mainland Greece, parts of Eastern Peloponnese, islands and coasts of Central Aegean and Crete, with drier summers and colder winters
- Continental Mediterranean Type: at the larger part of Northern Greece and similar to the climate of the Southern Balkans
- Mountainous Mediterranean: mostly at the mountainous regions of Greece.

Weather systems over the Eastern Mediterranean basin, are mostly controlled by the seasonal movement of semi-permanent systems of high pressure systems that are formed over the Atlantic, Europe, Asia and North Africa such as the anticyclone of Azores, the Siberian anticyclone and the primary and secondary depressions of the Mediterranean.

However, the variability of the geographical characteristics of the areas, with the form of topographical characteristics and water distribution, are responsible for the evolution of atmospheric circulation in a smaller and local scale. For example, the Gulf of Genoa is considered as the region with the most frequent intense cyclogenesis in the Mediterranean, but cyclones are also generated in the Adriatic Sea, in Cyprus and Aegean Sea, in the Black Sea and in several areas of the western Mediterranean Sea (Flocas and Karacostas, 1994; Trigo et al., 1999; Trigo et al., 2002; Lionello, Malanotte-Rizzoli, Boscolo, Alpert, et al., 2006; Lionello, Malanotte-Rizzoli, Boscolo, Tsimplis, et al., 2006; Lionello, Bhend, et al., 2006).

Some of the strong winds in the Mediterranean are characterized by locality and behaviors are shown in Figure 3.1.4 (Reiter, 1975) and are usually related with the Mediterranean cyclones. A low pressure system over Italy or westwards can result in Sirocco storms in the Adriatic Sea, with the channelling effect of Apennines and Dinaric Alps intensifying the flow that otherwise could be distributed on a larger front. In addition, air flow and orography can contribute to the development and evolution of local winds that can be noticed as downslope flows or formed due to channelling effects. Hot winds blowing from the desert across the Libyan and Egyptian segments of flat coast (Chill), strong easterlies over the Eastern Mediterranean and the Libeccio storms in the Tyrrhenian Sea, are examples of winds formed by the interactions of the aforementioned parameters (Saaroni et al., 1998; Lionello, Bhend, et al., 2006; Zenetos, 2005).

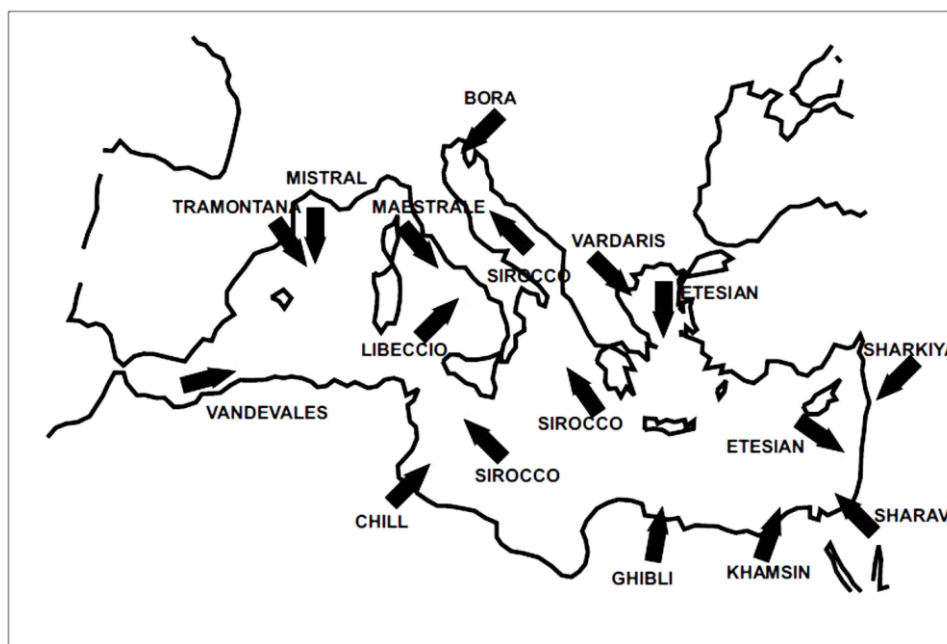


Figure 3.1.4: Main local winds of the Mediterranean (Lionello, Bhend, et al., 2006)

Wind patterns can be distinguished in two periods of maximum fluctuation, one during winter (DJF) and a secondary during summer (JJA). During winter, most of the cyclones are originated at Gulf of Lions, Gulf of Genoa, North Adriatic Sea and Eastern Mediterranean. The primary cyclones pass through southern Italy, towards Greece and over the Aegean Sea and then turn towards the Black Sea.

Secondary cyclones are usually formed over the desert region south of the Atlas mountain ranges of North Africa. These cyclones transfer tropical air masses that move eastward along the coast or enter the eastern Mediterranean. The west part of the Eastern Mediterranean region is characterized by high precipitation with the Ionian Sea receiving much more rain than the Aegean Sea and that is due to the blockage of the mountain ranges at the Hellenic Peninsula. Southeast anticyclonic activity over central Europe, low-pressure systems along with high-pressure systems over the Balkan Peninsula may form northerly flows that prevail in the Aegean Sea. Bora winds (called Vardaris in Thermaikos Gulf) are north to northwest cold and strong winds whose flow is blocked to the Aegean Sea by Rodopi Mountains to the north, the Pindos Mountains to the west, and the western Turkish Mountains to the east (Kallos et al. 1996; Poulos et al. 1997; Zenetos 2005) .

During summer, persistent northerlies govern the atmospheric circulation of the Eastern Mediterranean (Metaxas 1977, Maheras 1980). They are formed due to the east – west pressure variation of the pressure dipole of the Persian trough and the high pressure over Central Europe and Western Mediterranean (Saaroni et al. 1998, Tyrlis et al. 2013). Several researchers suggest that the Etesians control the Eastern Mediterranean climate during summer and that the southward directions of waves in the Aegean and Levantine are related with the impact of the Etesians on the water volumes (Lionello and Sanna, 2005; Zecchetto and De Biasio, 2007). Over the Northern Aegean, the winds are of north-easterly direction, over the Central and South Aegean they are north-westerly to southeast. Over the Ionian, they are mostly weakened, with NW directions at its southern areas (Klaic et al., 2009). The complex topography in the Aegean can alter the flows characteristics (e.g. channelling - funnelling) such as in Crete where the flow slows down at the upwind' side (Kotroni et al., 2001; Koletsis et al., 2009). In Tyrlis et al. (2013) and Tyrlis and Lelieveld (2013), it is suggested that the short-term variability of the Etesians, is controlled by dynamics of mid-latitudes and their interannual variability is linked with the formations of the South Asian monsoon. By examining Etesians outbreaks, the authors conclude that these outbreaks are more frequent in mid-July to mid-August, with the maxima in the beginning of August. Transient periods are considered the changes from / to winter and summer climate patterns. From winter to summer the period is that of March to May, with the decay of the Siberian anticyclone, stopping cold air and bringing warm weather in the Eastern Mediterranean. Cyclonic activity is not that common during spring and becomes less intense as summer approaches. Cyclones from North Africa are those that form southerly winds that in turn, bring the Saharan dust in the Eastern Mediterranean. Autumn is basically from the end of September to end of October with a change to winter conditions (Poulos et al., 1997; Zenetos, 2005; Flocas et al., 2010; Kouroutzoglou et al., 2011).

The initial fluctuations that lead to wave generations are caused from changes of the atmospheric pressure that result in very small amplitude waves (capillary waves). With the wind blowing and increasing speeds, waves become higher until when they reach the point where they start to break (Hasselmann 1968, LeBlond and Mysak 1978, Zenetos 2005; Holthuijsen 2007). In Lionello et al. (2006c), it is suggested that waves in the ocean are due to winds in a way that intense cyclones can generate extreme waves. Local parameters of winds such as duration and fetch should be kept in mind as well.

The tidal signal in the Aegean and the Ionian seas cannot be described separately from the Mediterranean tidal patterns as they are directly linked. The accurate description of the Mediterranean tidal signal is of importance especially due to its relation with climate change and for the last two decades this is done by data from satellite altimetry and precise tidal estimates from GPS stations. The tidal system of the Mediterranean can be described as the summing of the astronomical forcing per area and the Atlantic tidal wave that enters the Mediterranean via the Gibraltar Straits.

The tidal components can exceed 10 cm in certain areas such as the north Aegean Sea, the Adriatic Sea and the Gulf of Gabes. Euripus and Messina Straits are areas with enhanced tidal components (Tsimplis, 1994; Zenetos, 2005).

To provide sufficient information about the marine state of the Greek Seas, the following data sources are available:

- **in-situ measurements:** wave buoys of the POSEIDON project of the Hellenic Centre for Marine Research (HCMR) (Soukissian et al., 1999). More than twenty tide-gauges have been in operation in Hellas during the last decades by the Hellenic Navy Hydrographic Service (HNHS) (Tsimplis and Spencer, 1997). Data from the tide gauges can be found in monthly and annual values in www.psmml.org.
- **Satellite altimetry products:** these include wave measurements as obtained from Topex / Poseidon processed and can be provided by AVISO. It should be noted that areas of 3 to 5 kilometres from the coasts or islands are not covered.
- **Visual observations:** as obtained by trained personnel on board of Voluntary Observing Ships (V.O.S.) and include parameters such as visual wave height H_v , visual wave period T_v and visual wave direction. For the Greek Seas a relevant dataset has been published in the form of Wind - Wave Atlas, from various V.O.S. with observations from the mid-1850s and is considered with almost no lack of coverage and good quality (Athanasoulis and Skarsoulis, 1992). The spatial resolution considered finest for the atlas was that of $1^\circ \times 1^\circ$ (elementary regions) and from those 33 larger regions were created with homogeneous wave characteristics (Figure 3.1.5).

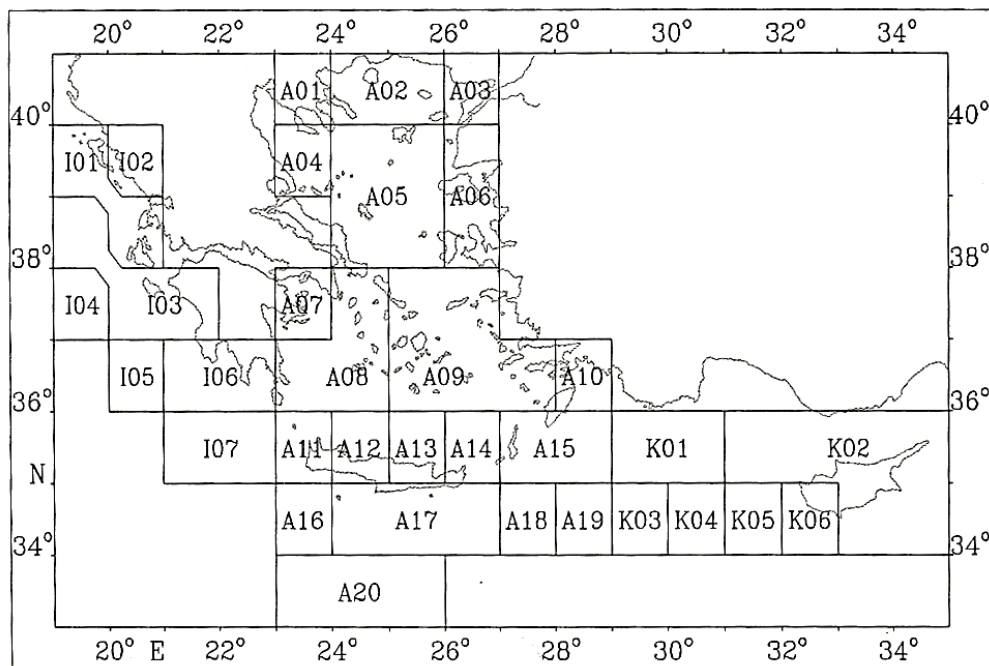


Figure 3.1.5: Regions of similar wave characteristics (Athanasoulis and Skarsoulis, 1992)

- **Wave model & hindcasts:** The first methods of wave forecasting have been established since 1947 (Sverdrup and Munk, 1947) and have evolved tremendously since then. A third generation wave model (WAM) was implemented and its description is given in (Komen et al., 1994).

Hindcasting is another form of numerical wave modelling, in the sense that it accumulates long-term wave data in spatial and temporal scales whilst using as inputs historic wind fields. The HCMR uses as basic model DAUT as developed by Christopoulos and Koutitas (1991), for wave forecasting a WAM-Cycle 4 model and SWAN for wave simulation at the coastal zone (Booij et al., 1999). A comparison of the results of WAM, DAUT, MIKE 21 OSW and data from buoys and satellites are given in Soukissian et al. (2001) and Kechris and Soukissian (2004). For WAM, the data used as inputs of the wind field are from the weather forecasting model (SKIRON) as developed by Kallos et al. (1997). WAM runs daily for 2 grids with 24 discrete directions and spectral density within the range 0.05054 – 0.66264 Hz, discretized logarithmically in 28 discrete frequencies (Soukissian et al., 2007):

- i) the Mediterranean with resolution $0.25^\circ \times 0.25^\circ$ with a time step of 720 s (Figure 3.1.6a)
- ii) The Greek Seas with resolution $0.05^\circ \times 0.05^\circ$ with a time-step of 180s and with boundary conditions the results of the Mediterranean ran (Figure 3.1.6b).

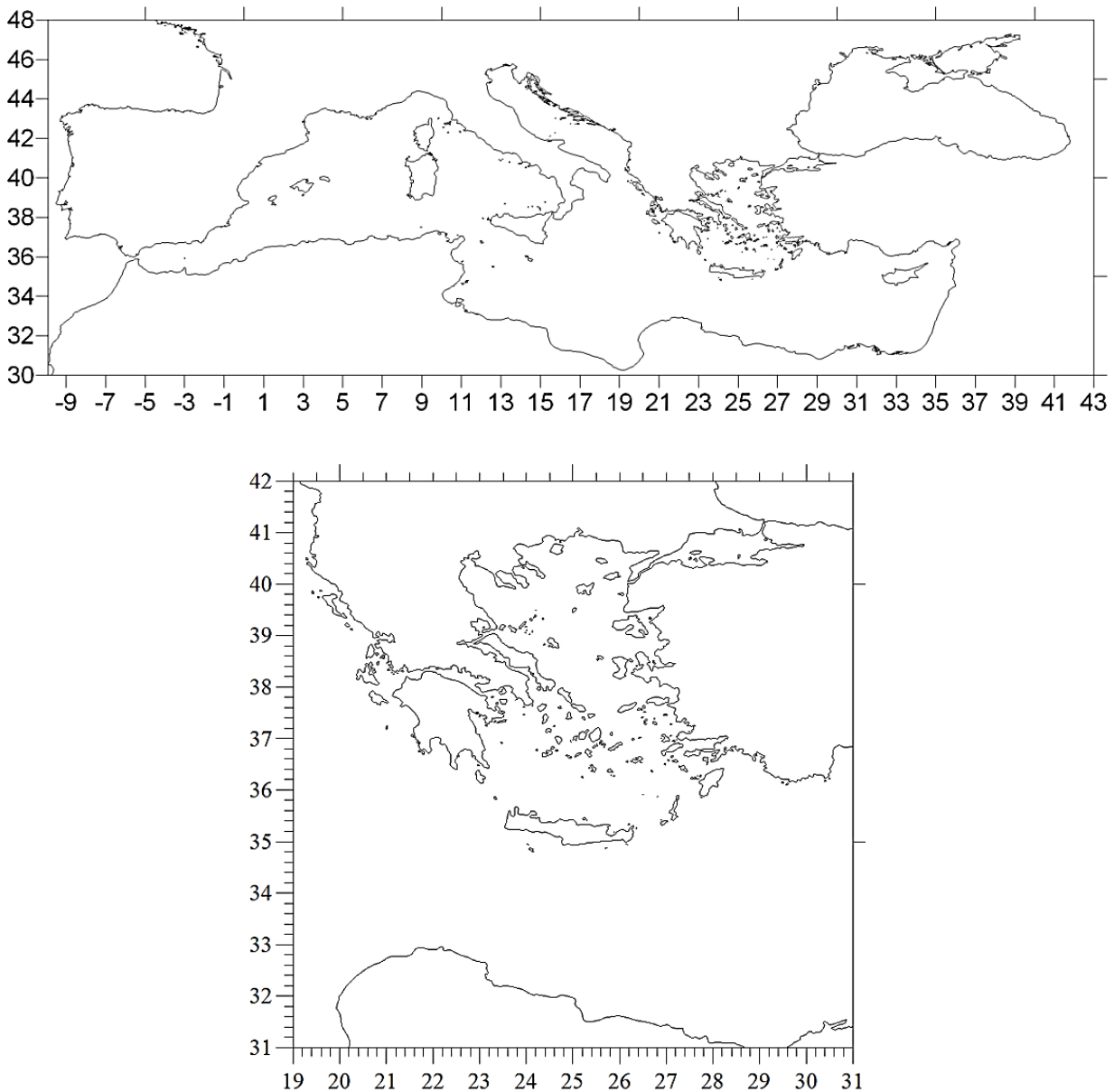


Figure 3.1.6: Grid of the WAM model for the Mediterranean (upper) and b) of the Greek Seas (lower)

3.1.2.1 Characteristics of the Greek Seas and Trends as given in previous studies

3.1.2.1.1 Wind and Wave Atlas V.O.S.

Data from selected boxes (see Figure 3.1.5) from the Wind and Wave Atlas (Athanasoulis and Skarsoulis 1992) shows that:

A01: Waves with heights of 0 to 0.5 m have frequencies of 82.29% with 98.8% of those having periods from 0 to 5 s. Waves with heights more than 2 m have frequencies of 0.65% and periods are all from 0 to 9 s. Winds with speeds from 2-8 m/s have frequencies of 61% and 44.88% are from NW to NE. Winds with more than 14 m/s have frequencies of 1.08% and are from NW to NE.

A02: 56.24% of the waves recorded have heights from 0 to 0.5m with 97% have periods of 0-5s. Waves with heights more than 3 m have frequencies of 2.19% and of those 42% have periods of 6-7s. Wind speeds of 2 - 8 m/s have frequencies of 59.62% and of those 50.27% have direction from N to E and 15.33% are from S. Winds of more than 14 m/s have frequencies of 4.78% and 73.33% of those are from N to E.

A05: Waves with heights from 0 to 1 m have frequencies of 65.93% and 92.34% has periods from 0 to 5 s. Waves with heights more than 3 m have frequencies of 3.73% and from those 32% is of 6 to 7 s. Speeds from 2 to 8 m/s have frequencies of 54.17% whilst from those 46.18% is from N-NE and 16.78% from S. Wind speeds higher than 14 m/s have frequencies of 6.68% and from those 66.02% is from N-NE.

A06: 56.98% of the recorded wave heights are from 0 to 0.5 m and from those 96% has periods from 0 - 5 s. Waves with heights more than 2 m have frequencies with 2.07% and of those 47.82% has periods from 0-5s. Wind speeds from 2-8 m/s have frequencies of 62.43% and 43.68% has direction from N to NE and 13.67% from S. Winds of more than 14 m/s have frequencies of 4% and 58.3% is from N-NE.

A07: 66.15% of the waves have heights from 0 to 0.5 m and from those 98.13% have periods from 0 to 5 s. Waves with heights of more than 3 m have frequencies of 1.3% and 53.45% have periods of 6-7 s. Wind speeds from 2-8 m/s are common (58.7%) and 48.03% are from NW to NE. Speeds greater than 14 m/s have frequencies of 2.79% and 6.54% of those are from N.

A09: 82.29% of the waves have heights 0-0.5 s and 98.8% has periods of 0-5 s. Waves with more than 2 m have frequencies of 0.65% and their periods are from 0 to 9 s. Winds have speeds from 2-8 m/s (61%) and from those 44.88% is from NW to NE. Winds with more than 14 m/s have frequencies of 1.08% and are from NW to N.

A13: 36.26% of the waves have heights from 0 to 0.5 m and 96.11% is with periods from 0 to 5 s. Waves with more than 3 m height, have frequencies of 3.13% and from those 35.3% has periods from 6-7 s and 30.4% 0-5 s. 64.48% of the winds have speeds from 2 – 8 m/s and from those 57.82% has direction from W to NW. Winds with more than 14 m/s have frequencies of 3.07% and 28.18% are from W and 22.72% from NW.

A14: 55.28% of the waves are with heights from 0 to 1m and 91% has periods of 0-5 s. Waves with more than 3 m heights have frequencies of 5.1% and 35.15% has periods of 6-7 s and 32.67% from 0 to 5 s. 58.5% has wind speeds from 2 to 8 m/s and from those 58.92% is from W and NW whilst 11.33% is from N. Winds of more than 14 m/s are have frequencies of 5.02% and 36.73% is from NW.

I03: 67.53% has waves with heights of 0 to 1 m and 91.41% has periods from 0-5 s. Waves with heights of more than 3 m, have frequencies of 3.55% and 40.71% is with periods of 6 to 7 s. Winds with speeds from 2 – 8 m/s have frequencies of 65% and 46.96% is from NW to N. Winds with more than 14 m/s have frequencies of 2.98% and 27.2% is from NW.

I06: 59.7% of the waves have heights of 0 to 1 m and 90.58% has periods of 0-5 s. Waves with heights more than 3 m have frequencies of 4.74% and 38.34% of those has periods 6 to 7 s. Winds with speeds of 2 to 8 m/s have frequencies of 63.35% and 49.04% have directions from W to NW and finally, winds with speeds more than 14 m/s have frequencies of 4.28% and 21.1% is from W.

3.1.2.1.2 Wind and Wave Atlas (HCMR) - Model

Mean annual wind speed distribution of the Greek Seas is shown in Figure 3.1.7a and for the wind directionality in Figure 3.1.7b (Soukissian et al., 2007). In North Aegean, the annual mean wind speeds range from 3 to 6 m/s, whilst in the Central Aegean they can reach up to 7 m/s. In South Aegean winds are up to 6 m/s, whilst they are greater in the areas of West and East of Crete, especially due to the channeling effects. In the area of North East Ionian, the winds range from 4 to 6 m/s whilst at the South-East Ionian from 5 to 6 m/s. As for wind direction, North Aegean has as dominant winds those blowing from NE, except in the case of Thermaikos Gulf where the winds are from NW. The NW winds are also dominant in the Central Aegean, while in South Aegean most of the winds are coming from the west. In North East Ionian, the winds are blowing from the NW turning to West until the South East Ionian, where at the area among Crete and Peloponnese they have west directionalities.

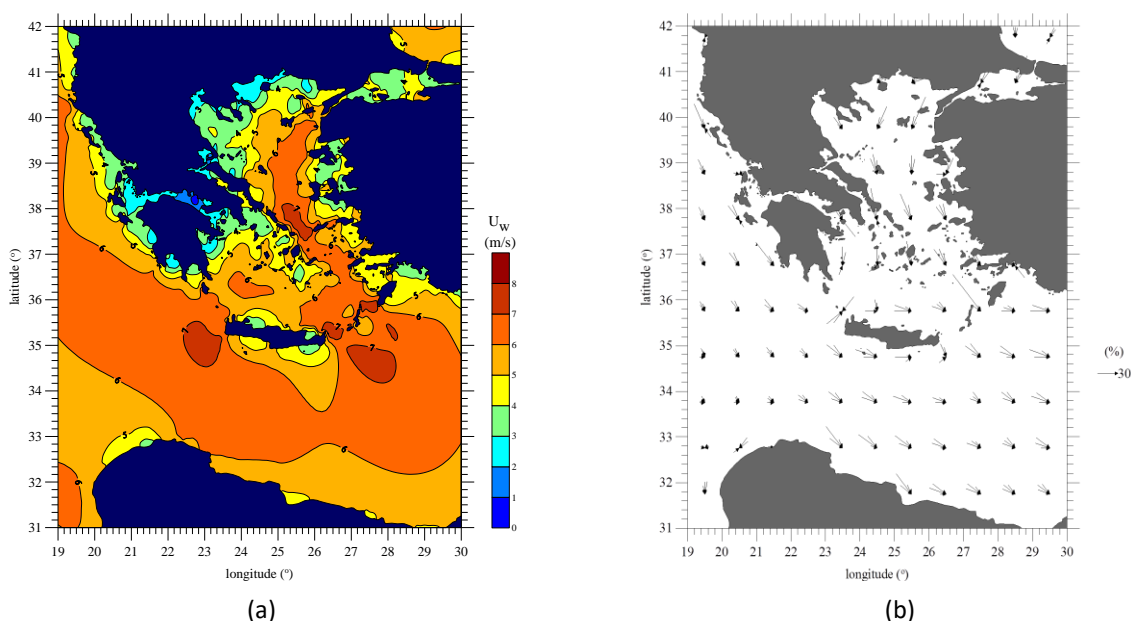


Figure 3.1.7: Annual wind speed (a), Annual wind direction (b) (Soukissian et al., 2007)

The mean annual wave height, period and direction distributions of the Greek Seas, as estimated from the model runs, are shown in Figure 3.1.8 a ,b and c respectively. North Aegean is characterized with waves of heights up to 0.9 m, peak periods of up to 4.6 s and waves' propagation from the North East, except in Thermaikos where waves come from NW. Central Aegean has heights that range of 0.9 up to 1.1 m, periods up to 5.6 s and directions from N-NW. In South Aegean waves have heights of 0.9 to 1.1 m with even higher waves of 1.2-1.3 m at the East and West of Crete. Associated periods are around 5.6 s and directions are from the west except the area of Kassos, Karpathos Rhodes, where they are from the NW. The North East Ionian has wave heights of 1 m, periods around 5.6 s and directions from NW. Finally, the South East Ionian, is described by waves with heights of up to 1.2 m, periods up to 6 s and directions NW turning west towards Crete.

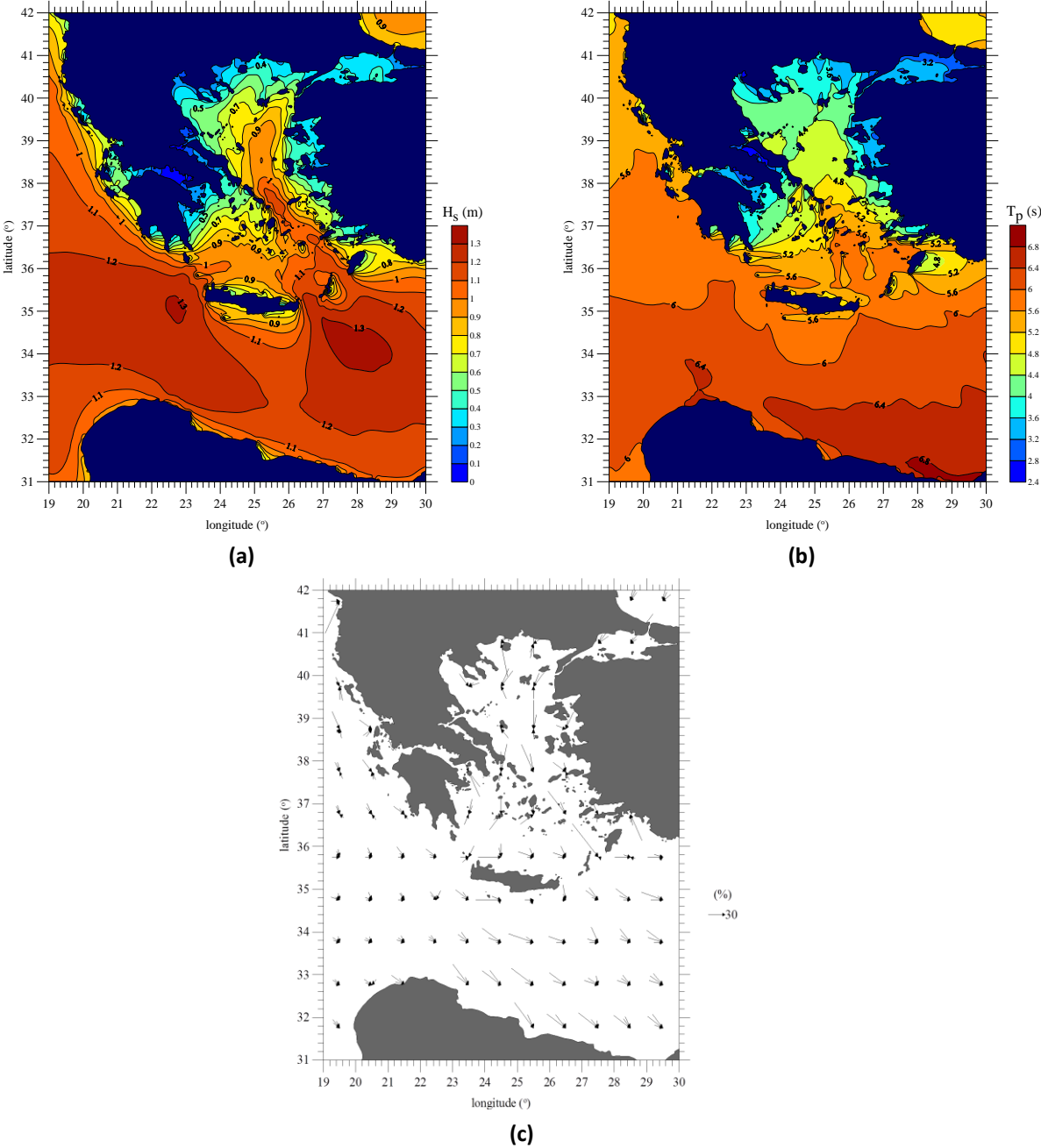


Figure 3.1.8: Annual Significant Wave Height (a), Annual Peak Period (b) and Annual Wave Direction (c) (Soukissian et al., 2007)

3.1.2.1.3 Wind and Wave Atlas (HCMR) - Buoys

The analysis of wind and wave data from 6 buoys of the POSEIDON network (for locations see Figure 3.1.9) provides the followings (Soukissian et al., 2007):

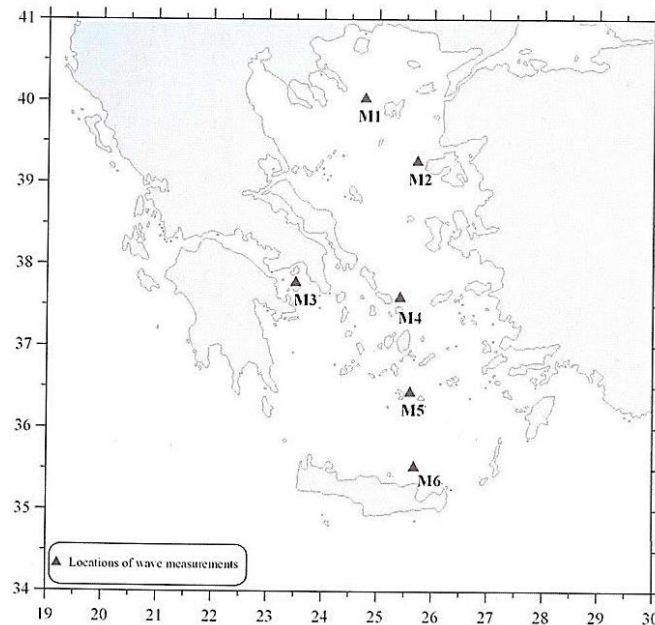


Figure 3.1.9: Buoys locations (Soukissian et al., 2007)

Athos (M1) is characterized with heights of 0-0.5 m (44.34%) from whom 58.75% has peak period (T_p) of 3.8 – 4.6 s while the higher waves (>3 m) have a frequency of 2.3% with 39.13% of them with period 7.4-8.1 s. From the waves with heights of 0 – 0.5 m, 29.47% has directions from the range 15 ° to 75 ° and 36.5% from 150 ° to 225 °. Additionally, 78.26% of the waves with heights more than 3 m have directions from 30 ° to 45 °. M1 shows that the most common winds are blowing from 30 ° to 45 ° with a frequency of 21.13%. The most frequent are winds with speeds of 2-5 m/s (36.89%); from which the 17.35% is from the sector 30 ° - 45 °. Higher wind speeds (>14 m/s) have frequencies of only 1.83% with 35.71% approaching from 30 ° - 45 °. Waves with heights of 0-0.5 m (43.24%) have the 37.96% being related to wind speeds of 2-4 m/s. Waves with heights >3 m have frequency of 2.4% from which the 33.33% is related with wind speeds > 16 m/s.

The area of Lesvos (M2) is characterized by 38.22% of wave heights of 0–0.5 m; from those the 50.6% has periods of 2.6-3.7 s, while waves with heights >3 m (0.6%) are related with periods >6.7 s. In addition, 84.47% of the waves with heights of 0 to 0.5 m have directions from 195 ° to 345 °, whilst waves with heights more than 3 m have directions from 165 ° to 195 °. The most common winds (41.8%) are from 0 ° to 30 °. Frequent winds (43.62%) have speed of 4-8 m/s blowing from 0 ° to 30 °. Winds with speeds >14 m/s have frequency of 1.52%, from which the 66.67% is also approaching from 0 ° to 30 °.

The area of Petrokaravo (M3) is characterized by waves with heights of 0-0.5 m (81.32%) from whom 70.5% is has periods of 1.9 – 3.8 s and 41.39% is propagating from 15 ° to 120 ° directions. Waves with heights of more than 1 m have a frequency of 0.5% and 40% is from 0 ° to 15 ° and another 40% from 270 ° to 285 °. Wind speeds from 2 to 8 m/s have frequencies of 59.47% and from those 36.11% is of 315 ° to 45 ° directions. Wind speeds greater than 12 m/s have frequency of 1.32% and 61.54% of them are from 0 ° to 15 °. Waves with heights of 0 to 0.5m (79.7%) are related with winds of 0 to 5 m/s speeds (76.57%). There is only one case of wave heights from 1.25 to 1.75 m and is related with winds more than 12 m/s.

The buoy of Mykonos (M4), is described with 58.39% of wave heights of 0 to 1 m with 52.49% of them having peak periods of 3.1 to 5 s. Waves higher than 3 m have frequencies of 1.61% and peak periods of more than 6.7 s. Additionally, 39.52% of the waves with heights of 0 to 1 m are from 330 ° to 360 ° and 56.25% of the waves with heights greater than 3 m are from 330 ° to 345 °. Winds with speeds from 2 to 8 m/s are of 49.19% frequency with 31.86% of them from 330 ° to 345 ° and the same with winds with speeds greater than 12 m/s (7.28%). Finally, heights of 0-1 m are related with winds from 2-8 m/s (71.4%) and heights greater than 3 m with wind speeds greater than 9 m/s.

For Santorini (M5), waves with heights from 0 to 1m have frequencies of 67.06% with 60.84% having peak periods of 3.1 to 5 s, 22.53% directions of 240 ° to 255 ° and 79.3% related with wind speeds of 2-8 m/s. Heights greater than 2.5 m have frequencies of 1.91% with peak periods greater than 6.1 s and 47.05% of those directions from 240 ° – 255 ° and 2.09 % is related with winds greater than 10 m/s. Wind speeds from 2 to 8 m/s have frequencies of 59.12% and from those 27.27% are of 330 ° to 360 ° while those with speeds greater than 12 m/s have frequencies of 2.53% and 32% is from North directions.

In the area of Avgo, waves with heights of 0 to 1m have frequencies of 59.92%, of those 62.52% has peak periods of 3.1 to 5 s, 33.33% has direction from 315 ° to 345 ° and 75.76% has wind speeds of 2 to 8 m/s. Waves with heights greater than 3 m, have frequencies of 1% with peak periods more than 6.7 s, 75% of 315 ° to 345 ° and related to wind speeds more than 10 m/s. Wind speeds of 2 to 8 m/s are common with frequencies of 66.53% and 27.05% is from 270 ° to 285° while those that have wind speeds more than 12 m/s have frequencies of 2.93% and from those 37.93% is from 330 to 345.

3.1.2.1.4 Reanalysis Datasets

Lionello and Sanna (2005) used wave models with initial inputs from the ERA-40 and NCEP datasets and presented wave characteristics of the Mediterranean Basin and their variability, as shown in Figure 3.1.10. More analytically, in January at the Gulf of Lyons waves with heights of more than 1 m had frequencies of as much as 70%, while waves higher than 2.5 m at the south-east of this zone were as frequent as 20%.

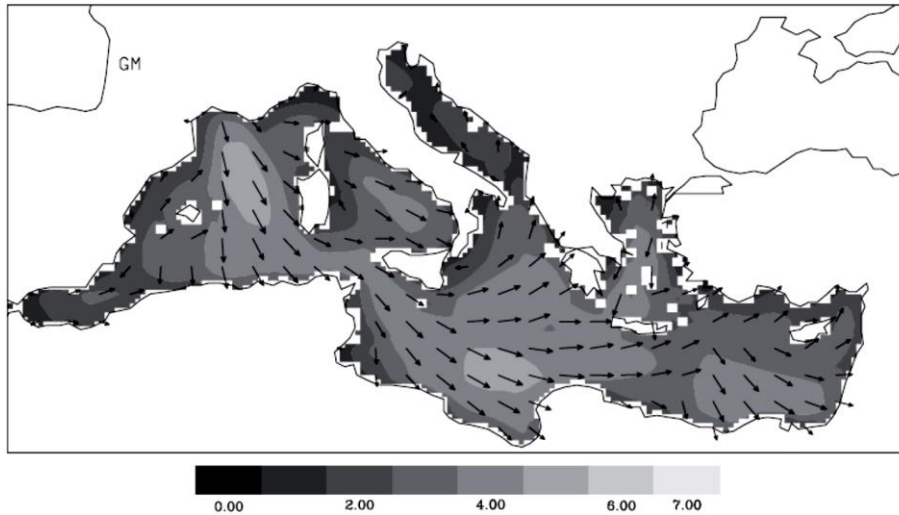
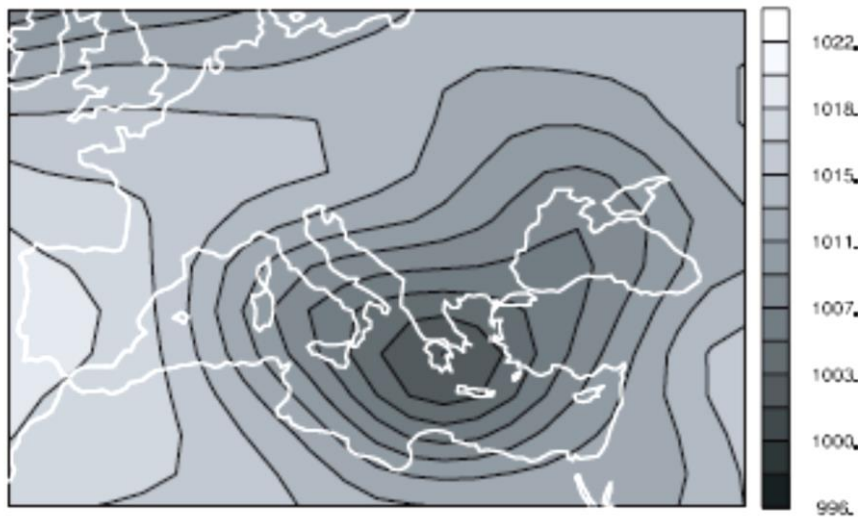
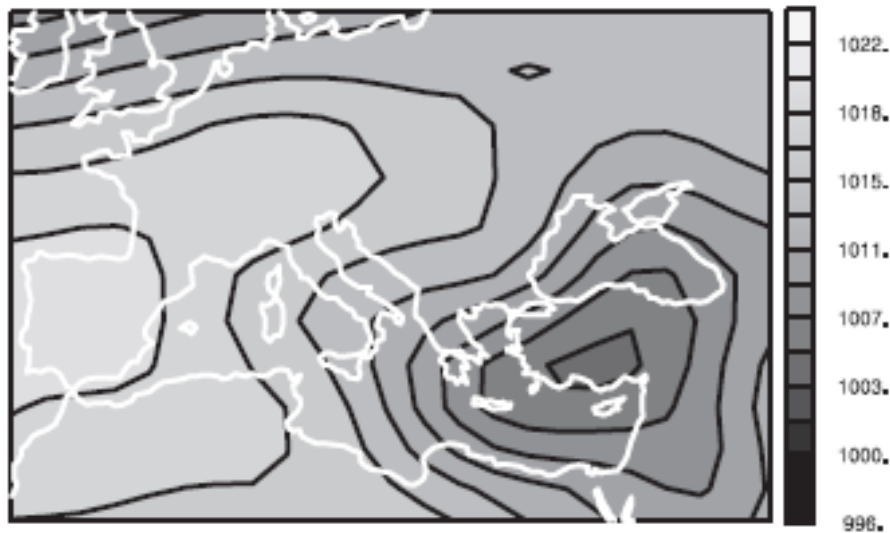


Figure 3.1.10: Distribution of maximum significant wave height (contours in m) and direction (arrows) (Lionello and Sanna, 2005)

The synoptic charts of mean sea level composites that are related with significant wave heights are presented for the area of Aegean and the Levantine in Figure 3.1.11. When strong wind and long fetch coincide then high waves can be present in most of the Mediterranean Sea. The largest wave heights can be found in the western Mediterranean and in the Ionian Sea where long fetch and strong winds present the best combination. The southern Adriatic and northern Ionian maximum wave heights are linked to Sirocco winds. The Etesians, due to the blocking of Cretan high mountains develop two wave maxima: one in the Aegean and the other in the Levantine Basin.



(a)



(b)

Figure 3.1.11: Synoptic charts of surface pressure related with maximum significant wave height, a) Ionian, b) Levantine basin (from Lionello and Sanna 2005)

Past and future trends of wind and wave regime are of importance for a variety of applications such as planning, environmental strategy, renewable energy etc. In Maheras et al. (2001), a reduction of the number of cyclones in the Western Mediterranean and an increase in the Eastern Mediterranean is shown for the period 1958-1997, even though the change is not homogeneous. However, for the period October to March a decrease is shown in Eastern Mediterranean. In addition, Poupkou et al. (2011) and Tyrlis and Lelieveld (2013) suggest that there are negative trends regarding the frequency of appearance and the wind speed of the Etesians, i.e. the number of Etesian days from June to September decrease by 1.48 per decade and the wind speeds by 0.28m/s per decade, as well. Moreover, Bagiorgas et al. (2012) suggest that trends of wind speed and wave heights vary per location in the Aegean and Ionian Seas, i.e. slightly decreasing trends were found at Lesbos and Santorini, but increasing trends at Athos and Mykonos. In Lionello and Sanna, (2005), wind wave extremes, as obtained from model simulations with inputs of ERA40 reanalysis dataset, show little to negligible significant trends. In Figure 3.1.12, their results show a decrease in the Ionian and Alboran Sea, consistent with the decrease of cyclone numbers in the western Mediterranean as suggested by (Maheras et al., 2001) while increase is rather limited at a region close to the coast of France.

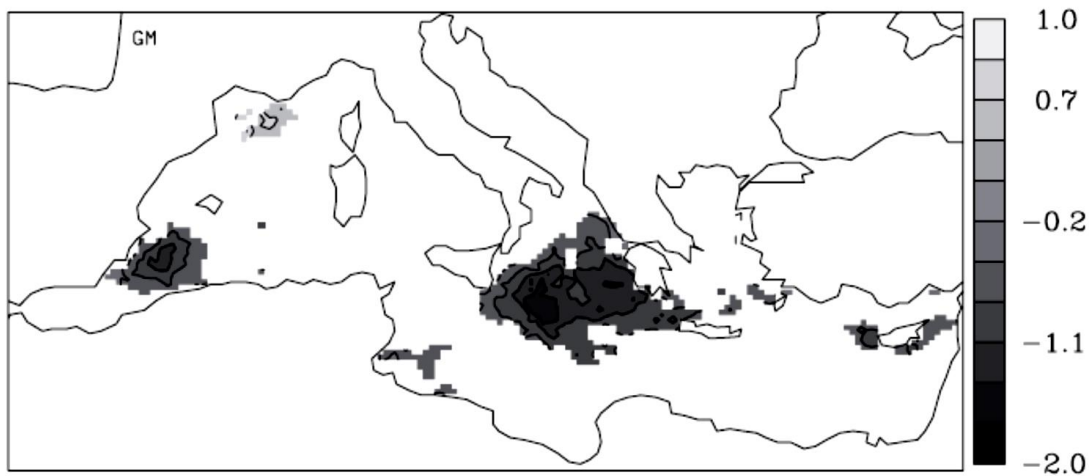


Figure 3.1.12: Variation of significant wave height as given from linear trends of ERA40 reanalysis (Lionello and Sanna, 2005)

Anagnostopoulou et al. (2014) compared the periods of 2021-2050 and 2071-2100 in respect to the reference period of 1961-1990 (with data from the RCM simulation of RegCM3) and showed that for the period June – July – August – September (JJAS) there are 3 distinct patterns of the Etesian winds summing up over 80% of the summer days of the Aegean. These patterns showed that the mean wind speed of the northerly winds is from 3.4 to 10.8 m/s. Weakening is indicated of the subsidence over eastern Mediterranean controlled from the deepening of the eastern Mediterranean / Middle East low pressure action centre that is in consistency with future weakening of South Asian monsoon and Hadley cell circulations.

3.1.3 Tides

As for the tidal characteristics, the semi-diurnal component (M2) is the most apparent in the Eastern Mediterranean (Tsimplis, 1994), while estimates of M2 amplitude and phase (based on numerical model) show that the highest amplitudes occur in North Aegean and Evvoikos and Korinthiakos Gulf (Figure 3.1.13a); this enhancement of the tidal signal is explained by coastal and seabed topography. The total tidal range is considered as the sum of the four tidal components M2, S2, K1 and O1 is given in Figure 3.1.13b. It is shown that the tides can be up to 0.5 m with the maxima estimated in North Aegean and the aforementioned semi-enclosed gulfs. The authors note that the annual and semi-annual variability of sea level can be considered numerically negligible and that they are caused mostly by non-astronomic factors.

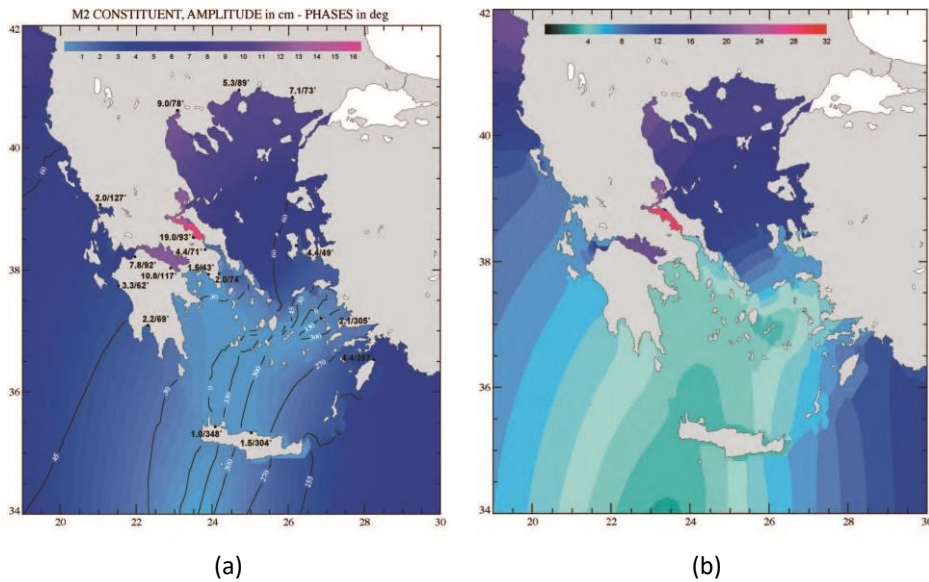


Figure 3.1.13: M2 tidal component from the models (contours) and the HNMS tide gauges (points) (a), sum of the four tidal components for the Hellenic Seas (b) (Tsimplis, 1994; Zenetos, 2005)

3.1.4 Storm Surge

Extreme storm surge events can result in high risk conditions especially at low-elevation areas along the Greek Coastline. In Krestenitis et al. (2015), Storm Surge Index (SSI) is estimated from model results and observations from tide gauges of the Hellenic Hydrographic Service (HNHS). This research provides information on a regional level for the Sea Level Height (SLH) of the Greek Seas. In Figure 3.1.14, trends of the temporal evolution of annual maxima SLH for the 6 regions of the Eastern Mediterranean for past and future periods are shown. The Ionian is affected mostly by high maximum SLH/s (> 60 cm) due to storm paths whilst it does not show decreasing trends on the 21st century. On the other hand, South Cretan and Levantine basing show weakening of storms during the future period.

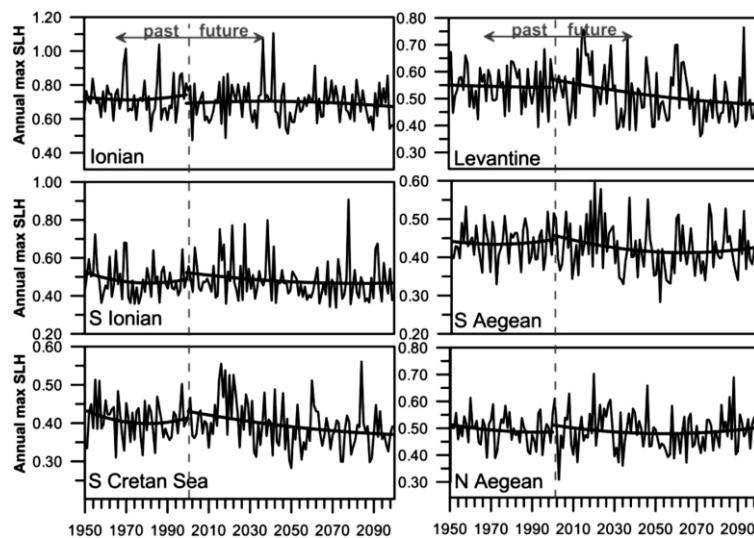


Figure 3.1.14: Evolution of annual maxima of SLH (m) for 6 Areas of the Eastern Mediterranean. The Solid lines represent past and future 2nd degree polynomials ((Krestenitis et al., 2015)

3.2 Pinios Case Study

3.2.1 Geomorphological Characteristics

The drainage area of Pinios river, and its deltaic plain, are located among 39° 05' to 40° 05' N and 21° 10' to 22° 55'E. The length of Pinios River is approximately 257km. The catchment of Pinios river exceeds the 10000 km² including the Thessalian Plain that is surrounded by the Olympus mountain in the north, Pindos at the west, Orthis in the south and Ossa at the East (Stournaras et al., 2011). It is characterized by a variety of geological formations with several lithological combinations, which vary on erosion rates (Stournaras and Galani, 1995). The lithology of the drainage area mostly consists by alluvial and clastic deposits (68%), metamorphic rocks (15.2%), igneous rocks (5.3%) and a variety of calcareous deposits (11.5%) (Foutrakis et al., 2007).

The deltaic area after the narrow area of Tempi valley is approximately 69 km² with gentle slopes from the mountains towards the sea. The Eastern boundary is that of Thermaikos Gulf, while the Olympus and Ossa mountains are the natural geomorphological boundaries of the delta from W to WSW and NNE, respectively. The mountains that surround the deltaic area have heights from 900 m to 1700 m. In contradiction to the surrounding mountainous region, the main zone of the deltaic sediments has milder topography with small slopes from the curbs of the basin towards the coastal zone. The mean height difference between the deltaic plain and the coast (approximately 7 km) is about 10 m. The evolution of the deltaic area is directly related with the geotectonic changes during Late Quaternary and the evolution of the river valley during this era (erosion-sedimentation). The deltaic plain is affected by the wave regime and associated nearshore currents, minimizing the fast progradation of the delta with respect also to water depths of the receiving basin (i.e. outer Thermaikos Gulf). The deltaic coastline is characterized by sandy to gravelly sand sediments and the formation of sand dunes that can reach up to 1.3 m. It is estimated that the river mouth has been moving seawards with a rate of 11 m/yr for the period 1959-1995, while the coastline north of Stomio, is under an erosive state with a rate of 4 m/yr for the same period (Karympalis and Gaki-Papanastasiou, 2008). The geomorphological map in Figure 3.2.1 shows the characteristic landforms and sedimentary deposits of the deltaic plain.

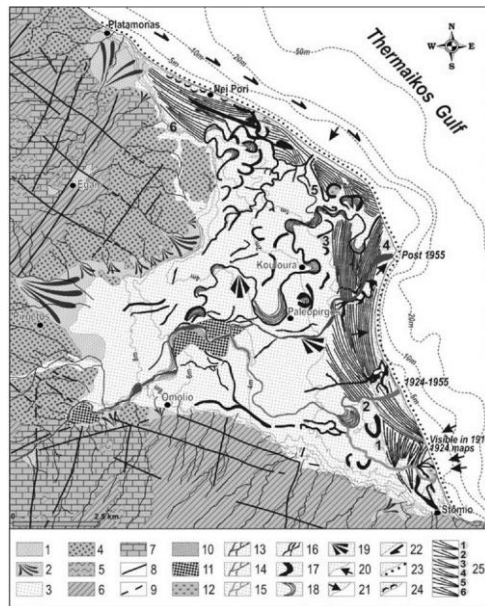


Figure 3.2.1: Geomorphological map of the Pinios Delta on a 1:5000 scale, 1: Alluvial deposits, 2: Alluvial cones, 3: Deposits of the deltaic plain, 4: Neogene formations, 5: Flysch, 6: Schists, gneiss, Amphibolite, 7:Marbles, Limestone , 8: Fault, 9: Possible fault, 9: Lower river terrace, 11: Upper river terrace, 12: Coastal slate, 13: Existing riverbed (since 1955), 14: River bed prior to 1955, 15: Riverbed during 1910-1924, 16: Abandoned beds, 17: Abandoned meanders, 18: Point ridges - bars, 19: Fragmented overflow fine-grained deposits, 20: flinch coastline, 21: Advancing coastline, 22: Currents, 23: Sandy seashore zone, 24: Active sand dunes, 25: Coastal ridges (Karympalis and Gaki-Papanastasiou, 2008)

It is rather important to mention that the geomorphology of the landward limit of the Pinios deltaic plain, both in the south and the west, is characterized by many secondary, torrential in character, small drainage areas that have resulted in the development of significant scree cones and created significant undercuts. From those, the most important are the stream of Pirgetos and Archontorrema to the west and southern fringes of the area, respectively (Panagopoulos et al., 2001).

3.2.2 Climatic Conditions

The climate at the coastal area of Pinios basin can be described, in general, as Mediterranean, whilst the central area as continental with less precipitation and bigger seasonal variations in atmospheric temperature. Furthermore, the mean annual temperature ranges from 17.0 to 17.5 °C, while on a monthly basis it can be from 7.5 to 33 °C (Zampakas, 1981). As for precipitation, the western part of the basin receives around 700 mm/yr, the central part 400 mm/yr, and in altitudes of more than 1000 m, precipitation can reach up to 1000 mm/yr. The overall mean annual precipitation of the basin is 710 mm.

3.2.3 Coastal Oceanography and Sedimentology

3.2.3.1 Oceanography

Pinios River discharges in the southwest coastline of Thermaikos gulf with the water masses having characteristics similar to the masses of the open Aegean Sea and those of the outer Thermaikos Gulf. Sea surface temperature ranges from 15 to 25°C and changes according to the periodic and seasonal variations of atmospheric temperature. Salinity is lower in the upper layers and ranges from 35 psu to 36 psu due to the intrusion of fresh water, while higher values are near the sea bottom and can be up to 38 psu. The seasonal thermocline is formed in depths that vary according to the seasonal climatological changes. When the water discharge is high, the full with sediment waters of the river can be traced in many kilometres away from the delta when there are calm sea conditions. The tidal height in Thermaikos Gulf is estimated to be around 19cm (Tsimplis, 1994). The delta is affected by significant wave dynamics, mostly due to the large fetch of waves, 58 km N, 60 km NE, 123 km E and 79 km SE. The submarine topography is characterized by slopes of 10% while the discharge basin can have depths of up to 100m (Poulos et al., 1996).

3.2.3.2 Wave and Wind Climate

Grid box AO4 of the wind and wave atlas of Athanasoulis and Skarsoulis (1992), is considered as representative for the offshore wind and wave conditions for the area of Pinios (see Figure 3.1.5). As shown in Table 3.2.1, for the annual values, 83.19% of the waves have heights of 0 to 1 m and 88.87% have periods of 0 to 5sec. Heights more than 2 m have frequency of appearance of 4.8% and periods longer than 8 sec have frequency of appearance of 4.15%. Furthermore, 97.14% of heights of 0 – 5 m is related to periods that range from 0 to 5 sec whilst heights greater than 4 m are related to periods 8-9 sec.

Table 3.2.1: Frequency Table (%) of Wave Height and Periods for the area of Pinios (from Athanasoulis and Skarsoulis, 1992)

| Wave Height (m) | Wave Period (s) | | | | | | | | Total |
|-----------------|-----------------|-------------|-------------|-------------|-------------|-------------|----------|----------|---------------|
| | 0 - 5 | 6-7 | 8 - 9 | 10-11 | 12-13 | 14-15 | 16-17 | >18 | |
| 0 - 0.5 | 59.39 | 0.87 | 0.44 | 0.44 | 0 | 0 | 0 | 0 | 61.14 |
| 0.5 - 1.0 | 20.09 | 1.75 | 0.22 | 0 | 0 | 0 | 0 | 0 | 22.05 |
| 1.0 - 1.5 | 6.33 | 1.31 | 0.44 | 0 | 0 | 0.44 | 0 | 0 | 8.52 |
| 1.5 - 2.0 | 1.75 | 1.53 | 0 | 0 | 0 | 0.22 | 0 | 0 | 3.49 |
| 2.0 - 2.5 | 0.44 | 1.31 | 0.44 | 0.22 | 0.22 | 0 | 0 | 0 | 2.62 |
| 2.5 - 3.0 | 0.87 | 0 | 0 | 0.22 | 0 | 0 | 0 | 0 | 1.09 |
| 3.0 - 4.0 | 0 | 0.22 | 0.22 | 0 | 0 | 0 | 0 | 0 | 0.44 |
| 4.0 - 5.0 | 0 | 0 | 0.66 | 0 | 0 | 0 | 0 | 0 | 0.66 |
| 5.0 - 6.0 | 0 | 0 | 0 | 0 | 0 | 0 | 0 | 0 | 0 |
| > 6.0 | 0 | 0 | 0 | 0 | 0 | 0 | 0 | 0 | 0 |
| Total | 88.86 | 6.99 | 2.40 | 0.87 | 0.22 | 0.66 | 0 | 0 | 100.00 |

The area of Pinios, as shown in Figure 3.2.2, is characterized by waves propagating from N, NE and E, with average heights of 0.6 m, 0.8 m and 0.9 m respectively. The frequencies of appearance of the waves for the aforementioned directions do not exceed 20%.

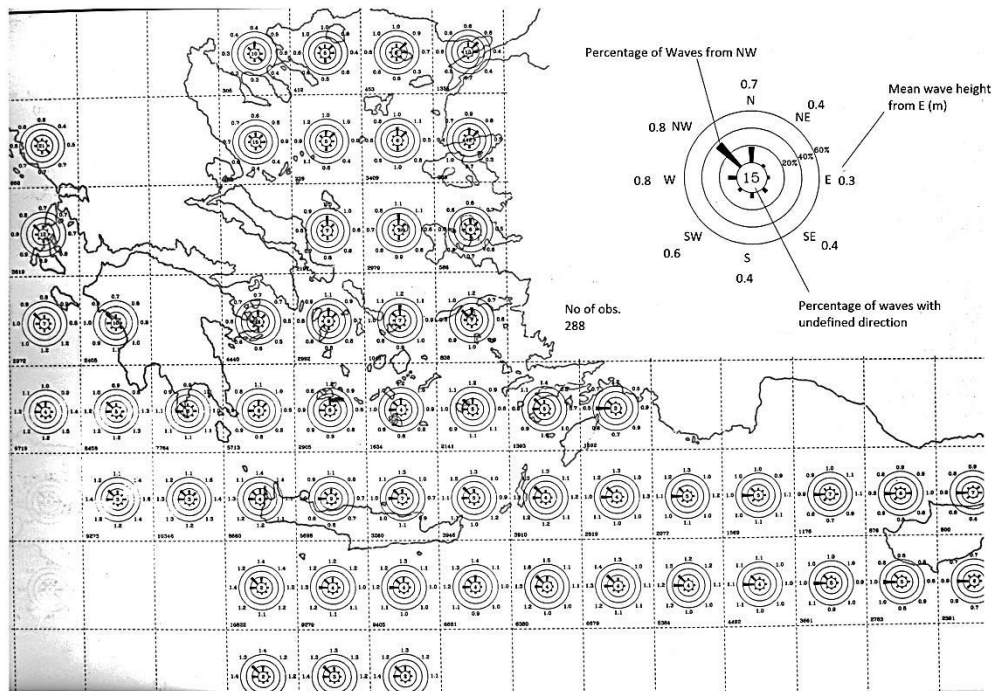


Figure 3.2.2: Annual wave directionality of the Greek Seas (from Athanasoulis and Skarsoulis, 1992)

In regards to the annual wind speed and direction (Table 3.2.2), the most frequent wind speeds are of 1.6 to 7.9 m/s (58.5%) whilst wind speeds greater than 20.8 m/s have frequency of 0.18 %. Furthermore, the most frequent winds blow from the N to E (44.91%) whilst those with speeds of more than 20.8 m/s blow from the E.

Table 3.2.2: Frequency (%) of Wind speed and Direction for the area of Pinios (from Athanasoulis and Skarsoulis, 1992)

| Wind Speed (m/s) | Wind Direction | | | | | | | | | Total | |
|------------------|----------------|-------|-------|------|------|------|------|-------|-------|-------|--------|
| | N | NE | E | SE | S | SW | W | NW | Calm | | |
| 0 | | | | | | | | | | 16.09 | 16.09 |
| 0.3-1.5 | 1.65 | 1.10 | 1.83 | 1.10 | 1.83 | 0.55 | 0.73 | 1.10 | 0 | 0 | 9.87 |
| 1.6-3.3 | 4.20 | 3.29 | 3.11 | 2.01 | 2.74 | 0.73 | 0.55 | 4.02 | 0 | 0 | 20.66 |
| 3.4-5.4 | 4.57 | 2.19 | 3.84 | 2.19 | 3.29 | 0.91 | 1.65 | 2.74 | 0 | 0 | 21.39 |
| 5.5-7.9 | 3.29 | 2.93 | 2.93 | 1.65 | 0.55 | 0.18 | 1.65 | 3.29 | 0 | 0 | 16.45 |
| 8.0-10.7 | 1.65 | 2.38 | 1.46 | 0.91 | 1.10 | 0 | 0.91 | 1.10 | 0 | 0 | 9.51 |
| 10.8-13.8 | 1.10 | 0.37 | 0.73 | 0.18 | 0.18 | 0.18 | 0 | 0.91 | 0 | 0 | 3.66 |
| 13.9-17.1 | 0.55 | 0.55 | 0.37 | 0 | 0 | 0 | 0 | 0 | 0 | 0 | 1.46 |
| 17.2-20.7 | 0 | 0.37 | 0.37 | 0 | 0 | 0 | 0 | 0 | 0 | 0 | 0.73 |
| 20.8-24.4 | 0 | 0 | 0.18 | 0 | 0 | 0 | 0 | 0 | 0 | 0 | 0.18 |
| Total | 17.00 | 13.16 | 14.81 | 8.04 | 9.69 | 2.56 | 5.48 | 13.16 | 16.09 | 16.09 | 100.00 |

In the Wind and Wave Atlas of Soukissian et al. (2007), maps of the spatial distribution of information obtained by numerical simulation of wind waves for the Greek Seas, are presented and discussed. From the annual map of significant wave height (H_s), the offshore area of Pinios delta is described by wave heights of 0.2-0.5 m (Figure 3.2.3a). Wave peak period (T_p) ranges from 3.6 s to 4.4 s (Figure 3.2.3b), while wave steepness is in the order of 1.6-1.8 (Figure 3.2.3c). Finally, most frequent waves propagate from NE to E as shown in (Figure 3.2.3d).

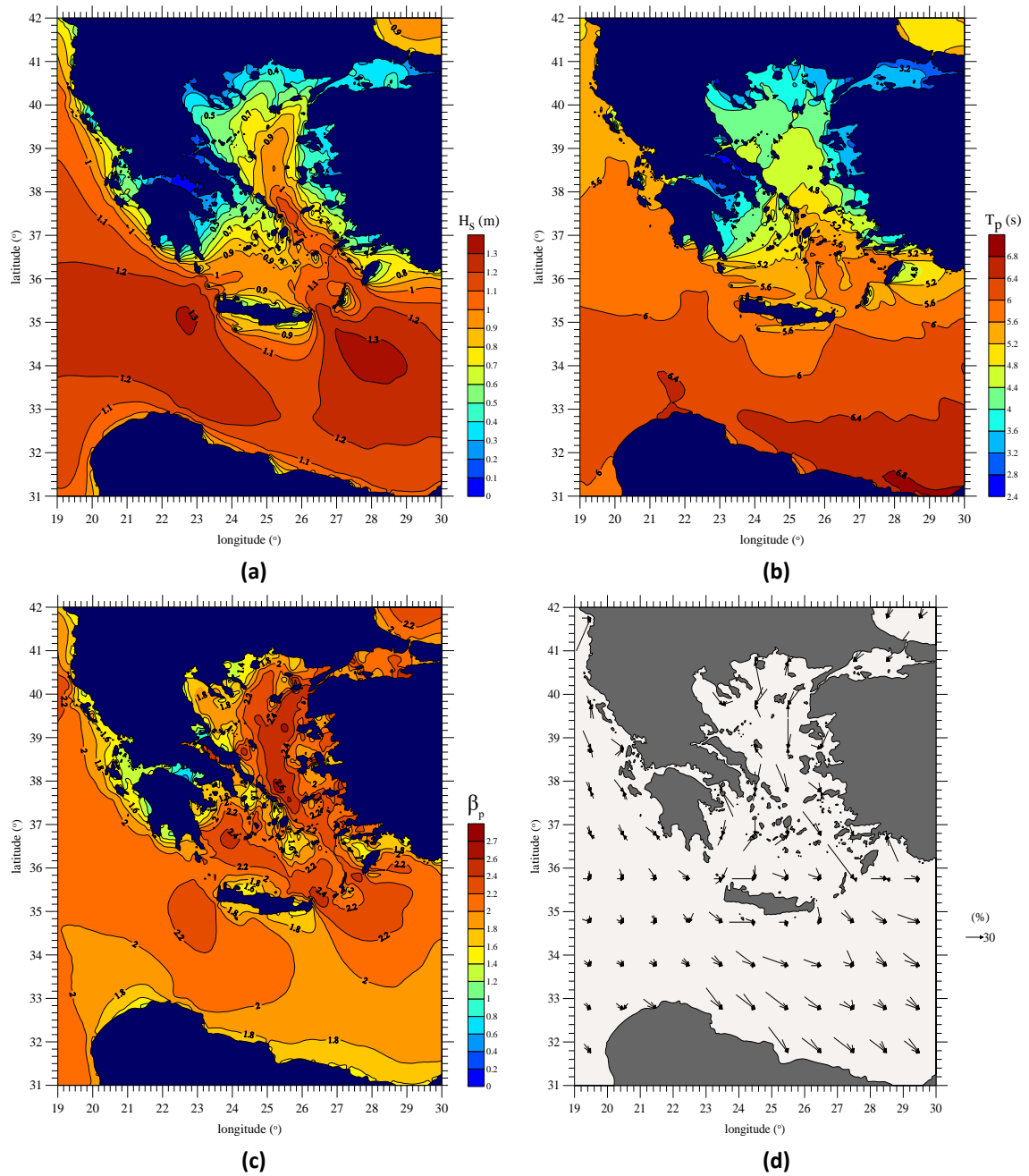


Figure 3.2.3: Annual Contours of significant wave height (a), wave period (b), wave steepness (c) and wave direction (d) (from Soukissian et al., 2007)

3.2.3.2.1 Thessaloniki Tidal Gauge

Sea level data presented here are from the tide gauge installed by the Hellenic Navy Hydrographic Office (coordinates: 40.63°, 22.93) for the period of 1969-2013. Caution is advised in the use of the equation of the linear fit due to changes in the methodology of recording and the missing values of the time series (Figure 3.2.4).

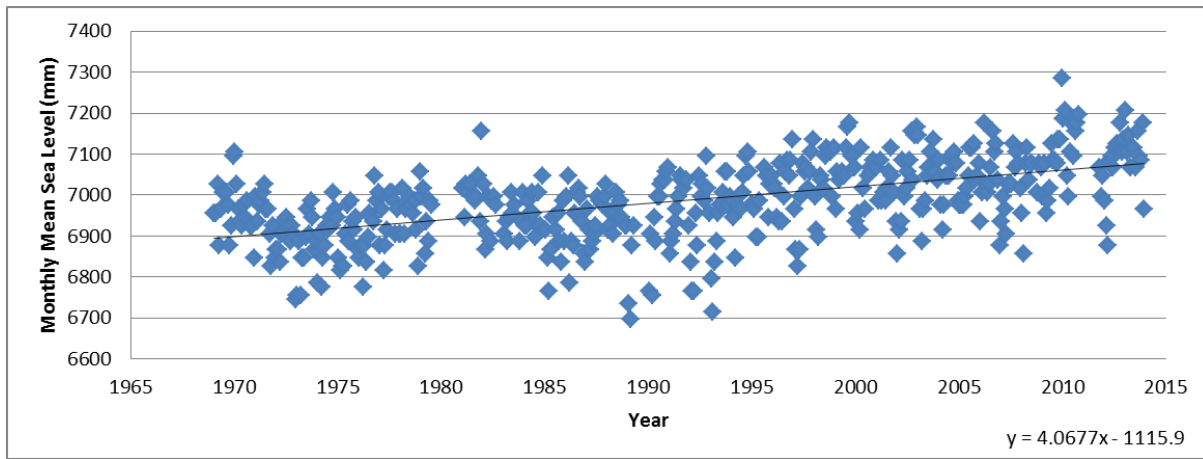


Figure 3.2.4: Monthly variation of sea level in Thessaloniki
 (<http://www.psmsl.org/data/obtaining/stations/373.php>)

Changes in the relative sea level through time for the gauge of Thessaloniki are given in Figure 3.2.5.

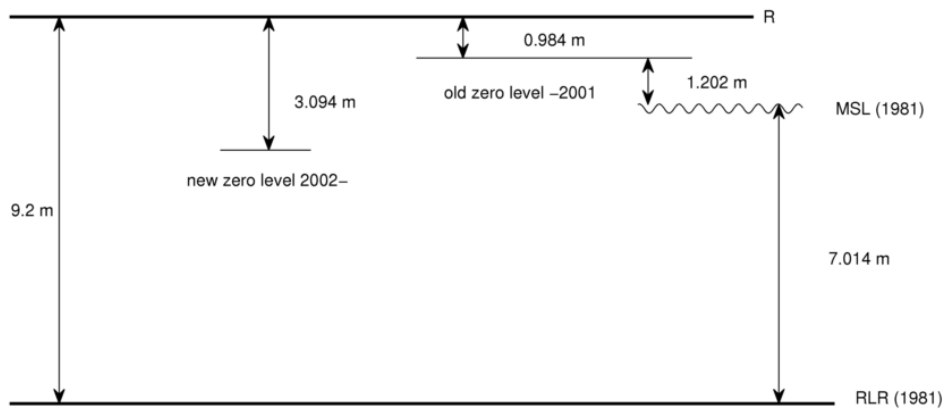


Figure 3.2.5: Relative sea level of the tide gauge of Thessaloniki
 (<http://www.psmsl.org/data/obtaining/rlr.diagrams/373.php>)

3.2.3.2.2 Skopelos Tidal Gauge

Sea level data presented here, are from the tide gauge installed by the Hellenic Navy Hydrographic Office (coordinates: 39.12°, 23.72°) and cover the period of 1999-2009 (Figure 3.2.6). As in Thessaloniki, caution should be given when using the linear equation.

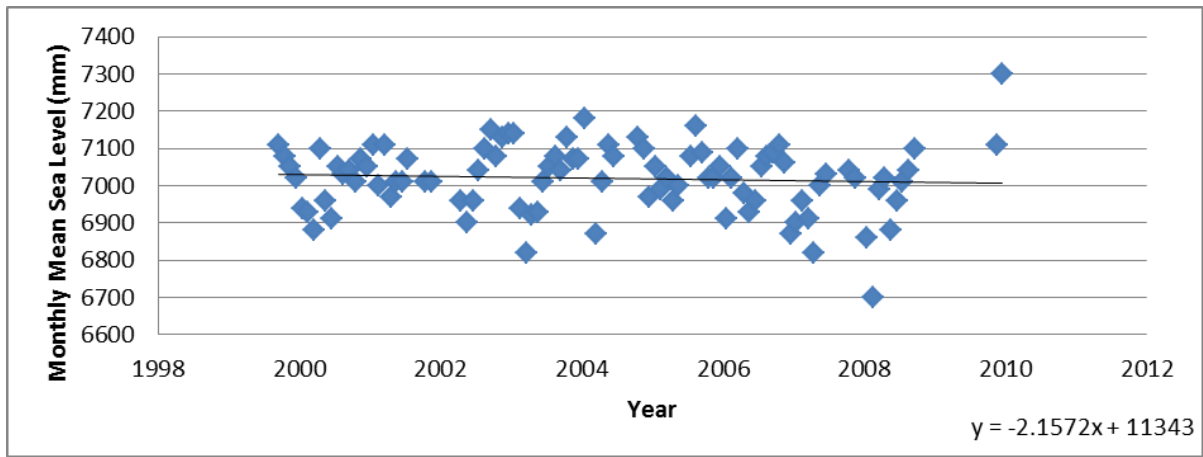


Figure 3.2.6: Monthly variation of sea level in Skopelos
 (<http://www.psmsl.org/data/obtaining/stations/1907.php>)

Changes in the relative sea level are given in Figure 3.2.7, for the different years from the gauge of Skopelos.

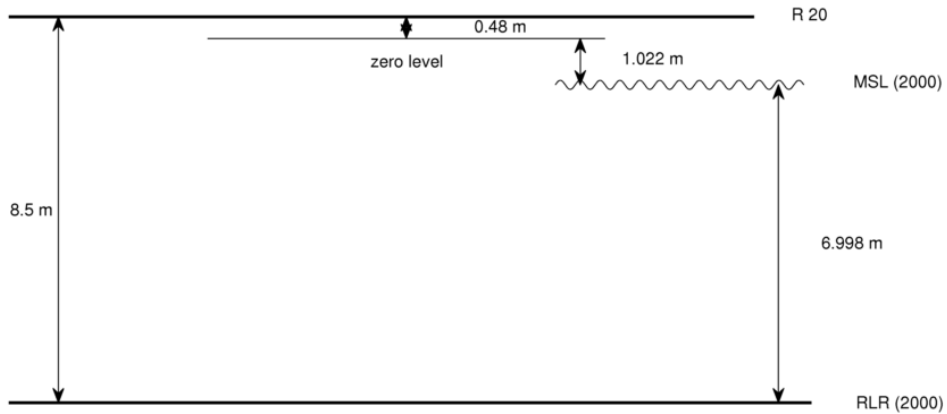
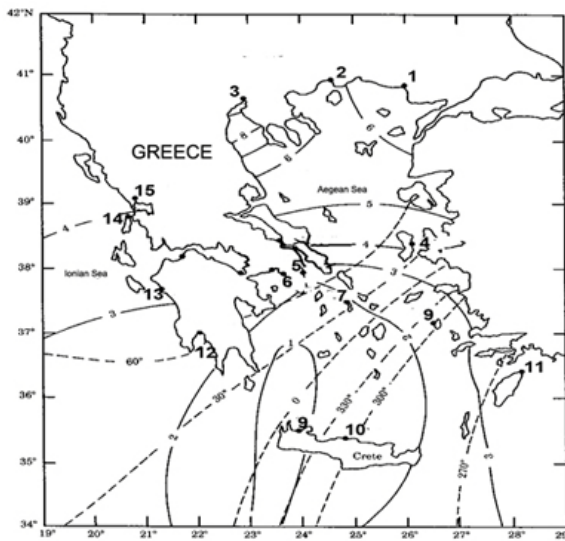


Figure 3.2.7: Relative sea level of the tide gauge of Skopelos
 (<http://www.psmsl.org/data/obtaining/rlr.diagrams/1907.php>)

3.2.3.2.3 Spatial Distribution of Tidal Signal (after Tsimplis, 1994)

Tidal components at the area of Pinios do not exceed the range of 0.15 to 0.22 m as shown in Figure 3.2.8.

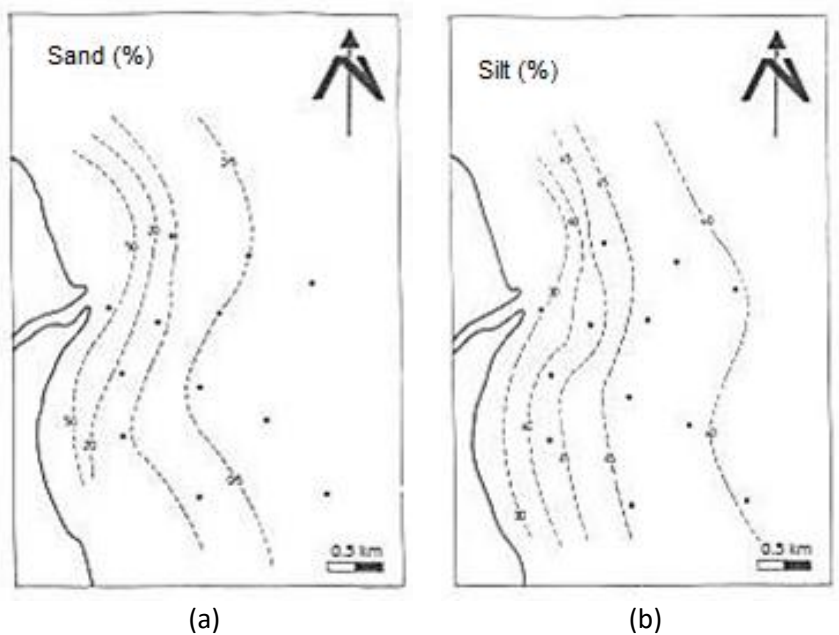


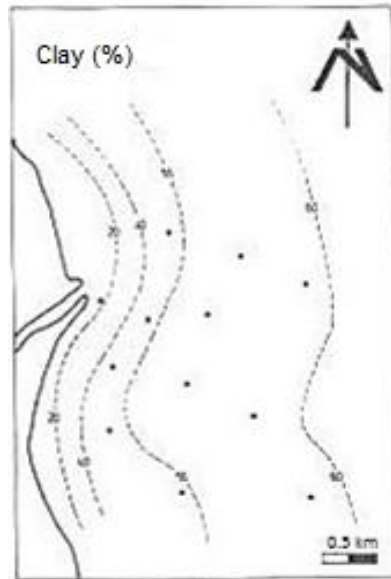
| No. | Gauge station | M2 | | S2 | | Mean water level variation |
|-----|-----------------|-----|---------|-----|---------|----------------------------|
| | | cm | degrees | cm | degrees | |
| 1 | Alexandroupolis | 7.1 | 73 | 5 | 92 | 0.66 |
| 2 | Kavala | 5.3 | 89 | 3.5 | 104 | 1.11 |
| 3 | Thessaloniki | 9 | 78 | 6.1 | 98 | 0.87 |
| 4 | Chios | 4.4 | 49 | 2.9 | 71 | 0.49 |
| 5 | Rafina | 2 | 74 | 1 | 86 | 0.63 |
| 6 | Piraeus | 1 | 63 | 0.5 | 63 | 0.61 |
| 7 | Syros | 2 | 42 | 1 | 57 | 0.52 |
| 8 | Leros | 2.1 | 305 | 1.3 | 316 | 0.40 |
| 9 | Souda | 1 | 348 | 1.8 | 368 | 0.44 |
| 10 | Heraklion | 1.5 | 304 | 1.1 | 69 | 0.45 |
| 11 | Rhodes | 4.4 | 257 | 2.7 | 268 | 0.59 |
| 12 | Kalamata | 2.2 | 69 | 1.1 | 69 | 0.60 |
| 13 | Katakolo | 3.3 | 62 | 1.7 | 35 | 0.50 |
| 14 | Lefkas | 4.0 | 79 | 2.2 | 85 | 0.46 |

Figure 3.2.8: Co-tidal (--) and co-range (-) contours for the M2 tidal component of the Greek Seas (Tsimplis, 1994; Zenetos, 2005)

3.2.3.3 Sedimentology

In the deltaic area of Pinios, the proportion of sand (Figure 3.2.9a) decreases with depth, i.e. 50% of sediment being sand near the mouth of the river and 20% at a depth of 10 m and 500 m distance from the shore. The corresponding percentage in depths of 30 m and 1 km distance from the mouth reaches only 1%. The sediments near the mouth of the river contain silt (Figure 3.2.9b) at a rate of about 30% that increases to 45% at depths of 5-30 m and gradually decreases to 40% at a depth of 60 m in a distance of 3.5 km. The amount of clay (Figure 3.2.9c) increases with depth starting from 20% near the mouth and reaching 55% in a depth of 30m, slowly increasing up to 60% at a depth of 60m and a distance of 3.5 km from the shore.





(c)

Figure 3.2.9: Pinios mouth: sand reposition (a), silt (b) and clay (c) in percent of total weight (*station positions) (originally from Poulos, 1989)

According to Shepard (1956), there are 4 types of sediment at the river's mouth (Figure 3.2.10). Sand is gathered directly at the mouth and parallel to the coastline where the nearshore sediment transport is dominated by waves. Seawards, sand is characterized at depths of 10m and 30m by zones of silty sand and sandy silt respectively covering the front of the delta. At bigger depths, sediments are mostly described as silty clay (Poulos, 1989).

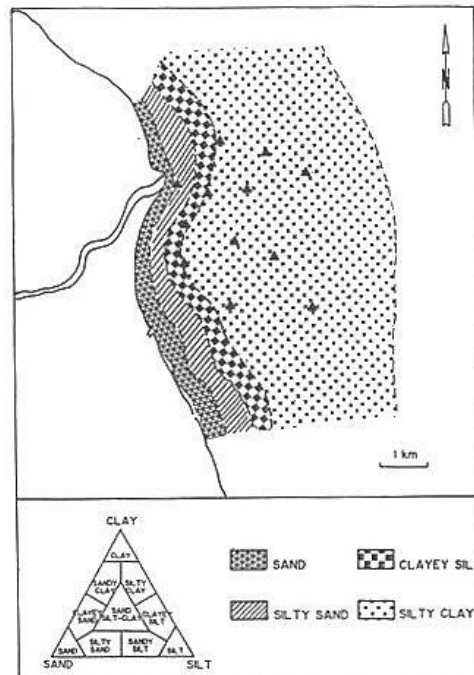


Figure 3.2.10: Pinios mouth: types of sediment according to Shepard, of the bottom of the basin (originally from Poulos, 1989)

Chapter 4 - Data Collection & Methodology

4 Data Collection & Methodology

4.1 Poseidon

POSEIDON is the first project that focuses on monitoring and assessing oceanographic data of the Greek Seas, jointly funded by the European Financial Mechanism (European Free Trade Association) through the European Investment Bank (85% of the total budget) and the Ministry of National Economy and run by the Hellenic Centre of Marine Research (HCMR). As given in Soukissian and Chronis (2000) its main objectives are to:

- remotely transmit data to the Operational Centre of HCMR
- monitor and measure marine and atmospheric parameters
- process the raw data and present the results in a user-friendly database
- forecast the sea state via numerical modelling
- disseminate the final products to the end-users and stakeholders.

4.1.1 Poseidon System Description

4.1.1.1 Poseidon - Hardware

POSEIDON has been based on the principles of OCEANOR's SeaWatch System, (Hansen and Stel, 1997), which is consisted of the following components:

1. Hardware on the buoys:
 - Sensors that monitor wind speed and direction, air pressure and temperature, surface water temperature, sea surface conductivity, sea surface current speed and direction, wave height and direction, water temperature and salinity from 0.50 m, sea surface radioactivity and light attenuation, dissolved oxygen, chlorophyll-a and nitrates
 - A computing system and the related software for the automated measurement in order to control, store, pre-process and prepare the data for near real-time remote transmission to the Operational Centre
 - Two-way telecommunication systems to transmit the data to the Operational Centre.
2. The Operational Centre in HCMR is equipped with a main frame UNIX computer, several PC's and peripheral devices, hardware and software for the remote connection with the POSEIDON network and the relevant software for data processing, storage, quality control, correction and finally presentation and distribution of the processed data to the users.
3. The Aegean Operational Forecasting System (AOFOS) provides numerical simulations and forecast models for the Greek seas. The Forecasting System is consisted by a weather prediction model; an open sea wave forecast model, a 3D hydrodynamic model, a shallow water wave prediction model and a buoyant pollutant transport model.

The in situ data are obtained by a network of 10 (+ 2 spare) oceanographic buoys and 10 wave buoys, located in offshore areas with a variety of sensors that monitor the marine environment.

There are three different types of buoys used for the Poseidon System (Figure 4.1.1):

- Seawatch is a multi-sensor wave directional data buoy for oceanographic and meteorological parameters, whilst its vertical stability makes it ideal for current measurements.
- Wavescan is a metocean data buoy that collects wave parameters (height and direction) and meteorological parameters and is installed mostly in deep water, remote locations and environments with high current speeds
- Wavescan-Deep Sea Module is designed especially for tsunami detection. It consists of a pressure sensor, a processor, batteries and an acoustic modem that is located on the seafloor. Along with the surface buoy it enables the collection of data sets for many meteorological and oceanographic parameters, giving a full description of the weather and sea state.

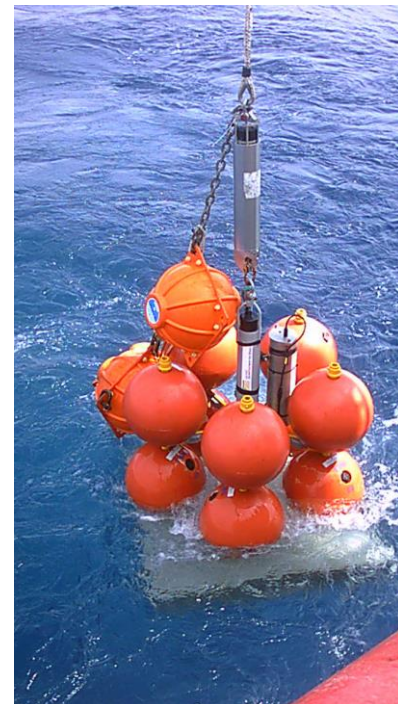


Figure 4.1.1: Photos of Seawatch Buoy (left), Wavescan (middle), Wavescan-Deep Sea Module (right) (<http://www.oceanor.com>)

4.1.1.2 Location and Buoys Deployment

Seven Seawatch buoys have been deployed in areas with water depth less than 300 m and are equipped with sensors for the basic meteorological and oceanographic parameters such as salinity, temperature, current speed and direction, a variety of wave parameters, air pressure, air temperature as well as wind speed and direction. Three Seawatch- Wavescan buoys have been deployed in deep offshore locations with CTD sensors adjusted on the mooring line providing salinity, temperature and pressure data down to 1000 m depth. Biochemical parameters such as oxygen and chlorophyll-a are also measured from the sea surface down to 100 m depth. ADCP profilers collect current data every 5 m from the sea surface to the depth of 50 m. In addition to the basic meteorological parameters, additional meteorological parameters are measured such as rainfall, radioactivity, radiance and irradiance.

A Wavescan buoy has been deployed at southern Ionian Sea (Pylos) and communicated through an acoustic modem with a Deep Sea Module platform (Figure 4.1.2). It is capable of recording sea pressure and detection of anomalies on the sea surface altimetry, which could indicate a tsunami incident over the specific sea area. The platform has also adjusted sensors measuring temperature and salinity down to the sea basin.

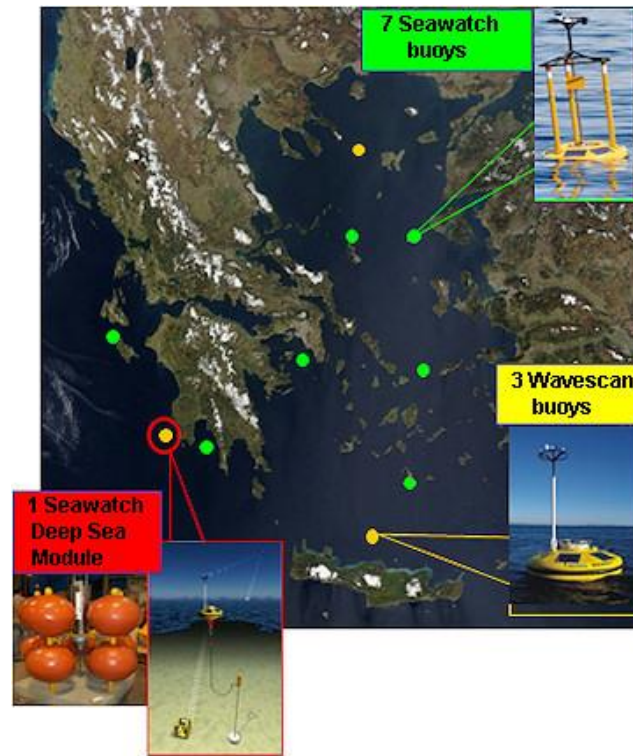


Figure 4.1.2: Initial locations of HCMR buoys (http://poseidon.hcmr.gr/article_view_no_news.php?id=117)

4.1.1.3 Data acquisition (Capabilities and Limitations)

The SeaWatch buoys used in the POSEIDON project are designed to measure oceanic variables in the upper 50 m and atmospheric variables at 3 m height above sea level. Wind speed and direction are recorded by a Lambrecht 145352 sensor (speed accuracy ± 1.05 m/s, direction accuracy $\pm 1^\circ$). A Vaisala PTB200 digital barometer is used for atmospheric pressure measurements (accuracy ± 0.2 hPa), while air temperature is recorded with an Omega Engineering ON90544036 sensor (range: 8 °C to 49.5 °C, accuracy: ± 0.1 °C). Every measurement is a 10 min average that reduces high frequency noise. The sampling interval is set to 3 hours for all variables. This interval allows an adequate representation of the daily cycle and eliminates power problems that occur when a 1-hour sampling interval is used. Data are transmitted to the operational centre of NCMR every 3 hours through Inmarsat-C satellite communication. An automatic quality control procedure removes spikes and erroneous data that are outside a predefined range of values. The maintenance procedure includes calibration of the sensors using reference in situ measurements.

As the replacement of all sensors per maintenance visit by new sensors and the use of the ship to do so, are rather costly the following sampling procedure has been adopted for in situ sensor calibration for the past years. On arriving at station and deploying the new, calibrated measuring platform, the old buoy is recovered and the ship moves towards the next position. On the way to the new deployment site, the buoy's sensors undergo the regular maintenance procedures. When this is done and the buoy is ready for redeployment at its new position, the calibration procedure takes place; the sampling interval for the SeaWatch buoy is temporarily set at 15 min, of which 5 min is reserved for sampling and 10 min is the interval between measurements, which allows us to move sensors to different water samples, dilute saline water to lower salinities, etc. 4–8 samples are taken, i.e., the calibration procedure for each SeaWatch buoy requires 1–2 hours. Afterwards, the sampling rate is turned back to 3 hours and the buoy is ready for redeployment (Nittis et al., 2001).

4.1.2 Poseidon Data & Methodology of Data Analysis

The data used for this research are obtained in 13 locations from the POSEIDON System located in several areas of the Greek Seas (Figure 4.1.3).



Figure 4.1.3: Buoys Locations

4.1.2.1 Wave Characteristics

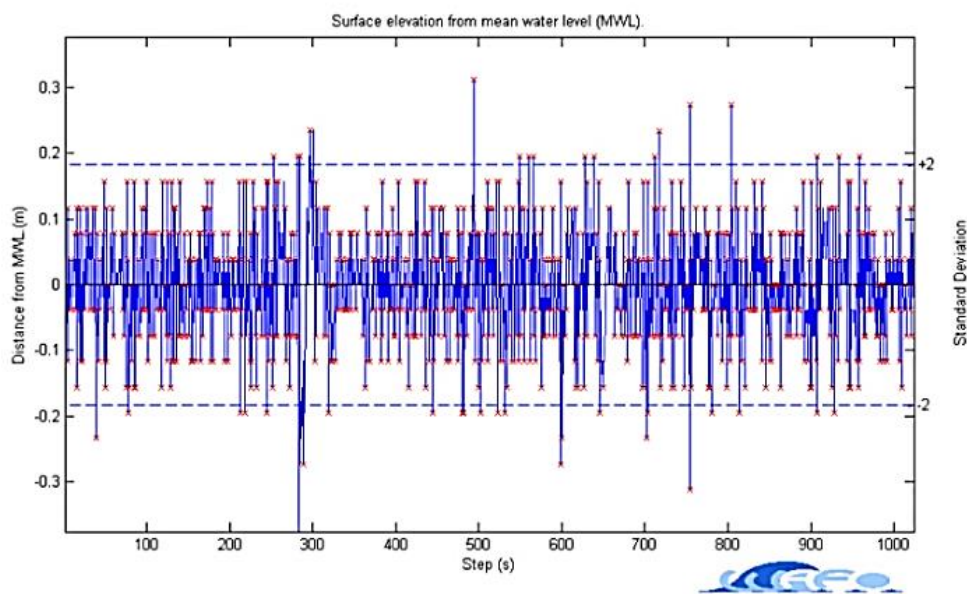
The parameters in Table 4.1.1 are obtained by the buoys every 3 hours. Prior to the analysis, the databases are checked for erroneous values and are accordingly filtered, i.e. values of -9999.99023 are replaced with NaN while for wave parameters the value -0.0001 or 7.50005 are excluded. Even though that the aforementioned procedure discarded these values the record is not deleted but kept even as empty. The analysis includes general statistics such as mean, max, standard deviation, wave charts (wave height - wave direction, swell height - swell direction, wind - wave height - wind - wave direction, and the same for period) and frequency tables (of wave height per wave period). Additionally, the following are also done, monthly means in the form of box-whisker plots, monthly means of every month for every year (in order to see the trends of the parameters and any extremes) and annual values to check the annual trends.

Table 4.1.1 Wave Characteristics as given by the SeaWatch buoys

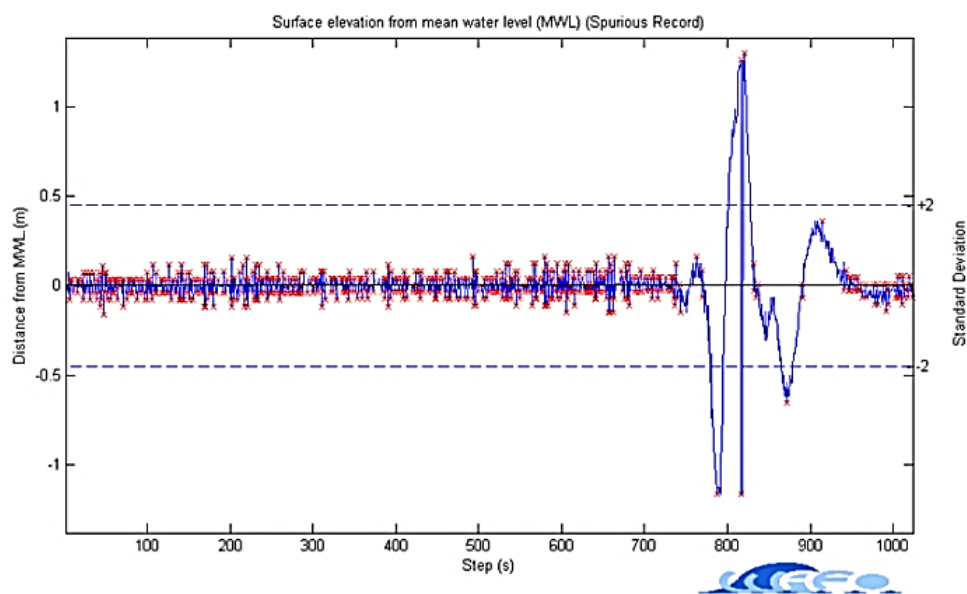
| Parameter | Description | Units (SI) |
|---------------|-----------------------------------------------------|-------------|
| Date | Date - time in the form of (DD-MM-YYYY hh:mm:ss) | |
| H_{m_0} | Significant wave height | m |
| $H_{m_{0a}}$ | Significant wave height for swells | m |
| $H_{m_{0b}}$ | Significant wave height for wind-waves | m |
| H_{max} | Maximum wave height | m |
| Lat. | Latitude | Degrees (°) |
| Lon. | Longitude | Degrees (°) |
| M_{dir} | Direction of waves (Clockwise from N) | Degrees (°) |
| M_{dir_a} | Direction of swells (Clockwise from N) | Degrees (°) |
| M_{dir_b} | Direction of wind-waves (Clockwise from N) | Degrees (°) |
| $SprT_p$ | Spreading at T_p | Degrees (°) |
| $ThHf$ | High frequency wave direction | Degrees (°) |
| $Thtp$ | Wave Direction at the Spectral Peak | Degrees (°) |
| $T_{m_{01}}$ | Mean period | s |
| $T_{m_{02}}$ | Mean Zero - crossing period | s |
| $T_{m_{02a}}$ | Mean Zero - crossing period of swells | s |
| $T_{m_{02b}}$ | Mean Zero - crossing period of wind waves | s |
| T_p | Peak period | s |
| UI | Unidirectivity index H3 | |
| Heave | Sea surface elevation (1024 values see Ch. 4.1.2.2) | m |

4.1.2.2 Sea Surface Elevation Data

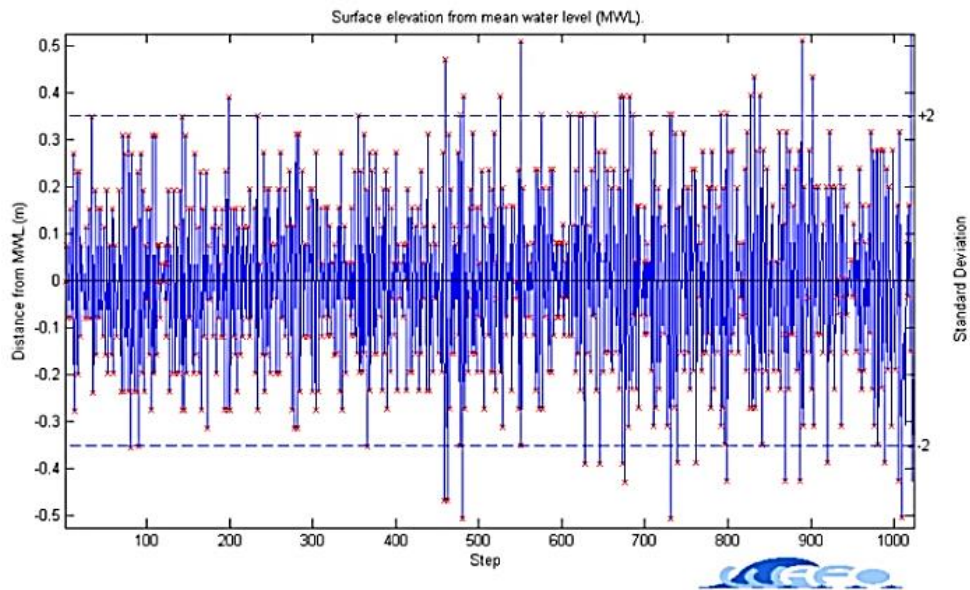
Sea surface elevation data (heave) are obtained by 7 offshore buoys located in North Aegean (Athos), North West Aegean (Skyros), Central Aegean (Mykonos), South Aegean (Santorini), North-East Ionian Sea (Zakynthos) and South East Ionian Sea (Pylos and Kalamata). The recording period of the buoys for wave data is of 17 min (i.e. 1024 sec) with recording intervals of 3hours and sampling frequency of the sea surface elevation measurements of 1 Hz. Prior to the analysis of the sea surface elevation, the data were analytically examined and filtered to discard erroneous values and outliers, following two basic criteria: (1) the record is of the nominal length of 17 - 20 min (Holthuijsen, 2007); and (2) there were no linear trends in the record. In the case of erroneous measurements found in a record, then the relevant heave time series was rejected. Examples of sea surface elevation records are shown in Figure 4.1.4.



(a)



(b)



(c)

Figure 4.1.4: SSE Records

In order to obtain the basic wave parameters, an algorithm based on WAFO toolbox of Matlab (Brodtkorb et al., 2000) is developed and implemented (see flow chart in Figure 4.1.5). All the input records are in form of time-series, i.e. one column was time (1-1023 sec) and the second column is the sea surface elevation.

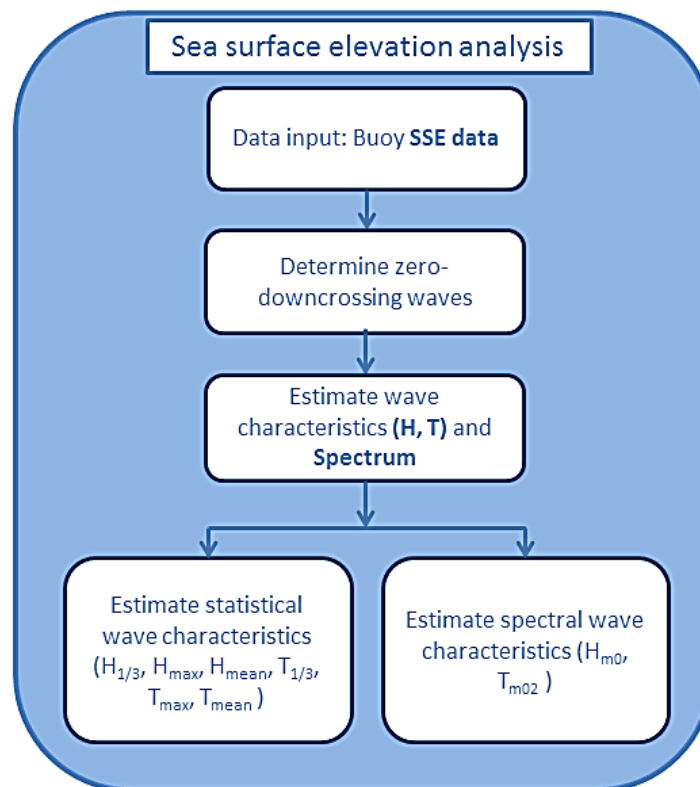


Figure 4.1.5: Basic structure of the algorithm used

Every record is de-trended in order to exclude any linear trends (function *detrend*). Afterwards, mean sea level is considered to be at 0 m and down-crossing waves are determined (*method=3*). With the *dat2steep* function the waves are identified and several characteristics, such as apparent wave height and period, are estimated and with *dat2wa* the sequence of wavelengths of the data are extracted assuming the deep water dispersion (Table 4.1.2). The spectrum is estimated with the function *dat2spec*, while *spec2char* estimates the chosen spectral characteristics of the wave. The *spec2mom* function estimates the spectral moments from the spectrum, up to the 4th order moment. Spectral bandwidth and irregularity factors are estimated with *spec2bw*. In order to estimate the statistical significant wave height $H_{1/3}$, wave heights of every recorded separately were sorted in descending order and the mean of the top 1/3 of the number of waves was estimated. The same procedure was followed for the case of $T_{1/3}$. Afterwards, the data provided from the aforementioned analysis are statistically examined in the form of mean, max and standard deviation. The monthly means are also estimated for the periods of recording.

Table 4.1.2: Basic functions and steps of the WAFO script

| Function | Outputs | Definition |
|-----------|-----------------|------------------------------------------------------|
| dat2steep | Steep | Steepness |
| | H | Wave height according to period |
| | Ac, At | Crest and trough amplitude |
| | Tcf, Tcb | Crest front and Crest rear period |
| dat2wa | T | Sequence of wave periods or wave lengths |
| dat2spec | S.S | Spectral density |
| | S.w | Angular frequency |
| | S.tr | Transformation |
| | S.h | Water depth |
| | S.type | freq |
| | S.note | Memorandum String |
| | S.date | Date and time of creation |
| | S.L | Maximum lag size of the window function |
| | S.Cl | Lower and upper confidence constant |
| | S.p | Confidence level |
| spec2mom | m | Vector of moments |
| | mtext | A cell array of strings describing the elements of m |
| spec2char | Hm ₀ | Significant wave height |
| | Tm01 | Mean wave period |
| | Tm02 | Mean zero-crossing period |
| | Tp | Peak period |
| | Ss | Significant wave steepness |
| spec2bw | eps2 | Narrowness factor |
| | eps4 | Broadness factor |

From the aforementioned script, the probability distribution with the best fit for the apparent wave height is examined (Soukissian et al. (2012)). Three closed upper boundary probability distributions Weibull, Rayleigh and Kumaraswamy are examined (Table 4.1.3).

Table 4.1.3: Rayleigh, Weibull and Kumaraswamy Distributions

| Distribution | Probability Density Function | Cumulative Distribution Function | Parameters |
|-------------------------------------------------------|-------------------------------------------------------------------------------------------------------------|----------------------------------------------------------------------|-------------------------------------------------------|
| Rayleigh (Pierson, 1952; Longuet-Higgins, 1952) | $f_x(x) = \frac{x}{\sigma^2} \exp\left\{\frac{-x^2}{2\sigma^2}\right\}, 0 \leq x < \infty, \sigma > 0$ | $F_x(x) = 1 - \exp\left\{\frac{-x^2}{2\sigma^2}\right\}$ | X a random variable, σ^2 the scale parameter |
| Weibull (Forristall, 1978) | $f_x(x) = \frac{c}{a} \left(\frac{x}{a}\right)^{c-1} \exp\left\{-\left(\frac{x}{a}\right)^c\right\}, x > 0$ | $F_x(x) = 1 - \exp\left\{-\left(\frac{x}{a}\right)^c\right\}, x > 0$ | c the shape parameter, a the scale parameter |
| Kumaraswamy (Kumaraswamy, 1980) | $f(x) = pqx^{p-1}(1-x^p)^{q-1}, 0 \leq x \leq 1, p > 0, q > 0$ | $F(x) = 1 - (1-x^p)^q$ | p, q are shape parameters |

For this, EasyFit software is used, examining the pre-chosen distributions via the goodness of fit tests Kolmogorov - Smirnov, Anderson - Darling and Chi- square.

Chi-Square Test

The chi-square test examines whether the observed frequencies O_1, O_2, \dots, O_k , of some possible events E_1, E_2, \dots, E_k are consistent with the expected (or theoretical) frequencies E_1, E_2, \dots, E_k , obtained from a particular theoretical distribution. The events considered must be mutually exclusive and should have the same sampling number, i.e.:

$$\sum_{j=1}^k E_j = \sum_{j=1}^k O_j = N \quad (4.1)$$

where, N is the total frequency. To estimate the difference of the observed and the expected frequencies, the statistic χ^2 is used and is calculated as:

$$\chi^2 = \sum_{j=1}^k \frac{(O_j - E_j)^2}{E_j} \quad (4.2)$$

Kolmogorov-Smirnov Test (K-S test)

The nonparametric Kolmogorov-Smirnov test (K-S test) tests the hypothesis that a given data set can be represented from a given distribution.

The null hypothesis to be tested is:

$$H_0 : F_n(x) = F(x), \text{ for all } x \quad (4.3)$$

where $F(\bullet)$ is a known cumulative distribution function. The K-S statistic estimates how the distribution function $F_n(x)$ and $F(\bullet)$ differ, via the statistic D_n :

$$D_n = \sup_{x \in \mathcal{R}} |F_n(x) - F(x)| \quad (4.4)$$

where, the distribution function $F_n(x)$ is estimated as:

$$F(x) = \frac{1}{n} \sum_{i=1}^n I_{X_i \leq x} \quad (4.5)$$

The indicator function $I_{X_i \leq x}$ is equal to 1 if $X_i \leq x$ or equal to 0 otherwise. If $D_n > D_{n,a}$, and $D_{n,a}$ is the critical K-S value and a is the risk level, then the null hypothesis is rejected.

Anderson - Darling Test (A-D test)

If the sample data x_1, x_2, \dots, x_n , is from a distribution with cumulative distribution function F , then it can be transformed to a uniform distribution. The uniformity is tested by a distance test. The test statistic A is compared with the critical values of the theoretical distribution defined as $A_2 = -n \cdot S$:

$$S = \sum_{k=1}^n \frac{2k-1}{n} \left[\ln F(Y_k) + \ln(1 - F(Y_{n+1-k})) \right] \quad (4.6)$$

and Y_k , $k=1, 2, \dots, n$ is the corresponding order statistic (i.e. $Y_1 < Y_2 < \dots < Y_n$) of $X_1, X_2, X_3, \dots, X_n$.

The A-D test is more sensitive to deviations in the tails of the distribution than the K-S test.

Finally, the relationship among the spectral and statistical parameters of wave height and period is examined in the forms of scatterplots and correlation coefficients. Ratios of several parameters are also examined from the sea surface elevation records analysis: $H_{m0} / H_{1/3}$, $H_{1/3} / \sqrt{m_0}$, H_{\max} / H_{m0} and $H_{\max} / H_{1/3}$. Main scope of this analysis is to provide information about the relation of the spectral and statistical parameters as well as the estimation of maximum wave height from the significant wave height (statistical or spectral) (Sifnioti et al., 2014).

4.1.2.3 Weather Characteristics

On a three hourly basis, the atmospheric parameters of Table 4.1.4 are obtained. The parameters are also filtered and checked for biases, whilst replacing erroneous records with NaN values. The descriptive statistics, as in the case of the wave parameters, are estimated for the weather characteristics: mean, max, standard deviation and coefficient of variation. In addition, wind charts are also created, to represent the directionality of the most common winds and the stronger ones as well. In addition, monthly means are presented in the form of box and whiskers plots, monthly means analytically for every year and finally, annual values are presented in scatterplots, to see any potential trends or events.

Table 4.1.4: Atmospheric Characteristics as given by the Poseidon buoys

| Parameters | Units (SI) |
|-----------------|--------------------------------------|
| Date-Time | DD-MM-YYYY hh:mm:ss |
| Air Pressure | hPa at 3 m |
| Air Temperature | °C at 3m |
| Latitude | degrees (°) |
| Longitude | degrees (°) |
| Wind Direction | degrees (°) at 3m (Clockwise from N) |
| Wind Gust | m/s at 3m |
| Wind Speed | m/s at 3m |

4.1.2.4 Wave - Weather Characteristics

The aforementioned wave and weather databases are merged, according to the time period of the atmospheric measurements, in order to obtain a full description of the wind and wave state of the Hellenic Seas (as provided by the buoys), only for matching time-periods (Sifnioti et al., 2013). This analysis includes a discussion on the relation of wave and atmospheric parameters per buoy in the means of charts, pivot tables and scatterplots along with the basic statistic parameters. The purpose of this analysis is to show the relation amongst wind speed and wave height especially, as well as wind directionality with wave height and period. To provide a categorization of wind speeds and the generation - characteristics of waves, the Beaufort wind scale on sea state is used (Table 2.2.1).

In addition, the upper 10% of the estimated wave heights and periods from the sea surface elevation data analysis are used in order to relate them with seasonal composite means of the vector wind from NCEP-NCAR dataset (Nastos and Sifnioti, 2012; Nastos et al., 2013). Analytically, 6291 measurements are selected, 4204 and 2719 for the Aegean and Ionian Seas, respectively. The NCEP-NCAR seasonal composite means of the vector wind were given for the matching dates of the upper 10% of daily means of wave height and period. The NCEP-NCAR data have spatial resolution of 1.9° latitude x 1.875° longitude (Kalnay et al., 1996).

4.2 ERA-Interim

ERA-Interim is the most recent global atmospheric reanalysis dataset produced by the European Centre for Medium-Range Weather Forecasts (ECMWF). The ERA-Interim dataset covers the period from 1 January 1979, is continued in real-time and updated every 2 months. The parameters produced are in forms of gridded datasets and describe surface parameters (weather, land and ocean every 3 hours) as well as 6 hourly upper-air characteristics from the troposphere and the stratosphere. Goal of this dataset is to describe the twentieth century, to overcome data assimilation issues that were found in previous datasets of ECMWF, such as ERA-40 and to provide much needed information on data selection - quality - biases and monitoring. More information can be found in the ERA-Interim archive (Berrisford et al., 2009) and in <http://www.ecmwf.int/research/era>.

4.2.1 Data Assimilation

In contradiction to weather forecast systems, reanalysis data are created by a data assimilation system, ran only once (Dee et al., 2011). As many observations as possible should be included and that is not an easy task as the lack of data in several temporal and spatial scales can be eminent even nowadays. Another requirement is to represent, the physical meaning of the data and to do this, a forecast model is used to assimilate and compare data from different sources and types. Localized observations and parameters are propagated in time via this model. Finally, the interpretation of interannual and decadal values should give trend estimates as accurately as possible and should include climatic patterns e.g. North Atlantic Oscillation (NAO). It should be noted that spurious climatic signals might be related to changes in the assimilation of the global observing system and to biases - errors in observations.

4.2.1.1 Atmospheric Analysis

The basic structure of the ERA-Interim is the 12-hourly 4D-Var assimilation system of the upper-air atmosphere (Courtier et al., 1994; Veerse and Thepaut, 1998). The outside loops of the nested loops of the system, form the nonlinear forecast model by estimating the 4D parameters and observations whilst the inner loops perform a quality control of the data (Trémolet, 2004). The original grid of ERA-Interim is T255 (~79 km) and there are two inner spectral resolutions at T95 (~210 km) and T159 (~125 km). The analysis of the surface parameters is performed separately from the main atmospheric analysis in many steps. Initially, an optimal interpolation (OI) scheme estimates every 6 hours temperature and dewpoint, by using synoptic observations. A similar scheme is used for ocean waves via the usage of satellite altimetry, when possible. A fully coupled 2D wave model describes the sea surface and gives the relevant wave heights according to pre specified thresholds for wind-sea and swell spectra (Lionello et al., 1992). The datasets of sea surface temperature (SST) and sea ice cover (SIC) that are used as boundary conditions for the atmospheric model in ERA-Interim are presented in Table 4.2.1.

Table 4.2.1: Datasets of SST and SIC, used in ERA-Interim (Dee et al., 2011)

| ERA-Interim period | SST and SIC |
|--------------------|---------------|
| 01/1979-06/2001 | NCEP 2D-Var |
| 07/2001-12/2001 | NCEP OISST v2 |
| 01/2002-01/2009 | NCEP RTG |
| After 02/2009 | OSTIA |

*NCEP: National Centre for Environmental Prediction, OISST: Optimal Interpolation Sea Surface Temperature, RTG: Real Time Global, OSTIA: Operational Sea Surface Temperature and Sea Ice Analysis

4.2.1.2 Forecast model

The Integrated Forecast System (IFS) has three components: atmosphere, land surface and ocean waves. Throughout the years, this model has changed accordingly (mostly due to maintenance and assimilation analysis); its' alterations can be found in www.ecmwf.int/products/data/operational_system/evolution and www.ecmwf.int/research/ifsdocs websites. The atmospheric model is based, among others, on a Lagrangean semi-implicit time stepping scheme and has a 30mins time step with a spectral T255 spectral resolution (horizontally) while vertically there are 60 model layers with the top of the atmosphere at 0.1hPa (Dee et al., 2011). A representation of daily counts in a logarithmic scale of several atmospheric parameters as given from ERA-Interim is shown in Figure 4.2.1.

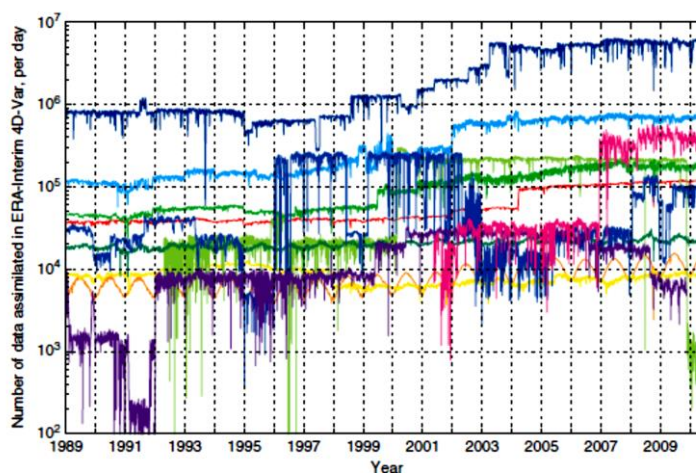


Figure 4.2.1: Daily observations assimilated by ERA-Interim atmospheric model, (after Dee et al., 2011)

The component of the wave model is described by including the evolution of wind fields and other atmospheric parameters that affect wave growth and supplying the model with details for the surface roughness of the sea state via the Charnock parameter (Janssen PAEM, 2004). The IFS wave model is based on WAM model (Komen et al., 1994) but is furthermore enhanced in physical and numerical aspects such as including a treating scheme for bathymetrical effects and dissipation sources (Bidlot et al., 2007). The horizontal grid of the ocean component is 110km, with a discretization of 24direction and 30 frequencies for the wave spectra.

4.2.2 Data Sources

Until 1989, the number of observations that were included in ERA-Interim were of 10^6 per day while from 2010 this amount has risen up to 10^7 per day; this increase was mostly due to the inclusion of satellite data and of measurements from the upper atmosphere as obtained mostly by radiosondes, pilot balloons, aircrafts and wind profiles (since 1998). Data from ships, buoys and land stations are also collected (Berrisford et al., 2011). The sources of conventional data used in ERA-Interim are shown in Figure 4.2.2. The observations of ERA-Interim before 2002 are mostly data collected for ERA-40 and can be found in (Uppala et al., 2005). The most notable differences from ERA-40 are:

- An automated scheme for bias corrections is applied for surface pressure observations.
- Bias corrections for temperature obtained by radiosondes are also applied.
- Scatterometer data of wind above ocean surface along with data from European Remote Sensing Satellites (ERS-1, ERS-2) and NASA Earth Observation Satellite (QuickSCAT) are also included.

For the ERA-Interim purposes, the following databases are also included:

- Altimeter wave height data from ERS-1, ERS-2 were correlated and calibrated with buoy measurements and then merged into a larger dataset.
- Several geostationary satellites of the European Organization for the Exploitation of Meteorological Satellites (EUMETSAT) such as the geostationary meteorological satellites Meteosat-3, Meteosat-4, Meteosat-5, and Meteosat-6 provided Atmospheric Motion Vector (AMV) wind data.

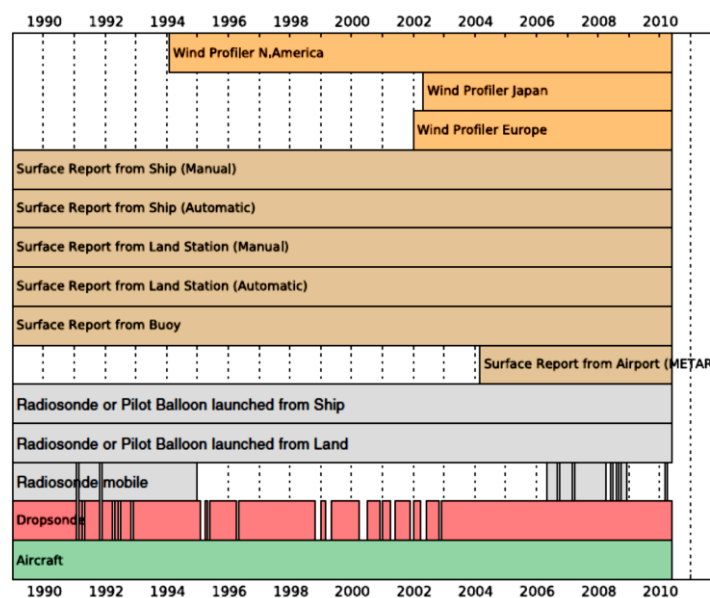


Figure 4.2.2: Timeline of conventional data included in ERA-Interim (Dee et al., 2011)

Data from satellites (sources shown in Figure 4.2.3) and especially from scatterometers that provide surface vector wind data over the global oceans in polar orbits of 25 km and widths of 550 km and 1800 km are checked for land and sea ice and backscatter corrections as provided by European Satellite Agency (ESA) over time.

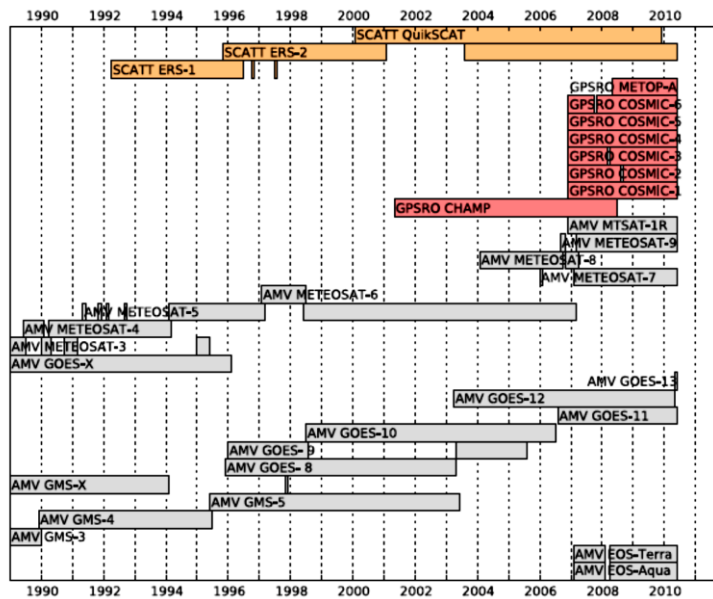


Figure 4.2.3: Scatterometer data sources included in ERA-Interim (Dee et al., 2011)

An optimal interpolation scheme is used to analyse in situ temperature data (with their count reaching more than 20000 per parameter for the complete ERA-Interim period). A similar optimal scheme is used for ocean waves to limit estimated wave spectra from wave height altimetry sessions. In Table 4.2.2 are shown the time periods of the satellites used for wave height estimation for ERA-Interim.

Table 4.2.2: Satellites used for ERA-Interim wave height data (Dee et al., 2011)

| | |
|---------|-------------------------|
| ERS-1 | 01/08/1991-03/06/1996 |
| ERS-2 | 03/05/1995-21/07/2003 |
| ENVISAT | 21/7/2003 (continuous) |
| Jason-1 | 20/08/2003 (continuous) |
| Jason-2 | 01/02/2010 (continuous) |

The data from altimeters undergo a background check for quality control, but before that an analysis of “along-track averaging procedure” is performed (Abdalla and Hersbach, 2004). The daily coverage of an altimeter represents almost 10% of the grid used in the model (2 altimeters give 20%). Therefore, it is possible that due to lack of coverages there will be orbits missing in the near-time archive. Space-borne altimeters ERS-1, ERS-2, ENVISAT, and Jason-1 constrain the wave spectra in ERA-Interim. In Figure 4.2.4 (a, c, e, g), time series of the normalised standard deviations and in (b, d, f, h) of the biases for significant wave height, peak period, zero-crossing mean wave period, and wind speed in 10m are shown. These data have been compared with quality - checked in situ data such as buoys, platforms, weather ships (Bidlot et al., 2002). It should be kept in mind, that the amount of information has increased through the years and any trend analysis should be treated with the relative detail.

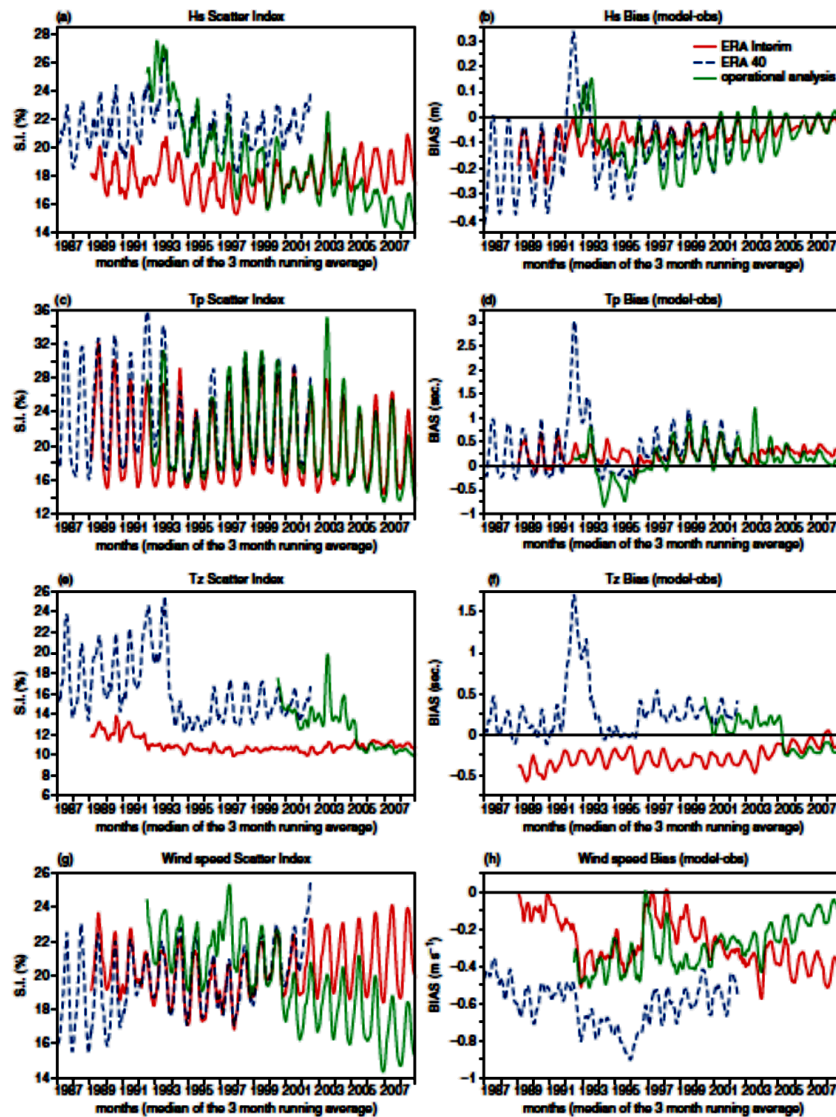


Figure 4.2.4: Normalized standard deviations of significant wave height (a), peak period (c), zero-crossing mean wave period (e) and wind speed in 10m (g) and biases of model and observations of wave parameters respectively (b, d, f, h) (Dee et al., 2011).

4.2.3 Data Quality and Selection

The observations in ERA-Interim go through quality control and several selection steps, in order to prevent any errors that can be produced during the transmission and recording of the data, such as air flight tracks, ship routes, duplicate reports etc. Any data that fail to pass these steps are excluded, but kept aside along with observations to be analysed for future needs. “Blacklists” rules are set to discriminate which data might cause a negative impact on the analysis. This can happen from types of data such as weather observations (such as visibility) and satellite measurements not accurately characterized by the forecast model. Quality control decisions for data usage and assimilation can be found in (Dee et al., 2011; Tavolato and Isaksen, 2010). Corrections of biases vary according to the parameter under-examination, e.g. surface pressure observations undergo an updating scheme in which the errors are assumed local and independent of the source of observation (i.e. ship, radiosondes etc.).

To do this an error of the previous 30day period is estimated and applied per observation per parameter independently and then crosschecked for any relation with estimates from nearby locations (Vasiljevic, 2005; Vasiljevic et al., 2006; Dee et al., 2011). As for the temperature correction as obtained from radiosondes, most of the departure statistics were derived from previous datasets such as ERA-40 and operational analyses from ECMWF (Andrae et al., 2004). The blacklist rules are constantly updated and maintained to include any changes in previous data manipulation and analysis.

4.2.4 Data Accumulation

ERA-Interim dataset is free for download after registering at the following site: http://apps.ecmwf.int/datasets/data/interim_full_daily/. Depending on the information that the user needs, the following are defined: time-period (e.g. 01/01/1979-31/12/1979), time (00:00, 06:00, 12:00, 18:00), step (0,3,6,9,12) and finally the parameter and the format of the output file (MARS,GRIBB, NetCDF) as shown in Figure 4.2.5.

The screenshot shows the 'ERA Interim, Daily fields' page on the ECMWF website. The page includes a navigation menu with 'About', 'Forecasts', 'Computing', 'Research', and 'Learning'. The main content area is titled 'ERA Interim, Daily fields' and contains a search form with the following sections:

- Select date:** A radio button to 'Select a date in the interval 1979-01-01 to 2014-10-31'. Below this are input fields for 'Start date: 1979-01-01' and 'End date: 2014-10-31', and a 'Reset' link.
- Select a list of months:** A radio button to 'Select a list of months'. Below this is a grid of checkboxes for each month (Jan to Dec) for each year from 1979 to 2014.
- Select time:** Radio buttons for '00:00:00', '06:00:00', '12:00:00', and '18:00:00'.
- Select step:** Radio buttons for '0', '3', '6', '9', and '12'.
- Select parameter:** A section for selecting the parameter, which is currently empty.

Figure 4.2.5: Website of ERA-Interim, ECMWF

Afterwards, the details of the job ready to be downloaded are shown along with the selection of the area of interest and the grid spacing (Figure 4.2.6).

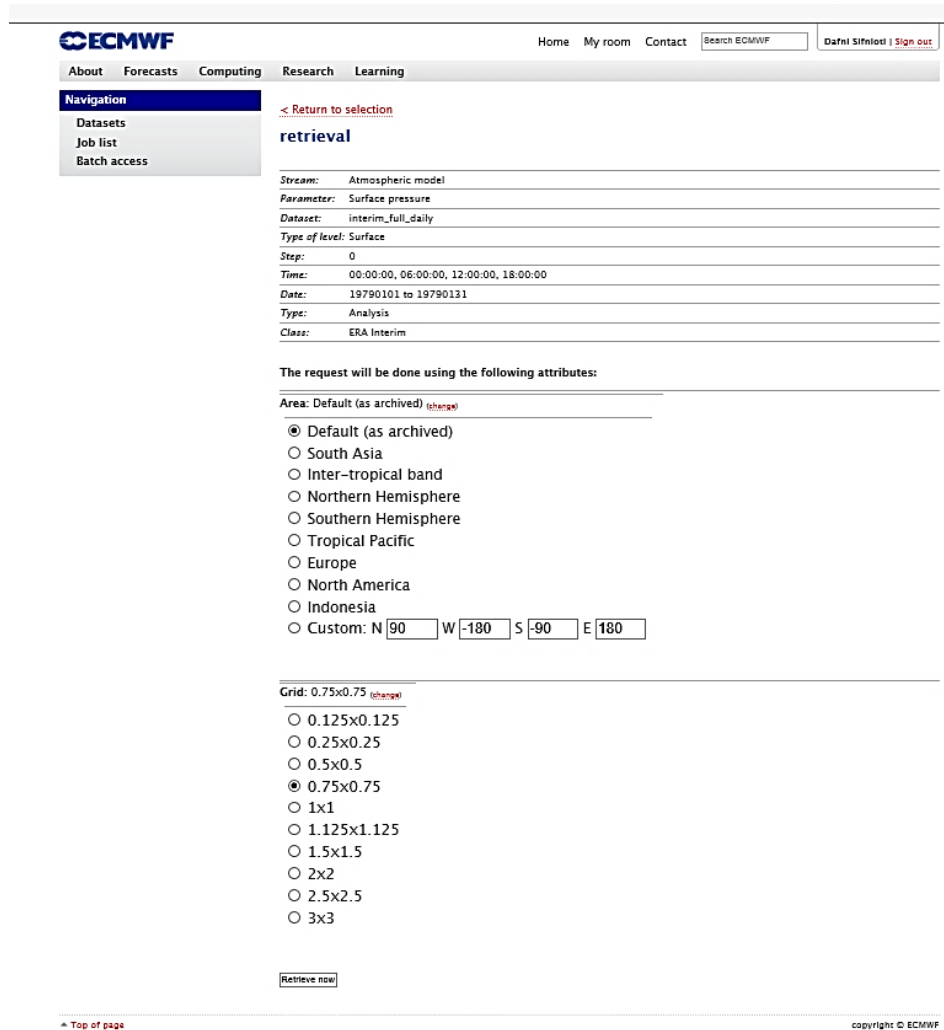


Figure 4.2.6: Choosing area and grid spacing

The characteristics of the data-files downloaded for this research are given in Table 4.2.3.

Table 4.2.3: Characteristics of data as downloaded from ERA-Interim, ECMWF

| Time- Period | Time | Step | Format | Area | Grid |
|-----------------------|------|-------|--------|------------------------------|-------------|
| 01/01/1979-31/12/2013 | 0 | 00:00 | NetCDF | 6°W to 37° E 30°N to 46°N | 0.125x0.125 |
| | | 06:00 | | | |
| | | 09:00 | | | |
| | | 12:00 | | | |

Due to limitation to the available data for download per file as set by the website, the above procedure is done per step for two time periods 01/01/1979 to 31/12/1999 and 01/01/2000 to 31/12/2013. The datasets are afterwards merged according to the Date and Time for the statistical analysis. The parameters downloaded are the following:

Table 4.2.4: Parameters downloaded from ERA-Interim database

| Long Name of Parameter | Short Name of Parameter | Units |
|-------------------------------------------------|-------------------------|---------|
| Significant Wave Height of Wind Waves and Swell | 'swh' | m |
| Mean Wave Period | 'mwp' | Pa |
| Mean Wave Direction (Clockwise from N) | 'mwd' | Degrees |
| Mean Sea Level Pressure | 'mslp' | Pa |
| Sea Surface Temperature | 'sst' | Kelvin |
| Temperature at 2m | 't2m' | Kelvin |
| Surface Pressure | 'sp' | Pa |
| Wind Zonal Velocity at 10m | 'u10' | m/s |
| Wind Meridional Velocity at 10m | 'v10' | m/s |

It should be mentioned here that the wind speed and wind speed direction are estimated via vector analysis and that pressure and temperature are converted to SI Units of °C and hPa. Further information about the parameters can be found here: <http://old.ecmwf.int/research/ifsdocs/CY40r1/IFSPart7.pdf>.

4.2.5 Buoy - Interim Data analysis

A variety of methods is performed in order to collocate and correlate the ERA-Interim database with eight Poseidon buoys. The methods are based on several researches (e.g., Stopa and Cheung, 2014; Mooney et al., 2011; Shanias and Sanil Kumar, 2013) and their results are considered representative of the under examination area and can be compared with the buoys. The methods are the following:

- 1) The grid point closest to the buoy's location (Figure 4.2.7, point B)
- 2) The weighted distance average of the four closest points to the buoy (Figure 4.2.7, points A, B, C, D).
- 3) The weighted distance average of the centres of the four grid boxes near the buoy (Figure 4.2.7, centre of boxes 1, 2, 3, 4).

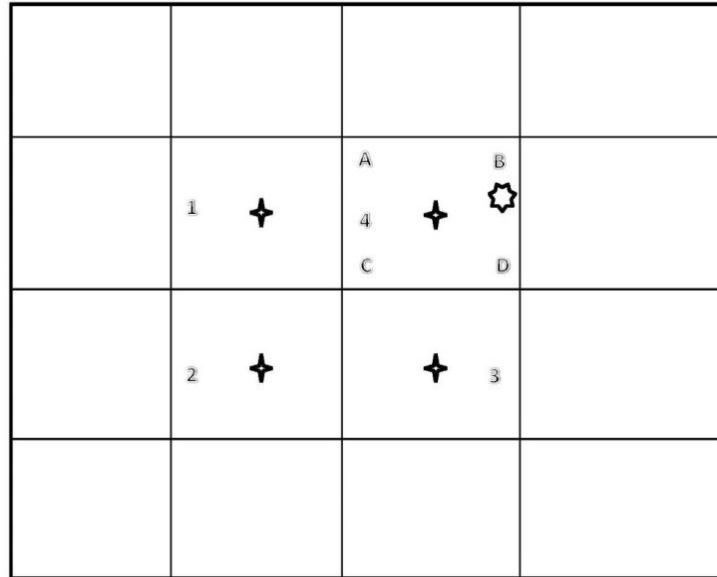


Figure 4.2.7: Methods of collocation (7-point star is the buoy)

The weighted distance average (WA) is calculated with the following equation:

$$WA = \frac{\frac{m_1}{r_1^2} + \frac{m_2}{r_2^2} + \frac{m_3}{r_3^2} + \frac{m_4}{r_4^2}}{\frac{1}{r_1^2} + \frac{1}{r_2^2} + \frac{1}{r_3^2} + \frac{1}{r_4^2}} \quad (4.7)$$

With, m the value of the parameter under examination per grid points A,B,C and D (for the weighted average) and 1,2,3,4 (for the Weighted Average of the Grid Boxes) and r the distance from the buoy to the grid points.

To compare the time-series of the buoys and ERA-Interim, the data are merged according to the time-series of the buoy (Date & Time). It should be mentioned that both datasets are on UTC time zone.

The parameters correlated are the following:

- Significant Wave Height (swh)
- Wind Speed at 10 m (w10)
- Temperature at 2 m (t2m)

It should also be noted that in order to collocate wind speed at 10 m, the wind speed of the buoys measured at 3m is converted to 10m elevation to match the data of wind speed as given from ERA-Interim. To do this, atmospheric stability has to be taken into account and methods such as described in by Monin and Obukhov (1954) should be applied. In order to do this though, measurements of pressure, relative humidity, air and sea surface temperature should be available, but in this case, they are not.

Thus, an alternative method of the logarithmic wind profile expression is applied, assuming that there are neutral stability conditions:

$$U_z = (U_{z_m}) * \frac{\ln \frac{z}{z_0}}{\ln \frac{z_m}{z_0}} \quad (4.8)$$

With U_z the wind speed at a height z (10 m), U_{z_m} wind velocity at the height of measurement (3 m), z_m and z_0 the roughness length of ocean surface equal to $1.52 \cdot 10^{-4}$ m (Carvalho et al., 2012).

The analysis includes bias, error and correlation estimates. Moreover, bias (*BIAS*) represents the data tendency, i.e. positive bias means that the simulated measurements underestimate the real observations while a negative bias overestimates them. The root mean square error (*RMSE*) gives a representation of the deviation amongst the observed and simulated data. The correlation coefficient (*COR*) shows how well the data correlate among each other.

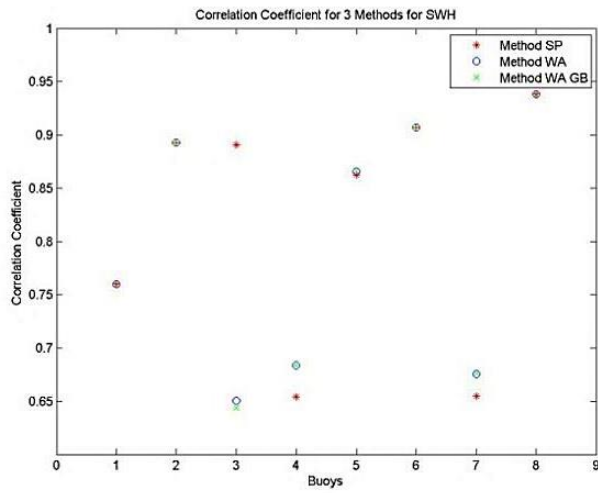
$$BIAS = (\bar{x} - \bar{y}) \quad (4.9)$$

$$RMSE = \sqrt{\frac{1}{n} \sum_{i=1}^n (y_i - x_i)^2} \quad (4.10)$$

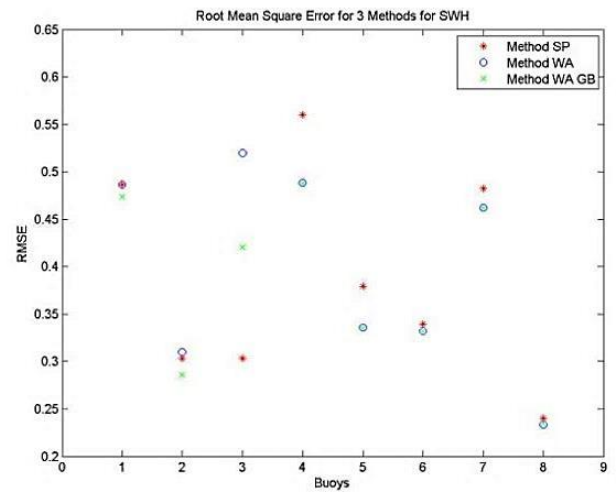
$$COR = \frac{\sum_{i=1}^n (y_i - \bar{y})(x_i - \bar{x})}{\sqrt{\sum_{i=1}^n (y_i - \bar{y})^2 \sum_{i=1}^n (x_i - \bar{x})^2}} \quad (4.11)$$

with x, y the buoy observations and the reanalysis data, respectively.

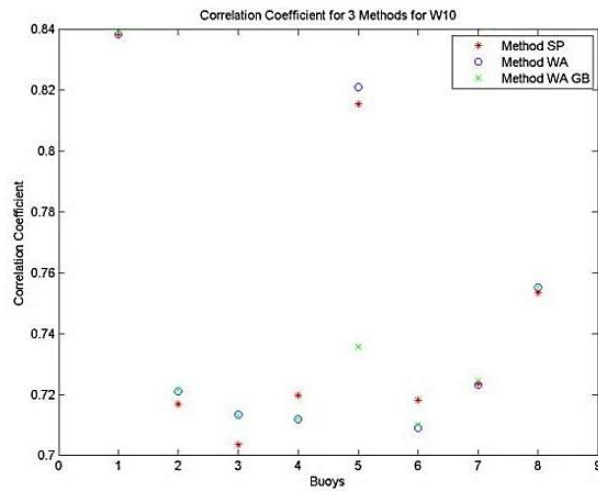
It should be mentioned, that errors can be due to amplitude errors (in relation to the mean weather state) or phase errors that can be related to the temporal consistency and the ability of the simulations to represent accurately the observations. The selection of the best method is based on the correlation coefficient and the root mean square, as represented in Figure 4.2.8:. Even though the method of the weighted averages of the centers of the 4 grid-boxes near the buoy presented good results, it is discarded due to the location of the boxes that occasionally are close to or on land.



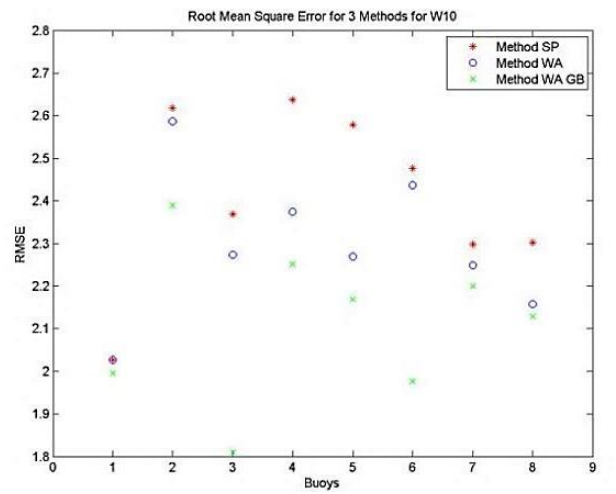
(a)



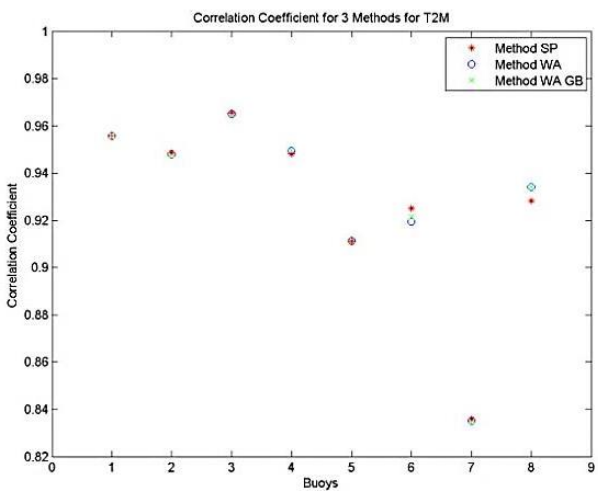
(b)



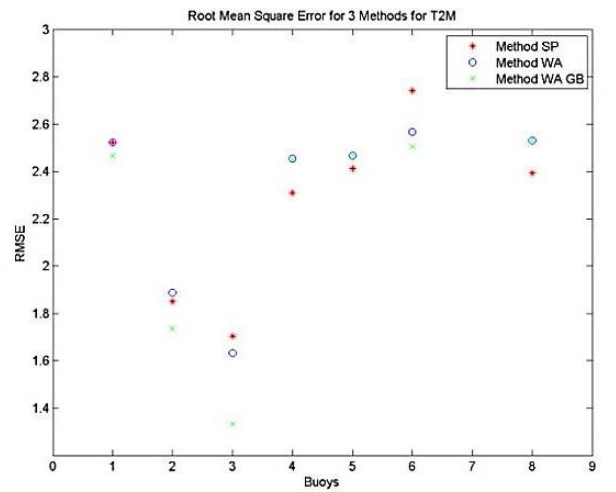
(c)



(d)



(e)



(f)

Figure 4.2.8: Correlation coefficients and root mean square error for the 8 stations between the buoy data and the ERA-Interim according to the 3 different collocation methods for wave height (a, b), wind speed (c, d) and temperature at 2 m (e, f). Stations are: 1: Athos, 2: Avgo, 3: E1M3A, 4: Lesvos, 5: Mykonos, 6: Pylos, 7: Santorini, 8: Skyros

4.2.5.1 Long Term Analysis

35 years statistical analysis for five selected points of the Greek Seas (Figure 4.2.9) is performed to provide information about the long-term wave and weather state in Aegean and Ionian Seas.

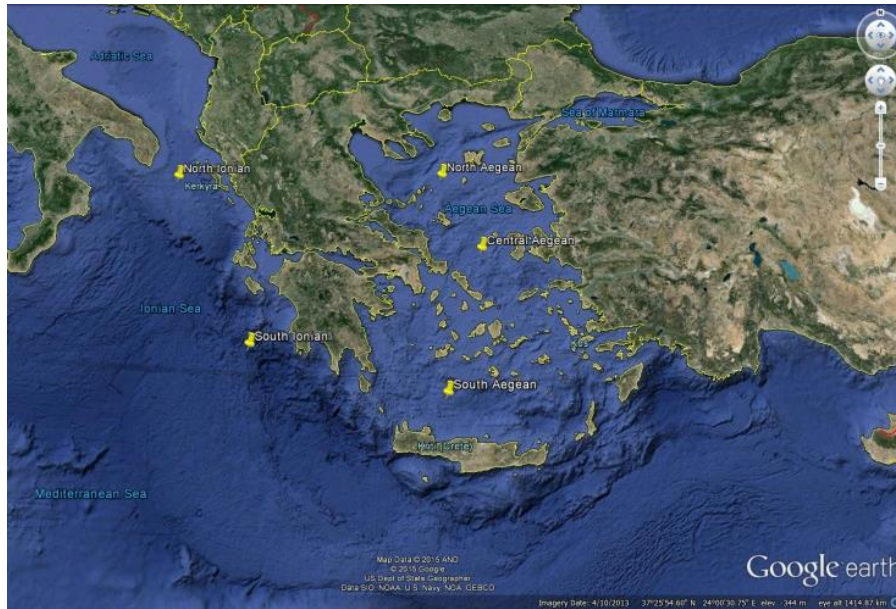


Figure 4.2.9: Locations of the 5 selected points of ERA-Interim

The analysis includes the monthly mean anomaly for the period 1979-2013 of the parameters of significant wave height, mean wave period, temperature at 2m and wind speed at 10m, as well as, annual values and monthly values per year. The trend of all aforementioned data is explained according to the likelihood of having a trend as given by the *p-value* of each analysis. In Mastrandrea et al. (2010), likelihood is suggested in order to quantify uncertainty and is used as “an expression of a probabilistic estimate of the occurrence of a single event or of an outcome (e.g., a climate parameter, observed trend, or projected change lying in a given range)”. The boundaries of the likelihood of an outcome, expressed in percentages are given in Table 4.2.5.

Table 4.2.5: Term and Likelihood of the Outcome (Mastrandrea et al., 2010)

| Term | Likelihood of the Outcome |
|------------------------|---------------------------|
| Virtually certain | 99-100% probability |
| Very likely | 90-100% probability |
| Likely | 66-100% probability |
| About as likely as not | 33 to 66% probability |
| Unlikely | 0-33% probability |
| Very unlikely | 0-10% probability |
| Exceptionally unlikely | 0-1% probability |

4.3 Pinios Methodology

4.3.1 Background Information

The area under examination extends from the southern part of the mouth of Pinios River to Stomio settlement. Analytically, the southern coastline extends from the geographical location is from N39.93°, E22.71° to N39.86°, E22.73° and is approximately of 7 km length, 40 m width at locations and an orientation of almost North to South. The shore area is mostly influenced by wind and waves from the NE, E and SE directions. The sediments are fine-grained, mostly sand with some mud, while mean sea level variations (such as tides and storm surges) for the purposes of this research are considered negligible. The offshore bathymetry has been abstracted from the DAPHNE project (hydrographic survey took place in October 2013).

4.3.2 Meteorological and Oceanographic Data

To describe the offshore conditions of Pinios River area, the point with geographical coordinates of 23°E, 39.875°N (with mean depth more than 200m (Krestenitis et al., 2015)), from ERA-Interim (0.125 x 0.125) grid is selected (Figure 4.3.1). The data cover the period from 01/01/1979 to 31/12/2013, are every 6 hours and consist of the parameters: wind speed at 10 m, wind direction (blowing from), temperature at 2 m, significant wave height of wind wave and swell, mean wave period and mean wave direction (propagating from). The analysis covers statistics of monthly data, annual data, and monthly anomalies for the 35 years period and a discussion on the trends of the aforementioned parameters. Fetch can be of 62 km (NE), 130 km (E) and 100 km (SE).

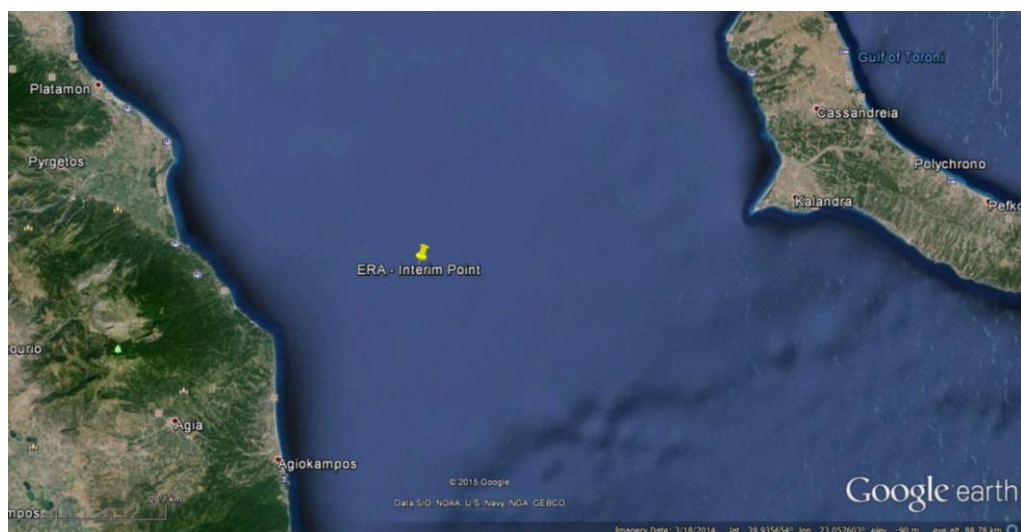


Figure 4.3.1: Location of selected point of ERA-Interim (23°E, 39.875°N)

4.3.3 Site Investigations

The present investigation focuses on the southern shore zone of the Pinios River facing eastwards along with two topographic profiles perpendicular to the shoreline (A and B; for locations see Figure 4.3.2) are utilised in order wave transformation from the deep-water condition to the breaking zone to be studied.

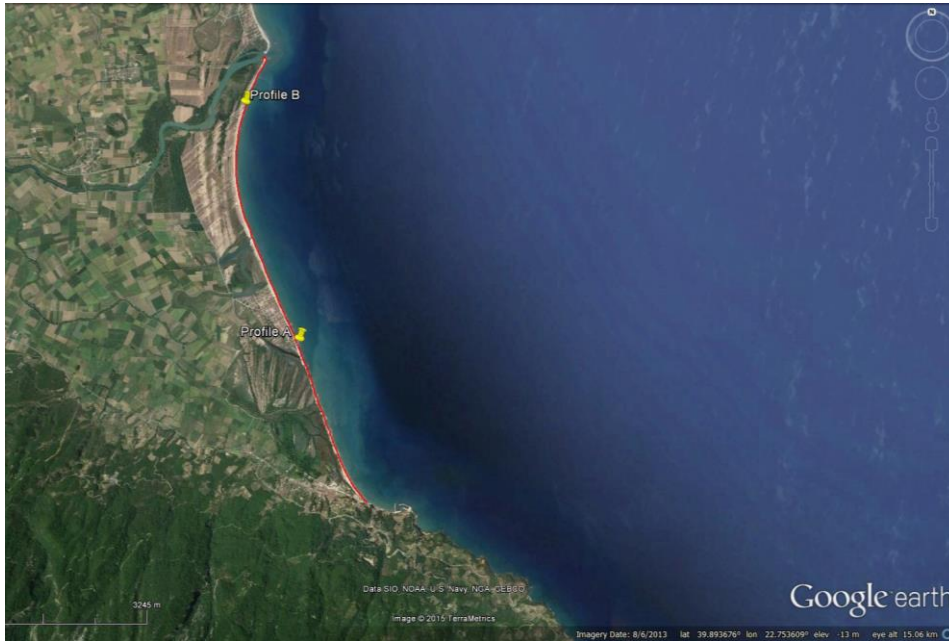


Figure 4.3.2: Locations of the Southern topographic surveys (yellow marks) and digital survey of the coastline (red line)

Profile A ($N^{\circ} 39.89$ and $E^{\circ} 22.72$) is located close to the settlement of Alexandrini and is characterized by at least 30m width (Figure 4.3.3).



(a)



(b)



(c)



(d)

Figure 4.3.3: Photographs of location 3, landwards (a), seawards (b), northwards (c) and southwards (d) - Survey Conducted in October 2013

Profile B ($N^{\circ} 39.92$ and $E^{\circ} 22.71$) is located close to the mouth of the river and as in profile, A has a width of some 30 m.(Figure 4.3.4).



(a)



(b)



(c)



(d)

Figure 4.3.4: Photographs of location 6, landwards (a), seawards (b), northwards (c) and southwards (d) Survey Conducted in October 2013

In addition to the topographic surveys, a bathymetry survey was conducted during October 2013 (Figure 4.3.5).

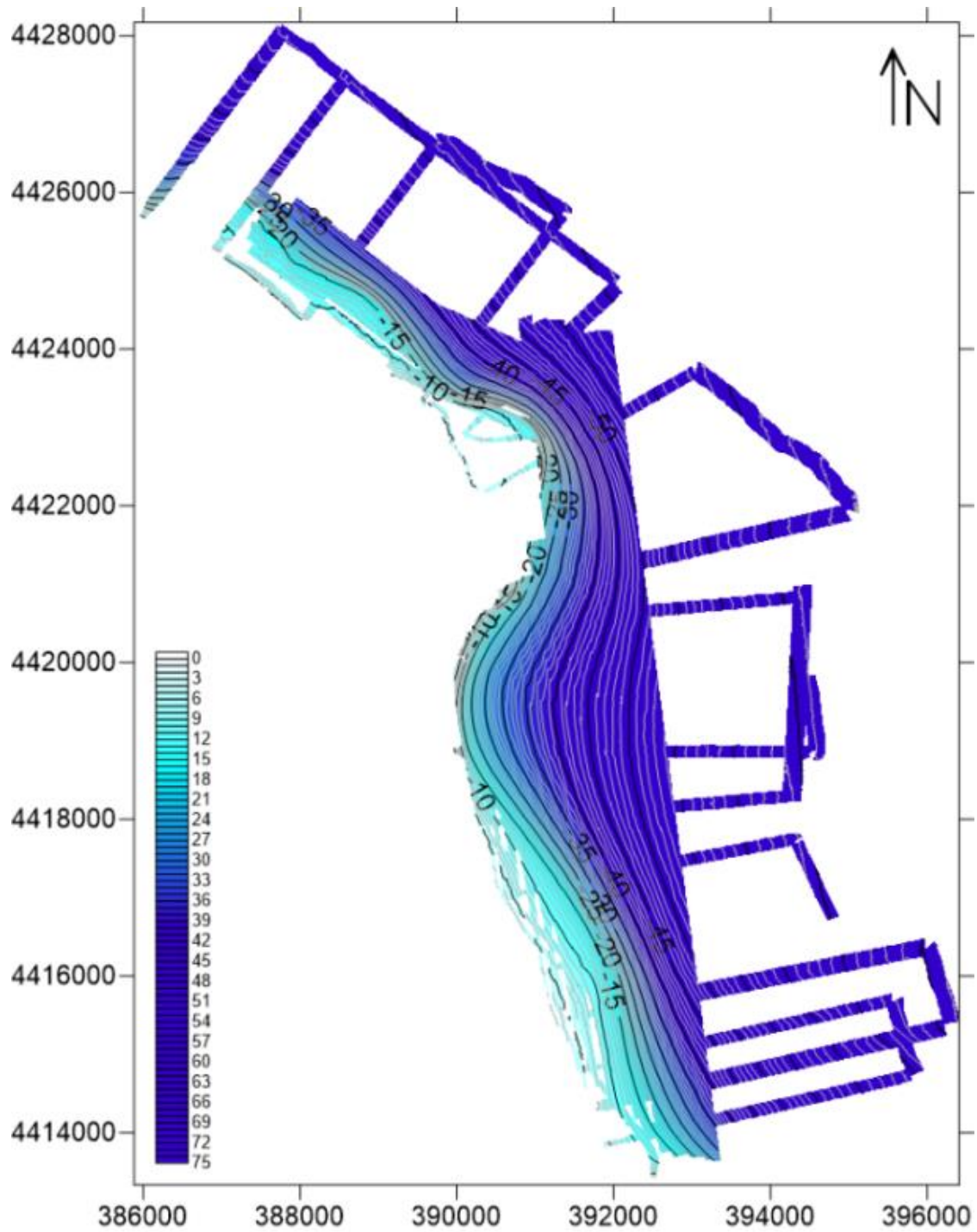


Figure 4.3.5: Isobaths from the bathymetric survey (Akti Engineering - THALIS- DAPHNE)

4.3.4 MIKE 21 PMS

To simulate the wave propagation from offshore to nearshore conditions the module Parabolic Mild - Slope (PMS) of MIKE 21 by DHI is used. PMS is a linear model describing refraction and diffraction, using a parabolic approximation to the elliptic mild slope equation. The output of the model can be the following: wave height, wave period, mean wave direction, surface elevation and radiation stresses. This module can be applied to any water depth on a gently sloping bathymetry and can be used to determine wave fields in open coastal areas, in coastal areas with structures where reflection and diffraction along the x-direction are negligible, in navigation channels, etc. Additionally, Mike 21 PMS can estimate the wave radiation stresses to simulate the wave-induced currents and subsequently the estimation of coastal sediment transport. It should be noted as PMS is a parabolic approximation; diffraction along the x-direction and backscatter are neglected. This model should not be used in areas where diffraction is the main phenomenon in the area, i.e. studying circulation in harbours. The model incorporates the following phenomena:

- Shoaling
- Refraction
- Diffraction
- Reflection
- Bottom dissipation
- Wave breaking
- Wind generation
- Frequency spreading
- Directional spreading
- Wave - wave interaction
- Wave - current interaction

4.3.4.1 Basic Equations

MIKE 21 PMS is based on a parabolic approximation of the elliptical mild slope equation. It takes in consideration the effects of refraction and shoaling due to changing depths, diffraction at the perpendicular to the dominant wave direction and energy dissipation due to bottom friction and wave breaking. The elliptic mild slope equation as given by (Berkhoff, 1972) is:

$$\nabla(C C_g \nabla \phi) + (k^2 C C_g + i\omega W)\phi = 0 \quad (4.12)$$

with $\nabla = \left(\frac{\partial}{\partial x}, \frac{\partial}{\partial y} \right)$ is the 2D gradient operator, $C(x, y)$ is the phase speed, $C_g(x, y)$ the group velocity, $\phi(x, y)$ the mean free surface velocity potential, related to the velocity potential as $\phi(x, y, z, t) = \frac{g}{\omega} \phi(x, y) \frac{\cosh k(z+d)}{\cosh kd} e^{-i\omega t}$, z the water level elevation measured from mean water level upwards, d the water depth, $k = 2\pi/L$ the wave number, $W = Ediss/E$ the dissipation term, $Ediss$ the mean energy dissipation rate per unit time per unit area, E the mean energy per unit area, $\omega = 2\pi f$ the circular frequency, L the wave length and f frequency. Sea surface elevation can also be written as (Dean and Dalrymple, 1984):

$$\eta = \frac{1}{g} \frac{\partial \phi}{\partial t} \text{ for } z=0 \quad (4.13)$$

and

$$\eta = \phi(x, y) e^{-i(\omega t + \pi/2)} \quad (4.14)$$

Mean free surface potential for plane progressive waves, is written as following:

$$\phi = A^*(x, y) e^{i\psi} \quad (4.15)$$

with

$$\psi = \int^x k \cos \theta dx + \int^y k \sin \theta dy \quad (4.16)$$

and θ is the angle between the direction of wave propagation and the x- axis. If the waves propagate at the x-direction then the phase function ψ is written as:

$$\psi = \int^x k dx \quad (4.17)$$

To obtain the parabolic approximation, a predominant wave direction at the x-axis is assumed and the back scatter is neglected. The simplest form of the parabolic approximation to the elliptic mild slope equation is the following:

$$A_x - i(k - k_o)A + \frac{a}{2C_g} (C_g)_x - \frac{i}{2\omega C_g} (CC_g A_y)_y + \frac{W}{2C_g} A = 0 \quad (4.18)$$

with $A(x, y)$ a slowly varying complex variable. This equation is valid only for waves propagating at the x axis or with a small angle. The wave number k_o is the average wave number at the y-axis. For large angles at the x axis (Kirby, 1986) derived the equation to the following:

$$A_x + i(k_o - \beta_1 k)A + \frac{a}{2C_g} (C_g)_x + \frac{\sigma_1}{\omega C_g} (CC_g A_y)_y + \frac{\sigma_2}{\omega C_g} (CC_g A_y)_{yx} + \frac{W}{2C_g} A = 0 \quad (4.19)$$

In which

$$\sigma_1 = i \left(\beta_2 - \beta_3 \frac{k_o}{k} \right) + \beta_3 \left(\frac{k_x}{k^2} + \frac{(C_g)_x}{2kC_g} \right) \quad (4.20)$$

$$\sigma_2 = -\frac{\beta_3}{k}$$

The coefficients are presented in Table 4.3.1 according to approximation (DHI, 2014).

Table 4.3.1: Coefficients of the mild slope equation (DHI, 2014)

| Approximation | β_1 | β_2 | β_3 |
|---------------|-------------|--------------|--------------|
| Simple | 1 | -0.50 | 0 |
| Padé | 1 | -0.75 | -0.25 |
| 10 ° | 0.999999972 | -0.752858477 | -0.252874920 |
| 20 ° | 0.999998178 | -0.761464683 | -0.261734267 |
| 30 ° | 0.999978391 | -0.775898646 | -0.277321130 |
| 40 ° | 0.999871128 | -0.796244743 | -0.301017258 |
| 50 ° | 0.999465861 | -0.822482968 | -0.335107575 |
| 60 ° | 0.985273164 | -0.854229482 | -0.383283081 |
| 70 ° | 0.994733030 | -0.890064831 | -0.451640568 |
| 80 ° | 0.985273164 | -0.925464479 | -0.550974375 |
| 90 ° | 0.956311082 | -0.943396628 | -0.704401903 |

4.3.4.2 Basic Parameters

Wave dissipation is estimated as follows in the parabolic mild-slope equation:

$$W = W_b + W_f \quad (4.21)$$

with W_b and W_f the dissipations due to breaking and bottom friction respectively.

Wave breaking can be described as the hydrodynamic instability of waves. This instability in offshore conditions is given by the tipping value of steepness (H/L) of the waves, whilst in shallow waters it depends on water depth (H/d). For MIKE 21 PMS, wave breaking depends on the model of Battjes and Janssen (1978), according to which the rate of energy dispersion of waves due to breaking is:

$$\frac{dE}{dt} = -\frac{\alpha}{8\pi} Q_b \omega H_{\max}^2 \quad (4.22)$$

where, $E = H_{rms}^2/8$ total energy, $\omega = \frac{2\pi}{T_m}$ angular frequency, T_m the energy averaged mean wave

period, $\frac{1-Q_b}{\ln(Q_b)} = -\left(\frac{H_{rms}}{H_{\max}}\right)^2$ the amount of breaking waves (of Rayleigh Distribution),

$H_{\max} = \gamma_1 k^{-1} \tanh(\gamma_2 k d / \gamma_1)$, γ_1 a factor controlling the maximum wave steepness before breaking, γ_2 the maximum H/d before breaking and α a constant from which the rate of energy dispersion depends on. For monochromatic waves, $Q_b=0$ for non-breaking waves, $H < H_{\max}$ or $Q_b=1$ for breaking waves $H \geq H_{\max}$. For monochromatic waves, MIKE 21 PMS uses the following equation for bottom dissipation:

$$\frac{dE}{dt} = -\frac{1}{6\pi} \frac{c_{fw}}{g} \left(\frac{\omega H}{\sinh(kd)} \right)^3 \quad (4.23)$$

where, $E = H_{rms}^2/8$, $c_{fw} = f_w/2$ the wave friction coefficient (Jonsson, 1966; Swart, 1974). For the unidirectional random waves (Rayleigh Distributed), (Dingemans, 1983) extended the equation to:

$$E_{diss} = \frac{-1}{8\sqrt{\pi}} \frac{c_{fw}}{g} \left(\frac{\omega H_{rms}}{\sinh kd} \right)^3 \quad (4.24)$$

Finally, wave energy dissipation to bottom friction is calculated as $W_f = E_{diss}/E$ depending if the waves are monochromatic or random.

4.3.4.3 Wave Parameters

For the output of the model, the following parameters are estimated:

Spectral significant wave height:

$$H_{m_0} = 4\sqrt{4E_1} \quad (4.25)$$

With total wave energy as: $E_1 = \int_{\theta_{min}}^{\theta_{max}} \int_{f_{min}}^{f_{max}} E(f, \theta) df d\theta$, where $\theta_{max}, \theta_{min}, f_{min}, f_{max}$ the limits of wave direction and of wave frequency in which energy is distributed. *Peak period* T_p is defined as the period where there is the max of the energy spectrum. *Mean wave direction* is estimated as:

$$\theta = \arctan\left(\frac{b}{a}\right) \quad (4.26)$$

With $a = \frac{1}{E_1} \int_0^{2\pi} \cos \theta E(\theta) d\theta$, $b = \frac{1}{E_1} \int_0^{2\pi} \sin \theta E(\theta) d\theta$. Finally, velocity vectors are also estimated as:

$$\begin{aligned} u &= H_{m_0} \cos \theta \\ v &= H_{m_0} \sin \theta \end{aligned} \quad (4.27)$$

4.3.4.4 Model Set-Up

The model requires the grid spacing to be able to represent the bathymetry and the wave field in the x-y dimensions. The grid for the specific application has chosen to be of 3 m spacing so for the area of 3600x7500 m there are 1200x2500 cells. PMS set up guide suggests that the wavelength L should cover 5 to 7 cells at least. In this case, the minimum L used is of approximately 30 m, fulfilling the aforementioned requirement. Furthermore, the grid should be rotated in a way that the waves propagate from the Western - offshore boundary of the grid.

- Basic Parameters

The bathymetry is used as an input here and a mode of 2D (area) is preferred (1D is for profiles). The bathymetric parameters (coordinates and orientation of the grid) are set from the input bathymetry file. When creating the bathymetry file, land is set with a default value of 10, (zero is avoided, especially for cases with tides and surge levels). For this research, the simulation period is chosen as stationary, as specific wave characteristics are examined and not events (quasi-stationary choice).

- Boundary Conditions

At the offshore boundary conditions, the boundary type is set according to the characteristics of the wave state under examination. The types are monochromatic, parameterized random, irregular & unidirectional, regular & directional and finally irregular & directional. In this study, the waves are considered as irregular and directional and the preferred wave states are set by the Generate Wave Energy Spectrum Tool of MIKE 21. Via this tool and the preferred set up a two-dimensional directional frequency spectrum is formed and used as input at the boundary conditions. In this study, the waves are considered as irregular and directional. The lateral boundaries are set to symmetrical, i.e. the gradient of the wave component is zero across the lateral boundaries, assuming the contours are relatively straight and parallel close to the boundary (the other choices are reflecting and absorbing).

- Model Parameters

For the surface elevation, the initial conditions consider the level to be at 0 m. In the case of the climate change, scenarios this changes accordingly (see Chapter Climate Change 4.3.5). There are three different types of the parabolic approximation: simple, Padé's and the minimax with varying aperture (Kirby, 1986; DHI, 2014). The simple model is the parabolic approximation to the elliptic mild slope model, with a requirement that there is a very small angle ($<10^\circ$) between the x-direction and the direction of the waves. The Padé's model allows wider angles $\pm 45^\circ$ (Kirby, 1986) and the minimax tries to minimize the error in the approximation for a given aperture width, i.e. for 60° , the model tries to minimise the error for waves coming within 60° to the x-axis. For this research, the Padé's model was selected. The dissipative interface was set as in default as exclude filtering. Bottom dissipation is included, with the coefficient format considered constant with the data selection using the Nikuradse roughness equal to 0.002 m. Finally, wave breaking is also included and set at the default values (constant) with $\gamma_1 = 1.0$, $\gamma_2 = 0.8$ and $\alpha = 1.0$.

- Output

The basic results of MIKE 21 PMS, are 2D arrays that include the following wave parameters: significant wave height H_{m_0} , peak wave period T_p , the mean wave direction θ_m and the vector components as in equation(4.27). The output area is defined according to the area under examination. To examine the wave height according to specific perpendicular to the beach profiles, the relevant 1D profile extraction tool of MIKE Zero is used. The latter is also used to see the bathymetry at the chosen profiles.

4.3.5 Scenarios

For the case of the module of PMS, runs for the mean condition and the 2% of the wave height are used and therefore presented per direction along with the results of the runs. Furthermore, for every run, sea level is also altered according to the worst scenario RCP 8.5 that changes for the period of 2046 – 2050 and 2081 – 2100. It should be noted that for all scenarios, the coastline is assumed stable. Therefore, for the directions of NE, E and SE the scenarios are:

1. Mean wave state condition
2. The average of the maximum 2% of wave conditions
3. The average of the maximum 2% of wave conditions with a sea level rise of 0.3 m as given by RCP 8.5 for the period 2046-2065
4. The average of the maximum 2% of wave conditions with a sea level rise of 0.63 m as given by RCP 8.5 for the period 2081-2100

In addition, for every perpendicular profile (A and B), plots of the wave height profiles are given according to the scenario along with the bottom bathymetry. The wave heights of the scenarios 1 and 2 at the breaking zone are compared to the results of the empirical equations as these are given in (CERC, 1984).

Chapter 5 - Results

5 Results

This chapter includes the results of the analyses that have been performed according the methodology presented in Chapter 4. Moreover, **SC5.1** is consisted of subchapters with results for each POSEIDON buoy with the sub-sections discretized according to: wave characteristics as given by the buoy's records, sea surface elevation records after data analysis, characteristics of the atmospheric parameters and a correlated analysis of wave and atmospheric data. In addition, **SC5.2** is divided in two main subchapters, the first with the correlation of buoys and ERA-Interim Reanalysis and the second with long-term analysis of 5 points considered representatives of the Greek Seas Finally, **SC5.3** presents the wave and wind state of Pinios area according to ERA-Interim and the results of the MIKE PMS analysis. An outline of the structure of **SC5.1** is given below:

| | | |
|--------|-------------------------|-----|
| 5.1 | POSEIDON Buoys..... | 102 |
| 5.1.1 | ATHOS..... | 102 |
| 5.1.2 | AVGO..... | 112 |
| 5.1.3 | DIA..... | 118 |
| 5.1.4 | E1M3A..... | 121 |
| 5.1.5 | KALAMATA..... | 127 |
| 5.1.6 | KATERINI..... | 137 |
| 5.1.7 | LESVOS..... | 144 |
| 5.1.8 | MYKONOS..... | 151 |
| 5.1.9 | PETROKARAVO..... | 160 |
| 5.1.10 | PYLOS..... | 167 |
| 5.1.11 | SANTORINI..... | 178 |
| 5.1.12 | SKYROS..... | 187 |
| 5.1.13 | ZAKYNTHOS..... | 197 |
| 5.1.14 | Seasonal Synoptics..... | 207 |

5.1 POSEIDON Buoys

5.1.1 ATHOS

The location of Athos buoy, its depth and the recording time periods per dataset are shown in Table 5.1.1.

Table 5.1.1: Location, depth of installation and time periods of recording per database for Athos

| Location | Depth (m) | Wave Characteristics | SSE data | Weather Characteristics |
|------------------------|-----------|-----------------------|---------------------------|-------------------------|
| 24.7226°E 39.9635°N | 220 | 01/01/2000-31/12/2011 | 05/02/2006- 31/12/2010 | 25/05/2000-31/12/2011 |

5.1.1.1 Wave Characteristics

The wave characteristics are presented in this session as estimated by the relevant analysis of data from the buoys for the period 01/01/2000-31/12/2011.

5.1.1.1.1 General Statistics

The statistics of the wave parameters give a general description of the wave state of the area of Athos buoy (Table 5.1.2). The mean significant wave height for Athos is of 0.8 m and the maximum recorded of 5.79 m, whilst the period has a mean of 3.64 s and a maximum of 7.85 s. The swells reach a mean height of 0.05 m, a maximum of 3.36 m and a period of 13.55 s with a maximum of 19.1 s. The wind waves have a mean height of 0.78 m, a maximum of 5.46 m with mean period of 3.63 s and 7.2 s maximum. The maximum wave height has a mean value of 1.48 m, with a maximum recorded value of 8.98 m whilst, the peak period, has a mean value of 4.58 s and a maximum of 16.52 s.

Table 5.1.2: Descriptive Statistics of Wave Parameters for Athos

| Parameters | Number of Records | Mean | Maximum | Std.Dev. |
|-------------------|-------------------|-------|---------|----------|
| H_{m_0} (m) | 28771 | 0.80 | 5.79 | 0.73 |
| $H_{m_{0a}}$ (m) | 27819 | 0.05 | 3.36 | 0.11 |
| $H_{m_{0b}}$ (m) | 26482 | 0.78 | 5.46 | 0.71 |
| H_{max} (m)* | 9451 | 1.48 | 8.98 | 1.09 |
| $T_{m_{02}}$ (s) | 28181 | 3.64 | 7.85 | 0.82 |
| $T_{m_{02a}}$ (s) | 26650 | 13.55 | 19.10 | 1.29 |
| $T_{m_{02b}}$ (s) | 28169 | 3.63 | 7.20 | 0.82 |
| T_p (s) | 27992 | 4.58 | 16.52 | 1.47 |

*The records of H_{max} are fewer as the buoys recorded the sea surface elevation only for the period 2006-2010.

From the wave charts, in Figure 5.1.1, it is shown that the main directions (42.02%) of waves are that of NE (Fetch length of 192 km) and SE to S (Fetch length of 220 km) with 24.73% frequency whilst swells have as primary direction (27.66%) N-NE and secondarily (15.44%) from S. Waves with heights of more than 3 m are from NE (71.83%) while swells with heights of more than 1 m (35.48%) propagate from S. The majority of mean wave periods and swell periods (43.44%, 43.91%) is from NE.

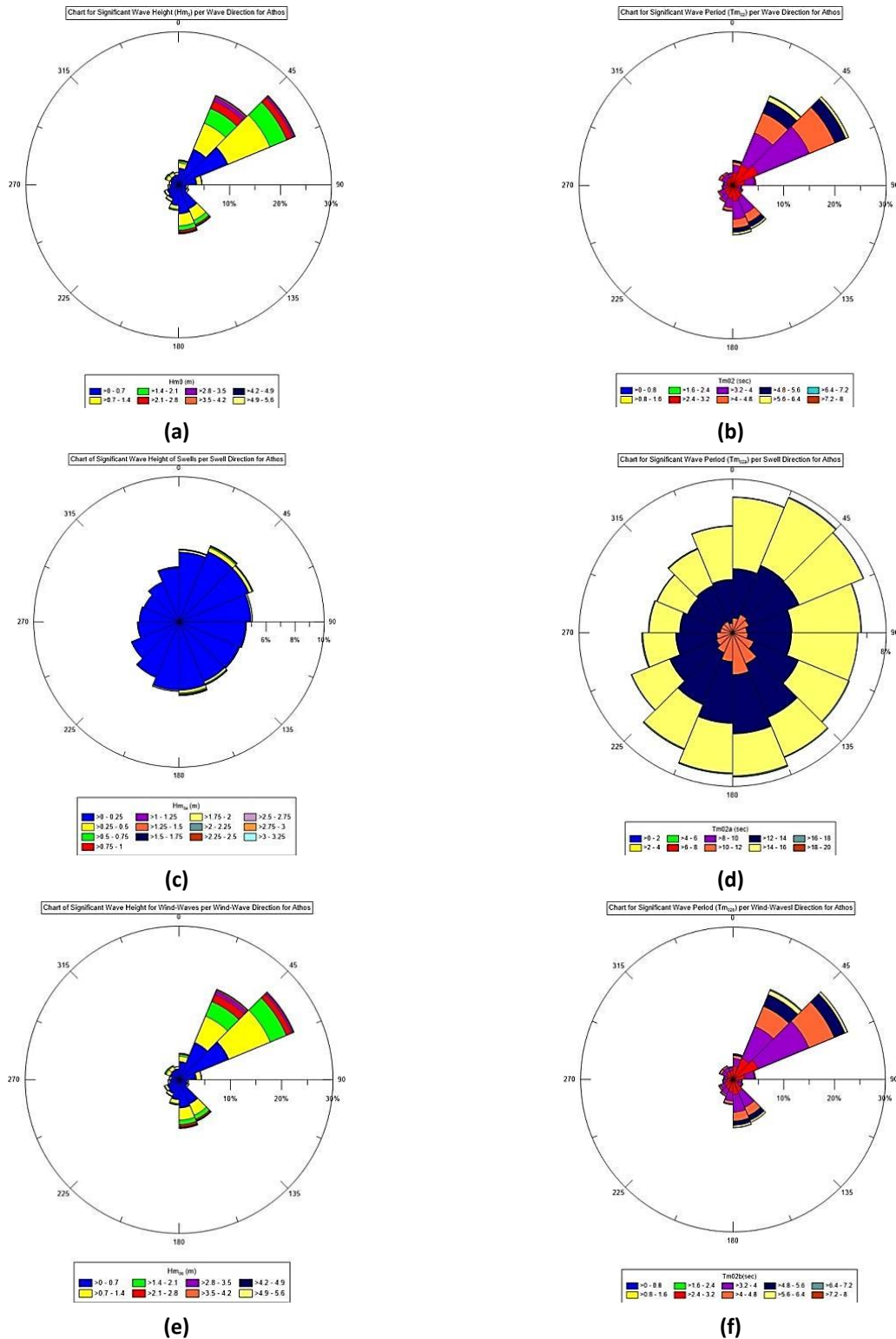


Figure 5.1.1: Rose Diagrams for Significant Wave Height and Wave period for all wave directions (a,b), swells (c,d) and wind waves (e,f) from Athos buoy

In Table 5.1.3, percentages of appearance of significant wave height according to wave period are shown. The highest waves (>3 m) have a frequency of 1.75% with 74.10% of those related with periods of 5 to 6.5 s. The most frequent waves (45.38%) are those with heights from 0 to 0.5 m, with 85.04% associated with periods of 2 to 3.5s.

Table 5.1.3: Pivot Table (%) for Significant Wave Height and Zero-crossing wave period for Athos Buoy

| Hm ₀ (m) | Tm ₀₂ (s) | | | | | Total |
|---------------------|----------------------|--------------|--------------|-------------|-------------|---------------|
| | <2 | 2-3.5 | 3.5-5 | 5-6.5 | 6.5-8 | |
| 0-0.5 | 1.55 | 38.59 | 5.23 | 0.01 | 0 | 45.38 |
| 0.5-1 | 0.91 | 10.29 | 15.46 | 0.05 | 0 | 26.71 |
| 1-1.5 | 0.52 | 0.10 | 12.56 | 0.23 | 0 | 13.42 |
| 1.5-2 | 0.37 | 0 | 5.70 | 0.77 | 0 | 6.83 |
| 2-2.5 | 0.29 | 0 | 1.16 | 2.29 | 0.01 | 3.75 |
| 2.5-3 | 0.14 | 0 | 0 | 1.91 | 0.01 | 2.06 |
| 3-3.5 | 0.05 | 0 | 0 | 0.95 | 0 | 1.00 |
| 3.5-4 | 0.03 | 0 | 0 | 0.34 | 0.06 | 0.43 |
| 4-4.5 | 0 | 0 | 0 | 0.07 | 0.15 | 0.22 |
| 4.5-5 | 0.01 | 0 | 0 | 0 | 0.12 | 0.13 |
| 5-5.5 | 0 | 0 | 0 | 0 | 0.04 | 0.04 |
| 5.5-6 | 0 | 0 | 0 | 0 | 0.02 | 0.02 |
| Total | 3.87 | 48.98 | 40.11 | 6.64 | 0.41 | 100.00 |

5.1.1.1.2 Monthly Means for the period 2000-2011

Wave heights are shown in Figure 5.1.2, where the minimum monthly means occur June (0.49 m), while the maximum monthly mean is in December (1.19 m). Furthermore, the minimum recorded value is in May (0.036 m) and the maximum is in April (5.79 m). For the wave period, the minimum monthly mean is in June (3.29 s) and the maximum monthly mean in December (4.11 s). The minimum recorded value for wave period is in June (2.22 s) and the maximum in December (7.27 s).

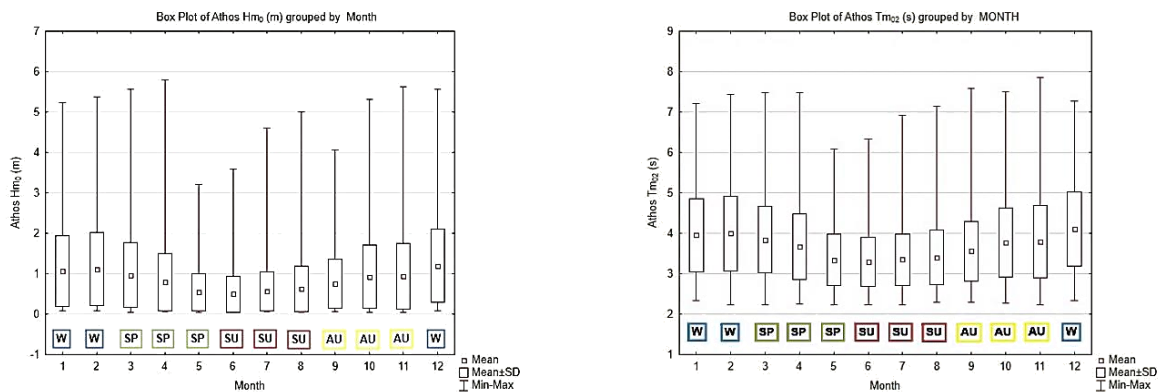


Figure 5.1.2: Box and Whiskers plots for Monthly Wave Height and Wave Period for Athos Buoy

5.1.1.2 Sea Surface Elevation (SSE)

In this section, a variety of results is given from the analysis of 8705 records of sea surface elevation (SSE). A random example of how SSE is plotted along with its spectral definition is shown in Figure 5.1.3. Via the analysis of spectrum and the timeseries, several wave characteristics could be estimated. For example, from this record the peak period of the spectrum (T_p) is around 10.2 s.

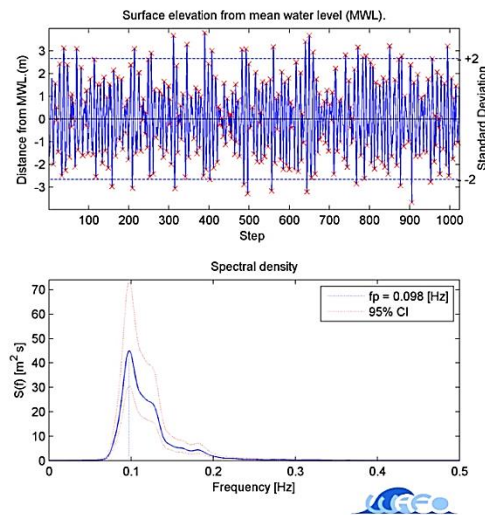


Figure 5.1.3: Random SSE record and its spectral definition for Athos Buoy

5.1.1.2.1 General Statistics

The basic statistics of the statistical and spectral analysis of the records are given in Table 5.1.4. The spectral significant wave height (H_{m0}) has a mean of 1.06 m, a maximum of 5.66 m while the statistical significant wave height ($H_{1/3}$) has a mean of 1.65 m and a maximum of 5.43m. The statistical wave period ($T_{1/3}$) has a mean of 5.43 s and a maximum of 10.61 s while the spectral wave period (T_{m02}) a mean of 3.99 s and a maximum of 7.82 s. Finally, the maximum wave height has a mean of 1.65 m and a maximum of 9.10 m whilst the peak period has a mean of 5.08 s and a maximum of 16.38 s.

Table 5.1.4: Descriptive Statistics as derived from SSE Analysis for Athos Buoy

| Parameters | Number of Records | Mean | Maximum | Std.Dev. |
|---------------|-------------------|------|---------|----------|
| H_{m0} (m) | 8705 | 1.06 | 5.66 | 0.67 |
| Hmax (m) | 8705 | 1.65 | 9.10 | 1.07 |
| $H_{1/3}$ (m) | 8705 | 0.99 | 5.43 | 0.65 |
| T_{m02} (s) | 8705 | 3.99 | 7.82 | 0.76 |
| $T_{1/3}$ (s) | 8705 | 5.43 | 10.61 | 1.03 |
| T_p (s) | 8705 | 5.08 | 16.38 | 1.26 |

In the case of Athos buoy, a correlation coefficient (r) of 0.99 is given for H_{m0} and $H_{1/3}$ and 0.97 for T_{m02} and $T_{1/3}$ (Figure 5.1.4).

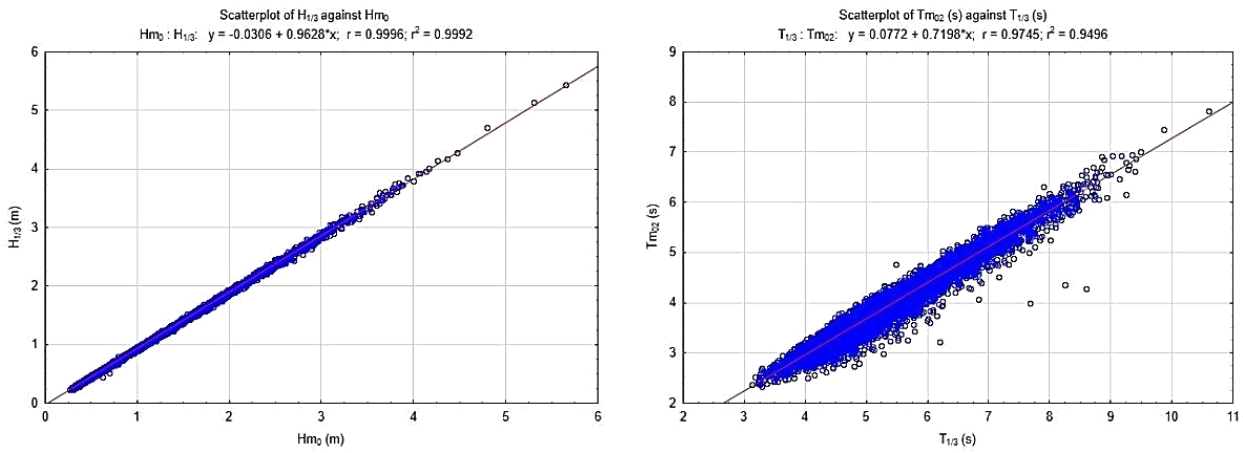


Figure 5.1.4: Scatterplots of statistical and spectral wave parameters for Athos Buoy

5.1.1.2.2 Monthly Means for the period 2006-2010

Box and Whiskers plots are shown for the spectral and wave statistical parameters per month (Figure 5.1.5).

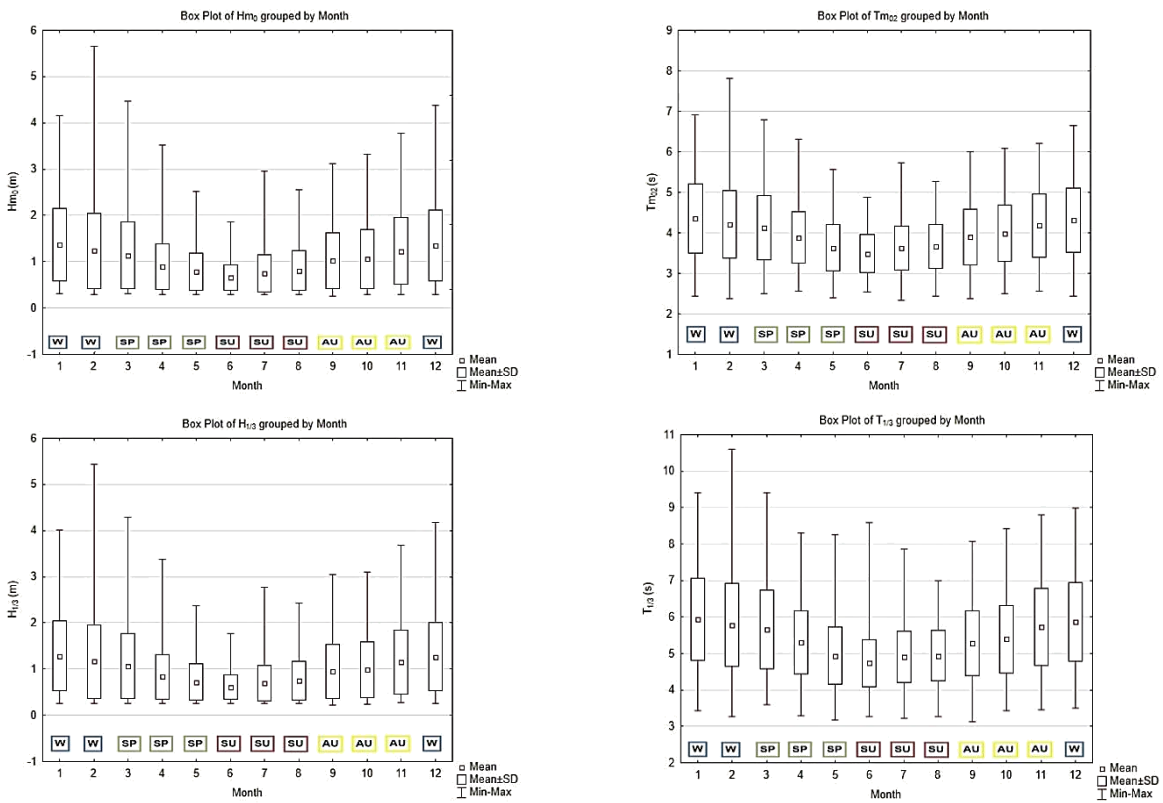


Figure 5.1.5: Spectral and Statistical Monthly Values per Wave Parameter for Athos Buoy

For the case of the spectral significant wave height (H_{m0}), the minimum monthly mean value is in June (0.66 m), the maximum monthly mean value is in January (1.36m), while the minimum recorded value is 0.26 m (September) and the maximum recorded 5.65 m (February). In regards to the spectral wave period (T_{m02}), the mean minimum monthly value is 3.48 s (June) and the maximum 4.35 s (January). The minimum recorded is 2.32 s (July) and the maximum is 7.81 s (February). As for the statistical significant wave height ($H_{1/3}$), the smallest monthly value is 0.61m (June), whilst the largest 1.29m (January). The smallest overall value is 0.23 m (September) and the maximum (5.43 m) in February. Finally, for the statistical significant wave period ($T_{1/3}$) the minimum monthly is 4.73 s in June and the maximum 5.93 s in January. The minimum recorded period is 3.13 s, in September and the maximum of 10.61 s in February.

5.1.1.2.3 Probability Distribution of Wave Height

Probability distributions of Weibull, Rayleigh and Kumaraswamy as well as the relevant QQ plots are shown in Figure 5.1.6. From the QQ plot it can be noted that Kumaraswamy distribution underestimates the larger values of wave heights whilst Weibull and Rayleigh distribution diverge from the mean values.

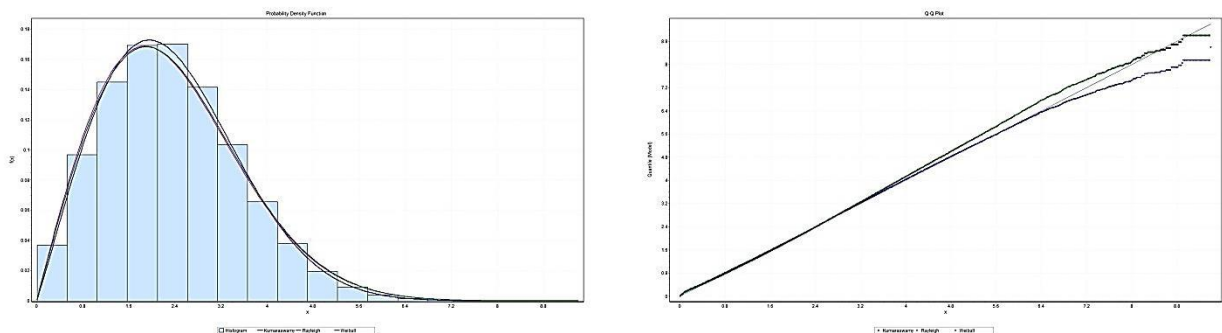


Figure 5.1.6: Probability Distributions and QQ plots for Athos Buoy for random wave heights

The statistics of goodness of fit tests for the distributions of Weibull, Rayleigh and Kumaraswamy are given in Table 5.1.5. For all three tests, the Kumaraswamy distribution represents best wave height.

Table 5.1.5: Statistics of Goodness of Fits according to K-S, A-D and χ^2 test for Athos Buoy

| Distribution | Kolmogorov Smirnov | Anderson Darling | Chi-Squared |
|--------------|--------------------|------------------|-------------|
| | Statistic | Statistic | Statistic |
| Kumaraswamy | 0.008 | 31.034 | 204.17 |
| Weibull | 0.015 | 179.05 | 1202.6 |
| Rayleigh | 0.019 | 228.43 | 1352.8 |

5.1.1.2.4 Ratios between Statistical and Spectral Parameters

The mean values of the ratios among spectral and statistical parameters for Athos are given in Table 5.1.6. A mean of 1.08 is given for the spectral and statistical wave height, 3.7 for the ratio of $H_{1/3} / \sqrt{m_0}$, 1.57 for the ratio of H_{max} / H_{m_0} and 1.7 the ratio of $H_{max} / H_{1/3}$.

Table 5.1.6: Statistics of various Ratios for Athos Buoy

| | Number of Records | Mean | Minimum | Maximum | Std.Dev. |
|------------------------|-------------------|------|---------|---------|----------|
| $H_{m_0} / H_{1/3}$ | 8705 | 1.08 | 0.99 | 1.34 | 0.03 |
| $H_{1/3} / \sqrt{m_0}$ | 8705 | 3.70 | 2.98 | 4.04 | 0.11 |
| H_{max} / H_{m_0} | 8705 | 1.57 | 1.22 | 2.44 | 0.15 |
| $H_{max} / H_{1/3}$ | 8705 | 1.70 | 1.29 | 2.72 | 0.17 |

5.1.1.3 Weather Characteristics

In this session, the atmospheric characteristics of the broader area of Athos buoy are presented in the form of statistics, wind charts, monthly values, monthly values per separate years and annual values.

5.1.1.3.1 General Statistics

The main statistics of atmospheric parameters for the Athos buoy are presented in Table 5.1.7. Minimum temperature can reach 0.0069 °C and the maximum 31.93 °C while the mean is 17.57 °C. Wind speed can be up to 21.96 m/s, while the mean is 4.96 m/s. Wind gust has a mean of 6.68 m/s and a maximum of 29.81 m/s. Finally, air pressure can be as low as 983.53 hPa, as high as 1037.96 hPa and is characterized by a mean of 1015.49 hPa.

Table 5.1.7: Descriptive Statistics of Atmospheric Parameters for Athos Buoy

| Parameters | Number of Records | Mean | Minimum | Maximum | Std.Dev. |
|---------------------|-------------------|---------|---------|---------|----------|
| Air Pressure(hPa) | 29734 | 1015.49 | 983.58 | 1037.96 | 6.61 |
| Air Temperature(°C) | 29468 | 17.57 | 0.0069 | 31.93 | 6.1 |
| Wind Gust (m/s) | 26711 | 6.68 | 0.028 | 29.81 | 4.39 |
| Wind Speed (m/s) | 26326 | 4.96 | 0 | 21.96 | 3.39 |

As given in wind chart of Figure 5.1.7, the main wind directions are in the range of N to NE (48.47%) and the secondary direction is from W to NW (15.25%). The most frequent winds range from 2.5 m/s to 5 m/s (31.85%) and from those 47.46% are of N to NE direction. Winds above 15 m/s are of 0.9% frequency and 62.45% is of NE directions.

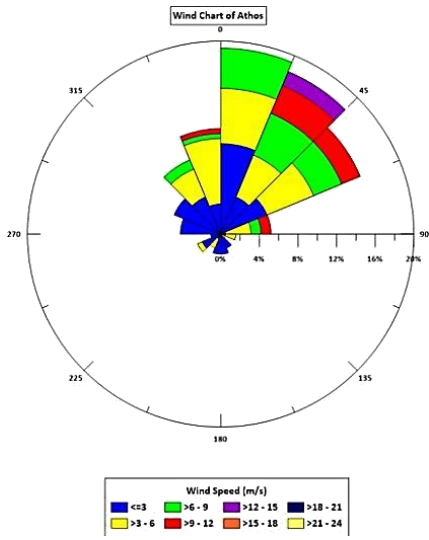


Figure 5.1.7: Wind Chart for Athos Buoy

5.1.1.3.2 Monthly Means for the period 2000-2011

Box and Whisker Plots of the monthly values for the atmospheric parameters of pressure, temperature, and wind speed and wind gust are shown in Figure 5.1.8.

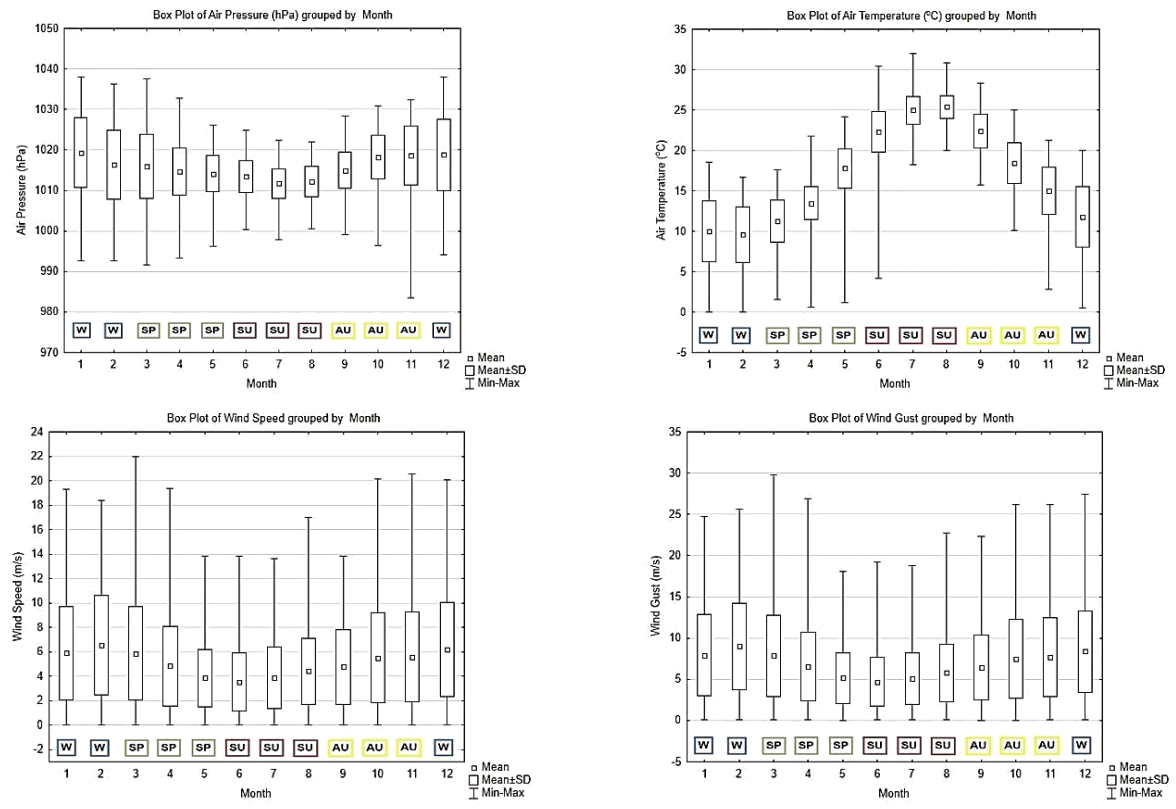


Figure 5.1.8: Monthly Box and Whiskers Plots for Atmospheric Parameters for Athos Buoy

For pressure, the minimum monthly value is in July (1011.7 hPa) and the maximum (1019.34 hPa) in January. For temperature, the minimum mean monthly 9.60 °C in February and the maximum in 25.4 °C during August. Minimum monthly values of wind speed and wind gust are in June (3.53 m/s and 4.69 m/s, respectively) and their maximum in February (6.54 m/s and 9.015 m/s, respectively).

5.1.1.4 Relation of Wind and Wave Data

In this section, an intercomparison of weather and wave parameters is presented, only for the dates that there are data available for the parameters under-consideration.

5.1.1.4.1 General Statistics

As shown in Table 5.1.8, the mean value wind speed (4.98 m/s) can be considered as gentle breeze (according to the Beaufort Scale) that will most likely result in breaking of wave crests with isolated whitecaps.

Table 5.1.8: Descriptive Statistics of Wave and Atmospheric Parameters for Athos Buoy

| Parameters | Number of Records | Mean | Minimum | Maximum | Std.Dev. |
|-----------------------|-------------------|---------|---------|---------|----------|
| Air Pressure (hPa) | 19224 | 1015.09 | 983.58 | 1037.96 | 6.55 |
| Air Temperature (°C) | 19224 | 18.16 | 0.01 | 30.40 | 6.07 |
| Wind Gust (m/s) | 19224 | 6.73 | 0.03 | 29.81 | 4.27 |
| Wind Speed (m/s) | 19224 | 4.96 | 0.00 | 21.00 | 3.31 |
| H _{m0} (m) | 19224 | 0.82 | 0.04 | 5.56 | 0.69 |
| H _{m0a} (m) | 19224 | 0.05 | 0.00 | 3.20 | 0.09 |
| H _{m0b} (m) | 19224 | 0.82 | 0.04 | 5.30 | 0.69 |
| H _{max} (m) | 6833 | 1.45 | 0.31 | 7.73 | 1.06 |
| T _{m02} (s) | 19224 | 3.65 | 2.23 | 7.50 | 0.79 |
| T _{m02a} (s) | 19224 | 13.64 | 10.27 | 18.87 | 1.25 |
| T _{m02b} (s) | 19224 | 3.64 | 2.23 | 7.19 | 0.79 |
| T _p (s) | 19224 | 4.61 | 1.99 | 16.52 | 1.43 |

Frequencies of wind speed and significant wave height are shown in Table 5.1.9. The most frequent waves of 43.54% have heights of 0-0.5 m and 40.04% are related to wind speeds of 2-4 m/s. Furthermore, the higher waves (>4m) have a frequency of 0.39% with a 22.55% related to wind speeds of more than 16m/s.

Table 5.1.9: Frequency Table (%) of Wind Speed and Significant Spectral Wave Height for Athos Buoy

| Wind Speed (m/s) | Hm ₀ (m) | | | | | | | | | | | | Total |
|------------------|---------------------|-------|-------|-------|-------|-------|-------|-------|-------|-------|-------|-------|--------|
| | 0-0.5 | 0.5-1 | 1-1.5 | 1.5-2 | 2-2.5 | 2.5-3 | 3-3.5 | 3.5-4 | 4-4.5 | 4.5-5 | 5-5.5 | 5.5-6 | |
| 0-2 | 14.95 | 3.51 | 0.73 | 0.33 | 0.11 | 0.13 | 0.09 | 0.02 | 0 | 0.01 | 0.01 | 0 | 19.91 |
| 2-4 | 17.43 | 6.98 | 1.43 | 0.40 | 0.12 | 0.09 | 0.04 | 0.01 | 0.03 | 0.02 | 0 | 0 | 26.55 |
| 4-6 | 7.85 | 9.32 | 2.88 | 0.64 | 0.15 | 0.10 | 0.03 | 0.01 | 0.02 | 0 | 0 | 0 | 20.99 |
| 6-8 | 2.02 | 5.98 | 4.76 | 1.40 | 0.37 | 0.14 | 0.06 | 0.02 | 0 | 0 | 0 | 0 | 14.76 |
| 8-10 | 0.59 | 1.44 | 3.14 | 2.26 | 0.85 | 0.21 | 0.08 | 0 | 0.01 | 0 | 0 | 0 | 8.60 |
| 10-12 | 0.30 | 0.33 | 0.73 | 1.72 | 1.41 | 0.58 | 0.10 | 0.05 | 0.01 | 0 | 0 | 0 | 5.24 |
| 12-14 | 0.20 | 0.10 | 0.13 | 0.25 | 0.74 | 0.67 | 0.24 | 0.09 | 0.04 | 0 | 0 | 0 | 2.46 |
| 14-16 | 0.12 | 0.06 | 0.03 | 0.04 | 0.09 | 0.20 | 0.33 | 0.15 | 0.06 | 0.04 | 0.01 | 0 | 1.14 |
| 16-18 | 0.06 | 0.01 | 0.01 | 0.01 | 0.01 | 0.02 | 0.04 | 0.05 | 0.04 | 0.03 | 0.01 | 0 | 0.28 |
| 18-20 | 0.01 | 0 | 0 | 0 | 0 | 0 | 0 | 0 | 0 | 0 | 0.01 | 0 | 0.03 |
| 20-22 | 0.01 | 0.01 | 0 | 0 | 0 | 0 | 0 | 0 | 0 | 0 | 0 | 0.01 | 0.03 |
| Total | 43.54 | 27.74 | 13.84 | 7.06 | 3.86 | 2.15 | 1.01 | 0.42 | 0.22 | 0.11 | 0.04 | 0.02 | 100.00 |

As shown in Figure 5.1.9, the highest and the most frequent waves are related to winds blowing from N to NE (70.09%) whilst the second most frequent winds are of NW (17.45%) and the same pattern applies for the most frequent periods as well.

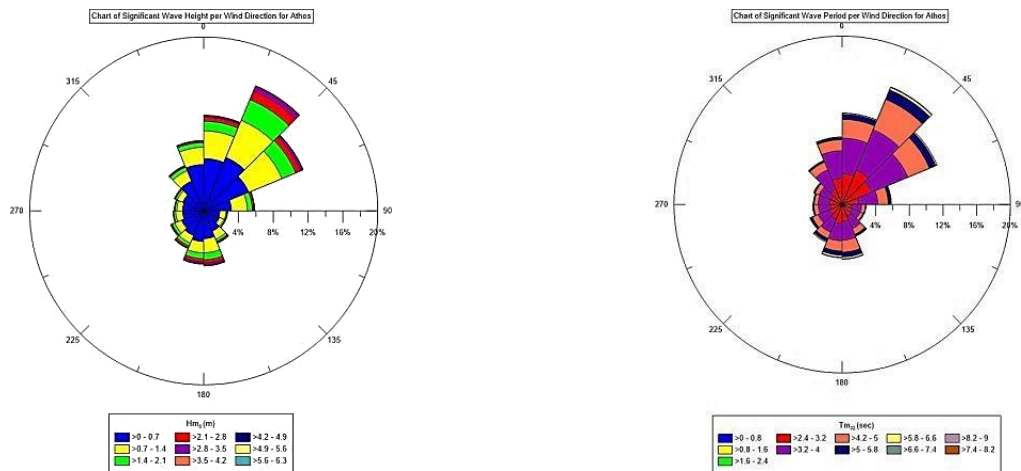


Figure 5.1.9: Charts of Wind Direction and Wave Height - period for Athos Buoy

5.1.2 AVGO

The location, depth of installation and periods of records for Avgo buoy are given in Table 5.1.10.

Table 5.1.10: Location, depth of installation and time periods of recording per database for Avgo Buoy

| Location | Depth (m) | Wave Parameters | SSE data | Atmospheric Parameters |
|---------------------|-----------|-----------------------|----------|------------------------|
| 25.6419°E 35.6216°N | 360 | 01/01/2000-31/12/2006 | -- | 22/05/2000-04/11/2006 |

5.1.2.1 Wave Characteristics

5.1.2.1.1 General Statistics

The descriptive statistics of wave parameters for the Avgo Buoy are shown, in Table 5.1.11. The mean significant wave height is 1 m, the maximum 5.43 m while the mean period is 3.87 s and the max 7.34 s. The height of swells is 0.07 m and the maximum of 2.51 m, whilst their period might reach is 13.48 s and maximum values of 15 s. The height of wind waves has a mean of 0.99 m, max of 5.25 m while the period reaches a mean of 3.86 s and a maximum 7.13 s . Finally, the peak period has a mean of 5.16 s and a maximum of 13.13 s .

Table 5.1.11: Descriptive Statistics of Wave Parameters for Avgo Buoy

| Parameters | Number of Records | Mean | Maximum | Std.Dev. |
|-------------------|-------------------|-------|---------|----------|
| H_{m_0} (m) | 16091 | 1.00 | 5.43 | 0.63 |
| $H_{m_{0a}}$ (m) | 16091 | 0.07 | 2.51 | 0.13 |
| $H_{m_{0b}}$ (m) | 16091 | 0.99 | 5.25 | 0.63 |
| $T_{m_{02}}$ (s) | 16091 | 3.87 | 7.34 | 0.73 |
| $T_{m_{02a}}$ (s) | 16091 | 13.48 | 15.00 | 1.37 |
| $T_{m_{02b}}$ (s) | 16091 | 3.86 | 7.13 | 0.71 |
| T_p (s) | 16091 | 5.16 | 13.13 | 1.45 |

The most frequent direction (84.9%) of incoming waves is from W to N (with a fetch-length of 954 km), whilst for swells (63.34%) is of W to NW (with a fetch- length of 277 km) as it shown in the wave charts of Figure 5.1.10. Waves with heights of more than 3 m have directions from NW to N (83.5%) with a fetch length of 120 km.

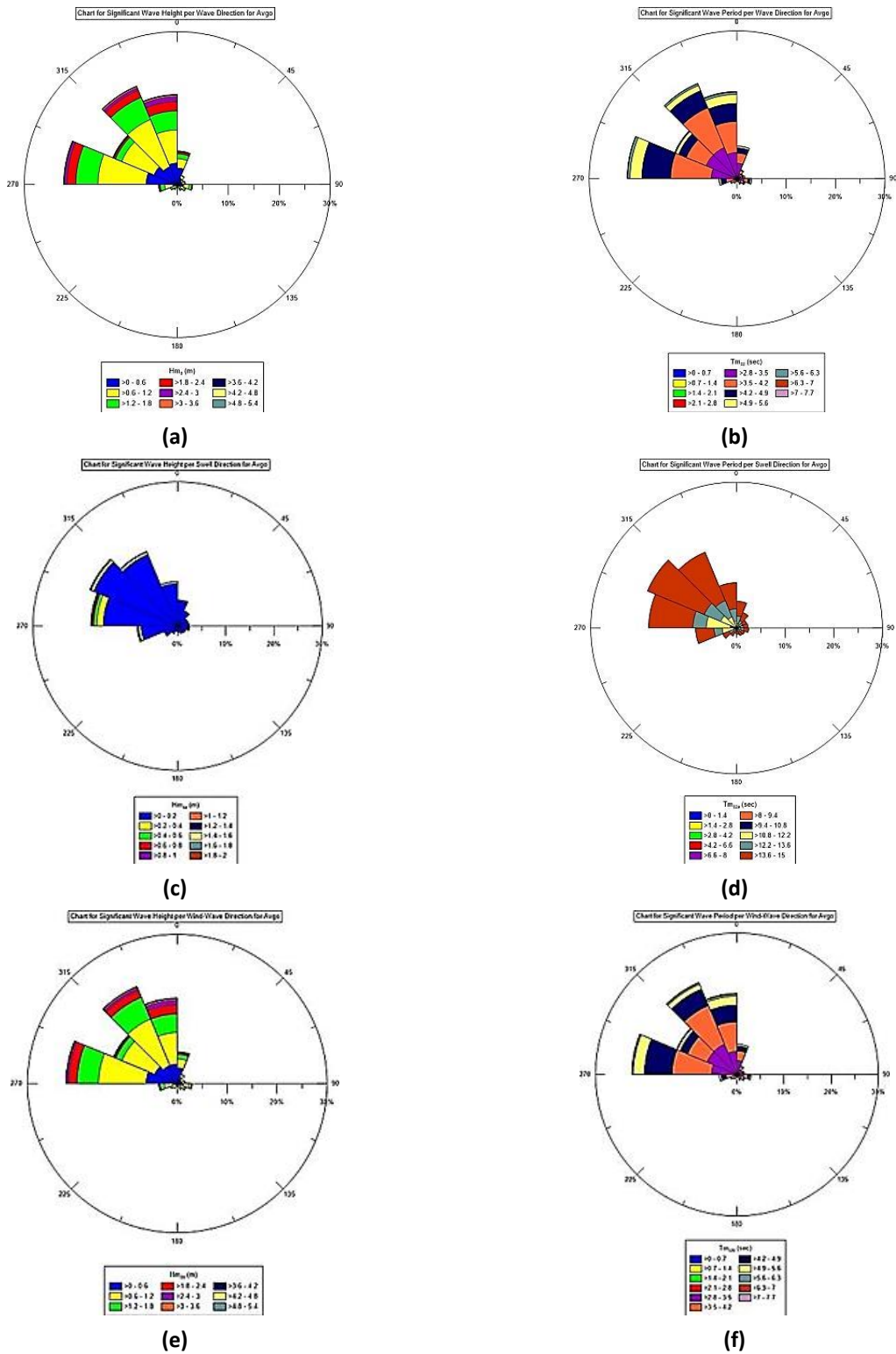


Figure 5.1.10: Rose Diagrams for Significant Wave Height and Wave period for all waves (a,b), swells (c,d) and wind waves (e,f) for Avgo Buoy

The pivot Table 5.1.12, shows that the most frequent waves are those with heights of 0.6-1.2 m (41.78%), with 55.64% of those having periods between 3.5-4.2 s. Waves with heights of >3 m have frequencies of 1.28%, while (70.39%) have periods of 5.6-6.3 s.

Table 5.1.12: Pivot Table for Significant Wave Height and Zero-crossing wave period for Avgo Buoy

| Hm ₀ (m) | Tm ₀₂ (s) | | | | | | | | |
|---------------------|----------------------|---------|---------|---------|---------|---------|-------|-------|--------|
| | 2.1-2.8 | 2.8-3.5 | 3.5-4.2 | 4.2-4.9 | 4.9-5.6 | 5.6-6.3 | 6.3-7 | 7-7.7 | Total |
| 0-0.6 | 3.44 | 18.29 | 6.56 | 1.16 | 0.24 | 0.02 | 0 | 0 | 29.71 |
| 0.6-1.2 | 0.02 | 13.22 | 23.24 | 4.51 | 0.70 | 0.07 | 0.01 | 0.01 | 41.78 |
| 1.2-1.8 | 0 | 0 | 6.29 | 10.65 | 1.21 | 0.12 | 0.01 | 0.01 | 18.28 |
| 1.8-2.4 | 0 | 0 | 0 | 3.20 | 3.13 | 0.16 | 0.01 | 0 | 6.49 |
| 2.4-3 | 0 | 0 | 0 | 0.01 | 1.95 | 0.48 | 0.01 | 0 | 2.45 |
| 3-3.6 | 0 | 0 | 0 | 0 | 0.03 | 0.77 | 0.02 | 0 | 0.83 |
| 3.6-4.2 | 0 | 0 | 0 | 0 | 0 | 0.13 | 0.16 | 0 | 0.29 |
| 4.2-4.8 | 0 | 0 | 0 | 0 | 0 | 0 | 0.08 | 0.02 | 0.11 |
| 4.8-5.4 | 0 | 0 | 0 | 0 | 0 | 0 | 0.02 | 0.03 | 0.05 |
| >6 | 0 | 0 | 0 | 0 | 0 | 0 | 0 | 0.01 | 0.01 |
| Total | 3.46 | 31.51 | 36.10 | 19.53 | 7.26 | 1.75 | 0.32 | 0.08 | 100.00 |

5.1.2.1.2 Monthly Means for the period 2000-2006

The minimum mean monthly value for wave height (0.84 m) is in September, while the maximum (1.19 m) is in February. The minimum recorded value of wave height is 0.08 m, in October and the maximum (5.43 m) in March. For the period, minimum mean monthly value is 3.71 s, in September and the maximum is 4.15 s, in February. The minimum recorded value is 2.32 s, in August and the maximum 7.33 s, in January (Figure 5.1.11).

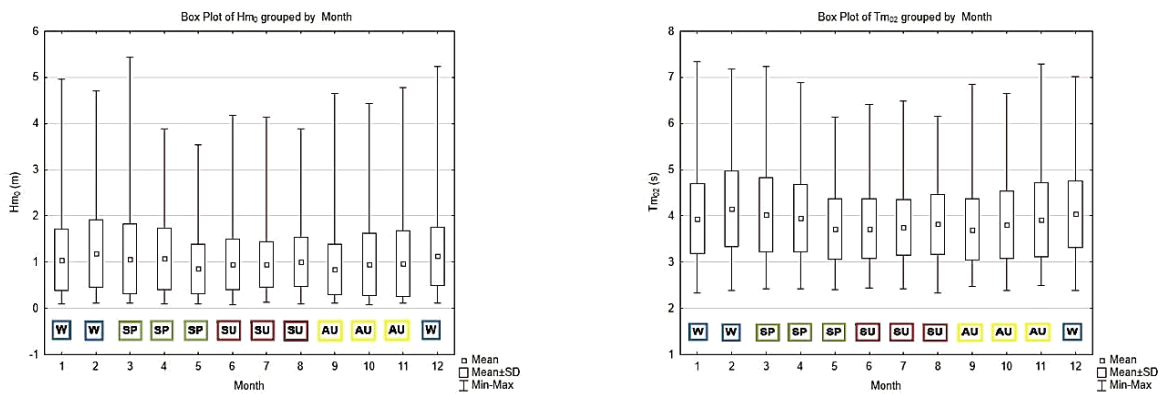


Figure 5.1.11: Box and Whiskers plots for Monthly Wave Height and Wave Period for Avgo Buoy

5.1.2.2 Weather Characteristics

The atmospheric characteristics of the area of Avgo buoy are presented here, in order to be able to discuss the atmospheric state in the form of wind charts and statistics.

5.1.2.2.1 General Statistics

Basic statistical parameters for atmospheric characteristics are given In Table 5.1.13. Minimum temperature reaches almost 1.51 °C and maximum reaches 34.33 °C, while wind speed varies from 0.01 to 19.75 m/s, with a mean of 5.51 m/s. Furthermore, the mean air pressure is of 1014.69 hPa, the minimum of 981.77 hPa and the maximum of 1031.37 hPa. Wind gusts may reach up to 25.63 m/s and have a mean of 7.39 m/s.

Table 5.1.13: Descriptive Statistics of Atmospheric Parameters for Avgo Buoy

| Parameters | Valid N | Mean | Minimum | Maximum | Std.Dev. |
|----------------------|---------|---------|---------|---------|----------|
| Air Pressure (hPa) | 16802 | 1014.69 | 981.77 | 1031.37 | 5.35 |
| Air Temperature (°C) | 14512 | 19.62 | 1.51 | 34.33 | 4.68 |
| Wind Gust (m/s) | 16660 | 7.39 | 0.01 | 25.63 | 4.03 |
| Wind Speed (m/s) | 16653 | 5.51 | 0.01 | 19.75 | 3.19 |

The wind chart in Figure 5.1.12, shows that the dominating winds (53.52%) in the area are blowing from W to NW. The most frequent winds have wind speeds 3-6 m/s (33.22%) with 61.36% of these with directions of W to NW. Wind speeds that are over 14 m/s have frequencies of occurrence of 1.07% with 64.25% of these blowing from NW to N.

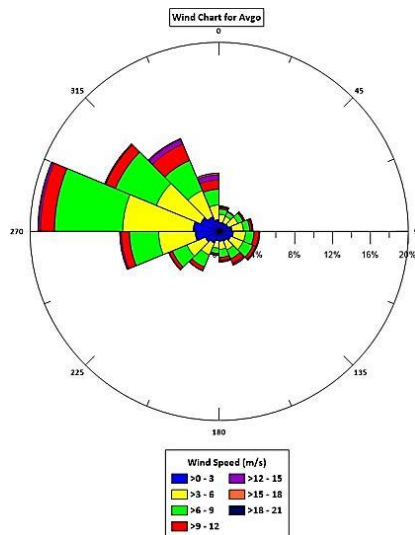


Figure 5.1.12: Wind Chart for Avgo Buoy

5.1.2.2.2 Monthly Means for the period 2000-2006

Minimum monthly mean value of atmospheric pressure occurs in July (1010.28 hPa), with the maximum in November (1017.87 hPa) as shown in Figure 5.1.13.

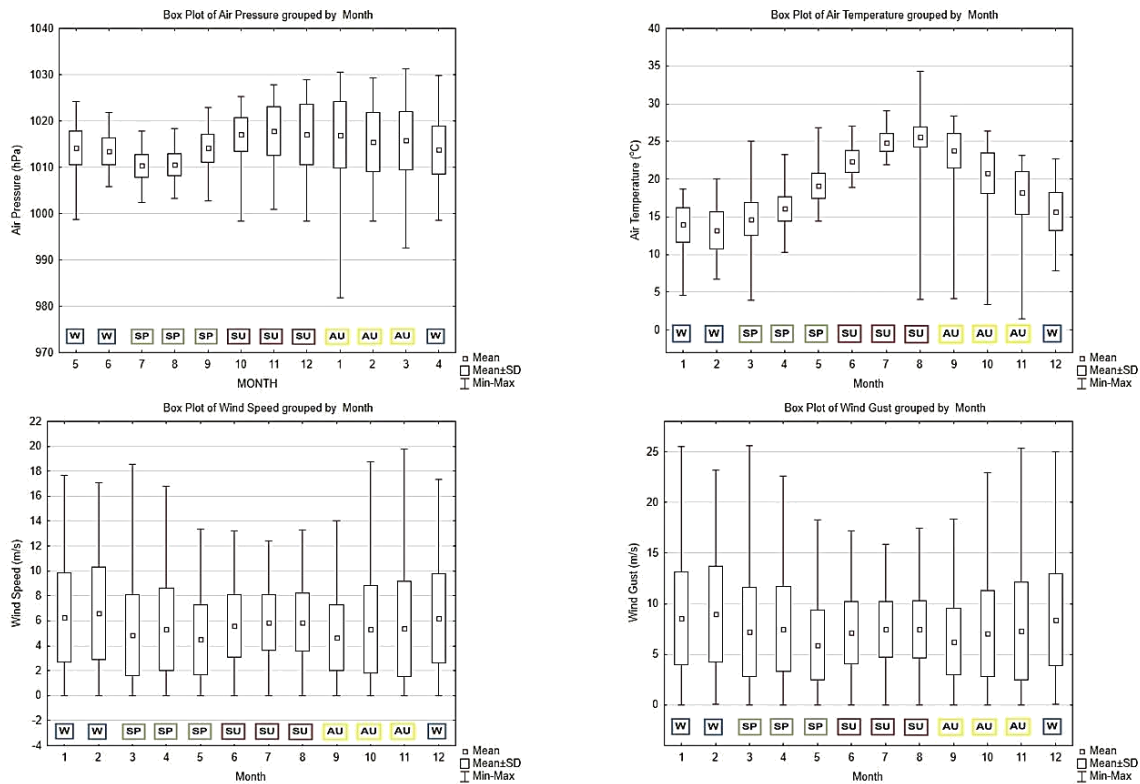


Figure 5.1.13: Monthly Box and Whiskers Plots for Atmospheric Parameters for Avgo Buoy

The temperature minimum monthly mean is observed in February (13.16 °C) while the maximum during August (25.56 °C). As regards to wind speed, minimum monthly mean value is in May (4.50 m/s), maximum in February (6.62 m/s); the same applies for wind gust (5.92 m/s and 8.99 m/s respectively).

5.1.2.3 Relation of Wind and Wave Data

An intercomparison of wind and wave data only for the common dates for the various parameters in wave and atmospheric datasets are considered.

5.1.2.3.1 General Statistics

In Table 5.1.14, the basic statistics of weather and wave parameters for the Avgo buoy are shown. The mean wind speed of 5.52m/s can be considered as moderate breeze that will lead to small and longer waves but with spreaded whitecaps.

Table 5.1.14: Descriptive Statistics of Wave and Atmospheric Parameters for the Avgo Buoy

| Parameters | Number of Records | Mean | Minimum | Maximum | Std.Dev. |
|-----------------------|-------------------|---------|---------|---------|----------|
| Air Pressure (hPa) | 14067 | 1014.37 | 992.52 | 1030.64 | 5.09 |
| Air Temperature (°C) | 14067 | 19.70 | 1.51 | 32.96 | 4.67 |
| Wind Gust (m/s) | 14067 | 7.33 | 0.01 | 25.63 | 3.83 |
| Wind Speed (m/s) | 14067 | 5.52 | 0 | 18.54 | 3.02 |
| Hm ₀ (m) | 14067 | 1.00 | 0.08 | 5.43 | 0.61 |
| Hm _{0a} (m) | 14067 | 0.07 | 0 | 2.16 | 0.12 |
| Hm _{0b} (m) | 14067 | 0.99 | 0.08 | 5.25 | 0.60 |
| Tm ₀₂ (s) | 14067 | 3.86 | 2.32 | 7.29 | 0.71 |
| Tm _{02a} (s) | 14067 | 13.56 | 10.10 | 15.00 | 1.35 |
| Tm _{02b} (s) | 14067 | 3.85 | 2.32 | 7.13 | 0.70 |
| T _p (s) | 14067 | 5.13 | 2.02 | 13.13 | 1.43 |

Wind speeds of 3-6 m/s are the most frequent (33.23%) with a 52.67% of those being related to wave heights of 0.6 to 1.2 m (Table 5.1.15). Additionally, wave heights greater than 4.2 m have a frequency of 0.16% of whom the 38.46% is associated with wind speeds of 15 - 18 m/s.

Table 5.1.15: Frequency Table (%) of Wind Speed and Significant Spectral Wave Height for Avgo

| Wind Speed (m/s) | Hm ₀ (m) | | | | | | | | | | Total |
|------------------|---------------------|---------|---------|---------|-------|-------|---------|---------|---------|-------|--------|
| | 0-0.6 | 0.6-1.2 | 1.2-1.8 | 1.8-2.4 | 2.4-3 | 3-3.6 | 3.6-4.2 | 4.2-4.8 | 4.8-5.4 | 5.4-6 | |
| 0-3 | 16.02 | 6.47 | 0.80 | 0.07 | 0.01 | 0 | 0 | 0 | 0 | 0 | 23.37 |
| 3-6 | 12.07 | 17.50 | 3.24 | 0.38 | 0.03 | 0.01 | 0 | 0 | 0 | 0 | 33.23 |
| 6-9 | 1.15 | 16.60 | 10.04 | 2.28 | 0.28 | 0.01 | 0.01 | 0 | 0.01 | 0 | 30.39 |
| 9-12 | 0.08 | 1.24 | 3.81 | 3.13 | 1.20 | 0.17 | 0.06 | 0.01 | 0.01 | 0.01 | 9.71 |
| 12-15 | 0 | 0.09 | 0.47 | 0.60 | 0.80 | 0.51 | 0.14 | 0.05 | 0.01 | 0 | 2.68 |
| 15-18 | 0 | 0.02 | 0.06 | 0.09 | 0.16 | 0.10 | 0.08 | 0.04 | 0.02 | 0 | 0.57 |
| 18-21 | 0 | 0 | 0.01 | 0 | 0.01 | 0.03 | 0.01 | 0 | 0 | 0 | 0.04 |
| Total | 29.33 | 41.93 | 18.43 | 6.55 | 2.48 | 0.83 | 0.29 | 0.11 | 0.05 | 0.01 | 100.00 |

To give a representation of wind directionality along with wave height and wave period the relevant rose charts have been created (Figure 5.1.14). The most frequent wave heights and wave periods (54.47%) are associated with winds blowing from W to NW. Waves of heights of more than 3m are related to winds from NW to N (77.67%), and the same apply for period.

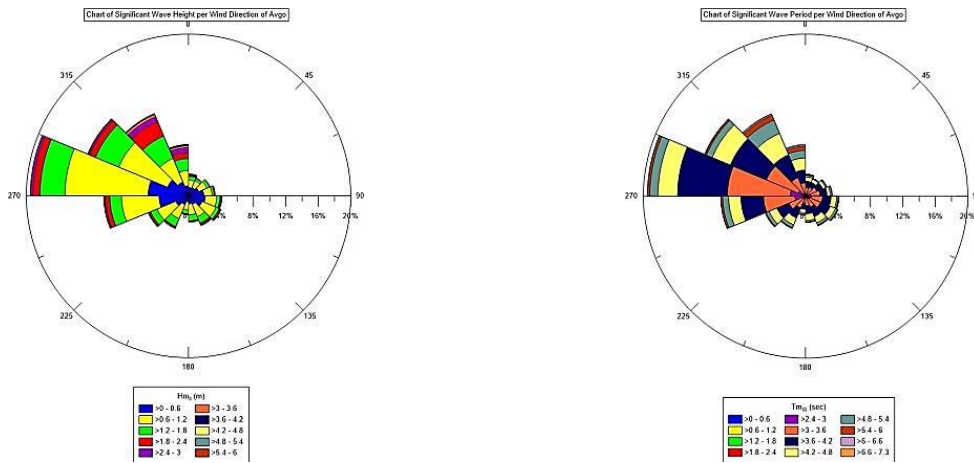


Figure 5.1.14: Charts of Wind Direction and Wave Height - period for the Avgo Buoy

5.1.3 DIA

The location, depth of installation and the recording periods for the DIA buoy are given in Table 5.1.16.

Table 5.1.16: Location, depth of installation and time periods of recording per database for Dia.

| Location | Depth (m) | Wave Parameters | SSE data | Atmospheric Parameters |
|------------------------|-----------|-----------------------|----------|------------------------|
| 25.14939°E, 35.43874°N | 360 | 01/01/2000-31/12/2000 | -- | - |

5.1.3.1 Wave Characteristics

The wave characteristics for the period 01/01/2000-31/12/2000 are presented and commented in this section.

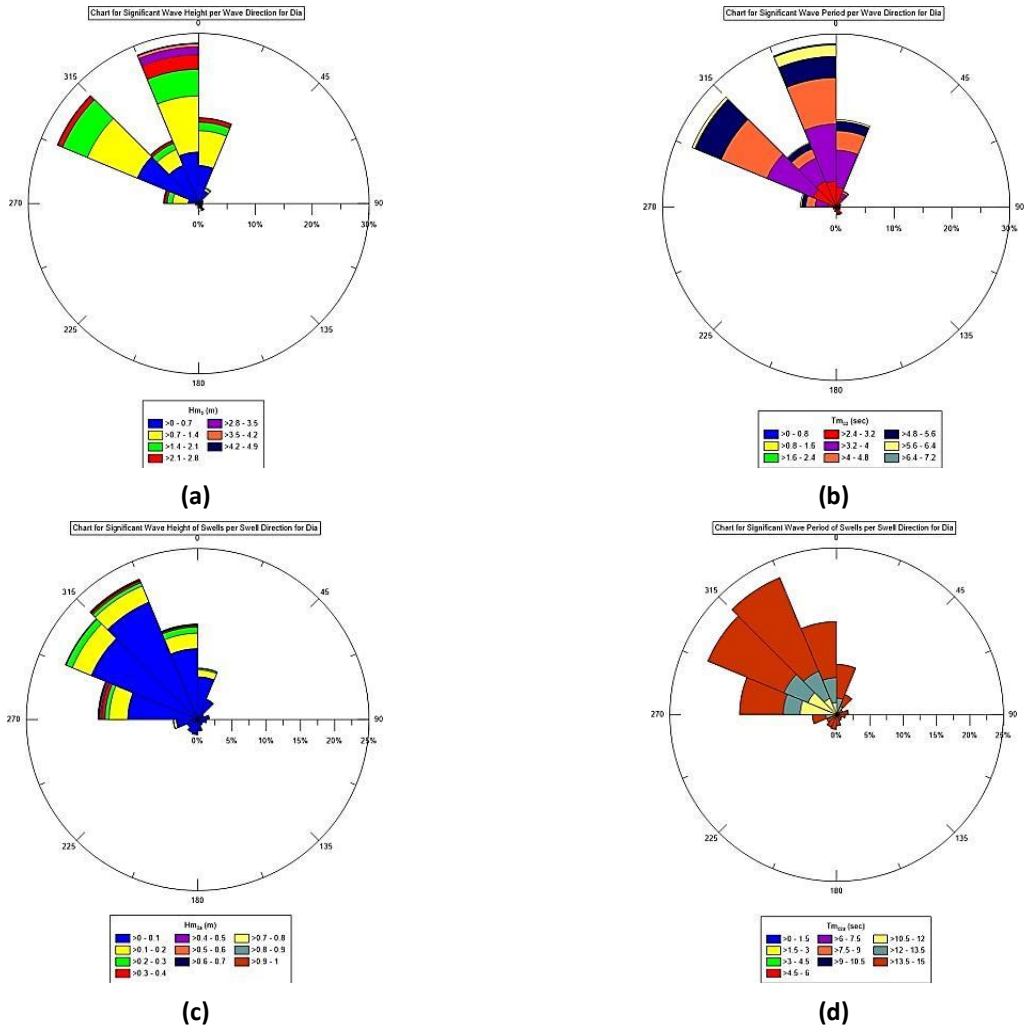
5.1.3.1.1 General Statistics

The descriptive statistics of wave parameters for Dia are given in Table 5.1.17. The mean significant wave height is 0.97 m, the maximum 4.68 m while the period reaches a mean value of 3.87 s, a maximum of 6.81 s. The height of swells has a mean of 0.06 m and a maximum of 0.96 m, while the period of swells is of 13.6 s and a maximum of 15 s. Additionally, the height of wind-waves is of 0.97 m, has a maximum of 4.58 m whilst their period has a mean of 3.86 s and a maximum of 6.72 s. Finally, the peak period has a mean of 5.14 s and a maximum of 10.45 s.

Table 5.1.17: Descriptive Statistics of Wave Parameters for Dia Buoy

| Parameters | Number of Records | Mean | Maximum | Std.Dev. |
|----------------|-------------------|-------|---------|----------|
| Hm_0 (m) | 1336 | 0.97 | 4.68 | 0.71 |
| Hm_{0a} (m) | 1336 | 0.06 | 0.96 | 0.09 |
| Hm_{0b} (m) | 1336 | 0.97 | 4.58 | 0.71 |
| Tm_{02} (s) | 1336 | 3.87 | 6.81 | 0.85 |
| Tm_{02a} (s) | 1336 | 13.60 | 15.00 | 1.32 |
| Tm_{02b} (s) | 1336 | 3.86 | 6.72 | 0.84 |
| T_p (s) | 1336 | 5.14 | 10.45 | 1.59 |

In Figure 5.1.15, charts of wave heights and periods are shown. The waves have as most frequent directions (43.47%) of incoming waves (and wind-waves) of N (with a fetch-length of 150 km) with a secondary direction NW (39.06%), whilst for swells (43.26%) is of NW (with a fetch-length of 290 km). This applies for higher waves and longer periods as well.



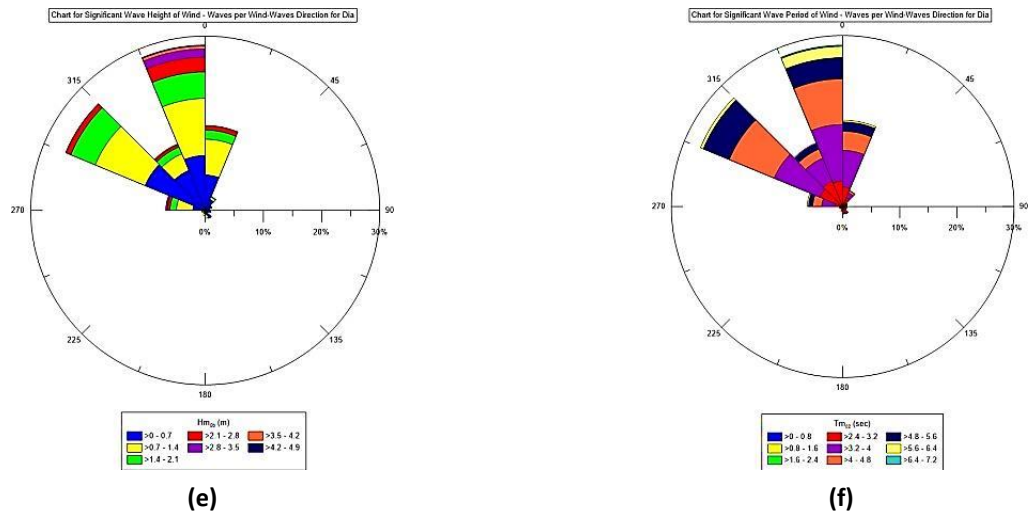


Figure 5.1.15: Rose Diagrams for Significant Wave Height and Wave period for all waves (a,b), swells (c,d) and wind waves (e,f) for Dia Buoy

The most frequent waves have heights from 0.5 to 1m (34.06%) and of those 77.63% has periods 2 – 4 s. Waves higher than 3.5 m have frequencies of 0.9% and of those 91.67% have periods of 6-8 s.

Table 5.1.18 Frequency (%) Table for Significant Wave Height and Zero-crossing wave period for Dia Buoy

| Hm ₀ (m) | Tm ₀₂ (s) | | | Total |
|---------------------|----------------------|--------------|-------------|---------------|
| | 2-4 | 4-6 | 6-8 | |
| 0-0.5 | 29.05 | 0.45 | 0 | 29.50 |
| 0.5-1 | 26.44 | 7.62 | 0 | 34.06 |
| 1-1.5 | 4.93 | 12.32 | 0 | 17.25 |
| 1.5-2 | 0 | 9.86 | 0 | 9.86 |
| 2-2.5 | 0 | 4.93 | 0 | 4.93 |
| 2.5-3 | 0 | 2.32 | 0 | 2.32 |
| 3-3.5 | 0 | 1.05 | 0.15 | 1.19 |
| 3.5-4 | 0 | 0.07 | 0.45 | 0.52 |
| 4-4.5 | 0 | 0 | 0.30 | 0.30 |
| 4.5-5 | 0 | 0 | 0.07 | 0.07 |
| Total | 60.42 | 38.61 | 0.97 | 100.00 |

5.1.3.1.2 Monthly Means for the period 01/01/2000-31/12/2000

In Figure 5.1.16, the variation of monthly values of wave height and period are shown for the year 2000. The minimum mean monthly value for wave height (0.69 m) is in September and the maximum in January (1.18 m). The minimum recorded value of wave height is 0.08 m (in November) and the maximum 4.68 m (in March). As for the period, minimum mean monthly value (3.46 s) occurs in August and the maximum (4.14 s) is in February. The minimum recorded value is 2.37 s (in March) and the maximum 6.8 s in March as well.

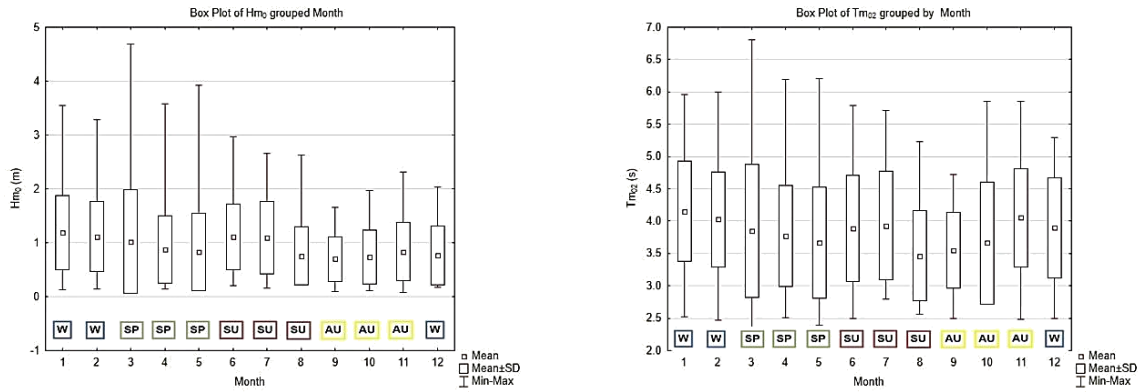


Figure 5.1.16: Box and Whiskers plots for Monthly Wave Height and Wave Period for Dia Buoy

5.1.4 E1M3A

The location, depth and the recording periods of the buoy E1M3A are shown in Table 5.1.19.

Table 5.1.19: Location, depth of installation and time periods of recording per database for E1M3A Buoy

| Location | Depth (m) | Wave Parameters | SSE data | Atmospheric Parameters |
|----------------------|-----------|-----------------------|----------|------------------------|
| 24.9342°E, 35.7910°N | 1440 | 01/01/2007-31/12/2011 | -- | 28/05/2007-03/11/2011 |

5.1.4.1 Wave Characteristics

The wave characteristics described in this section refer to the period of 2007-2011.

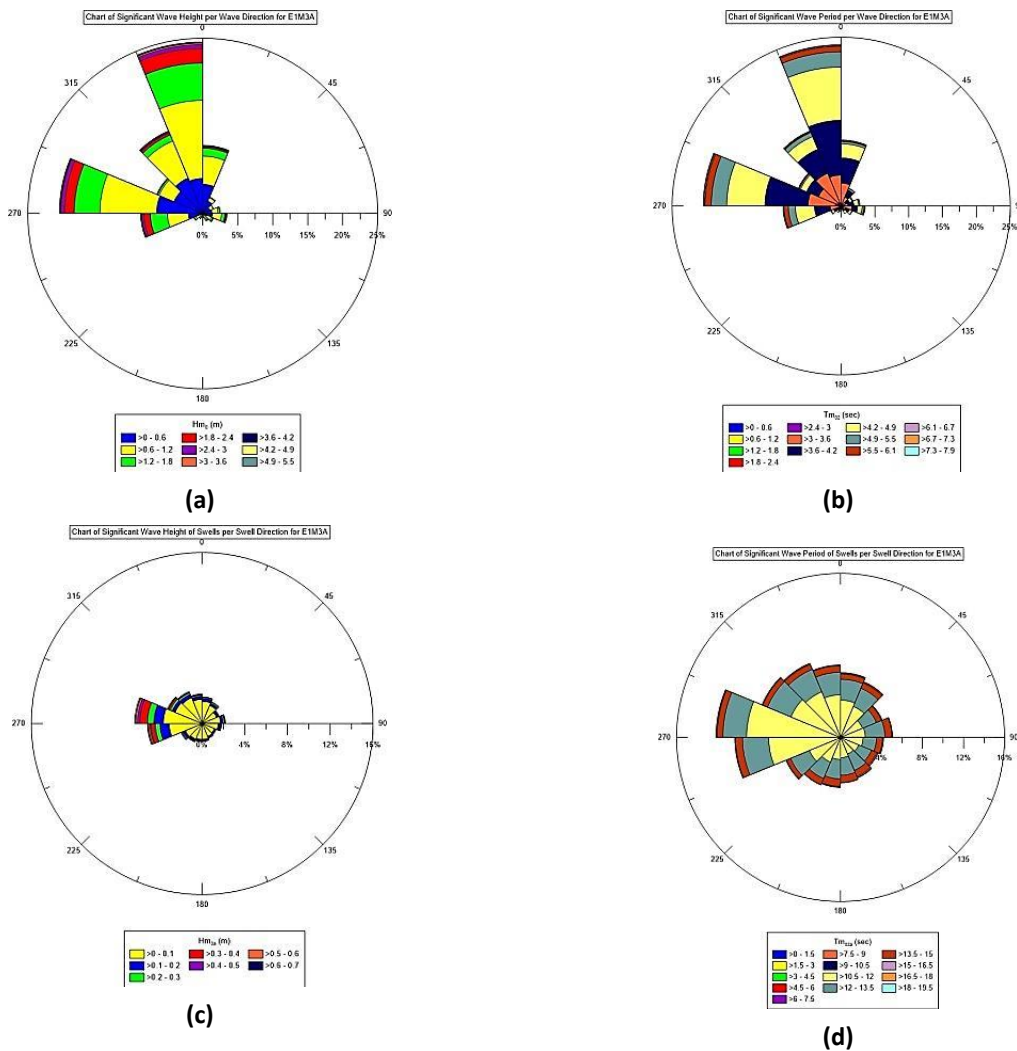
5.1.4.1.1 General Statistics

The basic statistics of wave parameters from the E1M3A Buoy are given in Table 5.1.20. Mean wave height is 0.99 m, maximum is 4.92 m while the mean period is 4.04 s and the maximum is 7.5 s. For the swells, heights have a mean value of 0.07 m, maximum of 2.89 m whilst the mean period has a mean of 12.14 s and a maximum of 18.63 s. Additionally, the wind induced waves have a height of 0.98 m, maximum of 4.84 m, mean period of 4.02 s and maximum of 7.15 s. The maximum wave height can reach up to 8.05 m while the peak period has a mean of 5.23 s and a maximum of 20.86 s.

Table 5.1.20: Descriptive Statistics of Wave Parameters for E1M3A Buoy

| Parameters | Number of Records | Mean | Maximum | Std.Dev. |
|----------------|-------------------|-------|---------|----------|
| Hm_0 (m) | 7319 | 0.99 | 4.92 | 0.61 |
| Hm_{0a} (m) | 7319 | 0.07 | 2.89 | 0.18 |
| Hm_{0b} (m) | 7319 | 0.98 | 4.84 | 0.59 |
| $Hmax$ (m) | 7319 | 1.41 | 8.05 | 0.93 |
| Tm_{02} (s) | 7319 | 4.04 | 7.50 | 0.70 |
| Tm_{02a} (s) | 7319 | 12.14 | 18.63 | 1.13 |
| Tm_{02b} (s) | 7319 | 4.02 | 7.15 | 0.67 |
| T_p (s) | 7319 | 5.23 | 20.86 | 1.53 |

In Figure 5.1.17, rose charts for wave height and period for the E1M3A buoy are presented. The most frequent directions (54.25%) are that of NW to N (Fetch length of 250 km). Waves with heights of more than 3 m have primary directions from N (50% and a fetch length of 150 km) and secondarily from W (35.71% and a fetch length of 135 km). Swells have as predominating direction (22.27%) from W (Fetch length of 135 km).



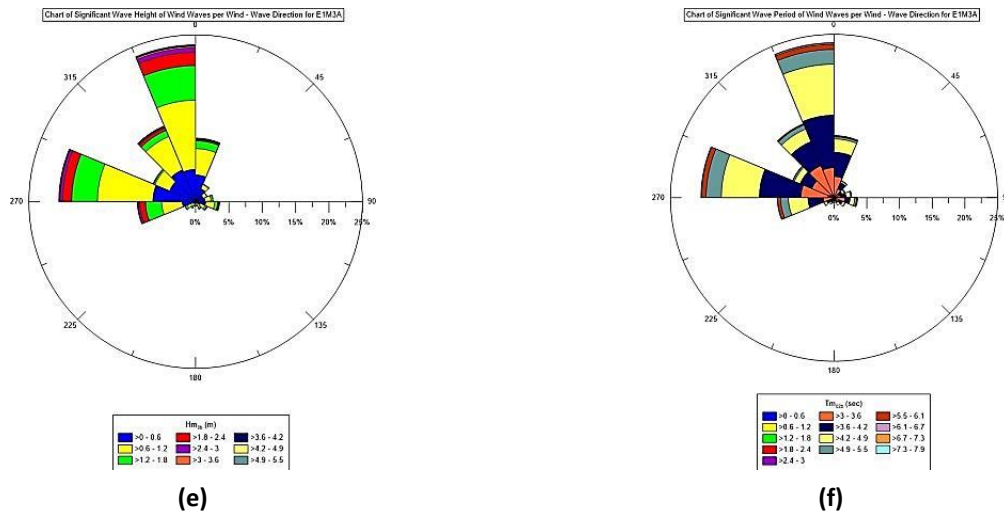


Figure 5.1.17: Rose Diagrams for Significant Wave Height and Wave period for all waves (a,b), swells (c,d) and wind waves (e,f) for E1M3A Buoy

In Table 5.1.21, percentages of appearance of significant wave height relative to wave period are shown. The highest waves (>4.2 m) have a frequency of 0.2% with periods of 6.8 to 8 s. The most frequent waves (40.31%) are those with height from 0.6 to 1.2 m with the majority of them (49.53%) related to periods of 3.8 to 4.4 s.

Table 5.1.21: Pivot Table for Significant Wave Height and Zero-crossing wave period for E1M3A Buoy

| H_{m0} (m) | T_{m02} (s) | | | | | | | | | | | Total |
|-----------------|---------------|-------|---------|---------|---------|-------|-------|---------|---------|---------|-------|--------|
| | <2 | 2-2.6 | 2.6-3.2 | 3.2-3.8 | 3.8-4.4 | 4.4-5 | 5-5.6 | 5.6-6.2 | 6.2-6.8 | 6.8-7.4 | 7.4-8 | |
| 0-0.6 | 0.63 | 0.17 | 11.12 | 18.00 | 4.59 | 0.61 | 0.14 | 0.05 | 0.01 | 0 | 0 | 35.32 |
| 0.6-1.2 | 0.76 | 0 | 0.63 | 15.21 | 19.96 | 3.08 | 0.51 | 0.12 | 0.02 | 0 | 0 | 40.31 |
| 1.2-1.8 | 0.23 | 0 | 0 | 0.01 | 5.17 | 9.18 | 1.13 | 0.26 | 0.01 | 0 | 0 | 15.99 |
| 1.8-2.4 | 0.08 | 0 | 0 | 0 | 0 | 1.80 | 3.08 | 0.47 | 0.05 | 0.01 | 0 | 5.49 |
| 2.4-3 | 0.04 | 0 | 0 | 0 | 0 | 0 | 0.81 | 0.94 | 0.07 | 0.02 | 0 | 1.89 |
| 3-3.6 | 0 | 0 | 0 | 0 | 0 | 0 | 0 | 0.42 | 0.14 | 0.01 | 0 | 0.57 |
| 3.6-4.2 | 0 | 0 | 0 | 0 | 0 | 0 | 0 | 0.01 | 0.18 | 0.02 | 0.01 | 0.23 |
| 4.2-4.8 | 0.01 | 0 | 0 | 0 | 0 | 0 | 0 | 0 | 0.06 | 0.06 | 0.01 | 0.14 |
| 4.8-5.4 | 0 | 0 | 0 | 0 | 0 | 0 | 0 | 0 | 0 | 0.06 | 0 | 0.06 |
| Total | 1.75 | 0.17 | 11.75 | 33.22 | 29.73 | 14.67 | 5.68 | 2.27 | 0.55 | 0.19 | 0.02 | 100.00 |

5.1.4.1.2 Monthly Means for the period 2007-2011

For the wave height, the box plots show that the minimum mean monthly value for the period 2007-2011 is in May (0.7 m) and the maximum is in December (1.16 m). In addition, the smallest recorded wave height (0.078 m) is in May and the maximum (4.92 m) is in January. As for the wave period, the minimum monthly mean (3.75 s) is in June and the maximum mean (4.11 s) is in December. The minimum recorded value for wave period (2.22 s) is in June and the maximum (4.24 s) is in December.

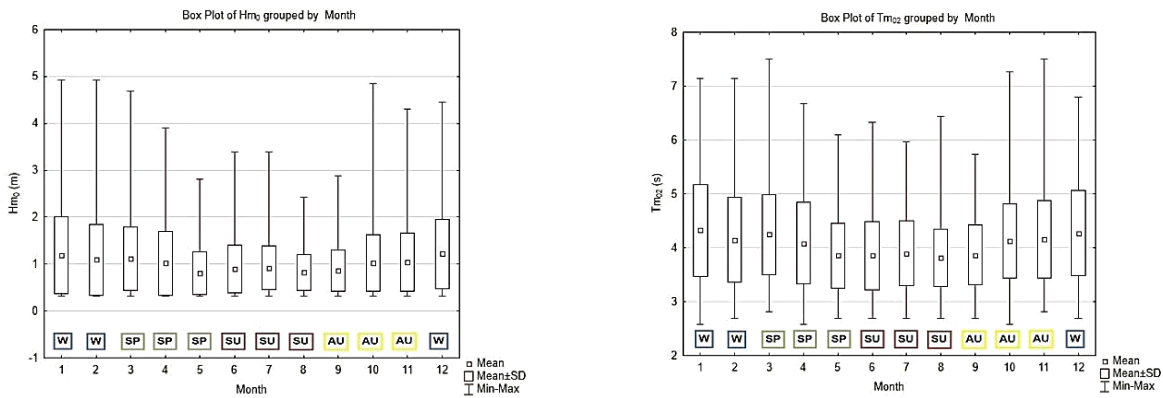


Figure 5.1.18: Box and Whiskers plots for Monthly Wave Height and Wave Period for E1M3A Buoy

5.1.4.2 Weather Characteristics

The atmospheric characteristics of the area of the E1M3A buoy for the period under examination are presented and commented in this section.

5.1.4.2.1 General Statistics

The basic statistics of atmospheric parameters measured at the E1M3A buoy are given in Table 5.1.22. The atmospheric pressure is characterized by a mean value of 1014.46 hPa, a minimum of 994.24 hPa and a maximum of 1033.17 hPa. The air temperature has a minimum of 3.89 °C and a maximum of 29.67 °C while the mean is of 19.73 °C. Wind speed has a mean of 5.31 m/s, a max of 18.75 m/s and wind gust has a mean of 7.14 m/s and a max of 49.81 m/s.

Table 5.1.22: Descriptive Statistics of Atmospheric Parameters for E1M3A Buoy

| Parameters | Number of Records | Mean | Minimum | Maximum | Std.Dev. |
|---------------------|-------------------|---------|---------|---------|----------|
| Air Pressure (hPa) | 9664 | 1014.46 | 994.24 | 1033.17 | 5.49 |
| Air Temperature(°C) | 9663 | 19.73 | 3.89 | 29.67 | 4.7 |
| Wind Speed (m/s) | 9399 | 5.31 | 0.19 | 18.75 | 2.74 |
| Wind Gust (m/s) | 9509 | 7.14 | 0.59 | 49.81 | 3.7 |

The area is dominated by winds blowing from W (28.8%) and NW (21.7%) as shown in Figure 5.1.19. The most common winds have wind speeds of 3-6 m/s (43.26%) and from those 30.05% is of W direction. Winds that have speeds over 15 m/s have a frequency of occurrence of 0.21% with 75% with directions of N.

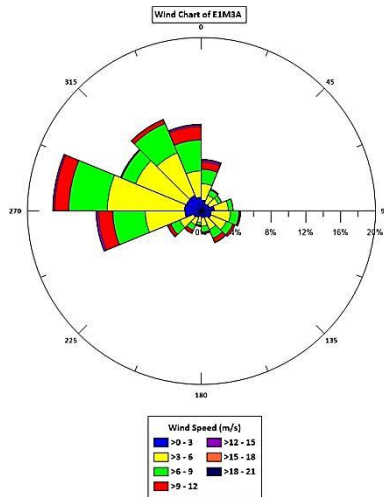


Figure 5.1.19: Wind Chart for E1M3A Buoy

5.1.4.2.2 Monthly Means for the period 2007-2011

For pressure, the minimum monthly mean value of atmospheric pressure (1010.24 hPa) is observed in July and the maximum (1018.7 hPa) in January (Figure 5.1.20). The minimum mean monthly temperature is 13.31 °C in February and the maximum is 25.77 °C in August. Minimum values of wind speed (4.51 m/s) and wind gust (5.74 m/s) are in May and the maximum (6.08 m/s and 8.65 m/s respectively) are in December.

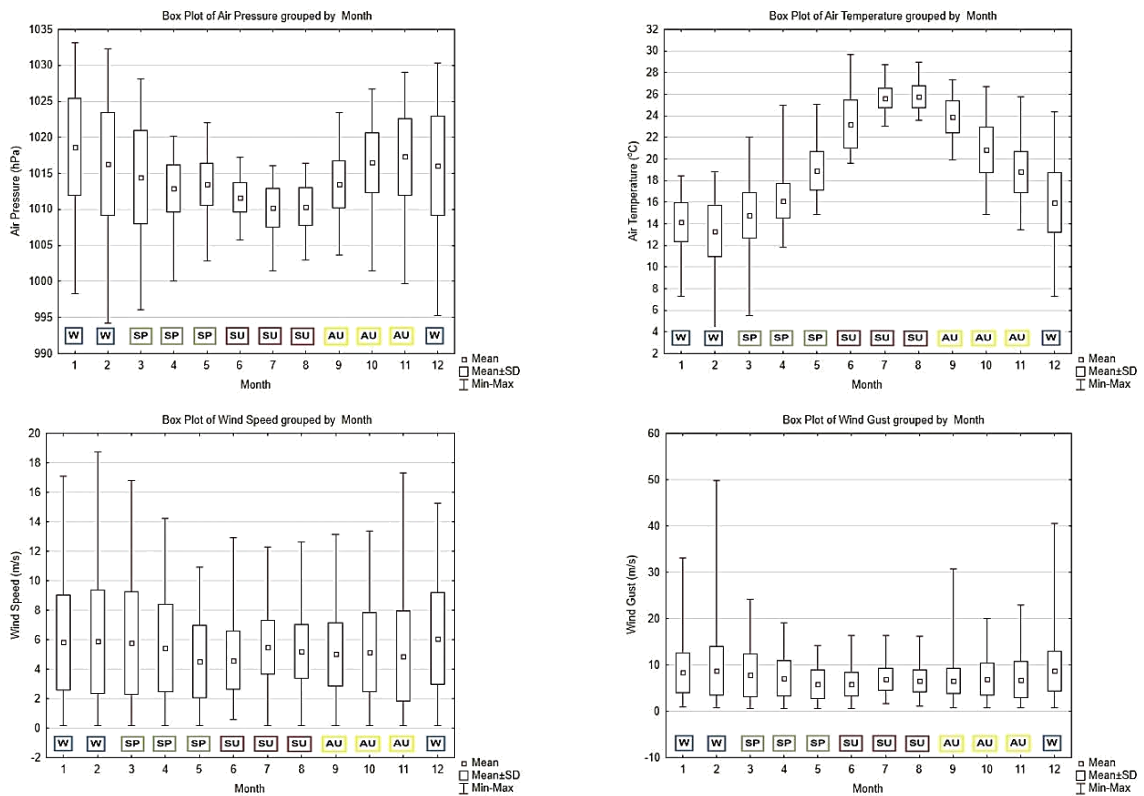


Figure 5.1.20: Monthly Box and Whiskers Plots for Atmospheric Parameters for E1M3A Buoy

5.1.4.3 Relation of Wind and Wave Data

The intercomparison of wind and wave datasets for the periods are there are dates for both is shown in this session.

5.1.4.3.1 General Statistics

In Table 5.1.23 the basic statistics of atmospheric and wave parameters are shown. The mean value wind speed (5.67m/s) can be categorized as moderate breeze that will generate small, longer waves with spreaded whitecaps.

Table 5.1.23: Descriptive Statistics of Wave and Atmospheric Parameters for E1M3A

| Parameters | Number of Records | Mean | Minimum | Maximum | Std.Dev. |
|-----------------------|-------------------|---------|---------|---------|----------|
| Air Pressure (hPa) | 7259 | 1014.12 | 994.24 | 1033.17 | 5.50 |
| Air Temperature (°C) | 7259 | 20.28 | 3.89 | 29.67 | 4.67 |
| Wind Gust (m/s) | 7259 | 7.46 | 0.59 | 49.80 | 3.52 |
| Wind Speed (m/s) | 7259 | 5.67 | 0.20 | 18.75 | 2.67 |
| Hm ₀ (m) | 7259 | 0.99 | 0.31 | 4.92 | 0.61 |
| Hm _{0a} (m) | 7259 | 0.07 | 0.00 | 2.89 | 0.18 |
| Hm _{0b} (m) | 7259 | 0.98 | 0.31 | 4.84 | 0.59 |
| H _{max} (m) | 7259 | 1.41 | 0.31 | 8.05 | 0.94 |
| Tm ₀₂ (s) | 7259 | 4.03 | 2.58 | 7.50 | 0.70 |
| Tm _{02a} (s) | 7259 | 12.14 | 10.20 | 18.63 | 1.13 |
| Tm _{02b} (s) | 7259 | 4.01 | 2.58 | 7.15 | 0.67 |
| T _p (s) | 7259 | 5.22 | 2.34 | 20.86 | 1.52 |

A frequency table of wind speed and significant wave height is shown in

Table 5.1.24. The most frequent waves of 40.57% have heights of 0.6-1.2 m and 52.83% of these are related with wind speeds of 3-6 m/s. Furthermore, the higher waves (>4.2 m) have a frequency of 0.2% with a 52.94% related with speeds of 15-18 m/s wind speeds.

Table 5.1.24: Frequency Table (%) of Wind Speed and Significant Spectral Wave Height for E1M3A

| Wind Speed (m/s) | Hm ₀ (m) | | | | | | | | | |
|------------------|---------------------|--------------|--------------|-------------|-------------|-------------|-------------|-------------|-------------|---------------|
| | 0-0.6 | 0.6-1.2 | 1.2-1.8 | 1.8-2.4 | 2.4-3 | 3-3.6 | 3.6-4.2 | 4.2-4.8 | 4.8-5.4 | Total |
| 0-3 | 14.00 | 5.13 | 0.45 | 0.01 | 0 | 0 | 0 | 0 | 0 | 19.59 |
| 3-6 | 19.46 | 21.43 | 2.81 | 0.18 | 0 | 0 | 0 | 0 | 0 | 43.89 |
| 6-9 | 1.32 | 13.33 | 9.33 | 1.85 | 0.34 | 0.01 | 0.01 | 0 | 0 | 26.19 |
| 9-12 | 0.05 | 0.66 | 3.39 | 3.25 | 1.11 | 0.25 | 0.07 | 0 | 0 | 8.79 |
| 12-15 | 0 | 0.01 | 0.13 | 0.25 | 0.45 | 0.31 | 0.07 | 0.08 | 0 | 1.32 |
| 15-18 | 0 | 0 | 0.01 | 0.01 | 0.01 | 0 | 0.07 | 0.05 | 0.06 | 0.22 |
| 18-21 | 0 | 0 | 0 | 0 | 0 | 0 | 0 | 0.01 | 0 | 0.01 |
| Total | 34.83 | 40.57 | 16.13 | 5.55 | 1.91 | 0.58 | 0.23 | 0.14 | 0.06 | 100.00 |

The charts in Figure 5.1.21, show that the most frequent waves are related with winds blowing from W (30.2%) while 50% of waves with heights more than 3 m are related with winds blowing from N. Frequent periods are related with winds with W directions.

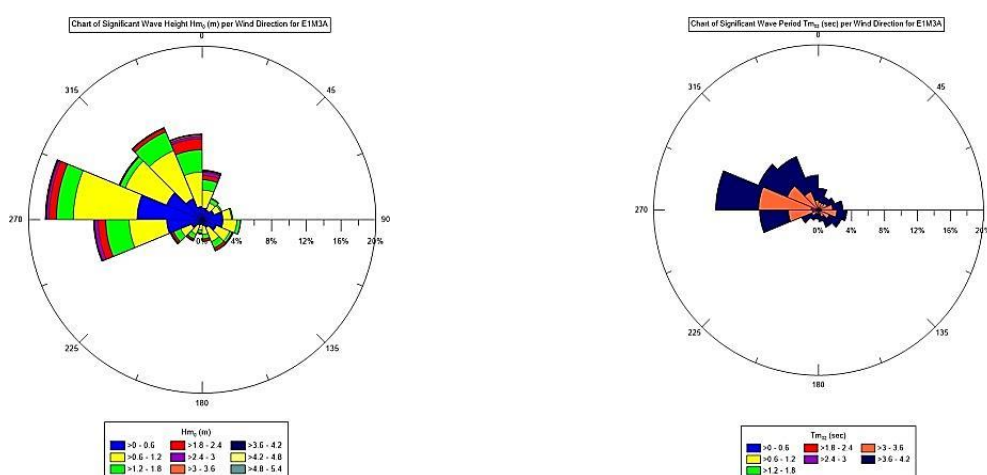


Figure 5.1.21: Charts of Wind Direction and Wave Height - Period for E1M3A Buoy

5.1.5 KALAMATA

The location, depth and time periods for Kalamata buoy are shown in Table 5.1.25.

Table 5.1.25: Location, depth of installation & time periods of recording per database for Kalamata Buoy

| Location | Depth (m) | Wave Parameters | SSE data | Atmospheric Parameters |
|---------------------------|-----------|---------------------------|---------------------------|---------------------------|
| 22.10693°E. 36.97266°N | 340 | 01/01/2007- 31/12/2011 | 15/05/2007- 02/01/2011 | 21/05/2007- 17/05/2011 |

5.1.5.1 Wave Characteristics

Wave characteristics are shown in this session as given by the analysis of the buoy records for the period 01/01/2007-31/12/2011.

5.1.5.1.1 General Statistics

The basic statistics of wave parameters for Kalamata Buoy are shown in Table 5.1.26. Mean significant wave height is 0.34 m while maximum wave height is 3.28 m. The period has a mean of 3.38 s and a maximum of 7.27 s. Swells have a mean height of 0.02 m and a maximum of 1.64 m whilst their period has a mean of 12.35 s and can reach up to 18.75 s. Wind waves have a mean height is of 0.34 m, a max of 2.81 m, mean period of 3.36 s that might reach up to 7.03 s. Finally, max wave height can reach up to 5.08 m while peak period has a mean 4.35 s and a maximum of 13.24s.

Table 5.1.26: Descriptive Statistics of Wave Parameters for Kalamata Buoy

| Parameters | Number of Records | Mean | Maximum | Std.Dev. |
|-------------------|-------------------|-------|---------|----------|
| H_{m_0} (m) | 11061 | 0.34 | 3.28 | 0.28 |
| $H_{m_{0a}}$ (m) | 11574 | 0.02 | 1.64 | 0.07 |
| $H_{m_{0b}}$ (m) | 11574 | 0.34 | 2.81 | 0.28 |
| H_{max} (m) | 11061 | 0.29 | 5.08 | 0.50 |
| $T_{m_{02}}$ (s) | 11579 | 3.38 | 7.27 | 0.92 |
| $T_{m_{02a}}$ (s) | 11430 | 12.35 | 18.75 | 1.13 |
| $T_{m_{02b}}$ (s) | 11574 | 3.36 | 7.03 | 0.91 |
| T_p (s) | 11579 | 4.35 | 13.24 | 2.12 |

The charts in Figure 5.1.22, show that the most frequent waves (77.62%) and swells (48.62%) propagate from S (Fetch can reach up to 550 km). The same pattern applies for wave period as well.

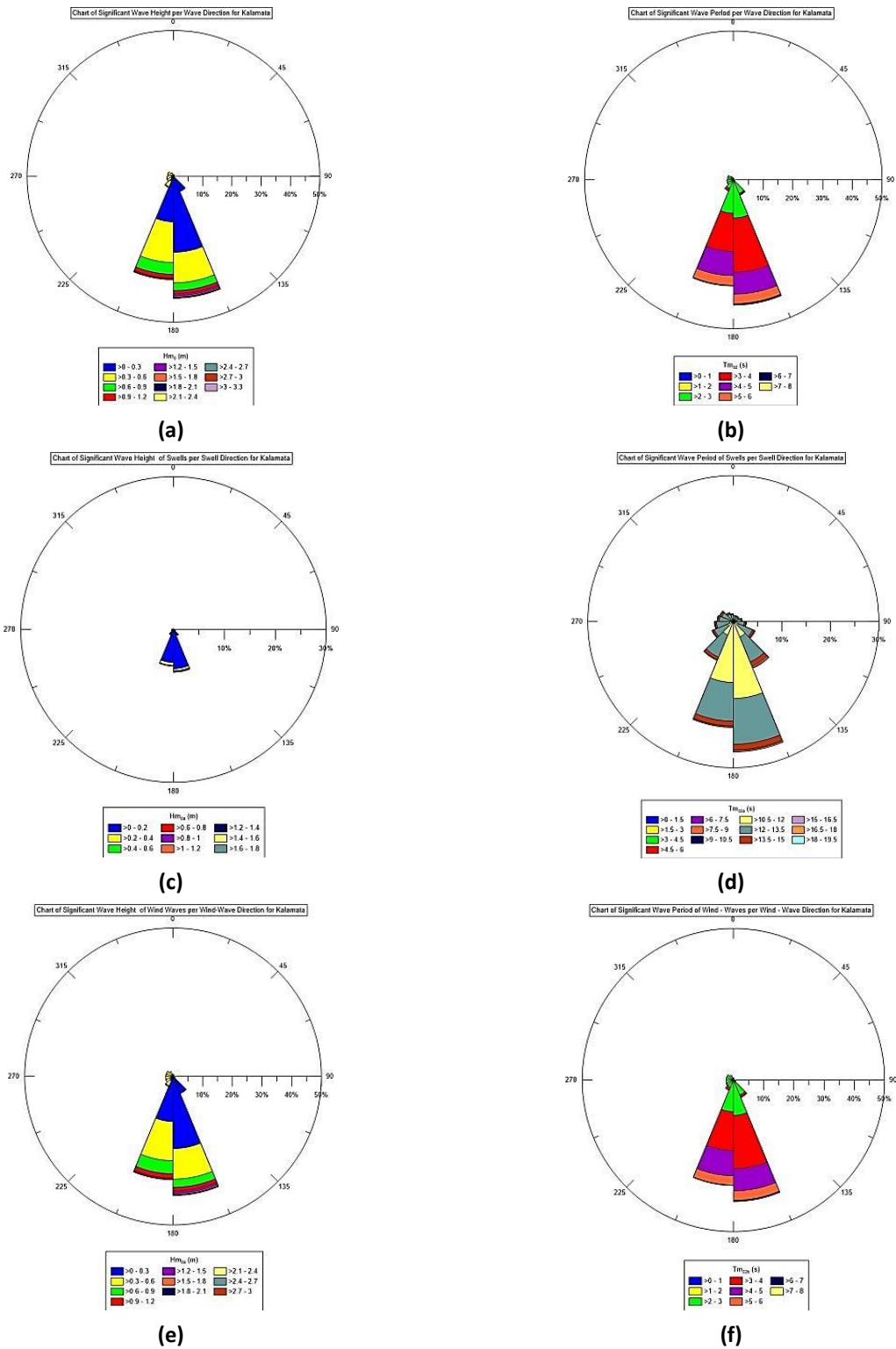


Figure 5.1.22: Rose Diagrams for Significant Wave Height and Wave period for all waves (a,b), swells (c,d) and wind waves (e,f) for Kalamata Buoy

The percentages of appearance of significant wave height according to wave period are shown in the Pivot Table 5.1.27. The highest waves (>3 m) have a frequency of 0.01% with periods of 6 to 7 s. The most frequent waves (96.13%) are those with heights from 0 to 1 m with the majority of them (46.92%) related to periods of 2 to 3 s.

Table 5.1.27: Pivot Table (%) for Significant Wave Height and Zero-crossing wave period for Kalamata Buoy

| Hm ₀ (m) | Tm ₀₂ (s) | | | | | | Total |
|---------------------|----------------------|-------|-------|------|------|------|--------|
| | 2-3 | 3-4 | 4-5 | 5-6 | 6-7 | 7-8 | |
| 0-1 | 45.10 | 32.75 | 13.70 | 4.43 | 0.15 | 0.00 | 96.13 |
| 1-2 | 0 | 0.37 | 1.04 | 1.70 | 0.46 | 0.04 | 3.61 |
| 2-3 | 0 | 0 | 0 | 0.12 | 0.11 | 0.03 | 0.25 |
| 3-4 | 0 | 0 | 0 | 0 | 0.01 | 0 | 0.01 |
| Total | 45.10 | 33.12 | 14.74 | 6.25 | 0.73 | 0.06 | 100.00 |

5.1.5.1.2 Monthly Means for the period 2007-2011

Mean monthly values of wave height are shown in Figure 5.1.23. The minimum mean monthly value for wave height is in August (0.26 m) while the maximum mean is in December (0.44 m). The minimum recorded value is in April (0.068 m) and the maximum is in December (3.28 m). For the wave period, the minimum monthly mean is in August (2.97 s) while the maximum monthly mean in December (3.74 s). The minimum recorded value for wave period is in August (2.22 s) and the maximum in December (7.27 s).

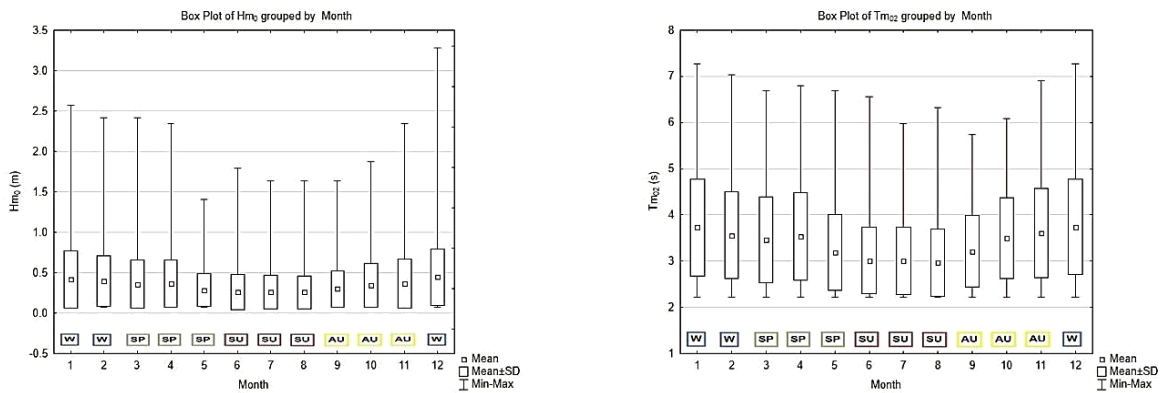


Figure 5.1.23: Box and Whiskers plots for Monthly Wave Height and Wave Period for Kalamata Buoy

5.1.5.2 Sea Surface Elevation (SSE)

In this section, results of the SSE analysis of 3423 records are shown for a variety of parameters. A random example of a record and its’ spectral analysis is shown in Figure 5.1.24. The peak period (T_p) of the spectrum shown is estimated to be 12.56 s.

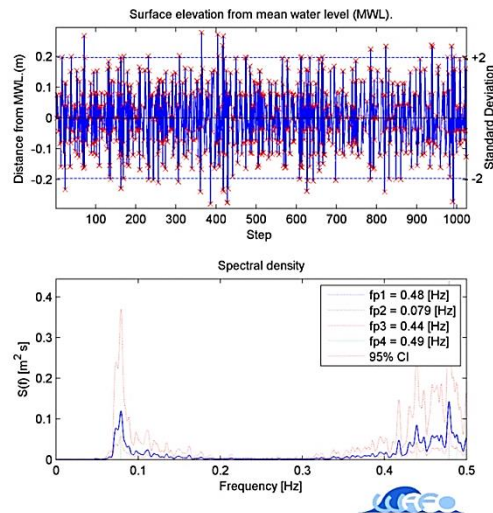


Figure 5.1.24: Random SSE record and its spectrum for Kalamata Buoy

5.1.5.2.1 General Statistics

The descriptive statistics of wave characteristics provided by SSE analysis from 3423 records are shown in Table 5.1.28. The spectral characteristics show that significant wave height has a mean of 0.68 m, a maximum of 3.27 m, mean wave period of 3.91 s and a max of 8.04 s. For the statistical characteristics, mean wave height is of 0.57 m with a max of 3.03 m while the mean wave period has a mean of 5.74 s and a max of 10.55 s. The apparent maximum wave height has a mean of 0.95 m with a max recorded of 4.99 m. Finally the peak period, has a mean of 5.26 s and a max of 12.56 s .

Table 5.1.28: Descriptive Statistics as derived from SSE Analysis for Kalamata Buoy

| Parameters | Number of Records | Mean | Maximum | Std.Dev. |
|------------------|-------------------|------|---------|----------|
| H_{m_0} (m) | 3423 | 0.68 | 3.27 | 0.32 |
| H_{max} (m) | 3423 | 0.95 | 4.99 | 0.52 |
| $H_{1/3}$ (m) | 3423 | 0.57 | 3.03 | 0.32 |
| $T_{m_{02}}$ (s) | 3423 | 3.91 | 8.04 | 0.87 |
| $T_{1/3}$ (s) | 3423 | 5.74 | 10.55 | 1.49 |
| T_p (s) | 3423 | 5.26 | 12.56 | 2.05 |

For Kalamata, a correlation coefficient (r) of 0.97 is shown for H_{m_0} and $H_{1/3}$ and a 0.91 for $T_{m_{02}}$ and $T_{1/3}$ as given in Figure 5.1.25.

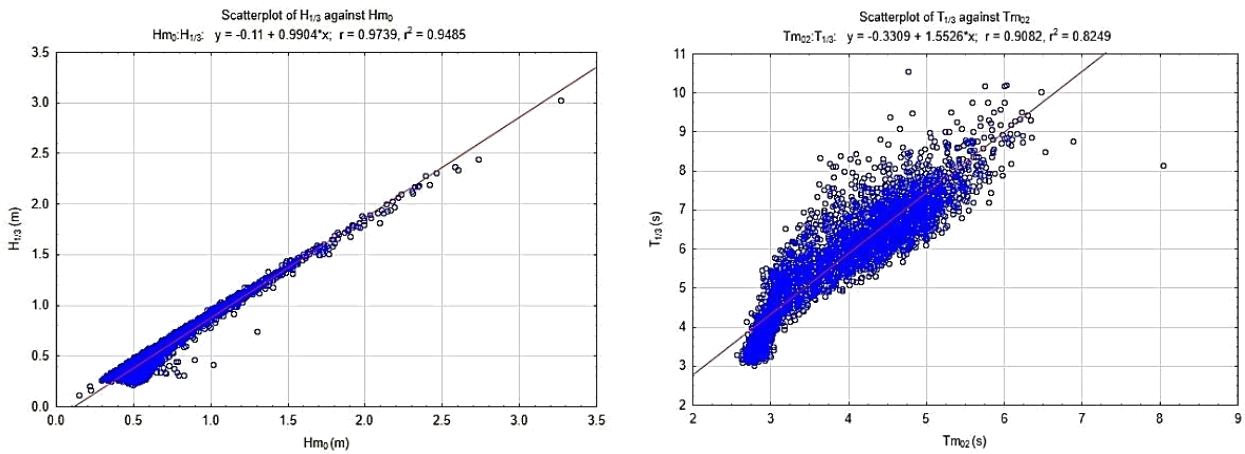


Figure 5.1.25: Scatterplots of statistical and spectral wave parameters for Kalamata Buoy

5.1.5.2.2 Monthly Means for the period 2007-2011

The monthly means of a variety of wave parameters as provided by the SSE analysis are shown in Figure 5.1.26.

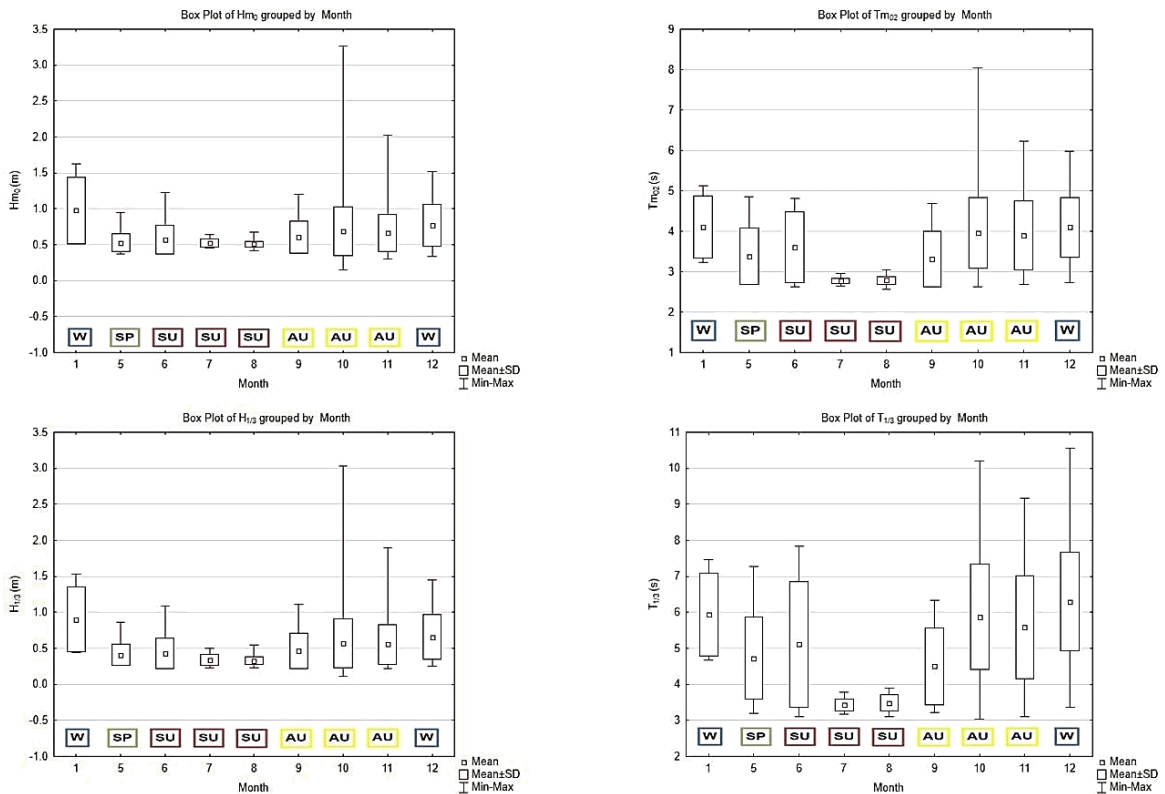


Figure 5.1.26: Spectral and Statistical Monthly Values per Wave Parameter for Kalamata Buoy

The spectral significant wave height H_{m0} , has a minimum mean monthly value in August (0.51 m), a maximum mean monthly value in January (0.98m), a minimum recorded value of 0.14 m (October) and a maximum 3.27 m (October). The statistical significant wave height $H_{1/3}$ has a minimum mean monthly value 0.33 m (August), a maximum mean monthly of 0.9 m (January), a minimum recorded 0.12 m

(October) and a max 3.03 m (October). The spectral wave period T_{m02} , has a minimum monthly mean of 2.78 s (July) and a maximum monthly mean of 4.11 s (January), a minimum recorded 2.56 s (August) and a maximum 8.04 s (October). Finally, the statistical wave period $T_{1/3}$ has a minimum mean monthly of 3.42 s (July), a max mean monthly of 6.29 s (December), minimum 3.02 s (October) and a maximum of 10.55 s (December).

5.1.5.2.3 Probability Distribution of Wave Height

The distributions of Weibull, Rayleigh and Kumaraswamy for a random set of wave height are shown in the forms of pdf and QQ plots in Figure 5.1.27. From the QQ plot it is shown that Kumaraswamy underestimates the most the higher values but deviates less from the mean values than the other two under-examination distributions.

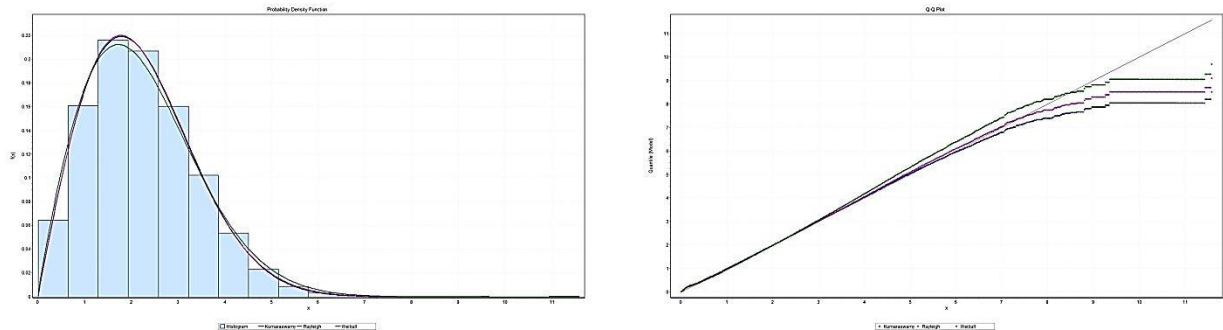


Figure 5.1.27: Probability Distributions and QQ plots for Kalamata Buoy for random wave heights

The statistics of goodness of fit tests are shown in Table 5.1.29, suggest that Kumaraswamy represents best wave height.

Table 5.1.29: Statistics of Goodness of Fits according to K-S, A-D and χ^2 test for Kalamata Buoy

| Distribution | Kolmogorov Smirnov | Anderson Darling | Chi-Squared |
|--------------|--------------------|------------------|-------------|
| | Statistic | Statistic | Statistic |
| Kumaraswamy | 0.007 | 35.97 | 254.66 |
| Weibull | 0.016 | 246.03 | 1750.5 |
| Rayleigh | 0.007 | 49.718 | 371.27 |

5.1.5.2.4 Ratios between Statistical and Spectral Parameters

Several ratios among spectral, statistical and apparent wave height parameters are shown in Table 5.1.30. A mean of 1.39 is given for H_{m0} and $H_{1/3}$, 1.28 for $H_{1/3}$ and $\sqrt{m_0}$, 1.72 for H_{max} and H_{m0} and 0.81 for H_{max} and $H_{1/3}$.

Table 5.1.30: Statistics of various Ratios for Kalamata Buoy

| | Number of Records | Mean | Minimum | Maximum | Std.Dev. |
|------------------------|-------------------|------|---------|---------|----------|
| $H_{m0} / H_{1/3}$ | 3423 | 1.39 | 0.72 | 2.25 | 0.24 |
| $H_{1/3} / \sqrt{m_0}$ | 3423 | 1.28 | 1.02 | 2.20 | 0.26 |
| H_{max} / H_{m0} | 3423 | 1.72 | 1.32 | 2.71 | 0.18 |
| $H_{max} / H_{1/3}$ | 3423 | 0.81 | 0.45 | 0.98 | 0.14 |

5.1.5.3 Weather Characteristics

The atmospheric characteristics as provided by the buoy of Kalamata, are shown in this section.

5.1.5.3.1 General Statistics

The main statistics of atmospheric parameters for Kalamata are shown in Table 5.1.31. Minimum temperature recorded is 2.47 °C, while the maximum is 36.41 °C and the mean is of 18.89 °C. Maximum wind speed is 15.67 m/s, mean is 3.7 m/s while for wind gust the maximum is 21.56 m/s and the mean of 4.9 m/s. The highest atmospheric pressure is of 1033.53 hPa, the lowest atmospheric pressure is 988.27 hPa and the mean 1013.13 hPa.

Table 5.1.31: Descriptive Statistics of Atmospheric Parameters for Kalamata Buoy

| Parameters | Number of Records | Mean | Minimum | Maximum | Std.Dev. |
|----------------------|-------------------|---------|---------|---------|----------|
| Air Pressure (hPa) | 11619 | 1013.13 | 988.27 | 1033.53 | 6.18 |
| Air Temperature (°C) | 11619 | 18.89 | 2.47 | 36.41 | 5.47 |
| Wind Gust (m/s) | 10989 | 4.92 | 0.23 | 21.56 | 2.81 |
| Wind Speed (m/s) | 10892 | 3.7 | 0.03 | 15.67 | 2.29 |

Main directions that winds are blowing from are in the range of NW (32.34%), there also winds from S (21.66%), as shown in the wind chart (Figure 5.1.28). The most frequent winds range from 0 to 3 m/s (43.49%) and from those 49.19% are of NW to N direction. Winds above 12 m/s are of 0.28% frequency with 80% from NW to NE.

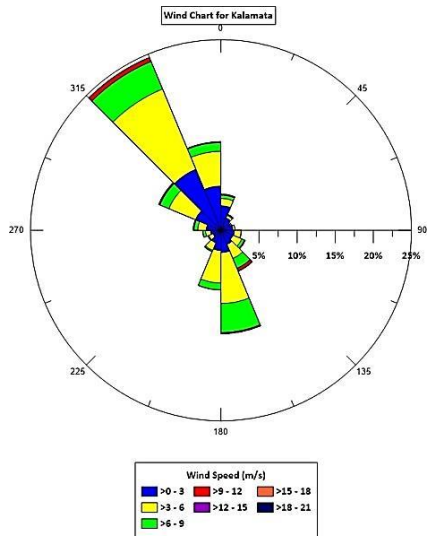


Figure 5.1.28: Wind Chart for Kalamata Buoy

5.1.5.3.2 Monthly Means for the period 2007-2011

The mean monthly values for atmospheric parameters for the period 2007-2011 are given in Figure 5.1.29.

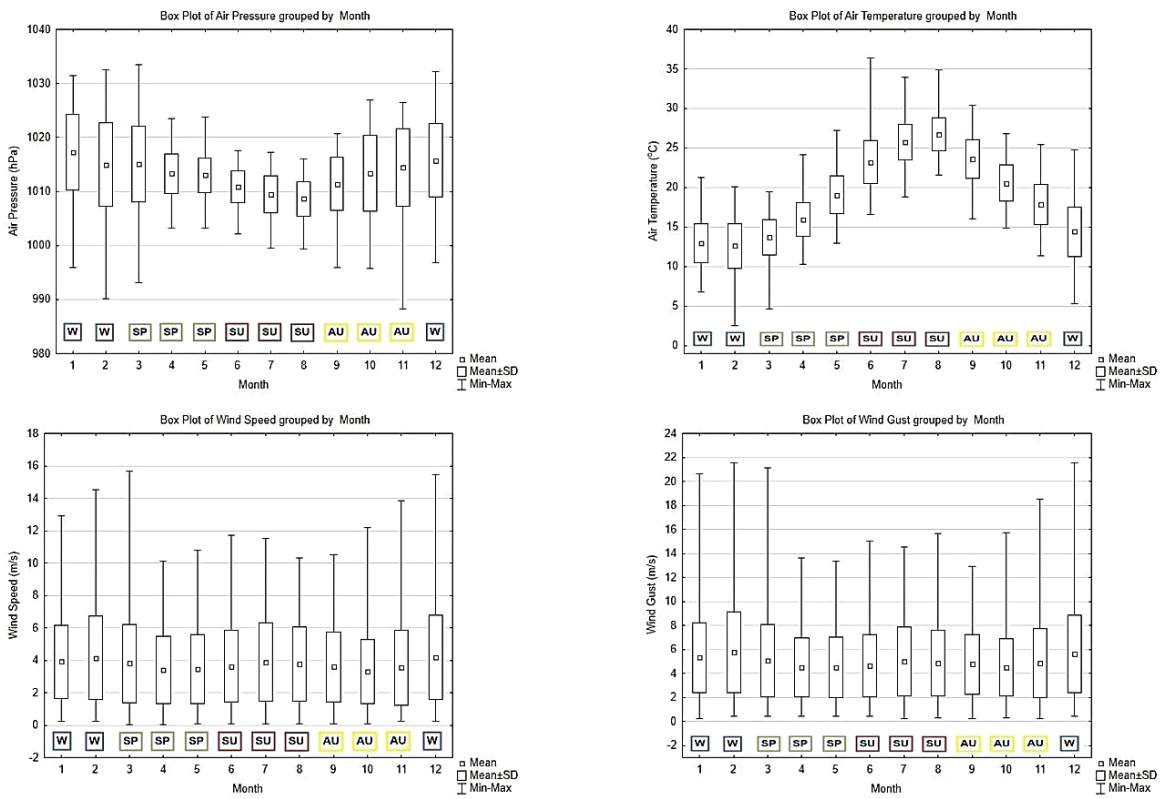


Figure 5.1.29: Monthly Box and Whiskers Plots for Atmospheric Parameters for Kalamata Buoy

For pressure the minimum value (1008.65 hPa) is in August and the maximum (1017.32 hPa) in January. For temperature the minimum mean monthly 12.58 °C is in February and the maximum is 26.74 °C in August. The minimum monthly mean value of wind speed (3.33 m/s) is in October and the maximum monthly mean (4.19 m/s) is in December. Wind gust minimum monthly mean is in April (4.49 m/s) and the maximum in 5.75 m/s in February.

5.1.5.4 Relation of Wind and Wave Data

The intercomparison of wind and wave datasets only for the dates that there were data available for the parameters under-consideration is shown in this session.

5.1.5.4.1 General Statistics

The statistics of atmospheric and wave parameters are given in Table 5.1.32. The mean value wind speed (3.7 m/s) can be considered as gentle breeze that will lead to isolated whitecaps .

Table 5.1.32: Descriptive Statistics of Wave and Atmospheric Parameters for Kalamata Buoy

| Parameters | Number of Records | Mean | Minimum | Maximum | Std.Dev. |
|-----------------------|-------------------|---------|---------|---------|----------|
| Air Pressure (hPa) | 10301 | 1012.92 | 988.28 | 1033.53 | 6.21 |
| Air Temperature (°C) | 10301 | 19.11 | 2.47 | 36.41 | 5.53 |
| Wind Gust (m/s) | 10301 | 4.94 | 0.45 | 21.56 | 2.79 |
| Wind Speed (m/s) | 10301 | 3.69 | 0.03 | 15.67 | 2.29 |
| Hm ₀ (m) | 10301 | 0.34 | 0.07 | 3.28 | 0.28 |
| Hm _{0a} (m) | 10301 | 0.02 | 0.00 | 1.64 | 0.07 |
| Hm _{0b} (m) | 10301 | 0.33 | 0.07 | 2.81 | 0.27 |
| H _{max} (m) | 10301 | 0.28 | 0.00 | 5.08 | 0.49 |
| Tm ₀₂ (s) | 10301 | 3.34 | 2.23 | 7.27 | 0.92 |
| Tm _{02a} (s) | 10301 | 12.38 | 10.31 | 18.75 | 1.15 |
| Tm _{02b} (s) | 10301 | 3.32 | 2.23 | 7.03 | 0.90 |
| T _p (s) | 10301 | 4.26 | 1.99 | 13.24 | 2.10 |

The pivot Table 5.1.33 shows that the most frequent waves of 52.82% have heights of 0-0.3 m and 57.57% of these are related with wind speeds of 0-3 m/s. The higher waves (>2.4 m) have a frequency of 0.06% and 50% of those are related with speeds of above 12 m/s wind speeds.

Table 5.1.33: Frequency Table (%) of Wind Speed and Significant Spectral Wave Height for Kalamata Buoy

| Wind Speed (m/s) | Hm0 (m) | | | | | | | | | | Total |
|------------------|---------|---------|---------|---------|---------|---------|---------|---------|---------|-------|--------|
| | 0-0.3 | 0.3-0.6 | 0.6-0.9 | 0.9-1.2 | 1.2-1.5 | 1.5-1.8 | 1.8-2.1 | 2.1-2.4 | 2.4-2.7 | 3-3.3 | |
| 0-3 | 30.41 | 9.12 | 2.98 | 0.77 | 0.24 | 0.06 | 0.01 | 0.01 | 0.01 | 0.00 | 43.60 |
| 3-6 | 20.97 | 14.43 | 2.85 | 0.92 | 0.34 | 0.12 | 0.07 | 0.03 | 0.00 | 0.00 | 39.72 |
| 6-9 | 1.44 | 10.81 | 1.14 | 0.60 | 0.34 | 0.20 | 0.06 | 0.02 | 0.00 | 0.00 | 14.61 |
| 9-12 | 0.00 | 0.78 | 0.35 | 0.26 | 0.23 | 0.08 | 0.05 | 0.06 | 0.02 | 0.00 | 1.81 |
| 12-15 | 0.00 | 0.01 | 0.11 | 0.05 | 0.01 | 0.00 | 0.02 | 0.03 | 0.02 | 0.00 | 0.24 |
| 15-18 | 0.00 | 0.00 | 0.00 | 0.00 | 0.01 | 0.00 | 0.00 | 0.00 | 0.00 | 0.01 | 0.02 |
| Total | 52.82 | 35.14 | 7.42 | 2.60 | 1.16 | 0.46 | 0.20 | 0.14 | 0.05 | 0.01 | 100.00 |

From the charts in Figure 5.1.30, the most frequent waves (50.42%) are related with winds blowing from NW to N and this applies for the most frequent periods as well. Secondary directions of wind speed blowing from S are also evident in relation to wave height with a frequency of 21.32%. Waves with heights of more than 2.4m (54.17%) are related to winds blowing from S.

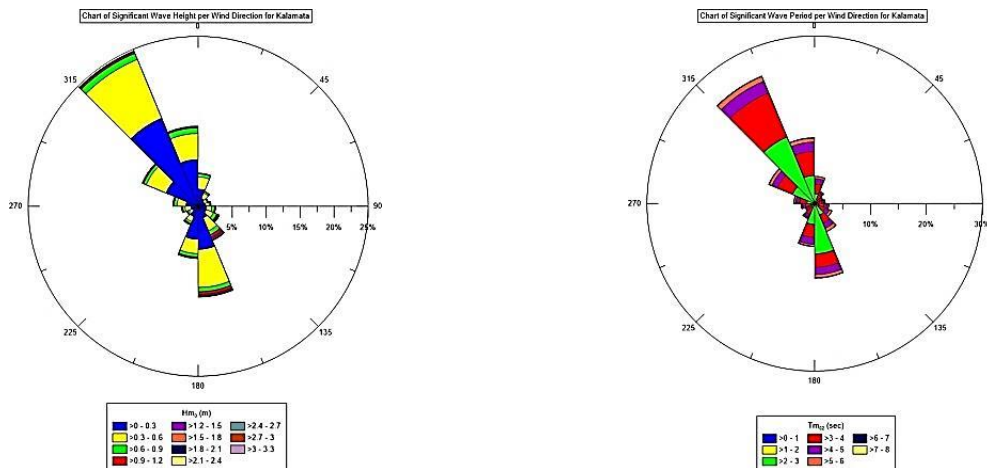


Figure 5.1.30: Charts of Wind Direction and Wave Height - Period for Kalamata Buoy

5.1.6 KATERINI

The location, depth and periods with records of Katerini are given in Table 5.1.34.

Table 5.1.34: Location, depth of installation and time periods of recording per database for Katerini Buoy

| Location | Depth (m) | Wave Parameters | SSE data | Atmospheric Parameters |
|--------------------------|-----------|---------------------------|----------|------------------------|
| 22.71685°E 40.25043°N | 54.5 | 01/01/2001- 31/12/2003 | -- | 08/09/2001-16/4/2003 |

5.1.6.1 Wave Characteristics

The wave characteristics are analysed in this subchapter as provided by the buoy for the period 2001-2003.

5.1.6.1.1 General Statistics

The basic statistics of wave parameters are presented for Katerini Buoy in Table 5.1.35. The mean significant wave height is 0.43 m and the max 2.79 m. The period has a mean of 2.94 s and a max of 5.36 s. The swells are described with mean heights of 0.02 m and periods of 14.13 s, while their maximum height and period can reach up to 0.36 m and 15 s respectively. Wind waves have mean height of 0.43 m and period of 2.93 s and maximum values of 2.78 m and 5.35 s. Finally, the peak period has a mean of 3.47 s and a max of 10.45 s.

Table 5.1.35: Descriptive Statistics of Wave Parameters for Katerini Buoy

| Parameters | Number of Records | Mean | Maximum | Std.Dev. |
|----------------|-------------------|-------|---------|----------|
| Hm_0 (m) | 4212 | 0.43 | 2.79 | 0.33 |
| Hm_{0a} (m) | 4131 | 0.02 | 0.36 | 0.03 |
| Hm_{0b} (m) | 4212 | 0.43 | 2.78 | 0.33 |
| Tm_{02} (s) | 4212 | 2.94 | 5.36 | 0.48 |
| Tm_{02a} (s) | 4212 | 14.13 | 15.00 | 0.99 |
| Tm_{02b} (s) | 4212 | 2.93 | 5.35 | 0.48 |
| T_p (s) | 4212 | 3.47 | 10.45 | 1.27 |

Charts for wave height and period for Katerini are given in Figure 5.1.31. Waves are coming from N (38.53% and Fetch length of 38 km) and from SE (32.45%) while heights of more than 2.1 m, propagate from SE (same pattern applies for wind-waves and for swells) with a fetch length of 335 km. Larger periods are also from SE directions.

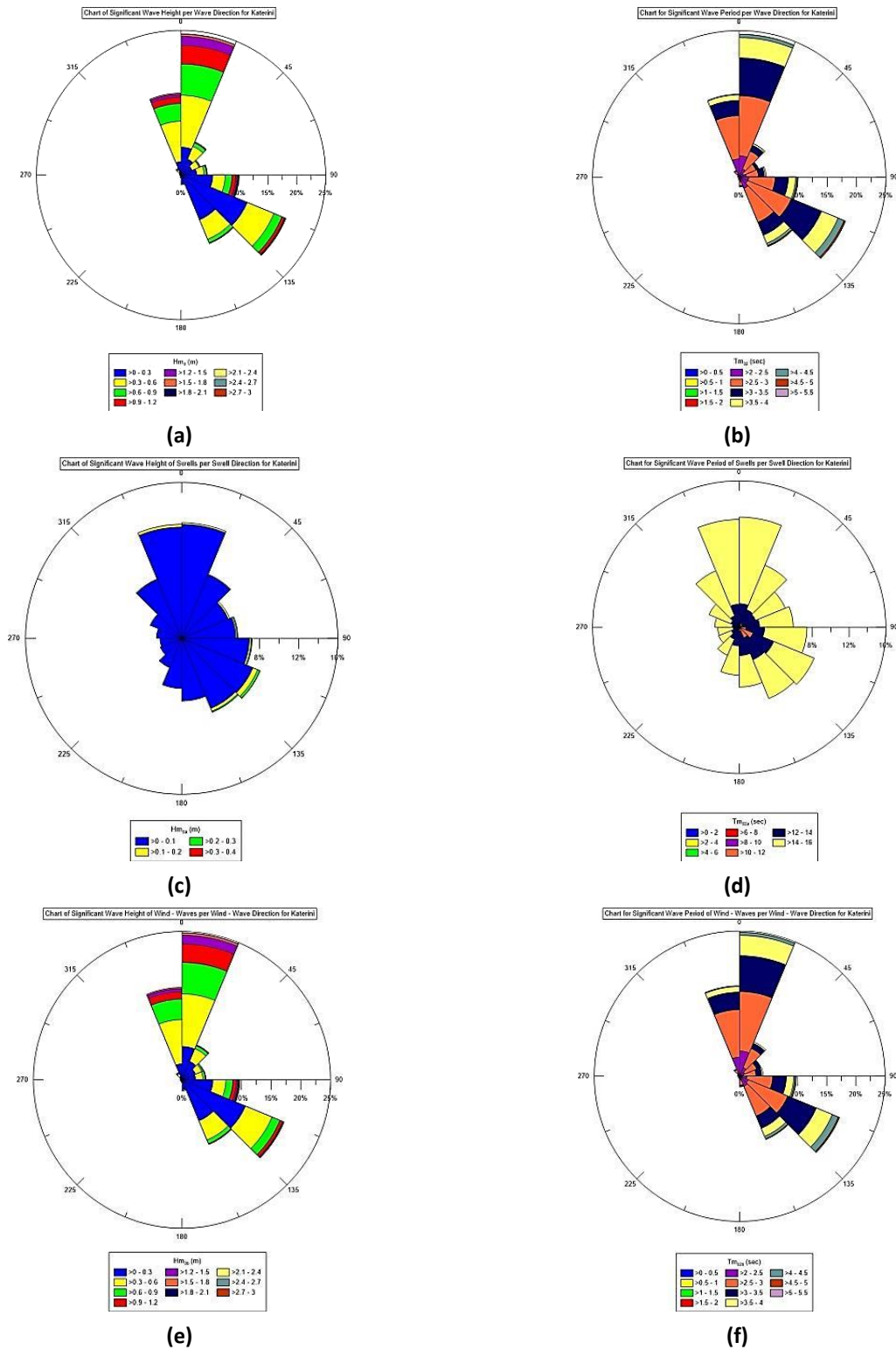


Figure 5.1.31: Rose Diagrams for Significant Wave Height and Wave period for all waves (a,b), swells (c,d) and wind waves (e,f) for Katerini Buoy

Percentages of appearance of significant wave height relative to wave period are given in Table 5.1.36. The most frequent waves (44.32%) have heights from 0 to 0.3m with 45.63% of them related with periods of 2.5 to 3 s. The highest waves (>2.7m) have a frequency of 0.05% with periods of 5 to 5.5 s.

Table 5.1.36: Pivot Table for Significant Wave Height and Zero-crossing wave period for Katerini Buoy

| Hm ₀ (m) | Tm ₀₂ (s) | | | | | | | Total |
|---------------------|----------------------|-------|-------|-------|-------|-------|-------|--------|
| | 2-2.5 | 2.5-3 | 3-3.5 | 3.5-4 | 4-4.5 | 4.5-5 | 5-5.5 | |
| 0-0.3 | 14.46 | 20.18 | 5.44 | 3.11 | 0.78 | 0.26 | 0 | 44.23 |
| 0.3-0.6 | 3.25 | 23.08 | 4.91 | 0.85 | 0.33 | 0.05 | 0.05 | 32.53 |
| 0.6-0.9 | 0 | 2.52 | 9.66 | 1.09 | 0.17 | 0.05 | 0 | 13.49 |
| 0.9-1.2 | 0 | 0 | 2.54 | 3.37 | 0.14 | 0 | 0 | 6.05 |
| 1.2-1.5 | 0 | 0 | 0 | 2.09 | 0.45 | 0.02 | 0 | 2.56 |
| 1.5-1.8 | 0 | 0 | 0 | 0.21 | 0.59 | 0 | 0 | 0.81 |
| 1.8-2.1 | 0 | 0 | 0 | 0 | 0.07 | 0.05 | 0 | 0.12 |
| 2.1-2.4 | 0 | 0 | 0 | 0 | 0 | 0.07 | 0 | 0.07 |
| 2.4-2.7 | 0 | 0 | 0 | 0 | 0 | 0.05 | 0.05 | 0.09 |
| 2.7-3 | 0 | 0 | 0 | 0 | 0 | 0 | 0.05 | 0.05 |
| Total | 17.71 | 45.77 | 22.55 | 10.73 | 2.54 | 0.55 | 0.14 | 100.00 |

5.1.6.1.2 Monthly Means for the period 2001-2003

The minimum monthly mean for wave height is in April (0.35 m) and the maximum monthly mean in December (0.61 m). The smallest recorded wave height is in April (0.026 m) and the maximum in July (2.79 m).

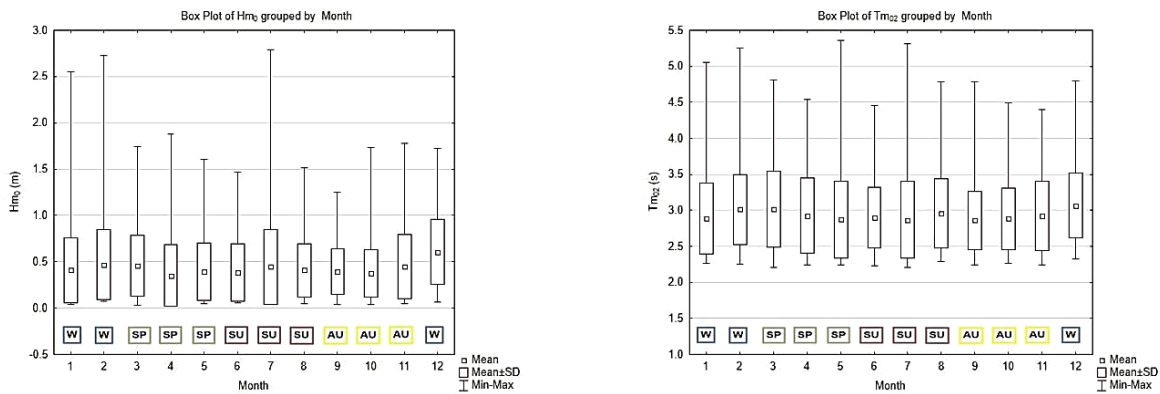


Figure 5.1.32: Box and Whiskers plots for Monthly Wave Height and Wave Period for Katerini Buoy

The minimum monthly mean of wave period is in September (2.86 s) and the maximum monthly mean in December (3.07 s). The minimum recorded value for wave period is in March (2.21 s) and the maximum in May (5.35 s) (Figure 5.1.32).

5.1.6.2 Weather Characteristics

The atmospheric parameters of the area of Katerini for the period 2001-2003 are analysed in this session.

5.1.6.2.1 General Statistics

Descriptive statistics of atmospheric parameters for Katerini are shown in Table 5.1.37. The mean temperature is of 14.86 °C and can reach a maximum of 31.59 °C. The mean wind speed is of 4.55 m/s and wind gust of 6.18 m/s. Pressure has a mean of 1017.06 hPa, but can range from 990.53 hPa to 1037.69 hPa.

Table 5.1.37: Descriptive Statistics of Atmospheric Parameters for Katerini Buoy

| Parameters | Number of Records | Mean | Minimum | Maximum | Std.Dev. |
|----------------------|-------------------|---------|---------|---------|----------|
| Air Pressure (hPa) | 4255 | 1017.06 | 990.53 | 1037.69 | 6.928 |
| Air Temperature (°C) | 4217 | 14.86 | 0.17 | 31.59 | 7.023 |
| Wind Gust (m/s) | 4039 | 6.18 | 0.02 | 24.71 | 4.05 |
| Wind Speed (m/s) | 4032 | 4.55 | 0.001 | 18.83 | 3.29 |

The wind chart in Figure 5.1.33 show that the most prevailing winds are blowing from NW to N (61.93%). Most common winds have speeds of 0-3m/s (37.48%) and from those 40.97% is of NW to N direction. Wind speeds >15 m/s have a frequency of occurrence of 0.52% with 42.86% of those blowing from E.

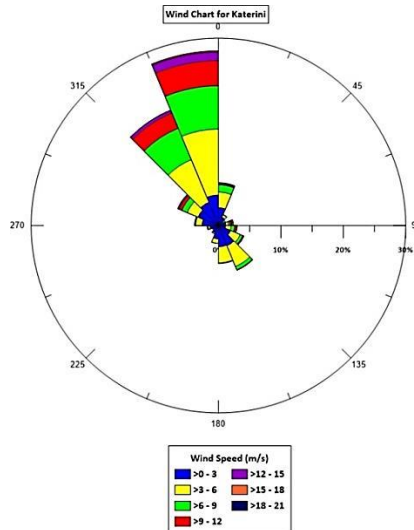


Figure 5.1.33: Wind Chart for Katerini Buoy

5.1.6.2.2 Monthly Means for the period 2001-2003

Box and whisker plots for the atmospheric parameters of Katerini buoy are given in Figure 5.1.34.

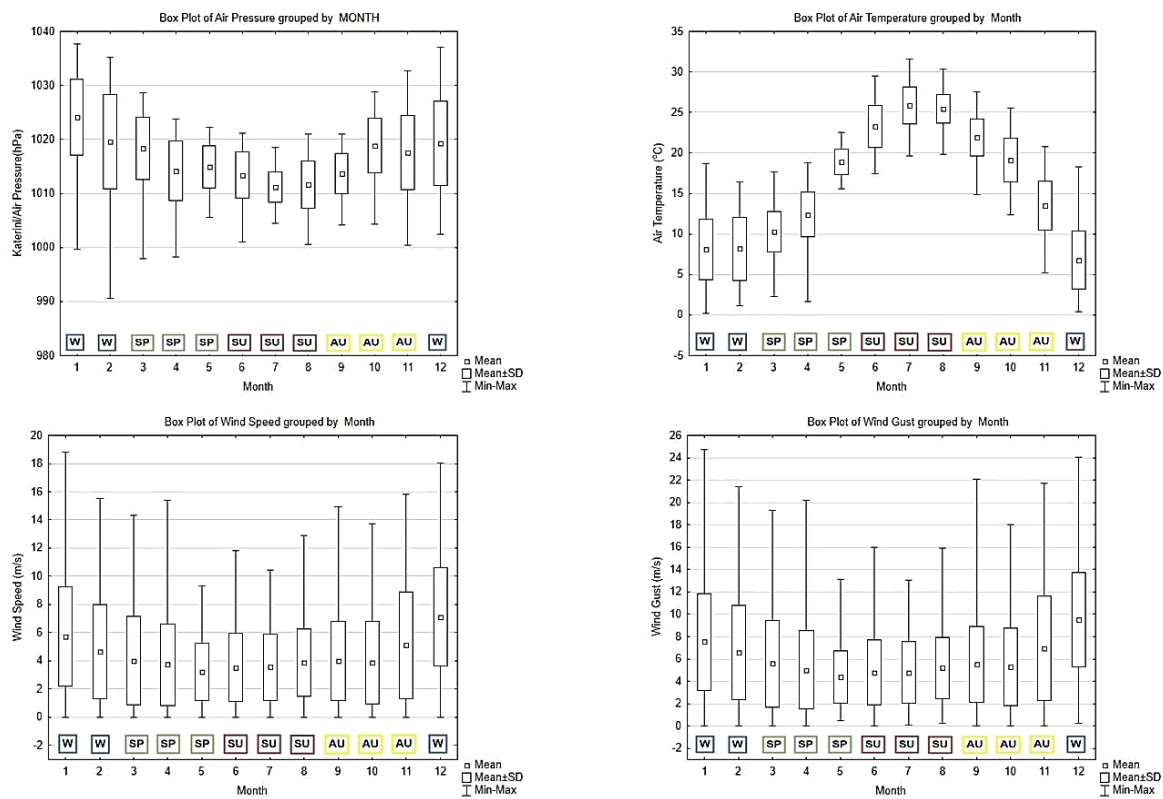


Figure 5.1.34: Monthly Box and Whiskers Plots for Atmospheric Parameters for Katerini Buoy

The minimum monthly mean is in July (1011.2 hPa) and the maximum (1024.08 hPa) in January. Minimum mean monthly temperature is 6.76 °C in December and the maximum in 25.83 °C during July. Minimum values of wind speed and wind gust are in May (3.23 m/s and 4.38 m/s respectively) and the maximum are in December (7.1 m/s and 9.51 m/s).

5.1.6.3 Relation of Wind and Wave Data

Results from the combined wind and wave datasets are shown in this subchapter.

5.1.6.3.1 General Statistics

Basic statistics of atmospheric and wave parameters are shown in Table 5.1.38. The area is influenced mainly by gentle breeze and waves with isolated whitecaps.

Table 5.1.38: Descriptive Statistics of Wave and Atmospheric Parameters for Katerini Buoy

| Parameters | Number of Records | Mean | Minimum | Maximum | Std.Dev. |
|--------------------|-------------------|---------|---------|---------|----------|
| Air Pressure (hPa) | 3891 | 1017.12 | 990.53 | 1037.69 | 6.98 |

| | | | | | |
|-----------------------|------|-------|-------|-------|------|
| Air Temperature (°C) | 3891 | 14.66 | 0.17 | 30.73 | 7.08 |
| Wind Gust (m/s) | 3891 | 6.17 | 0.02 | 24.71 | 4.02 |
| Wind Speed (m/s) | 3891 | 4.54 | 0.00 | 18.83 | 3.28 |
| Hm ₀ (m) | 3891 | 0.44 | 0.03 | 2.79 | 0.33 |
| Hm _{0a} (m) | 3891 | 0.02 | 0.00 | 0.36 | 0.03 |
| Hm _{0b} (m) | 3891 | 0.44 | 0.03 | 2.78 | 0.33 |
| Tm ₀₂ (s) | 3891 | 2.93 | 2.21 | 5.32 | 0.48 |
| Tm _{02a} (s) | 3891 | 14.13 | 10.59 | 15.00 | 1.00 |
| Tm _{02b} (s) | 3891 | 2.93 | 2.21 | 5.31 | 0.48 |
| T _p (s) | 3891 | 3.46 | 2.02 | 10.45 | 1.26 |

The frequency table of wind speed and significant wave height is given in Table 5.1.39. Most of the waves (41.52%) have heights of 0-0.3 m and 71.09% of these are related with wind speeds of 0-3 m/s. The higher waves (>2.4 m) have a frequency of 0.15% and are related with wind speeds of more than 15 m/s.

Table 5.1.39: Frequency Table (%) of Wind Speed and Significant Spectral Wave Height for Katerini Buoy

| Wind Speed (m/s) | Hm ₀ (m) | | | | | | | | | | Total |
|---------------------|---------------------|---------|---------|---------|---------|---------|---------|---------|---------|-------|-------|
| | 0-0.3 | 0.3-0.6 | 0.6-0.9 | 0.9-1.2 | 1.2-1.5 | 1.5-1.8 | 1.8-2.1 | 2.1-2.4 | 2.4-2.7 | 2.7-3 | |
| 0-3 | 29.52 | 6.99 | 0.70 | 0.10 | 0.03 | 0 | 0 | 0 | 0 | 0 | 37.33 |
| 3-6 | 11.68 | 19.62 | 2.61 | 0.40 | 0 | 0 | 0 | 0 | 0 | 0 | 34.30 |
| 6-9 | 0.30 | 7.12 | 7.97 | 1.48 | 0.15 | 0 | 0 | 0.03 | 0 | 0 | 17.04 |
| 9-12 | 0.03 | 0.18 | 2.88 | 3.86 | 1.28 | 0.20 | 0.03 | 0 | 0 | 0 | 8.44 |
| 12-15 | 0 | 0.08 | 0.05 | 0.55 | 1.15 | 0.50 | 0.03 | 0 | 0 | 0 | 2.36 |
| 15-18 | 0 | 0 | 0 | 0 | 0.10 | 0.15 | 0.08 | 0.03 | 0.08 | 0.05 | 0.48 |
| 18-21 | 0 | 0 | 0 | 0 | 0 | 0 | 0 | 0.03 | 0.03 | 0 | 0.05 |
| Total | 41.52 | 33.98 | 14.21 | 6.39 | 2.71 | 0.85 | 0.13 | 0.08 | 0.10 | 0.05 | 100 |

In Figure 5.1.35, wind direction / wave - period charts are given. Moreover, the most frequent waves (60.45%) and waves with heights more than 2.1 m are related with winds blowing from NW to N. The same pattern applies for periods as well.

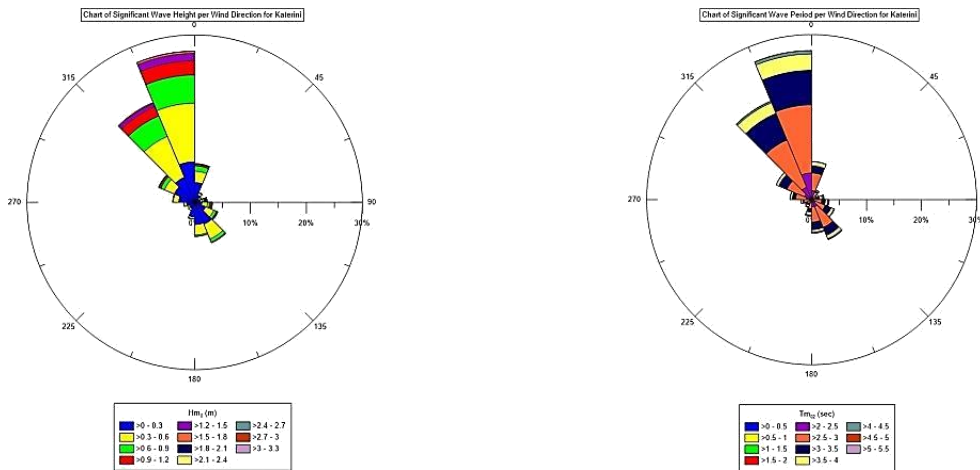


Figure 5.1.35: Charts of Wind Direction and Wave Height - Period for Katerini Buoy

5.1.7 LESVOS

Depth, location and time periods of Lesvos buoy are given in Table 5.1.40.

Table 5.1.40: Location, depth of installation and time periods of recording per database for Lesvos Buoy

| Location | Depth (m) | Wave Parameters | SSE data | Atmospheric Parameters |
|--------------------------|-----------|---------------------------|----------|------------------------|
| 25.81066°E 39.15078°N | 131 | 01/01/2000- 31/12/2011 | -- | 01/01/2000-31/12/2011 |

5.1.7.1 Wave Characteristics

This subchapter includes the analysis of wave parameters as provided by the buoy of Lesvos for the period 2000-2011.

5.1.7.1.1 General Statistics

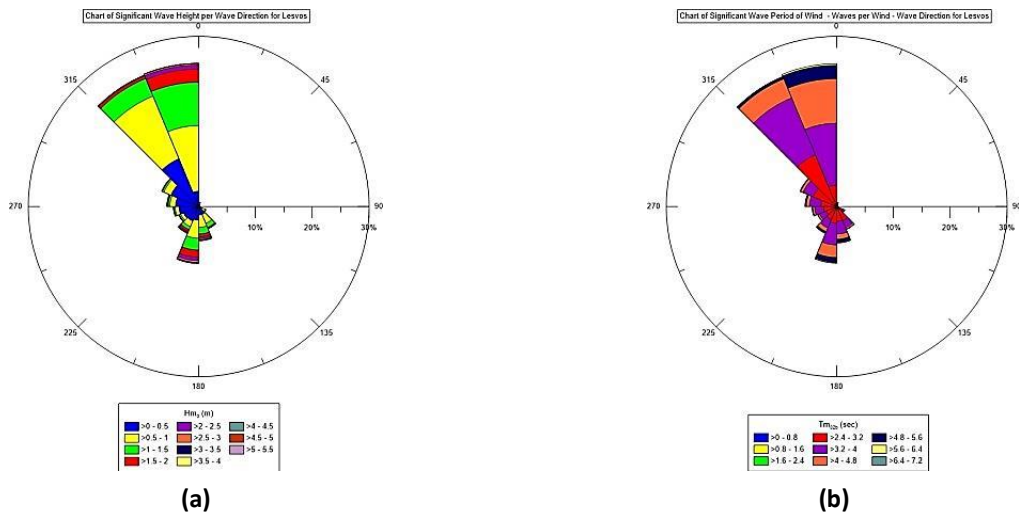
The basic statistics of wave parameters are shown in Table 5.1.41. Wave height has a mean of 0.77 m, maximum of 5.38 m while their period has a mean of 3.54 s and max of 8.83 s. Swells have mean height

of 0.04 m, max of 3.06 m, mean period of 13.85 s and max period of 16.88 s. The wind waves have heights of 0.78 m, max of 5.09 m, period of 3.53 s and max of 6.75 s. Finally, the peak period has a mean of 4.61 s and a max of 11.91 s while maximum wave height can have a mean of 1.22 m and a max of 5.94 m.

Table 5.1.41: Descriptive Statistics of Wave Parameters for Lesvos Buoy

| Parameters | Number of Records | Mean | Maximum | Std.Dev. |
|----------------|-------------------|-------|---------|----------|
| Hm_0 (m) | 28361 | 0.77 | 5.38 | 0.55 |
| Hm_{0a} (m) | 28333 | 0.04 | 3.06 | 0.08 |
| Hm_{0b} (m) | 28873 | 0.78 | 5.09 | 0.55 |
| $Hmax$ (m)* | 9780 | 1.22 | 5.94 | 0.76 |
| Tm_{02} (s) | 28514 | 3.54 | 8.83 | 0.72 |
| Tm_{02a} (s) | 28729 | 13.85 | 16.88 | 1.02 |
| Tm_{02b} (s) | 28873 | 3.53 | 6.75 | 0.71 |
| T_p (s) | 28833 | 4.61 | 11.91 | 1.37 |

Rose charts for wave height and period for Lesvos are given in Figure 5.1.36. Waves are mainly coming (58.04%) from NW to N (Fetch length of 242 km) and the same applies for swells (38.07%). Waves with heights of more than 3 m are from South (66.03%) and for swells with heights of more than 2 m are from NW.



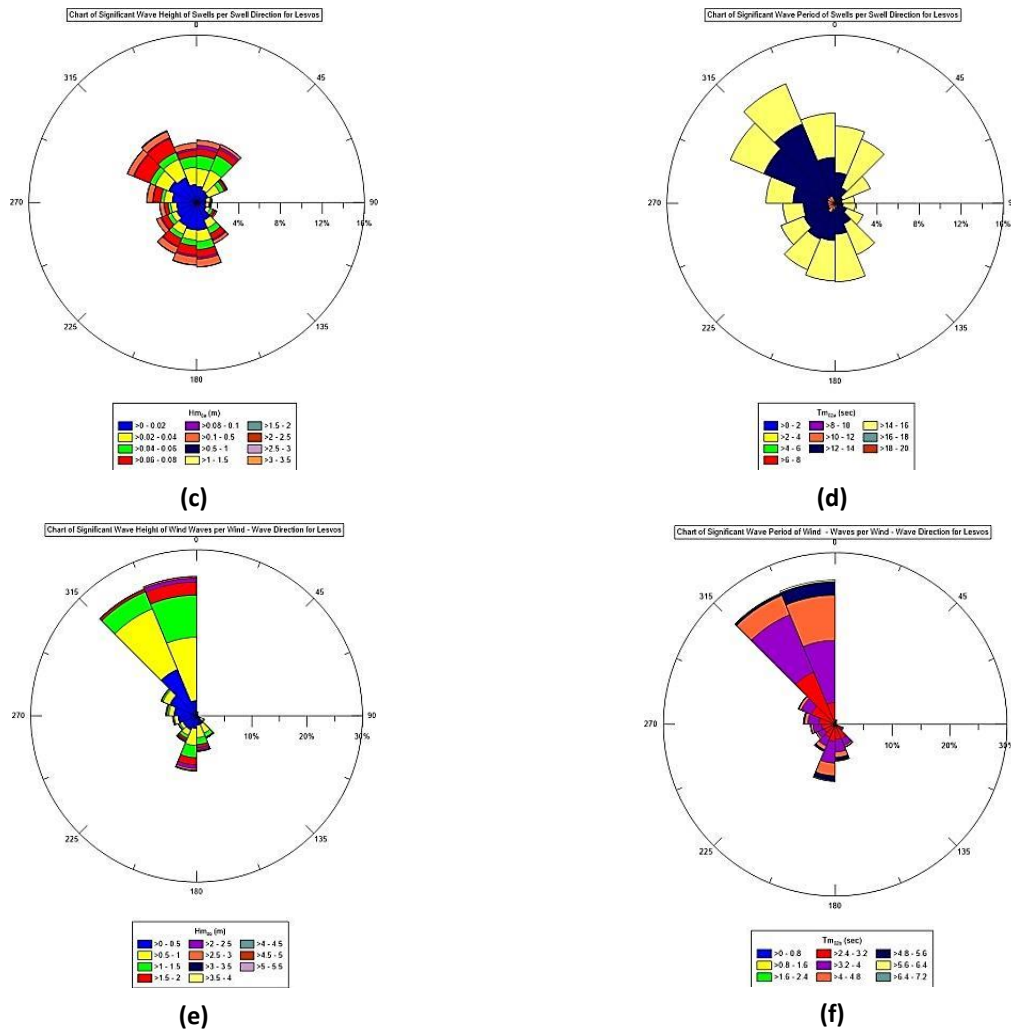


Figure 5.1.36: Rose Diagrams for Significant Wave Height and Wave period for all waves (a,b), swells (c,d) and wind waves (e,f) for Lesvos Buoy

In Table 5.1.42, the percentages of appearance of significant wave height relative to wave period are shown. The most frequent waves (37.23%) are those with height from 0 to 0.5 m with the majority of them (59.38%) described with periods of 2.8 to 3.6 s. The highest waves (>4 m) have a frequency of 0.7% with periods larger of 6 s.

Table 5.1.42: Pivot Table for Significant Wave Height and Zero-crossing wave period for Lesvos Buoy

| Hm ₀ (m) | Tm ₀₂ (s) | | | | | | | | Total |
|------------------------|----------------------|-------|---------|---------|---------|-------|-------|---------|-------|
| | <2 | 2-2.8 | 2.8-3.6 | 3.6-4.4 | 4.4-5.2 | 5.2-6 | 6-6.8 | 6.8-7.6 | |
| 0-0.5 | 0.70 | 12.80 | 22.11 | 1.55 | 0.06 | 0.01 | 0 | 0 | 37.23 |
| 0.5-1 | 0.50 | 0.41 | 22.10 | 13.13 | 0.34 | 0.01 | 0 | 0 | 36.49 |
| 1-1.5 | 0.08 | 0 | 0.66 | 12.41 | 3.84 | 0.02 | 0 | 0.01 | 17.02 |
| 1.5-2 | 0.01 | 0 | 0 | 1.17 | 4.09 | 0.26 | 0 | 0 | 5.54 |
| 2-2.5 | 0 | 0 | 0 | 0 | 1.51 | 0.63 | 0 | 0 | 2.15 |
| 2.5-3 | 0 | 0 | 0 | 0 | 0.22 | 0.79 | 0.02 | 0 | 1.03 |
| 3-3.5 | 0 | 0 | 0 | 0 | 0 | 0.32 | 0.06 | 0 | 0.38 |

| | | | | | | | | | |
|--------------|------|-------|-------|-------|-------|------|------|------|--------|
| 3.5-4 | 0 | 0 | 0 | 0 | 0 | 0.04 | 0.06 | 0 | 0.10 |
| 4-4.5 | 0 | 0 | 0 | 0 | 0 | 0 | 0.05 | 0 | 0.05 |
| 4.5-5 | 0 | 0 | 0 | 0 | 0 | 0 | 0.01 | 0.01 | 0.02 |
| 5-5.5 | 0 | 0 | 0 | 0 | 0 | 0 | 0 | 0 | 0 |
| Total | 1.30 | 13.21 | 44.86 | 28.26 | 10.05 | 2.08 | 0.20 | 0.03 | 100.00 |

5.1.7.1.2 Monthly Means for the period 2000-2011

The box whiskers charts in Figure 5.1.37, show that wave height minimum monthly mean is in June (0.57 m) while the maximum mean is in February (1.03 m). The smallest recorded wave height is in June (0.015 m) and the maximum is in May (5.37 m). As for wave period, the minimum mean is in June (3.29 s) and the maximum mean in February (3.82 s). Finally, the minimum value for wave period is in June (2.22 s) and the maximum in August (8.83 s).

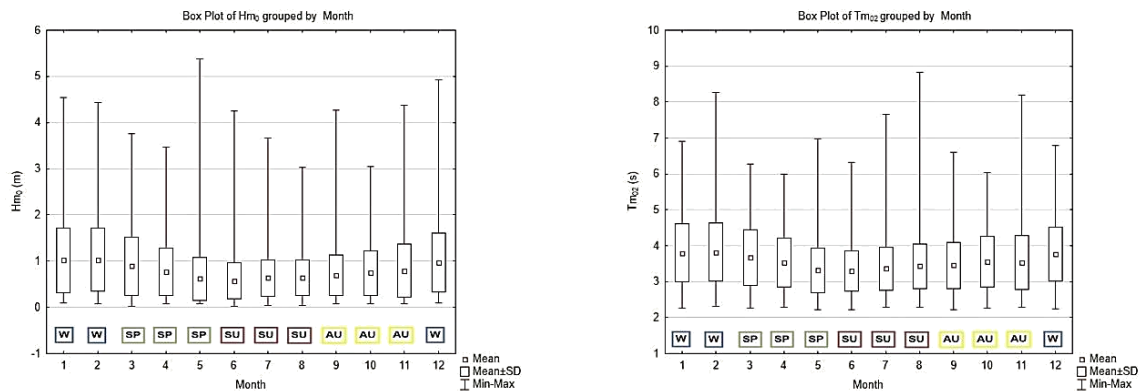


Figure 5.1.37: Box and Whiskers plots for Monthly Wave Height and Wave Period for Lesvos Buoy

5.1.7.2 Weather Characteristics

The atmospheric parameters as given by the buoy of Lesvos for the period 2000-2011, are analysed in this subchapter.

5.1.7.2.1 General Statistics

In Table 5.1.43 are shown the basic statistics of atmospheric parameters. Temperature is described by minimums of -1.19 °C, a maximum of 35.446 °C and a mean of 17.35 °C. Air pressure has a mean of 1014.67 hPa, a min of 980.78 hPa and a max of 1036.88 hPa. Wind speed has a mean of 6 m/s but can reach a max of 26.76 m/s while wind gust has a mean of 7.82 m/s and a max of 35.6 m/s.

Table 5.1.43: Descriptive Statistics of Atmospheric Parameters for Lesvos Buoy

| Parameters | Number of Records | Mean | Minimum | Maximum | Std.Dev. |
|---------------------|-------------------|---------|---------|---------|----------|
| Air Pressure (hPa) | 29081 | 1014.67 | 980.78 | 1036.88 | 6.4 |
| Air Temperature(°C) | 28738 | 17.35 | -1.19 | 35.44 | 5.34 |
| Wind Gust (m/s) | 26642 | 7.82 | 0.017 | 35.6 | 4.3 |
| Wind Speed (m/s) | 26635 | 6.0 | 0.03 | 26.76 | 3.39 |

The wind chart in Figure 5.1.38 gives a description of the dominating winds. Furthermore, the area's most frequent winds are blowing from N (40%). Wind speeds of 4-8 m/s (43.22%) are most common and from those 26.2% is of N to NNE direction. Winds with speeds over 16 m/s have a frequency of occurrence of 0.68% with 55.25% from directions of N.

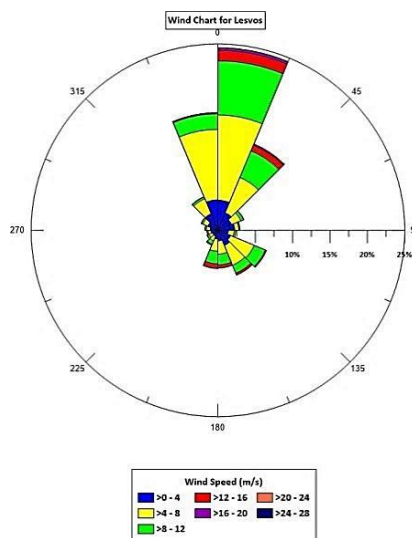
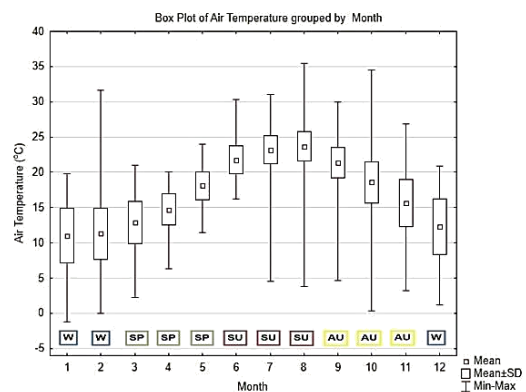
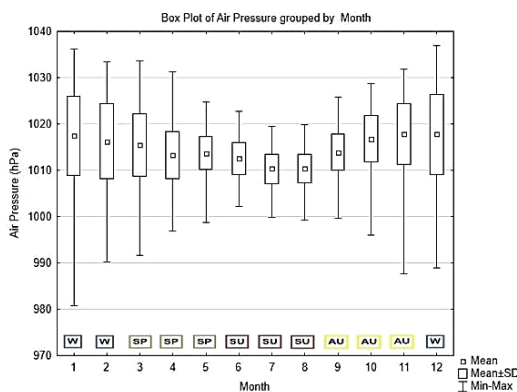


Figure 5.1.38: Wind Chart for Lesvos Buoy

5.1.7.2.2 Monthly Means of the period 2000-2011

The minimum monthly mean value of pressure is in July (1010.28 hPa) and the maximum (1017.89 hPa) in November (Figure 5.1.39).



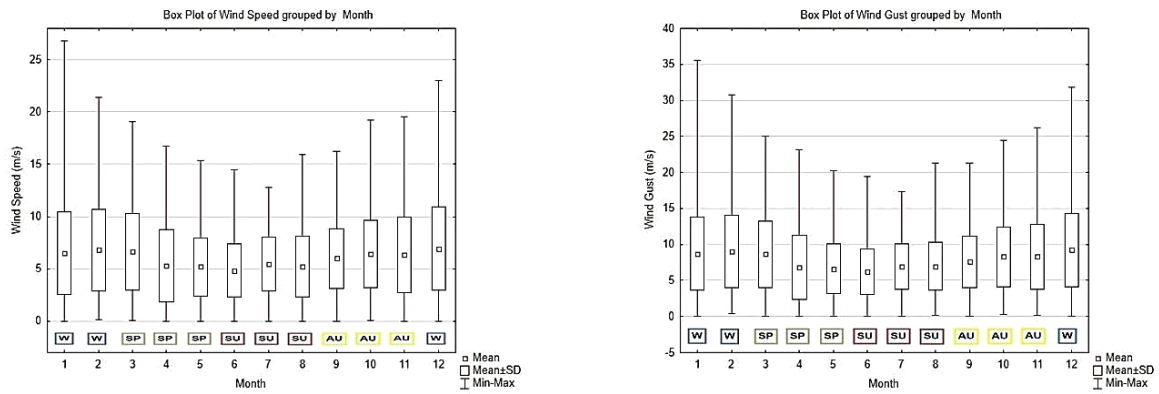


Figure 5.1.39: Monthly Box and Whiskers Plots for Atmospheric Parameters for Lesvos Buoy

Temperature minimum mean monthly value is 11.03 °C in January and the maximum in 23.68 °C during August. As for wind speed and wind gust the minima are in June (4.84 m/s and 6.18 m/s respectively) and the maxima are in December (6.94 m/s and 9.22 m/s).

5.1.7.3 Relation of Wind and Wave Data

An intercomparison of wind and wave data as given from Lesvos buoy for the period 2000-2011 are shown here.

5.1.7.3.1 General Statistics

Basic statistics of atmospheric and wave parameters are shown in Table 5.1.44. The mean value wind speed (6.01 m/s) can be categorized as moderate breeze that will generate small and longer waves with spreaded whitecaps.

Table 5.1.44: Descriptive Statistics of Wave and Atmospheric Parameters for Lesvos Buoy

| Parameters | Number of Records | Mean | Minimum | Maximum | Std.Dev. |
|----------------------|-------------------|---------|---------|---------|----------|
| Air Pressure (hPa) | 23741 | 1014.70 | 980.78 | 1036.88 | 6.55 |
| Air Temperature (°C) | 23741 | 17.14 | -1.19 | 34.61 | 5.40 |
| Wind Gust (m/s) | 23741 | 7.82 | 0.02 | 35.60 | 4.28 |
| Wind Speed (m/s) | 23741 | 6.01 | 0.00 | 26.76 | 3.37 |
| Hm ₀ (m) | 23741 | 0.80 | 0.02 | 5.38 | 0.56 |
| Hm _{0a} (m) | 23741 | 0.04 | 0.00 | 3.06 | 0.07 |
| Hm _{0b} (m) | 23741 | 0.80 | 0.02 | 5.09 | 0.56 |

| | | | | | |
|----------------|-------|-------|-------|-------|------|
| H_{max} (m) | 7717 | 1.27 | 0.23 | 5.94 | 0.79 |
| Tm_{02} (s) | 23741 | 3.55 | 2.23 | 6.97 | 0.72 |
| Tm_{02a} (s) | 23741 | 13.88 | 10.15 | 16.29 | 1.04 |
| Tm_{02b} (s) | 23741 | 3.55 | 2.23 | 6.75 | 0.71 |
| T_p (s) | 23741 | 4.63 | 1.99 | 11.91 | 1.37 |

The frequency table of wind speed and significant wave height in Table 5.1.45 shows that the most frequent waves of 36.77% have heights of 0.5-1 m and 60.28% of these are related with wind speeds of 4-8 m/s. The higher waves (>3.5 m) have a frequency of occurrence of 0.61% with a 65.96% related with speeds greater than 12 m/s.

Table 5.1.45: Frequency Table (%) of Wind Speed and Significant Spectral Wave Height for Lesvos Buoy

| Wind Speed (m/s) | Hm_0 (m) | | | | | | | | | | | Total |
|---------------------|--------------|--------------|--------------|-------------|-------------|-------------|-------------|-------------|-------------|-------------|----------|---------------|
| | 0-0.5 | 0.5-1 | 1-1.5 | 1.5-2 | 2-2.5 | 2.5-3 | 3-3.5 | 3.5-4 | 4-4.5 | 4.5-5 | 5-5.5 | |
| 0-4 | 19.93 | 7.53 | 1.89 | 0.64 | 0.24 | 0.12 | 0.04 | 0.02 | 0.02 | 0.01 | 0 | 30.41 |
| 4-8 | 14.59 | 22.16 | 5.64 | 0.85 | 0.31 | 0.07 | 0.02 | 0.00 | 0.01 | 0 | 0 | 43.66 |
| 8-12 | 1.43 | 6.80 | 8.98 | 3.03 | 0.79 | 0.26 | 0.05 | 0.01 | 0 | 0 | 0 | 21.35 |
| 12-16 | 0.32 | 0.25 | 0.65 | 1.21 | 0.78 | 0.44 | 0.24 | 0.05 | 0.02 | 0 | 0 | 3.96 |
| 16-20 | 0.08 | 0.03 | 0.03 | 0.03 | 0.13 | 0.15 | 0.06 | 0.02 | 0.02 | 0 | 0 | 0.56 |
| 20-24 | 0.02 | 0 | 0 | 0 | 0 | 0 | 0.02 | 0 | 0 | 0 | 0 | 0.04 |
| 24-28 | 0 | 0 | 0 | 0 | 0 | 0 | 0 | 0 | 0 | 0 | 0 | 0.01 |
| Total | 36.37 | 36.77 | 17.19 | 5.76 | 2.26 | 1.04 | 0.42 | 0.10 | 0.06 | 0.02 | 0 | 100.00 |

The charts in Figure 5.1.40 show that the most frequent and highest waves are related with winds blowing from N and the same occurs with the most frequent periods.

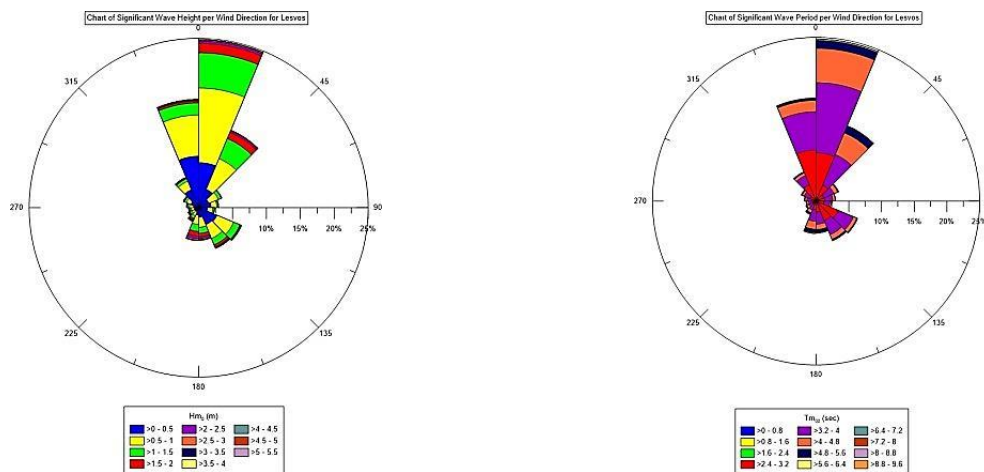


Figure 5.1.40: Charts of Wind Direction and Wave Height - Period for Lesvos Buoy

5.1.8 MYKONOS

Details about the location, depth and time periods of records for Mykonos buoy are shown in Table 5.1.46.

Table 5.1.46: Location, depth of installation & time periods of recording per database for Mykonos

| Location | Depth (m) | Wave Parameters | SSE data | Atmospheric Parameters |
|------------------------|-----------|-----------------------|-----------------------|------------------------|
| 25.46631°E, 37.51831°N | 140 | 01/01/2000-31/12/2011 | 01/01/2007-01/01/2011 | 01/01/2000-31/12/2011 |

5.1.8.1 Wave Characteristics

Information about the wave characteristics as these are provided from Mykonos buoy records is given in this subchapter for the period 2000-2011.

5.1.8.1.1 General Statistics

The descriptive statistics of wave parameters for Mykonos Buoy are shown in Table 5.1.47. Waves are described by a mean height of 1.01 m and max of 5.76 m whilst period has a mean of 3.66 s and a max of 7.73 s.

Swells have mean heights of 0.06 m, max of 3.83 m and periods of 13.43 s (mean) and 20.51 s (max). Wind-waves have heights of 0.99 m, max of 4.67 m and mean periods of 3.65 s and max of 6.9 s. The peak period has a mean of 4.9 s and a max of 12.34 s. Finally, the maximum height has a mean of 1.61 m and a maximum recorded of 8.28 m.

Table 5.1.47: Descriptive Statistics of Wave Parameters for Mykonos Buoy

| Parameters | Number of Records | Mean | Maximum | Std.Dev. |
|----------------|-------------------|-------|---------|----------|
| H_{m0} (m) | 27683 | 1.01 | 5.76 | 0.75 |
| H_{m0a} (m) | 26718 | 0.06 | 3.83 | 0.15 |
| H_{m0b} (m) | 26961 | 0.99 | 4.67 | 0.73 |
| H_{max} (m)* | 10751 | 1.61 | 8.28 | 1.04 |
| T_{m02} (s) | 26600 | 3.66 | 7.73 | 0.83 |
| T_{m02a} (s) | 26357 | 13.43 | 20.51 | 1.23 |
| T_{m02b} (s) | 26961 | 3.65 | 6.90 | 0.82 |
| T_p (s) | 26812 | 4.90 | 12.34 | 1.66 |

*The records of H_{max} are fewer as the buoys recorded the sea surface elevation only for the period 2007-2011

The charts in Figure 5.1.41, show that the main directions (64.96%) of waves are that of NW to N (Fetch length of 335 km) whilst swells have as predominating direction NW to N (48.55% frequency and Fetch length of 220 km). The same pattern applies for period as well.

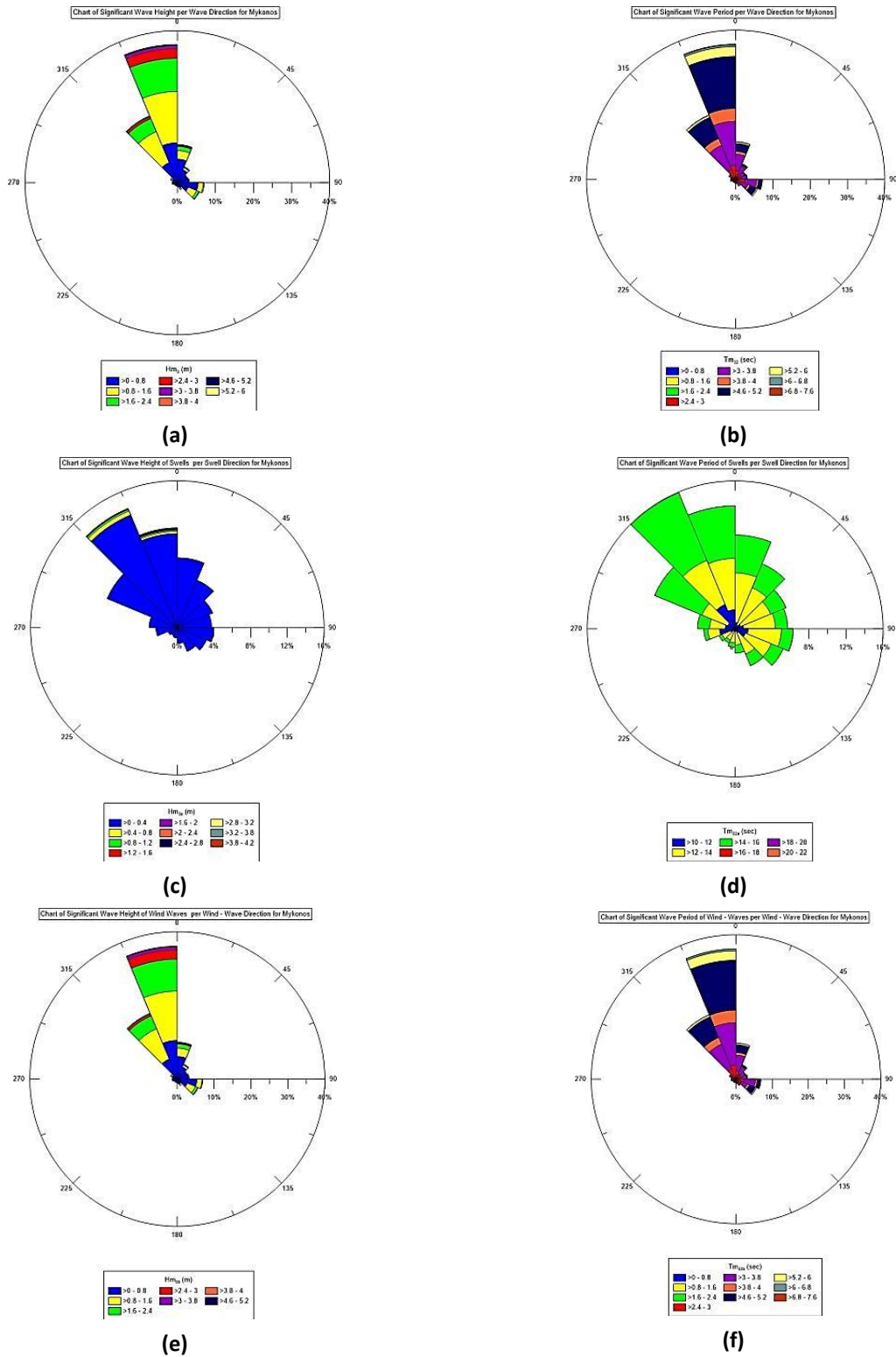


Figure 5.1.41: Rose Diagrams for Significant Wave Height and Wave period for all waves (a,b), swells (c,d) and wind waves (e,f) for Mykonos Buoy

The percentages of appearance of significant wave height according to wave period for Mykonos are given in Table 5.1.48.

Table 5.1.48: Pivot Table for Significant Wave Height and Zero-crossing wave period for Mykonos

| Hm ₀ (m) | Tm ₀₂ (s) | | | | | | | | | |
|---------------------|----------------------|-------|---------|---------|---------|-------|-------|---------|------|--------|
| | <2 | 2-2.8 | 2.8-3.6 | 3.6-4.4 | 4.4-5.2 | 5.2-6 | 6-6.8 | 6.8-7.6 | >7.6 | Total |
| 0-0.8 | 2.18 | 13.22 | 29.48 | 4.20 | 0.23 | 0.01 | 0 | 0 | 0 | 49.32 |
| 0.8-1.6 | 1.32 | 0 | 7.53 | 19.74 | 1.64 | 0.10 | 0 | 0 | 0 | 30.34 |
| 1.6-2.4 | 0.69 | 0 | 0 | 2.86 | 10.76 | 0.50 | 0.01 | 0 | 0 | 14.82 |
| 2.4-3.2 | 0.39 | 0 | 0 | 0 | 0.97 | 2.99 | 0.06 | 0 | 0 | 4.40 |
| 3.2-4 | 0.09 | 0 | 0 | 0 | 0 | 0.26 | 0.50 | 0.01 | 0 | 0.86 |
| 4-4.8 | 0.01 | 0 | 0 | 0 | 0 | 0 | 0.08 | 0.10 | 0 | 0.19 |
| 4.8-5.6 | 0 | 0 | 0 | 0 | 0 | 0 | 0 | 0.05 | 0 | 0.05 |
| 5.6-6.4 | 0 | 0 | 0 | 0 | 0 | 0 | 0 | 0 | 0.01 | 0.01 |
| Total | 4.67 | 13.22 | 37.01 | 26.81 | 13.60 | 3.87 | 0.65 | 0.17 | 0.01 | 100.00 |

The most frequent waves (49.32%) are those with height from 0 to 0.8m with 59.77% described with periods of 2.8 to 3.6 s. The highest waves (>4 m) have a frequency of 61.43% related with periods of 6.8-7.6 s.

5.1.8.1.2 Monthly Means for the period 2000-2011

The box and whisker plots of Figure 5.1.42 show the variation of the wave parameters. The minimum monthly mean is in May (0.76 m) while the maximum monthly mean is in December (1.19 m). The minimum recorded value is in May (0.05 m) and the maximum is in February (5.76 m). As for the wave period, the minimum mean monthly is in May (3.38 s) and the maximum monthly mean in December (3.92 s). The overall minimum value for wave period is in March (2.21 s) and the maximum in January (7.73 s).

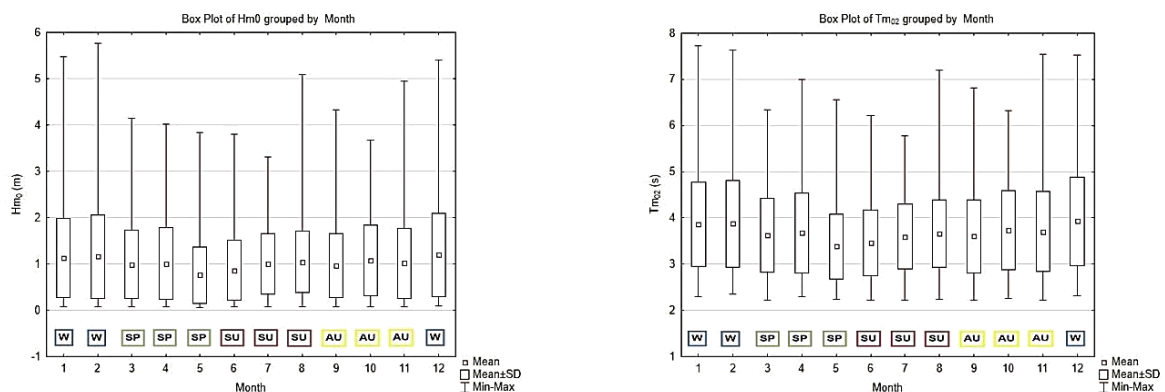


Figure 5.1.42: Box and Whiskers plots for Monthly Wave Height and Wave Period for Mykonos

5.1.8.2 Sea Surface Elevation (SSE)

For this subchapter, results of 7457 sea surface elevation records of Mykonos buoy are shown. An example of a SSE record is shown in Figure 5.1.43. For the specific example, the peak period of the Spectrum (T_p) can be estimated (10.1 s).

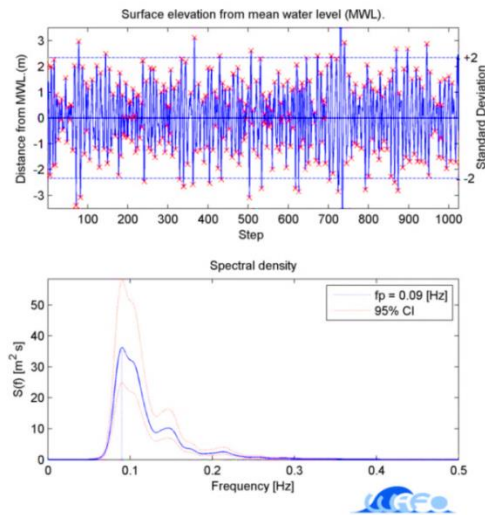


Figure 5.1.43: Random SSE record and its spectrum for Mykonos Buoy

5.1.8.2.1 General Statistics

Basic statistics of wave characteristics are shown in

Table 5.1.49 as derived from 7457 records of sea surface elevation analysis. The spectral wave height has a mean of 1.13 m and a max of 5.52 m while the statistical has a mean of 1.04 m and a max of 5.29 m. The maximum wave height has a mean of 1.72 m while it can reach a maximum of 8.19 m. The spectral wave period has a mean of 3.8 s and a max of 7.69 s while the statistical has a mean of 5.39 s and a max of 10.8 s. The peak period is described by a mean of 5.16 s and a max of 11.54 s.

Table 5.1.49: Descriptive Statistics as derived from SSE Analysis for Mykonos Buoy

| Parameters | Number of Records | Mean | Maximum | Std.Dev. |
|------------------|-------------------|------|---------|----------|
| H_{m_0} (m) | 7457 | 1.13 | 5.52 | 0.65 |
| H_{max} (m) | 7457 | 1.72 | 8.19 | 1.01 |
| $H_{1/3}$ (m) | 7457 | 1.04 | 5.29 | 0.63 |
| $T_{m_{02}}$ (s) | 7457 | 3.80 | 7.69 | 0.76 |
| $T_{1/3}$ (s) | 7457 | 5.39 | 10.80 | 1.08 |

| | | | | |
|-----------|------|------|-------|------|
| T_p (s) | 7457 | 5.16 | 11.54 | 1.46 |
|-----------|------|------|-------|------|

For the Mykonos buoy, the correlation coefficient (r) is 0.99 for H_{m0} and $H_{1/3}$ and 0.95 for T_{m02} and $T_{1/3}$ (Figure 5.1.44).

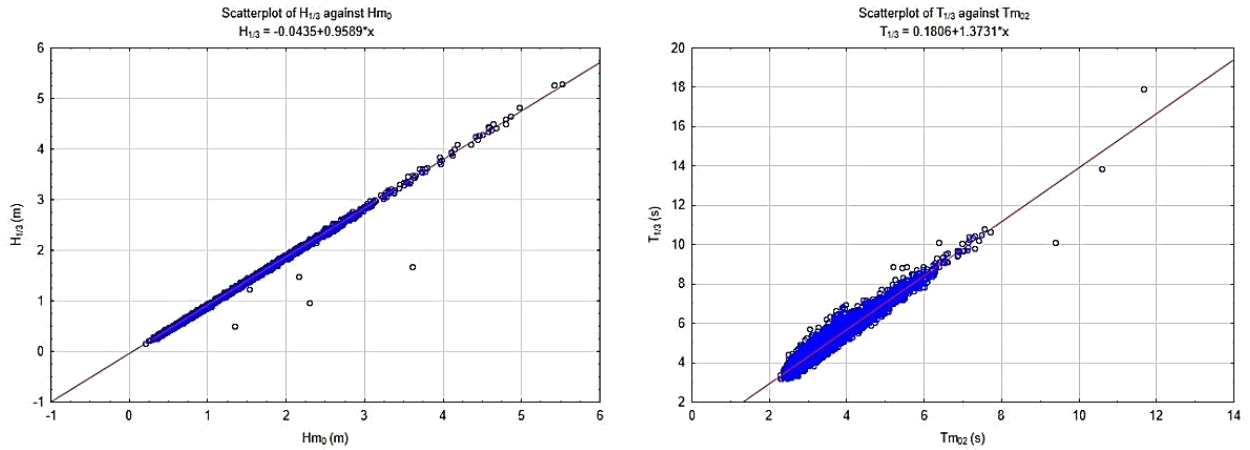
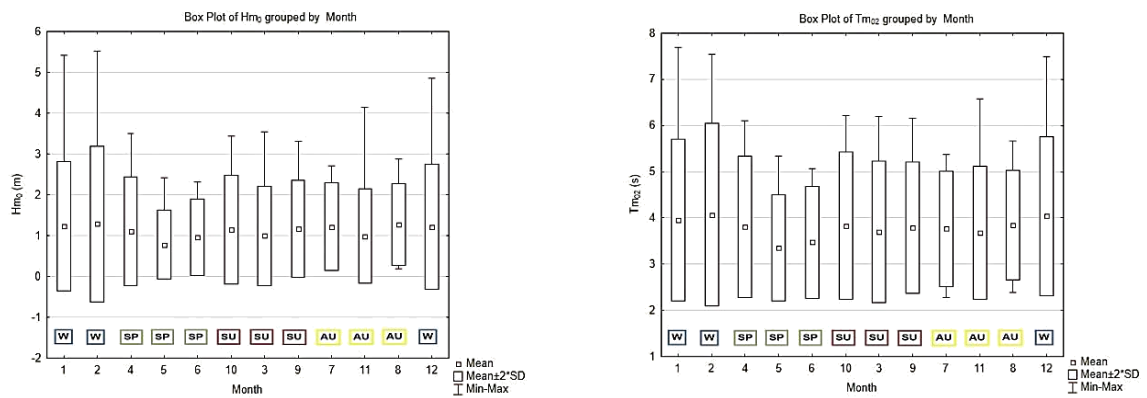


Figure 5.1.44: Scatterplots of statistical and spectral wave parameters for Mykonos Buoy

5.1.8.2.2 Monthly Means for the period 2000-2011

The monthly means for the period 2000-2011 for the wave parameters are given in Figure 5.1.45.



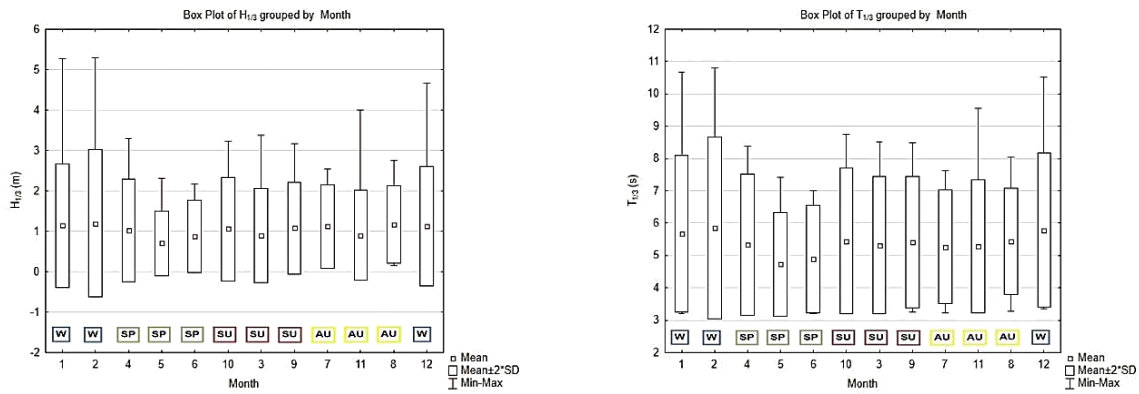


Figure 5.1.45: Spectral and Statistical Monthly Values per Wave Parameter for Mykonos Buoy

The spectral significant wave height H_{m0} , the minimum mean monthly value is in May (0.78 m), the maximum mean in February (1.28 m) while the minimum value recorded is in 0.19 m (August) and the maximum 5.52 m (February).

The spectral wave period (T_{m02}), shows a mean minimum monthly value in May (3.36 s) and a maximum in February (4.07 s). The minimum is 2.28 s (July) and the maximum 11.67 s (September). The statistical significant wave height $H_{1/3}$, presented the smallest monthly value in May (0.7 m) whilst the largest (1.19 m) is in February. The smallest overall value is 0.15 m (August) and the maximum (5.28 m) in February. The statistical significant wave period $T_{1/3}$ had a minimum monthly mean of 4.73 s on May and a maximum 5.85 s in February. Finally, the minimum recorded period is 3.2 s (October) and the maximum 17.91 s in September.

5.1.8.2.3 Probability Distribution of Wave Height

For Mykonos, Kumaraswamy distribution is in the top 3 probability distributions of wave height. In Figure 5.1.46, probability distributions of Weibull, Rayleigh and Kumaraswamy as well as the relevant QQ plots are shown. In this case, Kumaraswamy distribution underestimates the larger values of wave heights whilst Weibull and Rayleigh distribution overestimate them.

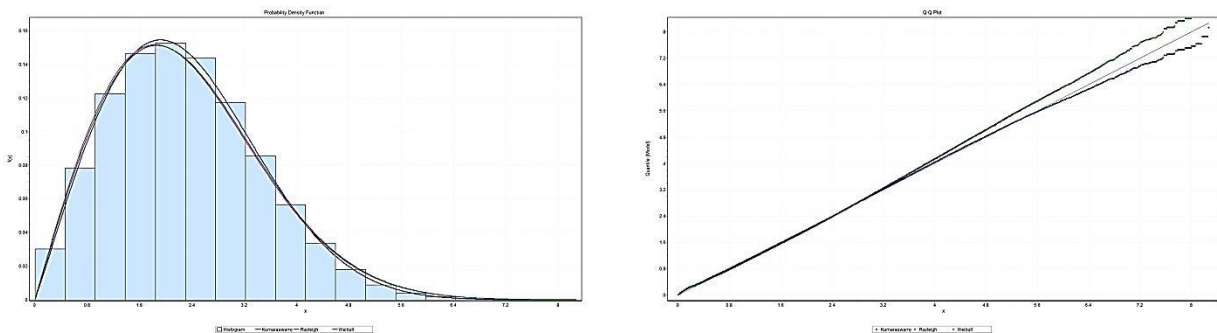


Figure 5.1.46: Probability Distributions and QQ plots for Mykonos for random wave heights

The statistics of goodness of fit for every distribution under examination are shown in Table 5.1.50.

Table 5.1.50: Statistics of Goodness of Fits according to K-S, A-D and χ^2 test for Mykonos Buoy

| Distribution | Kolmogorov Smirnov | Anderson Darling | Chi-Squared |
|--------------|--------------------|------------------|-------------|
| | Statistic | Statistic | Statistic |
| Kumaraswamy | 0.007 | 19.13 | 123.1 |
| Weibull | 0.015 | 128.08 | 931.64 |
| Rayleigh | 0.017 | 161.85 | 1022.3 |

5.1.8.2.4 Ratios between Statistical and Spectral Parameters

Mean values of the ratios among spectral and statistical parameters for Mykonos are shown in Table 5.1.51. A mean of 1.10 is given for the spectral and statistical wave height, 3.65 for the ratio of $H_{1/3} / \sqrt{m_0}$, 1.56 for H_{max} / H_{m0} and 1.70 $H_{max} / H_{1/3}$.

Table 5.1.51: Statistics of various Ratios for Mykonos Buoy

| Ratios | Number of Records | Mean | Minimum | Maximum | Std.Dev. |
|------------------------|-------------------|------|---------|---------|----------|
| H_{m0} / H_{13} | 7454 | 1.10 | 1.00 | 1.34 | 0.04 |
| $H_{1/3} / \sqrt{m_0}$ | 7454 | 3.65 | 2.97 | 3.98 | 0.14 |
| H_{max} / H_{m0} | 7454 | 1.56 | 1.18 | 5.56 | 0.16 |
| $H_{max} / H_{1/3}$ | 7454 | 1.70 | 1.29 | 7.40 | 0.19 |

5.1.8.3 Weather Characteristics

The atmospheric characteristics of the area of Mykonos are shown in this session for the period 2000-2011.

5.1.8.3.1 General Statistics

The main statistics of atmospheric parameters for Mykonos are shown in Table 5.1.52. A minimum temperature of 0.13 °C, a maximum of 41.86 °C and a mean of 18.6 °C are estimated. Pressure has a mean of 1013.23 hPa, a min of 875 hPa and a max of 1035.88 hPa. Finally, wind speed has a mean of 6.81 m/s and a max of 18.85 m/s while gust has a mean of 8.83 m/s and a max of 32.11 m/s.

Table 5.1.52: Descriptive Statistics of Atmospheric Parameters for Mykonos Buoy

| Parameters | Number of Records | Mean | Minimum | Maximum | Std.Dev. |
|---------------------|-------------------|---------|---------|---------|----------|
| Air Pressure(hPa) | 27899 | 1013.23 | 875.00 | 1035.88 | 6.80 |
| Air Temperature(°C) | 27303 | 18.60 | 0.13 | 41.86 | 4.88 |
| Wind Gust (m/s) | 26457 | 8.83 | 0.00 | 32.11 | 4.43 |
| Wind Speed (m/s) | 26390 | 6.81 | 0.00 | 18.85 | 3.52 |

The wind chart of Figure 5.1.47 shows the directionality of the most frequent waves to be of NW to N (62.32%). The most frequent winds have wind speeds of 4 m/s to 8 m/s (35.99%) of which 29.82% are of NW direction. Winds above 16 m/s are of 0.24% frequency and 61.9% is of the range NW to N.

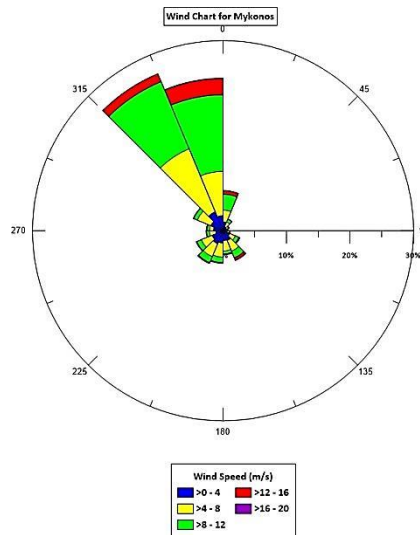


Figure 5.1.47: Wind Chart for Mykonos Buoy

5.1.8.3.2 Monthly Means for the period 2000-2011

The minimum mean monthly value is in August (1007.75 hPa) and the maximum (1018.05 hPa) in January (Figure 5.1.48). As for the temperature the minimum mean monthly 12.32 °C in February and the maximum in 24.81 °C during August. The minimum values of wind speed and wind gust are in May (5.51 m/s and 7.12 m/s respectively) and the maximum are in February (7.41 m/s and 10 m/s).

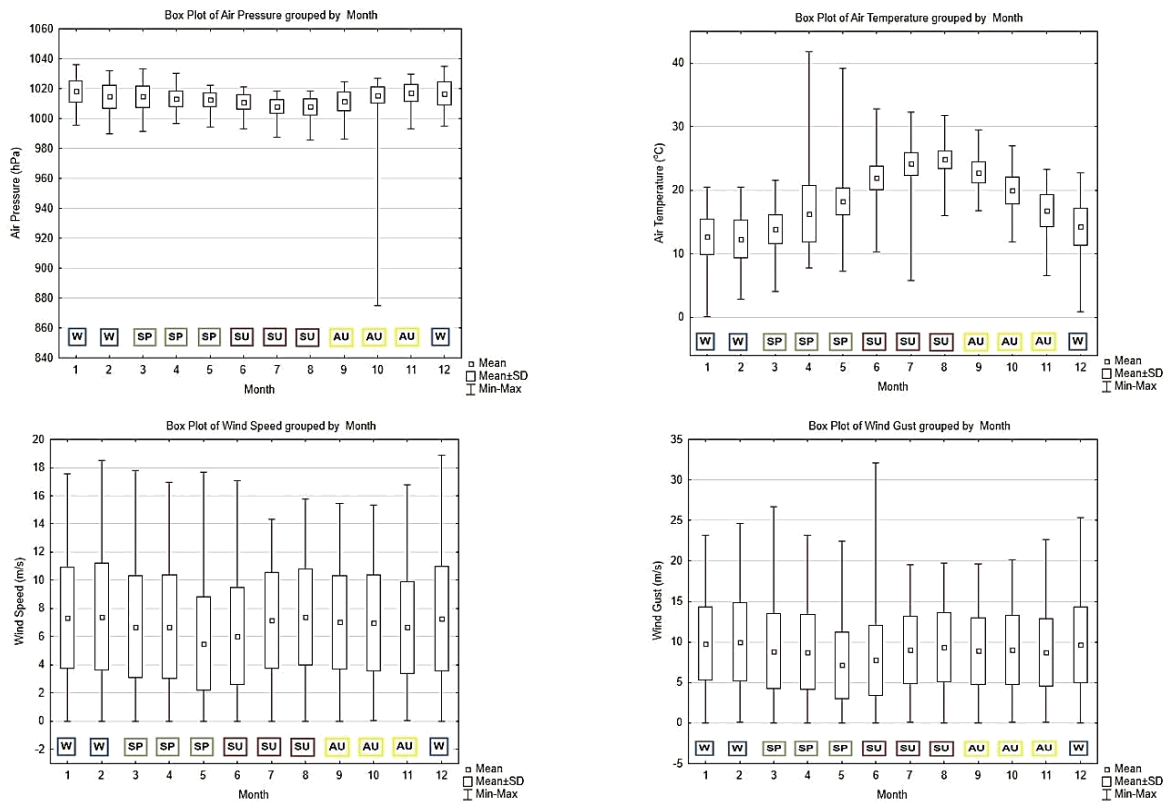


Figure 5.1.48: Monthly Box and Whiskers Plots for Atmospheric Parameters for Mykonos Buoy

5.1.8.4 Relation of Wind and Wave Data

5.1.8.4.1 General Statistics

The mean value wind speed (6.87 m/s) can be considered as moderate breeze that will generate small and longer waves with spreaded whitecaps (Table 5.1.53).

Table 5.1.53: Descriptive Statistics of Wave and Atmospheric Parameters for Mykonos Buoy

| Parameters | Number of Records | Mean | Minimum | Maximum | Std.Dev. |
|-----------------------|-------------------|---------|---------|---------|----------|
| Air Pressure (hPa) | 21236 | 1013.43 | 875.00 | 1033.53 | 6.51 |
| Air Temperature (°C) | 21236 | 18.93 | 0.13 | 41.86 | 4.95 |
| Wind Gust (m/s) | 21236 | 8.92 | 0.00 | 25.37 | 4.41 |
| Wind Speed (m/s) | 21236 | 6.87 | 0.00 | 18.85 | 3.51 |
| Hm ₀ (m) | 21236 | 1.03 | 0.05 | 5.76 | 0.76 |
| Hm _{0a} (m) | 21236 | 0.06 | 0.00 | 3.83 | 0.16 |
| Hm _{0b} (m) | 21236 | 1.03 | 0.05 | 4.67 | 0.74 |
| Tm ₀₂ (s) | 21236 | 4.20 | 0.00 | 29.99 | 2.57 |
| Tm _{02a} (s) | 21236 | 131.27 | 0.00 | 359.91 | 146.02 |
| Tm _{02b} (s) | 21236 | 3.78 | 2.24 | 8.32 | 0.89 |
| T _p (s) | 21236 | 4.26 | 2.02 | 12.34 | 1.43 |

As given in Table 5.1.54, the most frequent waves of 48.66% have heights of 0-08 m and 43.47% of these are related with wind speeds of 3-6 m/s. The higher waves (>4 m) have a frequency of 0.26% are related with speeds of more than 12m/s.

Table 5.1.54: Frequency Table (%) of Wind Speed and Significant Spectral Wave Height for Mykonos Buoy

| Wind Speed (m/s) | Hm ₀ (m) | | | | | | | | Total |
|---------------------|---------------------|--------------|--------------|-------------|-------------|-------------|-------------|-------------|---------------|
| | 0-0.8 | 0.8-1.6 | 1.6-2.4 | 2.4-3.2 | 3.2-4 | 4-4.8 | 4.8-5.6 | 5.6-6.4 | |
| 0-3 | 16.33 | 0.55 | 0.04 | 0 | 0 | 0 | 0 | 0 | 16.92 |
| 3-6 | 21.16 | 3.51 | 0.18 | 0.01 | 0.01 | 0 | 0 | 0 | 24.87 |
| 6-9 | 9.90 | 16.41 | 1.86 | 0.10 | 0.01 | 0 | 0 | 0 | 28.28 |
| 9-12 | 1.24 | 9.76 | 10.65 | 1.87 | 0.17 | 0 | 0 | 0 | 23.69 |
| 12-15 | 0.05 | 0.67 | 2.17 | 2.12 | 0.50 | 0.06 | 0 | 0 | 5.56 |
| 15-18 | 0 | 0.05 | 0.13 | 0.17 | 0.14 | 0.13 | 0.05 | 0 | 0.66 |
| 18-21 | 0 | 0 | 0 | 0 | 0 | 0 | 0.01 | 0 | 0.02 |
| Total | 48.66 | 30.94 | 15.03 | 4.27 | 0.83 | 0.19 | 0.06 | 0.01 | 100.00 |

The charts in Figure 5.1.49 show that the highest and the most frequent waves (61.67%) are related with winds blowing from NW to N and this applies for the most frequent periods.

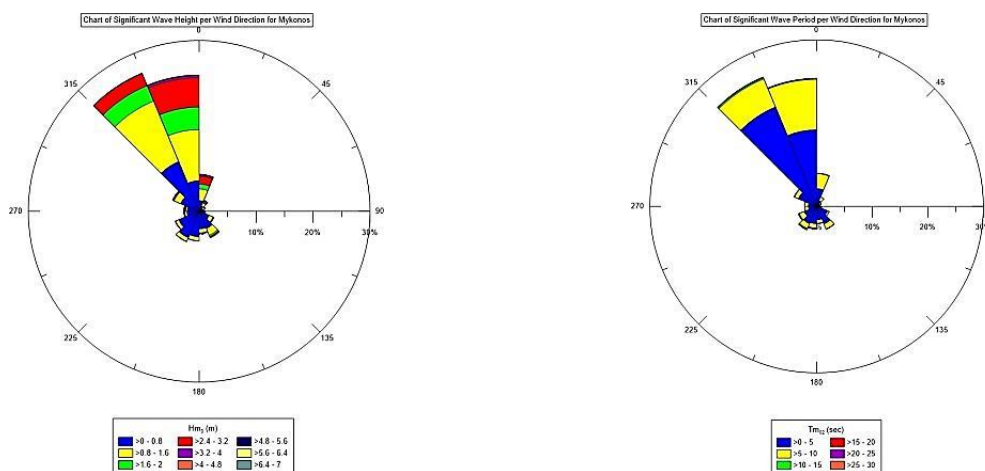


Figure 5.1.49: Charts of Wind Direction and Wave Height - Period for Mykonos Buoy

5.1.9 PETROKARAVO

Information about the location, depth and time periods of records for Petrokaravo buoy are shown in Table 5.1.55.

Table 5.1.55: Location, depth of installation & time periods of recording per database for Petrokaravo Buoy

| Location | Depth (m) | Wave Parameters | SSE data | Atmospheric Parameters |
|----------|-----------|-----------------|----------|------------------------|
|----------|-----------|-----------------|----------|------------------------|

| | | | | |
|-----------------------|-----|-----------------------|----|-----------------------|
| 23.56689°E 37.60742°N | 211 | 01/01/2000-31/12/2011 | -- | 28/08/2007-31/12/2011 |
|-----------------------|-----|-----------------------|----|-----------------------|

5.1.9.1 Wave Characteristics

The wave characteristics as presented from the records of the buoy for the period 2000-2011 are shown in this session.

5.1.9.1.1 General Statistics

The basic statistics of wave parameters for Petrokaravo are given Table 5.1.56. The waves have mean heights of 0.5 m that can reach 3.13 m and periods of 3.22 s and max 5.98 s. The swells have mean heights of 0.02 m and max of 0.31 m, whilst periods have means of 11.45 s and max of 17.19 s. The wind waves have mean heights of 0.5 m, max of 3.05 m and period with mean of 3.22 s and max of 5.86 s. The peak period can reach a mean of 4.21 s and max of 24.97 s while max wave height can have a mean of 0.54 m and a max of 5.31 m.

Table 5.1.56: Descriptive Statistics of Wave Parameters for Petrokaravo Buoy

| Parameters | Number of Records | Mean | Maximum | Std.Dev. |
|-----------------------|-------------------|-------|---------|----------|
| Hm ₀ (m) | 9645 | 0.50 | 3.13 | 0.30 |
| Hm _{0a} (m) | 9708 | 0.02 | 0.31 | 0.03 |
| Hm _{0b} (m) | 9361 | 0.50 | 3.05 | 0.30 |
| Hmax (m)* | 9645 | 0.54 | 5.31 | 0.51 |
| Tm ₀₂ (s) | 9717 | 3.22 | 5.98 | 0.48 |
| Tm _{02a} (s) | 9629 | 11.45 | 17.19 | 3.52 |
| Tm _{02b} (s) | 8995 | 3.22 | 5.86 | 0.48 |
| T _p (s) | 9717 | 4.21 | 24.97 | 1.71 |

As shown in the charts of Figure 5.1.50, the most frequent waves are coming from of N to NE (43.72% and Fetch length of 33 km), and SE (25.15%) and swells have as predominating direction E to SE (Fetch length 126 km, frequency 45.46%). The heights of waves greater than 2.1 m are from SE the same for swells. Same patterns apply for periods of swells and wind-waves.

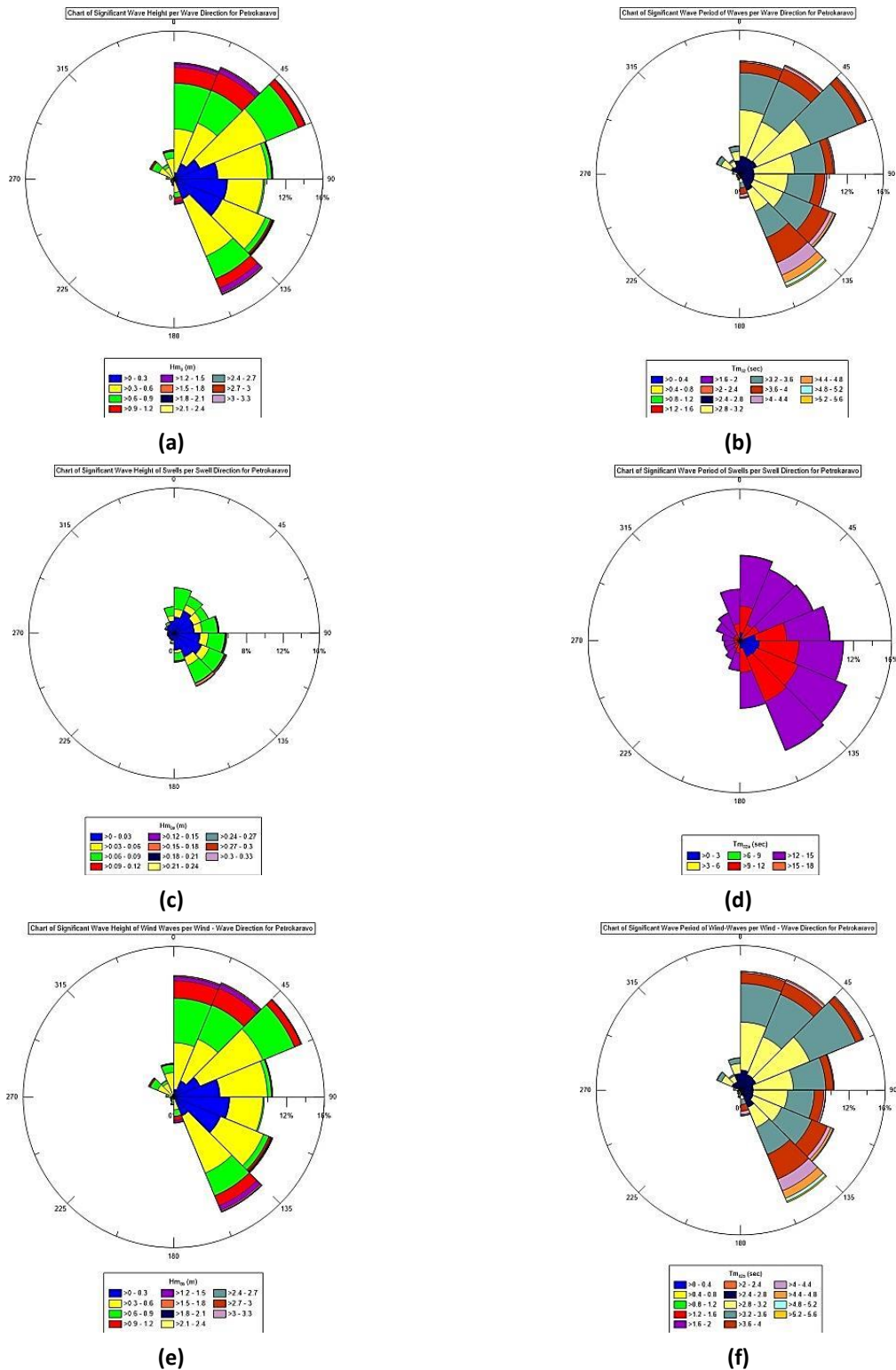


Figure 5.1.50: Rose Diagrams for Significant Wave Height and Wave period for all waves (a,b), swells (c,d) and wind waves (e,f) for Petrokaravo Buoy

In Table 5.1.57, the percentages of appearance of significant wave height relative to wave period are given. The most frequent waves (45.23%) are those with height from 0.3 to 0.6 m with the majority of them (42.98%) described with periods of 2.8 to 3.2 s. The highest waves (>1.8 m) have a frequency of 0.29% with periods of more than 4 s.

Table 5.1.57: Pivot Table for Significant Wave Height and Zero-crossing wave period for Petrokaravo Buoy

| Hm ₀ (m) | Tm ₀₂ (s) | | | | | | | | | | Total |
|------------------------|----------------------|---------|---------|---------|-------|-------|---------|---------|---------|-------|--------|
| | 2-2.4 | 2.4-2.8 | 2.8-3.2 | 3.2-3.6 | 3.6-4 | 4-4.4 | 4.4-4.8 | 4.8-5.2 | 5.2-5.6 | 5.6-6 | |
| 0-0.3 | 0.15 | 5.13 | 8.11 | 8.10 | 3.03 | 0.54 | 0.17 | 0.01 | 0 | 0 | 25.23 |
| 0.3-0.6 | 0.15 | 12.13 | 19.44 | 9.00 | 3.54 | 0.63 | 0.25 | 0.09 | 0 | 0 | 45.23 |
| 0.6-0.9 | 0 | 0.07 | 7.04 | 9.63 | 1.80 | 0.63 | 0.41 | 0.06 | 0.02 | 0 | 19.68 |
| 0.9-1.2 | 0 | 0 | 0.02 | 4.13 | 2.15 | 0.33 | 0.29 | 0.12 | 0.04 | 0 | 7.08 |
| 1.2-1.5 | 0 | 0 | 0 | 0.02 | 0.89 | 0.58 | 0.31 | 0.15 | 0.07 | 0 | 2.02 |
| 1.5-1.8 | 0 | 0 | 0 | 0 | 0.04 | 0.27 | 0.08 | 0.05 | 0.02 | 0.01 | 0.48 |
| 1.8-2.1 | 0 | 0 | 0 | 0 | 0 | 0.01 | 0.07 | 0.04 | 0.03 | 0.01 | 0.17 |
| 2.1-2.4 | 0 | 0 | 0 | 0 | 0 | 0 | 0 | 0.03 | 0.02 | 0 | 0.05 |
| 2.4-2.7 | 0 | 0 | 0 | 0 | 0 | 0 | 0 | 0 | 0 | 0.02 | 0.02 |
| 2.7-3 | 0 | 0 | 0 | 0 | 0 | 0 | 0 | 0 | 0.01 | 0.03 | 0.04 |
| 3-3.3 | 0 | 0 | 0 | 0 | 0 | 0 | 0 | 0 | 0 | 0.01 | 0.01 |
| Total | 0.29 | 17.34 | 34.61 | 30.88 | 11.45 | 3.00 | 1.59 | 0.56 | 0.22 | 0.08 | 100.00 |

5.1.9.1.2 Monthly Means for the period 2000-2011

The minimum monthly mean of wave height is in May (0.34 m) while the in January (0.65 m) as shown in Figure 5.1.51. The smallest recorded wave height is in May (0.078 m) and the maximum in December (3.12 m). The minimum mean value of wave period is in September (3.07 s) and the maximum mean in January (3.43 s). The minimum recorded value of wave period is in January (2.22 s) and the maximum in December (5.98 s).

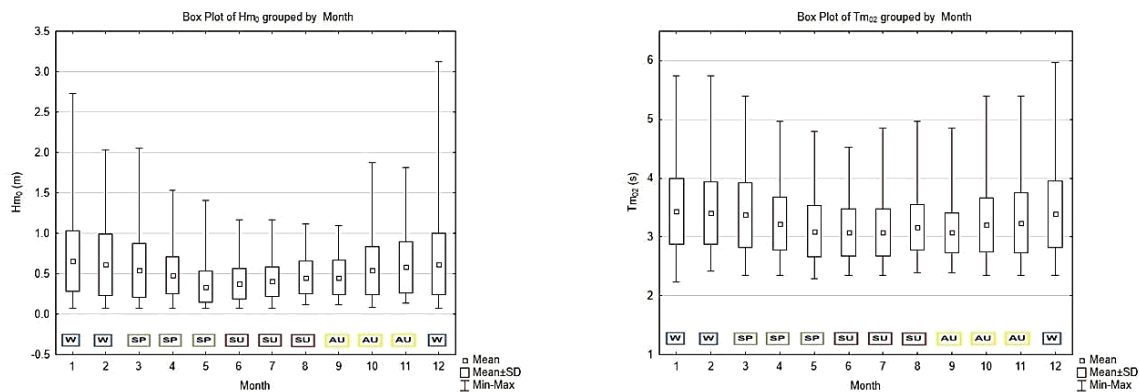


Figure 5.1.51: Box and Whiskers plots for Monthly Wave Height and Wave Period for Petrokaravo Buoy

5.1.9.2 Weather Characteristics

Weather characteristics of the area of Petrokaravo for the period 2007-2011 are shown in this session.

5.1.9.2.1 General Statistics

A minimum in temperature of 0.62 °C and a maximum of 41.53 °C, a mean wind speed of 4.73 m/s characterize the area as shown in Table 5.1.58.

Table 5.1.58: Descriptive Statistics of Atmospheric Parameters for Petrokaravo Buoy

| Parameters | Number of Records | Mean | Minimum | Maximum | Std.Dev. |
|---------------------|-------------------|---------|---------|---------|----------|
| Air Pressure (hPa) | 9792 | 1012.82 | 985.84 | 1034.98 | 6.63 |
| Air Temperature(°C) | 9791 | 19.52 | 0.62 | 41.53 | 6.28 |
| Wind Gust (m/s) | 9624 | 6.21 | 0.12 | 21.56 | 3.44 |
| Wind Speed (m/s) | 9609 | 4.73 | 0.01 | 16.41 | 2.77 |

The area of Petrokaravo is dominated by winds blowing from N (27.27%) and SE (12.04%) as shown in the wind chart of Figure 5.1.52. The most frequent winds have speeds of 2-4 m/s (26.53%) and from those 18.71% is of SE direction. Winds with speeds over 12 m/s have a frequency of occurrence of 0.82% with 49.37% with directions of N.

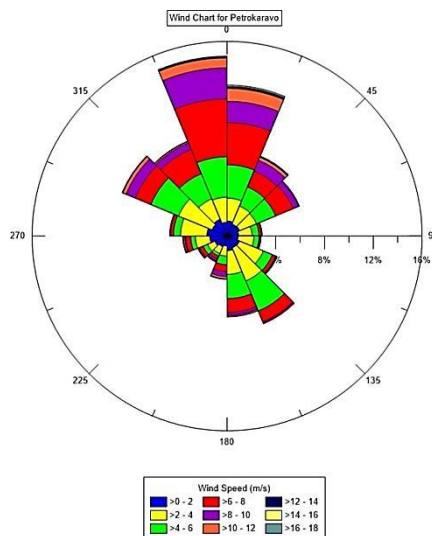


Figure 5.1.52: Wind Chart for Petrokaravo Buoy

5.1.9.2.2 Monthly Means for the period 2007-2011

Monthly means for the atmospheric parameters for the period 2007-2011 are shown in (Figure 5.1.53).

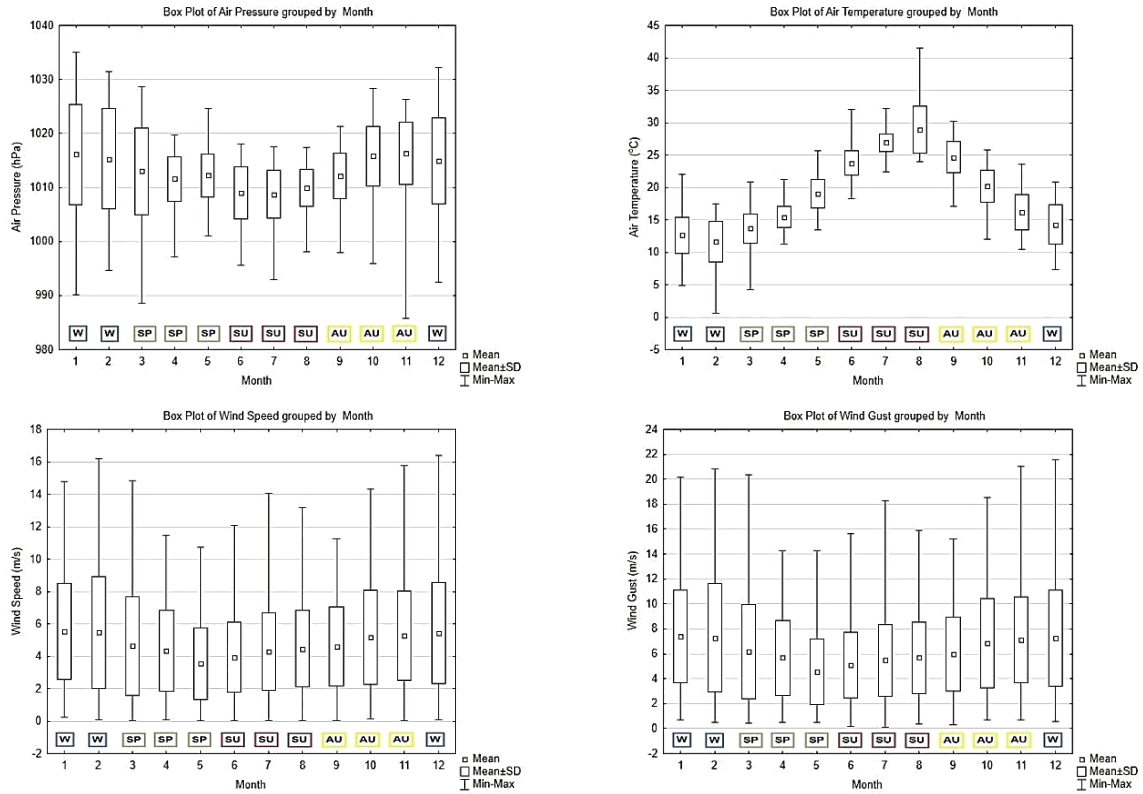


Figure 5.1.53: Monthly Box and Whiskers Plots for Atmospheric Parameters for Petrokaravo Buoy

For pressure the minimum value is in July (1008.74 hPa) and the maximum (1016.3 hPa) in November. The minimum mean monthly temperature 11.61 °C in February and the maximum in 28.89 °C during August. Minimum values of wind speed and wind gust are in May (3.53 m/s and 4.55 m/s respectively) and the maximum are in December (5.55 m/s and 7.38 m/s).

5.1.9.3 Relation of Wind and Wave Data

The relation between wind and wave data only for the same dates is shown here.

5.1.9.3.1 General Statistics

Descriptive statistics of atmospheric and wave parameters are given in Table 5.1.59. The mean value wind speed (4.75 m/s) can be categorized as gentle breeze that will generate small wave crests with isolated whitecaps.

Table 5.1.59: Descriptive Statistics of Wave and Atmospheric Parameters for Petrokaravo Buoy

| Parameters | Number of Records | Mean | Minimum | Maximum | Std.Dev. |
|-----------------------|-------------------|---------|---------|---------|----------|
| Air Pressure (hPa) | 8695 | 1012.94 | 985.84 | 1034.98 | 6.81 |
| Air Temperature (°C) | 8695 | 19.60 | 0.62 | 41.53 | 6.48 |
| Wind Gust (m/s) | 8695 | 6.26 | 0.41 | 21.56 | 3.44 |
| Wind Speed (m/s) | 8695 | 4.75 | 0.01 | 16.41 | 2.77 |
| Hm ₀ (m) | 8695 | 0.51 | 0.08 | 3.13 | 0.30 |
| Hm _{0a} (m) | 8695 | 0.02 | 0.00 | 0.31 | 0.03 |
| Hm _{0b} (m) | 8695 | 0.51 | 0.08 | 3.05 | 0.30 |
| H _{max} (m) | 8695 | 0.56 | 0.00 | 5.31 | 0.51 |
| Tm ₀₂ (s) | 8695 | 3.22 | 2.23 | 5.98 | 0.48 |
| Tm _{02a} (s) | 8695 | 11.44 | 1.17 | 17.19 | 3.54 |
| Tm _{02b} (s) | 8695 | 3.21 | 2.23 | 5.86 | 0.48 |
| T _p (s) | 8695 | 4.20 | 1.14 | 24.97 | 1.70 |

The most frequent waves of 45.54% have heights of 0.3-0.6m and 35.89% of these are related with wind speeds of 4-6 m/s. The higher waves (>1.8m) have a frequency of 0.3% with 78.57% of them related with speeds more than 10m/s.

Table 5.1.60: Frequency Table (%) of Wind Speed and Significant Spectral Wave Height for Petrokaravo

| Wind Speed (m/s) | Hm ₀ (m) | | | | | | | | | | | |
|------------------|---------------------|---------|---------|---------|---------|---------|---------|---------|---------|-------|-------|--------|
| | 0-0.3 | 0.3-0.6 | 0.6-0.9 | 0.9-1.2 | 1.2-1.5 | 1.5-1.8 | 1.8-2.1 | 2.1-2.4 | 2.4-2.7 | 2.7-3 | 3-3.3 | Total |
| 0-2 | 11.10 | 6.88 | 0.64 | 0.14 | 0 | 0.01 | 0 | 0 | 0 | 0 | 0 | 18.78 |
| 2-4 | 11.19 | 13.76 | 1.31 | 0.22 | 0.06 | 0 | 0 | 0 | 0 | 0 | 0 | 26.54 |
| 4-6 | 2.11 | 16.34 | 3.89 | 0.48 | 0.14 | 0.02 | 0.00 | 0.00 | 0.01 | 0 | 0 | 22.99 |
| 6-8 | 0.07 | 8.05 | 9.26 | 1.55 | 0.25 | 0.04 | 0.02 | 0.01 | 0 | 0 | 0 | 19.26 |
| 8-10 | 0 | 0.50 | 4.40 | 2.92 | 0.59 | 0.06 | 0.01 | 0.01 | 0 | 0 | 0 | 8.49 |
| 10-12 | 0 | 0 | 0.47 | 1.68 | 0.72 | 0.19 | 0.03 | 0.01 | 0.01 | 0.02 | 0.00 | 3.13 |
| 12-14 | 0 | 0 | 0 | 0.17 | 0.25 | 0.11 | 0.03 | 0.02 | 0 | 0 | 0 | 0.58 |
| 14-16 | 0 | 0 | 0 | 0.03 | 0.04 | 0.04 | 0.06 | 0 | 0 | 0.02 | 0 | 0.20 |
| 16-18 | 0 | 0 | 0 | 0 | 0 | 0.01 | 0.01 | 0 | 0 | 0 | 0.01 | 0.03 |
| Total | 24.47 | 45.54 | 19.97 | 7.19 | 2.06 | 0.48 | 0.17 | 0.05 | 0.02 | 0.04 | 0.01 | 100.00 |

The most frequent waves (height and period) are related with winds blowing from N while the highest with winds blowing from SE.

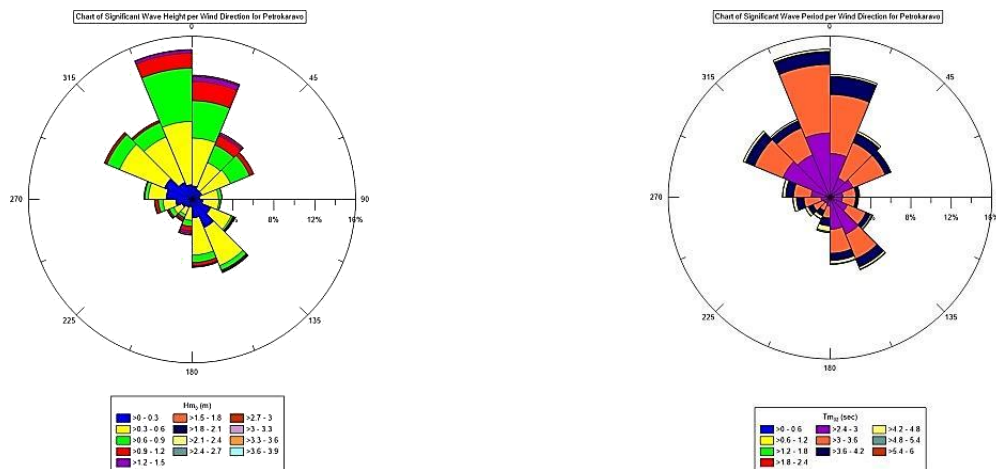


Figure 5.1.54: Charts of Wind Direction and Wave Height - Period for Petrokaravo Buoy

5.1.10 PYLOS

The location, depth of installation and time periods of Pylos buoy are shown in Table 5.1.61.

Table 5.1.61: Location, depth of installation and time periods of recording per database for Pylos Buoy

| Location | Depth (m) | Wave Parameters | SSE data | Atmospheric Parameters |
|------------------------|-----------|-----------------------|----------------------|------------------------|
| 21.60889°E, 36.83105°N | 1681 | 01/01/2007-31/12/2011 | 9/11/2007-31/12/2011 | 09/11/2007-31/12/2011 |

5.1.10.1 Wave Characteristics

The wave characteristics as these are given from the buoy of Pylos are shown through a variety of analyses in this subchapter for the period 2007-2011.

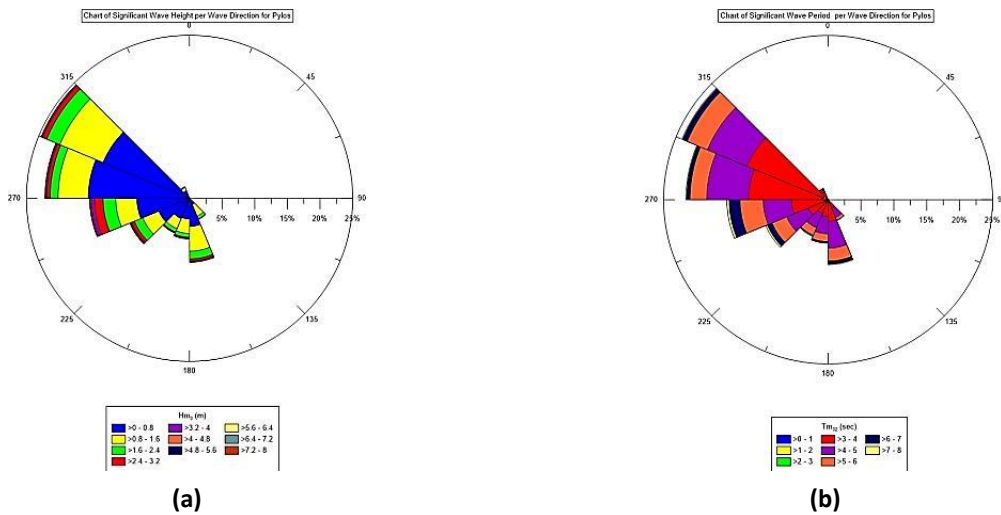
5.1.10.1.1 General Statistics

The statistics of wave parameters for Pylos are given in Table 5.1.62. The waves have mean height of 0.96 m, max of 7.58 m while periods have mean 4.33 s and max of 9.14 s. Wind waves have heights of 0.96 m, max of 4.77 m and mean period 4.3 s and max of 7.27 s. Swells have heights of 0.12 m, max of 6.17m and periods with means of 11.77 s and max of 18.87 s. Maximum wave height has a mean of 1.37 m, a max of 11.02 m whilst peak period has a mean of 5.81 s and a max of 13.83 s.

Table 5.1.62: Descriptive Statistics of Wave Parameters for Pylos Buoy

| Parameters | Number of Records | Mean | Maximum | Std.Dev. |
|----------------|-------------------|-------|---------|----------|
| H_{m0} (m) | 11020 | 0.96 | 7.58 | 0.74 |
| H_{m0a} (m) | 11529 | 0.12 | 6.17 | 0.34 |
| H_{m0b} (m) | 11529 | 0.96 | 4.77 | 0.69 |
| H_{max} (m)* | 11020 | 1.37 | 11.02 | 1.16 |
| T_{m02} (s) | 11541 | 4.33 | 9.14 | 0.95 |
| T_{m02a} (s) | 8867 | 11.77 | 18.87 | 1.04 |
| T_{m02b} (s) | 11529 | 4.30 | 7.27 | 0.89 |
| T_p (s) | 11541 | 5.81 | 13.83 | 1.69 |

The most frequent waves are propagating from the W to NW (64.84% and Fetch length of 550 km) while the swells from SW (42.87% and Fetch length of 815 km). Waves with heights of more than 4 m have directions W (54.41%) and the same applies for swells as well.



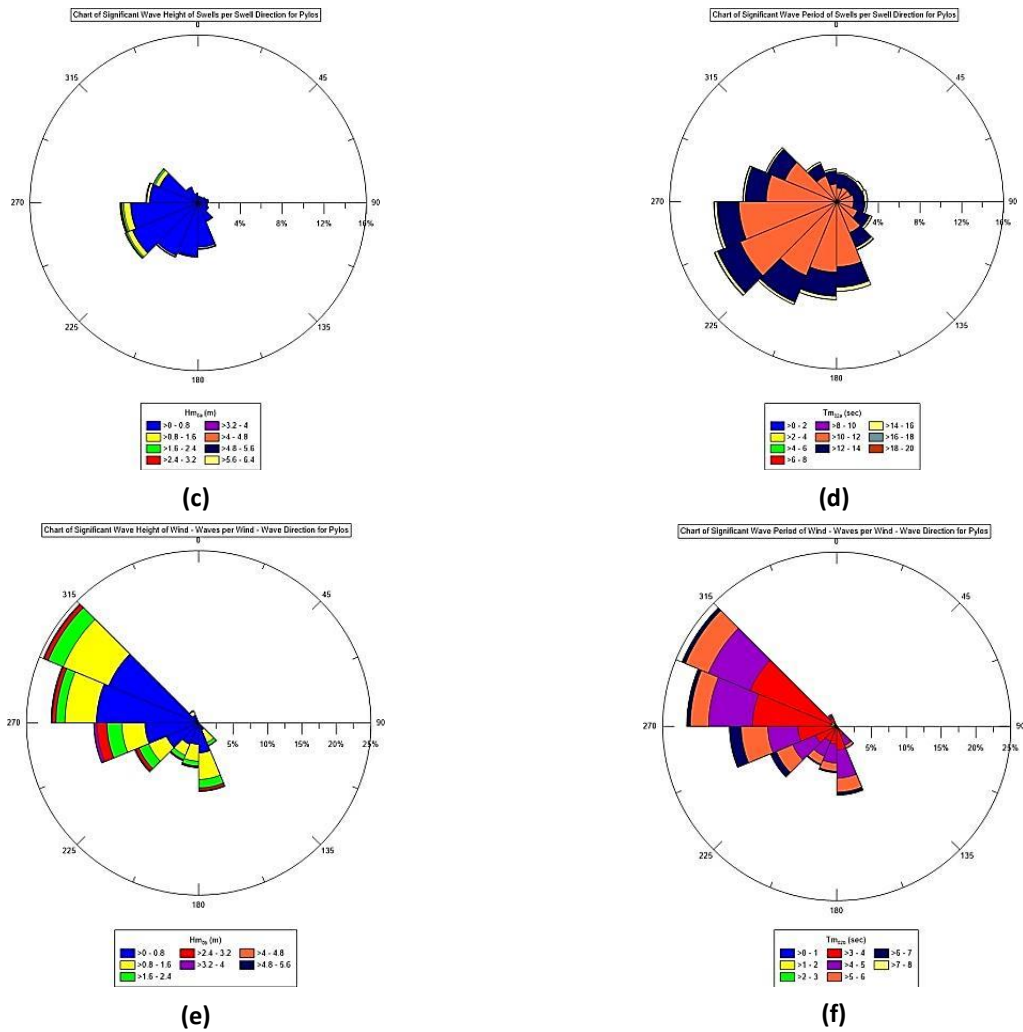


Figure 5.1.55: Rose Diagrams for Significant Wave Height and Wave period for all waves (a,b), swells (c,d) and wind waves (e,f) for Pylos Buoy

The pivot in Table 5.1.63 gives the frequency of occurrence of wave heights relative to their period. The most frequent waves (56.8%) have heights from 0 to 0.8 m with most of them (69.47%) with periods of 3 to 4 s. Waves with heights of more than 4 m, have frequencies of 0.62% with 66.18% related with periods of 7-8 s.

Table 5.1.63: Pivot Table for Significant Wave Height and Zero-crossing wave period for Pylos Buoy

| Hm ₀ (m) | Tm ₀₂ (s) | | | | | | | | |
|---------------------|----------------------|-------|-------|------|------|------|------|------|-------|
| | 2-3 | 3-4 | 4-5 | 5-6 | 6-7 | 7-8 | 8-9 | 9-10 | Total |
| 0-0.8 | 2.54 | 39.46 | 13.92 | 0.88 | 0 | 0 | 0 | 0 | 56.80 |
| 0.8-1.6 | 0 | 4.84 | 15.8 | 6.99 | 0.23 | 0 | 0 | 0 | 27.85 |
| 1.6-2.4 | 0 | 0 | 1.81 | 6.58 | 1.20 | 0.05 | 0 | 0 | 9.64 |
| 2.4-3.2 | 0 | 0 | 0 | 1.49 | 1.98 | 0.18 | 0.01 | 0 | 3.66 |
| 3.2-4 | 0 | 0 | 0 | 0.05 | 0.98 | 0.42 | 0 | 0 | 1.44 |
| 4-4.8 | 0 | 0 | 0 | 0 | 0.08 | 0.28 | 0.04 | 0 | 0.40 |
| 4.8-5.6 | 0 | 0 | 0 | 0 | 0 | 0.11 | 0.03 | 0.01 | 0.15 |
| 5.6-6.4 | 0 | 0 | 0 | 0 | 0 | 0.02 | 0.01 | 0.01 | 0.04 |

| | | | | | | | | | |
|----------------|-----|-------|-------|-------|------|------|------|------|--------|
| 6.4-7.2 | 0 | 0 | 0 | 0 | 0 | 0 | 0.03 | 0 | 0.03 |
| 7.2-8 | 0 | 0 | 0 | 0 | 0 | 0 | 0 | 0.01 | 0.01 |
| Total | 2.5 | 44.29 | 31.53 | 15.98 | 4.46 | 1.05 | 0.11 | 0.03 | 100.00 |

5.1.10.1.2 Monthly Means for the period 2007-2011

The monthly mean values are shown in Figure 5.1.56. The minimum mean monthly of wave height is in August (0.6 m) while the maximum mean is in December (1.52 m). The minimum value recorded is in June (0.07 m) and the maximum in November (7.57 m). As for the wave period, the minimum mean monthly is in July (3.71 s) and the maximum mean in December (5.07 s). The minimum value recorded for wave period is in November (2.46 s) and the maximum in November (9.14 s).

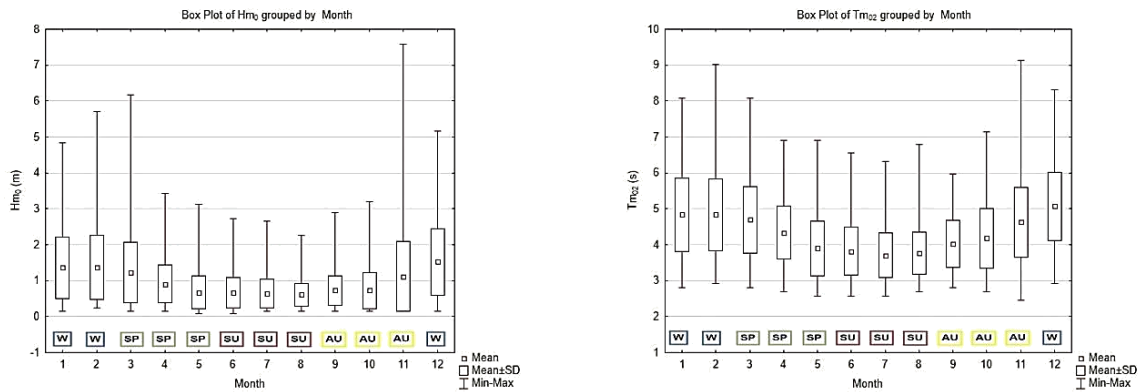


Figure 5.1.56: Box and Whiskers plots for Monthly Wave Height and Wave Period for Pylos Buoy

5.1.10.2 Sea Surface Elevation (SSE)

Several parameters are shown in this subchapter that have been obtained from the analysis of 6077 records of Sea Surface Elevation. An example of a record and its' spectral analysis are shown in Figure 5.1.57. The peak period (T_p) in this case is 12.84 s.

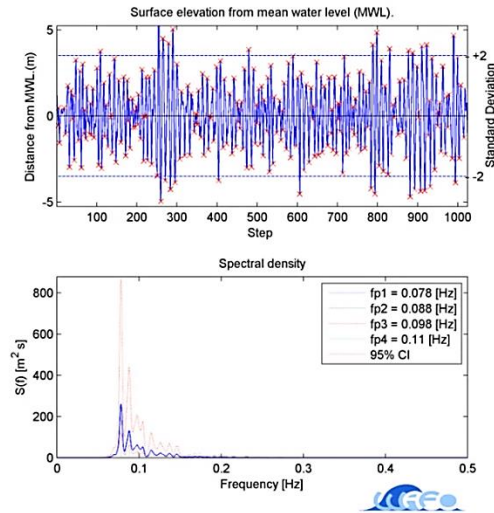


Figure 5.1.57: Random SSE record and its spectrum for Pylos Buoy

5.1.10.2.1 General Statistics

The descriptive statistics of wave characteristics as estimated from 6077 records of sea surface elevation analysis are given in Table 5.1.64.

Table 5.1.64: Descriptive Statistics as derived from SSE Analysis for Pylos Buoy

| Parameters | Number of Records | Mean | Maximum | Std.Dev. |
|---------------|-------------------|------|---------|----------|
| H_{m0} (m) | 6077 | 1.20 | 7.67 | 0.80 |
| Hmax (m) | 6077 | 1.82 | 11.36 | 1.26 |
| $H_{1/3}$ (m) | 6077 | 1.10 | 7.31 | 0.78 |
| T_{m02} (s) | 6077 | 4.51 | 8.85 | 0.94 |
| $T_{1/3}$ (s) | 6077 | 6.36 | 12.39 | 1.39 |
| T_p (s) | 6077 | 6.12 | 13.04 | 1.67 |

Spectral significant wave height has a mean of 1.2 m and a max of 7.67 m, while the statistical has a mean of 1.10 m and a max of 7.31 m. Spectral period has a mean of 4.51 s, and a max of 8.85 s while the statistical has a mean of 6.36 s and a max of 12.39 s. The max wave height has a mean of 1.82 m and a max of 11.36 m. The peak period has a mean of 6.12 s and a max of 13.04 s.

The correlations of the spectral and statistical parameters of Pylos buoy are given in Figure 5.1.58. Analytically, a correlation of 0.99 is given for H_{m0} and $H_{1/3}$ and 0.97 for T_{m02} and $T_{1/3}$.

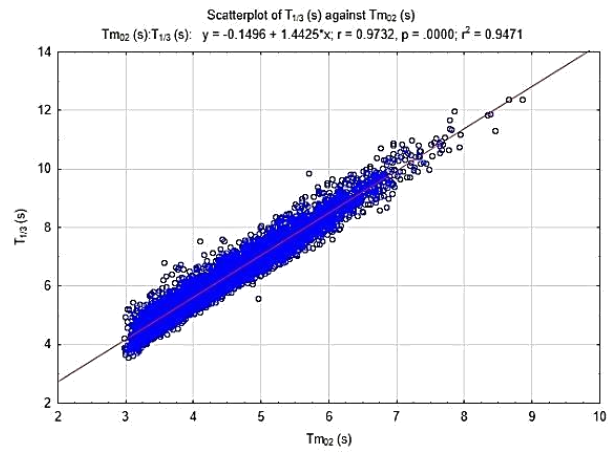
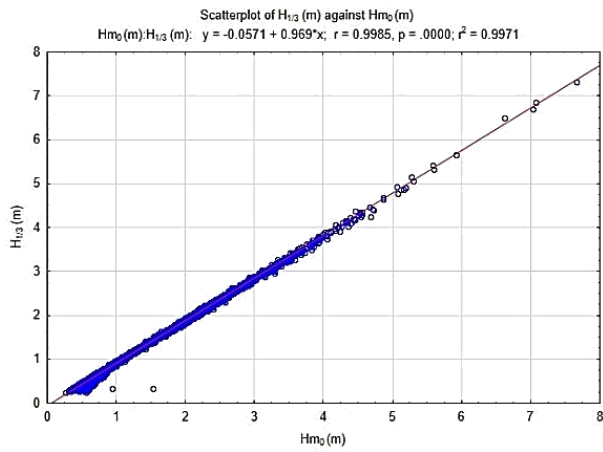


Figure 5.1.58: Scatterplots of statistical and spectral wave parameters for Pylos Buoy

5.1.10.2.2 Monthly Means for the period 2007-2011

In Figure 5.1.59, the monthly values of spectral and statistical wave parameters are shown for Pylos.

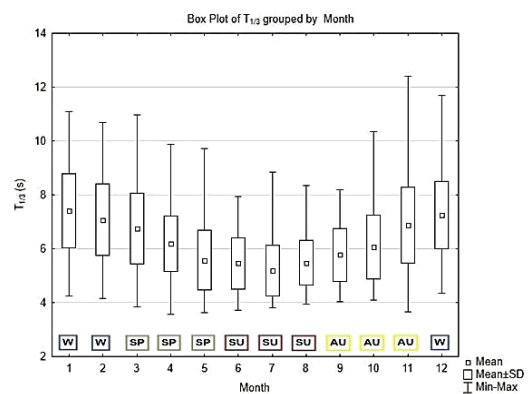
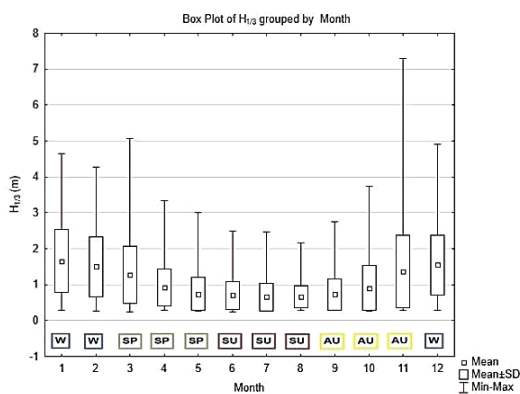
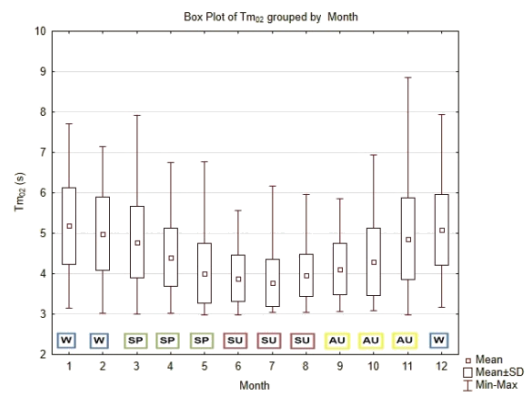
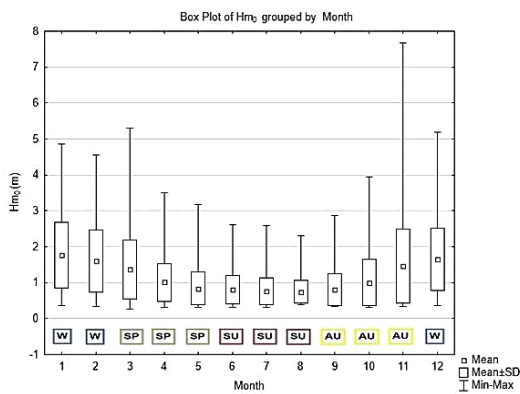


Figure 5.1.59: Spectral and Statistical Monthly Values per Wave Parameter for Pylos Buoy

For the spectral significant wave height H_{m0} , the minimum mean monthly value is in August (0.75 m), the maximum mean value is in January (1.77 m) while the minimum value is 0.27 m (March) and the maximum 7.67 m (November). As for the spectral wave period (T_{m02}), the mean minimum monthly value is 3.77 s (July) and the maximum 5.18 s (January). The minimum recorded value is in 2.97 s (May) and the maximum 8.85 s (November). In regards to the statistical significant wave height $H_{1/3}$, the smallest monthly value is 0.65 m (July) whilst the largest 1.66 m (January). The smallest overall value is 0.24 m (March) and the maximum (7.31 m) in November. Finally, for the statistical significant wave period $T_{1/3}$ the minimum monthly is 5.19 s in July and the maximum 7.4 s in January. In general, the minimum recorded period is 3.56 s (April) and the maximum 12.4 s in November.

5.1.10.2.3 Probability Distribution of Wave Height

In Figure 5.1.60, the probability distributions and the QQ plots of Weibull, Rayleigh for Pylos wave heights are shown. From the QQ plot one can detect that Kumaraswamy distribution overestimates the larger values of wave heights whilst Weibull and Rayleigh distribution diverge from the mean values.

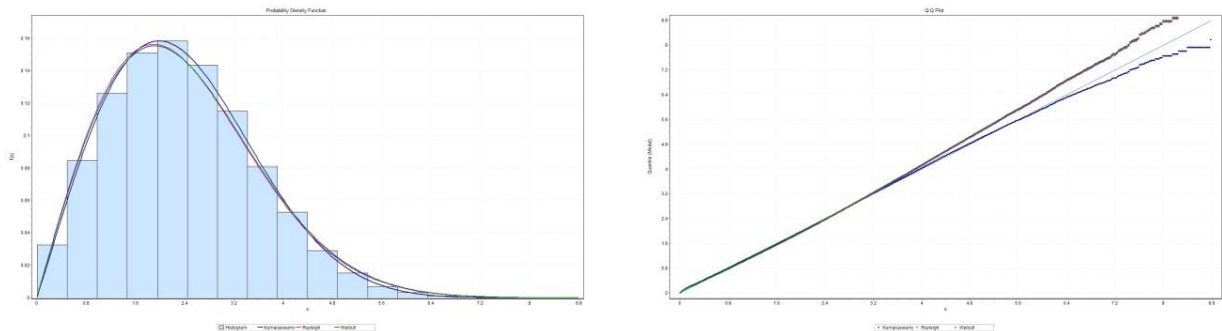


Figure 5.1.60: Probability Distributions and QQ plots for Athos for random wave heights

The statistics of goodness of fit for every distribution under examination are given in Table 5.1.65.

Table 5.1.65: Statistics of Goodness of Fits according to K-S, A-D and χ^2 test for Pylos Buoy

| Distribution | Kolmogorov - Smirnov | Anderson - Darling | Chi-Squared |
|--------------|----------------------|--------------------|-------------|
| | Statistic | Statistic | Statistic |
| Kumaraswamy | 0.008 | 20.6 | 143.13 |
| Weibull | 0.015 | 144.91 | 1061.4 |
| Rayleigh | 0.018 | 162.37 | 1045.2 |

5.1.10.2.4 Ratios between Statistical and Spectral Parameters

From the statistics in Table 5.1.66, mean values of the ratios among spectral and statistical parameters for Pylos are given. A mean of 1.07 is given for the spectral and statistical wave height, 3.73 for the ratio of $H_{1/3} / \sqrt{m_0}$, 1.55 for H_{max} / H_{m0} and $1.67H_{max} / H_{1/3}$.

Table 5.1.66: Statistics of various Ratios for Pylos Buoy

| Ratios | Number of Records | Mean | Minimum | Maximum | Std.Dev. |
|------------------------|-------------------|------|---------|---------|----------|
| $H_{m0} / H_{1/3}$ | 6077 | 1.07 | 1.01 | 1.22 | 0.03 |
| $H_{1/3} / \sqrt{m_0}$ | 6077 | 3.73 | 3.28 | 3.96 | 0.09 |
| H_{max} / H_{m0} | 6077 | 1.55 | 1.21 | 3.02 | 0.15 |
| $H_{max} / H_{1/3}$ | 6077 | 1.67 | 1.28 | 3.42 | 0.16 |

5.1.10.3 Weather Characteristics

The atmospheric characteristics that effect Pylos area as shown from the records of the buoy are given here.

5.1.10.3.1 General Statistics

In Table 5.1.67, the main statistics of atmospheric parameters for Pylos are shown. Minimum air pressure is of 989.36 hPa, the max of 1033.71 hPa and the mean of 1014.97 hPa. The mean temperature is of 19.52 °C while it can reach 31.82 °C. Wind speed has a mean of 4.93 m/s and can reach a maximum of 16.46 m/s while wind gust has a mean of 6.62 m/s and can go up to 41.43 m/s.

Table 5.1.67: Descriptive Statistics of Atmospheric Parameters for Pylos Buoy

| Parameters | Number of Records | Mean | Minimum | Maximum | Std.Dev. |
|---------------------|-------------------|---------|---------|---------|----------|
| Air Pressure(hPa) | 11571 | 1014.97 | 989.36 | 1033.71 | 5.61 |
| Air Temperature(°C) | 11571 | 19.52 | 3.50 | 31.82 | 4.98 |
| Wind Gust (m/s) | 11553 | 6.62 | 0.23 | 41.43 | 3.67 |
| Wind Speed (m/s) | 11528 | 4.93 | 0.06 | 16.46 | 2.84 |

In the wind chart of Figure 5.1.61, the most frequent (32.89%) winds are blowing from NW and 15.29% is from SE, with the wind speeds higher (60%) than 14 m/s blowing from SE.

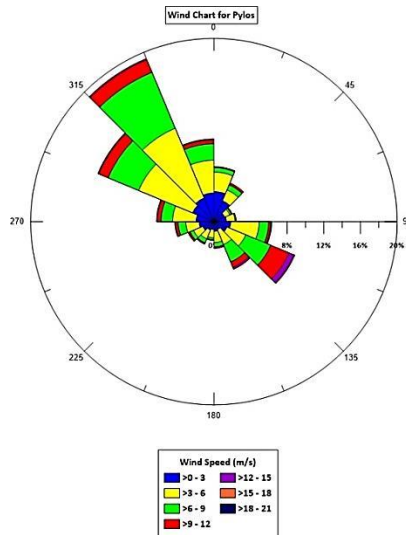


Figure 5.1.61: Wind Chart for Pylos Buoy

5.1.10.3.2 Monthly Means for the period 2007-2011

The monthly means are presented in (Figure 5.1.62).

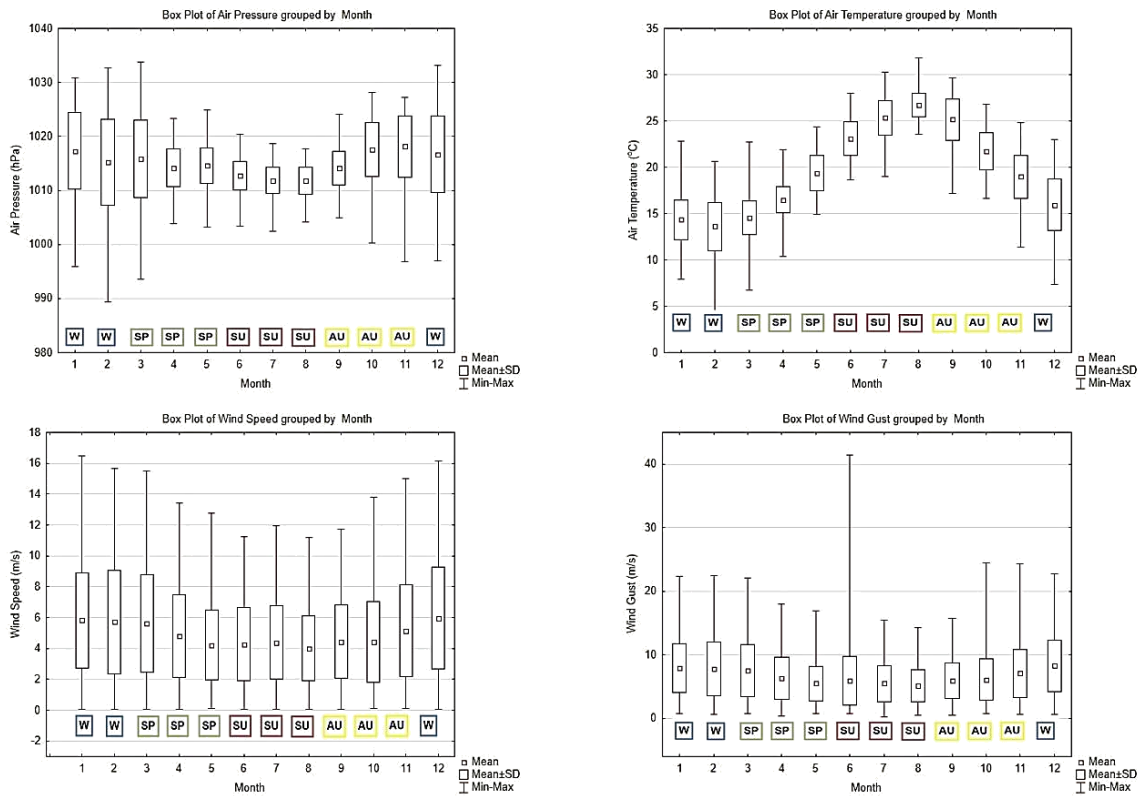


Figure 5.1.62: Monthly Box and Whiskers Plots for Atmospheric Parameters for Pylos Buoy

For pressure the minimum monthly mean value is in August (1011.7 hPa) and the maximum (1018.12 hPa) in January. For temperature the minimum mean monthly 13.60 °C in February and the maximum in 26.71 °C during August. Minimum values of wind speed and wind gust are in August (4 m/s and 5.15 m/s respectively) and the maximum are in December (5.97 m/s and 8.25 m/s).

5.1.10.4 Relation of Wind and Wave Data

Results of the intercomparison of wind and wave data are shown in this subchapter.

5.1.10.4.1 General Statistics

The mean value wind speed (4.9 m/s) can be considered as gentle breeze that will most likely result in breaking of wave crests with isolated whitecaps (Table 5.1.68).

Table 5.1.68: Descriptive Statistics of Wave and Atmospheric Parameters for Pylos Buoy

| Parameters | Number of Records | Mean | Minimum | Maximum | Std.Dev. |
|-----------------------|-------------------|---------|---------|---------|----------|
| Air Pressure (hPa) | 10968 | 1014.96 | 989.36 | 1033.71 | 5.64 |
| Air Temperature (°C) | 10968 | 19.52 | 3.50 | 31.82 | 5.05 |
| Wind Gust (m/s) | 10968 | 6.58 | 0.41 | 41.43 | 3.63 |
| Wind Speed (m/s) | 10968 | 4.90 | 0.06 | 16.46 | 2.82 |
| Hm ₀ (m) | 10968 | 0.97 | 0.08 | 7.58 | 0.74 |
| Hm _{0a} (m) | 10968 | 0.12 | 0.00 | 6.17 | 0.34 |
| Hm _{0b} (m) | 10968 | 0.95 | 0.08 | 4.77 | 0.68 |
| Tm ₀₂ (s) | 10968 | 1.38 | 0.00 | 11.02 | 1.16 |
| Tm _{02a} (s) | 10968 | 4.31 | 2.58 | 9.14 | 0.95 |
| Tm _{02b} (s) | 8306 | 11.79 | 10.31 | 18.87 | 1.05 |
| T _p (s) | 10968 | 4.27 | 2.58 | 7.27 | 0.89 |

The pivot Table 5.1.69 shows that the most frequent waves (56.8%) have heights of 0-0.8 and 38.34% of these are related with wind speeds of 2-4 m/s. Waves with heights more than 4m have a frequency of 0.62% with a 75% related with speeds of above 8m/s wind speeds.

Table 5.1.69: Frequency Table (%) of Wind Speed and Significant Spectral Wave Height for Pylos Buoy

| Wind Speed (m/s) | Hm ₀ (m) | | | | | | | | | | Total |
|------------------|---------------------|---------|---------|---------|-------|-------|---------|---------|---------|-------|--------|
| | 0-0.8 | 0.8-1.6 | 1.6-2.4 | 2.4-3.2 | 3.2-4 | 4-4.8 | 4.8-5.6 | 5.6-6.4 | 6.4-7.2 | 7.2-8 | |
| 0-2 | 12.17 | 2.63 | 0.46 | 0.09 | 0 | 0.01 | 0 | 0 | 0 | 0 | 15.36 |
| 2-4 | 21.86 | 5.50 | 1.13 | 0.37 | 0.05 | 0 | 0 | 0 | 0 | 0 | 28.92 |
| 4-6 | 14.80 | 6.52 | 1.68 | 0.52 | 0.14 | 0.03 | 0 | 0 | 0 | 0 | 23.68 |
| 6-8 | 6.74 | 7.46 | 2.41 | 0.70 | 0.32 | 0.10 | 0.02 | 0 | 0 | 0 | 17.75 |
| 8-10 | 1.05 | 4.35 | 2.22 | 0.96 | 0.26 | 0.10 | 0.03 | 0 | 0 | 0 | 8.97 |
| 10-12 | 0.07 | 1.17 | 1.30 | 0.69 | 0.39 | 0.08 | 0.02 | 0.03 | 0 | 0.01 | 3.77 |
| 12-14 | 0 | 0.23 | 0.31 | 0.26 | 0.19 | 0.04 | 0.05 | 0.01 | 0.03 | 0 | 1.12 |
| 14-16 | 0 | 0.04 | 0.15 | 0.07 | 0.08 | 0.05 | 0.03 | 0 | 0 | 0 | 0.41 |
| 16-18 | 0 | 0 | 0.01 | 0 | 0.01 | 0 | 0 | 0 | 0 | 0 | 0.02 |
| Total | 56.68 | 27.91 | 9.67 | 3.67 | 1.45 | 0.40 | 0.15 | 0.04 | 0.03 | 0.01 | 100.00 |

The most frequent waves are related with winds blowing from W (36.41%) and this applies for the most frequent periods (Figure 5.1.63). Waves with heights of more than 4 m (82.35%) are related with winds blowing from SW to W directions.

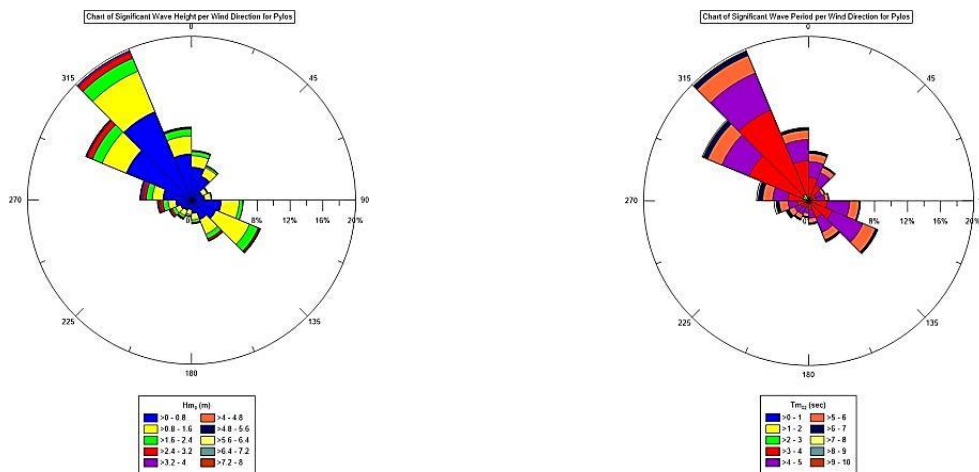


Figure 5.1.63: Charts of Wind Direction and Wave Height - Period for Pylos Buoy

5.1.11 SANTORINI

The depth of installation, location and time periods per dataset for Santorini buoy are shown in Table 5.1.70.

Table 5.1.70: Location, depth of installation and time periods of recording per database for Santorini Buoy

| Location | Depth (m) | Wave Parameters | SSE data | Atmospheric Parameters |
|---------------------------|-----------|-----------------------|-------------|------------------------|
| 25.49568°E, 36.26111°N | 320 | 01/01/2000-31/12/2000 | 2001 & 2008 | 01/01/2000-31/12/2011 |

5.1.11.1 *Wave Characteristics*

Wave characteristics are shown in this subchapter as these are obtained by the Santorini buoy for the period 2000-2011.

5.1.11.1.1 General Statistics

In Table 5.1.71, the descriptive statistics of wave parameters are shown for the Santorini Buoy. The waves have heights of mean of 0.9 m, max of 4.92 m and periods of mean 3.73 s and max of 9.04 s. The wind waves have mean 0.89 m, max of 4.69 m and periods of mean 3.72 s and max of 7.27 s. The swells have heights of mean of 0.06 m and max of 2.6m and as for periods, the mean is 13.16 s and max of 15.37 s. The max wave heights have mean of 1.28 m and maximum of 7.5 m. Finally the peak period, has a mean of 5.01 s and a a max of 14.63 s.

Table 5.1.71: Descriptive Statistics of Wave Parameters for Santorini Buoy

| Parameters | Number of Records | Mean | Maximum | Std.Dev. |
|-------------------|-------------------|-------|---------|----------|
| H_{m_0} (m) | 30867 | 0.90 | 4.92 | 0.55 |
| $H_{m_{0a}}$ (m) | 30866 | 0.06 | 2.60 | 0.12 |
| $H_{m_{0b}}$ (m) | 30866 | 0.89 | 4.69 | 0.54 |
| H_{max} (m) | 12335 | 1.28 | 7.50 | 0.77 |
| $T_{m_{02}}$ (s) | 30866 | 3.73 | 9.04 | 0.71 |
| $T_{m_{02a}}$ (s) | 30865 | 13.16 | 15.37 | 1.25 |
| $T_{m_{02b}}$ (s) | 30866 | 3.72 | 7.27 | 0.69 |
| T_p (s) | 30865 | 5.01 | 14.63 | 1.48 |

From the charts it is shown that the main directions of waves are that of N (33.21% and fetch 192 km) and SW to W (35.34% and Fetch length of 220 km) whilst swells have as predominating direction SW to W. The maximum heights for waves are from of W and N directions and the same applies for swells as well.

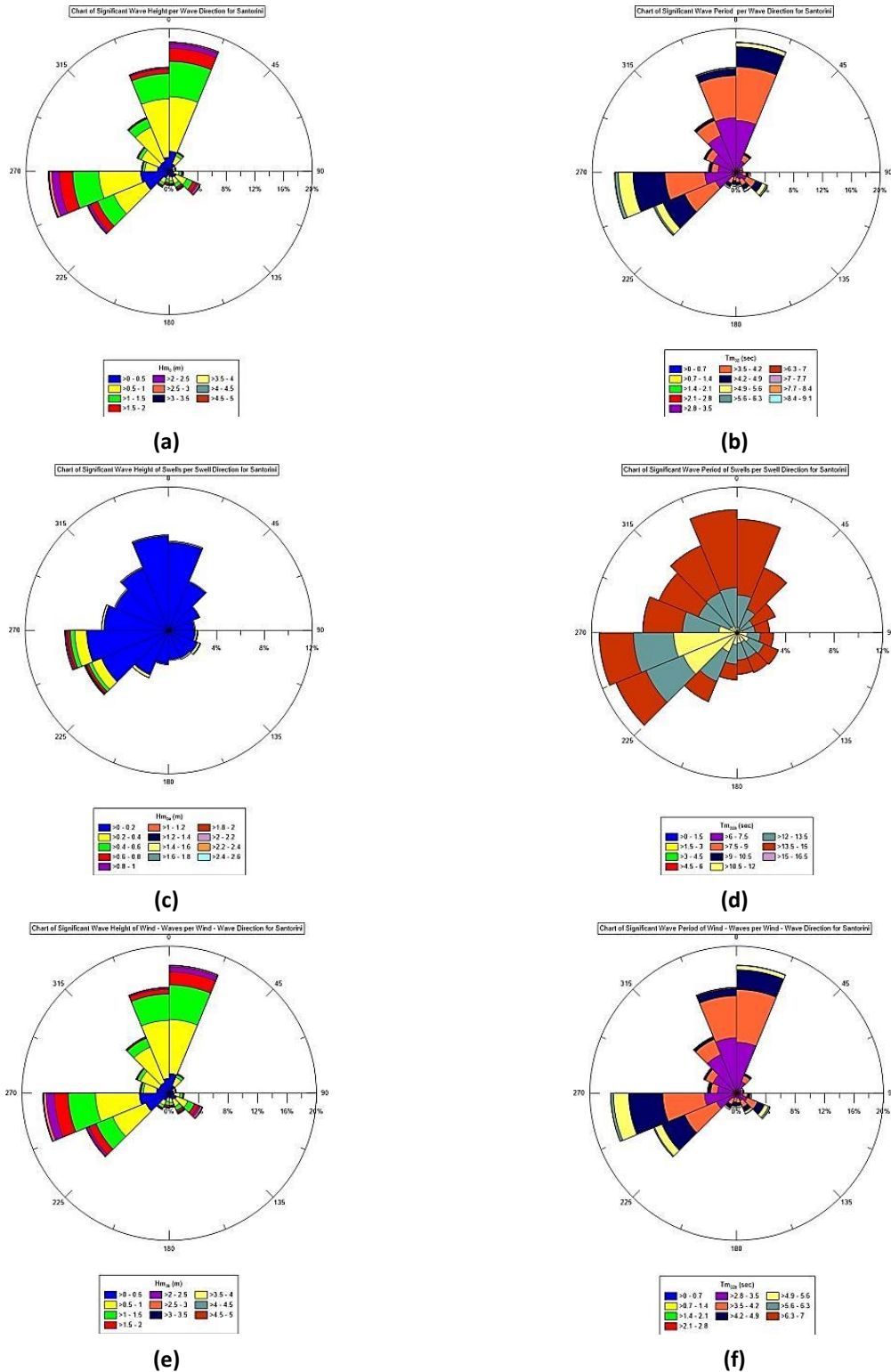


Figure 5.1.64: Rose Diagrams for Significant Wave Height and Wave period for all waves (a,b), swells (c,d) and wind waves (e,f) for Santorini Buoy

The pivot table (Table 5.1.72) shows the frequencies of occurrence of significant wave height according to wave period.

The highest waves (>3 m) have a frequency of 0.52% with periods greater than 4.7 s. The most frequent waves (42.33%) have heights from 0.5 to 1 m with the majority of them (77.78%) with periods of 2.9 to 3.8 s.

Table 5.1.72: Pivot Table for Significant Wave Height and Zero-crossing wave period for Santorini Buoy

| Hm ₀ (m) | Tm ₀₂ (s) | | | | | | | Total |
|---------------------|----------------------|---------|---------|---------|---------|---------|------|--------|
| | 2-2.9 | 2.9-3.8 | 3.8-4.7 | 4.7-5.6 | 5.6-6.5 | 6.5-7.4 | >7.4 | |
| 0-0.5 | 7.45 | 14.82 | 1.94 | 0.31 | 0.03 | 0 | 0 | 24.55 |
| 0.5-1 | 0.86 | 32.92 | 7.98 | 0.51 | 0.04 | 0.01 | 0 | 42.32 |
| 1-1.5 | 0 | 4.20 | 14.91 | 1.38 | 0.07 | 0 | 0 | 20.56 |
| 1.5-2 | 0 | 0 | 4.85 | 2.68 | 0.13 | 0.01 | 0 | 7.67 |
| 2-2.5 | 0 | 0 | 0.16 | 2.82 | 0.22 | 0.01 | 0 | 3.22 |
| 2.5-3 | 0 | 0 | 0 | 0.73 | 0.43 | 0 | 0 | 1.16 |
| 3-3.5 | 0 | 0 | 0 | 0.02 | 0.33 | 0 | 0 | 0.35 |
| 3.5-4 | 0 | 0 | 0 | 0 | 0.10 | 0.05 | 0 | 0.15 |
| 4-4.5 | 0 | 0 | 0 | 0 | 0 | 0.01 | 0 | 0.01 |
| 4.5-5 | 0 | 0 | 0 | 0 | 0 | 0.01 | 0 | 0.01 |
| Total | 8.31 | 51.94 | 29.84 | 8.44 | 1.35 | 0.11 | 0.01 | 100.00 |

5.1.11.1.2 Monthly Means for the period 2000-2011

For the wave height it shown that the minimum monthly mean is in May (0.71 m) while the maximum mean is in February (1.15 m) (Figure 5.1.65). Furthermore, the minimum value recorded is in May (0.015 m) and the maximum is in January (4.92 m). For the wave period, the minimum mean monthly is in July (3.49 s) and the maximum mean in February (4.1 s). The minimum value for wave period is in November (2.32 s) and the maximum in May (9.04 s).

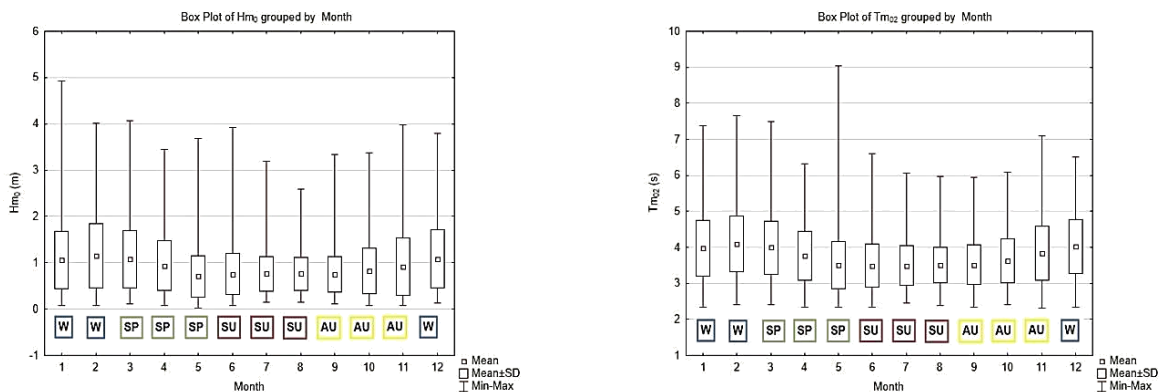


Figure 5.1.65: Box and Whiskers plots for Monthly Wave Height and Wave Period for Santorini Buoy

5.1.11.2 Sea Surface Elevation (SSE)

Data of 4308 sea surface elevation records analysis are presented in this chapter. The example of Figure 5.1.66. Via the analysis of spectrum and the timeseries, the aforementioned data of wave characteristics can be excluded. For the specific experiment, one can exclude the peak period of the Spectrum (T_p) which is around 8.98 s.

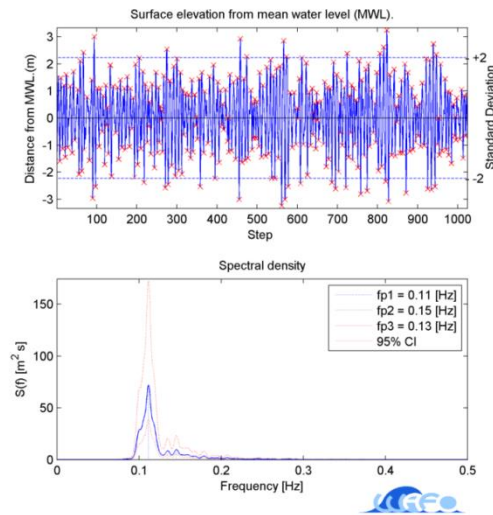


Figure 5.1.66: Random SSE record and its spectrum for Santorini Buoy

5.1.11.2.1 General Statistics

The descriptive statistics of wave characteristics as derived from 4308 records of sea surface elevation analysis are given in Table 5.1.73. The spectral significant wave height has a mean of 0.98 m and a maximum of 4.84 m whilst the statistical significant wave height has a mean of 3.84 m and a max of 7.37 m. The statistical wave period has a mean of 5.51 s and a max of 10.42 s while the spectral has a mean of 3.85 s and a max of 7.37 s. Furthermore, the apparent maximum wave height has a mean of 0.87 m and a maximum of 7.53 m whilst peak period has a mean of 5.2 s and a maximum of 12.84 s.

Table 5.1.73: Descriptive Statistics as derived from SSE Analysis for Santorini Buoy

| Parameters | Number of Records | Mean | Maximum | Std.Dev. |
|---------------|-------------------|------|---------|----------|
| H_{m0} (m) | 4308 | 0.97 | 4.85 | 0.54 |
| H_{max} (m) | 4308 | 0.87 | 7.53 | 0.72 |
| $H_{1/3}$ (m) | 4308 | 0.9 | 4.63 | 0.52 |
| T_{m02} (s) | 4308 | 3.85 | 7.37 | 0.71 |
| $T_{1/3}$ (s) | 4308 | 5.51 | 10.42 | 1.03 |
| T_p (s) | 4308 | 5.2 | 12.84 | 1.43 |

In the case of Santorini buoy, a correlation of 0.99 is given for H_{m0} and $H_{1/3}$ and 0.96 for T_{m02} and $T_{1/3}$ as shown in Figure 5.1.67.

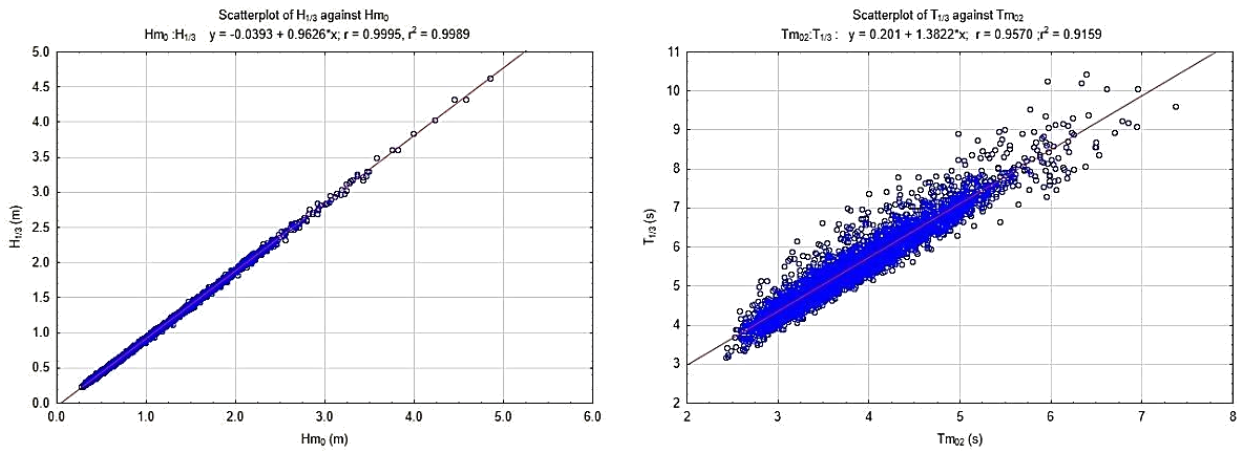


Figure 5.1.67: Scatterplots of statistical and spectral wave parameters for Santorini Buoy

5.1.11.2.2 Monthly Means for the period 2006-2011

The monthly means are presented in (Figure 5.1.68).

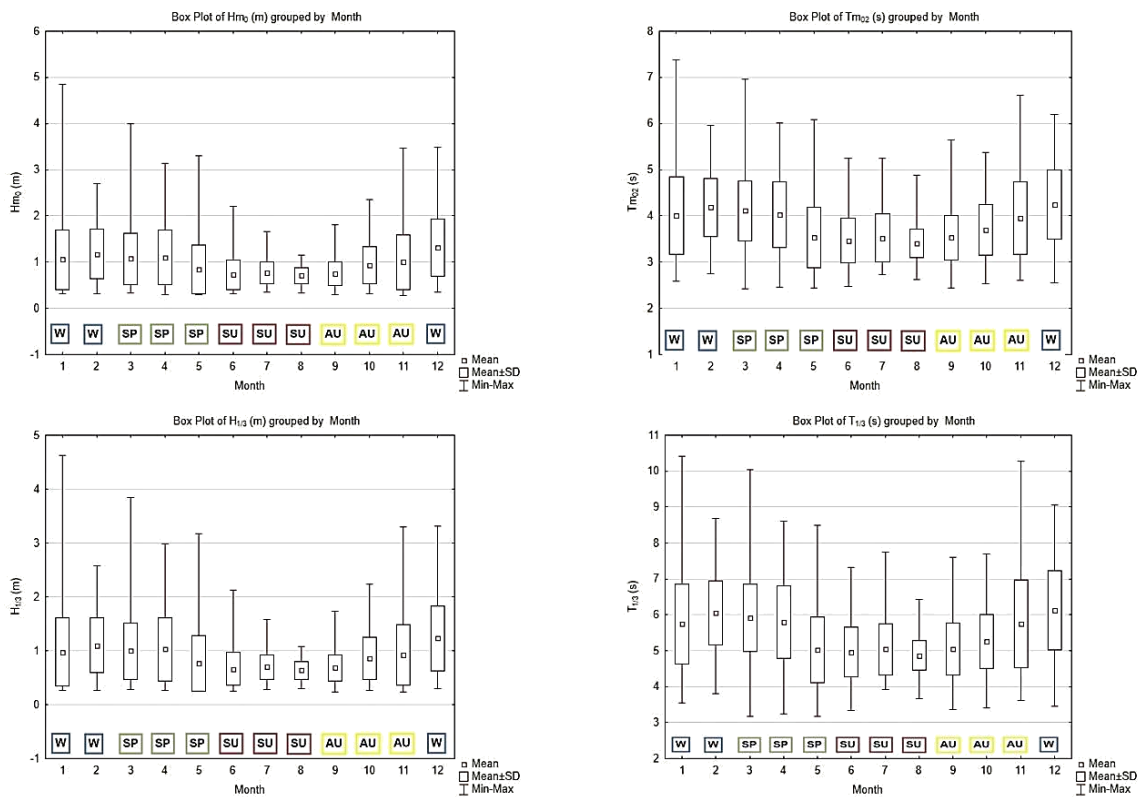


Figure 5.1.68: Spectral and Statistical Monthly Values per Wave Parameter for Santorini Buoy

The spectral significant wave height H_{m0} , the minimum mean monthly value is in August (0.71 m), the maximum mean value is in December (1.32 m) while the minimum value is 0.27 m (November) and the maximum 4.85 m (January). As for the spectral wave period (T_{m02}), the mean minimum monthly value is in 3.41 s (August) and the maximum in 4.25 s (December). The minimum is 2.43 s (March) and the maximum 7.37s (January). As for the statistical significant wave height $H_{1/3}$, the smallest mean monthly value is 0.64 m (August) whilst the largest 1.23 m (December). The smallest overall value is 0.24 m (September) and the maximum (4.63 m) in January. Finally, for the statistical significant wave period $T_{1/3}$ the minimum monthly is 4.87 s in August and the maximum 6.12 s in December. The minimum recorded period is 3.16 s (May) and the maximum 10.43 s in January.

5.1.11.2.3 Probability Distribution of Wave Height

Probability distributions of Weibull, Rayleigh and Kumaraswamy as well as the relevant QQ plots are shown in Figure 5.1.69. From the QQ plot one can detect that Kumaraswamy distribution underestimates the larger values of wave heights whilst Weibull and Rayleigh distribution diverge from the mean values and overestimate the higher ones.

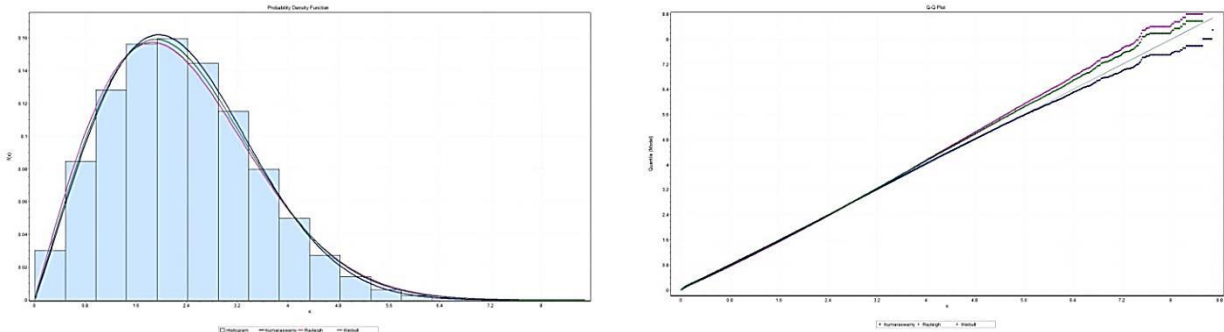


Figure 5.1.69: Probability Distributions and QQ plots for Santorini Buoy for random wave heights

The statistics of goodness of fit tests for Kumaraswamy, Weibull and Rayleigh are shown in Table 5.1.74.

Table 5.1.74: Statistics of Goodness of Fits according to K-S, A-D and χ^2 test for Santorini Buoy

| Distribution | Kolmogorov Smirnov | Anderson Darling | Chi-Squared |
|--------------|--------------------|------------------|-------------|
| | Statistic | Statistic | Statistic |
| Kumaraswamy | 0.005 | 18.36 | 129.3 |
| Weibull | 0.012 | 114.18 | 817.68 |
| Rayleigh | 0.019 | 283.83 | 1699.4 |

5.1.11.2.4 Ratios between Statistical and Spectral Parameters

The statistics of the ratios in Table 5.1.75, show that a mean of 1.1 is estimated for $H_{m0} / H_{1/3}$, 3.65 for $H_{1/3} / \sqrt{m_0}$, 1.53 H_{max} / H_{m0} and 1.68 for $H_{max} / H_{1/3}$.

Table 5.1.75: Statistics of Various Ratios for Santorini Buoy

| Ratios | Number of Records | Mean | Minimum | Maximum | Std.Dev. |
|------------------------|-------------------|------|---------|---------|----------|
| $H_{m0} / H_{1/3}$ | 4308 | 1.10 | 1.01 | 1.25 | 0.03 |
| $H_{1/3} / \sqrt{m_0}$ | 4308 | 3.65 | 3.20 | 3.98 | 0.11 |
| H_{max} / H_{m0} | 4308 | 1.53 | 1.18 | 2.30 | 0.15 |
| $H_{max} / H_{1/3}$ | 4308 | 1.68 | 1.27 | 2.61 | 0.16 |

5.1.11.3 Weather Characteristics

The atmospheric characteristics of the area of Santorini are presented in this session .

5.1.11.3.1 General Statistics

A minimum temperature of 0.29 °C and a maximum of 36.8 °C characterize the area along with mean wind speeds and wind gusts of 5.6m/s and 7.47m/s respectively (Table 5.1.76).

Table 5.1.76: Descriptive Statistics of Atmospheric Parameters for Santorini Buoy

| Parameters | Number of Records | Mean | Minimum | Maximum | Std.Dev. |
|---------------------|-------------------|---------|---------|---------|----------|
| Air Pressure(hPa) | 30914 | 1014.24 | 988.59 | 1036.33 | 5.74 |
| Air Temperature(°C) | 29951 | 19.66 | 0.29 | 36.80 | 5.18 |
| Wind Gust (m/s) | 30380 | 7.47 | 0.00 | 29.77 | 3.84 |
| Wind Speed (m/s) | 30280 | 5.60 | 0.00 | 19.03 | 3.00 |

The wind chart (Figure 5.1.70) shows that the most frequent winds are blowing from N (25.41%) with 36.3% of them having wind speeds of 6-9 m/s. The secondary directions are of NW with frequency of 24.16% The most common winds have speeds of 3-6 m/s (38.28%) and winds with speeds more than 15 m/s have a frequency of 0.36% with 26.17% of them of W direction.

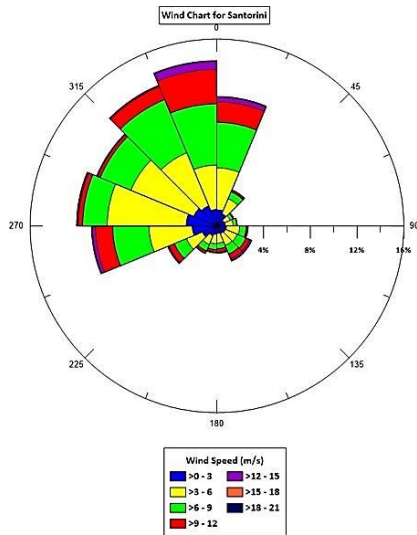


Figure 5.1.70: Wind Chart for Santorini Buoy

5.1.11.3.2 Monthly Means for the period 2000-2011

For pressure the minimum monthly mean value is in July (1009.52 hPa) and the maximum (1017.79 hPa) in November (Figure 5.1.71)Figure 5.1.71. The minimum mean monthly temperature is 13.94 °C in January and the maximum in 25.76 °C during August. Minimum values of wind speed and wind gust are in May (4.64 m/s and 6.14 m/s respectively) and the maximum are in February (6.8 m/s and 9.17 m/s).

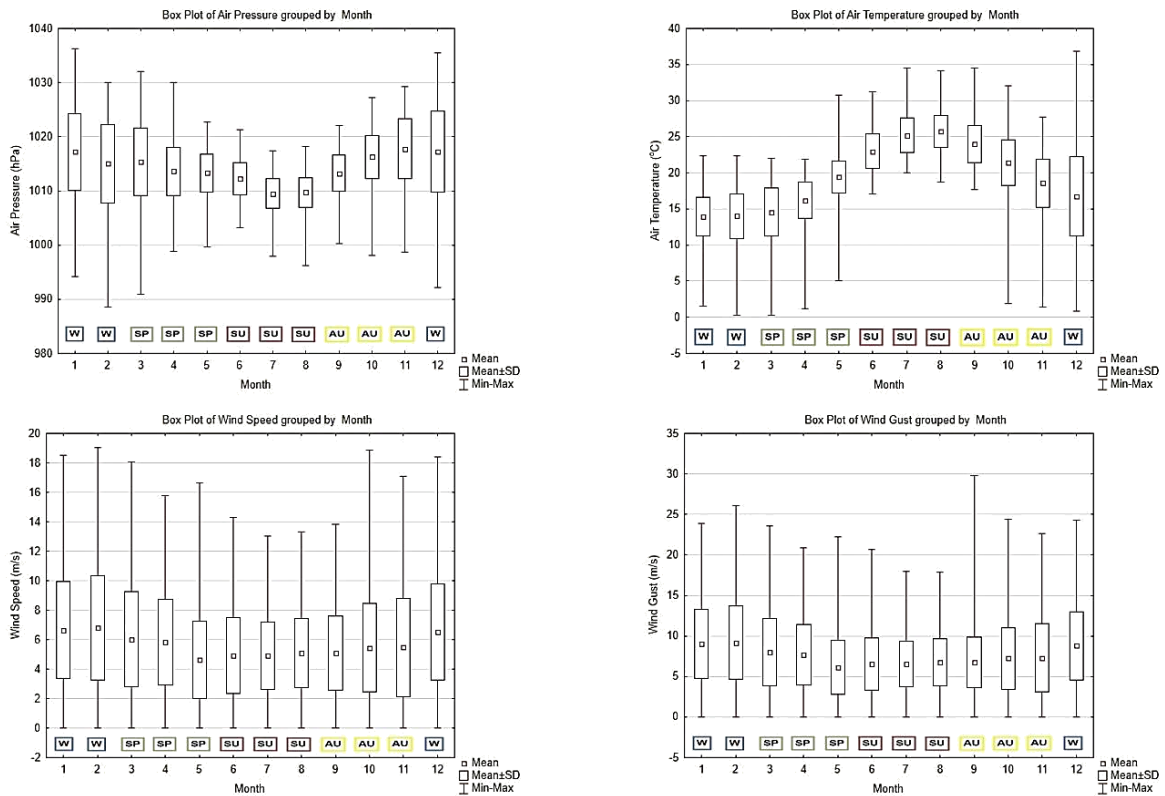


Figure 5.1.71: Monthly Box and Whiskers Plots for Atmospheric Parameters for Santorini Buoy

5.1.11.4 Relation of Wind and Wave Data

The intercomparison of the datasets of wave and atmospheric parameters is shown in this session, only for matching time periods.

5.1.11.4.1 General Statistics

The mean wind speed of (5.6 m/s), as given in Table 5.1.77, suggests that the area is influenced by moderate breeze that might lead to the generation of small and longer waves with spreaded whitecaps.

Table 5.1.77: Descriptive Statistics of Wave and Atmospheric Parameters for Santorini Buoy

| | Number of Records | Mean | Minimum | Maximum | Std.Dev. |
|-----------------------|-------------------|---------|---------|---------|----------|
| Air Pressure (hPa) | 11286 | 1012.94 | 988.59 | 1033.17 | 5.70 |
| Air Temperature (°C) | 11286 | 21.13 | 6.62 | 36.26 | 5.29 |
| Wind Gust (m/s) | 11286 | 7.65 | 0.00 | 29.77 | 3.38 |
| Wind Speed (m/s) | 11286 | 5.76 | 0.00 | 18.52 | 2.72 |
| Hm ₀ (m) | 11286 | 0.92 | 0.01 | 4.92 | 0.50 |
| Hm _{0a} (m) | 11286 | 0.05 | 0.00 | 2.60 | 0.13 |
| Hm _{0b} (m) | 11286 | 0.92 | 0.01 | 4.69 | 0.50 |
| H _{max} (m) | 11286 | 1.28 | 0.29 | 7.50 | 0.78 |
| Tm ₀₂ (s) | 11286 | 3.75 | 2.34 | 9.04 | 0.69 |
| Tm _{02a} (s) | 11286 | 12.89 | 10.20 | 15.37 | 1.03 |
| Tm _{02b} (s) | 11286 | 3.74 | 2.34 | 7.27 | 0.67 |
| T _p (s) | 11286 | 5.06 | 1.99 | 14.63 | 1.42 |

The frequency table of Table 5.1.78, suggests that the most frequent waves of 42.73% have heights of 0.5-1 m and 48.74% of these are related with wind speeds of 3-6 m/s. The higher waves (>3m) have a frequency of 0.54% with a 67.92% of those related with speeds of above 15 m/s wind speeds.

Table 5.1.78: Frequency Table (%) of Wind Speed and Significant Spectral Wave Height for Santorini Buoy

| Wind Speed (m/s) | Hm ₀ (m) | | | | | | | | | | |
|---------------------|---------------------|-------|-------|-------|-------|-------|-------|-------|-------|-------|--------|
| | 0-0.5 | 0.5-1 | 1-1.5 | 1.5-2 | 2-2.5 | 2.5-3 | 3-3.5 | 3.5-4 | 4-4.5 | 4.5-5 | Total |
| 0-3 | 10.75 | 7.25 | 1.50 | 0.34 | 0.20 | 0.03 | 0.03 | 0.01 | 0 | 0 | 20.11 |
| 3-6 | 11.23 | 20.83 | 4.88 | 0.97 | 0.35 | 0.11 | 0.03 | 0.01 | 0 | 0 | 38.41 |
| 6-9 | 1.60 | 13.11 | 9.99 | 2.68 | 0.65 | 0.16 | 0.02 | 0.01 | 0 | 0 | 28.21 |
| 9-12 | 0.50 | 1.33 | 3.80 | 2.95 | 1.35 | 0.48 | 0.07 | 0 | 0 | 0 | 10.49 |
| 12-15 | 0.14 | 0.19 | 0.22 | 0.60 | 0.66 | 0.39 | 0.16 | 0.06 | 0.01 | 0 | 2.43 |
| 15-18 | 0.04 | 0.02 | 0.02 | 0.02 | 0.04 | 0.07 | 0.07 | 0.05 | 0 | 0.01 | 0.33 |
| 18-21 | 0 | 0 | 0 | 0 | 0 | 0 | 0 | 0.01 | 0 | 0 | 0.02 |
| Total | 24.26 | 42.73 | 20.41 | 7.56 | 3.25 | 1.24 | 0.37 | 0.15 | 0.01 | 0.01 | 100.00 |

The most frequent waves are related with winds blowing from N, while waves with heights are related to wind speeds with directions from W. The most frequent and higher periods are related to winds with directions from N and W (Figure 5.1.72).

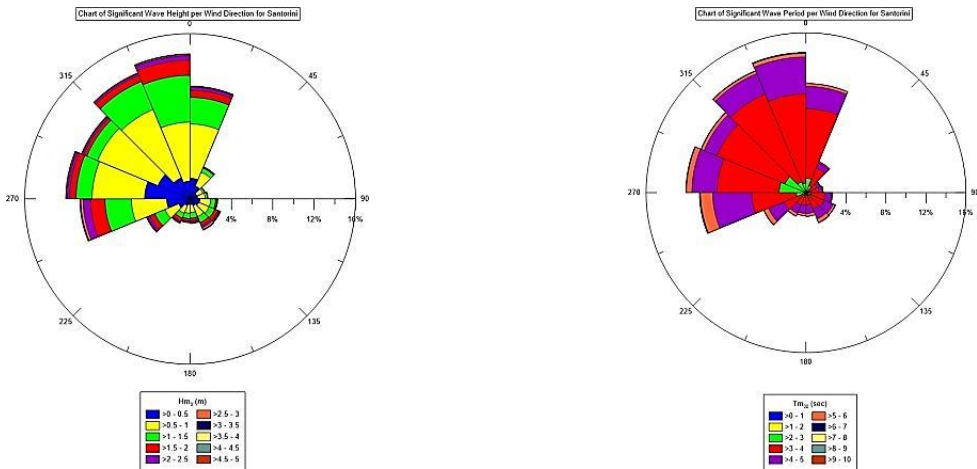


Figure 5.1.72: Charts of Wind Direction and Wave Height - Period for Santorini Buoy

5.1.12 SKYROS

Details about the buoy’s location, its depth of installation and the time periods of the data are shown in Table 5.1.79.

Table 5.1.79: Location, depth of installation and time periods of recording per database for Skyros Buoy

| Location | Depth (m) | Wave Parameters | SSE data | Atmospheric Parameters |
|------------------------|-----------|-----------------------|-----------------------|------------------------|
| 24.46777°E, 39.11133°N | 117 | 01/01/2007-31/12/2011 | 28/08/2007-02/01/2011 | 29/08/2007-31/12/2011 |

5.1.12.1 Wave Characteristics

Wave parameters and their analysis are shown in this session, for Skyros buoy for the period 2007-2011.

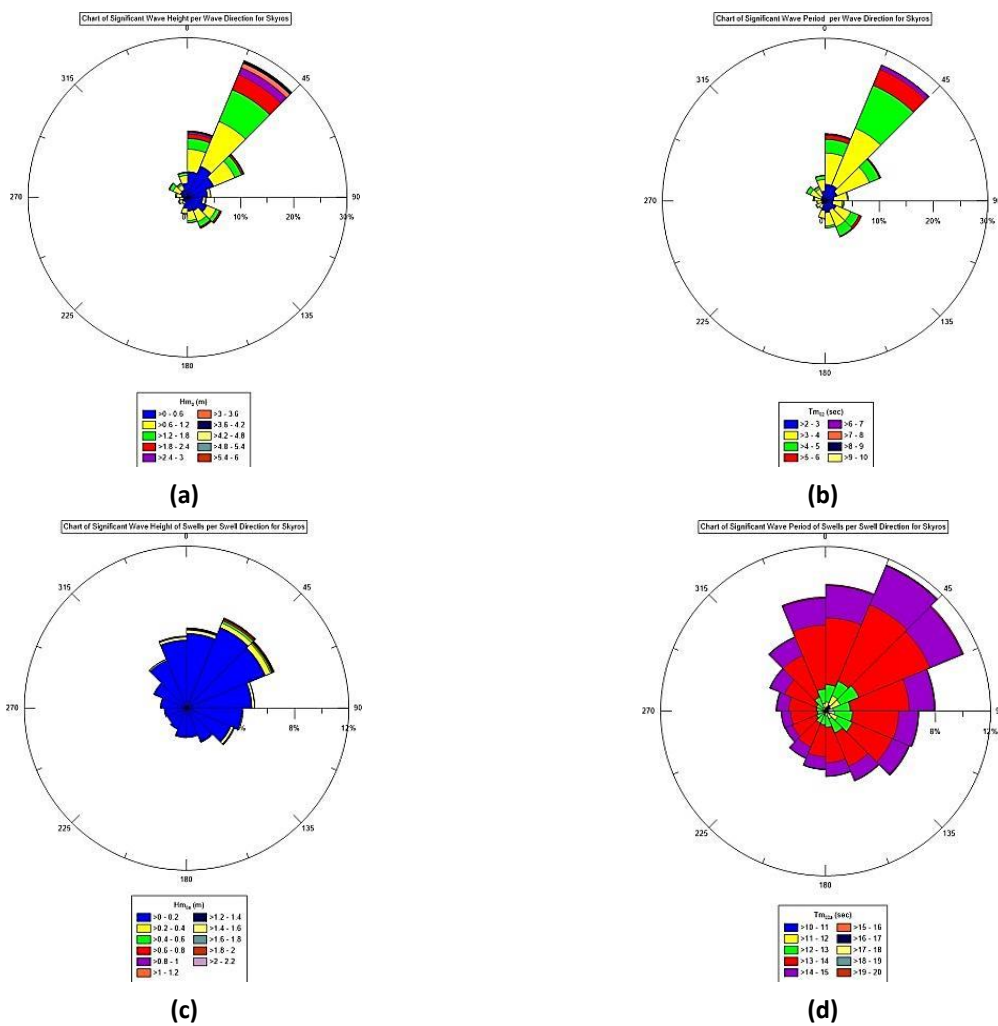
5.1.12.1.1 General Statistics

In Table 5.1.80, the descriptive statistics of wave parameters are shown for Skyros. The waves have mean heights of 0.98 m, that can reach 5.46 m while their mean period is 3.6 s and has a max of 7.52 s. The wind waves have mean heights of 0.85 s, max of 4.69 m and their period is of 3.59 s (mean) and 7.05 s (max). The swells have mean height of 0.04 m and 2.99 m (max), mean periods of 13.41 s (mean) and 19.57 s (max). Finally, the max wave height has a mean of 1.16 m and a max recorded of 7.51 m while the peak period has a mean of 4.63 s and a max of 10.43 s.

Table 5.1.80: Descriptive Statistics of Wave Parameters for Skyros Buoy

| | Number of Records | Mean | Maximum | Std.Dev. |
|----------------|-------------------|-------|---------|----------|
| H_{m0} (m) | 11251 | 0.87 | 5.46 | 0.70 |
| H_{m0a} (m) | 11761 | 0.04 | 2.99 | 0.11 |
| H_{m0b} (m) | 9733 | 0.85 | 4.69 | 0.67 |
| H_{max} (m)* | 11150 | 1.16 | 7.51 | 1.09 |
| T_{m02} (s) | 11772 | 3.60 | 7.52 | 0.82 |
| T_{m02a} (s) | 11280 | 13.41 | 19.57 | 0.88 |
| T_{m02b} (s) | 11761 | 3.59 | 7.05 | 0.81 |
| T_p (s) | 11772 | 4.63 | 10.43 | 1.49 |

From the charts in Figure 5.1.73, it is shown that the main directions of waves (40%) are of NE (Fetch length of 94 km) and the same applies for swells. Waves with heights of more than 3 m have a frequency of 1.77% and 82.91% is from NE.



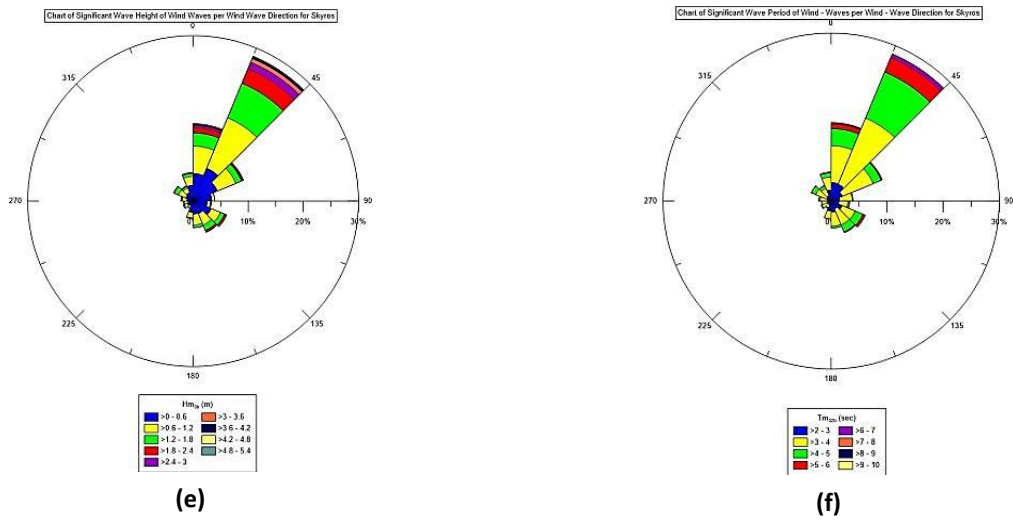


Figure 5.1.73: Rose Diagrams for Significant Wave Height and Wave period for all waves (a,b), swells (c,d) and wind waves (e,f) for Skyros Buoy

The percentages of appearance of significant wave height according to wave period are given in Table 5.1.81. The highest waves (>3.6 m) have a frequency of 0.74% with periods of more than 6 s. The most frequent waves (44.50%) are those with height from 0 to 0.6 m with the majority of them (58.22%) described with periods of 2 to 3 s.

Table 5.1.81: Pivot Table for Significant Wave Height and Zero-crossing wave period for Skyros Buoy

| Hm ₀ (m) | Tm ₀₂ (s) | | | | | | | Total |
|---------------------|----------------------|-------|-------|------|------|------|--------|-------|
| | 2-3 | 3-4 | 4-5 | 5-6 | 6-7 | 7-8 | | |
| 0-0.6 | 25.91 | 18.42 | 0.18 | 0 | 0 | 0 | 44.50 | |
| 0.6-1.2 | 0.90 | 26.67 | 3.82 | 0.05 | 0 | 0 | 31.45 | |
| 1.2-1.8 | 0 | 2.11 | 12.27 | 0.32 | 0 | 0 | 14.69 | |
| 1.8-2.4 | 0 | 0 | 3.20 | 2.16 | 0 | 0 | 5.36 | |
| 2.4-3 | 0 | 0 | 0 | 2.20 | 0.03 | 0 | 2.23 | |
| 3-3.6 | 0 | 0 | 0 | 0.62 | 0.41 | 0 | 1.03 | |
| 3.6-4.2 | 0 | 0 | 0 | 0 | 0.60 | 0 | 0.60 | |
| 4.2-4.8 | 0 | 0 | 0 | 0 | 0.11 | 0 | 0.11 | |
| 4.8-5.4 | 0 | 0 | 0 | 0 | 0 | 0.03 | 0.03 | |
| 5.4-6 | 0 | 0 | 0 | 0 | 0 | 0.01 | 0.01 | |
| Total | 26.81 | 47.20 | 19.46 | 5.36 | 1.14 | 0.04 | 100.00 | |

5.1.12.1.2 Monthly Means for the period 2007-2011

The minimum monthly mean of wave height is in July (0.48 m) while the maximum mean is in February (1.27 m).

Furthermore, the minimum value recorded is in June (0.05 m) and the maximum is in March (5.46 m). For the wave period, the minimum mean is in July (3.08 s) and the maximum mean in February (4.03 s). The minimum value for wave period is in September (2.22 s) and the maximum in March (7.52 s).

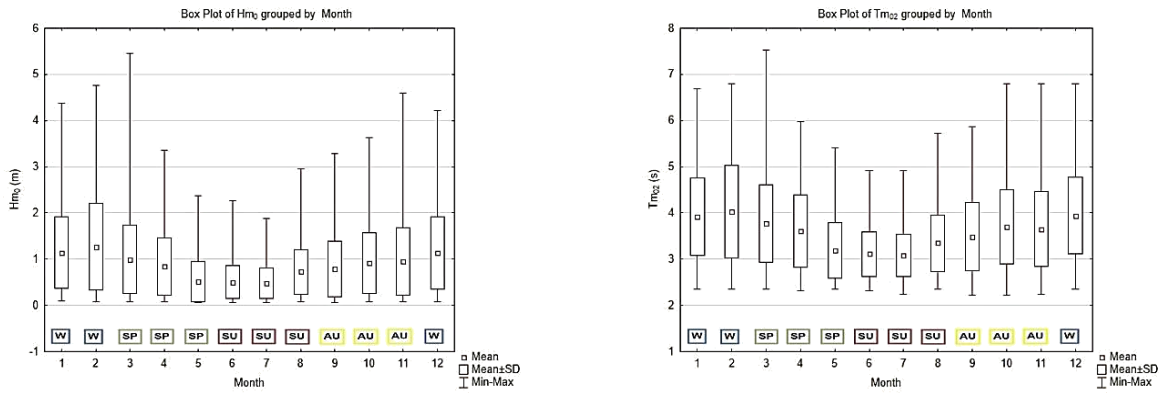


Figure 5.1.74: Box and Whiskers plots for Monthly Wave Height and Wave Period for Skyros Buoy

5.1.12.2 Sea Surface Elevation (SSE)

The results of the analysis of 6371 SSE records from Skyros buoy are shown in this chapter. For the example shown in Figure 5.1.75, the peak period of the Spectrum (T_p) is around 8.71 s.

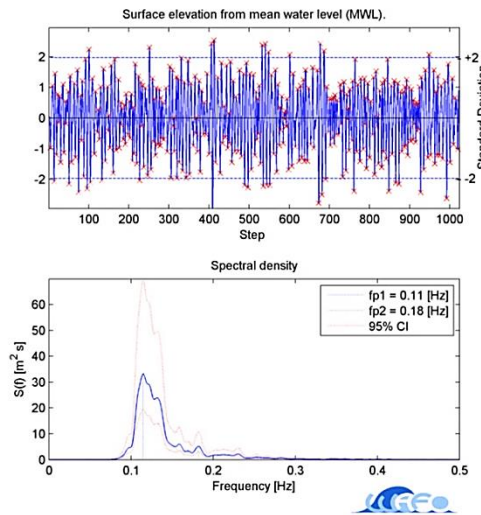


Figure 5.1.75: Random SSE record and its spectrum for Skyros Buoy

5.1.12.2.1 General Statistics

In Table 5.1.82, the descriptive statistics of wave characteristics as derived from 6371 records of sea surface elevation analysis are given.

The spectral significant wave height H_{m0} has a mean of 1.01 m and a max of 4.68 m while the statistical $H_{1/3}$ has a mean of 0.94 m and a max of 4.37 m. The spectral period T_{m02} has a mean of 3.76 s and a max of 6.78 s while the statistical $T_{1/3}$ has a mean of 5.24 s and a max of 9.38 s. Finally, the max wave height has a mean of 1.55 m and a max of 7.85 m while the peak period has a mean of 4.29 s and a max of 10.56 s.

Table 5.1.82: Descriptive Statistics as derived from SSE Analysis for Skyros Buoy

| Parameters | Number of Records | Mean | Maximum | Std.Dev. |
|---------------|-------------------|------|---------|----------|
| H_{m0} (m) | 6371 | 1.01 | 4.68 | 0.63 |
| Hmax (m) | 6371 | 1.55 | 7.85 | 0.97 |
| $H_{1/3}$ (m) | 6371 | 0.94 | 4.37 | 0.60 |
| T_{m02} (s) | 6371 | 3.76 | 6.78 | 0.75 |
| $T_{1/3}$ (s) | 6371 | 5.24 | 9.38 | 1.09 |
| T_p (s) | 6371 | 4.92 | 10.56 | 1.35 |

For Skyros, a correlation of 0.99 is given for H_{m0} and $H_{1/3}$ and 0.98 for T_{m02} and $T_{1/3}$ (Figure 5.1.76).

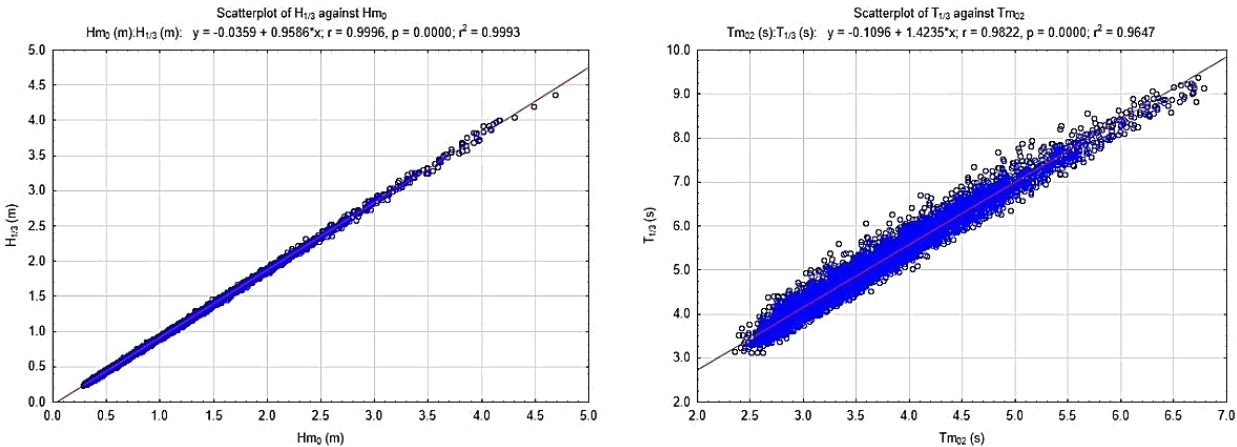


Figure 5.1.76: Scatterplots of statistical and spectral wave parameters for Skyros Buoy

5.1.12.2.2 Monthly Means for the period 2007-2011

Monthly means for the period 2007 – 2011 are shown in (Figure 5.1.77).

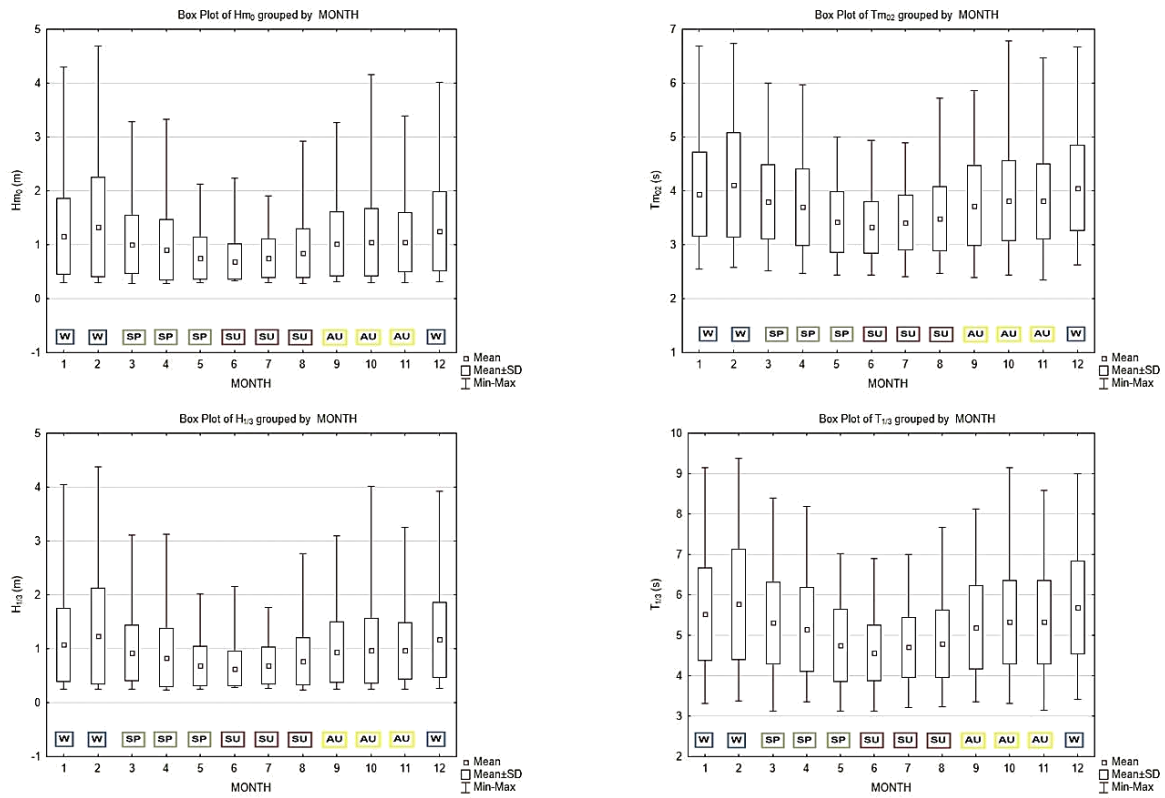


Figure 5.1.77: Spectral and Statistical Monthly Values per Wave Parameter for Skyros Buoy

As for the case of the spectral significant wave height H_{m0} , the minimum mean monthly value is in June (0.69 m), the maximum mean value is in February (1.32 m) while the minimum recorded value is 0.28 m (August) and the maximum 4.68 m (February). For the spectral wave period (T_{m02}), the mean minimum monthly value is 3.22 s (June) and the maximum 4.11 s (February). The minimum recorded value is in 2.34 s (November) and the maximum 6.77 s (October). As for the statistical significant wave height $H_{1/3}$, the smallest monthly value is 0.63 m (June) whilst the largest 1.24 m (February). The smallest overall value is 0.23 m (August) and the maximum (4.37 m) in February. Finally, for the statistical significant wave period $T_{1/3}$ the minimum monthly is 4.56 s on June and the maximum 5.76 s in February. In general, the minimum recorded period is 3.12 s (March) and the maximum 9.38 s in February.

5.1.12.2.3 Probability Distribution of Wave Height

From the QQ plot, in Figure 5.1.78, the Kumaraswamy distribution approximates the mean values better than Weibull and Rayleigh, while underestimates the higher values in contradiction to the other two distributions that overestimate them.

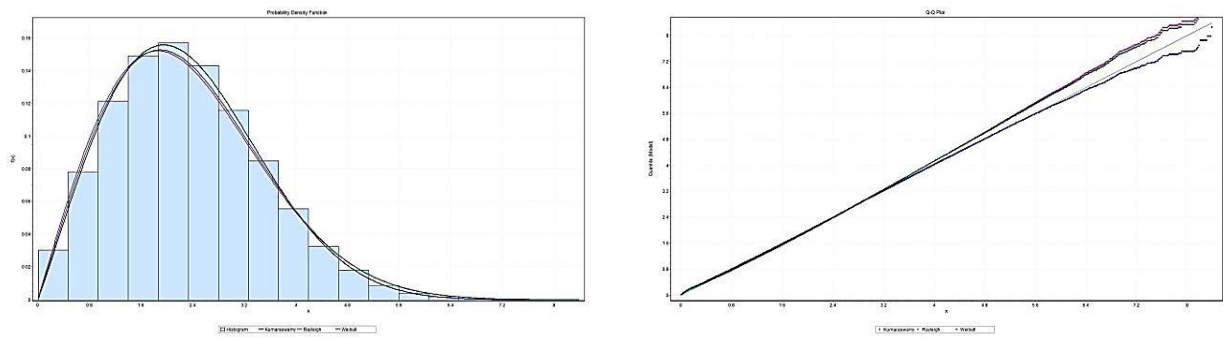


Figure 5.1.78: Probability Distributions and QQ plots for Skyros Buoy for random wave heights

The statistics of goodness of fit for every distribution under examination are given in Table 5.1.83.

Table 5.1.83: Statistics of Goodness of Fits according to K-S, A-D and χ^2 test for Skyros Buoy

| Distribution | Kolmogorov Smirnov | Anderson Darling | Chi-Squared |
|--------------|--------------------|------------------|-------------|
| | Statistic | Statistic | Statistic |
| Kumaraswamy | 0.00672 | 21.582 | 132.17 |
| Weibull | 0.01332 | 148.16 | 992.98 |
| Rayleigh | 0.01963 | 249.97 | 1456.1 |

5.1.12.2.4 Ratios between Statistical and Spectral Parameters

The statistics of the ratios in Table 5.1.84, show that a mean of 1.09 is estimated for $H_{m0} / H_{1/3}$, 3.67 for $H_{1/3} / \sqrt{m_0}$, 1.56 H_{max} / H_{m0} and 1.7 for $H_{max} / H_{1/3}$.

Table 5.1.84: Statistics of Various Ratios for Skyros Buoy

| Ratios | Number of Records | Mean | Minimum | Maximum | Std.Dev. | CV (%) |
|------------------------|-------------------|------|---------|---------|----------|--------|
| $H_{m0} / H_{1/3}$ | 6371 | 1.09 | 1.01 | 1.25 | 0.03 | 3.18 |
| $H_{1/3} / \sqrt{m_0}$ | 6371 | 3.67 | 3.20 | 3.95 | 0.11 | 3.10 |
| H_{max} / H_{m0} | 6371 | 1.56 | 1.21 | 2.54 | 0.15 | 9.60 |
| $H_{max} / H_{1/3}$ | 6371 | 1.70 | 1.28 | 2.74 | 0.17 | 9.87 |

5.1.12.3 Weather Characteristics

The atmospheric characteristics of the area of Skyros are shown in this chapter for the period of 2007-2011.

5.1.12.3.1 General Statistics

The main statistics of atmospheric parameters for Skyros are shown in Table 5.1.85. The area is described by minimum temperatures of 0.0069 °C and maximums of 31.93 °C while mean wind speeds of 4.96 m/s.

Table 5.1.85: Descriptive Statistics of Atmospheric Parameters for Skyros Buoy

| Parameters | Number of Records | Mean | Minimum | Maximum | Std.Dev. |
|---------------------|-------------------|---------|---------|---------|----------|
| Air Pressure(hPa) | 11825 | 1015.30 | 987.01 | 1036.88 | 6.92 |
| Air Temperature(°C) | 11209 | 17.19 | 1.79 | 30.33 | 6.17 |
| Wind Gust (m/s) | 10300 | 6.80 | 0.04 | 25.59 | 3.95 |
| Wind Speed (m/s) | 10209 | 5.13 | 0.01 | 18.68 | 3.12 |

As given in wind chart of Figure 5.1.79, the main directions of wind (47.86%) are in the range of N to NE. The most frequent winds range from 3 to 6 m/s (38.71%) and from those 33.27% are of N direction. Winds above 15 m/s are of 0.44% frequency and 86.67% of them are blowing from N-NE.

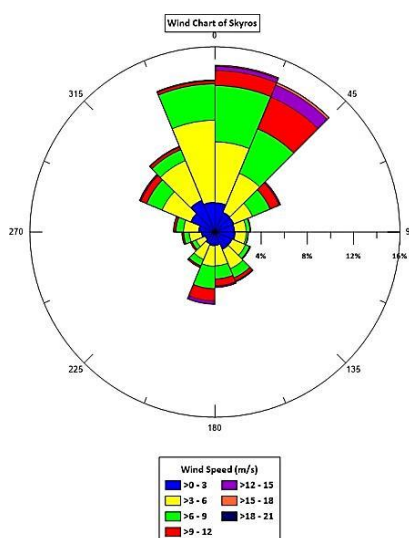


Figure 5.1.79: Wind Chart for Skyros Buoy

5.1.12.3.2 Monthly Means for the period 2007-2011

The minimum mean monthly value for pressure is in July (1010.29 hPa) and the maximum (1019.04 hPa) in January. For temperature the minimum mean monthly 9.95 °C is in February and the maximum 25.31 °C in August. Minimum values of wind speed and wind gust are in May (3.64 m/s and 4.65 m/s respectively) and the maximum are in February (6.51 m/s and 8.77 m/s).

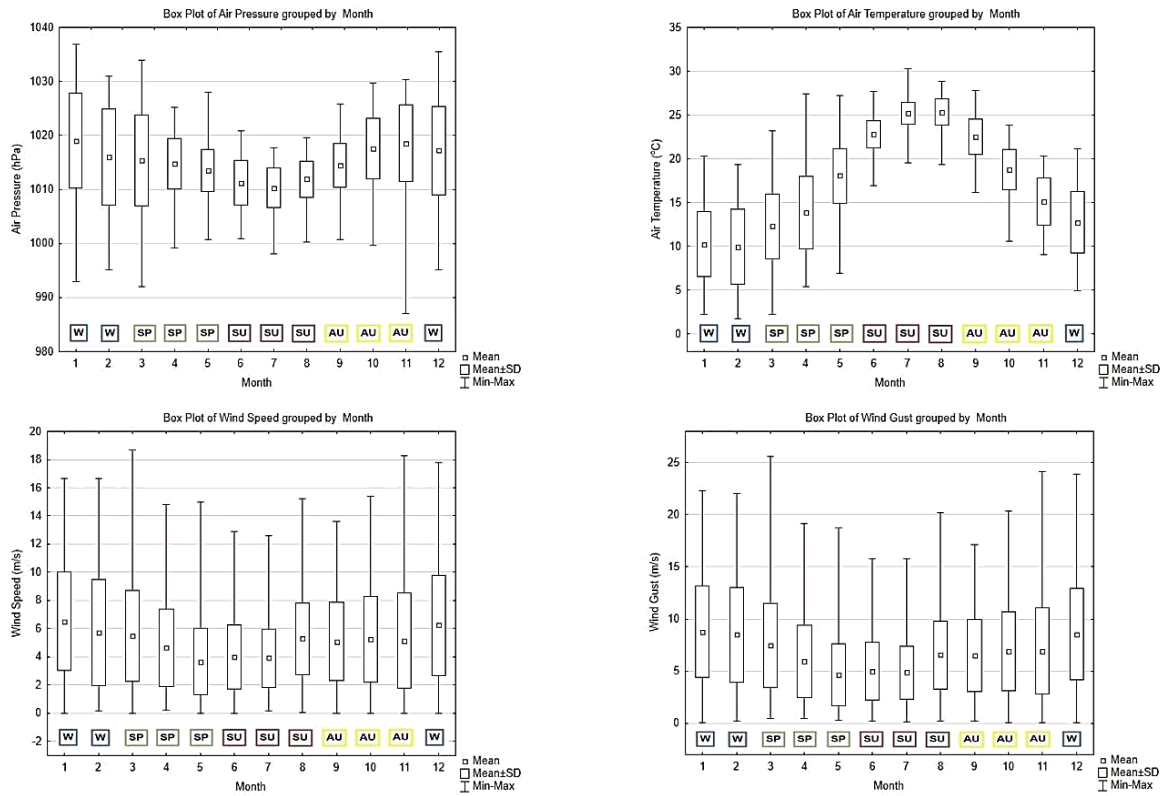


Figure 5.1.80: Monthly Box and Whiskers Plots for Atmospheric Parameters for Skyros Buoy

5.1.12.4 Relation of Wind and Wave Data

The relation of atmospheric and wave characteristics only for the same time period is shown in this chapter for Skyros area.

5.1.12.4.1 General Statistics

The mean value wind speed (5.32 m/s) can be considered as gentle breeze that will most likely result in breaking of wave crests with isolated whitecaps (Table 5.1.86).

Table 5.1.86: Descriptive Statistics of Wave and Atmospheric Parameters for Skyros Buoy

| | Number of Records | Mean | Minimum | Maximum | Std.Dev. |
|-----------------------|-------------------|---------|---------|---------|----------|
| Air Pressure (hPa) | 8530 | 1014.59 | 987.01 | 1036.88 | 6.85 |
| Air Temperature (°C) | 8530 | 18.36 | 1.79 | 30.33 | 5.61 |
| Wind Gust (m/s) | 8530 | 6.94 | 0.42 | 24.14 | 3.89 |
| Wind Speed (m/s) | 8530 | 5.32 | 0.01 | 18.28 | 3.08 |
| Hm ₀ (m) | 8530 | 0.87 | 0.05 | 4.77 | 0.68 |
| Hm _{0a} (m) | 8530 | 0.04 | 0.00 | 1.72 | 0.09 |
| Hm _{0b} (m) | 8530 | 0.87 | 0.05 | 4.69 | 0.68 |
| H _{max} (m) | 8530 | 1.15 | 0.00 | 7.19 | 1.06 |
| Tm ₀₂ (s) | 8530 | 3.57 | 2.23 | 6.80 | 0.81 |
| Tm _{02a} (s) | 8530 | 13.44 | 10.31 | 17.81 | 0.87 |
| Tm _{02b} (s) | 8530 | 3.57 | 2.23 | 6.72 | 0.81 |
| T _p (s) | 8530 | 4.59 | 1.99 | 10.43 | 1.49 |

The most frequent waves of 50.25% have heights of 0-0.7m and 48.19% of these are related with wind speeds of 3-6 m/s. Furthermore, the higher waves (>3.5m) have a frequency of 0.99% with 69.79% related with speeds of above 12m/s wind speeds.

Table 5.1.87: Frequency Table (%) of Wind Speed and Significant Spectral Wave Height for Skyros Buoy

| Wind Speed (m/s) | Hm ₀ (m) | | | | | | | | Total |
|---------------------|---------------------|---------|---------|---------|---------|---------|---------|---------|--------|
| | 0-0.7 | 0.7-1.4 | 1.4-2.1 | 2.1-2.8 | 2.8-3.5 | 3.5-4.2 | 4.2-4.9 | 4.9-5.6 | |
| 0-3 | 23.13 | 2.64 | 0.78 | 0.38 | 0.22 | 0.18 | 0.02 | 0.00 | 27.34 |
| 3-6 | 24.22 | 11.75 | 1.27 | 0.18 | 0.07 | 0.05 | 0.01 | 0.00 | 37.55 |
| 6-9 | 2.84 | 14.20 | 5.69 | 0.53 | 0.03 | 0.00 | 0.00 | 0.00 | 23.30 |
| 9-12 | 0.05 | 1.83 | 4.54 | 2.18 | 0.33 | 0.03 | 0.00 | 0.00 | 8.95 |
| 12-15 | 0.01 | 0.12 | 0.50 | 0.67 | 0.76 | 0.33 | 0.01 | 0.00 | 2.40 |
| 15-18 | 0.00 | 0.00 | 0.01 | 0.02 | 0.06 | 0.24 | 0.09 | 0.00 | 0.42 |
| 18-21 | 0.00 | 0.00 | 0.00 | 0.01 | 0.00 | 0.00 | 0.00 | 0.02 | 0.03 |
| Total | 50.25 | 30.54 | 12.79 | 3.97 | 1.47 | 0.83 | 0.13 | 0.02 | 100.00 |

The charts in Figure 5.1.81, shows that 40.99% of waves with heights up to 1.4 m are related to winds blowing from N to NE and the same applies for waves with heights of more than 3.5 m. The same pattern applies for periods as well.

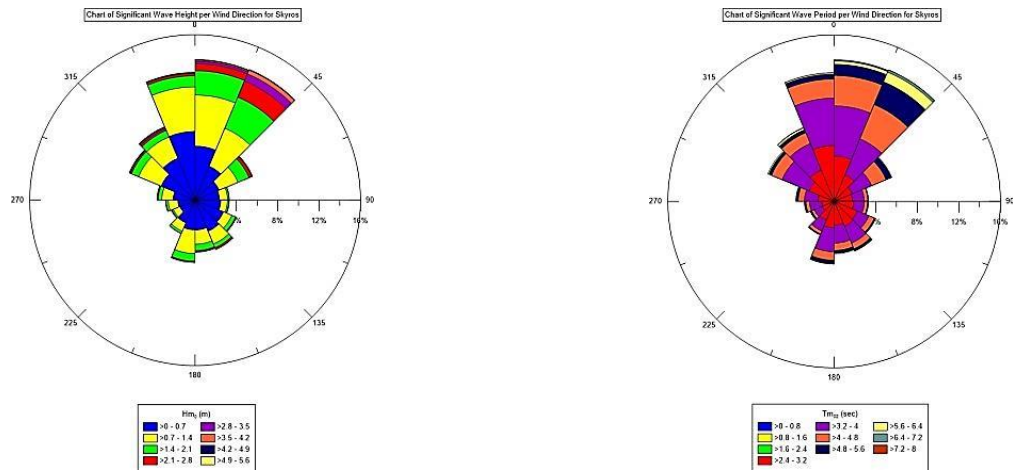


Figure 5.1.81: Charts of Wind Direction and Wave Height - Period for Skyros Buoy

5.1.13 ZAKYNTHOS

The location, depth of installation and the time of recordings for Zakynthos are shown in Table 5.1.88.

Table 5.1.88: Location, depth of installation and time periods of recording per database for Zakynthos Buoy

| Location | Depth (m) | Wave Parameters | SSE data | Atmospheric Parameters |
|--------------------------|-----------|-----------------------|----------------------|------------------------|
| 20.61035°E, 37.9541°N | 313 | 01/01/2007-31/12/2011 | 08/11/200731/12/2011 | 08/11/200731/12/2011 |

5.1.13.1 Wave Characteristics

The wave characteristics as given by the buoy's records are presented in this session for the period of 2007-2011.

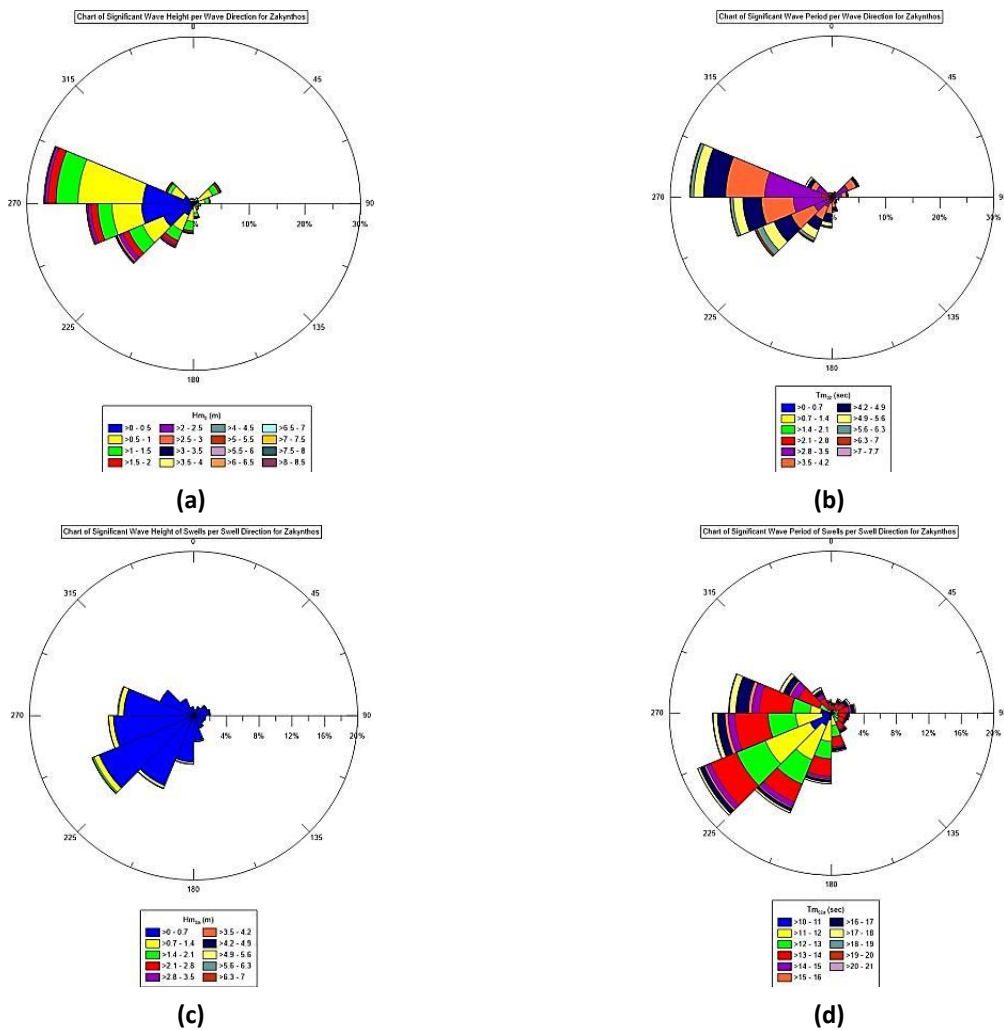
5.1.13.1.1 General Statistics

The descriptive statistics of wave parameters for Zakynthos are given in Table 5.1.89. The wind waves have mean heights of 0.81 m and max of 4.38 m and mean periods of 3.81 s and max of 6.91 s. Swells have mean heights of 0.11 m, max of 5.94 m and mean periods of 13.07 s and max of 20.86 s. Waves have mean heights of 0.82 m and max of 7.19 m whilst periods of 3.86 s and max of 8.09 s. Max wave height has a mean of 1.12 m and can reach up to 16.02 m. Peak period has a mean of 5.35 s and a max of 12.3 s.

Table 5.1.89: Descriptive Statistics of Wave Parameters for Zakynthos Buoy

| | Number of Records | Mean | Maximum | Std.Dev. |
|----------------|-------------------|-------|---------|----------|
| H_{m0} (m) | 10803 | 0.82 | 7.19 | 0.57 |
| H_{m0a} (m) | 10602 | 0.11 | 5.94 | 0.27 |
| H_{m0b} (m) | 11078 | 0.81 | 4.38 | 0.54 |
| H_{max} (m) | 10802 | 1.12 | 16.02 | 0.99 |
| T_{m02} (s) | 10966 | 3.86 | 8.09 | 0.88 |
| T_{m02a} (s) | 11087 | 13.07 | 20.86 | 1.73 |
| T_{m02b} (s) | 11078 | 3.81 | 6.91 | 0.82 |
| T_p (s) | 10780 | 5.35 | 12.30 | 1.77 |

The charts of Figure 5.1.82, provide information about the directionality of waves for Zakynthos. The most frequent waves propagate from SW to W (69.27% with a fetch length of 360km) and their majority (39.69%) is of 0-0.5m wave height. The higher waves (>3m) have a frequency of occurrence of 0.77% with 85.54% of them from the SW-W. Periods are 2.7-3.4s (32.03%) and 50.23% of the waves propagate from W. The longer periods (>7.6 s) are from SW (66.67%).



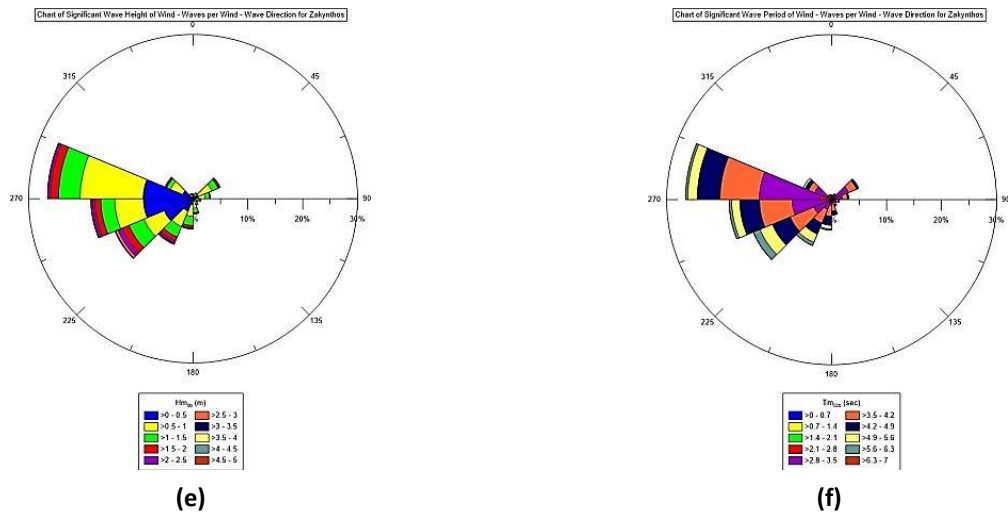


Figure 5.1.82: Rose Diagrams for Significant Wave Height and Wave period for all waves (a,b), swells (c,d) and wind waves (e,f) for Zakynthos Buoy

The percentages of appearance of significant wave height according to wave period for Zakynthos are shown in Table 5.1.90. The most frequent waves (46.24%) are those with heights of 0.5 to 1m with the majority of them described with periods of 2.7 to 3.4s. The higher waves (>3m) are related with periods of more than 6.2s.

Table 5.1.90: Pivot Table for Significant Wave Height and Zero-crossing wave period for Zakynthos Buoy

| Hm ₀ (m) | Tm ₀₂ (s) | | | | | | | | | Total |
|---------------------|----------------------|---------|---------|---------|---------|---------|---------|---------|---------|--------|
| | 2-2.7 | 2.7-3.4 | 3.4-4.1 | 4.1-4.8 | 4.8-5.5 | 5.5-6.2 | 6.2-6.9 | 6.9-7.6 | 7.6-8.3 | |
| 0-0.5 | 5.23 | 20.00 | 8.25 | 1.38 | 0.05 | 0 | 0 | 0 | 0 | 34.91 |
| 0.5-1 | 0.11 | 12.29 | 14.26 | 8.28 | 1.27 | 0.01 | 0.01 | 0 | 0 | 36.24 |
| 1-1.5 | 0 | 0.07 | 4.98 | 7.98 | 4.19 | 0.61 | 0.00 | 0 | 0 | 17.83 |
| 1.5-2 | 0 | 0 | 0.02 | 1.84 | 3.32 | 1.22 | 0.08 | 0.01 | 0 | 6.49 |
| 2-2.5 | 0 | 0 | 0 | 0.05 | 1.13 | 1.22 | 0.32 | 0.02 | 0 | 2.73 |
| 2.5-3 | 0 | 0 | 0 | 0 | 0.11 | 0.56 | 0.31 | 0.05 | 0 | 1.03 |
| 3-3.5 | 0 | 0 | 0 | 0 | 0 | 0.08 | 0.28 | 0.07 | 0.02 | 0.45 |
| 3.5-4 | 0 | 0 | 0 | 0 | 0.01 | 0 | 0.10 | 0.09 | 0.01 | 0.22 |
| 4-4.5 | 0 | 0 | 0 | 0 | 0 | 0 | 0 | 0.02 | 0 | 0.02 |
| 4.5-5 | 0 | 0 | 0 | 0 | 0 | 0 | 0.01 | 0.04 | 0.02 | 0.07 |
| 5-5.5 | 0 | 0 | 0 | 0 | 0 | 0 | 0.01 | 0 | 0.01 | 0.02 |
| 7-7.5 | 0 | 0 | 0 | 0 | 0 | 0 | 0.01 | 0 | 0 | 0.01 |
| Total | 5.35 | 32.37 | 27.51 | 19.51 | 10.08 | 3.70 | 1.13 | 0.29 | 0.06 | 100.00 |

5.1.13.1.2 Monthly Means for the period 2007-2011

For the wave height it is shown (Figure 5.1.83) that the minimum mean monthly is in May (0.56 m) while the maximum mean is in February (1.23 m). The minimum recorded value is in May (0.07 m) and the maximum is in November (7.18 m). As for the wave period, the minimum monthly mean is in July (3.41 s) and the maximum mean in February (4.49 s). The minimum recorded value for wave period is in July (2.31 s) and the maximum in November (8.09 s).

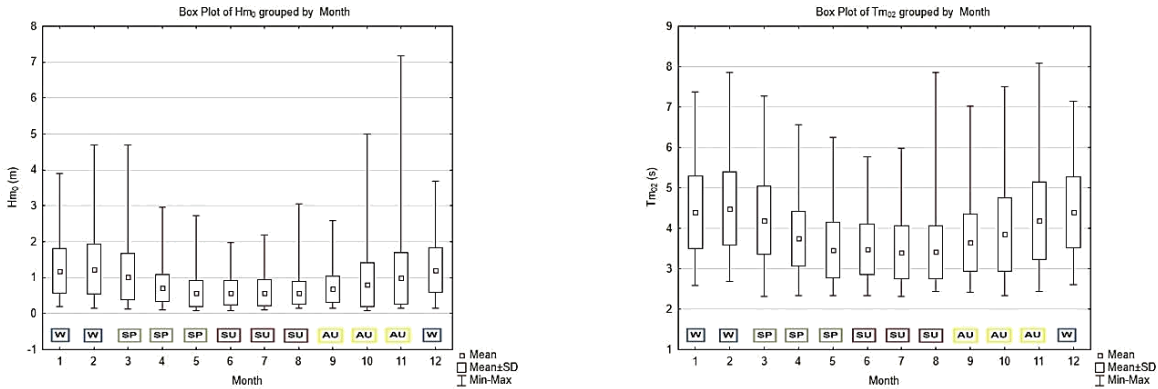


Figure 5.1.83: Box and Whiskers plots for Monthly Wave Height and Wave Period for Zakynthos Buoy

5.1.13.2 Sea Surface Elevation (SSE)

Wave parameters as derived from the analysis of 6332 records of sea surface elevation as obtained by the Santorini buoy are shown in this subchapter. An example of a record of sea surface analysis and its spectral analysis is given in Figure 5.1.84. For this case, the peak period of the Spectrum (T_p) is around 9.43 s.

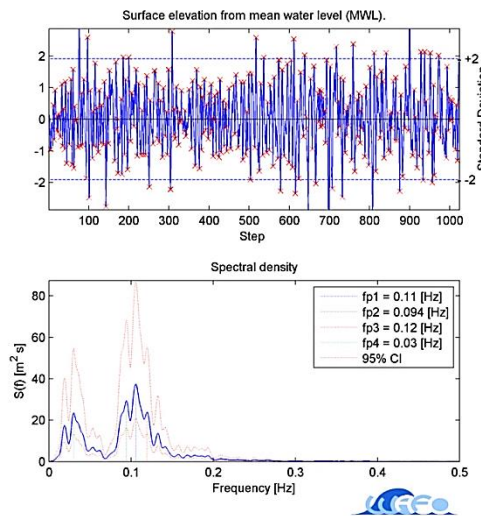


Figure 5.1.84: Random SSE record and it's spectrum for Zakynthos Buoy

5.1.13.2.1 General Statistics

In Table 5.1.91 are shown the descriptive statistics of wave characteristics as derived from 6332 records of sea surface elevation analysis. The spectral wave height H_{m0} has a mean of 0.99 m and a max of 5.77 m while the statistical wave height $H_{1/3}$ has a mean of 0.89 m and a max of 5.21 m. The statistical wave period has a mean period of 6.15 s and a max of 13.64 s while the spectral has a mean period of 4.14 s and a max of 10.28 s. The max wave height has a mean of 1.51 m and a max of 11.92 m whilst the peak period has a mean of 5.81 s and a max of 12.8 s.

Table 5.1.91: Descriptive Statistics as derived from SSE Analysis for Zakynthos Buoy

| | Number of Records | Mean | Maximum | Std.Dev. |
|---------------|-------------------|------|---------|----------|
| H_{m0} (m) | 6332 | 0.99 | 5.77 | 0.59 |
| Hmax (m) | 6332 | 1.51 | 11.92 | 0.98 |
| $H_{1/3}$ (m) | 6332 | 0.89 | 5.21 | 0.55 |
| T_{m02} (s) | 6332 | 4.14 | 10.28 | 0.92 |
| $T_{1/3}$ (s) | 6332 | 6.15 | 13.64 | 1.43 |
| T_p (s) | 6332 | 5.81 | 12.80 | 1.70 |

A correlation of 0.99 is given for H_{m0} and $H_{1/3}$ and 0.95 for T_{m02} and $T_{1/3}$ (Figure 5.1.85).

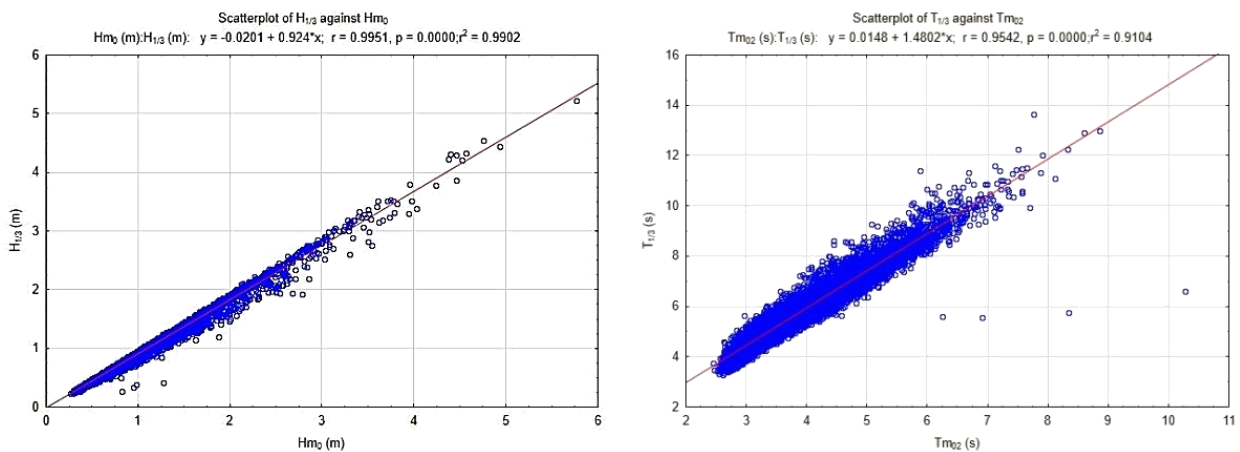


Figure 5.1.85: Scatterplots of statistical and spectral wave parameters for Zakynthos Buoy

5.1.13.2.2 Monthly Means for the period 2007-2011

For the case of the spectral significant wave height H_{m0} , the minimum mean value is in June (0.65 m), the maximum mean value is in February (1.3 m) while the minimum estimated value is 0.27 m (May) and the maximum 5.77 m (November).

As for the spectral wave period (T_{m02}), the mean minimum monthly value is 3.6 s (May) and the maximum 4.64 s (February). The minimum estimated period is 2.45 s (May) and the maximum 10.28 s (July). As for the statistical significant wave height $H_{1/3}$, the smallest monthly value is 0.59 m (June) whilst the largest 1.19 m (December). The smallest overall value is 0.23 m (January) and the maximum (5.21 m) in November. Finally, for the statistical significant wave period $T_{1/3}$ the minimum monthly is 5.23 s on May and the maximum 6.89 s in February. In general, the minimum recorded period is 3.29 s (June) and the maximum 13.64 s in September.

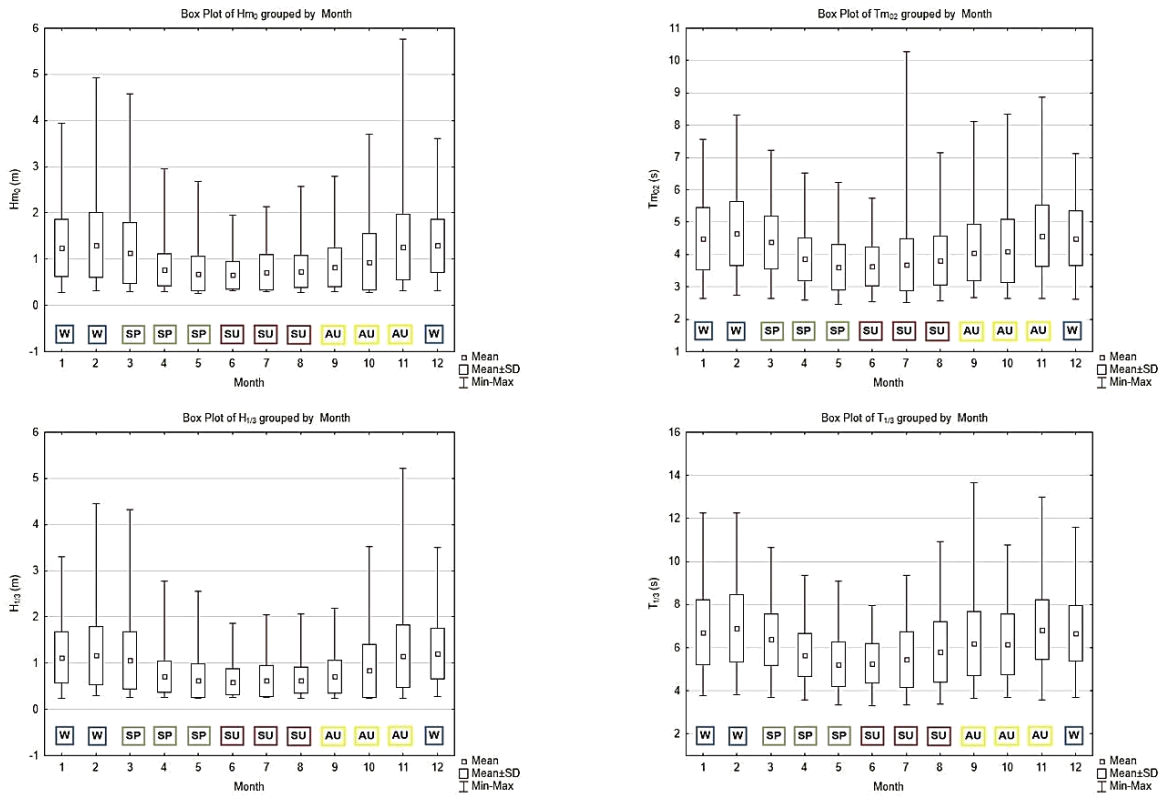


Figure 5.1.86: Spectral and Statistical Monthly Values per Wave Parameter for Zakynthos Buoy

5.1.13.2.3 Probability Distribution of Wave Height

From the QQ plot (Figure 5.1.87) one can detect that Kumaraswamy distribution underestimates the larger values of wave heights whilst Weibull and Rayleigh distribution diverge from the mean values.

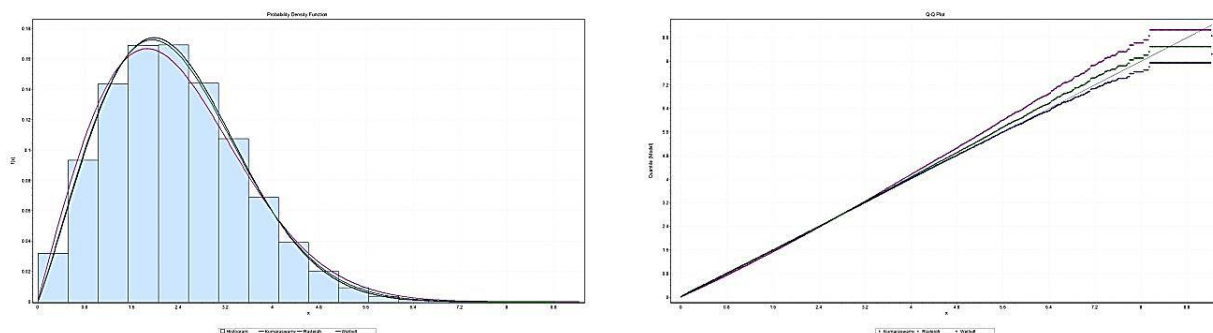


Figure 5.1.87: Probability Distributions and QQ plots for Zakynthos Buoy for random wave heights

The statistics of goodness of fit for every distribution under examination are given in Table 5.1.92.

Table 5.1.92: Statistics of Goodness of Fits according to K-S, A-D and χ^2 test for Zakynthos Buoy

| Distribution | Kolmogorov Smirnov | Anderson Darling | Chi-Squared |
|--------------|--------------------|------------------|-------------|
| | Statistic | Statistic | Statistic |
| Kumaraswamy | 0.00361 | 4.579 | 39.737 |
| Weibull | 0.00751 | 28.402 | 226.5 |
| Rayleigh | 0.02186 | 282.04 | 1675.8 |

5.1.13.2.4 Ratios between Spectral and Statistical Parameters

The statistics of the ratios in Table 5.1.93, show that a mean of 1.11 is estimated for $H_{m0} / H_{1/3}$, 3.62 for $H_{1/3} / \sqrt{m_0}$, 1.54 H_{max} / H_{m0} and 1.7 for $H_{max} / H_{1/3}$.

Table 5.1.93: Statistics of Various Ratios for Skyros Buoy

| | Number of Records | Mean | Minimum | Maximum | Std.Dev. |
|------------------------|-------------------|------|---------|---------|----------|
| $H_{m0} / H_{1/3}$ | 6333 | 1.11 | 1.00 | 6.96 | 0.10 |
| $H_{1/3} / \sqrt{m_0}$ | 6333 | 3.62 | 0.57 | 3.98 | 0.17 |
| H_{max} / H_{m0} | 6333 | 1.54 | 1.12 | 2.88 | 0.16 |
| $H_{max} / H_{1/3}$ | 6329 | 1.70 | 1.27 | 4.62 | 0.19 |

5.1.13.3 Weather Characteristics

The atmospheric characteristics of the area of Zakynthos are shown here for the period 2007-2011.

5.1.13.3.1 General Statistics

In Table 5.1.94, the main statistics of atmospheric parameters for Zakynthos are shown. The mean temperature is 19.15 °C, the mean pressure of 1013.31 hPa while wind gust has a mean of 6.49 m/s and wind speed 4.93 m/s.

Table 5.1.94: Descriptive Statistics of Atmospheric Parameters for Zakynthos Buoy

| | Number of Records | Mean | Minimum | Maximum | Std.Dev. |
|---------------------|-------------------|---------|---------|---------|----------|
| Air Pressure(hPa) | 11171 | 1013.31 | 989.90 | 1033.58 | 6.15 |
| Air Temperature(°C) | 11171 | 19.15 | 3.40 | 31.28 | 4.89 |
| Wind Gust (m/s) | 10591 | 6.49 | 0.16 | 25.08 | 3.68 |
| Wind Speed (m/s) | 10568 | 4.93 | 0.01 | 17.81 | 2.97 |

As given in wind chart of Figure 5.1.88 the main directions of wind are in the range of W (24.89%) and the secondary direction is from E (19.99%). The most frequent winds range from 2m/s to 4m/s (27.11%) and from those 43.56% is from W. Winds above 14m/s are of 0.48% frequency and 56.86% have directions of NE.

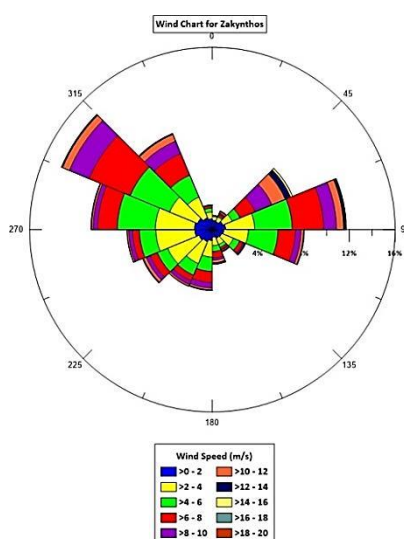


Figure 5.1.88: Wind Chart for Zakynthos Buoy

5.1.13.3.2 Monthly Means for the period 2007-2011.

For pressure the minimum monthly value is in August (1009.89 hPa) and the maximum (1016.72 hPa) in January. For temperature the minimum mean monthly 12.71 °C in February and the maximum in 25.9 °C during August. Minimum values of wind speed and wind gust are in May (3.94 m/s and 5.14 m/s respectively) and the maximum are in January (6.42 m/s) and December (8.815 m/s) respectively.

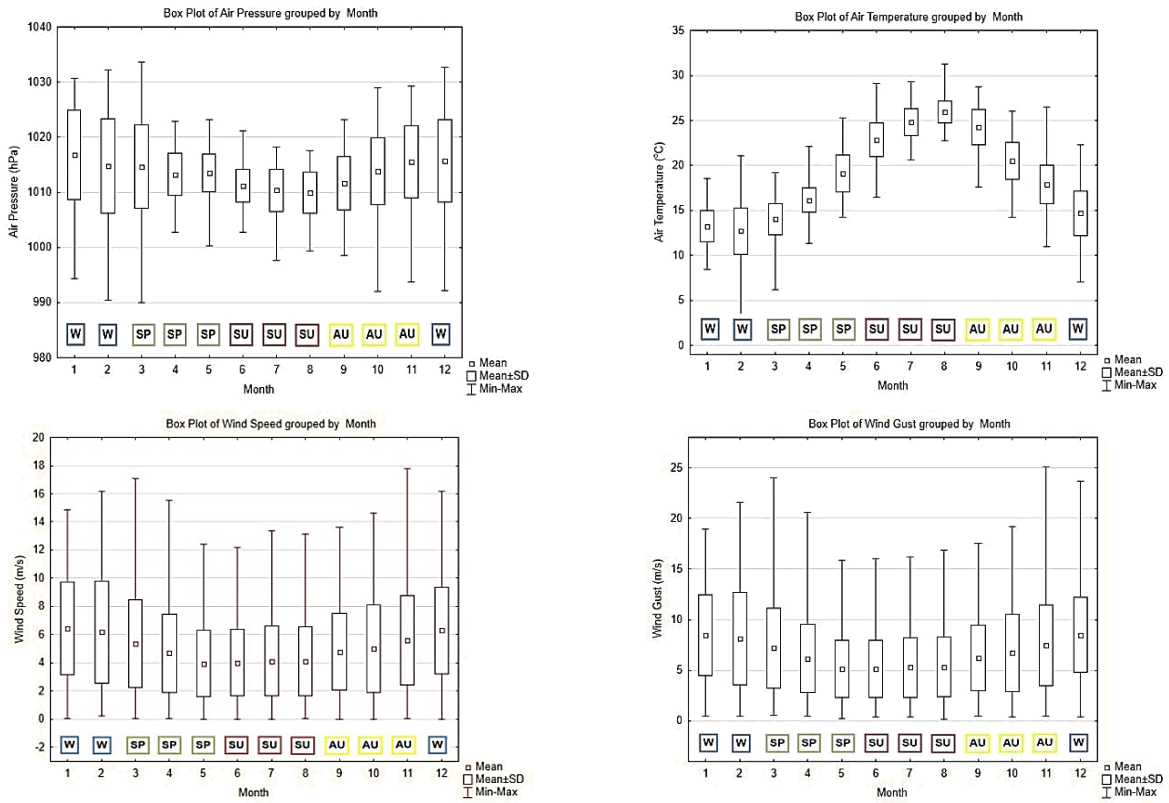


Figure 5.1.89: Monthly Box and Whiskers Plots for Atmospheric Parameters for Zakyntos Buoy

5.1.13.4 Relation of Wind and Wave Data

The relation of wind and wave data for the matching time periods of Zakyntos is shown in this subchapter.

5.1.13.4.1 General Statistics

The mean value wind speed (5.29 m/s) can be considered as gentle breeze that will most likely result in breaking of wave crests with isolated whitecaps (Table 5.1.95).

Table 5.1.95: Descriptive Statistics of Wave and Atmospheric Parameters for Zakynthos Buoy

| | Number of Records | Mean | Minimum | Maximum | Std.Dev. |
|-----------------------|-------------------|---------|---------|---------|----------|
| Air Pressure (hPa) | 6402 | 1012.09 | 989.90 | 1033.58 | 6.08 |
| Air Temperature (°C) | 6402 | 19.47 | 3.40 | 31.16 | 4.96 |
| Wind Gust (m/s) | 6402 | 6.99 | 0.32 | 25.08 | 3.89 |
| Wind Speed (m/s) | 6402 | 5.29 | 0.01 | 17.81 | 3.13 |
| Hm ₀ (m) | 6402 | 0.91 | 0.09 | 5.31 | 0.60 |
| Hm _{0a} (m) | 6402 | 0.11 | 0.00 | 3.75 | 0.23 |
| Hm _{0b} (m) | 6402 | 0.89 | 0.09 | 4.38 | 0.57 |
| H _{max} (m) | 6402 | 1.24 | 0.00 | 15.31 | 0.97 |
| Tm ₀₂ (s) | 6402 | 3.94 | 2.31 | 8.09 | 0.90 |
| Tm _{02a} (s) | 6402 | 12.88 | 10.31 | 19.57 | 1.79 |
| Tm _{02b} (s) | 6402 | 3.90 | 2.31 | 6.91 | 0.86 |
| T _p (s) | 6402 | 5.54 | 1.99 | 12.30 | 1.85 |

A frequency table of wind speed and significant wave height is shown in Table 5.1.96. The most frequent waves of 62.67% have heights of 0-0.8 and 35.54% of these are related with wind speeds of 2-4 m/s. Furthermore, the higher waves (>3.2m) have a frequency of 0.48% and 61.22% are related with speeds of above 10m/s wind speeds.

Table 5.1.96: Frequency Table (%) of Wind Speed and Significant Spectral Wave Height for Zakynthos Buoy

| Wind Speed (m/s) | Hm ₀ (m) | | | | | | | | Total |
|---------------------|---------------------|---------|---------|---------|-------|-------|---------|---------|--------|
| | 0-0.8 | 0.8-1.6 | 1.6-2.4 | 2.4-3.2 | 3.2-4 | 4-4.8 | 4.8-5.6 | 6.4-7.2 | |
| 0-2 | 15.19 | 2.00 | 0.14 | 0.01 | 0.02 | 0 | 0 | 0 | 17.35 |
| 2-4 | 22.27 | 4.60 | 0.36 | 0.02 | 0.00 | 0 | 0 | 0 | 27.26 |
| 4-6 | 15.37 | 6.43 | 0.69 | 0.07 | 0.02 | 0.01 | 0 | 0.01 | 22.60 |
| 6-8 | 8.20 | 7.45 | 1.68 | 0.20 | 0.03 | 0 | 0.01 | 0 | 17.57 |
| 8-10 | 1.47 | 5.03 | 1.85 | 0.34 | 0.09 | 0 | 0 | 0 | 8.78 |
| 10-12 | 0.17 | 2.79 | 1.05 | 0.52 | 0.13 | 0.03 | 0 | 0 | 4.68 |
| 12-14 | 0 | 0.62 | 0.55 | 0.05 | 0.05 | 0.01 | 0 | 0 | 1.27 |
| 14-16 | 0 | 0.08 | 0.25 | 0.04 | 0.03 | 0.01 | 0.01 | 0 | 0.42 |
| 16-18 | 0 | 0 | 0.04 | 0 | 0.01 | 0 | 0.02 | 0 | 0.07 |
| Total | 62.67 | 29.00 | 6.61 | 1.24 | 0.37 | 0.06 | 0.04 | 0.01 | 100.00 |

Waves with heights of 0 to 0.8 m (frequency 60.91%) are related to winds blowing from W to NW (41.47%) whilst waves with heights for more than 4 m, a percentage of 33.33% is related to winds from W. The same applies for most frequent periods and longer ones.

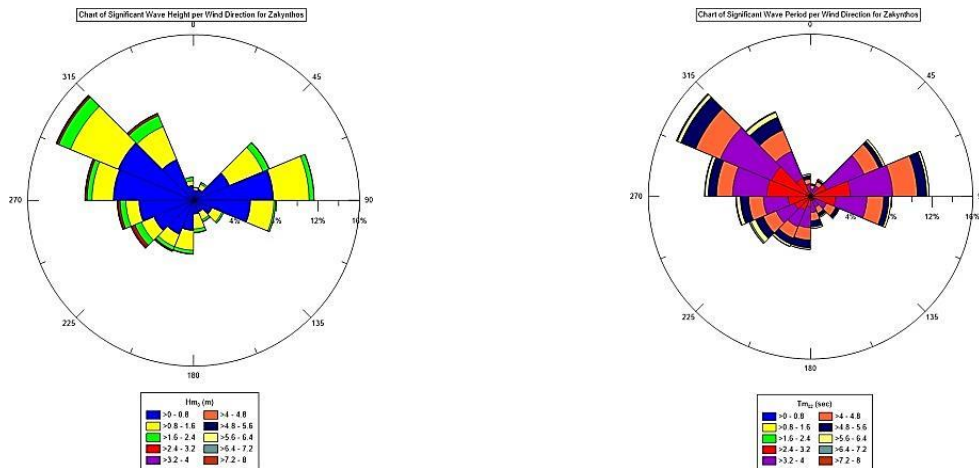


Figure 5.1.90: Charts of Wind Direction and Wave Height - Period for Zakynthos Buoy

5.1.14 Seasonal Synoptics

From the analysis of the Sea Surface Elevation records, the upper 10% of wave heights and periods along with their dates of appearance are selected from the buoys Athos, Mykonos, Santorini, Pylos and Zakynthos.

It is shown, that during winter north winds are formed in the Aegean Sea with average speeds of 2-3 m/s that are due to Arctic or Polar continental air masses descending through the valleys of Axios, Strimon and Evros, towards the Central Aegean (Poulos et al., 1997). The upper 10% analysis presents means of 1.41 m wave height and 5.54 s period. A mostly zonal wind pattern is formed in the Ionian, along the (east-west) direction of the basin. Wind has mean velocity of 2-3 m/s whilst at the south west of Greece (near to Libyan coast), the composite wind pattern, presents higher wind speeds (7-8 m/s), with the corresponding mean wave height and period of 1.21m and 6.08sec, respectively.

In spring, in both the Aegean and the Ionian, the most frequent winds are south and southwest (Poulos et al., 1997) and can reach up to 5 m/s. Mean wave height is around 1.32 m and mean period is about 5.4 s. In the Aegean Sea the S-SW winds are blocked from the island of Crete and cannot develop high waves in contradiction to the Ionian Sea. The Ionian Sea is characterized by mean wave height of 1.19 m and period of 5.95 s.

In summer, the Aegean is characterized by the local Etesian winds that are north winds (up to 8 m/s). Winds blowing from the NW (up to 6m/s) are dominant over the Ionian, with their maximum values at the south. The Aegean Sea is characterized by 1.06 m, 5.19 sec, while the Ionian Sea by 0.88 m and 5.27 sec, respectively.

In autumn, the winds are blowing from the west in the Ionian and can be up to 8 m/s, while in the Aegean Sea winds have north directions and are up to 4 m/s. Wave heights and periods are of 1.35 m and 5.47 s, respectively, while in the Ionian Sea of 1.03 m and 5.91 s.

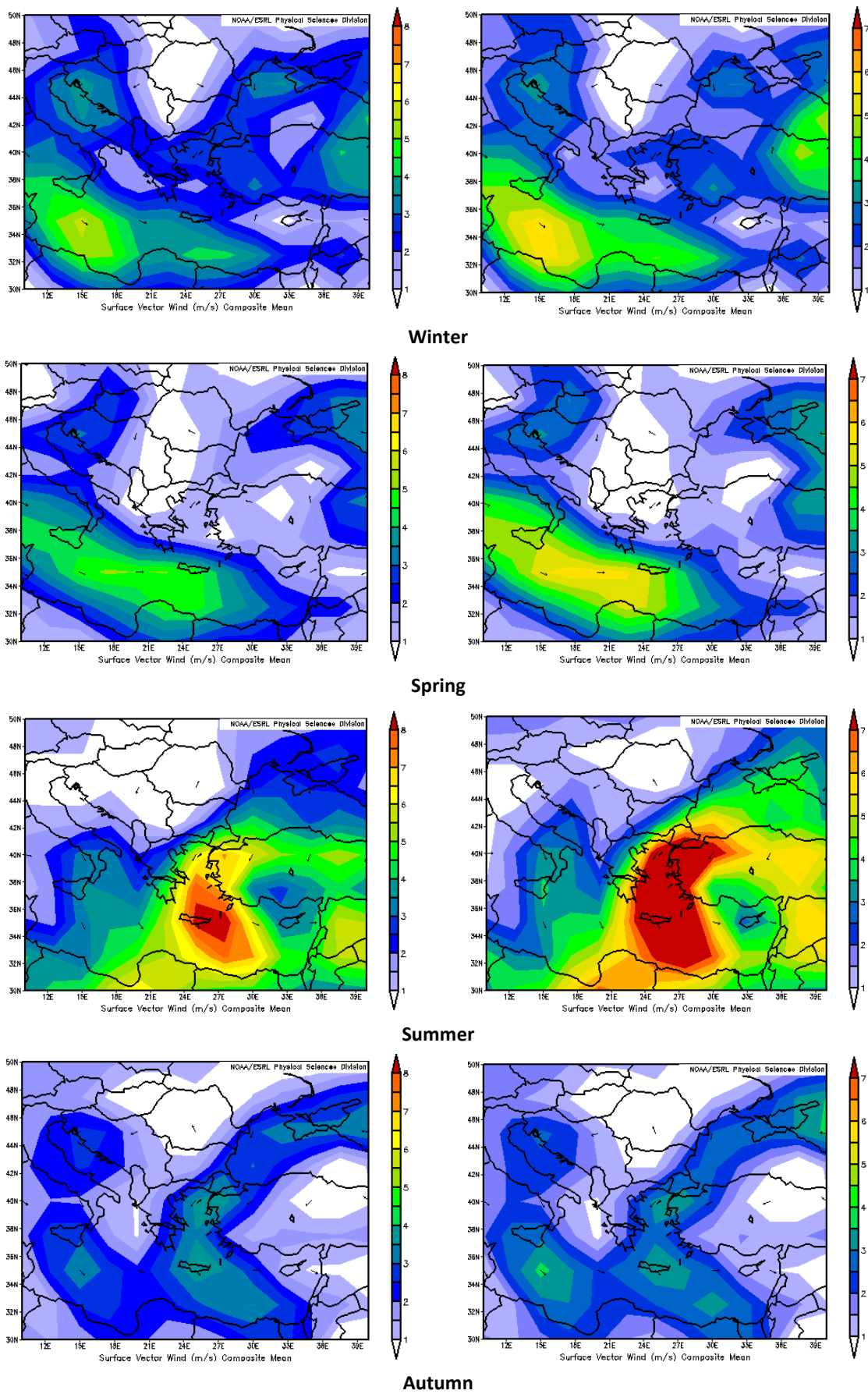


Figure 5.1.91: Seasonal synoptic composite means of the surface vector wind (m/s) associated with the upper 10% of wave height (left graphs) and period (right graphs) for the Aegean Sea

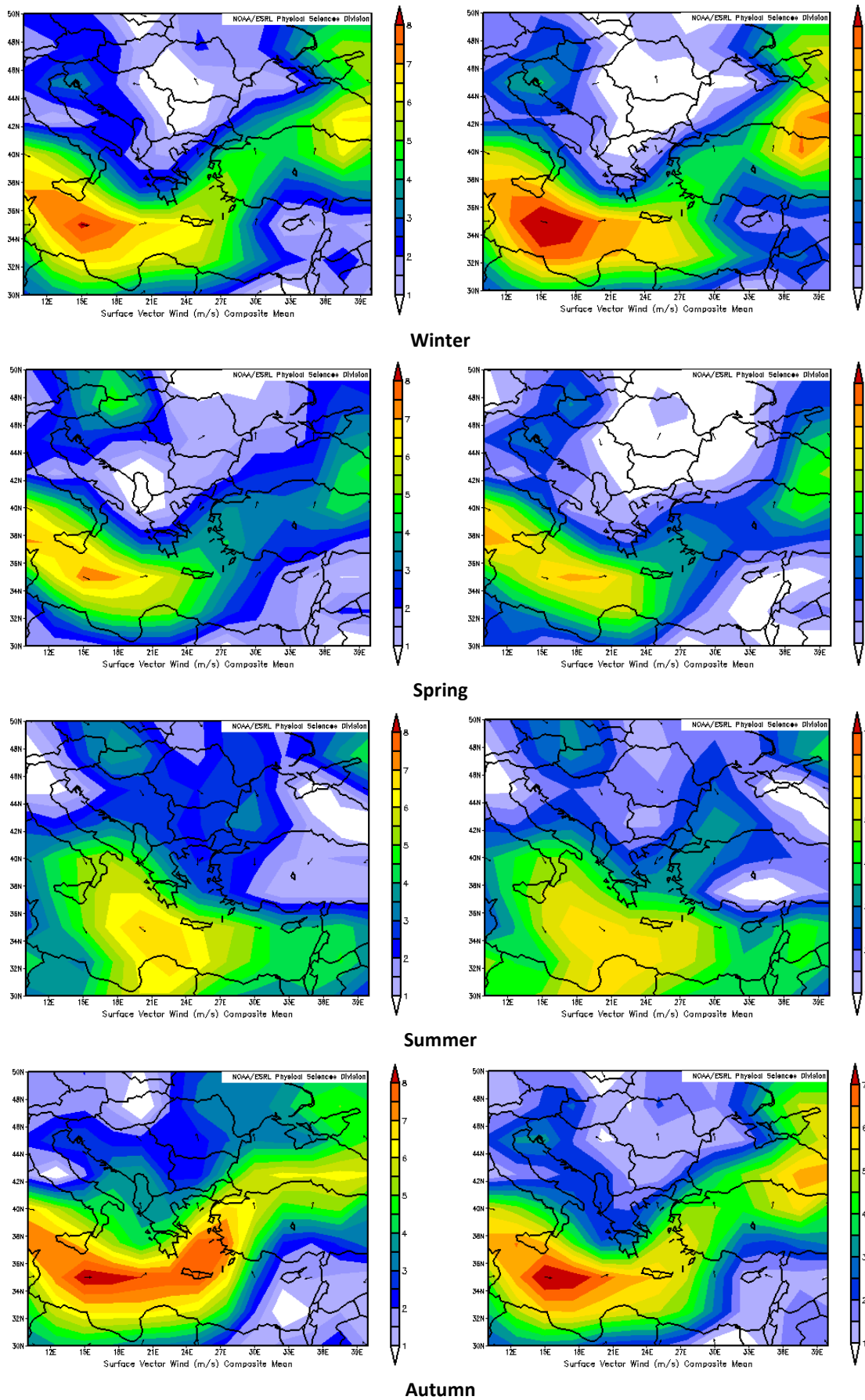


Figure 5.1.92: Seasonal synoptic composite means of the surface vector wind (m/s) associated with the upper 10% of wave height (left graphs) and period (right graphs) for the Ionian Sea

5.2 ERA-Interim

5.2.1 Buoy - Interim Correlation

5.2.1.1 Athos

The buoy's location and the 4 nearby points are shown in Figure 5.2.1.



Figure 5.2.1: Athos Buoy and the 4 nearby points of ERA-Interim grid

5.2.1.1.1 Significant Wave Height (SWH)

According to the method of Weighted Distance Average of the 4 closest ERA-Interim grid points to the Athos buoy location (see Figure 5.2.1) the correlation and the descriptive statistics for significant wave height are presented in Table 5.2.1, while the monthly variability for the period 2000 - 2010 of the 2 datasets is presented in Figure 5.2.2.

The mean significant wave height of the buoy is greater than that of the ERA-Interim by a bias of 0.08 m. The maximum height is also greater in the case of the buoy by 0.38 m and the same applies for standard deviation by 0.09 m.

Table 5.2.1: Statistics of Significant Wave Height of Athos Buoy and ERA-Interim data as estimated by the method WA and their relation.

| Parameter | N | Corr. | RMSE | Bias | Mean | Max | Std.Dev. |
|--------------------------|-------|-------|------|------|------|------|----------|
| Hm ₀ (m) Buoy | 13842 | 0.76 | 0.49 | 0.08 | 0.8 | 5.63 | 0.73 |
| SWH (m) ERA- Interim | | | | | 0.72 | 5.25 | 0.64 |

The mean monthly values of significant wave height of ERA-Interim are lower in relation to that given from the buoy. The smallest difference is in December with 0.03 m and the larger is in January with 0.19 m. The annual variability of the ERA-Interim dataset is also lower in relation to the buoy, with the smallest difference observed in year 2011 (0.04 m) and the largest in 2002 (0.15 m).

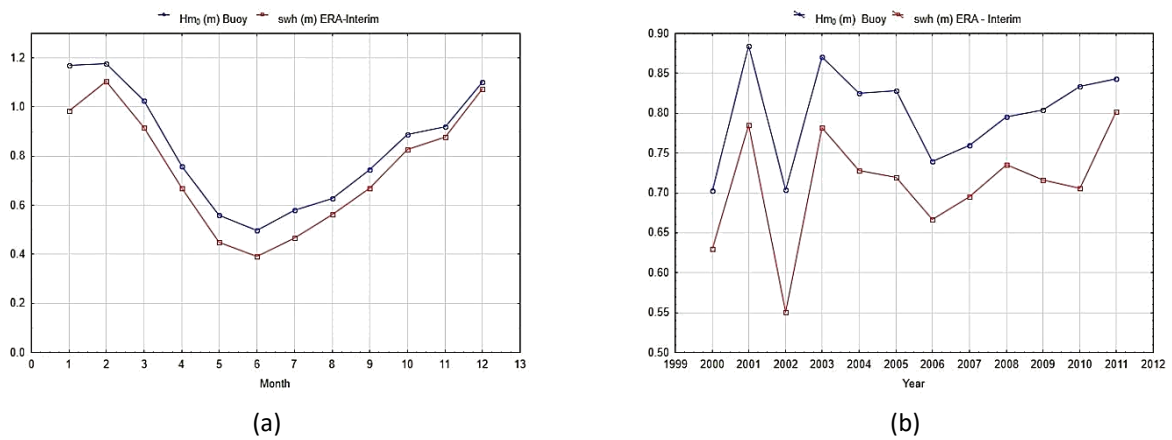


Figure 5.2.2: Mean monthly (a) and annual (b) significant wave height values (Hm₀) from the buoy and ERA-Interim, as estimated from the method of WA (swh)

5.2.1.1.2 Wind Speed (W10)

For the comparison of the wind speed, the method of selected point is used, which in this case is point 4. The correlation statistics between the buoy and the ERA-Interim dataset are presented in Table 5.2.2, whilst the mean monthly variation of wind speed as estimated from the buoy and the selected point of ERA-Interim dataset is shown in Figure 5.2.3. From the statistics of the datasets it is shown, that there is a bias of 0.33 m/s and a correlation of 0.84. Max values are larger estimated by the buoy that from the Interim by 2.83 m/s.

Table 5.2.2: Statistics of Wind Speed for Buoy and ERA-Interim Method SP

| Parameter | N | Corr. | RMSE | Bias | Mean | Max | Std.Dev. |
|-----------------------|-------|-------|------|------|------|-------|----------|
| Wind Speed (m/s) Buoy | 12582 | 0.84 | 2.00 | 0.33 | 5.77 | 23.89 | 3.9 |
| W10 (m/s) ERA-Interim | | | | | 5.44 | 21.06 | 3.26 |

The monthly values of ERA-Interim dataset are lower than those of the buoy, except in the case of July where it is higher, but only by 0.05 m/s. The smallest difference is in June with 0.03 m/s and the largest in December with 0.85 m/s. The annual variability presents an overall higher variability compared to the mean monthly values; thus, the highest buoy values (>6.5 m/s) observed in 2005 and in 2010 while its lowest is in 2002 (<4 m/s). The ERA Interim values are generally lower with the exception of the years 2000 and 2001.

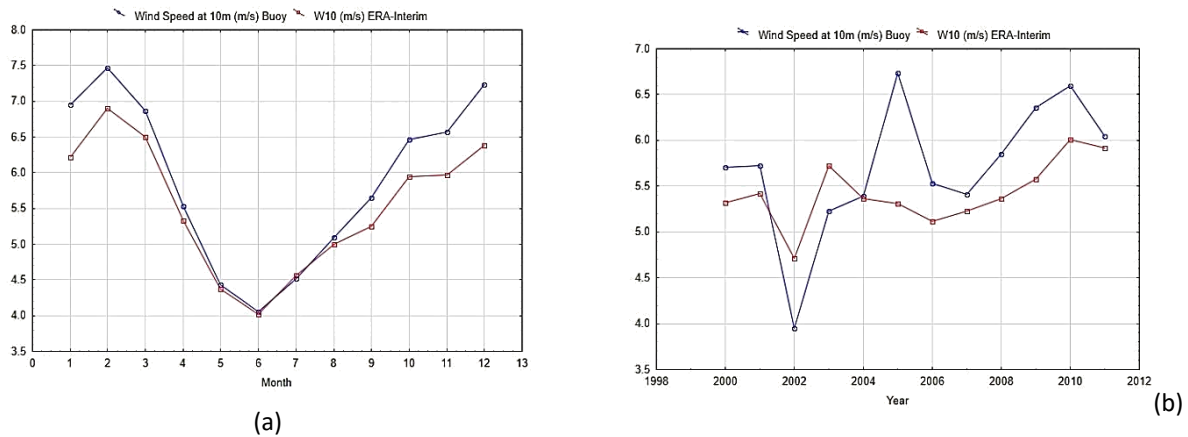


Figure 5.2.3: Mean monthly (a) and annual (b) wind speed values (10 m above sea level) from the buoy and ERA-Interim, as estimated from the method of SP (W10)

5.2.1.1.3 Temperature at 2m (T2M)

The method chosen for the collocation of the buoy and the ERA-Interim dataset is that of the selected point, with point 4. The relationship of temperature of the 2 datasets is presented in Table 5.2.3, while their mean monthly and annual variation is shown in Figure 5.2.4. As given by the statistics presented in Table 5.2.3, the ERA-Interim are higher than the buoy's estimates of temperature at 2 m (negative bias) by 0.28 °C. The correlation is very good with a value of 0.96 and the deviation is approximately of 1 °C difference.

Table 5.2.3: Statistics of Temperature at 2m for Buoy and ERA-Interim Method SP

| Parameter | N | Corr. | RMSE | Bias | Mean | Max | Std.Dev. |
|-----------------------------|-------|-------|------|-------|-------|-------|----------|
| Temperature at 2m (°C) Buoy | 14055 | 0.96 | 2.14 | -0.28 | 17.54 | 30.16 | 6.08 |
| T2M (°C) ERA-Interim | | | | | 17.82 | 33.74 | 7.02 |

In general, the values of ERA-Interim are higher (1-2 °C) than the buoy's from March to September and lower (<2 °C) for the rest of year. For the annual variation, ERA-Interim are higher than the buoy with the smallest difference observed in 2007 (the ERA-Interim is higher by only 0.05 °C) and the largest in 2005 ((1.43 °C).

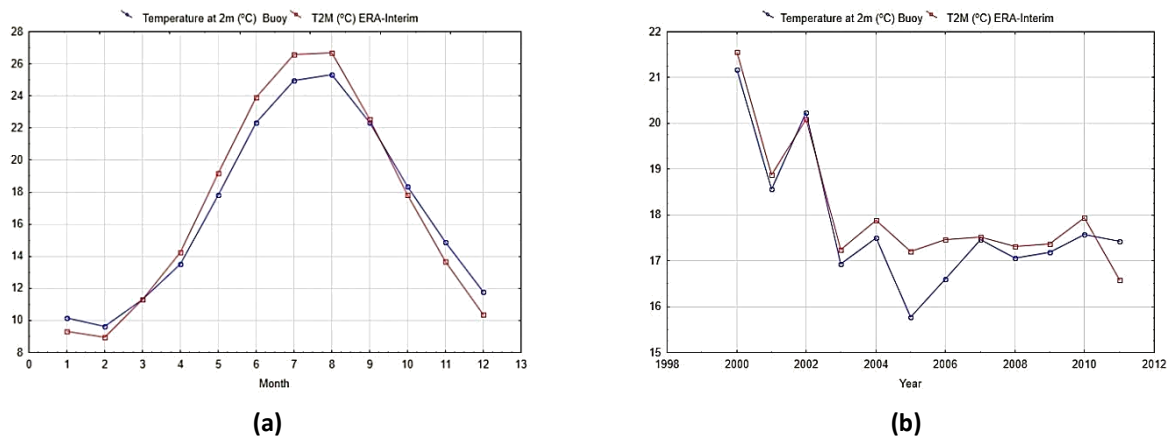


Figure 5.2.4 Mean monthly (a) and annual (b) temperature values (at 2 m above sea level) from the buoy and ERA-Interim, as estimated from the method of SP (T2M)

5.2.1.2 Avgo

The location of the buoy and the 4 nearest grid points are shown in Figure 5.2.5.



Figure 5.2.5: Avgo Buoy and the 4 nearby points of ERA-Interim grid

5.2.1.2.1 Significant Wave Height (SWH)

In the case of the significant wave height, the point of Avgo 2 is proven best for the collocation and correlation with the buoy and the relevant statistics are shown in Table 5.2.4.

From the comparison of 8046 records, there is a correlation of 0.89 among the two datasets. It is shown that the data from the Selected Point of ERA-Interim are higher than those of the buoy, with a bias of 0.1 m. Furthermore, the maximum are lower from the ERA-Interim dataset by 0.44 m while the deviation is of 0.01 m difference.

Table 5.2.4: Statistics of Significant Wave Height of Avgo Buoy and ERA-Interim Method SP

| Parameter | N | Corr. | RMSE | Bias | Mean | Max | Std.Dev. |
|--------------------------|------|-------|------|------|------|------|----------|
| Hm ₀ (m) Buoy | 8046 | 0.89 | 0.3 | -0.1 | 1 | 5.4 | 0.63 |
| SWH (m) ERA- Interim | | | | | 1.09 | 4.96 | 0.64 |

The mean monthly variation of significant wave height is presented in Figure 5.2.6 with ERA-Interim higher than the buoy. The smallest difference is during April (0.03 m) and the largest in February (0.17 m). For the annual variation, the ERA-Interim values are higher than the buoy with the largest difference is in 2004 (0.14 m) and the smallest (0.001 m) in 2002.

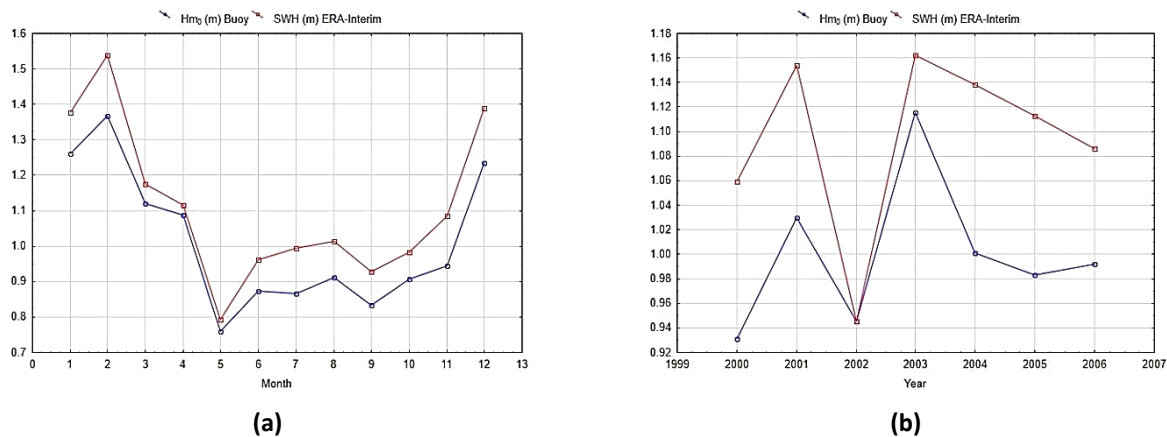


Figure 5.2.6: Mean monthly (a) and annual (b) significant wave height values from the buoy (Hm₀) and ERA-Interim as estimated from the method of SP (swh)

5.2.1.2.2 Wind Speed (W10)

For wind speed, the method of weighted distance average of the 4 points closest to the buoy is chosen. The statistics in Table 5.2.5 show that the wind speed from the buoy is lower than that of the ERA-Interim by 0.38 m/s while at the maximum value the data from the buoy are higher than that of ERA-Interim.

Table 5.2.5: Statistics of Wind Speed for Buoy and ERA-Interim Method WA

| Parameter | N | Corr. | RMSE | Bias | Mean | Max | Std.Dev. |
|-----------------------|------|-------|------|-------|------|-------|----------|
| Wind Speed (m/s) Buoy | 7972 | 0.72 | 2.59 | -0.38 | 6.43 | 22.62 | 3.68 |
| W10 (m/s) ERA-Interim | | | | | 6.81 | 18.44 | 2.98 |

The monthly mean variation is shown in Figure 5.2.7. The reanalysis is higher in relation to the buoy data with the smallest difference in October (0.02 m/s) and the largest in March (0.98 m/s). The annual variation of wind speed shows that the reanalysis dataset is higher than the values of the buoy except in the years 2002 and 2003 where it is lower. The smallest difference is in 2002 (0.04 m/s) and the largest in 2004 (1.10 m/s).

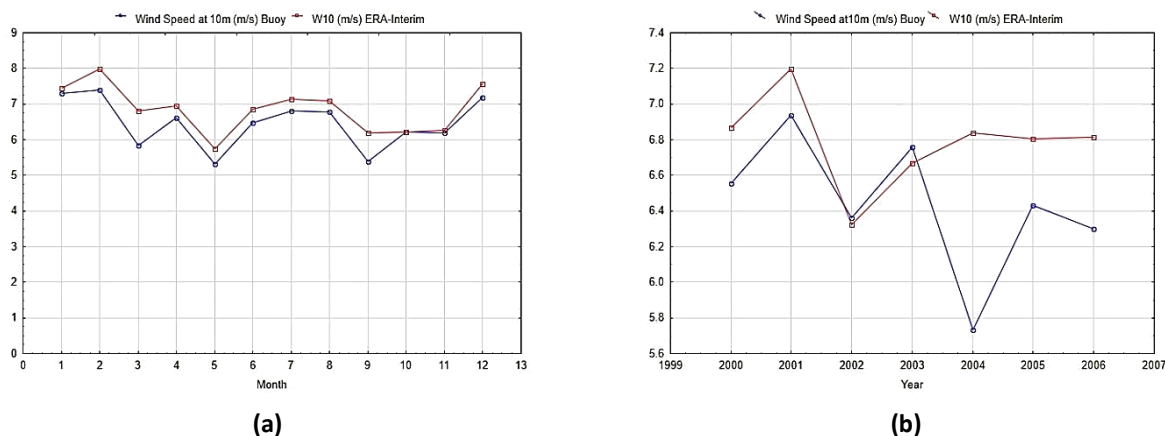


Figure 5.2.7: Mean monthly (a) and annual (b) wind speed values from the buoy (Wind speed at 10m) and ERA-Interim as estimated from the method of WA (W10)

5.2.1.2.3 Temperature at 2m (T2M)

For temperature, the method chosen is that of the selected point (point 2). The relationship of the reanalysis and the buoy is shown in Table 5.2.6. The buoy values of temperature at 2 m are lower than those from the ERA-Interim by 0.82 °C and the same applies for the max values by 0.42 °C.

Table 5.2.6: Statistics of Temperature at 2m for Buoy and ERA-Interim Method SP

| Parameter | N | Corr. | RMSE | Bias | Mean | Max | Std.Dev. |
|-----------------------------|------|-------|------|-------|-------|-------|----------|
| Temperature at 2m (°C) Buoy | 7262 | 0.95 | 1.85 | -0.82 | 19.6 | 32.12 | 4.66 |
| T2M (°C) ERA-Interim | | | | | 20.42 | 32.54 | 5.48 |

The mean monthly variation of temperature is given in Figure 5.2.8. For the months of March to October the reanalysis data are higher in relation to the buoy whilst for the other months are lower. The smallest difference is in November (0.14 °C) and the largest in July (1.92 °C). The annual variation shows that the reanalysis data are higher than the data from the buoy. The smallest difference is in 2003 (0.11 °C) and the largest is in 2004 (1.81 °C).

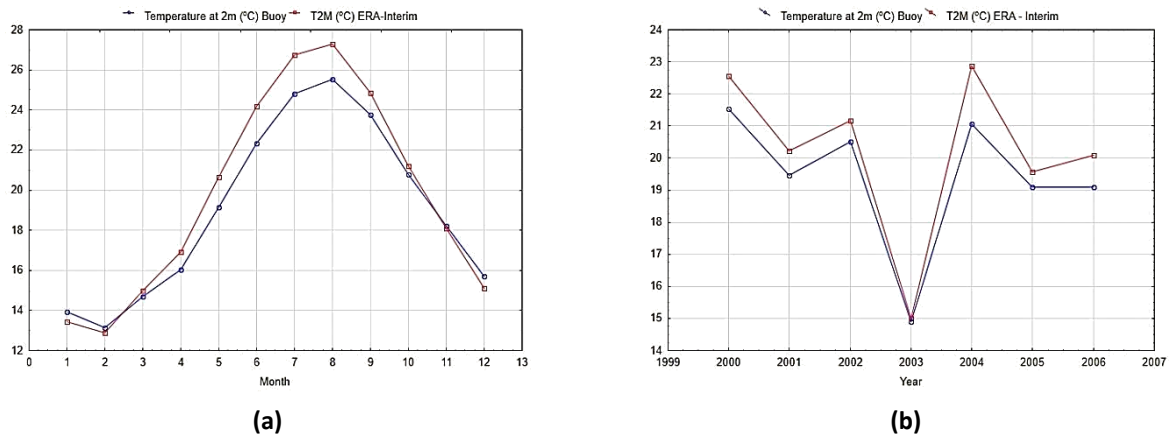


Figure 5.2.8: Mean monthly (a) and annual (b) temperature values from the buoy (Temperature at 2m) and ERA-Interim as estimated from the method of SP (T2M)

5.2.1.3 E1M3A

The location of E1M3A buoy and the 4 closest grid points of ERA-Interim dataset are shown in Figure 5.2.9.



Figure 5.2.9: E1M3A Buoy and the 4 nearby points of ERA-Interim grid

5.2.1.3.1 Significant Wave Height (SWH)

For the case of significant wave height the method of selected point is chosen (point 1). The statistics of the correlation with the buoy dataset are shown in Table 5.2.7. From the statistics of the relation between the 2 datasets it is shown that there is a correlation of 0.89 and a negative bias of 0.15m (ERA-Interim are higher than the buoy). Finally, maximum values are very close with a difference of 0.01 m.

Table 5.2.7: Statistics of Significant Wave Height of E1M3A Buoy and ERA-Interim Method SP

| Parameter | N | Corr. | RMSE | Bias | Mean | Max | Std.Dev. |
|--------------------------|------|-------|------|-------|------|------|----------|
| Hm ₀ (m) Buoy | 4146 | 0.89 | 0.3 | -0.15 | 0.93 | 4.92 | 0.62 |
| SWH (m) ERA- Interim | | | | | 1.08 | 4.91 | 0.60 |

For the mean monthly variation, it is shown that the reanalysis dataset is higher than the data of the buoy, with the smallest difference in April (0.05 m) and the largest in August (0.22 m). In the case of the annual variability of significant wave height, it is shown that the reanalysis dataset is higher than the buoy data with the largest difference in 2009 (0.19 m) and the smallest in 2011 (0.09 m).

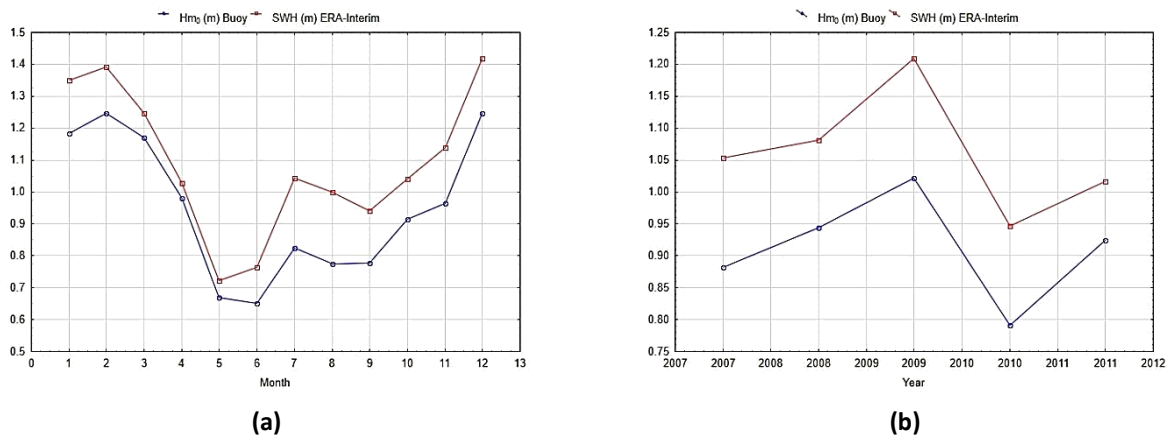


Figure 5.2.10: Mean monthly (a) and annual (b) significant wave height values from the buoy (Hm₀) and ERA-Interim as estimated from the method of SP (swh)

5.2.1.3.2 Wind Speed (W10)

For wind speed the preferred method is that of the weighted distance average of the 4 nearest points to the buoy. The statistics in Table 5.2.8 show that there is a correlation of 0.71 between the two datasets and that the buoy is lower than the ERA Interim by 0.29 m/s. On the other hand, the maximum values of wind speed are higher from the buoy than that of the reanalysis dataset by 3.71 m/s .

Table 5.2.8: Statistics of Wind Speed for Buoy and ERA-Interim Method WA

| Parameter | N | Corr. | RMSE | Bias | Mean | Max | Std.Dev. |
|-----------------------|------|-------|------|-------|------|-------|----------|
| Wind Speed (m/s) Buoy | 3214 | 0.71 | 2.27 | -0.29 | 6.33 | 21.75 | 3.25 |
| W10 (m/s) ERA-Interim | | | | | 6.62 | 18.04 | 2.97 |

For the monthly mean variation, the reanalysis is higher than the buoy, except in the case of December where it is lower. The smallest difference is in June (0.05 m/s) and the largest in July (0.81 m/s). For the annual variability, the reanalysis dataset only for the years 2007 and 2011 is lower than the buoy and higher for the rest of the years. The smallest difference is in 2007 (~0 m/s) and the largest in 2010 (0.97 m/s).

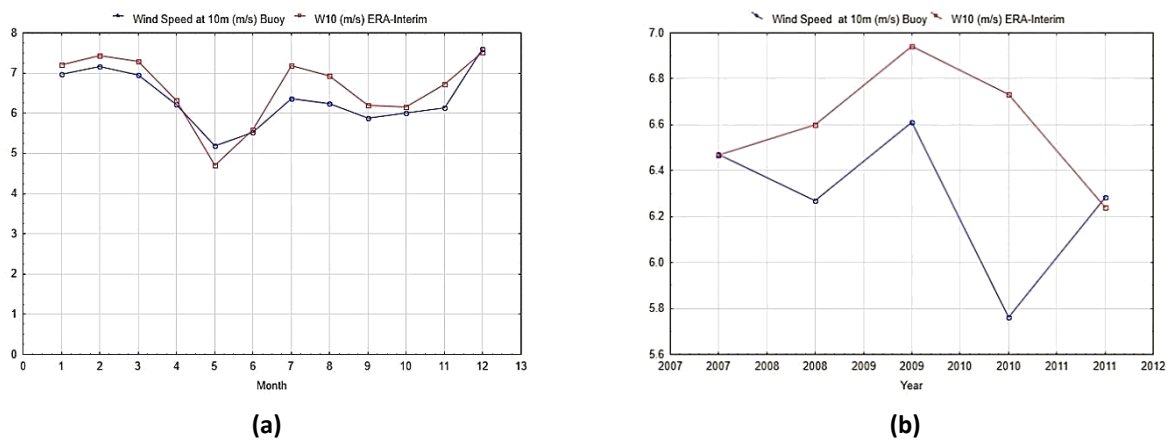


Figure 5.2.11: Mean monthly (a) and annual (b) wind speed values from the buoy (Wind speed at 10m) and ERA-Interim as estimated from the method of WA (W10)

5.2.1.3.3 Temperature at 2m (T2M)

In the case of temperature, the method of selected point is chosen (point 1) and the statistics are shown in Table 5.2.9. Temperature presents a very good correlation of 0.97 but the buoy is lower than that of ERA-Interim by 0.64 °C. Furthermore, the maximum also present that ERA-Interim is higher than that of the buoy by 4.19 °C.

Table 5.2.9: Statistics of Temperature at 2m for Buoy and ERA-Interim Method SP

| Parameter | N | Corr. | RMSE | Bias | Mean | Max | Std.Dev. |
|-----------------------------|------|-------|------|-------|-------|-------|----------|
| Temperature at 2m (°C) Buoy | 4774 | 0.97 | 1.7 | -0.64 | 19.83 | 29.67 | 4.62 |
| T2M (°C) ERA-Interim | | | | | 20.48 | 33.86 | 5.46 |

The mean monthly variability of temperature is shown in Figure 5.2.12 . The ERA-Interim are higher than the buoy for the months of March to October with the largest difference in June (2.31 °C) and the smallest in November (0.13 °C). The annual variability shows that ERA-Interim is higher in relation to the buoy. The smallest difference is in 2009 (0.22 °C) and the largest in 2007 (0.89 °C).

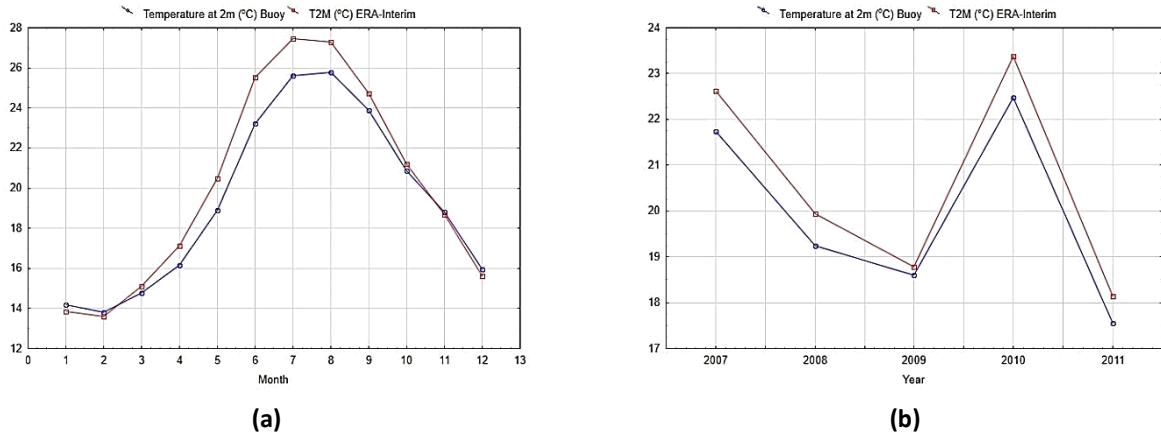


Figure 5.2.12: Mean monthly (a) and annual (b) temperature values from the buoy (Temperature at 2m) and ERA-Interim as estimated from the method of SP (T2M)

5.2.1.4 Lesvos

The location of the buoy is presented in Figure 5.2.13. The method preferred for the parameters is that of the selected point and in this case it is the weighted distance average of points 1 and 2.

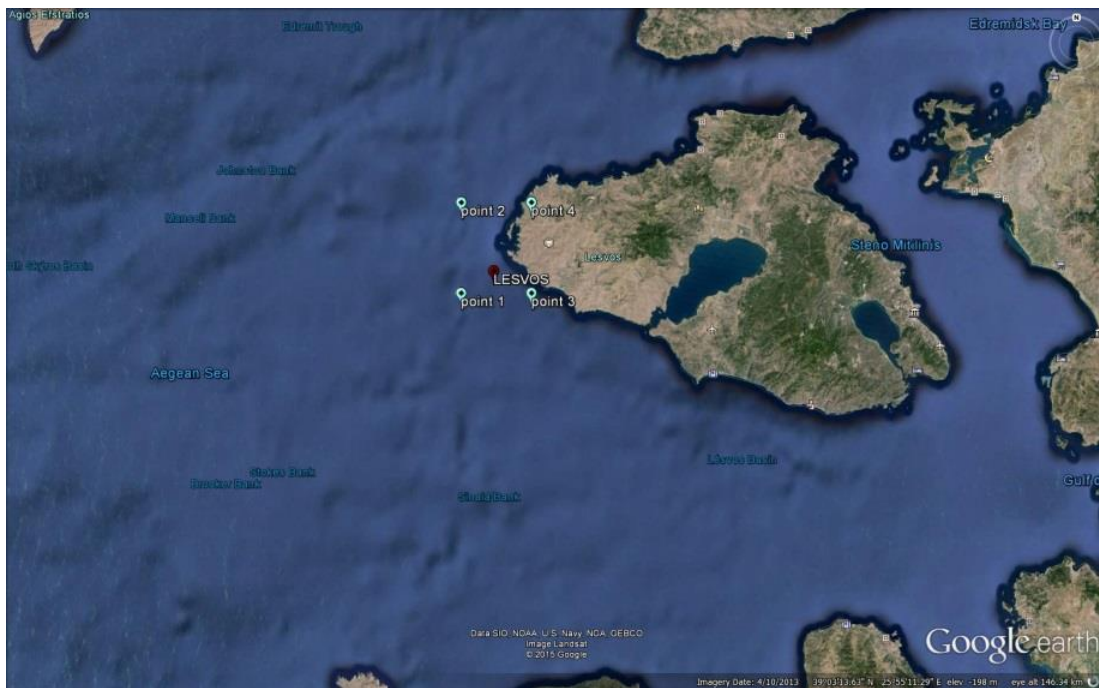


Figure 5.2.13: Lesvos Buoy and the 4 nearby points of ERA-Interim grid

5.2.1.4.1 Significant Wave Height (SWH)

The relation among the significant wave height from the weighted distance average of the 2 points of ERA-Interim and from the buoy is shown in Table 5.2.10. The correlation of significant wave height from both datasets is of 0.65 and the bias presents that the buoy is lower than that of ERA-Interim by 0.17 m. For the maximum values, the ERA-Interim are higher than the buoy by 1.12 m.

Table 5.2.10: Statistics of Significant Wave Height of Lesvos Buoy and ERA-Interim Method WA

| Parameter | N | Corr. | RMSE | Bias | Mean | Max | Std.Dev. |
|--------------------------|-------|-------|------|-------|------|------|----------|
| Hm ₀ (m) Buoy | 14229 | 0.65 | 0.56 | -0.17 | 0.77 | 4.92 | 0.55 |
| SWH (m) ERA- Interim | | | | | 0.94 | 6.04 | 0.72 |

For the monthly mean values, the reanalysis data is higher than the buoy, except in May where it is lower. The smallest difference is in May (0.001 m) and the largest in December (0.32 m). The annual variation, shows that the reanalysis data is higher than the buoy data with the largest variation in 2011 (0.25 m) and the smallest in 2002 (0.10 m).

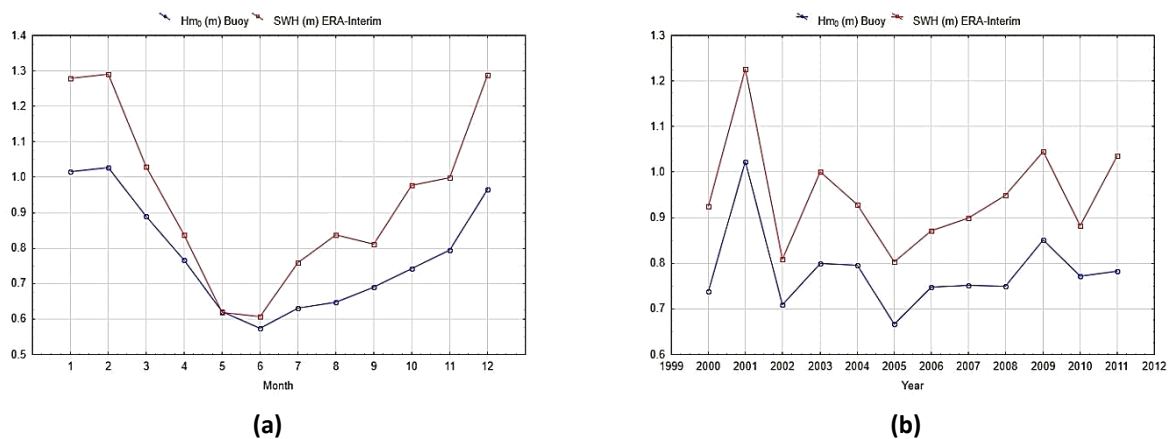


Figure 5.2.14: Mean monthly (a) and annual (b) significant wave height values from the buoy (Hm0) and ERA-Interim as estimated from the method of SP (swh)

5.2.1.4.2 Wind Speed (W10)

The relation among the data from the buoy and the reanalysis data for wind speed for the method of weighted distance average are presented in Table 5.2.11. The correlation is of 0.72 for the 2 datasets whilst the buoy is higher by a bias of 0.21 m/s than that of the reanalysis data. The buoy maximum is higher than that of the ERA-Interim by 5.68 m/s.

Table 5.2.11: Statistics of Wind Speed for Buoy and ERA-Interim Method WA

| Parameter | N | Corr. | RMSE | Bias | Mean | Max | Std.Dev. |
|-----------------------|-------|-------|------|------|------|-------|----------|
| Wind Speed (m/s) Buoy | 13322 | 0.72 | 2.64 | 0.21 | 6.96 | 30.24 | 3.92 |
| W10 (m/s) ERA-Interim | | | | | 6.76 | 24.56 | 3.45 |

In the case of the monthly mean variation, it is shown that the reanalysis data are lower than those from the buoy except for the months of January, July and August. The smallest difference is in December (0.06 m/s) while the largest is in March (0.86 m/s). For the annual variability of wind speed, the ERA-Interim is lower than the data from the buoy except for the years of 2003, 2005 and 2007. The smallest variation is in 2005 (0.10 m/s) and the largest in 2002 (0.85 m/s).

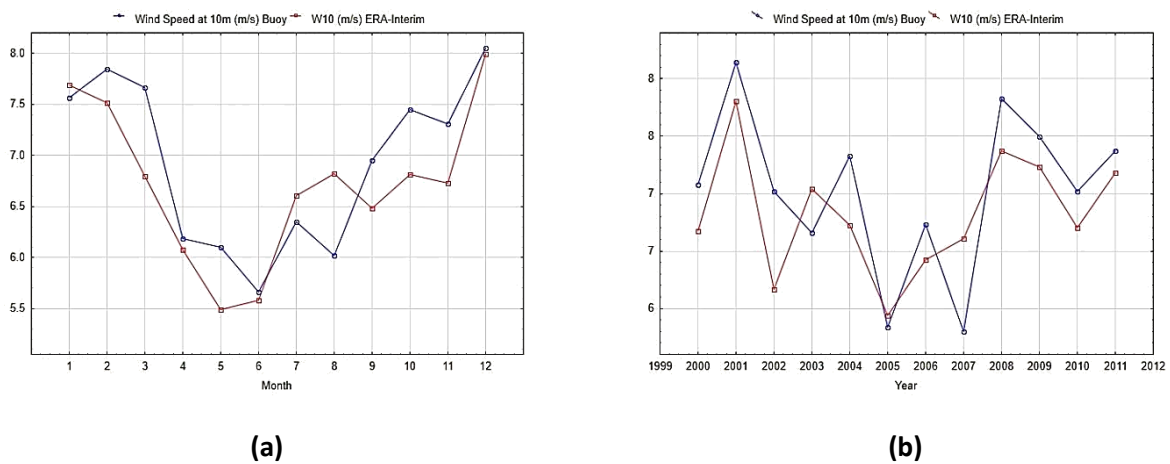


Figure 5.2.15: Mean monthly (a) and annual (b) wind speed values from the buoy (Wind speed at 10m) and ERA-Interim as estimated from the method of SP (W10)

5.2.1.4.3 Temperature at 2m (T2M)

The statistics of the relationship of the buoy data and the reanalysis data (WA of points 1, 2) are shown in Table 5.2.12. The correlation of the temperature is 0.95 while the ERA-Interim are higher than the buoy by 0.52 °C. In contradiction, the maximum of the buoy is higher than that of the reanalysis by 1.69 °C.

Table 5.2.12: Statistics of Temperature at 2m for Buoy and ERA-Interim Method SP

| Parameter | N | Corr. | RMSE | Bias | Mean | Max | Std.Dev. |
|-----------------------------|-------|-------|------|-------|-------|-------|----------|
| Temperature at 2m (°C) Buoy | 14379 | 0.95 | 2.31 | -0.52 | 17.36 | 34.79 | 5.35 |
| T2M (°C) ERA-Interim | | | | | 17.92 | 33.10 | 6.63 |

The monthly variation of temperature at 2m is given in Figure 5.2.16 from the buoy and the weighted distance average from points 1 and 2. The ERA-Interim is higher than the data from the buoy in the months of March to September. The smallest variation is in October (0.06 °C) and the largest in July (2.88 °C). For the annual mean values, the data from ERA-Interim, is higher than the data from the buoy with the largest difference in 2005 (1.53 °C) and the smallest in 2002 (0.02 °C).

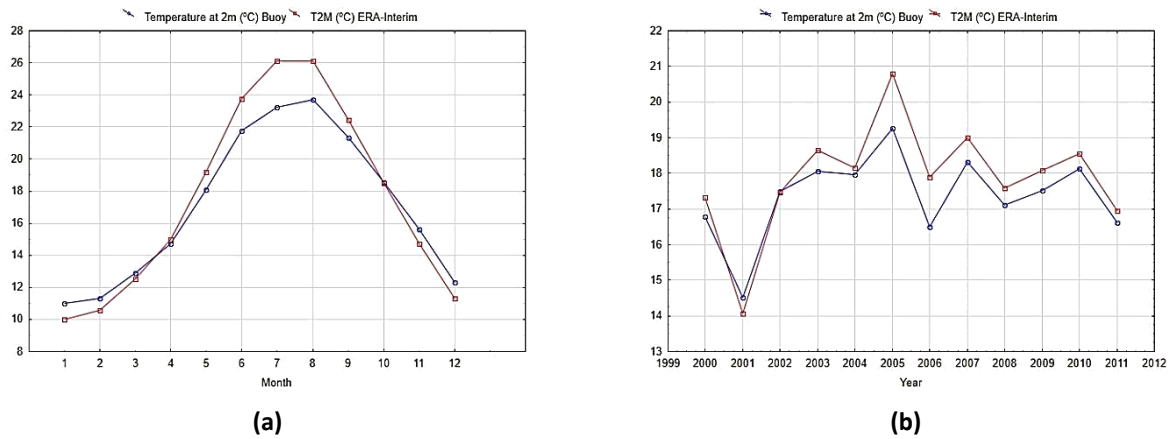


Figure 5.2.16: Mean monthly (a) and annual (b) temperature values from the buoy (Temperature at 2m) and ERA-Interim as estimated from the method of SP (T2M)

5.2.1.5 Mykonos

The location of the buoy and the 4 near grid points are presented in Figure 5.2.17.

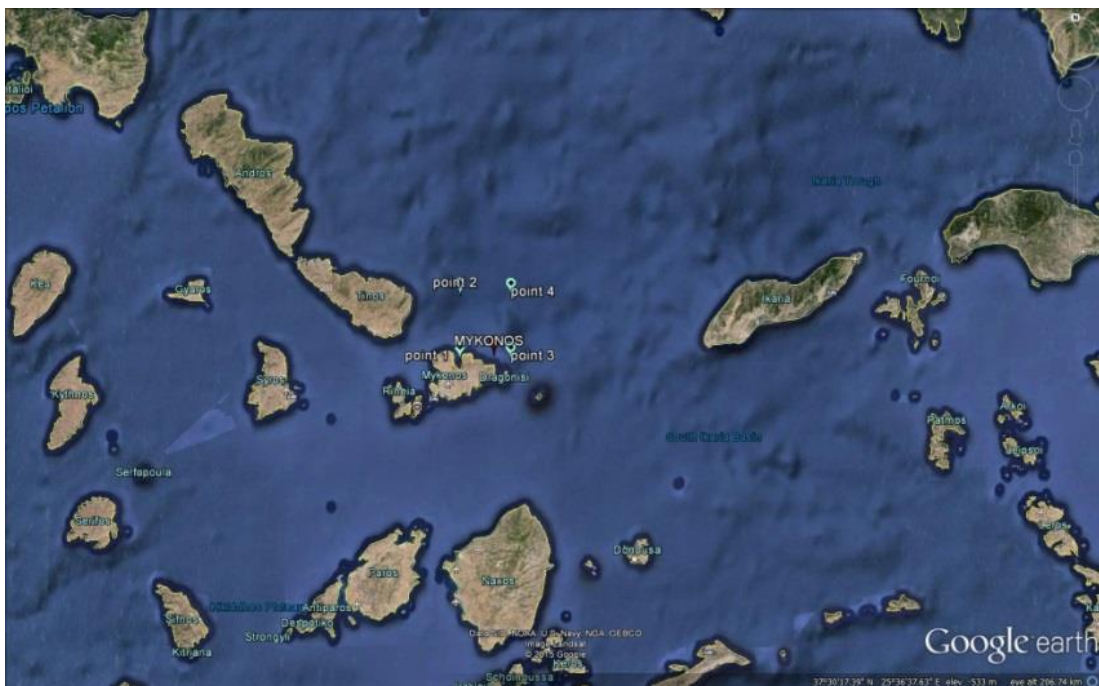


Figure 5.2.17: Mykonos Buoy and the 4 nearby points of ERA-Interim grid

5.2.1.5.1 Significant Wave Height (SWH)

For significant wave height the method of weighted distance average is chosen and the relevant statistics are shown in Table 5.2.13. In Mykonos, the correlation of the buoy and the ERA-Interim for significant wave height is 0.87 with the buoy higher than that of the reanalysis by 0.04 m. This applies for the maximum values where they differ by 0.02 m.

Table 5.2.13: Statistics of Significant Wave Height of Mykonos Buoy and ERA-Interim Method WA

| Parameter | N | Corr. | RMSE | Bias | Mean | Max | Std.Dev. |
|--------------------------|-------|-------|------|------|------|------|----------|
| Hm ₀ (m) Buoy | 13702 | 0.87 | 0.34 | 0.04 | 1.01 | 5.63 | 0.75 |
| SWH (m) ERA- Interim | | | | | 0.96 | 5.61 | 0.65 |

Mean monthly variation shows that ERA-Interim is higher for winter and March and November, whilst lower for the rest of the year. The smallest difference is in March (0.03 m) and the largest in July (0.13 m). The annual variation of significant wave height shows that the buoy is higher than ERA-Interim except in the case of 2009. The smallest difference is 0.003 m in 2001 and the largest 0.10 m in 2002.

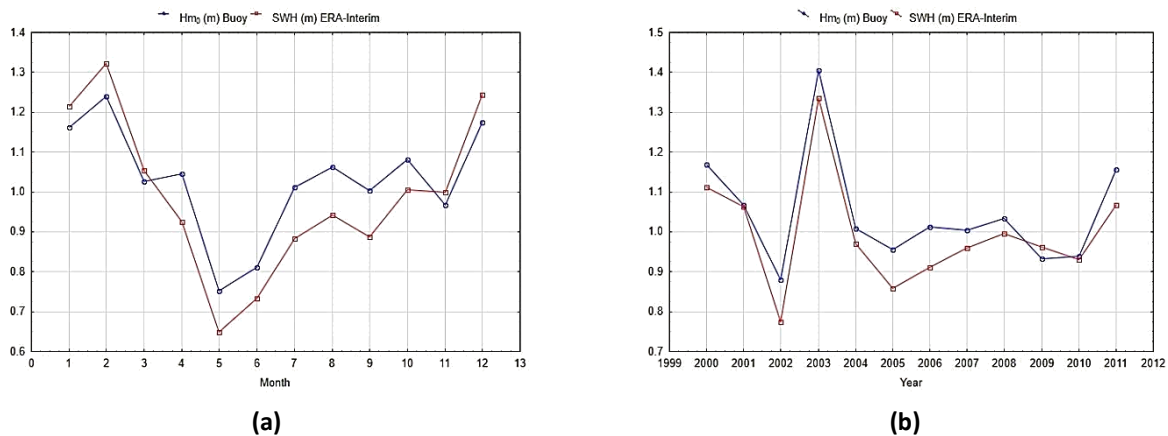


Figure 5.2.18: Mean monthly (a) and annual (b) significant wave height values from the buoy (Hm₀) and ERA-Interim as estimated from the method of WA (swh)

5.2.1.5.2 Wind Speed (W10)

For wind speed, the weighted distance average method is also chosen and the statistics are shown in Table 5.2.14. For wind speed, the correlation is 0.82 with a positive bias of 1.21 m/s (buoy is higher than the reanalysis). The maximum values differ by 0.91 m/s with buoy data higher.

Table 5.2.14: Statistics of Wind Speed for Buoy and ERA-Interim Method WA

| Parameter | N | Corr. | RMSE | Bias | Mean | Max | Std.Dev. |
|-----------------------|-------|-------|------|------|------|-------|----------|
| Wind Speed (m/s) Buoy | 12974 | 0.82 | 2.27 | 1.21 | 7.89 | 21.87 | 4.1 |
| W10 (m/s) ERA-Interim | | | | | 6.69 | 20.96 | 3.27 |

From the variation of the monthly means of wind speed, it is shown that the reanalysis data is lower in relation to the data from the buoy, with the smallest difference is in February (0.73 m/s) and the largest in September (1.69 m/s). The annual wind speed is lower for the reanalysis data in relation to the buoy with the smallest different in 2003 (0.45 m/s) and the largest in 2006 (1.93 m/s).

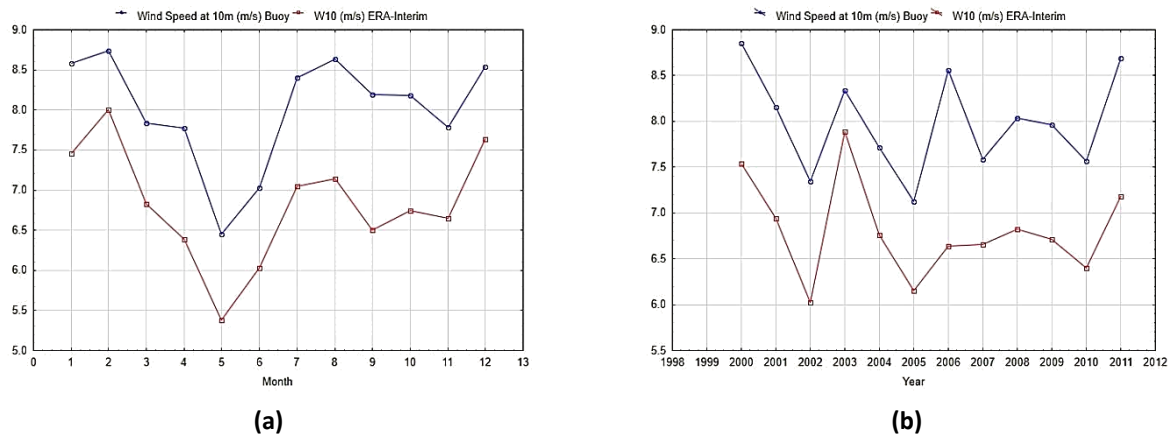


Figure 5.2.19: Mean monthly (a) and annual (b) wind speed values from the buoy (Wind speed at 10m) and ERA-Interim as estimated from the method of WA (W10).

5.2.1.5.3 Temperature at 2m (T2M)

The method of the selected point (point 3) is chosen for temperature and the according statistics are given in Table 5.2.15. The correlation is 0.91 and it is shown that the ERA-Interim temperature is higher than that of the buoy by 0.47 °C. On the other hand, the maximum value recorded by the buoy is significantly higher than that of ERA-Interim by 8.89 °C.

Table 5.2.15: Statistics of Temperature at 2m for Buoy and ERA-Interim Method SP

| Parameter | N | Corr. | RMSE | Bias | Mean | Max | Std.Dev. |
|-----------------------------|-------|-------|------|-------|-------|-------|----------|
| Temperature at 2m (°C) Buoy | 13814 | 0.91 | 2.41 | -0.47 | 18.54 | 41.86 | 4.87 |
| T2M (°C) ERA-Interim | | | | | 19.01 | 32.97 | 5.74 |

In the case of the monthly mean value of temperature at 2m, it is shown that the ERA-Interim is higher than the buoy data from May to September. The smallest difference is in October (0.02 °C) and the maximum in July (2.04 °C).

Additionally, for the mean annual variation it is shown that the reanalysis data is higher in relation to the buoy except for the year 2011, where it is lower. The minimum difference is in 2009 (0.28 °C) and the maximum in 2006 (1.10 °C).

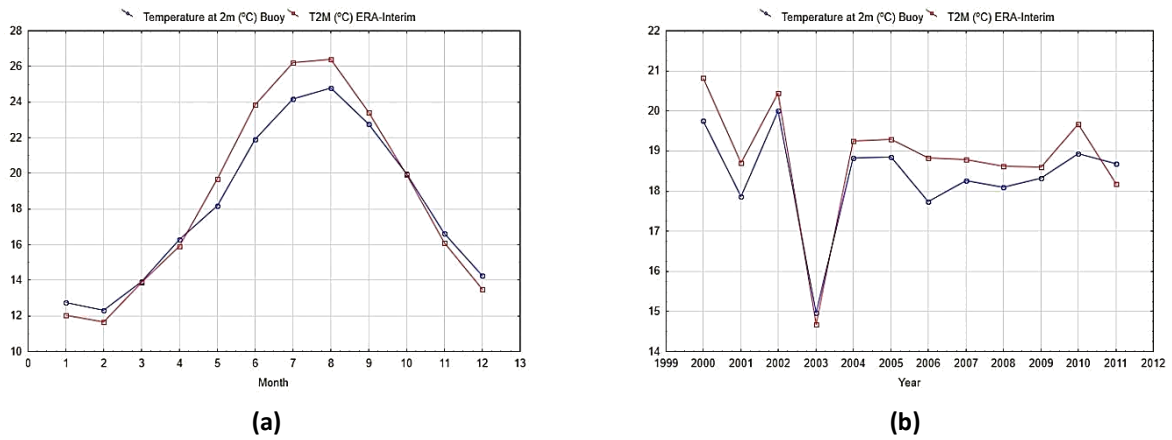


Figure 5.2.20: Mean monthly (a) and annual (b) temperature values from the buoy (Temperature at 2m) and ERA-Interim as estimated from the method of SP (T2M)

5.2.1.6 Pylos

The location of the buoy and the 4 points of the ERA-Interim grid box are shown in Figure 5.2.21.

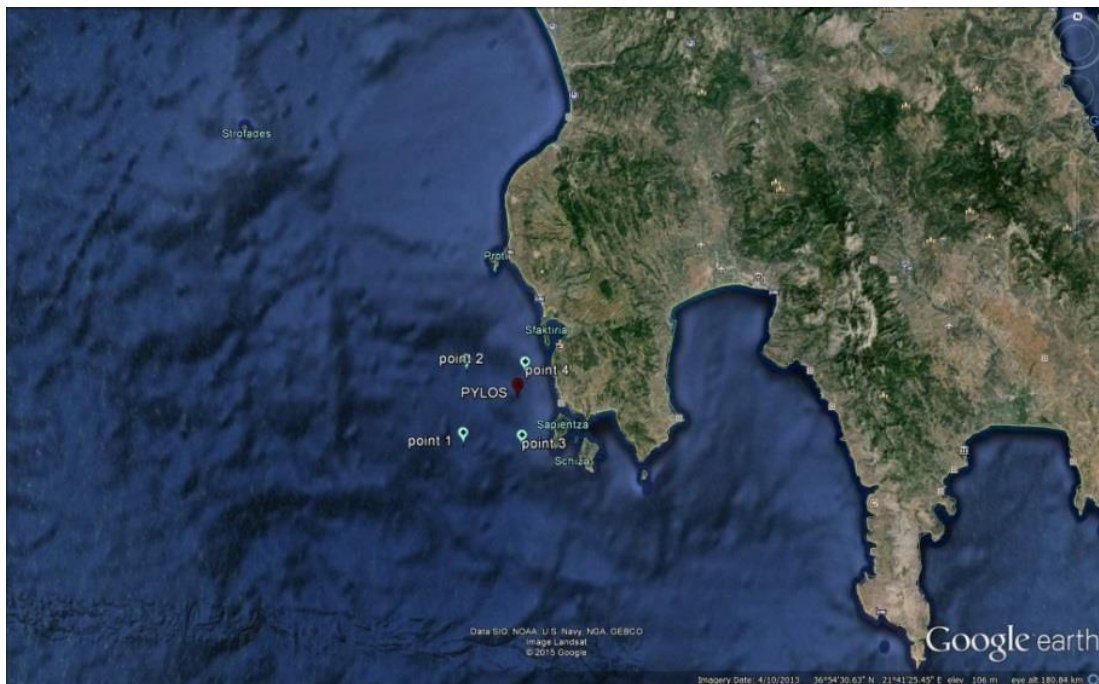


Figure 5.2.21: Pylos Buoy and the 4 nearby points of ERA-Interim grid

5.2.1.6.1 Significant Wave Height (SWH)

The method of distance weighted average (WA) is chosen for Pylos for the case of significant wave height and the statistics are shown in Table 5.2.16. For the significant wave height the correlation is of 0.91 and the bias of 0.12 m with the buoy data higher than the reanalysis. The same apply for the maximum wave height but with a very large difference of 2.62 m.

Table 5.2.16: Statistics of Significant Wave Height of Pylos Buoy and ERA-Interim Method WA

| Parameter | N | Corr. | RMSE | Bias | Mean | Max | Std.Dev. |
|--------------------------|------|-------|------|------|------|------|----------|
| Hm ₀ (m) Buoy | 5548 | 0.91 | 0.33 | 0.12 | 0.97 | 7.58 | 0.75 |
| SWH (m) ERA- Interim | | | | | 0.85 | 4.96 | 0.59 |

In the monthly variation (see Figure 5.2.22a) of significant wave height the pattern is similar for the buoy and ERA-Interim, with the first being higher than the latter with the smallest difference observed of 0.02 m in July and the largest 0.24 m in December. Similar to the monthly variation, in the case of interannual variability (see Figure 5.2.22b), both datasets present decreasing patterns, with the buoy higher than the ERA-Interim and the largest difference in 2007 by 0.20 m whilst the smallest is in 2010 by 0.10 m.

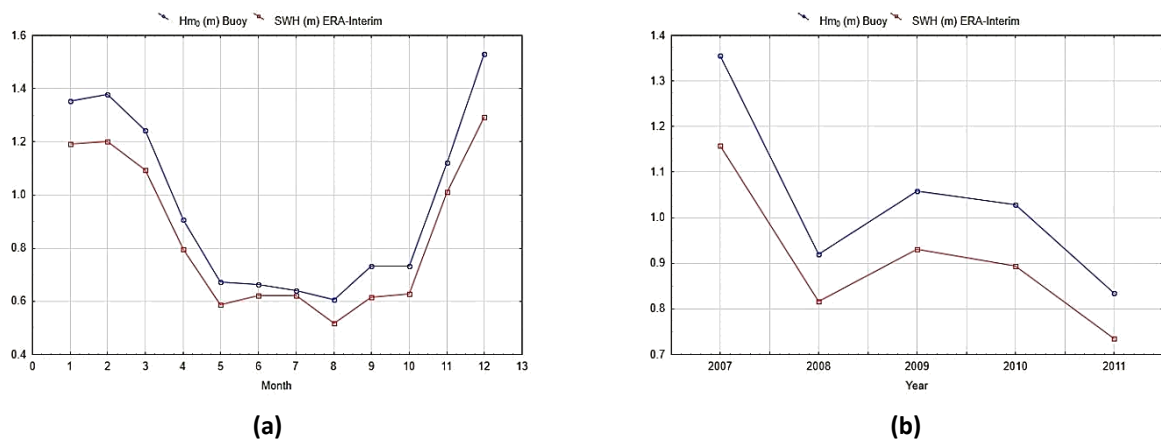


Figure 5.2.22: Mean monthly (a) and annual (b) significant wave height values from the buoy (Hm0) and ERA-Interim as estimated from the method of SP (swh)

5.2.1.6.2 Wind Speed (W10)

Wind speed is described best in relation to the buoy by the ERA-Interim as these are estimated by the method of selected point which in this case is the distance weighted average of points 1 and 2. The statistics of the interrelation of the data from the buoy and ERA-Interim (SP) are presented in Table 5.2.17. The correlation is of 0.72 and the positive bias of 0.91 m/s shows that the buoy data are higher than that of the ERA-Interim. The same is for the maximum values as well, with a difference of 1.83 m/s.

Table 5.2.17: Statistics of Wind Speed for Buoy and ERA-Interim Method SP

| Parameter | N | Corr. | RMSE | Bias | Mean | Max | Std.Dev. |
|-----------------------|------|-------|------|------|------|-------|----------|
| Wind Speed (m/s) Buoy | 5767 | 0.72 | 2.48 | 0.91 | 5.73 | 18.28 | 3.3 |
| W10 (m/s) ERA-Interim | | | | | 4.82 | 16.45 | 2.59 |

Both datasets present similar patterns in the case of monthly variation, with the wind speed from the buoy higher than that given by ERA-Interim. The smallest difference is in May by 0.16 m/s and the largest in August by 1.34 m/s. The annual patterns are similar for both datasets, with the wind speed from the buoy higher than the ERA-Interim, with the smallest difference 0.64 m/s in 2007 and the higher 1.12 m/s in 2011.

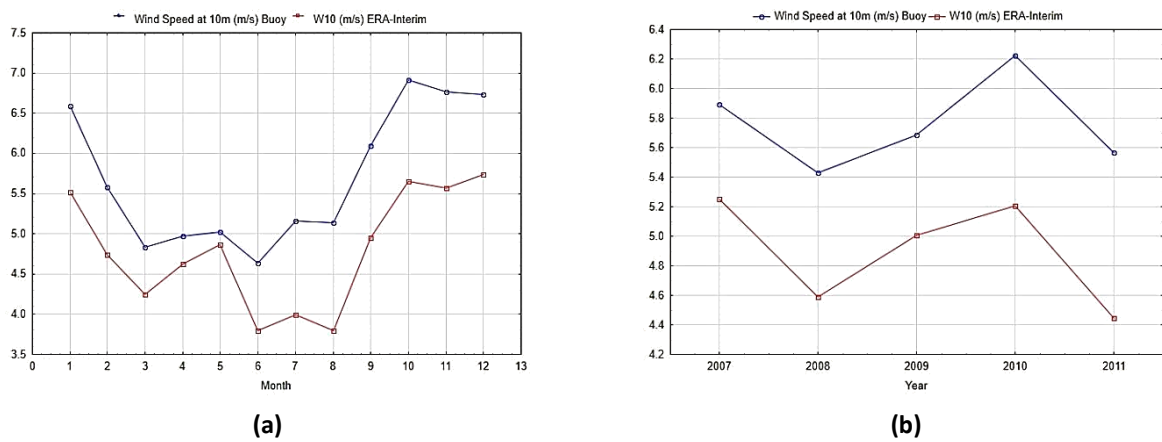


Figure 5.2.23: Mean monthly (a) and annual (b) wind speed values from the buoy (Wind speed at 10m) and ERA-Interim as estimated from the method of SP (W10).

5.2.1.6.3 Temperature at 2m (T2M)

Temperature at 2m is estimated with the method of weighted distance average of the 4 nearest points. The relationship with the data given from the buoy is shown in Table 5.2.18. The correlation of the two datasets is 0.92 with a positive bias of 0.36 °C (buoy data higher than the reanalysis). In contradiction, the maximum of the ERA-Interim is higher than that of the buoy by 2.41 °C.

Table 5.2.18: Statistics of Temperature at 2m for Buoy and ERA-Interim Method WA

| Parameter | N | Corr. | RMSE | Bias | Mean | Max | Std.Dev. |
|-----------------------------|------|-------|------|------|-------|-------|----------|
| Temperature at 2m (°C) Buoy | 5548 | 0.92 | 2.57 | 0.36 | 19.51 | 31.82 | 5.03 |
| T2M (°C) ERA-Interim | | | | | 19.15 | 34.23 | 6.40 |

For the monthly variation, the data from the ERA-Interim are higher than those of the buoy for the months April to August and lower for the rest.

The smallest difference is in April by 0.18 °C and the largest in November by 2.24 °C. Regarding the annual variation, the data from the buoy are higher except in the years 2008 and 2009. The smallest difference is 0.03 °C in 2010 and the largest 1.67 °C in 2007.

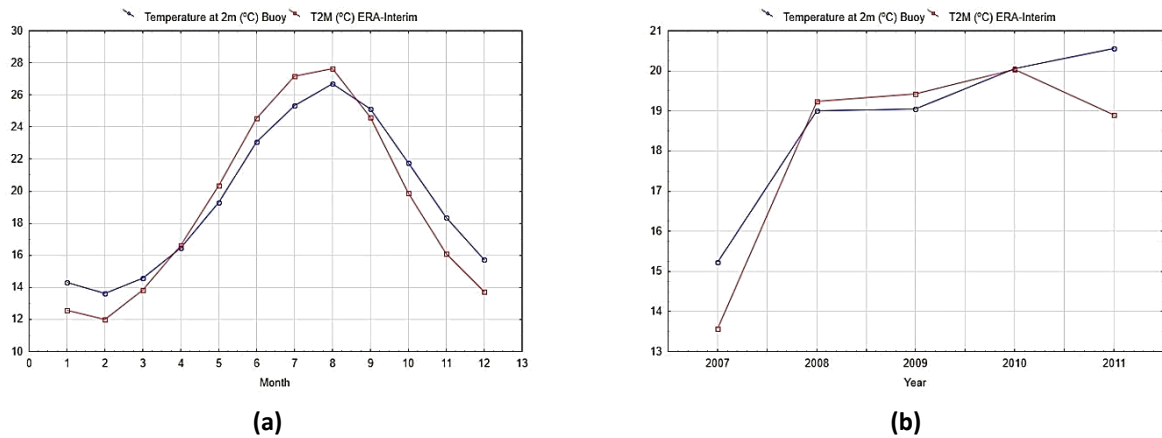


Figure 5.2.24: Mean monthly (a) and annual (b) temperature values from the buoy (Temperature at 2m) and ERA-Interim as estimated from the method of SP (T2M)

5.2.1.7 Santorini

The location of the buoy and the 4 points of the ERA-Interim grid are shown in Figure 5.2.25. For all of the parameters the method of weighted distance average is chosen.



Figure 5.2.25: Santorini Buoy and the 4 nearby points of ERA-Interim grid

5.2.1.7.1 Significant Wave Height (SWH)

The relation of the ERA-Interim dataset and the buoy dataset are shown in Table 5.2.19. The correlation of the two datasets in Santorini is 0.68 with a negative bias of 0.16 m (buoy is lower than the reanalysis). The maximum values are very close, with a difference of 0.02 m.

Table 5.2.19: Statistics of Significant Wave Height of Santorini Buoy and ERA-Interim Method WA

| Parameter | N | Corr. | RMSE | Bias | Mean | Max | Std.Dev. |
|--------------------------|-------|-------|------|-------|------|------|----------|
| Hm ₀ (m) Buoy | 15086 | 0.68 | 0.46 | -0.16 | 0.89 | 4.92 | 0.55 |
| SWH (m) ERA- Interim | | | | | 1.05 | 4.9 | 0.61 |

The monthly variation of the wave height has the same pattern in both of the datasets, with the ERA-Interim higher than the buoy. The smallest difference is in May by 0.05 m and the largest in August by 0.24 m. The annual variation is similar for the 2 datasets, with ERA-Interim higher than the buoy, as in the case of the monthly variation. The smallest difference is in 2002 by 0.08 m and the largest in 2000 by 0.25 m.

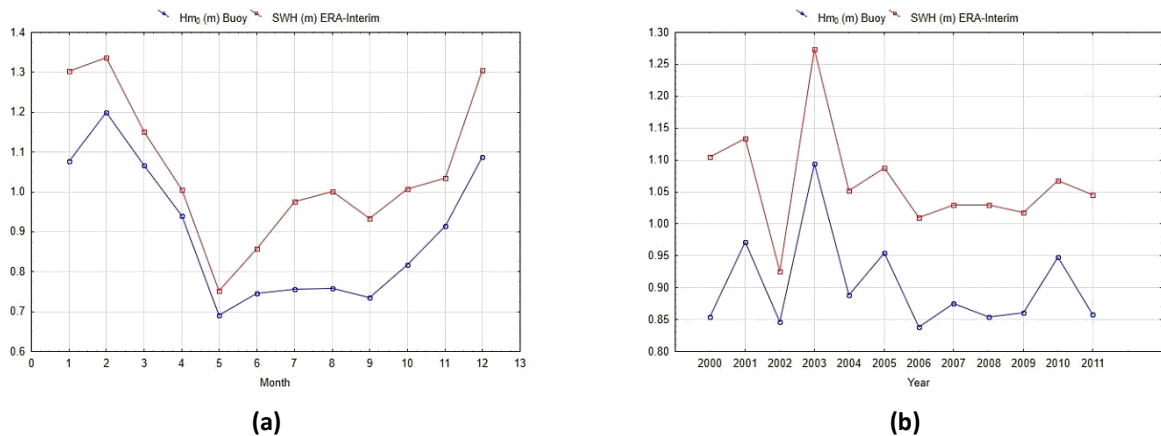


Figure 5.2.26: Mean monthly (a) and annual (b) significant wave height values from the buoy (Hm₀) and ERA-Interim as estimated from the method of WA (swh)

5.2.1.7.2 Wind Speed (W10)

The statistical characteristics of wind speed from the buoys and ERA-Interim and their relation is shown in Table 5.2.20. In the case of wind speed the correlation is 0.72 with a bias of 0.01 m/s (buoy higher than the reanalysis). The maximum values are higher at the buoys than the ERA-Interim by 3.23 m/s.

Table 5.2.20: Statistics of Wind Speed for Buoy and ERA-Interim Method WA W10

| Parameter | N | Corr. | RMSE | Bias | Mean | Max | Std.Dev. |
|-----------------------|-------|-------|------|------|------|-------|----------|
| Wind Speed (m/s) Buoy | 14765 | 0.72 | 2.25 | 0.01 | 6.49 | 21.48 | 3.48 |
| W10 (m/s) ERA-Interim | | | | | 6.48 | 18.25 | 3.00 |

The monthly variation shows that wind speed of ERA-Interim is higher than that of the buoy for the months of June to September and lower for the rest of the period. The smallest difference is in May by 0.07 m/s and the highest in July by 1.08 m/s. The annual variation has similar patterns in both datasets, with the ERA-Interim being higher than the buoy in the years 2000, 2001, 2003, 2005, 2006, 2008 and 2009, whilst lower for the rest. The minimum difference is in 2005 by 0.01 m/s and the maximum in 2006 by 0.42 m/s.

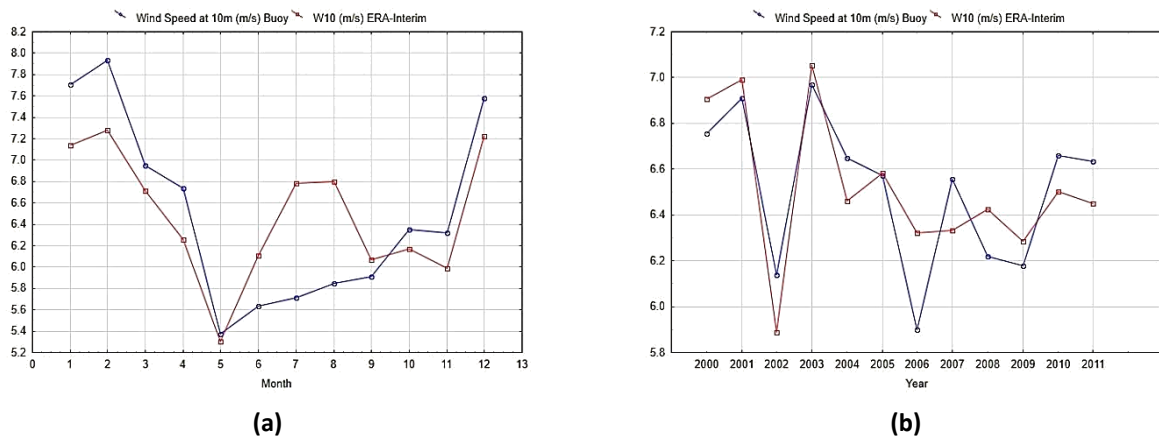


Figure 5.2.27: Mean monthly (a) and annual (b) wind speed values from the buoy (Wind speed at 10m) and ERA-Interim as estimated from the method of WA (W10).

5.2.1.7.3 Temperature at 2m (T2M)

The relation of the two datasets for the case of temperature at 2m is shown in Table 5.2.21. The correlation for wind speed is of 0.84 with a negative bias of 0.64 °C (buoy is lower than the reanalysis). The maximum value of temperature is higher at the buoy than at the reanalysis by 2.91 °C.

Table 5.2.21: Statistics of Temperature at 2m for Buoy and ERA-Interim Method WA

| Parameter | N | Corr. | RMSE | Bias | Mean | Max | Std.Dev. |
|-----------------------------|-------|-------|------|-------|-------|-------|----------|
| Temperature at 2m (°C) Buoy | 14645 | 0.84 | 2.88 | -0.64 | 19.65 | 36.26 | 5.18 |
| T2M (°C) ERA-Interim | | | | | 20.29 | 33.35 | 5.51 |

From March to October, the temperature of ERA-Interim is higher than that the buoy, with the smallest difference in February by 0.01 °C and the largest in July by 2.12 °C.

The annual variation is similar for both datasets with ERA-Interim higher than the buoy data except in the years 2010 and 2011 where it is lower. The smallest difference is in 2010 by 0.11 °C and the largest in 2011 by 4.45 °C.

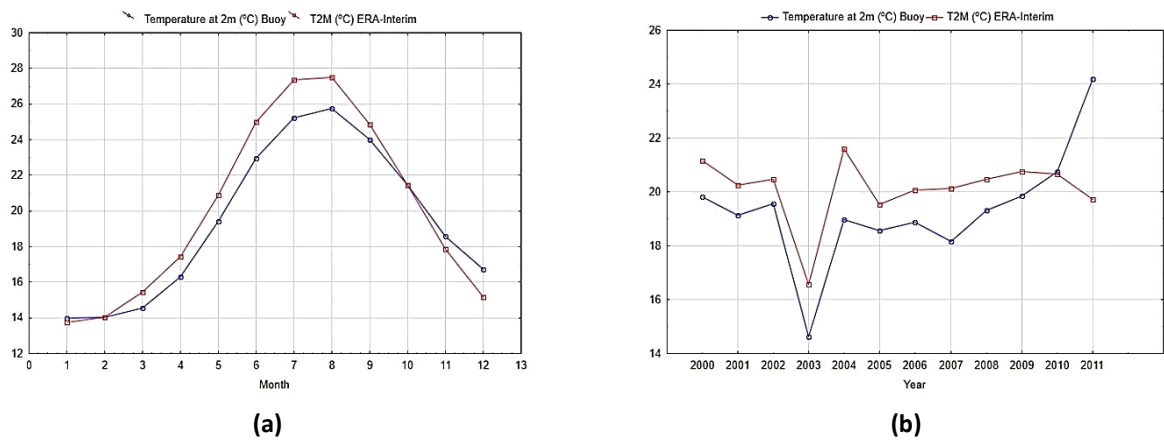


Figure 5.2.28: Mean monthly (a) and annual (b) temperature values from the buoy (Temperature at 2m) and ERA-Interim as estimated from the method of WA (T2M)

5.2.1.8 Skyros

The location of the buoy and the 4 nearest grid points are shown in Figure 5.2.29.

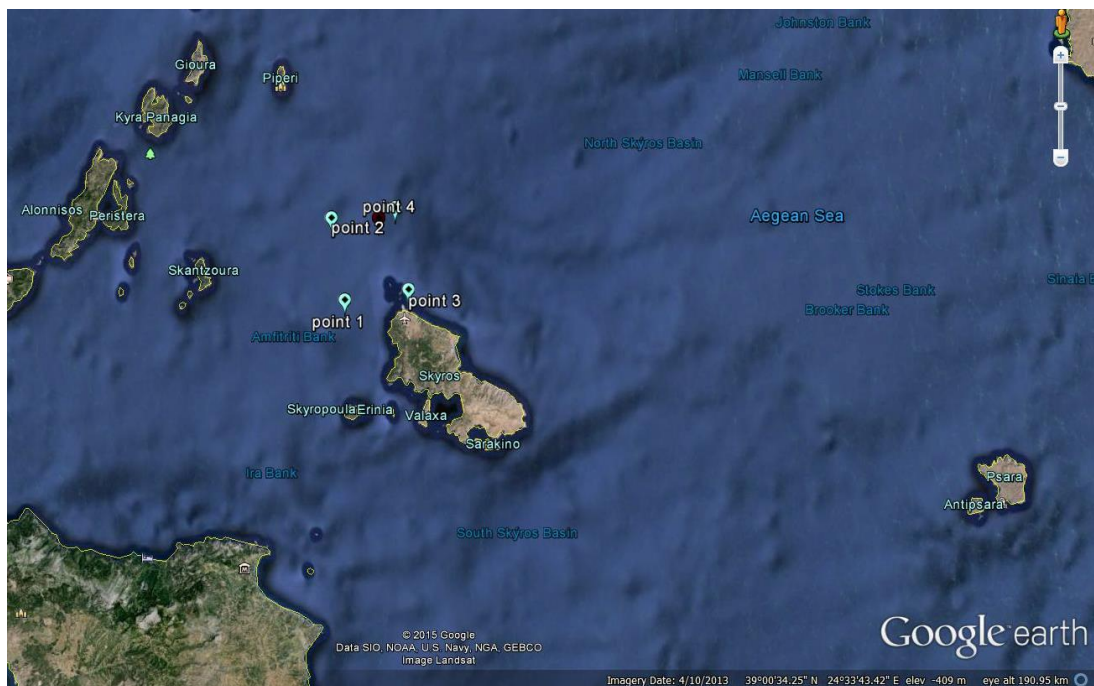


Figure 5.2.29: Skyros Buoy and the 4 nearby points of ERA-Interim grid

5.2.1.8.1 Significant Wave Height (SWH)

Statistics of the data from the buoy and the ERA-Interim dataset as provided from the method of WA are shown in Table 5.2.22. The correlation for the significant wave height is very good, 0.94 with a negative bias of 0.002m (the buoy data are lower than the reanalysis). Furthermore, the max values are higher from the ERA-Interim, in relation to the buoy, with a 0.62 m difference.

Table 5.2.22: Statistics of Significant Wave Height of Skyros Buoy and ERA-Interim Method WA

| Parameter | N | Corr. | RMSE | Bias | Mean | Max | Std.Dev. |
|--------------------------|------|-------|------|--------|------|------|----------|
| Hm ₀ (m) Buoy | 5666 | 0.94 | 0.23 | -0.002 | 0.87 | 4.85 | 0.69 |
| SWH (m) ERA- Interim | | | | | 0.87 | 5.47 | 0.7 |

The monthly variation is rather similar for both datasets with ERA-Interim being higher in the months January and from August to December. The smallest difference is 0.01 m in December and the largest in April by 0.08 m. The annual variation is similar as well with the ERA-Interim lower than the buoy in the years 2009 and 2010. The smallest difference is in 2008 by 0.004 m and the largest in 2007 by 0.03 m.

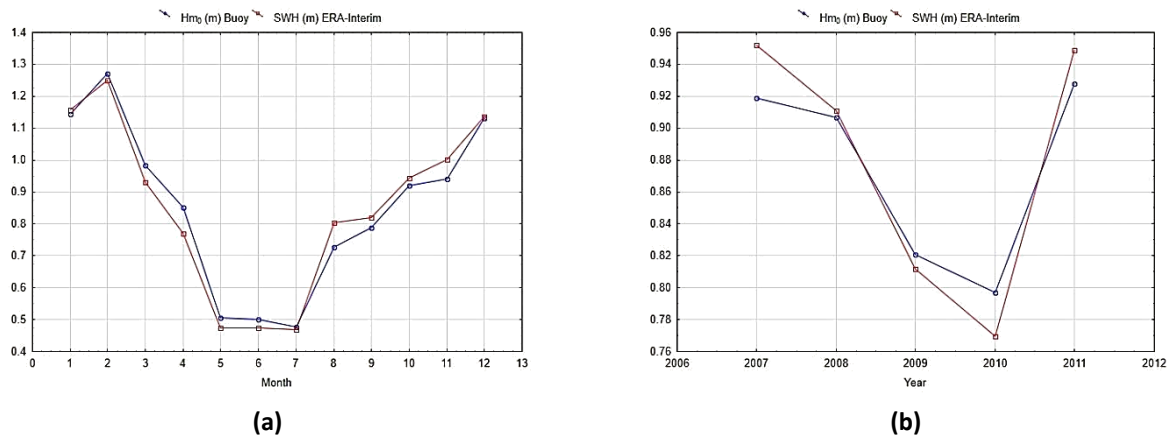


Figure 5.2.30: Mean monthly (a) and annual (b) significant wave height values from the buoy (Hm₀) and ERA-Interim as estimated from the method of WA (swh)

5.2.1.8.2 Wind Speed (W10)

The statistics of the relation of data of wind speed from the buoy of Skyros and the weighted average data of ERA-Interim are shown in Table 5.2.23. The correlation is around 0.72 with a bias of 0.01 m/s (the buoy is higher than the reanalysis). The buoy has higher maximum value of wind speed than the ERA-Interim by 3.23 m/s.

Table 5.2.23: Statistics of Wind Speed for Buoy and ERA-Interim Method WA W10

| Parameter | N | Corr. | RMSE | Bias | Mean | Max | Std.Dev. |
|-----------------------|------|-------|------|------|------|-------|----------|
| Wind Speed (m/s) Buoy | 4908 | 0.72 | 2.25 | 0.01 | 6.49 | 21.48 | 3.48 |
| W10 (m/s) ERA-Interim | | | | | 6.48 | 18.25 | 3.00 |

Both of the datasets have similar patterns in the monthly variation, with ERA-Interim being higher than the buoy during the months February, May, October and November. The minimum difference is 0.004 m/s in May and the maximum 0.68 m/s in February. The annual variation is also the same for both datasets, with the buoy being higher than the ERA-Interim except the year 2011. The smallest difference is 0.18 m/s in 2007 and the maximum 1.57 m/s in 2011.

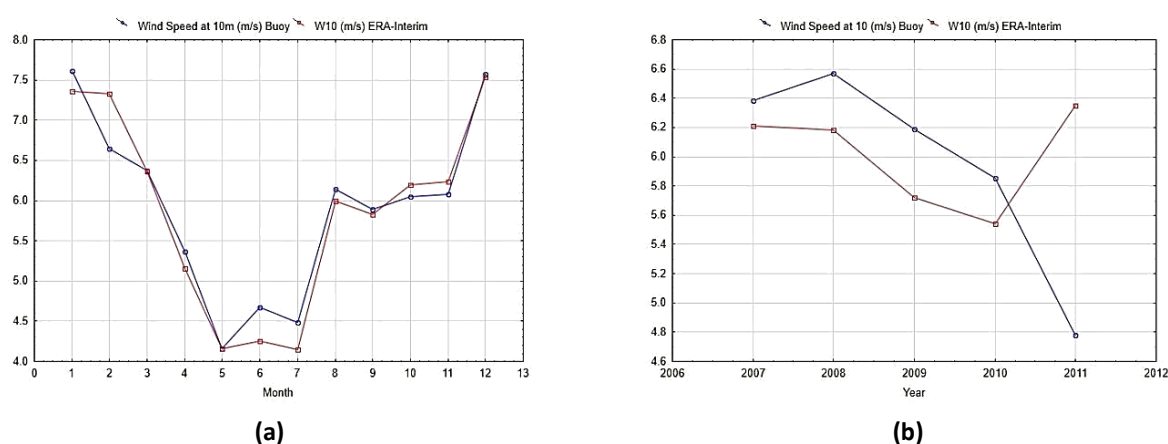


Figure 5.2.31: Mean monthly (a) and annual (b) wind speed values from the buoy (Wind speed at 10m) and ERA-Interim as estimated from the method of WA (W10).

5.2.1.8.3 Temperature at 2m (T2M)

For temperature at 2 m, the method of weighted average of points 2 and 4 is used. The statistics in Table 5.2.24, show that there is a correlation of 0.93 for the two datasets, with a negative bias of 0.4 °C. As for the maximum values, ERA-Interim is higher than the buoy by 1.76 °C.

Table 5.2.24: Statistics of Temperature at 2m for Buoy and ERA-Interim Method SP

| Parameter | N | Corr. | RMSE | Bias | Mean | Max | Std.Dev. |
|-----------------------------|------|-------|------|-------|-------|-------|----------|
| Temperature at 2m (°C) Buoy | 5604 | 0.93 | 2.39 | -0.40 | 17.17 | 30.33 | 6.17 |
| T2M (°C) ERA-Interim | | | | | 17.57 | 32.09 | 6.53 |

The mean monthly variation is similar for both datasets, with ERA-Interim higher than the buoys except for the months March and October to December. The smallest difference is in March by 0.13 °C and the largest in July by 1.46 °C. The annual variation is similar for both datasets with ERA-Interim lower than

the buoy except the years 2010 and 2011. The smallest difference is 0.06 °C in 2009 and the largest in 2011 by 1.62 °C.

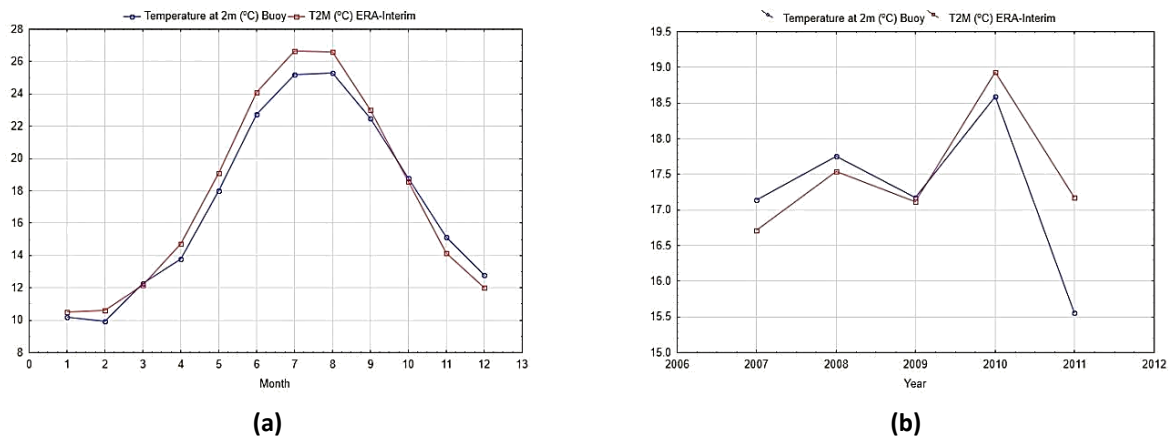


Figure 5.2.32: Mean monthly (a) and annual (b) temperature values from the buoy (Temperature at 2m) and ERA-Interim as estimated from the method of SP (T2M)

5.2.2 35 years analysis

5.2.2.1 North Aegean

5.2.2.1.1 Wave Characteristics

Wave characteristics (height and period) of the North Aegean are presented in Table 5.2.25, as provided by ERA-Interim dataset, while, their monthly and annual means and related monthly anomalies, for the period 1979-2013, are shown in Figure 5.2.34.

Table 5.2.25: Wave Characteristics of North Aegean as given from ERA-Interim

| Coordinates | Parameter | N | Mean | Maximum | Std.Dev. |
|------------------|-----------|-------|------|---------|----------|
| 39.5°N 24.5°E | SWH (m) | 51136 | 0.78 | 5.62 | 0.67 |
| | MWP (s) | 51136 | 4.11 | 9.18 | 1.15 |

According to the ERA-Interim data set, the most frequent wave directions are from NE (52.46%) (Fig. 5.35), while secondary directions are from S (16.3%). A percent of 40.8% of waves with heights of 0 to 0.5 m are from NE while heights of more than 4 m are mostly (85.37%) from N22.5 ° to N45°.

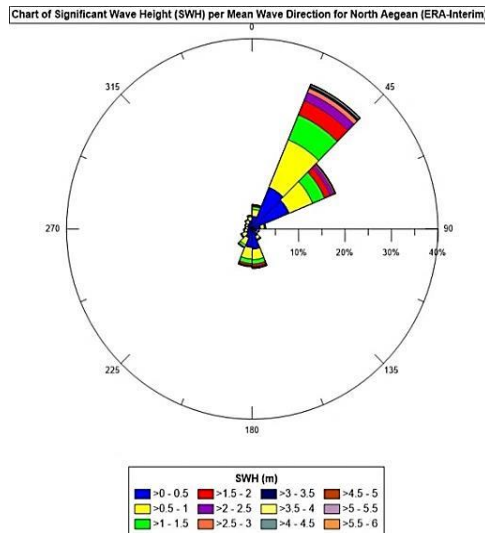


Figure 5.2.33: Wave Chart of North Aegean from ERA-Interim

The area of North Aegean is characterized by waves with heights of 0 to 0.5 m with a frequency of 44.4% and periods with range of 2-4 s with a frequency of 50.82% (Table 5.26). Waves with heights of more than 4 m have frequency of 0.24% and periods longer than 8 s of 0.21%.

Table 5.2.26: Frequency (%) table of significant wave height (SWH) and mean wave period (MWP) for North Aegean (ERA-Interim)

| SWH (m) | MWP (s) | | | | | |
|--------------|---------|-------|-------|------|------|--------|
| | 0-2 | 2-4 | 4-6 | 6-8 | 8-10 | Total |
| 0-0.5 | 0.39 | 38.74 | 5.26 | 0 | 0 | 44.40 |
| 0.5-1 | 0 | 11.96 | 17.52 | 0.08 | 0 | 29.56 |
| 1-1.5 | 0 | 0.12 | 12.80 | 0.35 | 0 | 13.27 |
| 1.5-2 | 0 | 0 | 5.41 | 1.18 | 0 | 6.60 |
| 2-2.5 | 0 | 0 | 0.71 | 2.61 | 0 | 3.31 |
| 2.5-3 | 0 | 0 | 0.01 | 1.55 | 0 | 1.56 |
| 3-3.5 | 0 | 0 | 0 | 0.75 | 0 | 0.75 |
| 3.5-4 | 0 | 0 | 0 | 0.27 | 0.03 | 0.30 |
| 4-4.5 | 0 | 0 | 0 | 0.06 | 0.09 | 0.16 |
| 4.5-5 | 0 | 0 | 0 | 0 | 0.05 | 0.05 |
| 5-5.5 | 0 | 0 | 0 | 0 | 0.03 | 0.03 |
| 5.5-6 | 0 | 0 | 0 | 0 | 0 | 0 |
| Total | 0.39 | 50.82 | 41.72 | 6.85 | 0.21 | 100.00 |

With respect to the trend of period 1979-2013, the means per month (Figure 5.2.34a) show that it is virtually certain (99.67%) to have had a decrease of 0.003 m/yr for significant wave height during February and very likely (93.05%) an increase of 0.004 m/yr in April.

For mean wave period (Figure 5.2.34b), it is virtually certain (99.96%) in April to have had an increase of 0.016 s/yr and very likely (97.21%) in June to have presented an increasing trend by 0.009 s/yr. In regards of the annual values, significant wave height (Figure 5.2.34c) was unlikely to change (11.36%) while mean wave period (Figure 5.2.34d) is virtually certain (99.94%) to had increased by 0.005 s/yr. Moreover, the monthly anomalies show that it is unlikely (12.52%) to have had a trend in the case of significant wave height (Figure 5.2.34e), whilst it is virtually certain (99.94%) that there had been an increase of 0.00001 s/yr of mean wave period (Figure 5.2.34f).

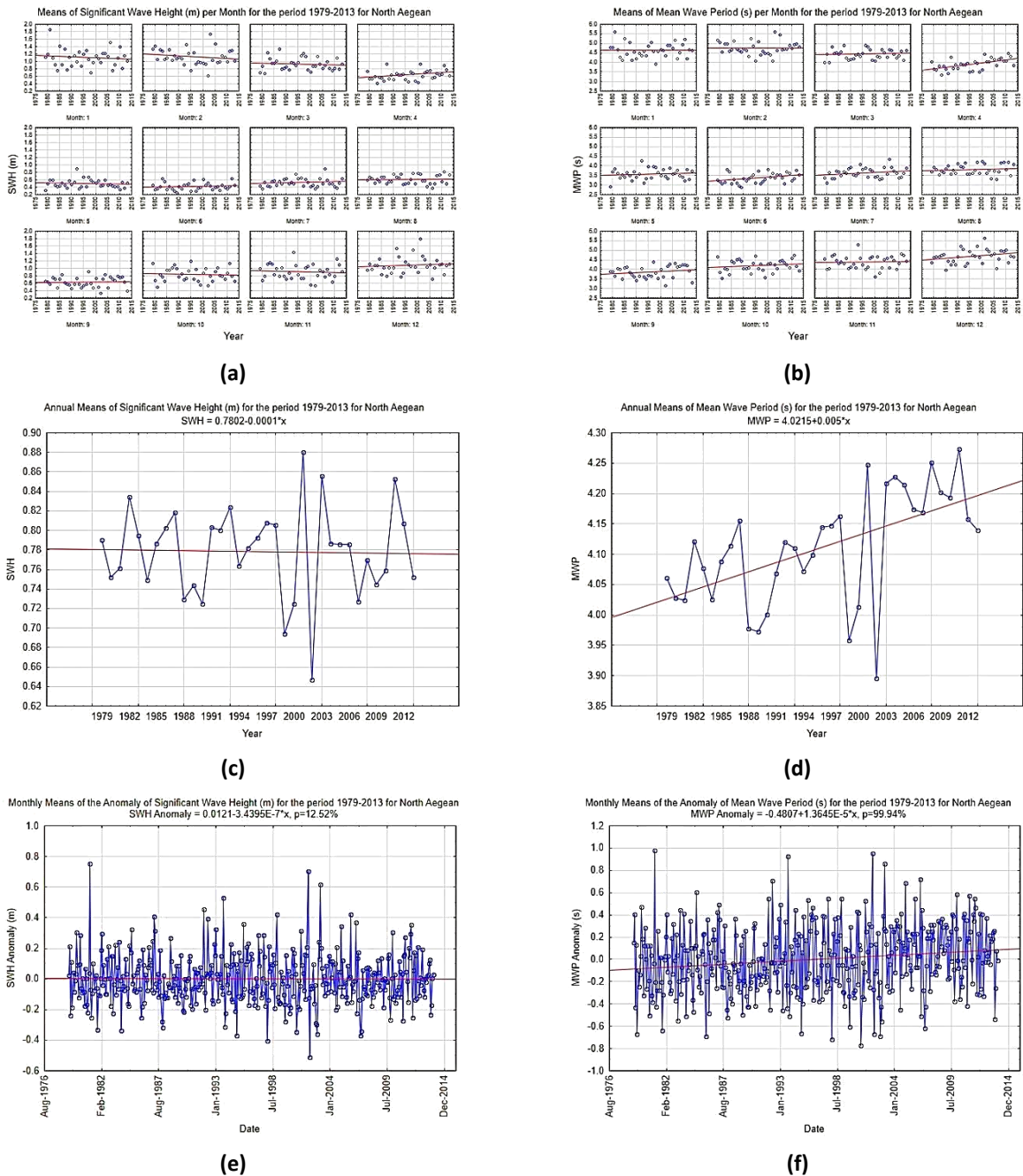


Figure 5.2.34: Monthly and annual means and monthly anomalies for the period 1979-2013 for significant wave height (a, c, e) and wave period (b, d, f) for North Aegean.

5.2.2.1.2 Weather Characteristics

The statistics of atmospheric characteristics (wind speed and air temperature at 10 m and 2 m, above sea level) of the North Aegean are shown in Table 5.2.27, as provided by ERA-Interim dataset.

Table 5.2.27: Weather Characteristics of North Aegean as given from ERA-Interim

| Coordinates | Parameter | Valid N | Mean | Maximum | Std.Dev. |
|-------------|-----------|---------|-------|---------|----------|
| 39.5°N | W10 (m/s) | 51136 | 5.71 | 21.94 | 3.46 |
| 24.5°E | T2M (°C) | 51136 | 18.27 | 35.62 | 6.52 |

The primary direction from where the winds are blowing in the area of North Aegean is NE with a frequency of 51.10% and the secondary is from S with frequency of 7.66% (Figure 5.2.35). The most common wind speeds are from 2 to 6 m/s with frequency of 46.46% and with the 60.92% of those is from N0° to N67.5°. Winds with speeds of more than 14 m/s have frequencies of only 2.10%, from which the 43.67% are related to NE directions.

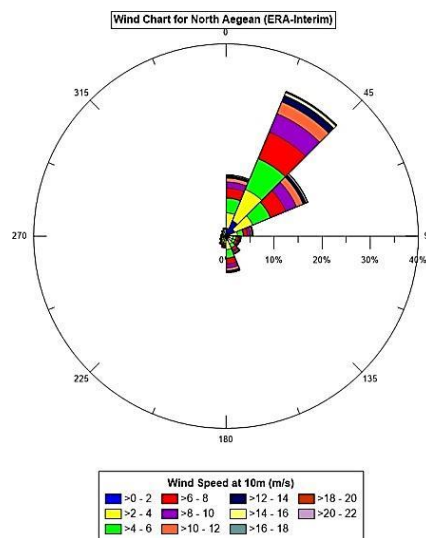
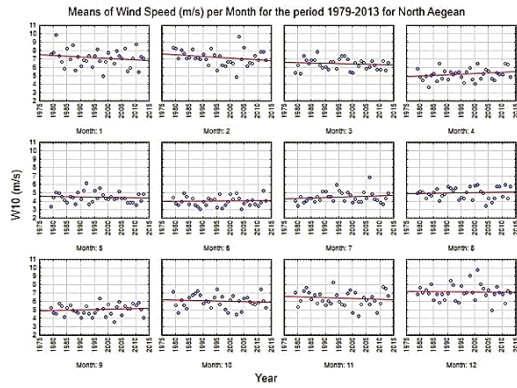
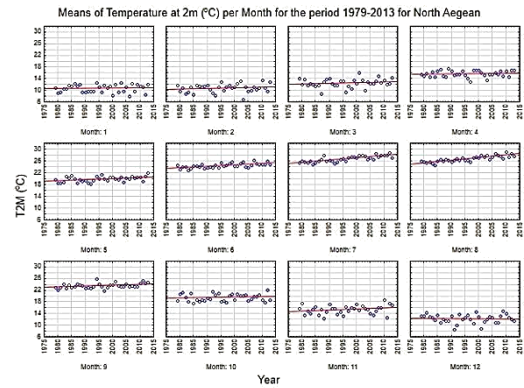


Figure 5.2.35: Wind Chart of North Aegean from ERA-Interim

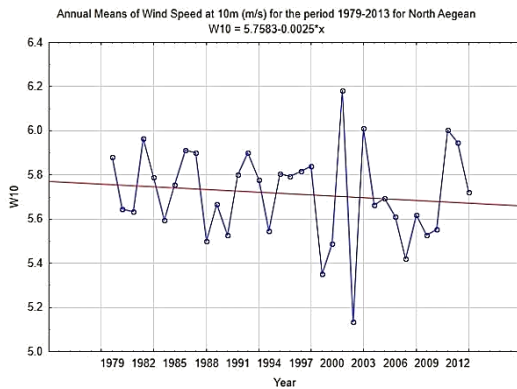
The monthly means of wind speeds for the period 1979-2013, is likely (82.63%) to had shown an increase of 0.016 m/s per year, while temperature is virtually certain and very likely (97-100%) to had increased from May to September in ranges of 0.03 to 0.08 °C per year (Figure 5.2.36a,b). Additionally, in the annual values, it is about likely as not (50.6%) for wind speed to have presented a trend whilst virtually certain for temperature to had increased by 0.032 °C per year (99.94%) (Figure 5.2.36c,d). In addition, the mean monthly anomalies show that wind speed is about likely as not (50.73%) to had presented a trend, while temperature is virtually certain (100%) to had shown an increasing trend of 0.001 °C/yr (Figure 5.2.36 e,f).



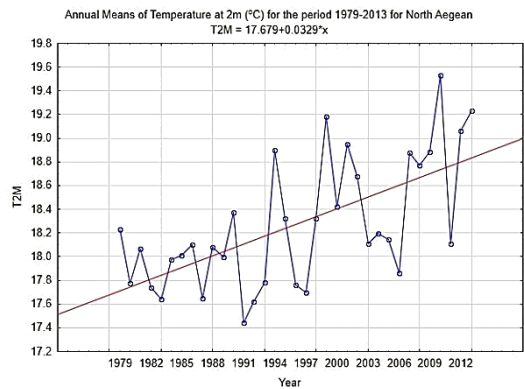
(a)



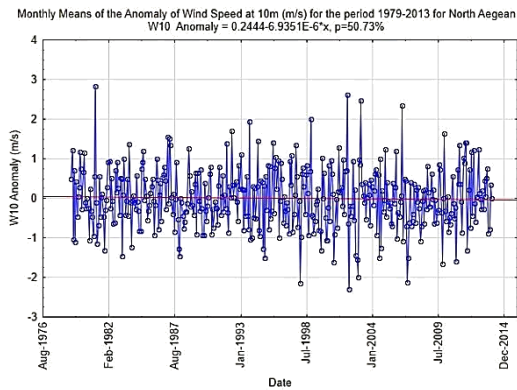
(b)



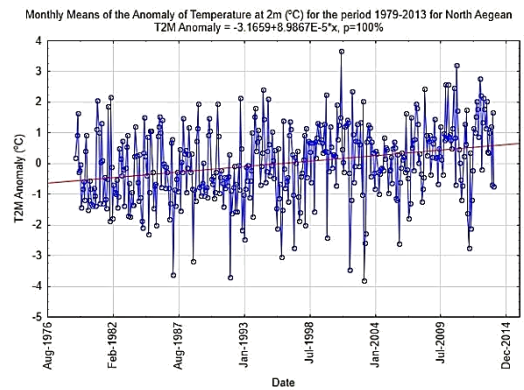
(c)



(d)



(e)



(f)

Figure 5.2.36: Monthly and annual means and monthly anomalies, for the period 1979-2013 for wind speed at 10m (a, c, e) and temperature at 2m (b, d, f) for North Aegean.

5.2.2.1.3 Wave and Wind Characteristics

The interrelationship between the significant wave height and the wind speeds in the North Aegean Sea is presented in Table 5.2.28. From the most frequent waves of <0.5 m, a 70.26% is related to wind speeds of 2-6 m/s, while the 86.99% of waves with heights >4 m are related with speeds of more than 16 m/s.

Table 5.2.28: Frequency table (%) of significant wave height (SWH) and wind speed at 10m (W10) for North Aegean (ERA-Interim)

| SWH (m) | W10 (m/s) | | | | | | | | | | | |
|--------------|-----------|-------|-------|-------|-------|-------|-------|-------|-------|-------|-------|--------|
| | 0-2 | 2-4 | 4-6 | 6-8 | 8-10 | 10-12 | 12-14 | 14-16 | 16-18 | 18-20 | 20-22 | Total |
| 0-0.5 | 11.97 | 20.10 | 11.10 | 1.20 | 0.03 | 0 | 0 | 0 | 0 | 0 | 0 | 44.40 |
| 0.5-1 | 0.88 | 4.17 | 10.10 | 11.39 | 2.84 | 0.17 | 0.01 | 0 | 0 | 0 | 0 | 29.56 |
| 1-1.5 | 0.02 | 0.13 | 0.82 | 3.93 | 6.15 | 2.01 | 0.19 | 0.01 | 0 | 0 | 0 | 13.27 |
| 1.5-2 | 0 | 0.01 | 0.03 | 0.29 | 2.08 | 3.33 | 0.78 | 0.06 | 0 | 0 | 0 | 6.60 |
| 2-2.5 | 0 | 0 | 0 | 0.01 | 0.12 | 1.24 | 1.70 | 0.22 | 0.01 | 0 | 0 | 3.31 |
| 2.5-3 | 0 | 0 | 0 | 0 | 0.01 | 0.12 | 0.84 | 0.53 | 0.06 | 0 | 0 | 1.56 |
| 3-3.5 | 0 | 0 | 0 | 0 | 0 | 0 | 0.10 | 0.48 | 0.15 | 0.01 | 0 | 0.75 |
| 3.5-4 | 0 | 0 | 0 | 0 | 0 | 0 | 0 | 0.10 | 0.18 | 0.02 | 0 | 0.30 |
| 4-4.5 | 0 | 0 | 0 | 0 | 0 | 0 | 0 | 0 | 0.09 | 0.06 | 0 | 0.16 |
| 4.5-5 | 0 | 0 | 0 | 0 | 0 | 0 | 0 | 0 | 0.01 | 0.04 | 0.01 | 0.05 |
| 5-5.5 | 0 | 0 | 0 | 0 | 0 | 0 | 0 | 0 | 0 | 0.02 | 0.01 | 0.03 |
| 5.5-6 | 0 | 0 | 0 | 0 | 0 | 0 | 0 | 0 | 0 | 0 | 0 | 0 |
| Total | 12.87 | 24.41 | 22.05 | 16.83 | 11.23 | 6.89 | 3.63 | 1.42 | 0.51 | 0.15 | 0.03 | 100.00 |

5.2.2.2 Central Aegean

5.2.2.2.1 Wave Characteristics

The area of Central Aegean is described by the wave state given in Table 5.2.29 as shown by the ERA-Interim dataset.

Table 5.2.29: Wave Characteristics of Central Aegean as given from ERA-Interim

| Coordinates | Parameter | N | Mean | Maximum | Std.Dev. |
|------------------|-----------|-------|------|---------|----------|
| 38.25N 25.25E | SWH (m) | 51136 | 1.00 | 6.06 | 0.75 |
| | MWP (s) | 51136 | 4.46 | 9.48 | 1.17 |

In the area of Central Aegean, 62.43% of the waves propagate from N and 19.71% from W. Wave heights range from 0-1 m with a frequency of 60.23%, with 53.84% of those from the N. Waves with heights of more than 4 m have frequencies of 0.46% and 99.16% are from 0° – 22.5°.

Chart of Significant Wave Height (SWH) per Mean Wave Direction for South Aegean (ERA-Interim)

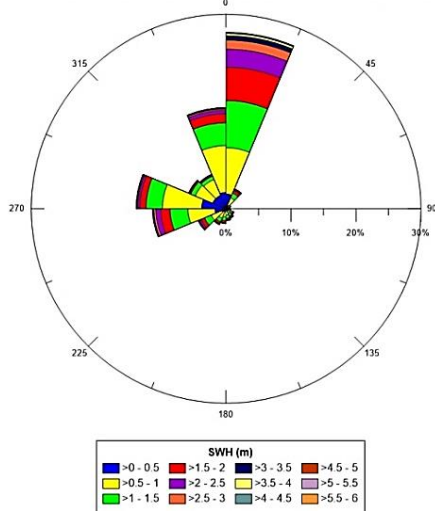
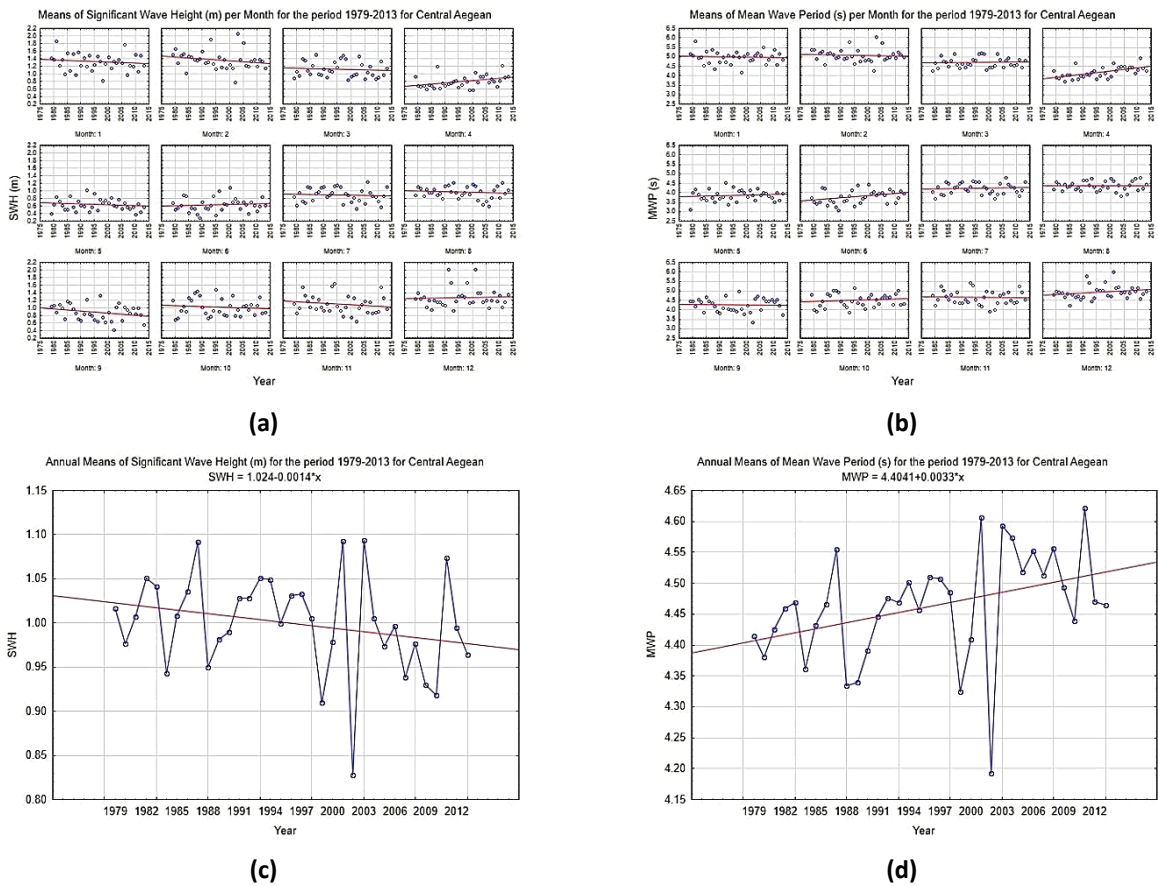
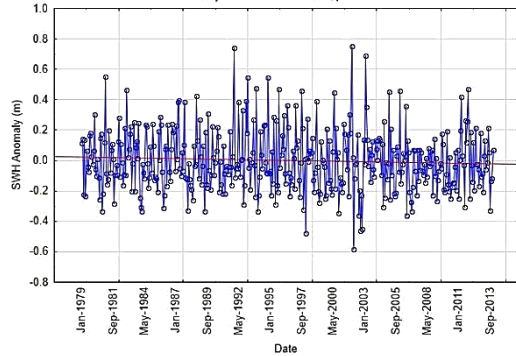


Figure 5.2.37: Wave Chart of Central Aegean from ERA-Interim

Monthly means, annual means and anomalies are given in Figure 5.2.38.

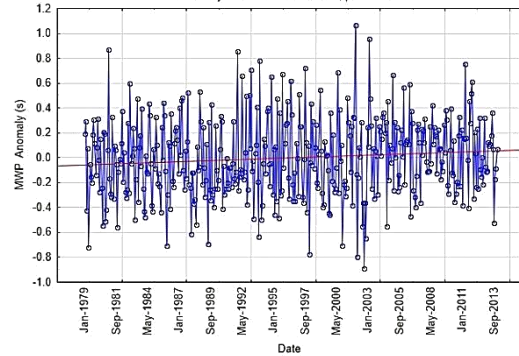


Monthly Means of the Anomaly of Significant Wave Height (m) for the period 1979-2013 for Central Aegean
 SWH Anomaly = $0.1317-3.7387E-6^*x$, $p=84.01\%$



(e)

Monthly Means of the Anomaly of Mean Wave Period (s) for the period 1979-2013 for Central Aegean
 MWP Anomaly = $-0.3135+8.8987E-6^*x$, $p=99.97\%$



(f)

Figure 5.2.38: Monthly and annual means and monthly anomalies, for the period 1979-2013 for significant wave height (a, c, e) and wave period (b, d, f) for Central Aegean.

The monthly means of significant wave height show that during April, it is very likely (97.94%) to have had an increase of 0.006 m and likely (85.56%) a decrease in September by 0.005 m (Figure 5.2.38a). In the case of mean wave period, it is virtually certain (99.98%) to have had an increase of 0.0168 s in April and very likely (95.11%) of 0.0112 s in June (Figure 5.2.38b). The annual values show that it is likely (84.41%) to have had a decreasing trend of significant wave height of 0.0014 m (Figure 5.2.38c) whilst it is very likely (97.44%) an increase in the mean wave period by 0.0033 s (Figure 5.2.38d). The anomaly of the monthly means for the period 1979-2013, shows that it is likely (84.01%) to have had a decrease of almost 0 m per year (Figure 5.2.38e), whilst for mean wave period it is virtually certain (99.97%) to have presented an increase of around 0.0001 s per year (Figure 5.2.38f).

In Central Aegean waves with heights of 0 to 1 m have frequencies of 60.23% and 99.78% are related with periods of 2-6 s. Waves with heights of more than 4 m have frequency of 0.46% and periods longer than 8 s of 0.48%.

Table 5.2.30: Frequency (%) table of significant wave height (SWH) and mean wave period (MWP) for Central Aegean

| SWH (m) | MWP (s) | | | | | Total |
|--------------|---------|-------|-------|-------|------|--------|
| | 0-2 | 2-4 | 4-6 | 6-8 | 8-10 | |
| 0-0.5 | 0.10 | 25.56 | 4.71 | 0 | 0 | 30.37 |
| 0.5-1 | 0 | 12.82 | 17.01 | 0.03 | 0 | 29.87 |
| 1-1.5 | 0 | 0.10 | 18.29 | 0.21 | 0 | 18.61 |
| 1.5-2 | 0 | 0 | 9.56 | 1.38 | 0 | 10.93 |
| 2-2.5 | 0 | 0 | 1.33 | 3.99 | 0 | 5.32 |
| 2.5-3 | 0 | 0 | 0.02 | 2.51 | 0.01 | 2.55 |
| 3-3.5 | 0 | 0 | 0 | 1.33 | 0.01 | 1.35 |
| 3.5-4 | 0 | 0 | 0 | 0.46 | 0.09 | 0.55 |
| 4-4.5 | 0 | 0 | 0 | 0.08 | 0.21 | 0.29 |
| 4.5-5 | 0 | 0 | 0 | 0.01 | 0.13 | 0.13 |
| 5-5.5 | 0 | 0 | 0 | 0 | 0.03 | 0.03 |
| 5.5-6 | 0 | 0 | 0 | 0 | 0.01 | 0.01 |
| 6-6.5 | 0 | 0 | 0 | 0 | 0 | 0 |
| Total | 0.10 | 38.48 | 50.93 | 10.01 | 0.48 | 100.00 |

5.2.2.2.2 Weather Characteristics

The atmospheric state of Central Aegean is described in Table 5.2.31, as provided by ERA-Interim dataset.

Table 5.2.31: Weather Characteristics of Central Aegean as given from ERA-Interim

| Coordinates | Parameter | Valid N | Mean | Maximum | Std.Dev. |
|-------------|-----------|---------|-------|---------|----------|
| 38.25N | W10 (m/s) | 51136 | 6.81 | 22.32 | 3.52 |
| 25.25E | T2M (°C) | 51136 | 18.79 | 33.78 | 6.05 |

In the area of Central Aegean winds are blowing from is NW to NE with a frequency of 56.41% and from SE to SW with frequency of 20.02%. Wind speeds from 2 to 8 m/s have frequencies of 55.11% and 49.86% of those are from N. Winds with speeds of more than 14 m/s have frequencies of 2.56% and 78.50% of those are from 0° to 22.5°.

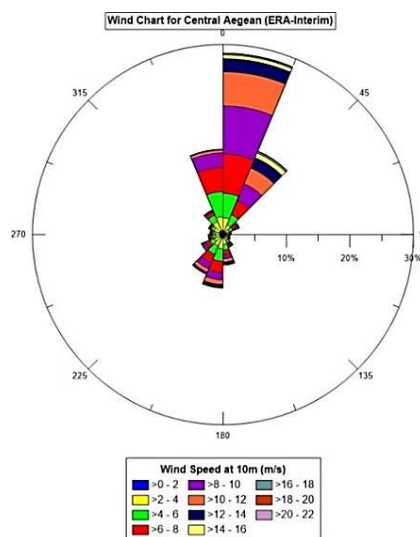
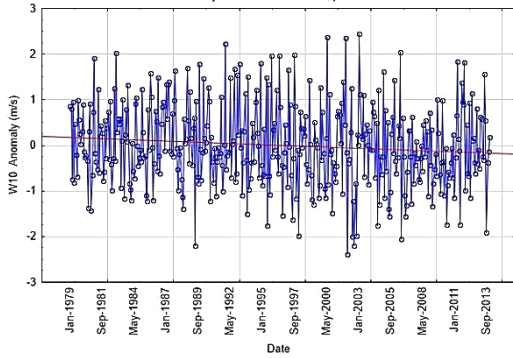


Figure 5.2.39: Wind Chart of Central Aegean from ERA-Interim

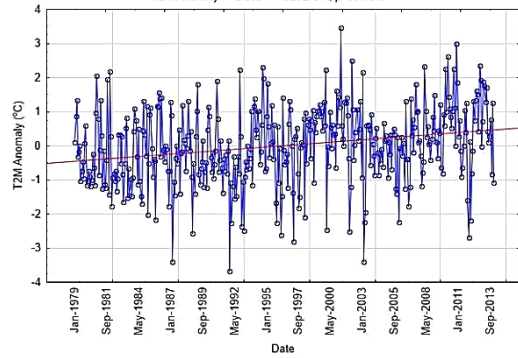
In the case of wind speed, the monthly values for the period 1979-2013 show that wind speed is very likely (90.32%) to have had an increase around 0.0195 m/s in April and very likely (95.54%) a decrease by 0.0346 m/s in September (Figure 5.2.40a). As for temperature, it is likely to virtually certain (88.55% to 100%) to have had an increase during the months May to September in a range of 0.02 to 0.06 °C (Figure 5.2.40b). Finally, the annual values present that it is very likely (97.38%) to have had a decrease in wind speed by 0.009 m/s (Figure 5.2.40c) and virtually certain (99.9%) to have had an increase in temperature of 0.026 °C (Figure 5.2.40d). The monthly anomaly means show that it is virtually certain (99.92%) that there had been a decrease of 0.0003 m/s per year in wind speed (Figure 5.2.40e) and virtually certain (99.78%) that temperature have had an increase by 0.0009 °C per year (Figure 5.2.40f).

Monthly Means of the Anomaly of Wind Speed at 10m (m/s) for the period 1979-2013 for Central Aegean
 $W10 \text{ Anomaly} = 0.9376 - 2.6606E-5 \cdot x$, $p=99.92\%$



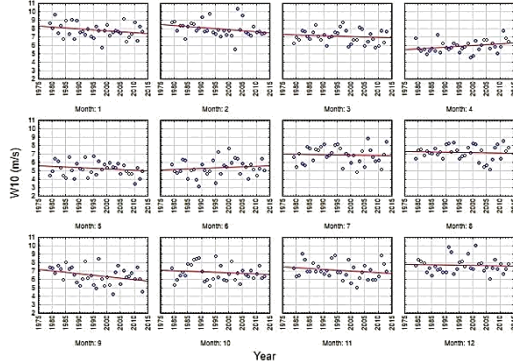
(a)

Monthly Means of the Anomaly of Temperature at 2m (°C) for the period 1979-2013 for Central Aegean
 $T2M \text{ Anomaly} = -2.5804 + 7.325E-5 \cdot x$, $p=99.78\%$



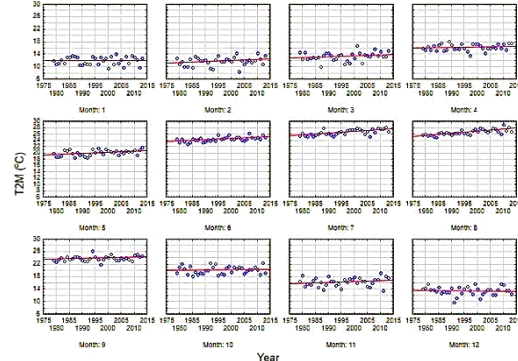
(b)

Means of Wind Speed (m/s) per Month for the period 1979-2013 for Central Aegean



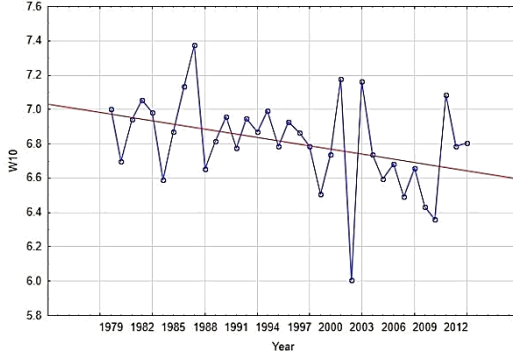
(c)

Means of Temperature at 2m (°C) per Month for the period 1979-2013 for Central Aegean



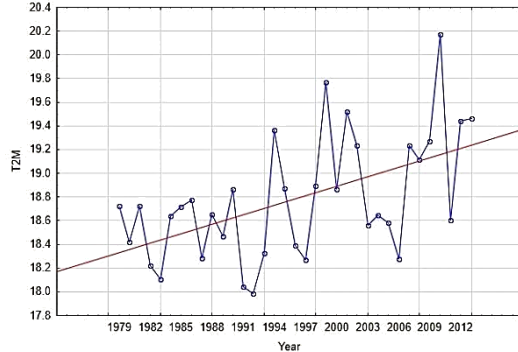
(d)

Annual Means of Wind Speed at 10m (m/s) for the period 1979-2013 for Central Aegean
 $W10 = 6.9813 - 0.0097 \cdot x$



(e)

Annual Means of Temperature at 2m (°C) for the period 1979-2013 for Central Aegean
 $T2M = 18.3042 + 0.0267 \cdot x$



(f)

Figure 5.2.40: Monthly anomalies, monthly and annual means for the period 1979-2013 for wind speed at 10m (a, c, e) and temperature at 2m (b, d, f) for Central Aegean.

5.2.2.2.3 Wave and Weather Characteristics

An 81.52% of waves with heights of 0 to 1 m are related to wind speeds of 2 to 8 m/s. A 67.51% of waves with heights of 4 to 4.5 m are related with speeds that range from 16 to 18 m/s.

Table 5.2.32: Frequency table (%) of significant wave height (SWH) and wind speed at 10m (W10) for Central Aegean

| SWH (m) | W10 (m/s) | | | | | | | | | | | | |
|--------------|-----------|-----------|-----------|-----------|-----------|-----------|-------|-------|-------|-------|-------|-------|------------|
| | 0-2 | 2-4 | 4-6 | 6-8 | 8-10 | 10-12 | 12-14 | 14-16 | 16-18 | 18-20 | 20-22 | 22-24 | Total |
| 0-0.5 | 7.4 7 | 13.4 1 | 8.74 | 0.75 | 0 | 0 | 0 | 0 | 0 | 0 | 0 | 0 | 30.37 |
| 0.5-1 | 0.7 5 | 2.84 | 9.43 | 13.9 3 | 2.84 | 0.06 | 0.01 | 0 | 0 | 0 | 0 | 0 | 29.87 |
| 1-1.5 | 0.0 2 | 0.18 | 0.75 | 4.61 | 10.8 7 | 2.10 | 0.08 | 0 | 0 | 0 | 0 | 0 | 18.61 |
| 1.5-2 | 0 | 0.02 | 0.04 | 0.36 | 3.48 | 6.29 | 0.72 | 0.02 | 0 | 0 | 0 | 0 | 10.93 |
| 2-2.5 | 0 | 0 | 0.01 | 0.02 | 0.23 | 2.68 | 2.22 | 0.14 | 0.01 | 0 | 0 | 0 | 5.32 |
| 2.5-3 | 0 | 0 | 0 | 0 | 0.01 | 0.25 | 1.81 | 0.44 | 0.03 | 0 | 0 | 0 | 2.55 |
| 3-3.5 | 0 | 0 | 0 | 0 | 0 | 0.01 | 0.42 | 0.83 | 0.08 | 0 | 0 | 0 | 1.35 |
| 3.5-4 | 0 | 0 | 0 | 0 | 0 | 0 | 0.02 | 0.36 | 0.16 | 0.01 | 0 | 0 | 0.55 |
| 4-4.5 | 0 | 0 | 0 | 0 | 0 | 0 | 0 | 0.06 | 0.22 | 0.02 | 0 | 0 | 0.29 |
| 4.5-5 | 0 | 0 | 0 | 0 | 0 | 0 | 0 | 0 | 0.09 | 0.04 | 0 | 0 | 0.13 |
| 5-5.5 | 0 | 0 | 0 | 0 | 0 | 0 | 0 | 0 | 0.01 | 0.02 | 0 | 0 | 0.03 |
| 5.5-6 | 0 | 0 | 0 | 0 | 0 | 0 | 0 | 0 | 0 | 0 | 0 | 0 | 0.01 |
| 6-6.5 | 0 | 0 | 0 | 0 | 0 | 0 | 0 | 0 | 0 | 0 | 0 | 0 | 0 |
| Total | 8.2 4 | 16.4 5 | 18.9 7 | 19.6 8 | 17.4 2 | 11.3 9 | 5.28 | 1.86 | 0.59 | 0.10 | 0.01 | 0 | 100.0 0 |

5.2.2.3 South Aegean

5.2.2.3.1 Wave Characteristics

The wave state of South Aegean can be described as given in Table 5.2.33.

Table 5.2.33: Wave Characteristics of South Aegean as given from ERA-Interim

| Coordinates | Parameter | N | Mean | Maximum | Std.Dev. |
|--------------|-----------|-------|------|---------|----------|
| 36N 24.5E | SWH (m) | 51136 | 1.08 | 5.27 | 0.68 |
| | MWP (s) | 51136 | 4.95 | 10.45 | 1.05 |

The primary direction waves are propagating from N by 42.83% and the secondary (25.18%) is from W. 56.04% of waves have heights of 0-1 m, with 34.18% propagating from the N. Waves with heights of more than 4 m have frequencies of 0.25% and 80.16% are from N.

Chart of Significant Wave Height (SWH) per Mean Wave Direction for South Aegean (ERA-Interim)

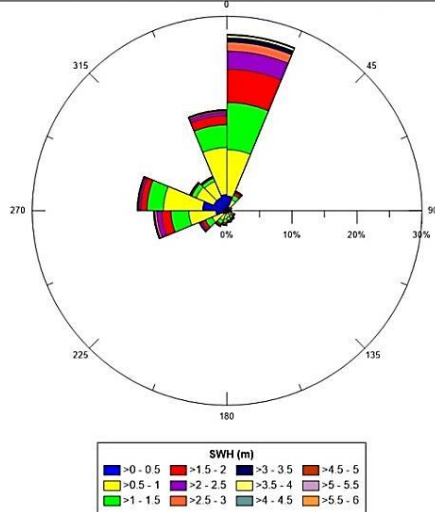
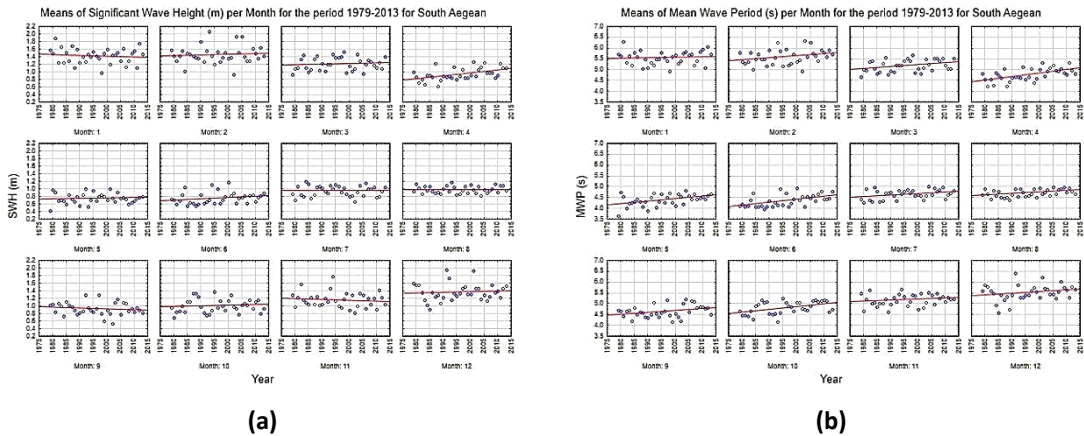


Figure 5.2.41: Wave Chart of South Aegean from ERA-Interim

For South Aegean, the monthly means per year, present that for significant wave height it is virtually certain (99.81%) that during April there had been an increase of 0.0079 m and likely (80.21%) an increase in June by 0.0034 m (Figure 5.2.42a). Mean wave period is very likely to virtually certain (93.31 to 99.96%) to have presented increasing trends from 0.0093 to 0.0159 s for the months February to October (Figure 5.2.42b). It is also likely (82.02%) to have had decreasing trend in December by 0.0082 s. In the annual values, significant wave height is likely (82.68%) to have had an increasing trend of 0.001 m (Figure 5.2.42c) while mean wave period is virtually certain (100%) to have had an increase by 0.0092 s (Figure 5.2.42d). Additionally, the monthly means of anomalies show that it is likely (78.39%) that there had been an increase of 0.00003 m per year of significant wave height (Figure 5.2.42e) while for mean wave period it is virtually certain (100%) that an increase of 0.0003 s per year (Figure 5.2.42f).



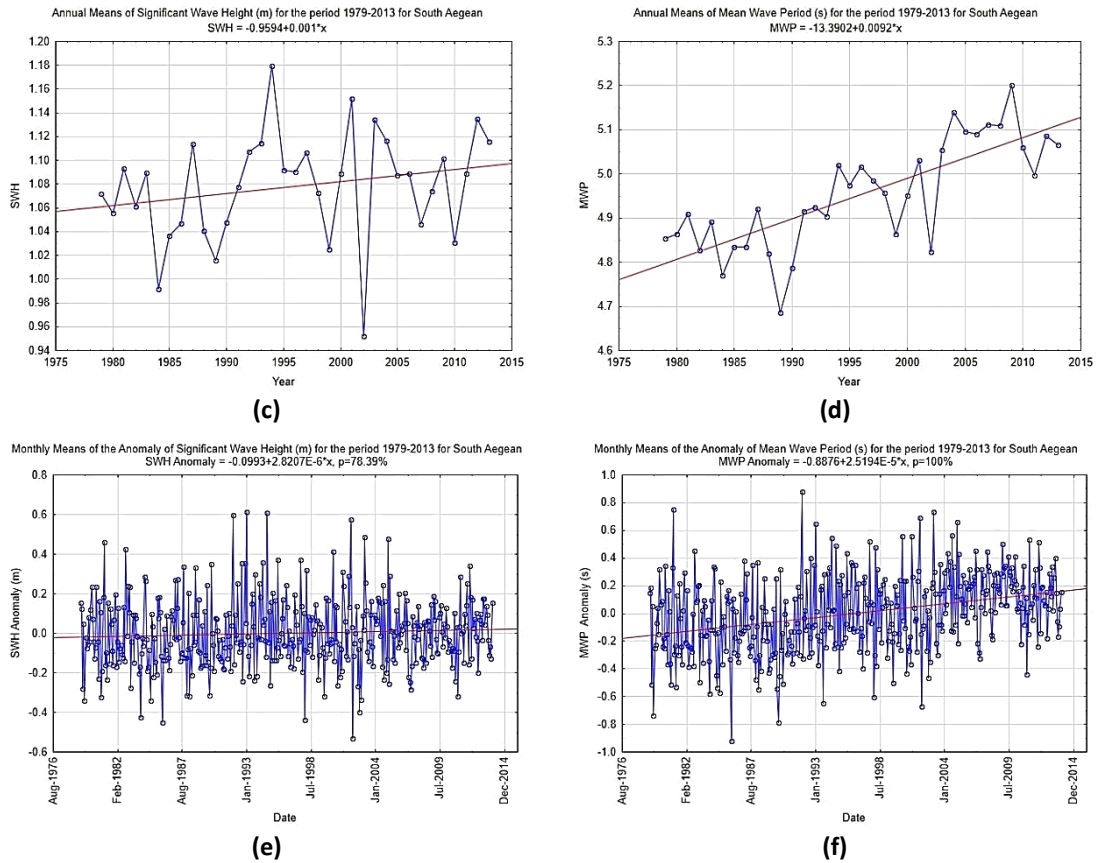


Figure 5.2.42: Monthly and annual means and monthly anomalies for the period 1979-2013 for significant wave height (a, c, e) and wave period (b, d, f) for South Aegean.

Waves with heights of 0 to 1 m have frequencies of 56.04% with 98.38% related with periods of 2-6 s. Periods longer than 8 s have frequency of 0.61% and waves with heights of more than 4 m have of 0.25%.

Table 5.2.34: Frequency (%) table of significant wave height (SWH) and mean wave period (MWP) for South Aegean (ERA-Interim)

| SWH (m) | MWP (s) | | | | | |
|--------------|--------------|--------------|--------------|-------------|----------|---------------|
| | 2-4 | 4-6 | 6-8 | 8-10 | 10-12 | Total |
| 0-0.5 | 11 | 7.22 | 0.05 | 0 | 0 | 18.27 |
| 0.5-1 | 7.52 | 29.40 | 0.85 | 0 | 0 | 37.77 |
| 1-1.5 | 0.02 | 19.85 | 2.23 | 0.04 | 0 | 22.14 |
| 1.5-2 | 0 | 8.30 | 3.38 | 0.04 | 0 | 11.72 |
| 2-2.5 | 0 | 0.81 | 4.81 | 0.06 | 0 | 5.68 |
| 2.5-3 | 0 | 0.01 | 2.44 | 0.08 | 0 | 2.54 |
| 3-3.5 | 0 | 0 | 1.02 | 0.07 | 0 | 1.10 |
| 3.5-4 | 0 | 0 | 0.42 | 0.11 | 0 | 0.53 |
| 4-4.5 | 0 | 0 | 0.04 | 0.14 | 0 | 0.18 |
| 4.5-5 | 0 | 0 | 0 | 0.05 | 0 | 0.05 |
| 5-5.5 | 0 | 0 | 0 | 0.01 | 0 | 0.01 |
| Total | 18.53 | 65.60 | 15.26 | 0.61 | 0 | 100.00 |

5.2.2.3.2 Weather Characteristics

The atmospheric state of South Aegean is described in Table 5.2.35, as provided by ERA-Interim dataset.

Table 5.2.35: Weather Characteristics of South Aegean as given from ERA-Interim

| Coordinates | Parameter | Valid N | Mean | Maximum | Std.Dev. |
|-------------|-----------|---------|------|---------|----------|
| 36N | W10 (m/s) | 51136 | 6.53 | 19.19 | 3.12 |
| 24.5E | T2M (°C) | 51136 | 19.6 | 34.84 | 5.5 |

In South Aegean winds are blowing from is N by 52.47% while 13.09% is blowing from W. Wind speeds ranging with 2 to 8 m/s have frequencies of 64.11% and 54.77% of those are from N. Winds with speeds of more than 14 m/s have frequencies of 1.51% with 71.60% blowing from N.

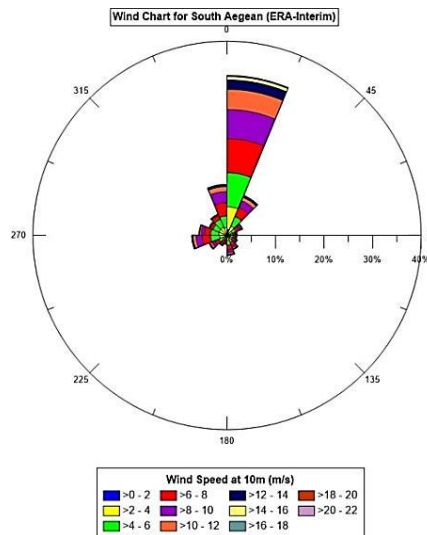
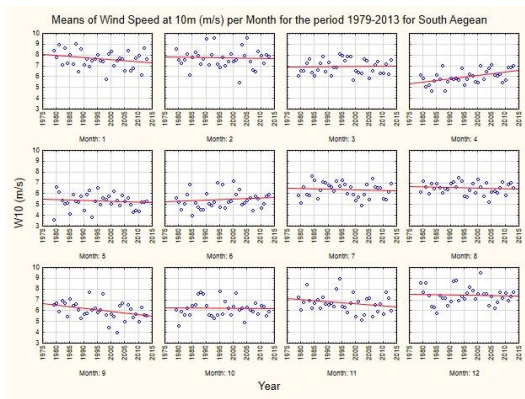
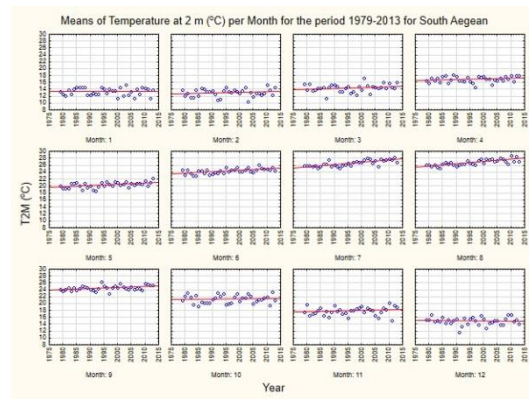


Figure 5.2.43: Wind Chart of South Aegean from ERA-Interim

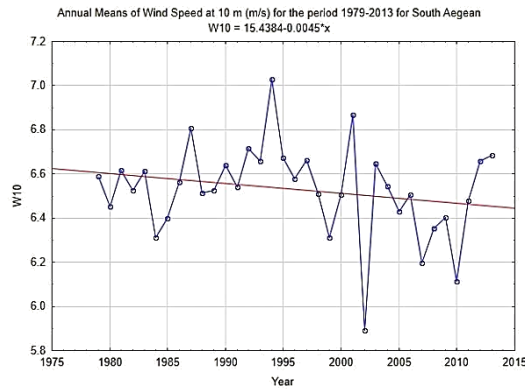
In the case of South Aegean, the monthly means show that wind speed (Figure 5.2.44a) is virtually certain (99.7%) to have had an increase by 0.0309 m/s in April while very likely (97.59%) a decrease by 0.0295 m/s in September and likely (85.16%) a decrease by 0.0204 m/s in November. Temperature monthly means (Figure 5.2.44b) show that it is very likely to virtually certain (97.76% to 100%) to have had an increase in ranges of 0.02 to 0.06 °C during the months May to September. Finally, as for the annual values, wind speed (Figure 5.2.44c) is likely (79.22%) have had a decrease by 0.0045 m/s while the temperature is virtually certain (99.97%) to have had an increase by 0.0265 °C (Figure 5.2.44d). The monthly mean anomaly of wind speed is likely (78.68%) to have presented a decreasing trend of 0.0001 m/s per year (Figure 5.2.44e) while it is virtually certain (100%) that temperature at 2m an increase by 0.0008 °C per year (Figure 5.2.44f).



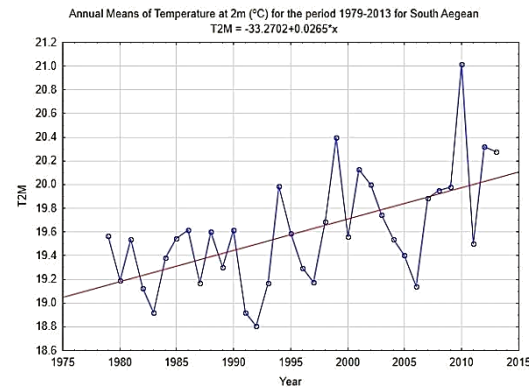
(a)



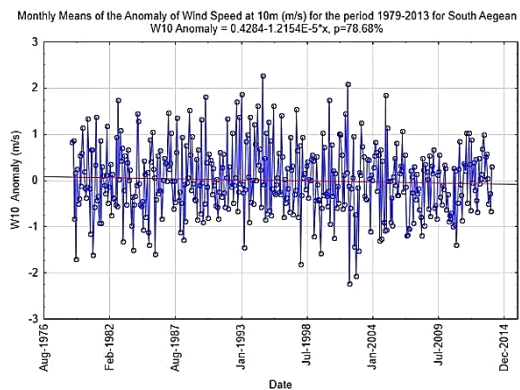
(b)



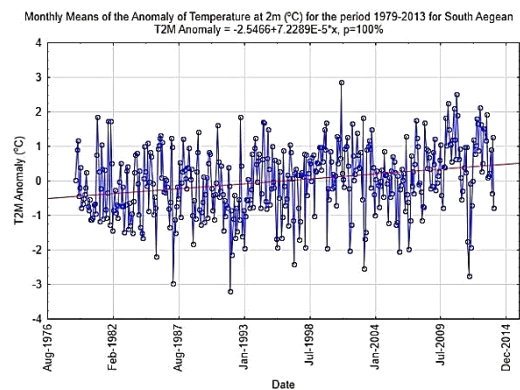
(c)



(d)



(e)



(f)

Figure 5.2.44: Monthly and annual means and monthly anomalies, for the period 1979-2013 for wind speed at 10m (a, c, e) and temperature at 2m (b, d, f) for South Aegean.

5.2.2.3.3 Wave and Weather Characteristics

Waves with heights of 0 to 1 m are related by 89.34% to wind speeds of 2 to 8 m/s while waves with heights of more than 4m, are related by 57.94% with wind speeds that range from 16 to 18 m/s.

Table 5.2.36: Frequency table (%) of significant wave height (SWH) and wind speed at 10m (W10) for South Aegean

| SWH (m) | W10 (m/s) | | | | | | | | | | |
|--------------|-----------|-------|-------|-------|-------|-------|-------|-------|-------|-------|--------|
| | 0-2 | 2-4 | 4-6 | 6-8 | 8-10 | 10-12 | 12-14 | 14-16 | 16-18 | 18-20 | Total |
| 0-0.5 | 3.56 | 9.95 | 4.63 | 0.13 | 0 | 0 | 0 | 0 | 0 | 0 | 18.27 |
| 0.5-1 | 1.44 | 7.44 | 16.53 | 11.38 | 0.97 | 0.01 | 0 | 0 | 0 | 0 | 37.77 |
| 1-1.5 | 0.13 | 0.63 | 2.83 | 8.89 | 8.89 | 0.75 | 0.02 | 0 | 0 | 0 | 22.14 |
| 1.5-2 | 0.01 | 0.06 | 0.20 | 1.24 | 5.42 | 4.53 | 0.25 | 0.01 | 0 | 0 | 11.72 |
| 2-2.5 | 0 | 0.01 | 0.05 | 0.12 | 0.78 | 3.37 | 1.30 | 0.04 | 0.01 | 0 | 5.68 |
| 2.5-3 | 0 | 0 | 0.01 | 0.01 | 0.07 | 0.60 | 1.62 | 0.22 | 0.01 | 0 | 2.54 |
| 3-3.5 | 0 | 0 | 0 | 0 | 0.01 | 0.05 | 0.53 | 0.47 | 0.03 | 0 | 1.10 |
| 3.5-4 | 0 | 0 | 0 | 0 | 0 | 0 | 0.05 | 0.39 | 0.09 | 0 | 0.53 |
| 4-4.5 | 0 | 0 | 0 | 0 | 0 | 0 | 0.01 | 0.06 | 0.10 | 0.01 | 0.18 |
| 4.5-5 | 0 | 0 | 0 | 0 | 0 | 0 | 0 | 0.01 | 0.03 | 0.01 | 0.05 |
| 5-5.5 | 0 | 0 | 0 | 0 | 0 | 0 | 0 | 0 | 0.01 | 0.01 | 0.01 |
| Total | 5.15 | 18.09 | 24.25 | 21.77 | 16.15 | 9.32 | 3.77 | 1.19 | 0.29 | 0.03 | 100.00 |

5.2.2.4 North Ionian

5.2.2.4.1 Wave Characteristics

Wave characteristics of North Ionian are given in Table 5.2.37.

Table 5.2.37: Wave Characteristics of North Ionian as given from ERA-Interim

| Coordinates | Parameter | N | Mean | Maximum | Std.Dev. |
|--------------|-----------|-------|------|---------|----------|
| 39.5N 19E | SWH (m) | 51136 | 0.78 | 5.31 | 0.61 |
| | MWP (s) | 51136 | 4.33 | 10.23 | 1.23 |

In the North Ionian, waves are primarily propagating from NW by 35.47% and secondarily from SW by 27.01%. The most common waves (73.9%) have heights from 0 to 1 m, with 37.66% coming from the N and 26.32% from SW. Waves with heights of more than 4 m have frequencies of 0.12% and 58.33% are from SE.

Chart of Significant Wave Height (SWH) per Mean Wave Direction for North Ionian (ERA-Interim)

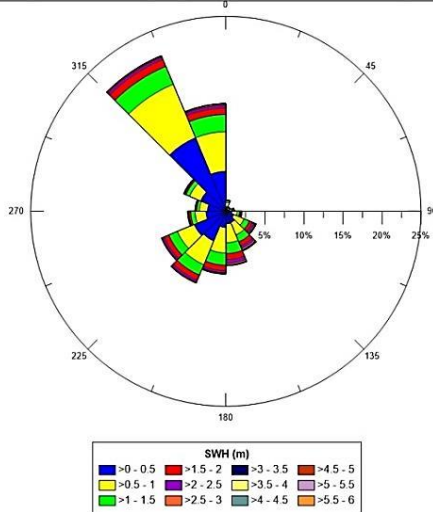
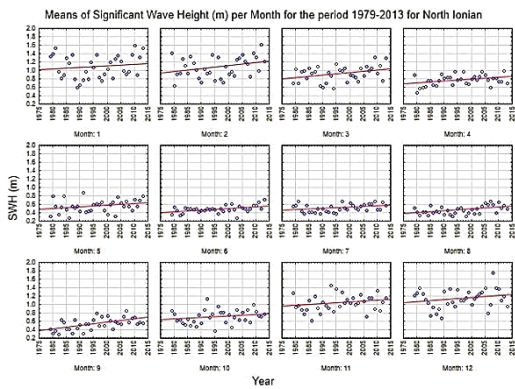
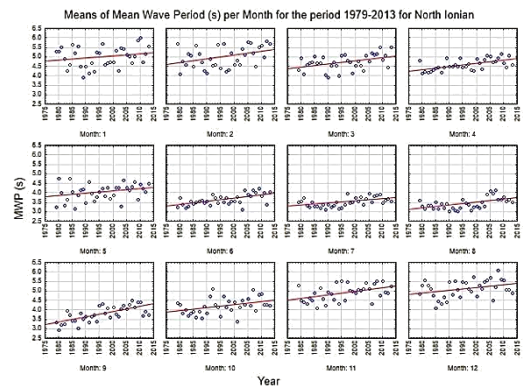


Figure 5.2.45: Wave Chart of North Ionian from ERA-Interim

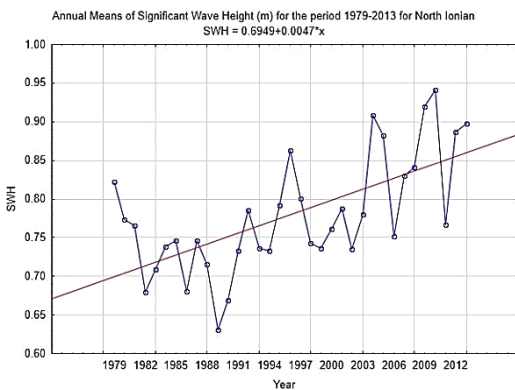
For the monthly means per year, significant wave height is likely to virtually certain (82.99% to 99.94%) to have had an increasing trend, ranging from 0.0031 to 0.0076 m for the months February to October (Figure 5.2.46a). Mean wave period, very likely to virtually certain (95.27% to 100%) to have had an increasing trend from February to December that ranges from 0.0123 to 0.0277 s (Figure 5.2.46b).



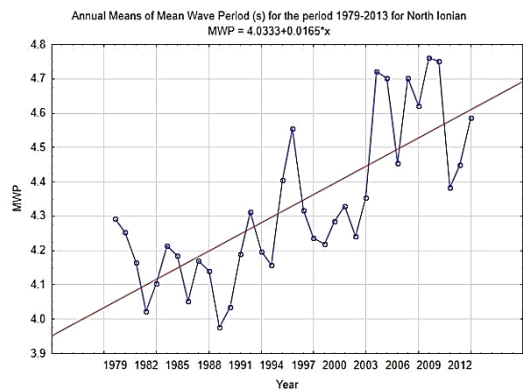
(a)



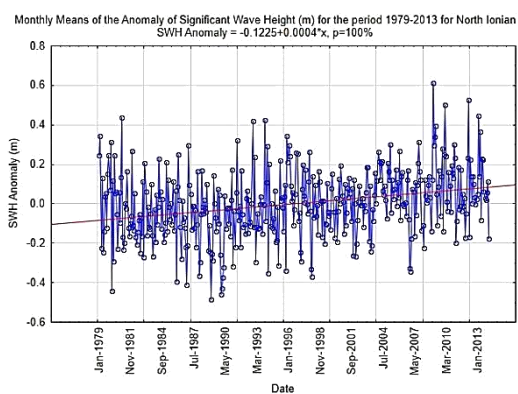
(b)



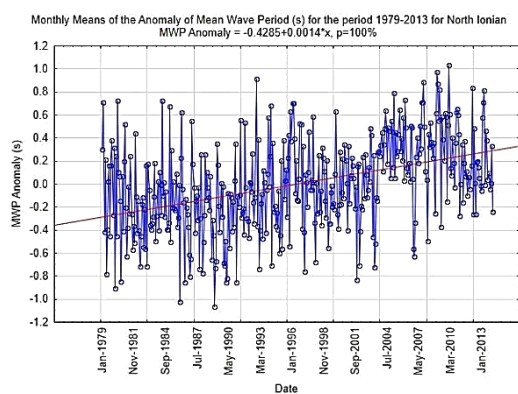
(c)



(d)



(e)



(f)

Figure 5.2.46: Monthly anomalies, monthly and annual means for the period 1979-2013 for significant wave height (a, c, e) and wave period (b, d, f) for North Ionian.

For the annual values, it is virtually certain (99.96%) that significant wave height have had an increase by 0.0047m (Figure 5.2.46c) while virtually certain (100%) that mean wave period an increase by 0.0165 s (Figure 5.2.46d). Finally, the mean monthly anomaly of significant wave height in North Ionian is virtually certain (100%) to have presented an increasing trend of 0.0048 m per year (Figure 5.2.46e). Similarly, mean wave period is virtually certain to have presented an increasing trend of 0.0017 s per year (Figure 5.2.46f).

Waves with heights of 0 to 1 m are rather common (73.9%) with 97.16% related with periods of 2-6 s. Periods longer than 8 s have frequencies of 0.49% and waves with heights of more than 4 m have of 0.12%.

Table 5.2.38: Frequency (%) table of significant wave height (SWH) and mean wave period (MWP) for North Ionian (ERA-Interim)

| SWH (m) | MWP (s) | | | | | | Total |
|--------------|---------|-------|-------|-------|------|-------|--------|
| | 0-2 | 2-4 | 4-6 | 6-8 | 8-10 | 10-12 | |
| 0-0.5 | 0.30 | 33.17 | 7.72 | 0.07 | 0 | 0 | 41.26 |
| 0.5-1 | 0 | 12.23 | 18.68 | 1.73 | 0.01 | 0 | 32.65 |
| 1-1.5 | 0 | 0.09 | 11.58 | 2.54 | 0.04 | 0 | 14.25 |
| 1.5-2 | 0 | 0 | 4.14 | 2.43 | 0.09 | 0 | 6.66 |
| 2-2.5 | 0 | 0 | 0.63 | 2.29 | 0.08 | 0 | 3.01 |
| 2.5-3 | 0 | 0 | 0.01 | 1.23 | 0.06 | 0 | 1.31 |
| 3-3.5 | 0 | 0 | 0 | 0.49 | 0.06 | 0 | 0.56 |
| 3.5-4 | 0 | 0 | 0 | 0.13 | 0.06 | 0 | 0.19 |
| 4-4.5 | 0 | 0 | 0 | 0.03 | 0.05 | 0 | 0.08 |
| 4.5-5 | 0 | 0 | 0 | 0 | 0.02 | 0 | 0.03 |
| 5-5.5 | 0 | 0 | 0 | 0 | 0 | 0 | 0.01 |
| Total | 0.30 | 45.50 | 42.76 | 10.96 | 0.49 | 0 | 100.00 |

5.2.2.4.2 Weather Characteristics

The atmospheric state of North Ionian is described in Table 5.2.39, as provided by ERA-Interim dataset.

Table 5.2.39: Weather Characteristics of North Ionian as given from ERA-Interim

| Coordinates | Parameter | Valid N | Mean | Maximum | Std.Dev. |
|--------------|-----------|---------|-------|---------|----------|
| 39.5N 19E | W10 (m/s) | 51136 | 5.34 | 19.2 | 3.00 |
| | T2M (°C) | 51136 | 18.98 | 34.71 | 5.79 |

Winds in North Ionian are blowing primarily (34.98%) from NW to N and secondarily (23.17%) from SE to S. Wind speeds range between 2 to 8 m/s have frequencies of 70.31% with 37.79% blowing from NW to N. Winds with speeds of more than 14 m/s have frequencies of 0.97% with 53.83% blowing from SE to S.

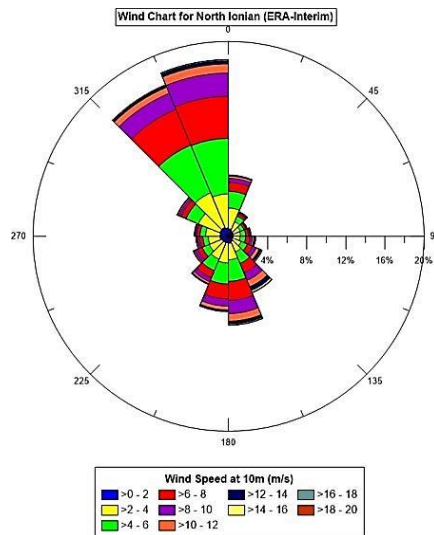
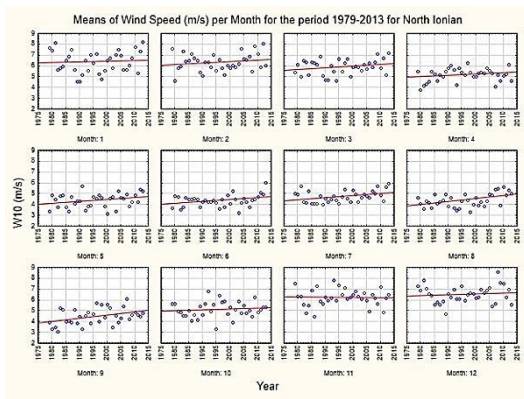
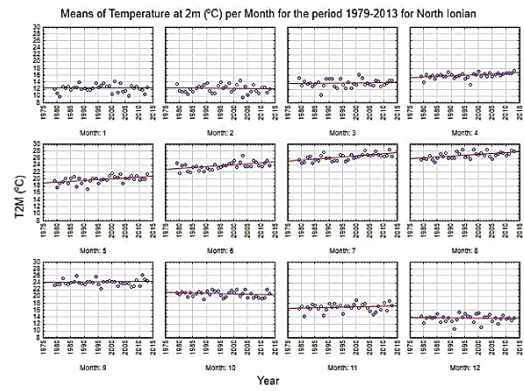


Figure 5.2.47: Wind Chart of North Ionian from ERA-Interim

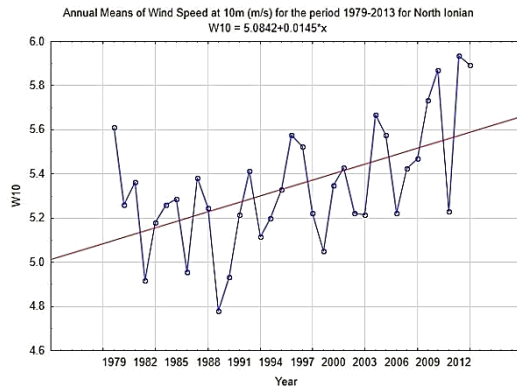
The monthly means per year show that wind speed (Figure 5.2.48a) is likely to virtually certain (87.12% to 99.45%) to have had an increasing trend, ranging from 0.008 to 0.0295 m/s during the months May to September. Temperature is virtually certain (99.33% to 99.94%) to have had an increase by 0.0369 to 0.059 °C for the months April to August (Figure 5.2.48b). For the annual values, wind speed (Figure 5.2.48c) is virtually certain (99.92%) to have shown an increase of 0.0145 m/s and temperature (99.81%) an increase of 0.022 °C (Figure 5.2.48d). Wind speed monthly mean anomaly is virtually certain (99.82%) to have had an increasing trend of 0.0144 m/s per year (Figure 5.2.48e) and virtually certain (99.9%) for the temperature an increase by 0.0216 °C per year (Figure 5.2.48f).



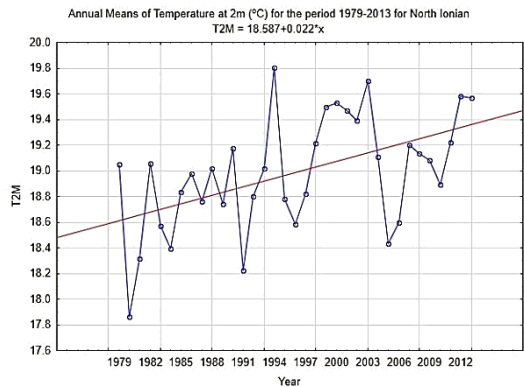
(a)



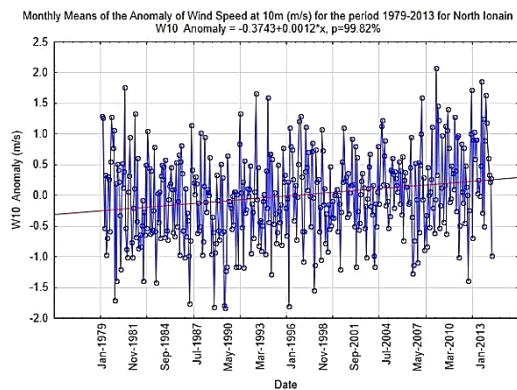
(b)



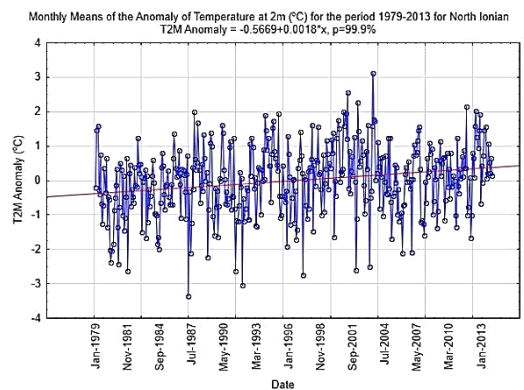
(c)



(d)



(e)



(f)

Figure 5.2.48: Monthly and annual means and monthly anomalies for the period 1979–2013 for wind speed at 10m (a, c, e) and temperature at 2m (b, d, f) for North Ionian.

5.2.2.4.3 Wave and Weather Characteristics

Waves with heights of 0 to 1 m are related by 81.94% to wind speeds ranging between 2 to 8 m/s. Waves with heights more than 4m, are related by 68.33% with wind speeds that range from 16 to 20 m/s.

Table 5.2.40: Frequency table (%) of significant wave height (SWH) and wind speed at 10m (W10) for North Ionian

| SWH (m) | W10 (m/s) | | | | | | | | | | |
|--------------|-----------|-------|-------|-------|-------|-------|-------|-------|-------|-------|--------|
| | 0-2 | 2-4 | 4-6 | 6-8 | 8-10 | 10-12 | 12-14 | 14-16 | 16-18 | 18-20 | Total |
| 0-0.5 | 9.49 | 19.74 | 10.95 | 1.07 | 0.01 | 0 | 0 | 0 | 0 | 0 | 41.26 |
| 0.5-1 | 1.70 | 5.72 | 12.07 | 11.01 | 2.07 | 0.08 | 0 | 0 | 0 | 0 | 32.65 |
| 1-1.5 | 0.27 | 0.91 | 2.24 | 4.49 | 5.03 | 1.23 | 0.10 | 0 | 0 | 0 | 14.25 |
| 1.5-2 | 0.04 | 0.18 | 0.45 | 1.12 | 2.24 | 2.17 | 0.41 | 0.04 | 0 | 0 | 6.66 |
| 2-2.5 | 0 | 0.01 | 0.06 | 0.25 | 0.62 | 1.16 | 0.77 | 0.13 | 0.01 | 0 | 3.01 |
| 2.5-3 | 0 | 0 | 0.01 | 0.02 | 0.13 | 0.31 | 0.57 | 0.24 | 0.03 | 0 | 1.31 |
| 3-3.5 | 0 | 0 | 0 | 0.01 | 0.01 | 0.07 | 0.20 | 0.22 | 0.05 | 0 | 0.56 |
| 3.5-4 | 0 | 0 | 0 | 0 | 0 | 0.01 | 0.03 | 0.10 | 0.05 | 0.01 | 0.19 |
| 4-4.5 | 0 | 0 | 0 | 0 | 0 | 0 | 0.01 | 0.03 | 0.04 | 0.02 | 0.08 |
| 4.5-5 | 0 | 0 | 0 | 0 | 0 | 0 | 0 | 0 | 0.02 | 0.01 | 0.03 |
| 5-5.5 | 0 | 0 | 0 | 0 | 0 | 0 | 0 | 0 | 0 | 0 | 0.01 |
| Total | 11.50 | 26.56 | 25.77 | 17.98 | 10.11 | 5.02 | 2.09 | 0.75 | 0.18 | 0.03 | 100.00 |

5.2.2.5 South Ionian

5.2.2.5.1 Wave Characteristics

For the area of South Ionian, characteristics of the wave state are given in Table 5.2.41.

Table 5.2.41: Wave Characteristics of South Ionian as given from ERA-Interim

| Coordinates | Parameter | N | Mean | Maximum | Std.Dev. |
|-------------|-----------|-------|------|---------|----------|
| 36.75N | SWH (m) | 51136 | 0.89 | 5.96 | 0.63 |
| 20.75E | MWP (s) | 51136 | 4.72 | 11.04 | 1.23 |

In the area of South Ionian, the most common waves (62.19%) are propagating from W to NW. Waves with heights from 0 to 1 m have frequency of 68.9%, with 66.05% coming from the W to NW. Waves with heights of more than 4 m have frequencies of 0.18% with 78.89% from W.

Chart of Significant Wave Height (SWH) per Mean Wave Direction for South Ionian (ERA-Interim)

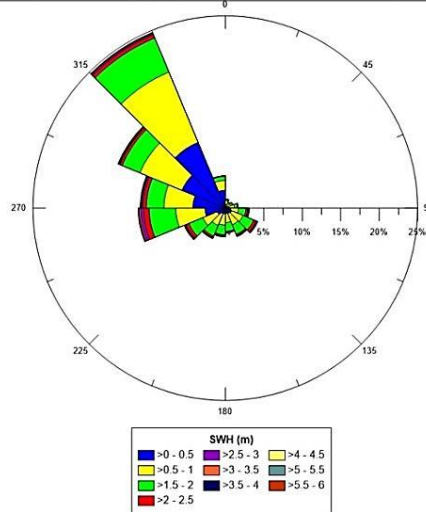
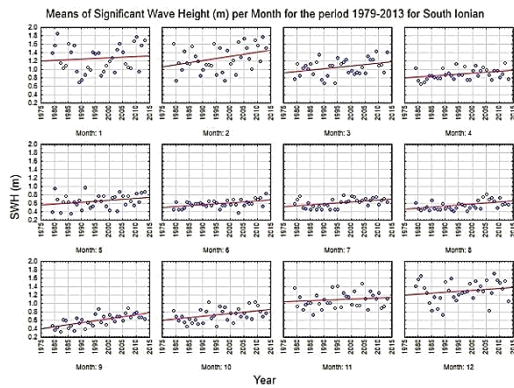
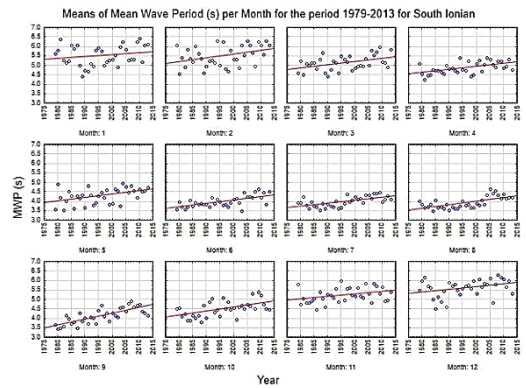


Figure 5.2.49: Wave Chart of South Ionian from ERA-Interim

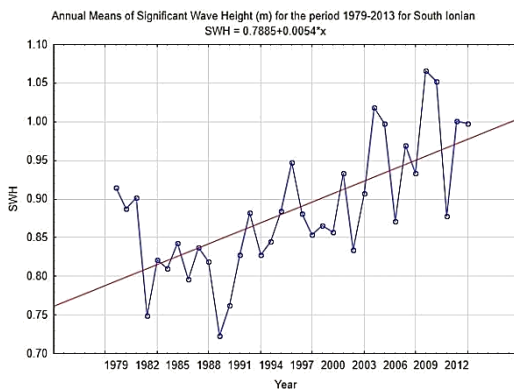
In the case of South Ionian, the mean monthly values for the period 1979-2013 show that it is likely to virtually certain (88.11% to 99.99%) to have had increasing trends in significant wave height (Figure 5.2.50a) for the months February to October ranging from 0.0042 to 0.01 m. It is also very likely to virtually certain (94.94% to 100%) to have had an increase in mean wave period in the range of 0.0128 s to 0.0304 s during the months February to December (Figure 5.2.50b).



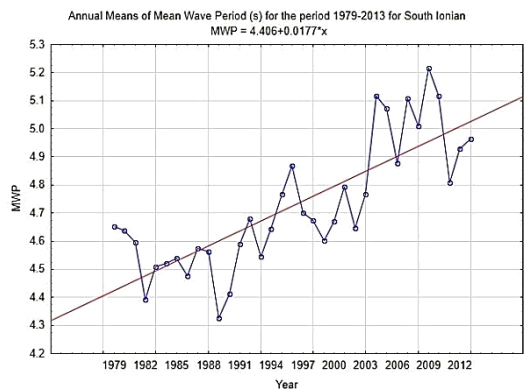
(a)



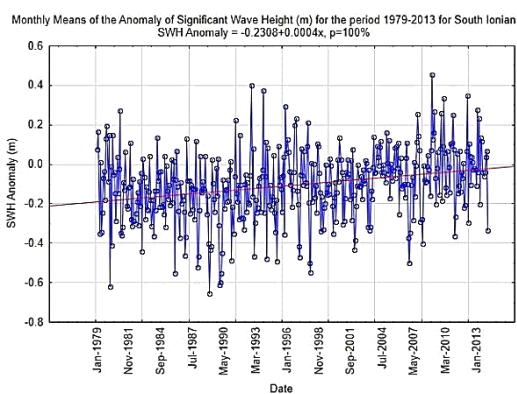
(b)



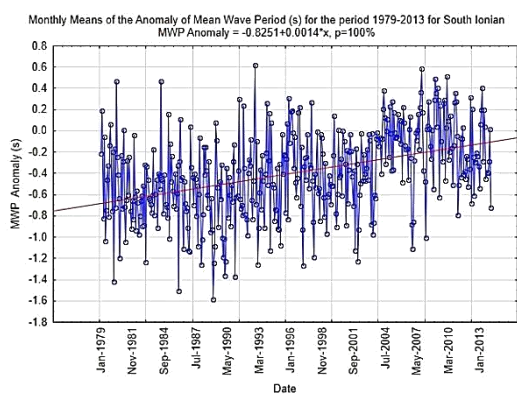
(c)



(d)



(e)



(f)

Figure 5.2.50: Monthly and annual means and mean anomalies for the period 1979-2013 for significant wave height (a, b,e) and wave period (c, d,f) for South Ionian.

In the case of the annual values, it is virtually certain to have had an increase of 0.0054 m for wave height (Figure 5.2.50c) and 0.0177 s (Figure 5.2.50d) for wave period (99.99% and 100% respectively). Finally, the mean monthly anomaly is virtually certain (100%) to have presented an increasing trend for significant wave height of 0.0048 m per year (Figure 5.2.50e) and of 0.0168 s per year for mean wave period (Figure 5.2.50f).

Waves that have heights of 0 to 1 m are rather common (68.99%) with 98.26% related with periods of 2-6 s. Periods longer than 8 s have frequencies of 1.16% and waves with heights of more than 4 m have of 0.18%.

Table 5.2.42: Frequency (%) table of significant wave height (SWH) and mean wave period (MWP) for South Ionian

| SWH (m) | MWP (s) | | | | | Total |
|--------------|---------|-------|-------|------|-------|--------|
| | 2-4 | 4-6 | 6-8 | 8-10 | 10-12 | |
| 0-0.5 | 23.65 | 8.35 | 0.01 | 0 | 0 | 32.01 |
| 0.5-1 | 9.23 | 26.55 | 1.19 | 0 | 0 | 36.97 |
| 1-1.5 | 0.02 | 12.61 | 3.92 | 0.01 | 0 | 16.55 |
| 1.5-2 | 0 | 3.23 | 4.45 | 0.06 | 0 | 7.74 |
| 2-2.5 | 0 | 0.27 | 3.38 | 0.18 | 0 | 3.83 |
| 2.5-3 | 0 | 0 | 1.43 | 0.25 | 0 | 1.68 |
| 3-3.5 | 0 | 0 | 0.44 | 0.27 | 0 | 0.72 |
| 3.5-4 | 0 | 0 | 0.10 | 0.21 | 0 | 0.31 |
| 4-4.5 | 0 | 0 | 0 | 0.11 | 0 | 0.12 |
| 4.5-5 | 0 | 0 | 0 | 0.03 | 0 | 0.04 |
| 5-5.5 | 0 | 0 | 0 | 0.01 | 0 | 0.02 |
| 5.5-6 | 0 | 0 | 0 | 0 | 0 | 0.01 |
| Total | 32.90 | 51.01 | 14.93 | 1.15 | 0.01 | 100.00 |

5.2.2.5.2 Weather Characteristics

The atmospheric state of South Ionian is described in Table 5.2.43, as provided by ERA-Interim dataset.

Table 5.2.43: Weather Characteristics of South Ionian as given from ERA-Interim

| Coordinates | Parameter | Valid N | Mean | Maximum | Std.Dev. |
|-------------|-----------|---------|-------|---------|----------|
| 36.75N | W10 (m/s) | 51136 | 5.68 | 20.84 | 2.97 |
| 20.75E | T2M (°C) | 51136 | 19.96 | 35.08 | 5.22 |

In the South Ionian winds have as main directionality (37.97%) from NW. A 70.97% of the winds have speeds between 2 to 8 m/s with 58.97% blowing from W to N. Winds with speeds of more than 14 m/s have frequencies of 1.03% with 38.97% blowing from W to NW and 33.46% from SE.

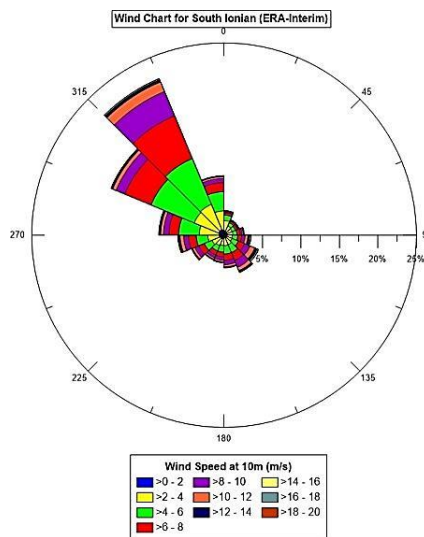
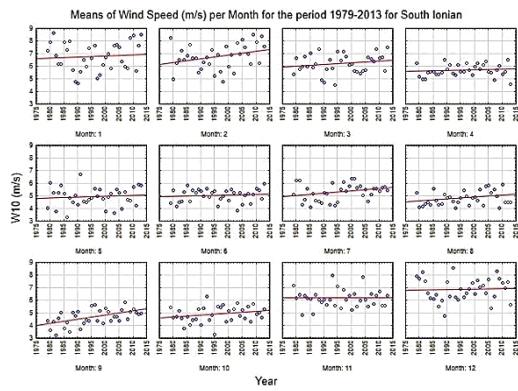
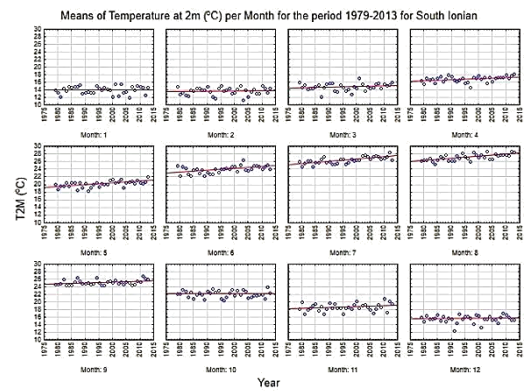


Figure 5.2.51: Wind Chart of South Ionian from ERA-Interim

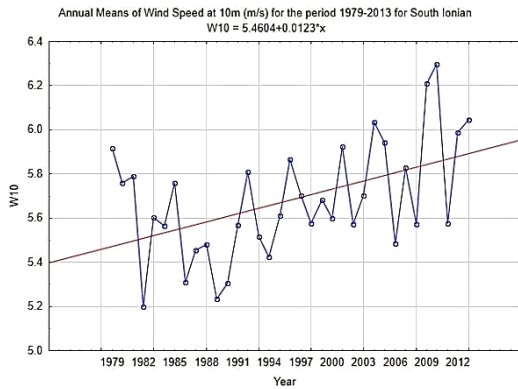
In the case of the monthly values wind speed is likely to virtually certain (81.68% to 99.9%) to have had an increase with a range of 0.0142 to 0.0326 m/s during the months July to October (Figure 5.2.52a). Temperature is very likely to virtually certain (93.51% to 100%) to have had an increase by 0.0197 to 0.0589 °C during the months April to September (Figure 5.2.52b). The annual values, it is virtually certain (99.68% and 99.94%) to have had increasing trends for wind speed and temperature by 0.0123 m/s and 0.0247 °C respectively (Figure 5.2.52 c, d). The monthly mean anomalies show that it is virtually certain (99.9%) for wind speed and temperature to have had increasing trends of 0.0144 m/s and 0.0216 °C per year (Figure 5.2.52e,f).



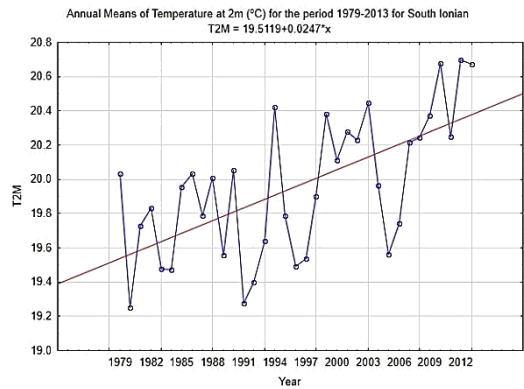
(a)



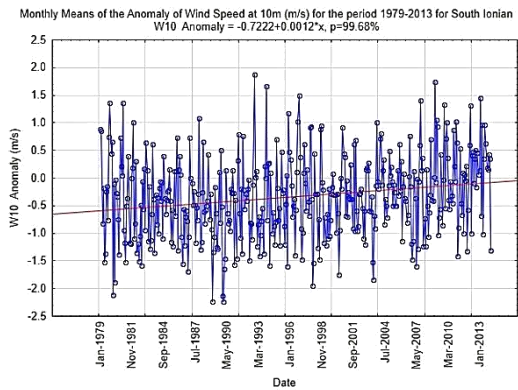
(b)



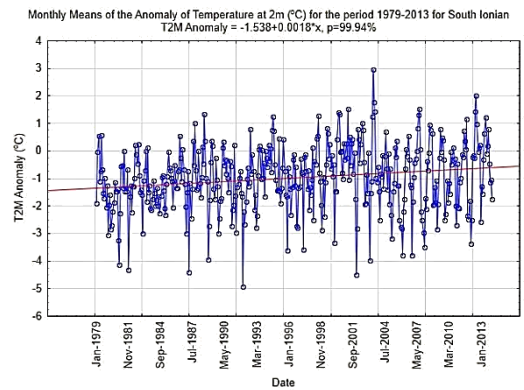
(c)



(d)



(e)



(f)

Figure 5.252: Monthly anomalies, monthly and annual means for the period 1979-2013 for wind speed at 10m (a, c, e) and temperature at 2m (b, d, f) for South Ionian.

5.2.2.5.3 Wave and Weather Characteristics

Waves with heights of 0 to 1 m can be related by 85.22% to wind speeds from 2 to 8 m/s. Wind speeds that range from 14 to 16 m/s can be related to wave heights of more than 4 m.

Table 5.2.44: Frequency table (%) of significant wave height (SWH) and wind speed at 10m (W10) for South Ionian

| SWH (m) | W10 (m/s) | | | | | | | | | | | |
|--------------|-----------|-------|-------|-------|-------|-------|-------|-------|-------|-------|-------|--------|
| | 0-2 | 2-4 | 4-6 | 6-8 | 8-10 | 10-12 | 12-14 | 14-16 | 16-18 | 18-20 | 20-22 | Total |
| 0-0.5 | 5.94 | 14.58 | 10.77 | 0.72 | 0 | 0 | 0 | 0 | 0 | 0 | 0 | 32.01 |
| 0.5-1 | 2.27 | 7.37 | 13.52 | 11.82 | 1.95 | 0.03 | 0 | 0 | 0 | 0 | 0 | 36.97 |
| 1-1.5 | 0.27 | 1.14 | 2.92 | 5.35 | 5.58 | 1.24 | 0.05 | 0 | 0 | 0 | 0 | 16.55 |
| 1.5-2 | 0.05 | 0.19 | 0.53 | 1.49 | 2.71 | 2.35 | 0.40 | 0.02 | 0 | 0 | 0 | 7.74 |
| 2-2.5 | 0.01 | 0.04 | 0.09 | 0.33 | 0.88 | 1.50 | 0.88 | 0.10 | 0.01 | 0 | 0 | 3.83 |
| 2.5-3 | 0 | 0.01 | 0.01 | 0.06 | 0.22 | 0.50 | 0.59 | 0.25 | 0.04 | 0 | 0 | 1.68 |
| 3-3.5 | 0 | 0 | 0 | 0.01 | 0.03 | 0.13 | 0.28 | 0.23 | 0.03 | 0.01 | 0 | 0.72 |
| 3.5-4 | 0 | 0 | 0 | 0 | 0 | 0.03 | 0.09 | 0.12 | 0.07 | 0.01 | 0 | 0.31 |
| 4-4.5 | 0 | 0 | 0 | 0 | 0 | 0 | 0.01 | 0.05 | 0.04 | 0.01 | 0 | 0.12 |
| 4.5-5 | 0 | 0 | 0 | 0 | 0 | 0 | 0 | 0.01 | 0.01 | 0 | 0 | 0.04 |
| 5-5.5 | 0 | 0 | 0 | 0 | 0 | 0 | 0 | 0 | 0.01 | 0 | 0 | 0.02 |
| 5.5-6 | 0 | 0 | 0 | 0 | 0 | 0 | 0 | 0 | 0 | 0 | 0 | 0.01 |
| Total | 8.54 | 23.34 | 27.85 | 19.78 | 11.37 | 5.78 | 2.31 | 0.78 | 0.21 | 0.03 | 0.01 | 100.00 |

5.3 Case Study: Pinios

5.3.1 Wave and Weather Climate in Offshore Conditions

5.3.1.1 Wave Characteristics

The descriptive statistics show that the area of Pinios has a mean significant wave height of 0.41 m and period of 3.84 s. Furthermore, the maxima can be up to 3.34 m and 8.53 s, respectively.

Table 5.3.1: Wave Characteristics of Pinios as given from ERA-Interim for the period 1979-2013

| Coordinates | Parameter | Valid N | Mean | Maximum | Std.Dev. |
|------------------|-----------|---------|------|---------|----------|
| 23°E 39.875°N | SWH (m) | 51136 | 0.41 | 3.34 | 0.34 |
| | MWP (s) | 51136 | 3.84 | 8.53 | 1.11 |

The most frequent wave directions (propagating from) are from NE to E (59.68%), while secondary directions are from SE to S (22.23%). Additionally, 34.22% of waves with heights of 0 to 0.5 m are from NE while heights of more than 3 m have frequencies of 0.01% with directions from NE to E.

Chart of Significant Wave Height (SWH) per Mean Wave Direction for Pinios (ERA-Interim)

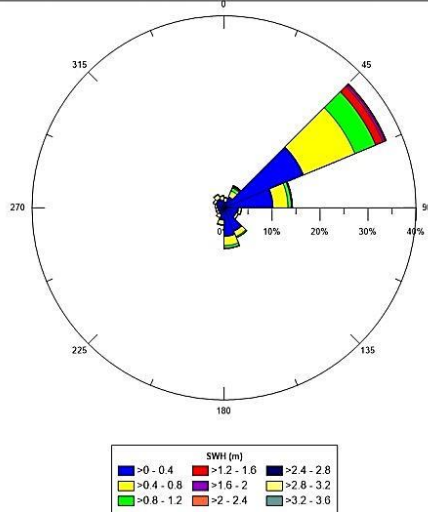
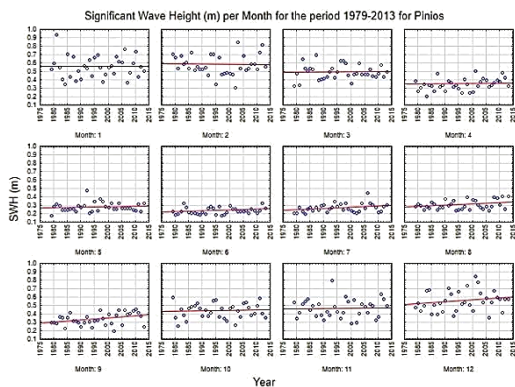
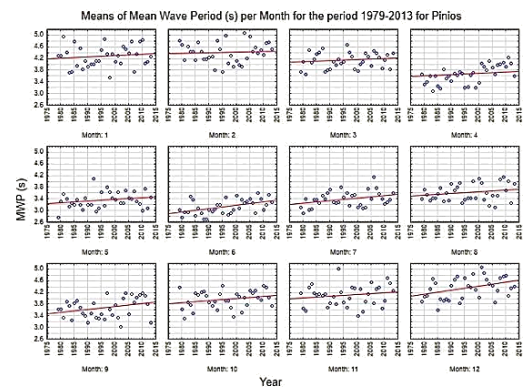


Figure 5.3.1: Wave Chart of Pinios from ERA-Interim

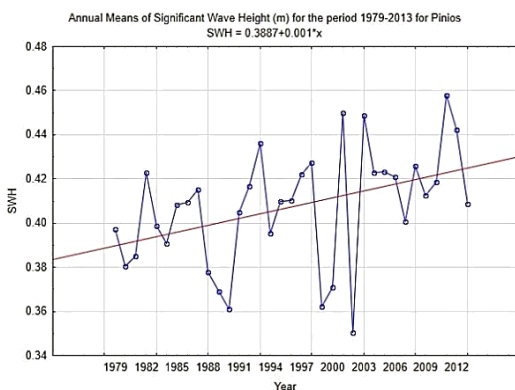
The means per month for the period 1979-2013, present that it is likely (81.62%) to very likely (95.97%) to have had an increase ranging from 0.0009 to 0.0024 m during the months June to September. Mean wave period is virtually certain (99.66%) and very likely (94.98%) to have had an increase by 0.0118 s and 0.0086 s during June and July respectively.



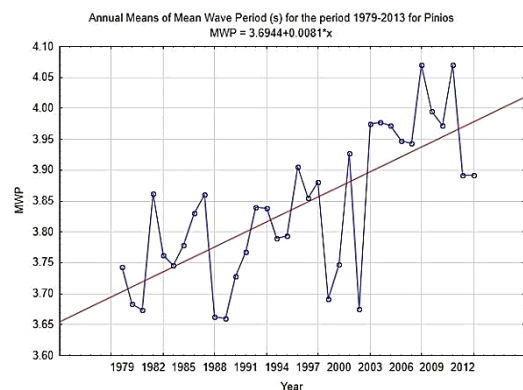
(a)



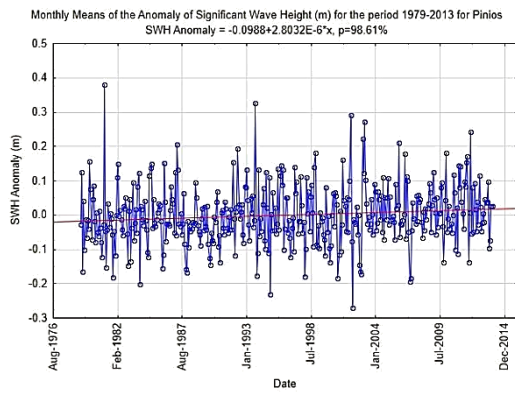
(b)



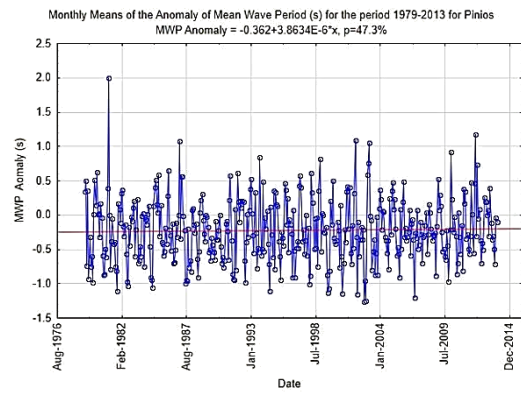
(c)



(d)



(e)



(f)

Figure 5.3.2: Monthly and annual means and monthly anomalies for the period 1979-2013 for significant wave height (a, c, e) and wave period (b, d, f) for Pinios.

The annual means show that it is very likely (98.37%) to have had an increase of 0.001 m in significant wave height and virtually certain (100%) to have had an increase of about 0.0081 s in mean wave period. In the case of the monthly mean anomalies of significant wave height it is shown that it is very likely (98.61%) to have had an increase, while it is about as likely as not to have an increase in mean wave period (47.3%).

The area of Pinios is characterized by wave with heights of 0 to 0.5 m by 72.76% and with periods that range up to 4 s with 58.05% frequency. Furthermore, waves with heights of more than 2.5 m have frequency of 0.11% and periods of more than 6 s have frequencies of 3.51%.

Table 5.3.2: Frequency (%) table of significant wave height (SWH) and mean wave period (MWP) for Pinios

| SWH (m) | MWP (s) | | | | | Total |
|--------------|---------|--------|--------|-------|-------|--------|
| | 0-2 | 2-4 | 4-6 | 6-8 | 8-10 | |
| 0-0.5 | 2.27% | 52.72% | 17.72% | 0.04% | 0% | 72.76% |
| 0.5-1 | 0% | 3.03% | 17.18% | 0.54% | 0% | 20.76% |
| 1-1.5 | 0% | 0.02% | 3.32% | 1.61% | 0% | 4.95% |
| 1.5-2 | 0% | 0% | 0.21% | 0.89% | 0% | 1.09% |
| 2-2.5 | 0% | 0% | 0.01% | 0.31% | 0% | 0.33% |
| 2.5-3 | 0% | 0% | 0% | 0.10% | 0% | 0.10% |
| 3-3.5 | 0% | 0% | 0% | 0% | 0% | 0.01% |
| Total | 2.27% | 55.77% | 38.44% | 3.50% | 0.01% | 100% |

5.3.1.2 Weather Characteristics

The atmospheric state of Pinios River area as described by ERA-Interim is given in Table 5.3.3. Mean wind speed is of 3.61 m/s, max can reach 17.59 m/s whilst temperature has a mean of 17.01 °C and maximum can be of 40.48 °C.

Table 5.3.3: Weather Characteristics of Pinios as given from ERA-Interim for the period 1979-2013

| Coordinates | Parameter | Valid N | Mean | Maximum | Std.Dev. |
|-------------|-----------|---------|-------|---------|----------|
| 39.5°N | W10 (m/s) | 51136 | 3.61 | 17.59 | 1.97 |
| 24.5°E | T2M (°C) | 51136 | 17.01 | 40.48 | 7.6 |

For wind, the primary direction is of NE to E (47.89%) with a secondary direction from SE to S (26.82%). The most frequent wind speeds are those from 0 to 6 m/s (88.47%) with 47.47% blowing from NE to E. Wind speeds higher than 12 m/s have a frequency of 0.16% and 43.9% of those is blowing from the NE.

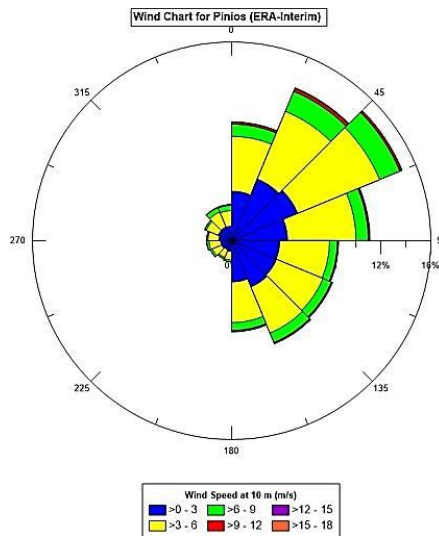
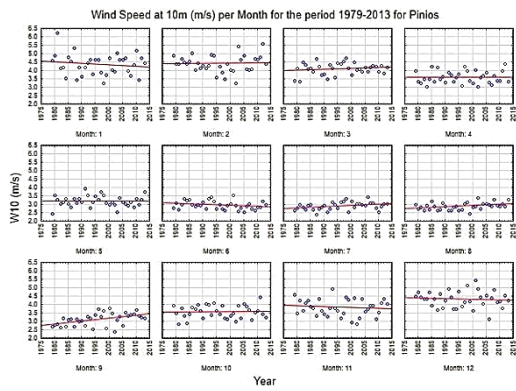
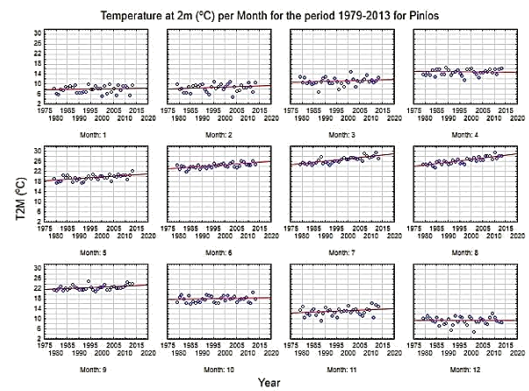


Figure 5.3.3: Wind Chart for Pinios from ERA-Interim

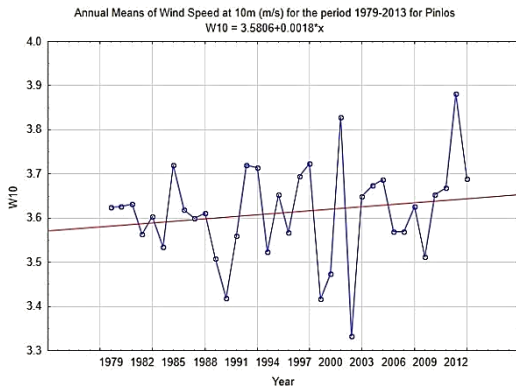
For the monthly means, wind speed is very likely (95.81%) to virtually certain (99.61%) to have had an increase in the ranges of 0.0079 m/s to 0.0172 m/s during the months July to September. In the case of temperature, it is virtually certain to have had an increase in the ranges of 0.04 °C to 0.11 °C during the months May to September. As for the annual values, it is likely (66%) for wind speed to have had an increase about 0.0018 m/s and virtually certain for temperature an increase by 0.0431 °C. Monthly mean anomalies for the period 1979-2013, show that there is virtually certain to have had an increase of 0.00004 m/s for wind speed and 0.0012 °C for temperature.



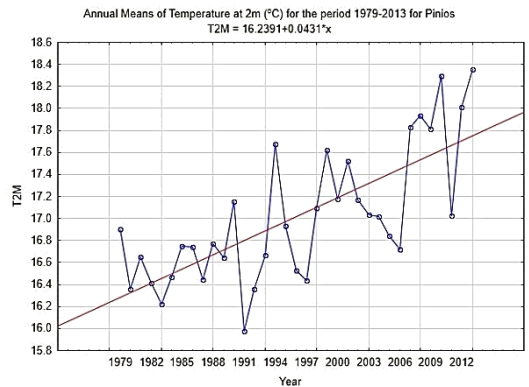
(a)



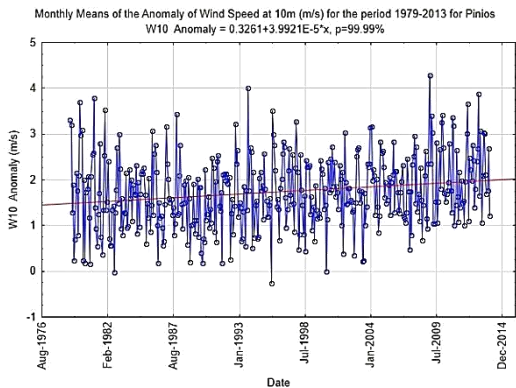
(b)



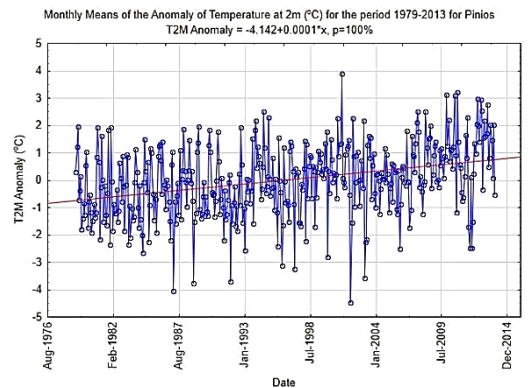
(c)



(d)



(e)



(f)

Figure 5.3.4: Monthly and annual means and monthly anomalies, for the period 1979-2013 for wind speed at 10m (a, c, e) and temperature at 2m (b, d, f) for Pinios.

5.3.1.3 Wave and Weather Characteristics

The most frequent waves (72.76%) are that with heights of 0 to 0.5 m with 40.13% related to wind speeds of 0 to 3 m/s. In addition, 65.45% waves with heights of more than 2.5 m are related to wind speeds of more than 12 m/s.

Table 5.3.4: Frequency table (%) of significant wave height (SWH) and wind speed at 10m (W10) for Pinios

| SWH (m) | W10 (m/s) | | | | | | Total |
|--------------|---------------|---------------|--------------|--------------|--------------|-----------|-------------|
| | 0-3 | 3-6 | 6-9 | 9-12 | 12-15 | 15-18 | |
| 0-0.5 | 40.13% | 31.54% | 1.09% | 0% | 0% | 0% | 72.76% |
| 0.5-1 | 2.61% | 12.97% | 4.99% | 0.19% | 0.01% | 0% | 20.76% |
| 1-1.5 | 0.02% | 1.19% | 3.28% | 0.46% | 0.01% | 0% | 4.95% |
| 1.5-2 | 0% | 0.01% | 0.60% | 0.45% | 0.02% | 0% | 1.09% |
| 2-2.5 | 0% | 0% | 0.03% | 0.24% | 0.05% | 0% | 0.33% |
| 2.5-3 | 0% | 0% | 0% | 0.04% | 0.06% | 0% | 0.10% |
| 3-3.5 | 0% | 0% | 0% | 0% | 0.01% | 0% | 0.01% |
| Total | 42.76% | 45.71% | 9.99% | 1.38% | 0.16% | 0% | 100% |

5.3.2 Wave propagation to the Nearshore Zone (MIKE 21 PMS)

In order to have the necessary file of bathymetry, all the information of the nearshore zone were gathered and added to the .batsf file after converted to the coordinates of the Greek Grid. More analytically, the geographical survey of the coastline, bathymetrical data of profiles perpendicular to the shoreline and the bathymetry as collected by Akti-Engineering were assimilated and afterwards interpolated into the bathymetry file (Figure 5.3.5a). This file was afterwards rotated clockwise to 180 degrees in order for the model start to be at the south-west boundary (Figure 5.3.5b).

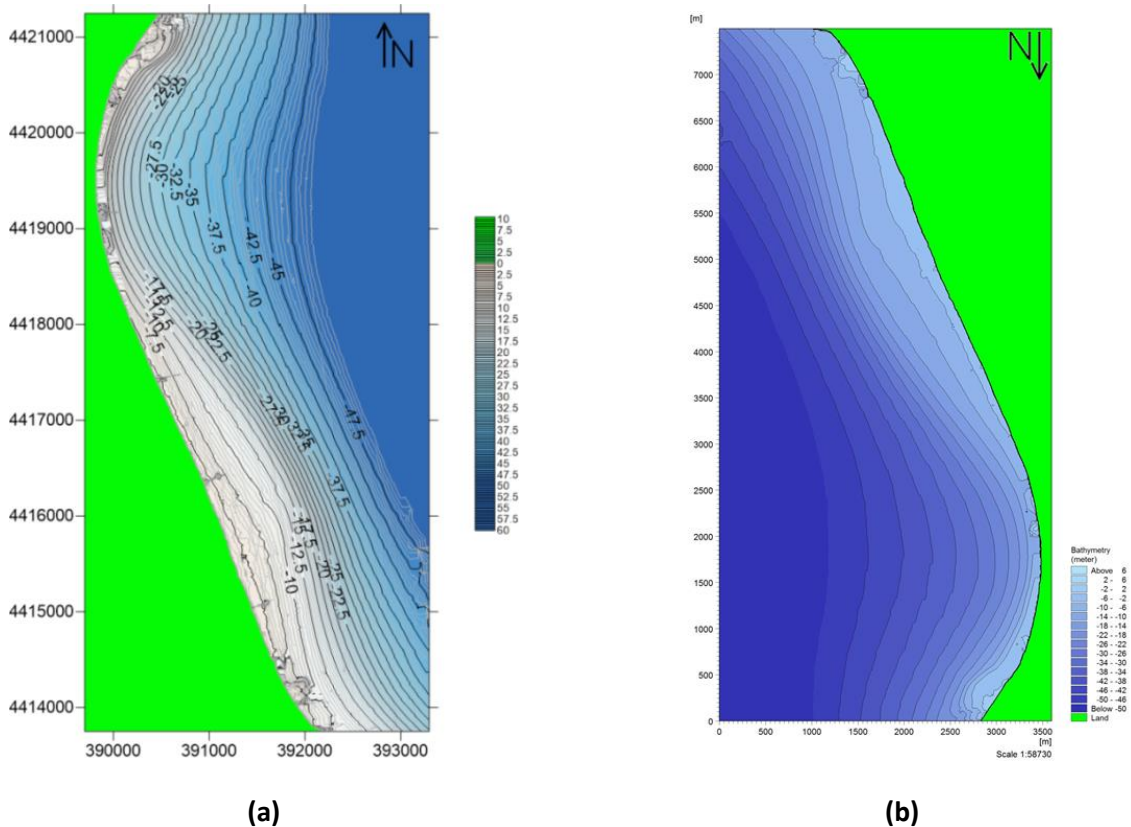


Figure 5.3.5: a) Bathymetry Data of the area, b) the rotated bathymetry used in MIKE21PMS

From the aforementioned ERA-Interim point, wave characteristics for specific directions (propagating from) have been analysed. The directionality of the waves in relation to their heights is presented in Table 5.3.5, with the most frequent directions are NE, E and SE.

Table 5.3.5: Frequency (%) of Wave Direction and Wave heights for Pinios River Offshore Area (ERA-Interim)

| Wave Direction | Wave Height (m) | | | | | | | Total |
|------------------|-----------------|--------|-------|-------|-------|-------|-------|---------|
| | 0-0.5 | 0.5-1 | 1-1.5 | 1.5-2 | 2-2.5 | 2.5-3 | 3-3.5 | |
| 0-22.5 | 1.56% | 0.56% | 0.07% | 0.02% | 0.00% | 0.00% | 0.00% | 2.21% |
| 22.5-45 | 2.97% | 1.26% | 0.56% | 0.20% | 0.07% | 0.03% | 0.00% | 5.09% |
| 45-67.5 | 21.93% | 10.44% | 3.23% | 0.73% | 0.23% | 0.06% | 0.00% | 36.64% |
| 67.5-90 | 11.54% | 2.28% | 0.36% | 0.09% | 0.01% | 0.01% | 0.00% | 14.29% |
| 90-112.5 | 3.26% | 0.33% | 0.06% | 0.00% | 0.00% | 0.00% | 0.00% | 3.66% |
| 112.5-135 | 2.99% | 0.24% | 0.04% | 0.01% | 0.00% | 0.00% | 0.00% | 3.28% |
| 135-157.5 | 5.75% | 0.86% | 0.13% | 0.02% | 0.00% | 0.00% | 0.00% | 6.76% |
| 157.5-180 | 6.62% | 1.64% | 0.24% | 0.02% | 0.00% | 0.00% | 0.00% | 8.52% |
| 180-202.5 | 2.99% | 0.63% | 0.04% | 0.00% | 0.00% | 0.00% | 0.00% | 3.67% |
| 202.5-225 | 1.88% | 0.38% | 0.02% | 0.00% | 0.00% | 0.00% | 0.00% | 2.27% |
| 225-247.5 | 1.47% | 0.29% | 0.02% | 0.00% | 0.00% | 0.00% | 0.00% | 1.79% |
| 247.5-270 | 1.50% | 0.22% | 0.02% | 0.00% | 0.00% | 0.00% | 0.00% | 1.74% |
| 270-292.5 | 1.74% | 0.19% | 0.01% | 0.00% | 0.00% | 0.00% | 0.00% | 1.94% |
| 292.5-315 | 2.15% | 0.31% | 0.03% | 0.00% | 0.00% | 0.00% | 0.00% | 2.49% |
| 315-337.5 | 2.48% | 0.55% | 0.06% | 0.00% | 0.00% | 0.00% | 0.00% | 3.09% |
| 337.5-360 | 1.91% | 0.59% | 0.06% | 0.00% | 0.00% | 0.00% | 0.00% | 2.56% |
| Total | 72.76% | 20.76% | 4.95% | 1.09% | 0.33% | 0.10% | 0.01% | 100.00% |

5.3.2.1 NE Waves

The number of records with waves propagating from the NE is 21337 of 51136 records. The mean height of the waves propagating from the NE is of 0.53 m and the period of 4.39 sec whilst the upper 2% is estimated 2.06 m and 6.93 s for wave height and period respectively (Table 5.3.6).

Table 5.3.6: Mean and max 2% of Significant Wave Height (SWH) and Mean Wave Period (MWP) of waves propagating from the NE

| | SWH (m) | MWP (s) |
|------|---------|---------|
| Mean | 0.53 | 4.39 |
| 2% | 2.06 | 6.93 |

For the mean conditions (Figure 5.3.6), it is shown that the directionality of the waves does not change that much in the nearshore zone, except in areas that are characterized with milder slopes with the waves' directionality becomes almost perpendicular to the shore.

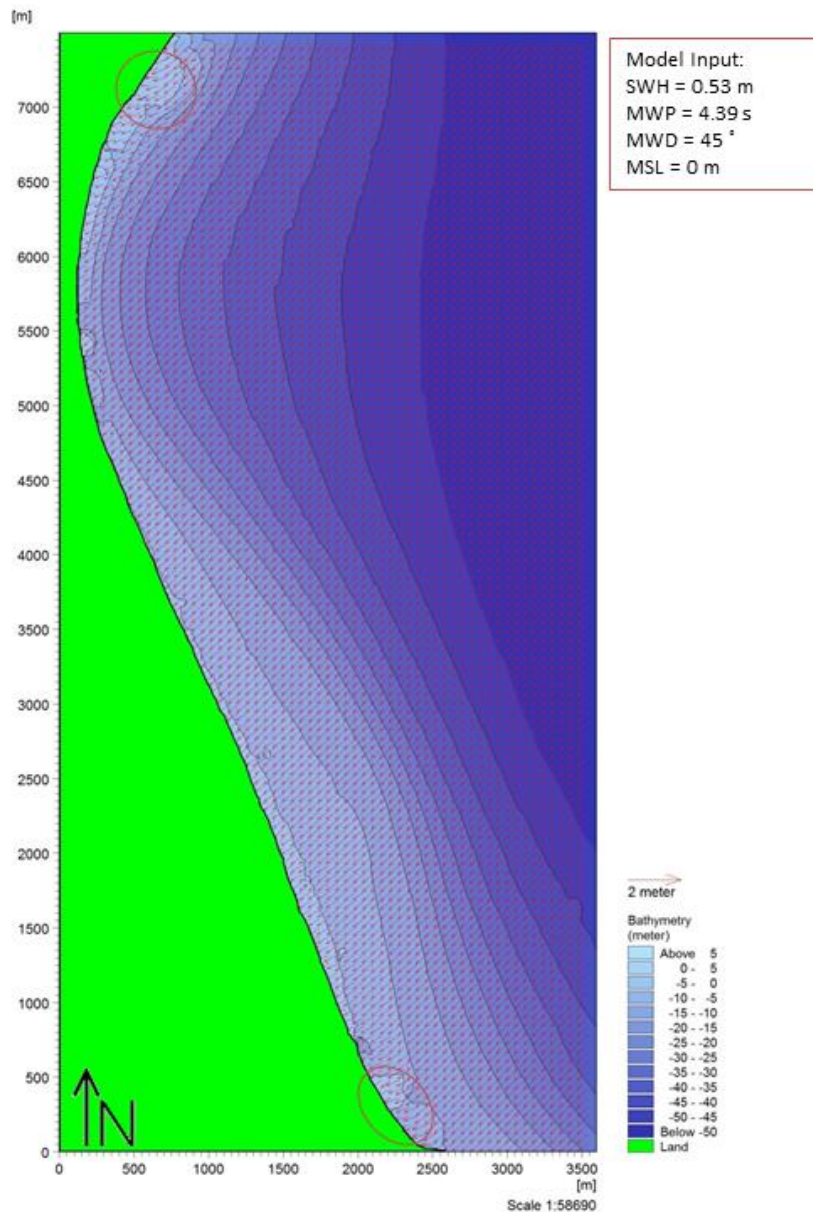


Figure 5.3.6: Wave propagation at mean NE conditions

For the mean of the upper 2% of the wave heights (Figure 5.3.7), the difference in wave directionality is more evident than in the case of the mean conditions. There are more areas with these changes (4 circles) and especially more evident in the North. As estimated from the empirical equations (CERC, 1984), the transient zone from offshore to nearshore for a wave length of 75 m ranges from 37.5 m to 3.75 m depth. Furthermore, these alterations can be subject to high resolution of the bathymetry, i.e. changing in specific areas the directionality of the wave (see Figure 4.5).

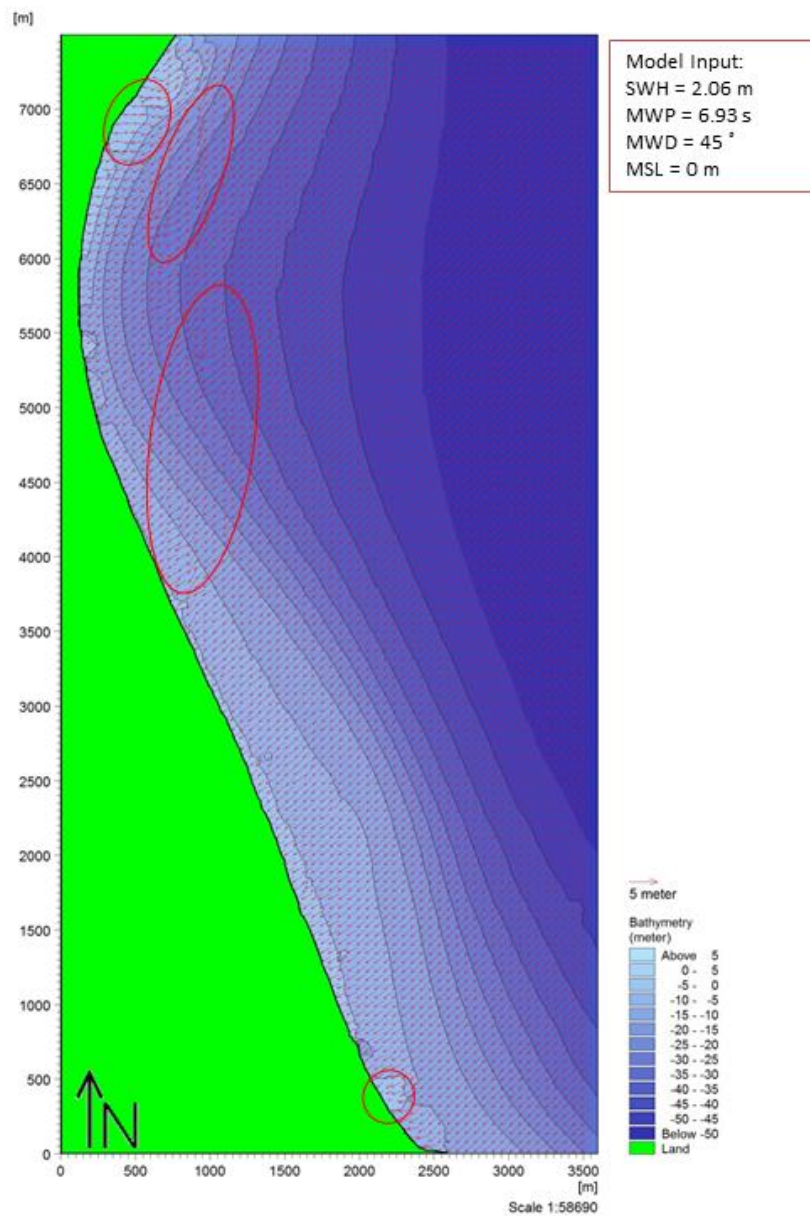


Figure 5.3.7: Wave propagation at the upper 2% of waves propagating from NE

At the 3rd scenario (Figure 5.3.8), with sea level rising around 0.3 m for the period 2046-2065, the areas with wave change directionality become more wide and it is shown that the waves have directions almost perpendicular to the shore from distances even further away from the coastline and bigger depths (even at 35m).

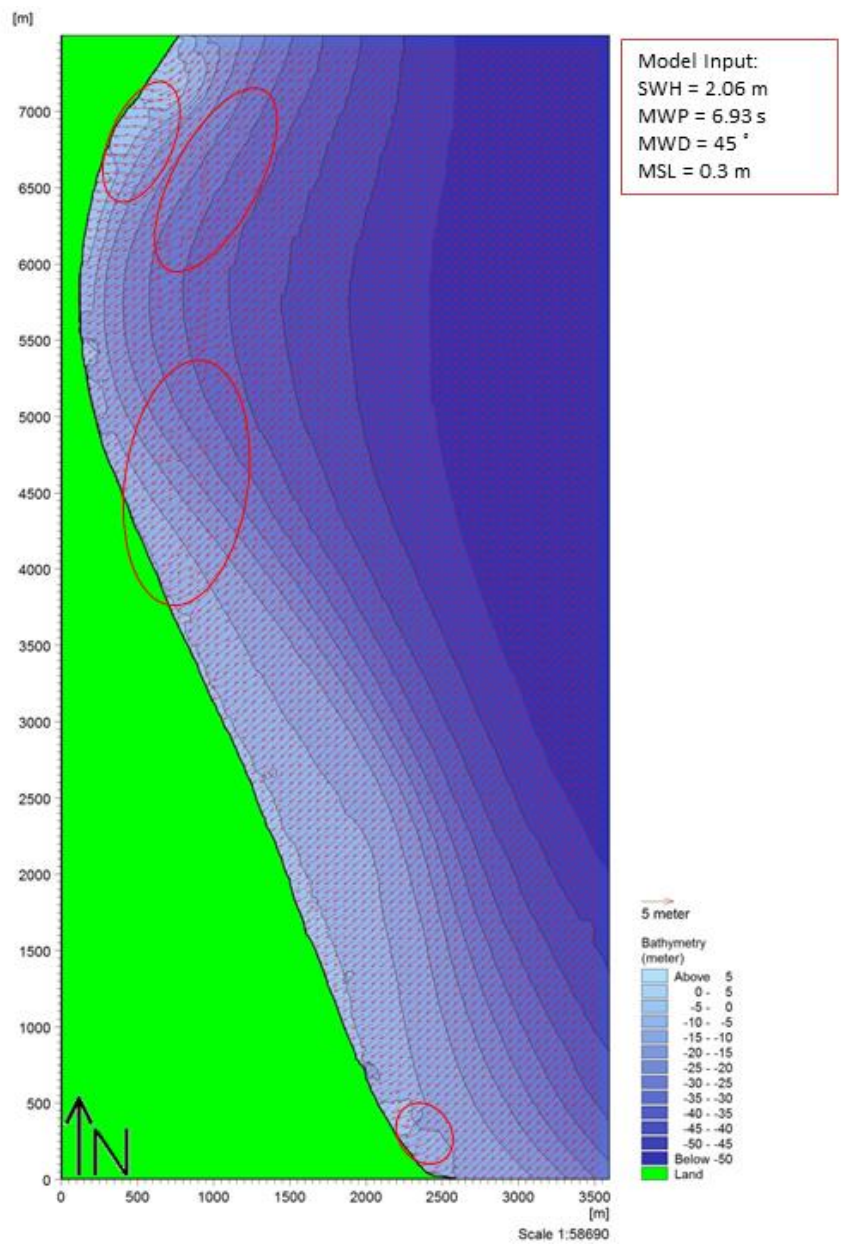


Figure 5.3.8: Wave propagation at the upper 2% of waves propagating from NE with a sea level rise of 0.3 m (RCP 8.5, 2046-2065)

For the case of sea level rise with 0.63 m for the period 2085-2100, the areas are wider than the 3rd scenario but more or less the change in the wave directionality remains the same (Figure 5.3.9), as previously.

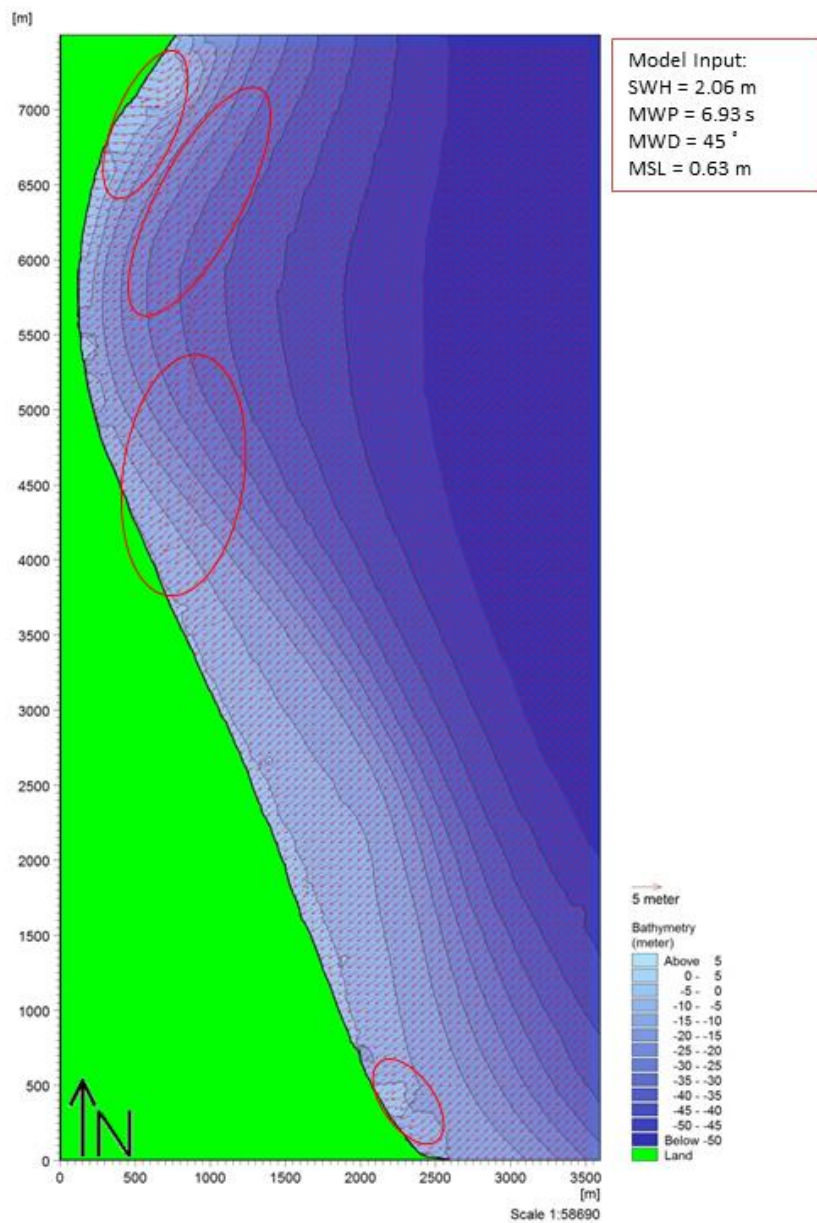


Figure 5.3.9: Wave propagation at the upper 2% of waves propagating from NE with a sea level rise of 0.63 m (RCP 8.5, 2081-2100)

The estimates of the wave characteristics in the offshore and the nearshore zone from the empirical equations presented in CERC (1984) are shown in Table 5.3.7. Analytically, with a wave height of 0.53 m, period 4.39 s, wavelength of 30.1 m and offshore depth of 50 m, the wave will break at 0.86 m depth and will have a height of 0.67 m. In the case of the mean of the upper 2% of wave height, a wave with height of 2.06 m, period of 6.93 s and wavelength of 75.02 m will eventually break at the depth of 3.05 m and will have height of 2.38 m.

Table 5.3.7: Wave Characteristics of NE direction as estimated from (CERC, 1984) in offshore and nearshore conditions

| NE-MEAN | | NE-2% | |
|-----------|-------|-----------|-------|
| Offshore | | Offshore | |
| d (m) | 50.00 | d (m) | 50.00 |
| H_o (m) | 0.53 | H_o (m) | 2.06 |
| T_o (s) | 4.39 | T_o (s) | 6.93 |
| L_o (m) | 30.10 | L_o (m) | 75.02 |
| Nearshore | | Nearshore | |
| H_b (m) | 0.67 | H_b (m) | 2.38 |
| d_b (m) | 0.86 | d_b (m) | 3.05 |

Wave height profiles for each wave scenario are presented along with bottom topography in Figure 5.3.10. For profile A (Figure 5.3.10), the breaking depth is estimated at -3.86m with wave height of 0.57 m (Scenario 1), at -3.67 m with wave height of 2.25 m (Scenario 2), at -3.86 m with height of 2.31 m (Scenario 3) and at -3.62 m with 2.32 m (Scenario 4).

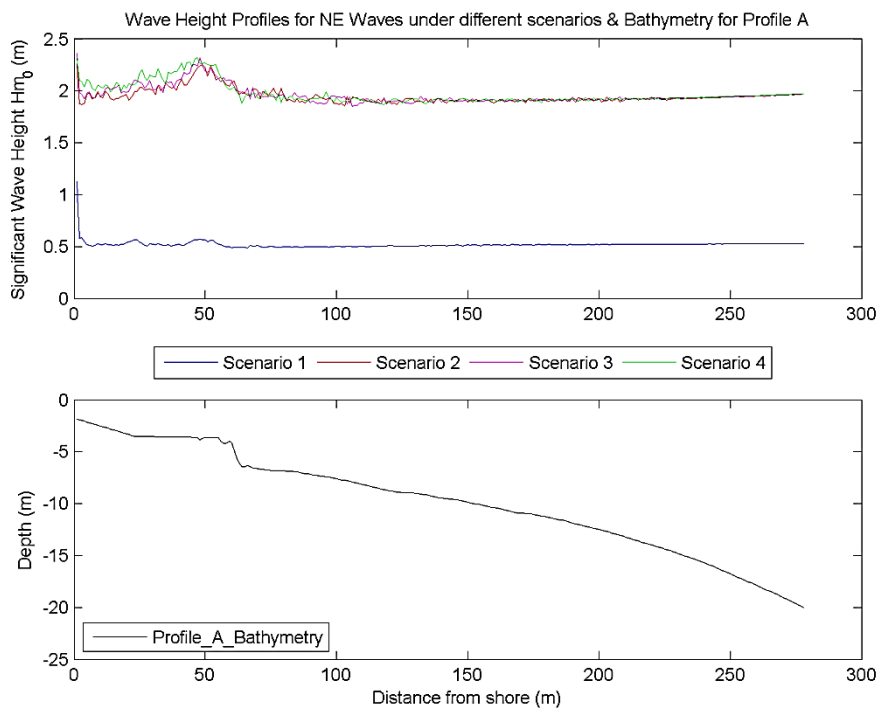


Figure 5.3.10: Wave Height Profiles for the NE under different scenarios for Location A. (Note: Distance from shore should be multiplied with 3, due to the grid size of 3m).

In the case of profile B (Figure 5.3.11), it is evident that the waves are influenced more from the steeper bottom topography than in the case of profile A. It should be kept in mind that due to the detail of the

bathymetry these changes in wave height might have a large uncertainty. The breaking depth is estimated at -0.86 m with heights of 0.52 m (Scenario 1), at -4.07 with height 1.76 m (Scenario 2), at -4.48 m with wave height 1.8 m (Scenario 3) and at -1.9 m with height 1.75 m (Scenario 4). The peaks from 2.75 m to 2.86 m that appear in depths ranging from -22 m to -23.7 m (i.e. in the transitional zone from nearshore to offshore) are due to the effect of the irregular bottom bathymetry as shown in Figure 4.3 and in Figure 5.3.9.

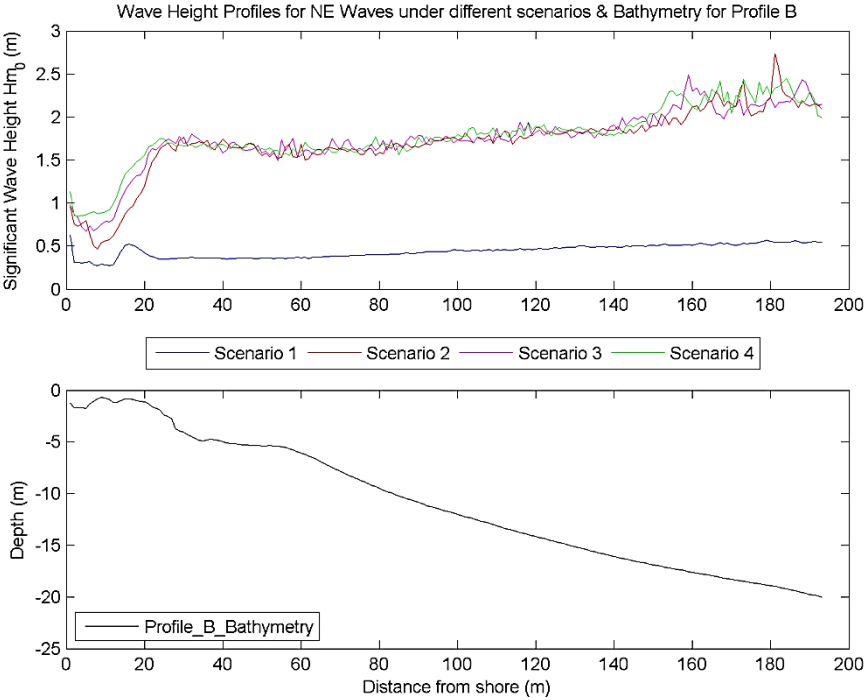


Figure 5.3.11: Wave Height Profiles for the NE under different scenarios for Location B. Note: Distance from shore should be multiplied with 3, due to the grid size of 3m.

5.3.2.2 E Waves

The secondary frequent wave direction in the area is that of E with 9180 records of 51136. The mean conditions have wave height of 0.34 m and period 3.55 s, while the upper 2% of 1.48 m and 5.68 s (Table 5.3.8).

Table 5.3.8: Mean and max 2% of Significant Wave Height (SWH) and Mean Wave Period (MWP) of waves propagating from the E

| | SWH (m) | MWP (s) |
|------|---------|---------|
| Mean | 0.34 | 3.55 |
| 2% | 1.48 | 5.68 |

The mean wave conditions of E direction are shown in Figure 5.3.12. There is not a significant change in wave directionality

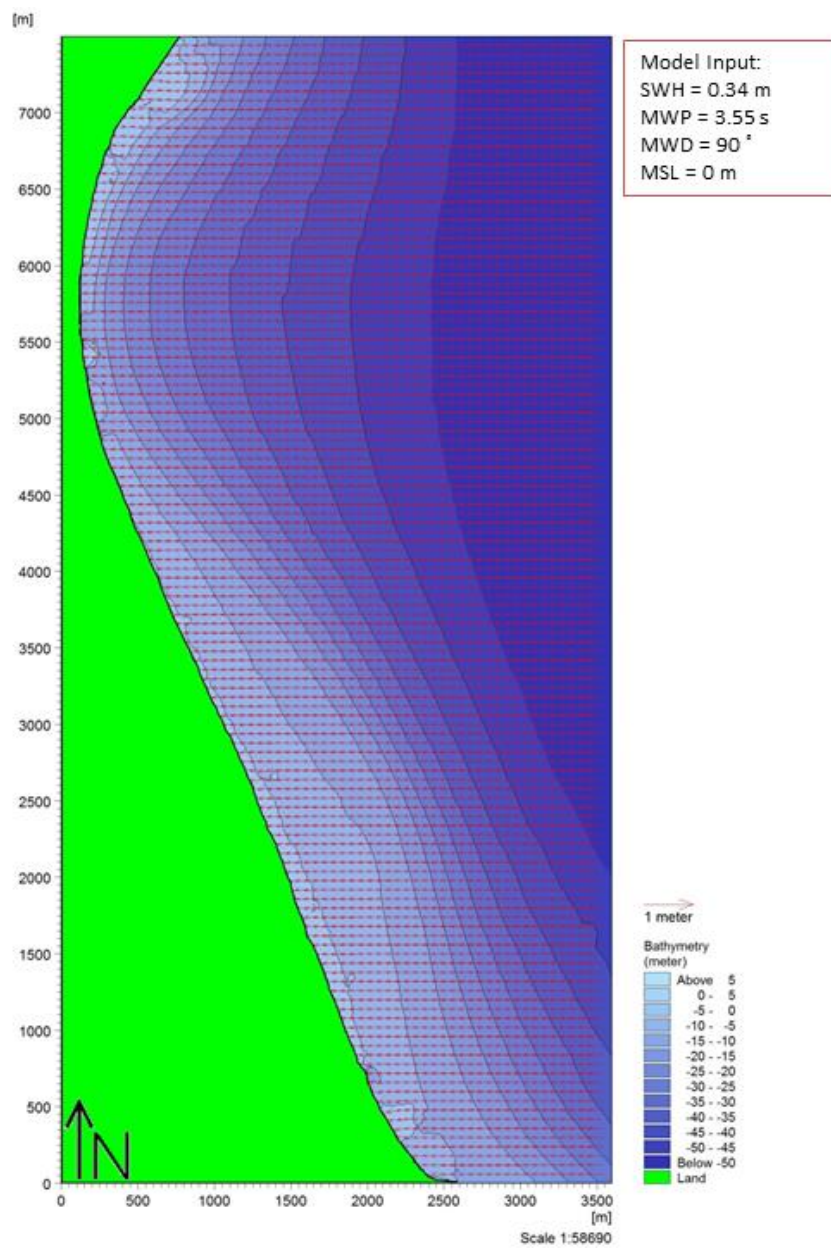


Figure 5.3.12: Wave propagation at mean E conditions

For the case of the mean of upper 2% of waves, the waves in 2 areas (Figure 5.3.13), slightly turn northwards (north circled area) and southwards (south circled area) close to the shore.

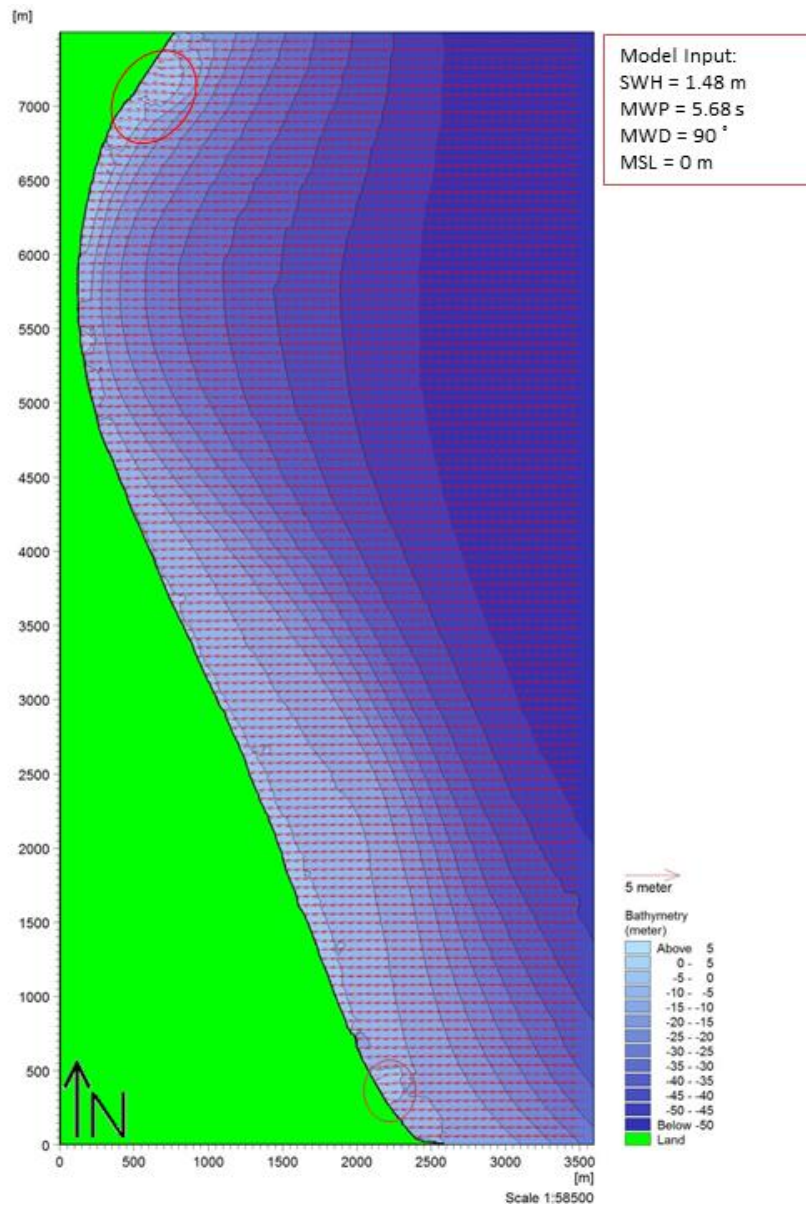


Figure 5.3.13: Wave propagation at the upper 2% of waves propagating from E

In the case of the 3rd scenario, the areas with changes in wave direction become wider Figure 5.3.14.

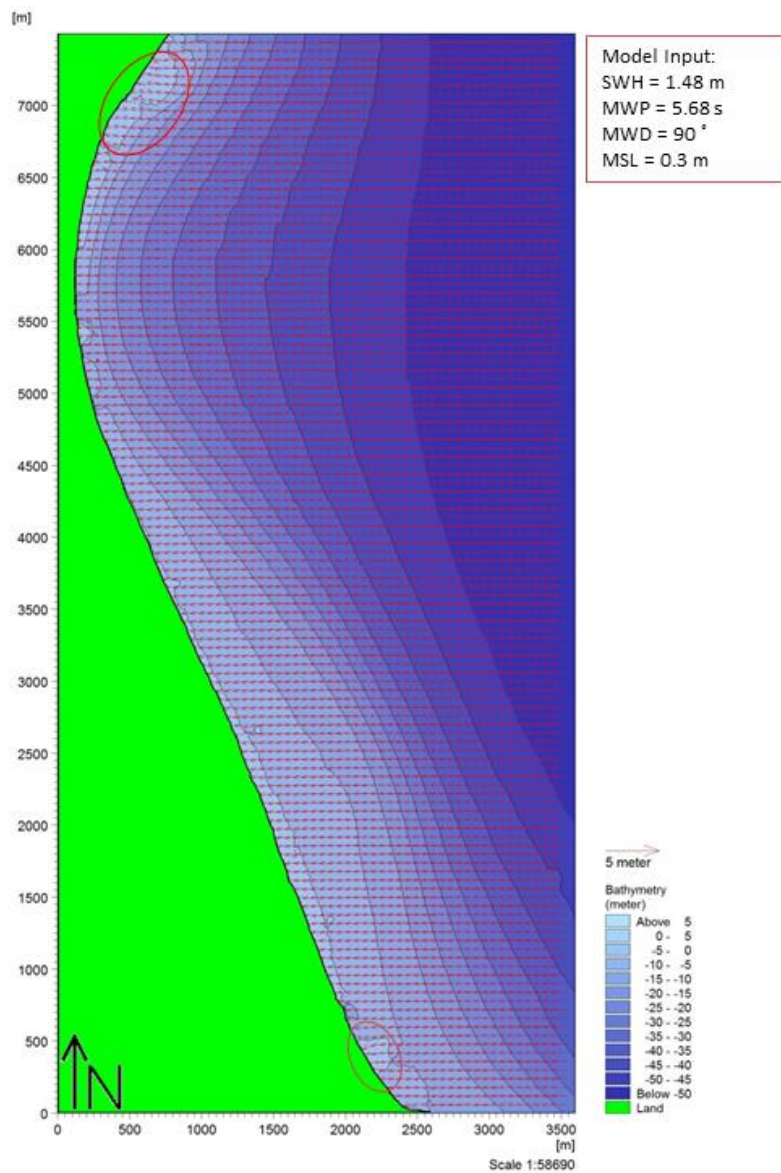


Figure 5.3.14: Wave propagation at the upper 2% of waves propagating from E with a sea level rise of 0.3 m (2046-2065)

Finally, in the case of the sea level rise of 0.63m, the areas are slightly wider (Figure 5.3.15).

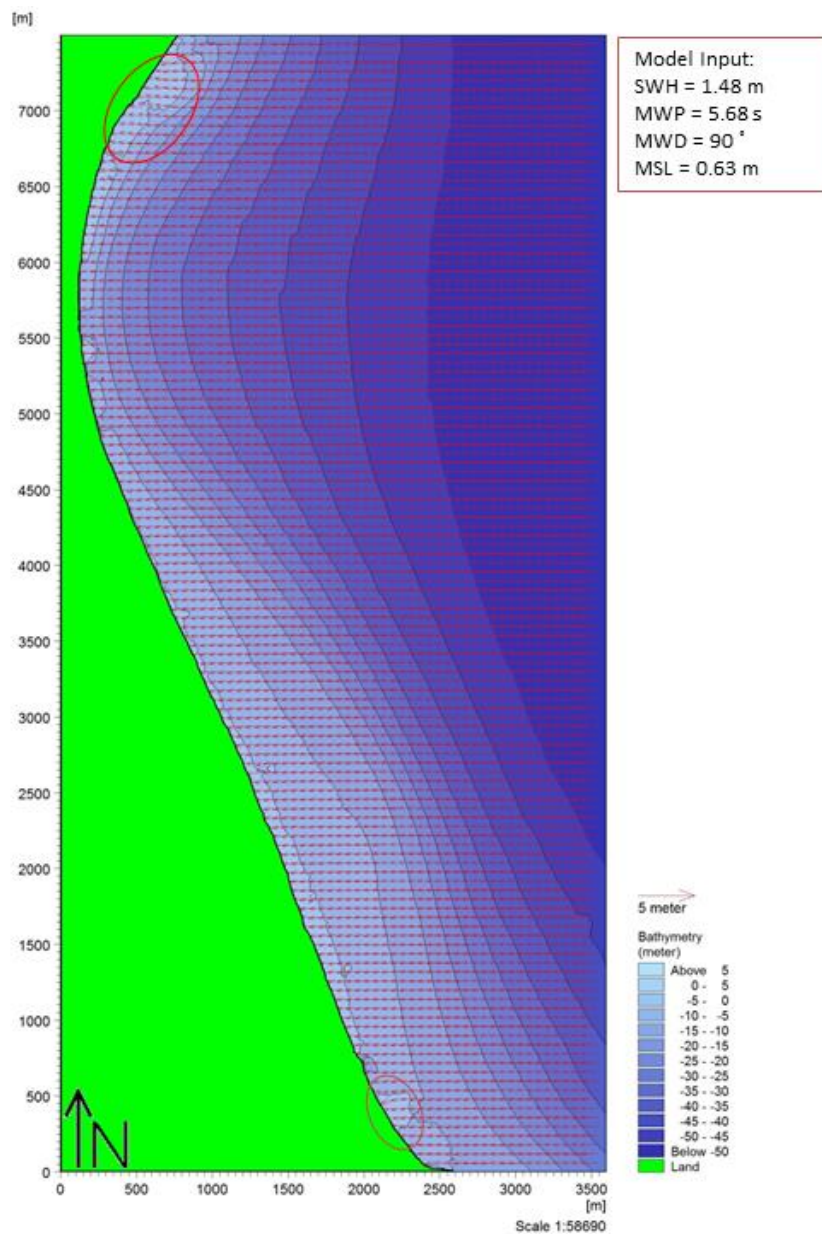


Figure 5.3.15: Wave propagation at the upper 2% of waves propagating from E with a sea level rise of 0.63 m (2085-2100).

Wave characteristics as estimated (CERC, 1984) for the mean conditions and the upper 2% for E waves, are shown in Table 5.3.9. Analytically, for a wave with characteristics of height of 0.32 m, period 3.55 s, wavelength of 19.69 m and offshore depth of 50 m, the wave is estimated to break at a depth of 0.53 m with a height of 0.41 m. For a wave characterized by a height of 1.48 m, period of 5.68 s, wavelength of 50.40 m and offshore depth of 50 m, it will break at the depth of 2.16 m and will have height of 1.69 m.

Table 5.3.9: Wave Characteristics of E direction as estimated from (CERC, 1984) in offshore and nearshore conditions

| E-MEAN | | E-2% | |
|-----------|-------|-----------|-------|
| Offshore | | Offshore | |
| d (m) | 50.00 | d (m) | 50.00 |
| H_o (m) | 0.32 | H_o (m) | 1.48 |
| T_o (s) | 3.55 | T_o (s) | 5.68 |
| L_o (m) | 19.69 | L_o (m) | 50.40 |
| Nearshore | | Nearshore | |
| H_b (m) | 0.41 | H_b (m) | 1.69 |
| d_b (m) | 0.53 | d_b (m) | 2.16 |

For profile A (Figure 5.3.16), for the 1st scenario, the wave will break at -3.51 m and have a height of 0.34 m, for the 2nd scenario at -3.86 m with height of 1.59 m, at the 3rd scenario at -2.77 m with wave height of 1.55 m and finally at the 4th scenario it will break at the depth of -3.86 m with a height of 1.56 m.

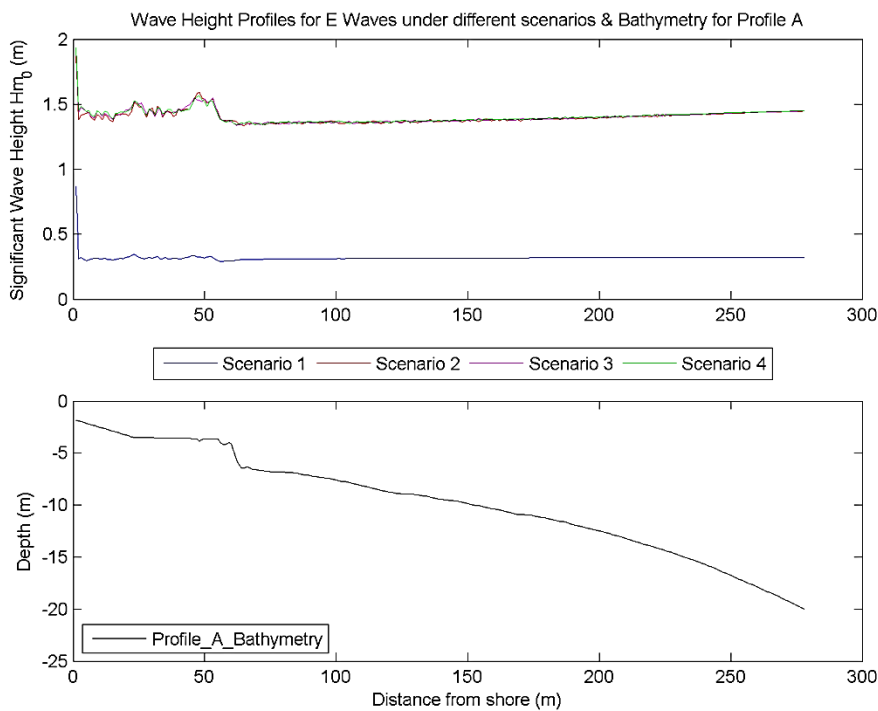


Figure 5.3.16: Wave Height Profiles for the E under different scenarios for Location A (Note: Distance from shore should be multiplied with 3, due to the grid size of 3m).

At profile B (Figure 5.3.17), the model estimates that for the mean conditions (Scenario 1), the wave breaks at -0.86 m with height of 0.41 m, for the upper 2% (Scenario 2) it will break at -4.89 m with

height of 1.35 m, for the sea level of 0.3 m (Scenario 3) at -1.9 m with height of 1.36 m and finally, at the Scenario 4 (sea level rise of 0.63 m) at -1.9 with height of 1.36 m.

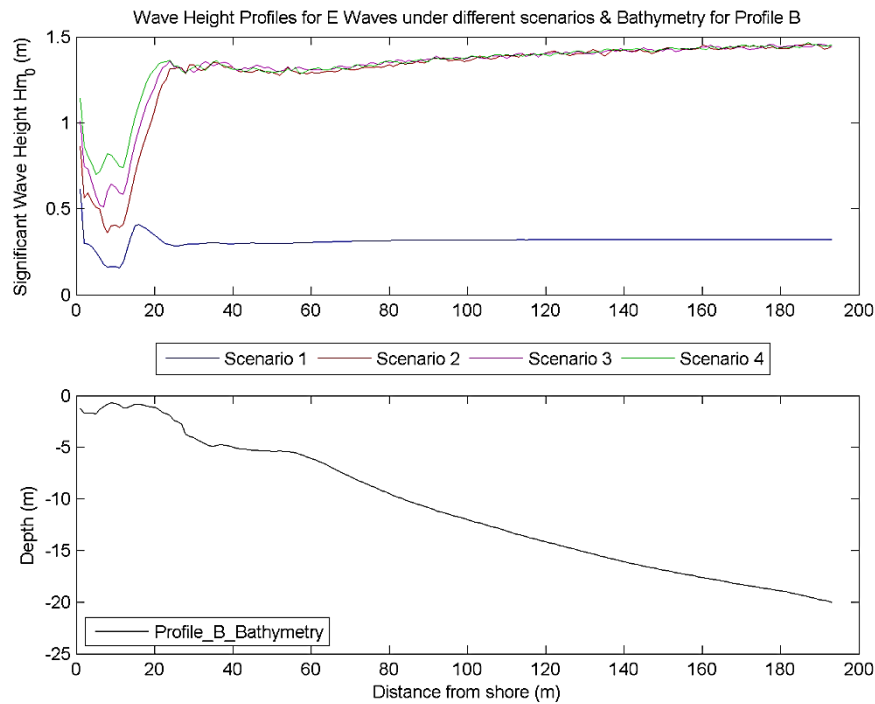


Figure 5.3.17: Wave Height Profiles for the E under different scenarios for Location B (Note: Distance from shore should be multiplied with 3, due to the grid size of 3m).

5.3.2.3 SE Waves

From the analysis of the ERA-Interim it is shown that there are 5136 records with waves propagating from the SE. The mean conditions are characterized by wave height of 0.28 m and period of 3.36 s, while the upper 2% of wave height of 1.24 m and period of 5.65 s (Table 5.3.10).

Table 5.3.10: Mean and max 2% of Significant Wave Height (SWH) and Mean Wave Period (MWP) of waves propagating from the SE

| | SWH (m) | MWP (s) |
|------|---------|---------|
| Mean | 0.28 | 3.36 |
| 2% | 1.24 | 5.65 |

For the mean wave conditions for the SE waves, there is only one area where waves change their directionality and become more perpendicular to the shore (see south circle in Figure 5.3.18).

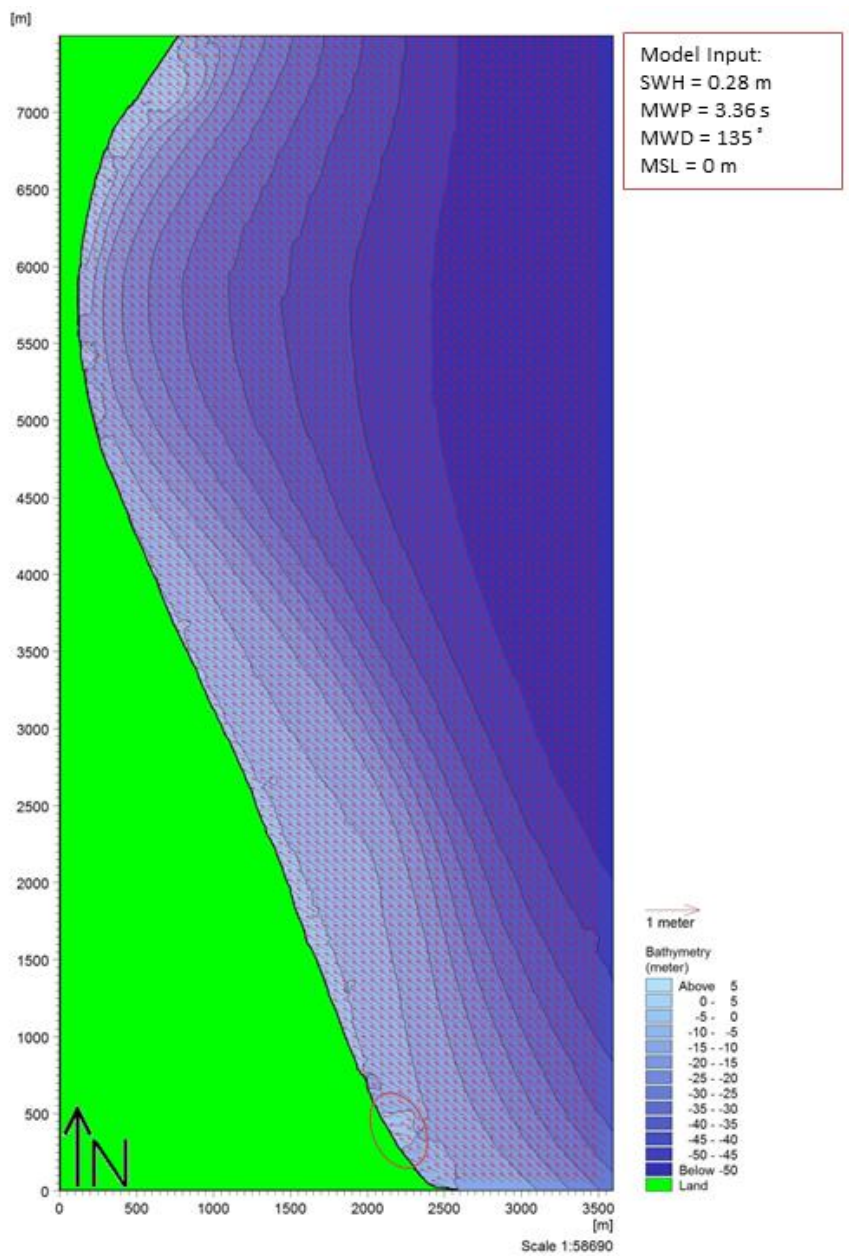


Figure 5.3.18: Wave propagation at mean SE conditions

In the case of the upper 2%, another area is evident with the waves becoming more perpendicular to the shore (north circle Figure 5.3.19). Additionally, the southern area is becoming wider.

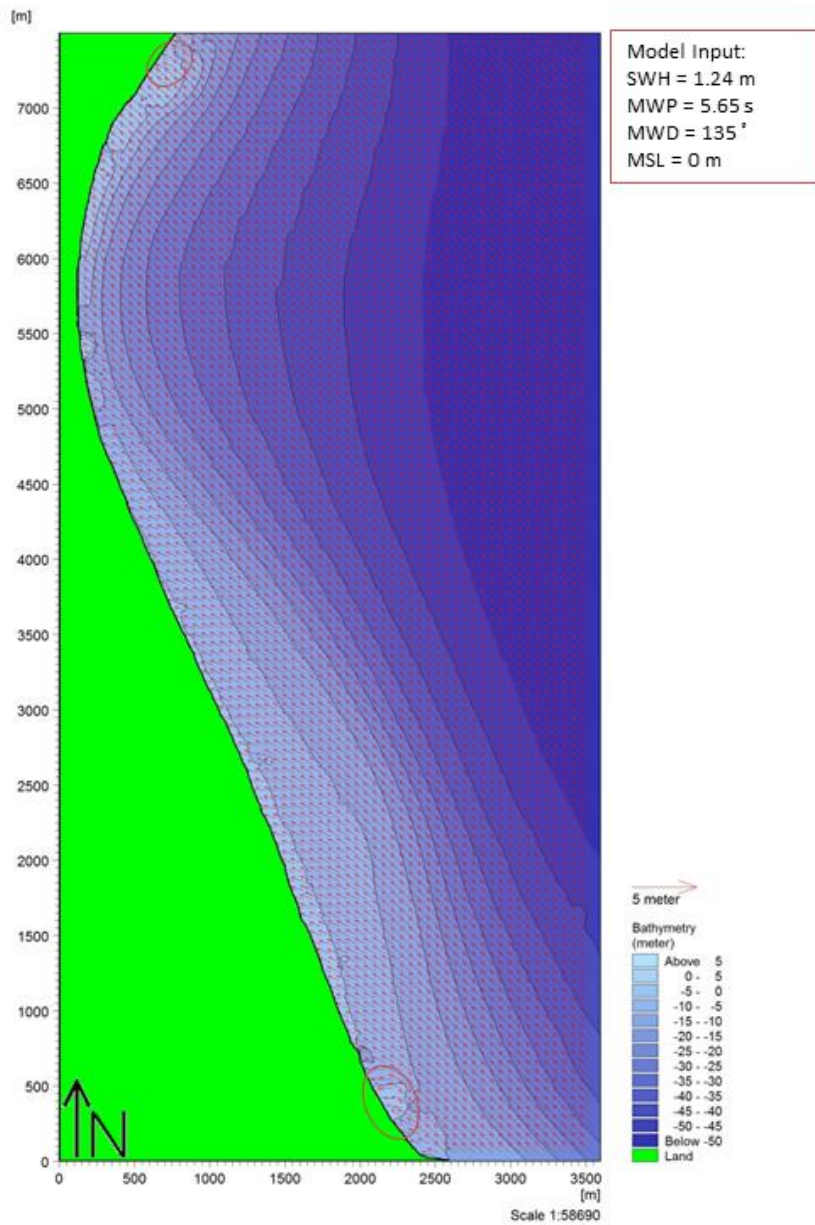


Figure 5.3.19: Wave propagation at the upper 2% of waves propagating from SE

Both of the aforementioned areas are even wider in the 3rd scenario, whilst a 3rd area is generated (centre circle Figure 5.3.20).

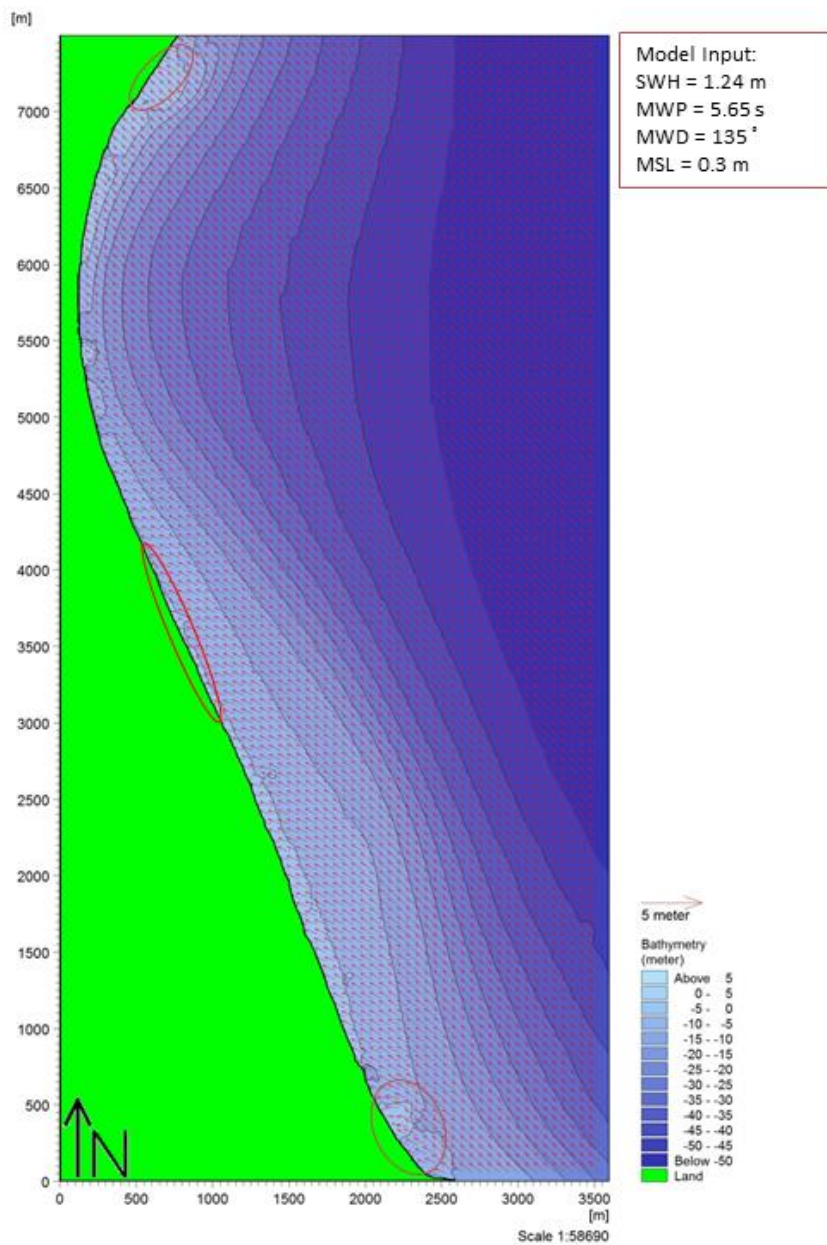


Figure 5.3.20: Wave propagation at the upper 2% of waves propagating from SE for a sea level rise of 0.3 m (RCP 8.5 2046-2065)

In the case of sea level rise of 0.63 m, there are even more areas with changes in wave direction as shown in Figure 5.3.23. It should be noted though that in the southern area, wave change their direction at greater depths than before, for example at 5-10 m.

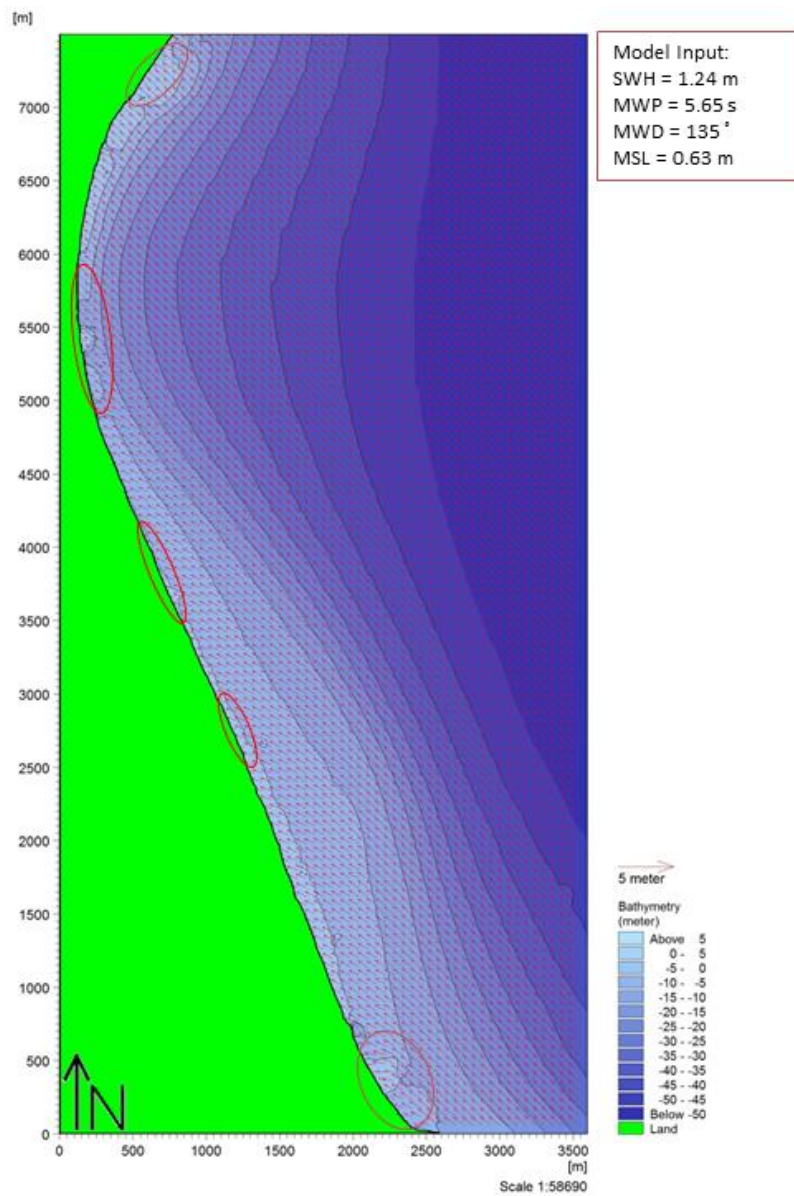


Figure 5.3.21: Wave propagation at the upper 2% of waves propagating from SE for a sea level rise of 0.63 m (RCP 8.5 2081-2100)

The wave characteristics of mean conditions and upper 2 % in the nearshore and the offshore zone for SE waves as estimated (CERC, 1984) are given in Table 5.3.11. Furthermore, for a wave height of 0.28 m, period 3.36 s, wavelength of 17.64 m and offshore depth of 50 m, the wave will probably break at a depth of 0.46 m with height of 0.36 m. Additionally, if a wave has a height of 1.24 m, period of 5.65 s, wavelength of 49.87 m and offshore depth of 50 m, the breaking zone will be at the depth of 1.87 m and the wave will have a height of 1.46 m.

Table 5.3.11: Wave Characteristics of SE direction as estimated (CERC, 1984) in offshore and nearshore conditions

| SE-MEAN | | SE-2% | |
|-----------|-------|-----------|-------|
| Offshore | | Offshore | |
| d (m) | 50.00 | d (m) | 50.00 |
| H_o (m) | 0.28 | H_o (m) | 1.24 |
| T_o (s) | 3.36 | T_o (s) | 5.65 |
| L_o (m) | 17.64 | L_o (m) | 49.87 |
| Nearshore | | Nearshore | |
| H_b (m) | 0.36 | H_b (m) | 1.46 |
| d_b (m) | 0.46 | d_b (m) | 1.87 |

For profile A (Figure 5.3.22), it is estimated at the mean conditions (1st scenario), the breaking depth will be at -2.77 m and the wave height will be 0.27 m, for the upper 2% (2nd scenario) at -2.77 m with height of 1.11 m, at the 3rd scenario at -2.77 m with wave height of 1.11 m and for the 4th scenario the depth will be at 2.77 m with a height of 1.08 m.

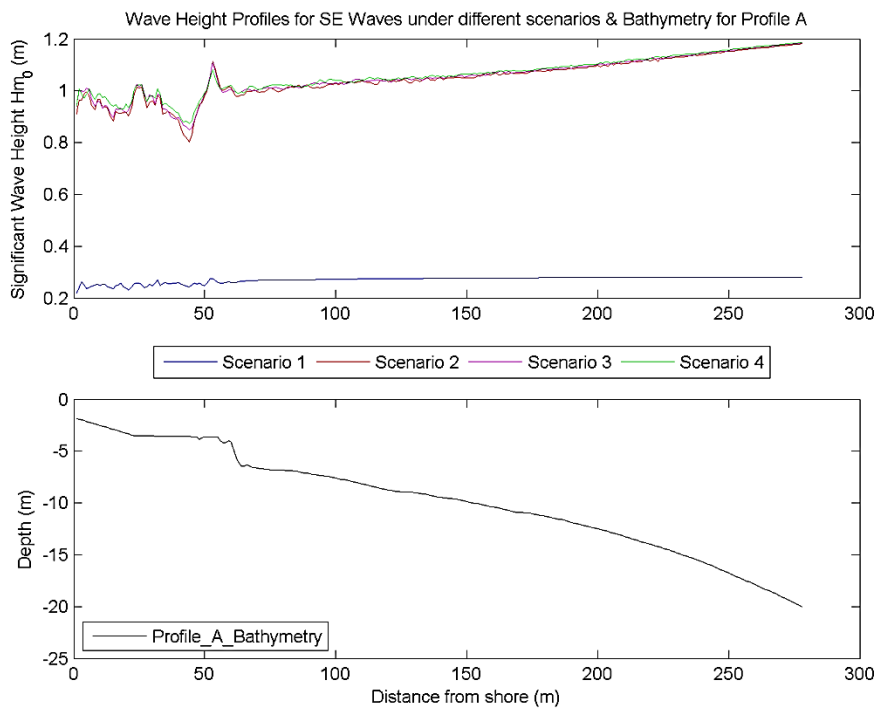


Figure 5.3.22: Wave Height Profiles for the SE under different scenarios for Location A (Note: Distance from shore should be multiplied with 3, due to the grid size of 3m).

As for profile B (Figure 5.3.23), the model estimates that for mean conditions, the waves will break at the depth of -1.12 m and will have a height of 0.28 m, for the 2nd Scenario (upper 2%), the waves will

break at -1.91 m with height of 1.25 m, at the 3rd Scenario (sea level rise of 0.3 m) the breaking depth is of -1.91 m with height of 1.25m, whilst finally, at the 4th scenario (sea level rise of 0.63 m), the wave will break at -1.29 m with height of 1.28 m.

As in the case of the NE waves, due to the incoming wave directionality, profile B shows changes in wave height even at the transitional zone that in this case ranges from -25 m to -28 m.

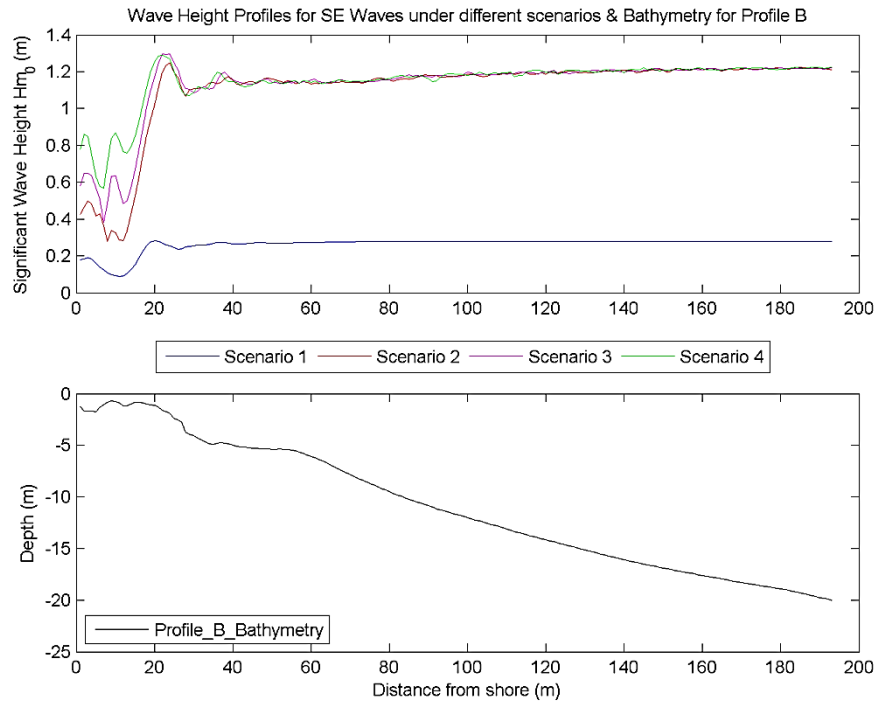


Figure 5.3.23: Wave Height Profiles for the SE under different scenarios for Location B (Note: Distance from shore should be multiplied with 3, due to the grid size of 3m).

Chapter 6 - Discussion

6 Discussion

6.1 Poseidon Buoys

For the discussion of the results concerning the data from the Poseidon buoys, the Greek Seas have been divided in the following sub-basins:

- 1) North Aegean: described by the buoys of Athos, Katerini, Lesvos and Skyros
- 2) Central Aegean: described by the buoys of Mykonos, and Petrokaravo
- 3) South Aegean: described by the buoys of Avgos, Dia, E1M3A and Santorini
- 4) North-East Ionian: described by Zakynthos
- 5) South-East Ionian: described by Pylos and Kalamata

It should be noted that the analyses in the different areas from different buoys do not coincide in time periods and the number of samples differs per site; this might lead to discrepancies and to inaccurate comparisons amongst buoys and, therefore, between the different regions. In addition, the results do not necessarily present a full description of the Greek Seas, especially due to the variation of the sea state in temporal and spatial scales, but every result could be considered as representative only of the nearby area that is under-examination.

6.1.1 North Aegean Sea

The North Aegean Sea is characterized by complex topography and significant variation of wave and atmospheric characteristics across its region. Furthermore, the case of Athos buoy (Figure 6.1.1) that is located between Limnos Isl. and Chalkidiki, it is more likely not to be representative for waves approaching from easterly directions. The Katerini buoy, as it is located close to the west coast of the NW part of Thermaikos Gulf, is expected to record smaller waves due to fetch limitation. Lesvos buoy, being located very close to the west coast of the island (almost 5 km) is not expected to monitor waves from NE-E. Finally, Skyros buoy is located north of the island and shows a blockage of waves approaching from the S and NW directions.

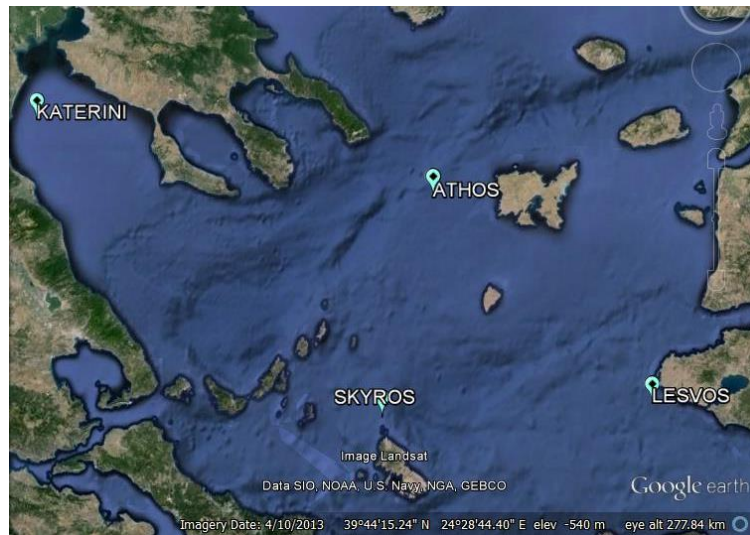


Figure 6.1.1: Location of the four buoys in the North Aegean Sea

The North Aegean Sea is described by mean spectral significant wave height (H_{m0}) of 0.43 m to 1.06 m and statistical significant wave height ($H_{1/3}$) of 1.01-1.06 m (Table 6.1.1). The buoy at Katerini gives the smallest mean height (0.43 m) amongst the 4 buoys, whilst the highest mean value (0.87 m) is recorded by Skyros buoy. The mean values of the maximum height of the area of the North Aegean vary from 1.16 m to 1.48 m, as given by the buoys, and from 1.55 m to 1.65 m, according to Sea Surface Elevation (SSE) analysis. The swells have smaller heights being from 0.02 m to 0.05m, with Athos providing the highest (0.05 m). The wind-induced waves have heights from 0.43 m to 0.85 m, with the highest measured in Skyros.

Table 6.1.1: Mean values of wave height parameters for the North Aegean Sea

| North Aegean | H_{m0} (m) | | $H_{1/3}$ (m) | H_{max} (m) | | H_{m0a} (m) | H_{m0b} (m) |
|--------------|--------------|--------------|---------------|---------------|--------------|---------------|---------------|
| | Buoy Records | SSE Analysis | SSE Analysis | Buoy Records | SSE Analysis | Buoy Records | Buoy Records |
| Athos | 0.80 | 1.06 | 0.99 | 1.48 | 1.65 | 0.05 | 0.78 |
| Katerini | 0.43 | – | – | – | – | 0.02 | 0.43 |
| Lesvos | 0.77 | – | – | 1.22 | – | 0.04 | 0.78 |
| Skyros | 0.87 | 1.01 | 0.94 | 1.16 | 1.55 | 0.04 | 0.85 |

*Buoy records= data directly from the buoys; SSE=data as given by the sea surface elevation analysis

The significant spectral wave period (T_{m02}) is from 2.94 to 3.64 s, while the statistical wave period ($T_{1/3}$) has a range of 3.76-3.99 s. Peak period (T_p) varies from 3.47 s to 4.63 s, as given by the buoy data and from 4.92 s to 5.08 s from the SSE analysis. The swells have periods from 13.41 s to 14.13 s, with Katerini recording the largest. The wind-induced waves have periods from 2.93 s to 6.75 s, with Lesvos recording the largest.

Table 6.1.2: Means of wave period parameters for the North Aegean Sea

| North Aegean | T _{m02} (s) | | T _{1/3} (s) | T _p (s) | | T _{m02a} (s) | T _{m02b} (s) |
|--------------|----------------------|--------------|----------------------|--------------------|--------------|-----------------------|-----------------------|
| | Buoy Records | SSE Analysis | SSE Analysis | Buoy Records | SSE Analysis | Buoy Records | Buoy Records |
| Athos | 3.64 | 3.99 | 5.43 | 4.58 | 5.08 | 13.55 | 3.63 |
| Katerini | 2.94 | – | – | 3.47 | – | 14.13 | 2.93 |
| Lesvos | 3.54 | – | – | 4.61 | – | 13.85 | 6.75 |
| Skyros | 3.6 | 3.76 | 5.24 | 4.63 | 4.92 | 13.41 | 3.59 |

*Buoy records= data from the buoys directly; SSE=data as given by the sea surface elevation analysis

The most frequent wave heights in the North Aegean are up to 0.5 m except in the case of Katerini, where they are up to 0.3 m and these heights are related to periods from 2 to 4 s. The maximum heights (more than 2.7 m) are most frequent in the case of Athos, whilst Katerini presents the smallest frequency in these heights and this applies for periods longer than 6 sec. The wave charts of the buoys of the North Aegean, present that the most frequent waves propagate mostly from the North and especially in the case of Skyros, waves that propagate from the South are absent due to the blockage from nearby land and islands.

The minima mean monthly values for wave height and period are during June (Table 6.1.3), except for Katerini where they are in April and September, respectively. The maximum mean monthly wave height values are in December for buoy data (H_{m0}) and in January for the SSE analysis (H_{m0}-H_{1/3}). The time lag can be due to the fact that SSE records cover half of the period of the buoys (i.e. SSE records in Athos are from 2007 – 2011 while the buoy record from 2000 – 2011)

Table 6.1.3: Seasonal Description of wave height for the North Aegean Sea

| North Aegean | H _{m0} (m) | | | | H _{1/3} (m) | |
|--------------|---------------------|------------|--------------|------------|----------------------|------------|
| | Buoy | | SSE | | SSE | |
| | Mean Monthly | | Mean Monthly | | Mean Monthly | |
| | Min | Max | Min | Max | Min | Max |
| Athos | JUN (0.49) | DEC (1.19) | JUN (0.66) | JAN (1.36) | JUN (0.61) | JAN (1.29) |
| Katerini | APR (0.35) | DEC (0.61) | – | – | – | – |
| Lesvos | JUN (0.57) | FEB (1.03) | – | – | – | – |
| Skyros | JUL (0.48) | FEB (1.27) | JUN (0.69) | FEB (1.32) | JUN (0.63) | FEB (1.24) |

The maximum mean values of spectral wave period (SSE and Buoy) and statistical wave period are presented during winter for Athos. The minimum value of spectral wave period is in Katerini in September as shown in Table 6.1.4.

Table 6.1.4: Seasonal Description of wave period for the North Aegean Sea

| North Aegean | T _{m02} (s) | | | | T _{1/3} (s) | |
|--------------|----------------------|------------|--------------|------------|----------------------|------------|
| | Buoy | | SSE | | SSE | |
| | Mean Monthly | | Mean Monthly | | Mean Monthly | |
| | Min | Max | Min | Max | Min | Max |
| Athos | JUN (3.29) | DEC (4.11) | JUN (3.48) | JAN (4.35) | JUN (4.73) | FEB (5.93) |
| Katerini | SEPT (2.86) | DEC (3.07) | – | – | – | – |
| Lesvos | JUN (3.29) | FEB (3.82) | – | – | – | – |
| Skyros | JUL (3.08) | FEB (4.03) | JUN (3.22) | FEB (4.11) | JUN (4.56) | FEB (5.76) |

The atmospheric characteristics of the North Aegean have mean values of atmospheric pressure from 1014.67 hPa to 1017.06 hPa, air temperature from 14.86 °C to 17.57, wind speed 4.55 to 6.00 m/s and of wind gust 6.18 to 7.82 m/s. The maximum mean values of wind speed and wind gust are observed in Lesvos and the minimum in Katerini.

Table 6.1.5: Mean values of Atmospheric Parameters for the North Aegean Sea

| North Aegean | Atmospheric Pressure (hPa) | Air Temperature (°C) | Wind Speed (m/s) | Wind Gust (m/s) |
|--------------|----------------------------|----------------------|------------------|-----------------|
| Athos | 1015.49 | 17.57 | 4.96 | 6.68 |
| Katerini | 1017.06 | 14.86 | 4.55 | 6.18 |
| Lesvos | 1014.67 | 17.35 | 6.00 | 7.82 |
| Skyros | 1015.30 | 17.19 | 5.13 | 6.80 |

The North Aegean is affected mostly by winds that have speeds from 3 to 8 m/s and are of northerly directions. The maximum speeds (>15m/s) are most evident in the area of Athos and Lesvos and are from N – NE directions except in the case of Katerini, where the higher winds are blowing from NE to E.

On a seasonal basis, the North Aegean presents higher pressure during January (except in Lesvos where is in November) and minimum in July for all the four buoys. Temperature has the regular seasonal pattern with lower values in winter (Jan-Feb) and higher in summer (Jul-Aug). Wind speed and wind gust have their maxima during winter season (Feb and Dec) and the minima during May and June.

Table 6.1.6: Seasonal atmospheric parameters for the North Aegean Sea

| North Aegean | Atmospheric Pressure (hPa) | | Air Temperature (°C) | | Wind Speed (m/s) | | Wind Gust (m/s) | |
|--------------|----------------------------|---------------|----------------------|-------------|------------------|------------|-----------------|-------------|
| | Min | Max | Min | Max | Min | Max | Min | Max |
| Athos | JUL (1011.7) | JAN (1019.34) | FEB (9.60) | AUG (25.4) | JUN (3.53) | FEB (6.54) | JUN (4.69) | FEB (9.015) |
| Katerini | JUL (1011.2) | JAN (1024.08) | DEC(6.76) | JUL (25.83) | MAY (3.23) | DEC (7.10) | MAY (4.38) | DEC (9.51) |
| Lesvos | JUL (1010.28) | NOV (1017.89) | JAN (11.03) | AUG (23.68) | JUN (4.84) | DEC (6.94) | JUN (6.18) | DEC (9.22) |
| Skyros | JUL (1010.29) | JAN (1019.04) | FEB (9.95) | AUG (25.31) | MAY (3.64) | FEB (6.51) | MAY (4.65) | FEB (8.77) |

In general, North Aegean waves with heights up to 1 m are related to wind speeds that are up to 8 m/s. Waves with heights of more than 3 m are related to winds with speeds of more than 12 m/s.

For Athos and Skyros buoy, it is shown that Kumaraswamy has the best fit according to all three tests and that it underestimates the higher values in contradiction to Weibull and Rayleigh that deviate even from the mean values and overestimate the higher ones. From the ratios given for Athos and Skyros (as those buoys recorded SSE for the North Aegean), the following can be established for North Aegean:

$$\frac{H_{m_0}}{H_{1/3}} = 1.085, \frac{H_{1/3}}{\sqrt{m_0}} = 3.7, \frac{H_{max}}{H_{m_0}} = 1.5, \frac{H_{max}}{H_{1/3}} = 1.7$$

6.1.2 Central Aegean Sea

In the case of Mykonos, the buoy is located in the northeastern part of the Island, with the Cyclades Isles acting as a blockage to the Southerly winds and especially from directions of S, SE and SW. Petrokaravo is located at the Argosaronikos Gulf, very close to SSE part of Aegena Island and SSW from the southern suburbs of Attiki. The islands of the Gulf block waves propagating from the W of the buoy (possibly from S to N of the buoy). Furthermore, the western part of the Cyclades can also block waves from that direction.

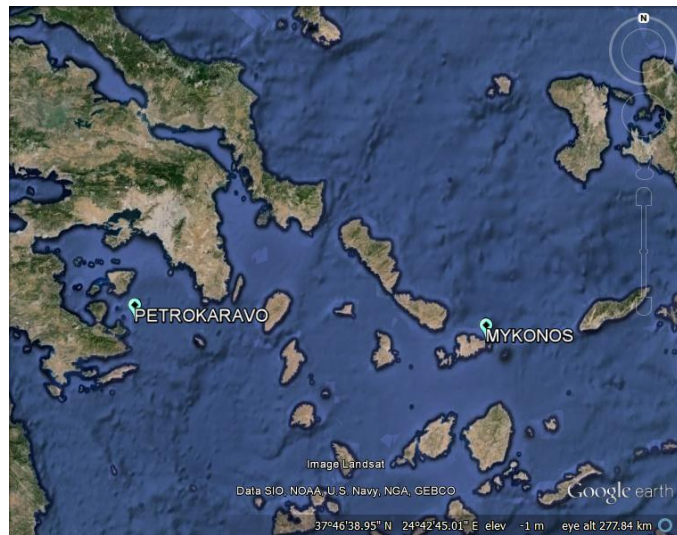


Figure 6.1.2: Location of the 2 buoys in Central Aegean Sea

For the Central Aegean, the spectral significant wave height, as given by the buoy records, can be of the range 0.5 m to 1.01 m, whilst it can reach up to 1.13 m as provided by the Mykonos sea surface elevation data analysis. Maximum wave height can be of 0.54 m to 1.61 m and 1.72 m as shown from the SSE. The wind waves have heights from 0.99 m (Mykonos) and 0.5 m (Petrokaravo), whilst swells can be of 0.02 (Petrokaravo) to 0.06 m (Mykonos).

Table 6.1.7: Means of wave height parameters for the Central Aegean Sea

| Central Aegean | H _{m0} (m) | | H _{1/3} (m) | H _{max} (m) | | H _{m0a} (m) | H _{m0b} (m) |
|----------------|---------------------|--------------|----------------------|----------------------|--------------|----------------------|----------------------|
| | Buoy Records | SSE Analysis | SSE Analysis | Buoy Records | SSE Analysis | Buoy Records | Buoy Records |
| Mykonos | 1.01 | 1.13 | 1.04 | 1.61 | 1.72 | 0.06 | 0.99 |
| Petrokaravo | 0.5 | – | – | 0.54 | – | 0.02 | 0.5 |

*Buoy records= data from the buoys directly; SSE=data as given by the sea surface elevation analysis

For the wave period, the spectral significant is from 3.22 s to 3.66 s, as provided by the buoys records and 3.8 s from the SSE analysis. The statistical significant wave period is of 5.39 s whilst the peak period ranges from 4.21 s to 4.9 s (buoys) and 5.16 s (SSE). Wind waves have periods from 3.22 s to 3.65 s and the swells from 11.45 s (Petrokaravo) to 13.43 s (Mykonos).

Table 6.1.8: Means of wave period parameters for the Central Aegean Sea

| Central Aegean | T _{m02} (s) | | T _{1/3} (s) | T _p (s) | | T _{m02a} (s) | T _{m02b} (s) |
|----------------|----------------------|--------------|----------------------|--------------------|--------------|-----------------------|-----------------------|
| | Buoy Records | SSE Analysis | SSE Analysis | Buoy Records | SSE Analysis | Buoy Records | Buoy Records |
| Mykonos | 3.66 | 3.8 | 5.39 | 4.9 | 5.16 | 13.43 | 3.65 |
| Petrokaravo | 3.22 | – | – | 4.21 | – | 11.45 | 3.22 |

*Buoy records= data from the buoys directly; SSE=data as given by the sea surface elevation analysis

The most frequent waves in the Central Aegean have heights of up to 0.8 m that are related to periods from 2 to 3.6 s. Higher waves (>1.8 m for Petrokaravo and >4 m in Mykonos) are related to periods of up to 7 s. The direction of waves in Mykonos is of N, whilst in Petrokaravo the direction waves are propagating from is of NE and swells from SE.

The seasonal characteristics of the Central Aegean show that the minimum wave height is in May and can be of 0.7 m (Mykonos) and 0.34 m (Petrokaravo). The maximum spectral wave height can be of 0.65 m (January, from Petrokaravo buoy) and 1.19 m (December in Mykonos buoy) to 1.28 (February - SSE). The statistical wave height can reach up to 1.19 m in February as shown from the SSE analysis of Mykonos records.

Table 6.1.9: Seasonal Description of wave height for the Central Aegean Sea

| Central Aegean | H _{m0} (m) | | | | H _{1/3} (m) | |
|----------------|---------------------|------------|--------------|------------|----------------------|------------|
| | Buoy | | SSE | | SSE | |
| | Mean Monthly | | Mean Monthly | | Mean Monthly | |
| | Min | Max | Min | Max | Min | Max |
| Mykonos | MAY (0.76) | DEC (1.19) | MAY (0.78) | FEB (1.28) | MAY (0.7) | FEB (1.19) |
| Petrokaravo | MAY (0.34) | JAN (0.65) | – | – | – | – |

For the period, the minimum is estimated in May for Mykonos buoy and can be of 3.38 s (buoy records) and up to 4.73 s (Statistical wave period - SSE analysis). For Petrokaravo, the period is 3.07 s for September. The maximum periods are generally in winter months, i.e. December and February for Mykonos, January for Petrokaravo.

Table 6.1.10: Seasonal Description of wave period for the Central Aegean Sea

| Central Aegean | T _{m02} (s) | | | | T _{1/3} (s) | |
|----------------|----------------------|------------|--------------|------------|----------------------|------------|
| | Buoy | | SSE | | SSE | |
| | Mean Monthly | | Mean Monthly | | Mean Monthly | |
| | Min | Max | Min | Max | Min | Max |
| Mykonos | MAY (3.38) | DEC (3.92) | MAY (3.36) | FEB (4.07) | MAY (4.73) | FEB (5.85) |
| Petrokaravo | SEPT (3.07) | JAN (3.43) | – | – | – | – |

For the Central Aegean, atmospheric pressure ranges from 1012.82 to 1013.23 hPa and air temperature from 18.6 to 19.5 °C. Wind speed and gust are greater in Mykonos (6.81 m/s and 8.83 m/s, respectively).

Table 6.1.11: Mean of Atmospheric Parameters for the Central Aegean Sea

| Central Aegean | Atmospheric Pressure (hPa) | Air Temperature (°C) | Wind Speed (m/s) | Wind Gust (m/s) |
|----------------|----------------------------|----------------------|------------------|-----------------|
| Mykonos | 1013.23 | 18.6 | 6.81 | 8.83 |
| Petrokaravo | 1012.82 | 19.52 | 4.73 | 6.21 |

In Mykonos, the most frequent winds blow from the North and are mostly 4-8 m/s. Winds in Petrokaravo are blowing from NW to NE and are from 2- 4 m/s. Minimum air pressure is estimated during the summer months of August (Mykonos) and July (Petrokaravo) whilst the higher at January (Mykonos) and November (Petrokaravo). Air Temperature presents the same pattern at both locations, i.e. the maxima in August and minima in February. Minimum wind speed is during May, while maximum in February for Mykonos and December in Petrokaravo. The same apply for wind gust.

Table 6.1.12: Seasonal Description of atmospheric parameters for the Central Aegean Sea

| Central Aegean | Atmospheric Pressure (hPa) | | Air Temperature (°C) | | Wind Speed (m/s) | | Wind Gust (m/s) | |
|----------------|----------------------------|---------------|----------------------|-------------|------------------|------------|-----------------|------------|
| | Min | Max | Min | Max | Min | Max | Min | Max |
| Mykonos | AUG (1007.75) | JAN (1018.05) | FEB (12.32) | AUG (24.81) | MAY (5.51) | FEB (7.41) | MAY (7.12) | FEB (10.0) |
| Petrokaravo | JUL (1008.74) | NOV (1016.3) | FEB (11.61) | AUG (28.89) | MAY (3.53) | DEC (5.55) | MAY (4.55) | DEC (7.38) |

The most frequent waves in Mykonos have heights of 0-0.8 m and are related with wind speeds of 3-6 m/s. The higher waves (>4 m) are related with speeds of more than 12m/s. The highest and the most frequent waves are related with winds blowing from NW to N. For Petrokaravo, the most frequent waves have heights of 0.3-0.6m and are related with wind speeds of 4-6 m/s. The higher waves (>1.8m) are related with speeds more than 10 m/s. The most frequent waves (height and period) are related with winds blowing from NE while the highest with winds of SE.

For Mykonos, Kumaraswamy distribution underestimates the larger values of wave heights whilst Weibull and Rayleigh distribution overestimate them. From the ratios given for Mykonos, the following can be established for Central Aegean:

$$\frac{H_{m_0}}{H_{1/3}} = 1.1, \frac{H_{1/3}}{\sqrt{m_0}} = 3.65, \frac{H_{max}}{H_{m_0}} = 1.56, \frac{H_{max}}{H_{1/3}} = 1.7$$

6.1.3 South Aegean Sea

As shown in Figure 6.1.3, the buoys of E1M3A and Avgo are located between the Southern Cyclades and Northern Crete. The buoy of Santorini is located at the SSW of the island and that might lead for the absence of waves from the NNE and the small frequency of waves coming from the North due to the blockage from the Cyclades. The buoy of Dia is located between the Isle Dia and Heraklion leading to blockage of the waves coming from the NNE. Caution should be taken with waves coming from the NW - NE due to wave reflections and alteration of their characteristics due to the many islands that of the Central and South Aegean.



Figure 6.1.3: Location of the buoys in the South Aegean Sea

The means of the wave height parameters are shown in Table 6.1.13.

Table 6.1.13: Means of wave height parameters for the South Aegean Sea

| South Aegean | H _{m0} (m) | | H _{1/3} (m) | H _{max} (m) | | H _{m0a} (m) | H _{m0b} (m) |
|--------------|---------------------|--------------|----------------------|----------------------|--------------|----------------------|----------------------|
| | Buoy Records | SSE Analysis | SSE Analysis | Buoy Records | SSE Analysis | Buoy Records | Buoy Records |
| Avgo | 1.00 | – | – | – | – | 0.13 | 0.63 |
| Dia | 0.97 | – | – | – | – | 0.06 | 0.97 |
| E1M3A | 0.99 | – | – | 1.41 | – | 0.07 | 0.98 |
| Santorini | 0.9 | 0.98 | 0.9 | 1.28 | 1.5 | 0.06 | 0.89 |

*Buoy records= data from the buoys directly; SSE=data as given by the sea surface elevation analysis

The wave height in the South Aegean ranges from 0.97 to 1 m (H_{m0}) and 0.9 m for H_{1/3}. The maximum wave height ranges from 1.28 to 1.5 m. The wind waves have heights from 0.63 to 0.98 m with the highest in E1M3A and the lowest in Avgo. Swells have heights from 0.06 to 0.13 m with the highest in Avgo and the lowest in Dia and Santorini.

The spectral wave period is from 3.73 to 4.04 s, the lowest in Santorini and the highest in E1M3A. The statistical period can be up to 5.51 s as shown from Santorini buoy. The peak period is from 5 to 5.23 s with the lowest in Santorini and the highest in E1M3A. The wind waves have periods from 3.7 to 7 s, the highest in Avgo and the smallest in Santorini, whilst swells have periods from 12.14 s to 15 s with the highest in Avgo.

Table 6.1.14: Means of wave period parameters for the South Aegean Sea

| South Aegean | T _{m02} (s) | | T _{1/3} (s) | T _p (s) | | T _{m02a} (s) | T _{m02b} (s) |
|--------------|----------------------|--------------|----------------------|--------------------|--------------|-----------------------|-----------------------|
| | Buoy Records | SSE Analysis | SSE Analysis | Buoy Records | SSE Analysis | Buoy Records | Buoy Records |
| Avgo | 3.87 | – | – | 5.16 | – | 15.00 | 7.13 |
| Dia | 3.87 | – | – | 5.14 | – | 13.6 | 3.86 |
| E1M3A | 4.04 | – | – | 5.23 | – | 12.14 | 4.02 |
| Santorini | 3.73 | 3.84 | 5.51 | 5.01 | 5.2 | 13.16 | 3.72 |

*Buoy records= data from the buoys directly; SSE=data as given by the sea surface elevation analysis

The most frequent waves in the South Aegean Sea have heights that range from 0.5 to 1 m and are related to periods up to 4 s. Waves with heights of more than 3 m are related to periods of more than 5 s. Most of the waves propagate from westerly directions except in the case of Santorini where there are waves propagating from the North as well (this applies for wind-waves and swells as well). Higher waves are mostly propagating from the West for all buoys. Lower wave heights are apparent during calmer months such as September and May, whilst higher waves are during winter months.

Table 6.1.15: Seasonal Description of wave height for South Aegean Sea

| South Aegean | H _{m0} (m) | | | | H _{1/3} (m) | |
|--------------|---------------------|------------|--------------|------------|----------------------|------------|
| | Buoy | | SSE | | SSE | |
| | Mean Monthly | | Mean Monthly | | Mean Monthly | |
| | Min | Max | Min | Max | Min | Max |
| Avgo | SEPT (0.84) | FEB (1.19) | – | – | – | – |
| Dia | SEPT (0.69) | JAN (1.18) | – | – | – | – |
| E1M3A | MAY (0.7) | DEC (1.16) | – | – | – | – |
| Santorini | MAY (0.71) | FEB (1.15) | AUG (0.71) | DEC (1.32) | AUG (0.64) | DEC (1.23) |

For wave period, the minima are mostly during summer months and even beginning of autumn (September in Avgo). As in the case of wave height the maxima are during winter months with the highest from the statistical wave period T_{1/3} in Santorini in December.

Table 6.1.16: Seasonal Description of wave period for the South Aegean Sea

| South Aegean | T _{m02} (s) | | | | T _{1/3} (s) | |
|--------------|----------------------|------------|--------------|------------|----------------------|------------|
| | Buoy | | SSE | | SSE | |
| | Mean Monthly | | Mean Monthly | | Mean Monthly | |
| | Min | Max | Min | Max | Min | Max |
| Avgo | SEP (3.71) | FEB (4.15) | – | – | – | – |
| Dia | AUG (3.46) | FEB (4.14) | – | – | – | – |
| E1M3A | JUN (3.75) | DEC (4.11) | – | – | – | – |
| Santorini | JUL (3.49) | FEB (4.1) | AUG (3.41) | DEC (4.25) | AUG (4.87) | DEC (6.12) |

For the South Aegean, atmospheric pressure is around 1014.45 hPa and air temperature around 19.67 °C. Wind speed is approximately 5.48 m/s and wind gust 7.3 m/s with the higher in Santorini.

Table 6.1.17: Mean of Atmospheric Parameters for the South Aegean Sea

| South Aegean | Atmospheric Pressure (hPa) | Air Temperature (°C) | Wind Speed (m/s) | Wind Gust (m/s) |
|--------------|----------------------------|----------------------|------------------|-----------------|
| Avgo | 1014.69 | 19.62 | 5.51 | 7.39 |
| Dia | – | – | – | – |
| E1M3A | 1014.46 | 19.73 | 5.31 | 7.14 |
| Santorini | 1014.24 | 19.66 | 5.6 | 7.47 |

The wind direction of South Aegean is mostly from W (for the most frequent speeds of 3 – 6 m/s) except in the case of Santorini where the most frequent winds (6–9 m/s) are blowing from the North. Maximum wind speeds are mostly from W to NW direction for all 4 buoys.

Seasonal description of the atmospheric parameters for the South Aegean Sea is shown in Table 6.1.18.

Table 6.1.18: Seasonal Description of atmospheric parameters for the South Aegean Sea

| South Aegean | Atmospheric Pressure (hPa) | | Air Temperature (°C) | | Wind Speed (m/s) | | Wind Gust (m/s) | |
|--------------|----------------------------|---------------|----------------------|-------------|------------------|------------|-----------------|------------|
| | Min | Max | Min | Max | Min | Max | Min | Max |
| Avgo | JUL (1010.28) | NOV (1017.87) | FEB (13.16) | AUG (22.56) | MAY (4.5) | FEB (6.62) | MAY (5.92) | FEB (8.99) |
| Dia | – | – | – | – | – | – | – | – |
| E1M3A | JUL (1010.24) | JAN (1018.7) | FEB (13.31) | AUG (25.77) | MAY (4.51) | DEC (6.08) | MAY (5.71) | DEC (8.65) |
| Santorini | JUL (1009.52) | NOV (1017.79) | JAN (13.94) | AUG (25.76) | MAY (4.64) | FEB (6.8) | MAY (6.14) | FEB (9.17) |

The minima pressure is during July for all buoys whilst the maxima are in November (Avgo and Santorini) and January for E1M3A. Air temperature has the lowest monthly means in the winter months and the

highest in August. Wind speed and gust are low during May while the higher ones are during winter months such as February and December.

The South Aegean Sea is characterized by waves with heights of 0.5 to 1 m that are related to wind speeds of 3 to 6 m/s. Higher waves (> 3m) are related to winds of more than 15 m/s.

For Santorini, it is shown that Kumaraswamy distribution underestimates the larger values of wave heights, whilst Weibull and Rayleigh distribution diverge from the mean values and overestimate the higher ones. From the ratios given for Santorini buoy, the following can be established South Aegean:

$$\frac{H_{m_0}}{H_{1/3}} = 1.1, \frac{H_{1/3}}{\sqrt{m_0}} = 3.65, \frac{H_{max}}{H_{m_0}} = 1.53, \frac{H_{max}}{H_{1/3}} = 1.68$$

6.1.4 Northeast Ionian Sea

The buoy of Zakynthos that is considered as representative of the northeast Ionian is located between the islands of Kefallonia and Zakynthos, at the NW part of the latter.

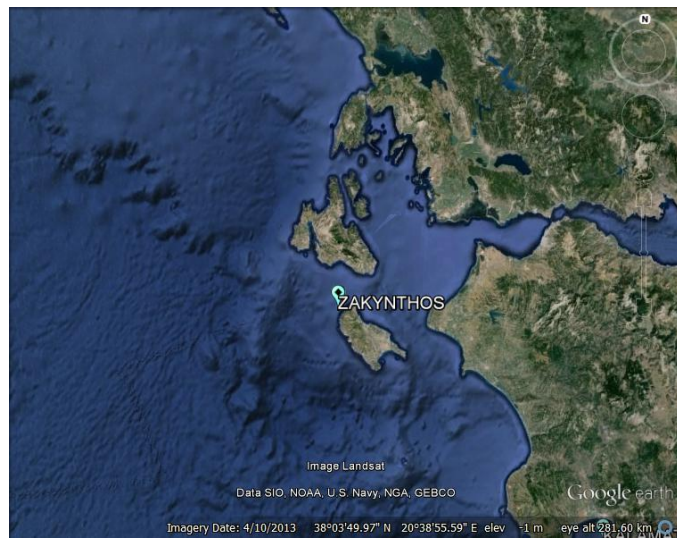


Figure 6.1.4: Location of the buoys in the Northeast Ionian Sea

For the Northeast Ionian, the significant spectral wave height ranges from 0.8 to 0.99 m, while the statistical is around 0.89 m. The maximum wave height might have means that range from 1.5 to 3.9 m as shown from the records and the SSE analysis of Zakynthos buoy. The swells have heights of 0.11 m and the wind induced waves 0.81 m. As for the period, the spectral mean period is from 3.9 to 4.14 s, while the statistical is around 6.15 s. The peak period is around 5.35 s to 5.81 s, while the period of swells can be around 13.1 s and wind waves of 3.81 s.

Table 6.1.19: Means of wave height and period parameters for the Northeast Ionian Sea

| North East Ionian | Hm ₀ (m) | | H _{1/3} (m) | H _{max} (m) | | Hm _{0a} (m) | Hm _{0b} (m) |
|-------------------|----------------------|--------------|----------------------|----------------------|--------------|-----------------------|-----------------------|
| | Buoy Records | SSE Analysis | SSE Analysis | Buoy Records | SSE Analysis | Buoy Records | Buoy Records |
| Zakynthos | 0.82 | 0.99 | 0.89 | 3.86 | 1.51 | 0.11 | 0.81 |
| | Tm ₀₂ (s) | | T _{1/3} (s) | T _p (s) | | Tm _{02a} (s) | Tm _{02b} (s) |
| Zakynthos | 3.86 | 4.14 | 6.15 | 5.35 | 5.81 | 13.07 | 3.81 |

*Buoy records= data from the buoys directly; SSE=data as given by the sea surface elevation analysis

The most frequent waves propagate from SW and most of them have heights of 0-0.5 m. The higher waves (>3m) are from the SW-W. Periods are 2.7-3.4 s mostly from W – NW, while the longer periods are from SW to W. Waves with heights of 0.5 to 1m are related to periods of 2.7 to 3.4s. The higher waves (>3m) are related with periods of more than 6.2s.

From the seasonal characteristics it is shown that the minima of wave height are apparent during late spring – early summer and range from 0.56 to 0.6 m. The maxima are during the winter season and range from 1.2 to 1.3 m. The period shows its minima during May and July and this range from 3.41 to 5.23 s, while the maxima are during February and range from 4.49 to 6.89 s.

Table 6.1.20: Seasonal Description of wave height and period for the Northeast Ionian Sea

| Northeast Ionian | Hm ₀ (m) | | | | H _{1/3} (m) | |
|-------------------|----------------------|------------|--------------|------------|----------------------|------------|
| | Buoy | | SSE | | SSE | |
| | Mean Monthly | | Mean Monthly | | Mean Monthly | |
| | Min | Max | Min | Max | Min | Max |
| Zakynthos | MAY (0.56) | FEB (1.23) | JUN (0.56) | FEB (1.3) | JUN (0.59) | DEC (1.19) |
| North East Ionian | Tm ₀₂ (s) | | | | T _{1/3} (s) | |
| | Buoy | | SSE | | SSE | |
| | Mean Monthly | | Mean Monthly | | Mean Monthly | |
| | Min | Max | Min | Max | Min | Max |
| Zakynthos | JUL (3.41) | FEB (4.49) | MAY (3.6) | FEB (4.64) | MAY (5.23) | FEB (6.89) |

The mean atmospheric parameters for the Northeast Ionian, as shown by Zakynthos buoy, are shown in Table 6.1.21.

Table 6.1.21: Mean of Atmospheric Parameters for the Northeast Ionian Sea

| Northeast Ionian | Atmospheric Pressure (hPa) | Air Temperature (°C) | Wind Speed (m/s) | Wind Gust (m/s) |
|------------------|----------------------------|----------------------|------------------|-----------------|
| Zakynthos | 1015.49 | 17.57 | 4.96 | 6.68 |

The main directions of wind are blowing from W to NE with the most frequent wind speeds ranging from 2m/s to 4m/s. Winds above 14m/s have directions of NE and this can be due to channelling effects or event coastal - catabatical winds.

Wind speed and wind gust present their minima during May and the maxima during winter months (January and December respectively). The atmospheric pressure has its minimum during August and the maxima during January, while air temperature has the minimum during February and the maximum during August.

Table 6.1.22: Seasonal Description of atmospheric parameters for the Northeast Ionian Sea

| Northeast Ionian | Atmospheric Pressure (hPa) | | Air Temperature (°C) | | Wind Speed (m/s) | | Wind Gust (m/s) | |
|------------------|----------------------------|---------------|----------------------|------------|------------------|------------|-----------------|------------|
| | Min | Max | Min | Max | Min | Max | Min | Max |
| Zakynthos | AUG (1009.89) | JAN (1016.72) | FEB (12.71) | AUG (25.9) | MAY (3.94) | JAN (6.42) | MAY (5.14) | DEC (8.82) |

The most frequent waves have heights of up to 0.8 m and most of them are related with wind speeds of 2-4 m/s. Furthermore, the higher waves (>3.2m) are related with speeds of above 10m/s wind speeds. The highest and the most frequent waves are related with winds blowing from W to NW and this applies for the most frequent periods.

For Zakynthos buoy, it is shown that Kumaraswamy distribution underestimates the larger values of wave heights whilst Weibull and Rayleigh distribution diverge from the mean values. From the ratios given for Zakynthos, the following can be established for Northeast Ionian:

$$\frac{H_{m_0}}{H_{1/3}} = 1.11, \frac{H_{1/3}}{\sqrt{m_0}} = 3.62, \frac{H_{max}}{H_{m_0}} = 1.54, \frac{H_{max}}{H_{1/3}} = 1.7$$

6.1.5 Southeast Ionian Sea

The buoy of Pylos is located at the southwestern part of the Peloponnese and due to its proximity to the coast; waves from the east and northeast might be absent. The buoy of Kalamata is located close to the harbour of Kalamata, at the Messinian Gulf and waves from N to E are blocked.

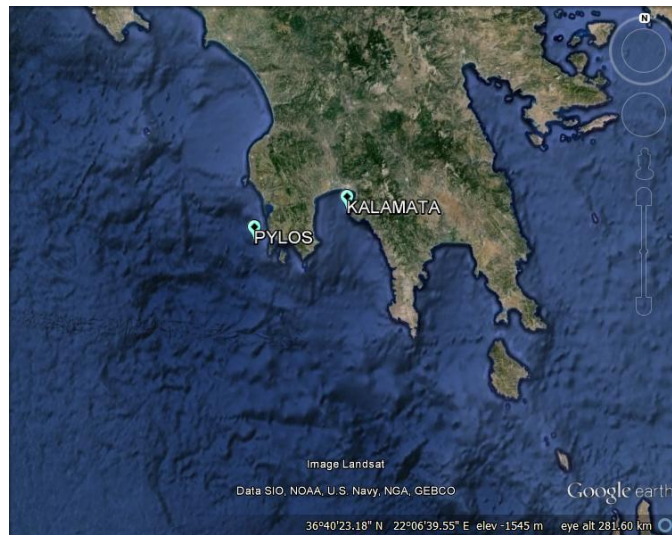


Figure 6.1.5: Location of the buoys in the Southeast Ionian Sea

The wave height of the Southeast Ionian is characterized by wave heights from 0.34 to 1.2 m (H_{m0}) and 0.57 to 1.1 m ($H_{1/3}$). The maximum wave height can be in the case of Pylos from 1.37 to 1.82 m and 0.29 to 0.95 m in Kalamata. The swells have heights from 0.02 to 0.12 m and the wind waves from 0.34 to 0.96 m.

Table 6.1.23: Means of wave height parameters for the Southeast Ionian Sea

| South East Ionian | H_{m0} (m) | | $H_{1/3}$ (m) | H_{max} (m) | | H_{m0a} (m) | H_{m0b} (m) |
|-------------------|--------------|--------------|---------------|---------------|--------------|---------------|---------------|
| | Buoy Records | SSE Analysis | SSE Analysis | Buoy Records | SSE Analysis | Buoy Records | Buoy Records |
| Pylos | 0.96 | 1.2 | 1.1 | 1.37 | 1.82 | 0.12 | 0.96 |
| Kalamata | 0.34 | 0.68 | 0.57 | 0.29 | 0.95 | 0.02 | 0.34 |

Spectral wave period ranges from 3.38 to 4.51 s while the statistical from 5.74 to 6.36 s. The peak period is from 4.35 to 6.12 s. The swells have periods from 11.77 to 12.35s and the wind waves from 3.36 s to 4.36s.

Table 6.1.24: Means of wave period parameters for the Southeast Ionian Sea

| South East Ionian | T_{m02} (s) | | $T_{1/3}$ (s) | T_p (s) | | T_{m02a} (s) | T_{m02b} (s) |
|-------------------|---------------|--------------|---------------|--------------|--------------|----------------|----------------|
| | Buoy Records | SSE Analysis | SSE Analysis | Buoy Records | SSE Analysis | Buoy Records | Buoy Records |
| Pylos | 4.33 | 4.51 | 6.36 | 5.81 | 6.12 | 11.77 | 4.36 |
| Kalamata | 3.38 | 3.91 | 5.74 | 4.35 | 5.26 | 12.35 | 3.36 |

*Buoy records= data from the buoys directly; SSE=data as given by the sea surface elevation analysis

For Pylos, the most frequent waves are propagating from the SW to NW while the swells from SW to W. The largest wave heights have directions of are from W and the same for swells as well. For Kalamata, the most frequent waves and swells have directions from SE to S (heights ranging from 0 to 1 m).

For the seasonal characteristics of the Southeast Ionian, it is shown that the minima in wave period and wave height are given for Pylos and Kalamata during summer. Whilst, the higher values of the parameters are shown in winter months, mostly December and January.

Table 6.1.25: Seasonal Description of wave height for the Southeast Ionian Sea

| Southeast Ionian | H _{m0} (m) | | | | H _{1/3} (m) | |
|------------------|---------------------|------------|--------------|------------|----------------------|------------|
| | Buoy | | SSE | | SSE | |
| | Mean Monthly | | Mean Monthly | | Mean Monthly | |
| | Min | Max | Min | Max | Min | Max |
| Pylos | AUG (0.6) | DEC (1.52) | AUG (0.75) | JAN (1.77) | JUL (0.65) | JAN (1.66) |
| Kalamata | AUG (0.26) | DEC (0.44) | AUG (0.51) | JAN (0.98) | AUG (0.33) | JAN (0.9) |

For Pylos, the most frequent waves have heights from 0 to 0.8 m with most of them related to periods of 3 to 4 s. Waves with heights of more than 4 m are mostly related to periods of 7-8 s. For Kalamata, the highest waves (>3 m) are related to periods of 6 to 7 sec while waves with heights from 0 to 1 m are related to periods of 2 to 3 s.

Table 6.1.26: Seasonal Description of wave period for the Southeast Ionian Sea

| South - East Ionian | T _{m02} (s) | | | | T _{1/3} (s) | |
|---------------------|----------------------|------------|--------------|------------|----------------------|------------|
| | Buoy | | SSE | | SSE | |
| | Mean Monthly | | Mean Monthly | | Mean Monthly | |
| | Min | Max | Min | Max | Min | Max |
| Pylos | JUL (3.71) | DEC (5.07) | JUL (3.77) | JAN (5.18) | JUL (5.19) | JAN (7.4) |
| Kalamata | AUG (2.97) | DEC (3.74) | JUL (2.78) | JAN (4.11) | JUL (3.42) | DEC (6.29) |

The mean atmospheric parameters for the Southeast Ionian, as given by the buoys of Pylos and Kalamata, show that atmospheric pressure ranges from 1013 to 1015 hPa, temperature from 18.9 to 19.5 °C, wind speed from 3.7 to 4.9 m/s and gust from 4.92 to 6.62 m/s.

Table 6.1.27: Mean of Atmospheric Parameters for Southeast Ionian Sea

| Southeast Ionian | Atmospheric Pressure (hPa) | Air Temperature (°C) | Wind Speed (m/s) | Wind Gust (m/s) |
|------------------|----------------------------|----------------------|------------------|-----------------|
| Pylos | 1014.97 | 19.52 | 4.93 | 6.62 |
| Kalamata | 1013.13 | 18.89 | 3.7 | 4.92 |

For Pylos, the most frequent winds are blowing from NW and E / SE, with the higher winds blowing from SE. For Kalamata, winds are blowing from NW and from SE. The most frequent winds range from 0 to 3 m/s and most of them are of NW while winds above 12 m/s are blowing from SE.

For the Southeast Ionian, the seasonal description is the same for both buoys in the cases of atmospheric pressure and air temperature i.e. the minima of atm. pressure are in summer and the maxima in winter and vice versa for air temperature. Wind speed and wind gust have their minima during summer and their maxima in winter for Pylos, while Kalamata minima are for wind speed in autumn and wind gust in spring, while the maxima remain in winter.

Table 6.1.28: Seasonal Description of atmospheric parameters for the Southeast Ionian Sea

| Southeast Ionian | Atmospheric Pressure (hPa) | | Air Temperature (°C) | | Wind Speed (m/s) | | Wind Gust (m/s) | |
|------------------|----------------------------|---------------|----------------------|-------------|------------------|------------|-----------------|------------|
| | Min | Max | Min | Max | Min | Max | Min | Max |
| Pylos | AUG (1011.7) | JAN (1018.12) | FEB (13.6) | AUG (26.71) | AUG (4.0) | DEC (5.97) | AUG (5.15) | DEC (8.25) |
| Kalamata | AUG (1008.66) | JAN (1017.32) | FEB (12.58) | AUG (26.74) | OCT (3.33) | DEC (4.19) | APR (4.49) | FEB (5.75) |

The Southeast Ionian is characterized by waves with heights of 0 - 0.8 m (Pylos) and 0 - 0.3 m (Kalamata) that are related to wind speeds of 2 to 4 m/s. Higher waves (>2.4 m) are related to winds with speeds of more than 8 m/s.

From the analysis of the ratios the following are shown:

$$\begin{aligned}
 \text{Pylos: } & \frac{H_{m_0}}{H_{1/3}} = 1.07, \quad \frac{H_{1/3}}{\sqrt{m_0}} = 3.73, \quad \frac{H_{max}}{H_{m_0}} = 1.55, \quad \frac{H_{max}}{H_{1/3}} = 1.67, \\
 \text{Kalamata: } & \frac{H_{m_0}}{H_{1/3}} = 1.39, \quad \frac{H_{1/3}}{\sqrt{m_0}} = 1.28, \quad \frac{H_{max}}{H_{m_0}} = 1.55, \quad \frac{H_{max}}{H_{1/3}} = 1.67
 \end{aligned}$$

For the South East Ionian, the Kumaraswamy is considered best for the representation of the probability distribution of wave heights, with Kumaraswamy distribution overestimating the larger values of wave heights, whilst Weibull and Rayleigh distribution diverge from the mean values.

6.1.6 Remarks for the Greek Seas / Observations

The results of the aforementioned analysis provide information about the states of the 5 different subareas of the Greek Seas, but also emphasize the variability of those states. Either focusing on the wave state or the wind state, it is now evident that neither should be analyzed separately or considered representative of a wider area than that of the approximate area of the location of the buoy. Additionally, variations in the period of recording per buoy or lack of data for parameters should always be kept in mind. Furthermore, it is evident that the location of the buoy is highly important especially for the directionality and evolution of waves. Analytically, the buoys of Kalamata, Petrokaravo and Katerini are located in enclosed areas (Messiniac Gulf, Argosaronic Gulf and Thermaic Gulf) that block either the formation of higher waves (mostly up to 3 m in all cases) or the directionality of the waves (varies according to the buoy). By examining the period of the waves, there can be some conclusions on

swell or wind wave presence per area. For example, the buoy of Avgo presents the longest mean period of swell and the longest mean period of wind induced waves. The locality of Avgo buoy might suggest that wind waves and swells from all directions can be recorded by the buoy as it is one of the most offshore “open sea” buoys. Wave charts of the buoys of Mykonos, Skyros, Lesvos, Zakyntos, Pylos and Dia show the apparent blockage of waves from specific directions due to the nearby land. It is shown that Northerly waves are most frequent in the Aegean, whilst the Ionian is affected more by SW – NW waves. The directionality of these waves is mostly related to wind patterns known to form in the aforementioned regions. Specifically, literature suggests that the Aegean is dominated mostly by NE (in the North Aegean Sea) winds that turn to NW (in the South Aegean Sea) and this is shown in wave directionality as well (Poulos et al., 1997; Lionello, Malanotte-Rizzoli, Boscolo, Alpert, et al., 2006; Soukissian, 2008; Tyrlis and Lelieveld, 2013). The Ionian Sea is mostly effected by Sirocco winds and the cyclogenesis of the Adriatic Sea, i.e. wave directionality is from SW to NW (Bagiorgas et al., 2012; Nastos et al., 2013; Poulos et al., 2014). Wave directions should not be considered as a result of the wind dominant at the under-examination location and time but should be discussed according to previous temporal and non - local data i.e. swells recorded on a specific site that are generated elsewhere and their propagation might have altered their characteristics.

The most frequent waves in Greek Seas have heights up to 1 m and are related with periods of up to 4 sec and wind speeds of up to 8 m/s (depending on locality). Higher waves (more than 3 m) are evident in areas with large fetch (according to wind direction) and are related to periods of more than 5 s and wind speeds of more than 10 m/s. It should be noted again, that every area should be analyzed according to its microclimate (either wind or wave).

The seasonal characteristics, either for wind or for wave state, present that the higher values (for wave height and wind speeds) are during winter months, while the lower are mostly during late spring (May) – early summer (June) and even early autumn (September). Temperature follows a reasonable seasonality with the higher values during July – August and the lower during winter for Aegean and the Ionian Sea.

The surface elevation data analysis provides more information about the wave state than that of the direct measurements as provided by the buoy. Analytically, details about the apparent wave characteristics can result in remarks for maximum wave height, statistical wave height - period, wave steepness etc. The spectral characteristics can also lead to the determination of the wave state according to wave periods (i.e. different types of waves such as swells, wind-waves, and freak waves) that cannot be determined by records of only wave characteristics. Furthermore, from the sea surface elevation data in all locations, ratios among wave characteristics have been estimated. The importance shown here is that the empirical equation of $H_{\max} = 2 * H_s$ should not be applied in the Greek Seas as the ratio is shown to range from 1.5 to 1.7 either by using the spectral or the statistical significant wave height. Furthermore, it is proven that the statistical and the spectral significant wave height have a ratio of approximately 1, which is similar to what is suggested from literature (Holthuijsen, 2007) for offshore conditions. Considering the ratio of $H_{1/3} = 4 * \sqrt{m_0}$ it is also shown that the ratio is closer to the range of 3.5 to 3.7 than that of 4, so this should also be carefully applied. As for the wave period, further analysis is suggested to evaluate the relationships between statistical and spectral estimates in order to include parameters such as spectral width, moments but also maybe consider wave types as well (swells - wind waves).

6.2 ERA-INTERIM

To present the relation between the ERA-Interim dataset and the Poseidon Buoys, the Greek Seas have been divided in the following sub-basins:

- 1) North Aegean: described by the buoys of Athos, Lesvos and Skyros
- 2) Central Aegean: described by the buoy of Mykonos
- 3) South Aegean: described by the buoys of Avgo, E1M3A and Santorini
- 4) Southeast Ionian: described by Pylos

As in the case of the Poseidon buoys analysis, it should be mentioned that the correlated timeseries differ in time period and locations. Furthermore, as presented in the chapter of methodology (Ch. 4.2) and the chapter of the results (Ch. 5.2), different methods are shown and preferred per buoy and per parameter for the correlation of buoys and the reanalysis. In addition, remarks on the 35 year long term statistical analysis of selected points that are considered representatives of the Greek Seas for the wave and weather state, are also discussed in this chapter. This analysis showed any likely or not trends per parameter for the annual and monthly values, as well as the monthly anomalies. Northeast Ionian is not included in the correlation analysis of the buoys with the ERA-Interim dataset, as Zakynthos buoy is located amongst the islands of Zakynthos and Kefallonia and no collocation is possible with the gridded dataset.

6.2.1 North Aegean

The relation of the buoys and the weighted distance average data of ERA-Interim for the significant wave height are shown in Table 6.2.1, along with the differences for the monthly and the annual values.

Table 6.2.1: Significant Wave Height Statistics of buoys - ERA-Interim for the North Aegean Sea

| Location | N | Corr. | RMSE | Bias | Mean | Max | St. Dev. | Min Monthly Dif. | Max Monthly Dif. | Min Annual Dif. | Max Annual Dif. |
|----------------------------|-------|-------|------|--------|------|------|----------|-------------------------------|-------------------------------|--------------------------------|--------------------------------|
| Athos Hm ₀ (m) | 13842 | 0.76 | 0.49 | 0.08 | 0.8 | 5.63 | 0.73 | Buoy higher 0.03 (DEC) | Buoy higher 0.19 (JAN) | Buoy higher 0.04 (2011) | Buoy higher 0.15 (2002) |
| Athos SWH - WA (m) | | | | | 0.72 | 5.25 | 0.64 | | | | |
| Lesvos Hm ₀ (m) | 14229 | 0.65 | 0.56 | -0.17 | 0.77 | 4.92 | 0.55 | Buoy higher 0.001 (MAY) | ERA-I higher 0.32 (DEC) | ERA-I higher 0.10 (2002) | ERA-I higher 0.25 (2011) |
| Lesvos SWH - WA (m) | | | | | 0.94 | 6.04 | 0.72 | | | | |
| Skyros Hm ₀ (m) | 5666 | 0.94 | 0.23 | -0.002 | 0.87 | 4.85 | 0.69 | ERA-I higher 0.01 (DEC) | ERA-I higher 0.08 (APR) | Buoy higher 0.004 (2008) | Buoy higher 0.03 (2007) |
| Skyros SWH - WA (m) | | | | | 0.87 | 5.47 | 0.7 | | | | |

The correlation (r) varies from 0.65 to 0.94, the RMSE from 0.23 to 0.56 m and the bias from 0.002 to 0.17 m (absolute values). The mean values of wave height vary from 0.77 m to 0.94 m, whilst the maximum values from 4.8 m to 6 m. In the case of monthly means, the absolute differences can be up to 0.32 m and for the annual up to 0.25 m.

Statistics of the data of ERA-Interim and buoys for wind speed at 10 m are shown in Table 6.2.2 along with the differences for the monthly and the annual values. The correlation varies from 0.72 to 0.84, the RMSE from 2 m/s to 2.64 m/s and the bias from 0.01 m/s to 0.33 m/s. Mean wind speed varies according to location from 5.44 m/s to 6.96 m/s and the maximum wind speed from 18.25 m/s to 30.24 m/s. Additionally, monthly differences vary from 0.004 m/s to 0.85 m/s and the annual from 0.10 m/s to 6.5 m/s.

Table 6.2.2: Wind Speed at 10 m Statistics of buoys - ERA-Interim for the North Aegean Sea

| Location | N | Corr | RMSE | Bias | Mean | Max | St. Dev. | Min Monthly Dif. | Max Monthly Dif. | Min Annual Dif. | Max Annual Dif. |
|-------------------------|-------|------|------|------|------|-------|----------|--------------------------|-------------------------|-------------------------|-----------------------------|
| Athos Wind Speed (m/s) | 12582 | 0.84 | 2.00 | 0.33 | 5.77 | 23.89 | 3.9 | Buoy higher 0.03 (JUN) | Buoy higher 0.85 (DEC) | Buoy higher 4 (2002) | Buoy higher 6.5 (2005,2010) |
| Athos W10 SP (m/s) | | | | | 5.44 | 21.06 | 3.26 | | | | |
| Lesvos Wind Speed (m/s) | 13322 | 0.72 | 2.64 | 0.21 | 6.96 | 30.24 | 3.92 | Buoy higher 0.06 (DEC) | Buoy higher 0.86 (MAR) | Buoy higher 0.10 (2005) | Buoy higher 0.85 (2011) |
| Lesvos W10 WA (m/s) | | | | | 6.76 | 24.56 | 3.45 | | | | |
| Skyros Wind Speed (m/s) | 4908 | 0.72 | 2.25 | 0.01 | 6.49 | 21.48 | 3.48 | ERA-I higher 0.004 (MAY) | ERA-I higher 0.68 (FEB) | Buoy higher 0.18 (2007) | Buoy higher 1.57 (2011) |
| Skyros W10 WA (m/s) | | | | | 6.48 | 18.25 | 3.00 | | | | |

For temperature at 2 m above sea surface, correlation is 0.93 - 0.96, RMSE from 2.14 °C to 2.39 °C and absolute bias from 0.28 °C to 0.52 °C. For the mean monthly differences, there is a range of 0.06 °C to 2.88 °C and for the annual values from 0.02 °C to 1.62 °C.

Table 6.2.3: Temperature at 2m Statistics of buoys - ERA-Interim for the North Aegean

| Location | N | Corr . | RMSE | Bias | Mean | Max | St. Dev. | Min Monthly Dif. | Max Monthly Dif. | Min Annual Dif. | Max Annual Dif. |
|------------------------|-------|--------|------|--------|-------|-------|----------|----------------------------|---------------------------|--------------------------|----------------------------|
| Athos Temp. (°C) | 14055 | 0.96 | 2.14 | - 0.28 | 17.54 | 30.16 | 6.08 | ERA- I higher <2 (AUT-WIN) | ERA-I higher >2 (SPR-SUM) | ERA-I higher 0.05 (2007) | ERA-I higher 1.43 (2005) |
| Athos T2M SP (°C) | | | | | 17.82 | 33.74 | 7.02 | | | | |
| Lesvos Temp. (°C) | 14379 | 0.95 | 2.31 | - 0.52 | 17.36 | 34.79 | 5.35 | ERA-I higher 0.06 (OCT) | ERA-I higher 2.88 (JUL) | ERA-I higher 0.02 (2002) | ERA-I higher 1.53 (2005) |
| Lesvos T2M WA 1-2 (°C) | | | | | 17.92 | 33.10 | 6.63 | | | | |
| Skyros Temp. (°C) | 5604 | 0.93 | 2.39 | - 0.40 | 17.17 | 30.33 | 6.17 | ERA-I higher 0.13 (MAR) | ERA-I higher 1.46 (JUL) | Buoy higher 0.06 (2009) | ERA - I higher 1.62 (2011) |
| Skyros T2M SP (°C) | | | | | 17.57 | 32.09 | 6.53 | | | | |

Synopsis

The analysis of the data of the period 1979-2013 for the North Aegean Sea, presents that mean wave height is of 0.78 m, maximum can reach 5.62 m and mean wave period can be of 4.11 s. The wave directionality, as given by the wave chart, is shown to be mainly from N directions and secondarily from S, while winds blow from N to NE directions. The most frequent waves have heights that range from 0 to 0.5 m and periods of 2 - 4 s, with the most frequent winds to have speeds of 2-8 m/s. The seasonal analysis shows that wave heights and periods are lower in June and higher in December / January; the same pattern applies for winds.

The trends per month show that is virtually certain to have a decrease for the significant wave height during February and very likely to have an increase in April. For mean wave period, it is virtually certain to have an increase in April and very likely in June. The annual trends show that significant wave height is unlikely to have changed while mean wave period is virtually certain to increase. The monthly anomalies confirm that it is unlikely to have a trend for significant wave height, whilst it is virtually certain that mean wave period will increase. Mean wind speed is of 5.7 m/s and can be up to 22 m/s, whilst mean temperature is of 18 °C and can reach a maximum of 35.6°C. The main wind direction is of NE, while the secondary is from South. The monthly means of wind speeds are likely to show an increase, while temperature is virtually certain and very likely to increase from May to September. Additionally, in the annual values, it is about likely as not for wind speed to have changed whilst it is virtually certain for temperature to have increased. In addition, the mean monthly anomalies show that wind speed is about likely as not to present a trend, while temperature is virtually certain to have increased.

6.2.2 Central Aegean

The statistics of the relation between the Mykonos buoy and the data from the methods of ERA-Interim for the Central Aegean Sea are shown in the Table 6.2.4. The mean value of wave height is around 1 m, the maximum value is around 5.6 m, mean wind speed is from 6.7 m/s to 7.9 m/s and the maximum from 21 m/s to 21.87 m/s. Finally, temperature has a mean value of 18.5 °C to 19 °C and a maximum of 32.9 °C to 41.8 °C. For wave height, the correlation is 0.87, the RMSE is 0.34 m and the bias is 0.04 m. The mean monthly differences range from 0.03 m to 0.13 m, with the annual ones from 0.003 m to 0.10 m. Wind speed has a correlation of 0.82, a RMSE of 2.27 m/s and a bias of 1.21 m/s. The monthly differences are from 0.73 m/s to 1.69 m/s and the annual from 0.45 m/s to 1.96 m/s. Finally, temperature of buoy and ERA-Interim shows a correlation of 0.91, a RMSE of 2.41°C and an absolute bias of 0.47°C. Furthermore, the monthly differences range from 0.02 °C to 2.04 °C and the annual from 0.28 °C to 1.10°C.

Table 6.2.4: Statistics of Wave and Atmospheric Parameters Mykonos - ERA-Interim for the Central Aegean Sea

| Location | N | Corr | RMSE | Bias | Mean | Max | St. Dev. | Min Monthly Dif. | Max Monthly Dif. | Min Annual Dif. | Max Annual Dif. |
|--------------------------|-------|------|------|-------|-------|-------|----------|-------------------------|-------------------------|--------------------------|--------------------------|
| Mykonos H_{m0} (m) | 13702 | 0.87 | 0.34 | 0.04 | 1.01 | 5.63 | 0.75 | ERA-I higher 0.03 (MAR) | ERA-I higher 0.13 (JUL) | Buoy higher 0.003 (2001) | Buoy higher 0.10 (2002) |
| Mykonos SWH - WA (m) | | | | | 0.96 | 5.61 | 0.65 | | | | |
| Mykonos Wind Speed (m/s) | 12974 | 0.82 | 2.27 | 1.21 | 7.89 | 21.87 | 4.1 | Buoy higher 0.73 (FEB) | Buoy higher 1.69 (SEP) | Buoy higher 0.45 (2003) | Buoy higher 1.96 (2006) |
| Mykonos W10 WA (m/s) | | | | | 6.69 | 20.96 | 3.27 | | | | |
| Mykonos Temp. (°C) | 13814 | 0.91 | 2.41 | -0.47 | 18.54 | 41.86 | 4.87 | ERA-I higher 0.02 (OCT) | ERA-I higher 2.04 (JUL) | ERA-I higher 0.28 (2009) | ERA-I higher 1.10 (2006) |
| Mykonos T2M SP (°C) | | | | | 19.01 | 32.97 | 5.74 | | | | |

Synopsis

35-year analysis shows that the mean wave height of the Central Aegean is around 1 m, with period of 4.46 s, while maximum height is up to 6.06 m. The most frequent wave directions are from NE while secondary directions are from S. Mean wind speed is of 6.8 m/s and mean temperature of 18°C. The most frequent waves have heights that range from 0 to 1 m and are related to periods of 2 s to 6 s.

The most frequent wind speeds are those of 2 - 6 m/s blowing from the NW to NE. Waves heights and periods are lower during May, being higher during winter period (December – February). This pattern applies for wind speed as well.

The monthly means of wave height show that during April, it is very likely to have an increase and likely to have a decrease in September. In the case of mean wave period, it is virtually certain to have an increase in April and very likely in June. The annual values show that it is likely to have a decreasing trend of significant wave height of 0.0014 m, whilst it is very likely that there is an increase in the mean wave period. The anomaly of the monthly means for the period 1979-2013 shows that it is likely not to have a decrease in an annual basis, whilst for mean wave period it is virtually certain to present an increase. Wind speed is very likely to increase in April and very likely to decrease in September. Temperature is likely to virtually certain to increase during the period May to September. The annual values show that it is very likely to have a decrease in wind speed and virtually certain to have an increase in temperature. The monthly anomaly means show that it is virtually certain that there will be a decrease in wind speed and virtually certain that temperature will increase.

6.2.3 South Aegean

The statistics of the correlation between the buoy and the ERA-Interim dataset for significant wave height for the South Aegean are shown in Table 6.2.5. The correlation ranges from 0.68 to 0.89, the RMSE from 0.3 to 0.46 m and the absolute bias from 0.1 to 0.16 m. Mean wave height has a range from 0.8 m to 1 m and a maximum values from 4.9 m to 5.4 m. For the monthly differences ERA-I are higher than the buoys with the smallest differences in spring and the largest in February and August. The annual differences in significant wave height present that ERA-Interim are higher than the buoy values with differences from 0.001 m to 0.25 m.

Table 6.2.5: Significant Wave Height Statistics of buoys - ERA-Interim for the South Aegean

| Location | N | Corr. | RMSE | Bias | Mean | Max | St. Dev. | Min Monthly Dif. | Max Monthly Dif. | Min Annual Dif. | Max Annual Dif. |
|------------------------|-------|-------|------|------|------|------|----------|-------------------------------|-------------------------------|---------------------------------|--------------------------------|
| Avgo Hm0 (m) | 8046 | 0.89 | 0.3 | -0.1 | 1 | 5.4 | 0.63 | ERA-I higher 0.03 (APR) | ERA-I higher 0.17 (FEB) | ERA-I higher 0.001 (2002) | ERA-I higher 0.14 (2004) |
| Avgo SWH - SP (m) | | | | | 1.09 | 4.96 | 0.64 | | | | |
| E1M3A Hm0 (m) | 4146 | 0.89 | 0.3 | - | 0.93 | 4.92 | 0.62 | ERA-I higher 0.05 (APR) | ERA-I higher 0.22 (AUG) | ERA-I higher 0.09 (2011) | ERA-I higher 0.19 (2009) |
| E1M3A SWH - SP (m) | | | | | 1.08 | 4.91 | 0.60 | | | | |
| Santorini Hm0 (m) | 15086 | 0.68 | 0.46 | - | 0.89 | 4.92 | 0.55 | ERA-I higher 0.05 (MAY) | ERA-I higher 0.23 (AUG) | ERA-I higher 0.08 (2002) | ERA-I higher 0.25 (2000) |
| Santorini SWH - WA (m) | | | | | 1.05 | 4.9 | 0.61 | | | | |

In the case of wind speed, the correlation is around 0.7, the RMSE ranges from 2.25 m/s to 2.6 m/s and the absolute bias is from 0.01 m/s to 0.38 m/s. Mean wind speed ranges from 6.33 m/s to 6.81 m/s with the maximum values ranging from 18 m/s to 22.6 m/s. The monthly differences show that the ERA-Interim values are higher than the buoy, ranging from 0.02 m/s to 1.08 m/s. The annual differences range from 0 to 1.10 m/s.

Table 6.2.6 Wind Speed at 10 m Statistics of buoys - ERA-Interim for the South Aegean Sea

| Location | N | Corr. | RMSE | Bias | Mean | Max | St. Dev. | Min Monthly Dif. | Max Monthly Dif. | Min Annual Dif. | Max Annual Dif. |
|-----------------------------|-------|-------|------|-------|------|-------|----------|-------------------------|-------------------------|--------------------------|--------------------------|
| Avgo Wind Speed (m/s) | 7972 | 0.72 | 2.59 | -0.38 | 6.43 | 22.62 | 3.68 | ERA-I higher 0.02 (OCT) | ERA-I higher 0.98 (MAR) | Buoy higher 0.04 (2002) | ERA-I higher 1.10 (2004) |
| Avgo W10 WA (m/s) | | | | | 6.81 | 18.44 | 2.98 | | | | |
| E1M3A Wind Speed (m/s) | 3214 | 0.71 | 2.27 | -0.29 | 6.33 | 21.75 | 3.25 | ERA-I higher 0.05 (JUN) | ERA-I higher 0.81 (JUL) | Buoy higher ~0 (2007) | ERA-I higher 0.97 (2010) |
| E1M3A W10 WA (m/s) | | | | | 6.62 | 18.04 | 2.97 | | | | |
| Santori ni Wind Speed (m/s) | 14765 | 0.72 | 2.25 | 0.01 | 6.49 | 21.48 | 3.48 | ERA-I higher 0.07 (MAY) | ERA-I higher 1.08 (JUL) | ERA-I higher 0.01 (2005) | ERA-I higher 0.42 (2006) |
| Santori ni W10 WA (m/s) | | | | | 6.48 | 18.25 | 3.00 | | | | |

The correlation for temperature among the two datasets ranges from 0.84 to 0.97 (depending on location), the RMSE is from 1.7 °C to 1.85 °C and the absolute bias is from 0.64 °C to 0.82 °C. The mean monthly value of temperature ranges from 19.6 °C to 20.48 °C with the maximum from 29.7 °C to 32.54 °C. The monthly differences range from 0.01 °C to 0.14 °C and the annual from 0.11 °C to 4.45 °C.

Table 6.2.7: Temperature at 2 m Statistics of buoys - ERA-Interim for the South Aegean Sea

| Location | N | Corr | RMSE | Bias | Mean | Max | St. Dev. | Min Monthly Dif. | Max Monthly Dif. | Min Annual Dif. | Max Annual Dif. |
|-----------------------|-------|------|------|-------|-------|-------|----------|-------------------------|--------------------------|--------------------------|--------------------------|
| Avgo Temp. (°C) | 7262 | 0.95 | 1.85 | -0.82 | 19.6 | 32.12 | 4.66 | Buoy higher 0.14 (NOV) | ERA-I higher 1.92 (JUL) | ERA-I higher 0.11 (2003) | ERA-I higher 1.81 (2004) |
| Avgo T2M SP (°C) | | | | | 20.42 | 32.54 | 5.48 | | | | |
| E1M3A Temp. (°C) | 4774 | 0.97 | 1.7 | -0.64 | 19.83 | 29.67 | 4.62 | ERA-I higher 0.13 (NOV) | ERA-I higher 2.31 (JUN) | ERA-I higher 0.22 (2009) | ERA-I higher 0.89 (2007) |
| E1M3A T2M WA 1-2 (°C) | | | | | 20.48 | 33.86 | 5.46 | | | | |
| Santorini Temp. (°C) | 14645 | 0.84 | 2.88 | -0.64 | 19.65 | 36.26 | 5.18 | ERA-I higher 0.01 (FEB) | ERA-I higher 2.121 (JUL) | Buoy higher 0.22 (2010) | Buoy higher 4.45 (2011) |
| Santorini T2M WA (°C) | | | | | 20.29 | 33.35 | 5.51 | | | | |

Synopsis

For the South Aegean Sea, the primary wave direction is from the N and the secondary is from the W. Mean wave height is 1.08 m and the maximum value is 5.27 m, while wave period has a mean value of 4.95 s and a maximum of 10.45 s. Waves with heights from 0 to 1 m have frequencies of 56.04 % with the 98.38 % to be related to periods of 2-6 s. Mean temperature is more than 19.6 °C and maximum is more than 29.67 °C, while mean wind speed can be more than 6.33 m/s with maximum value of more than 19 m/s. In South Aegean winds blow from N and W directions, with wind speeds ranging from 2 m/s to 8 m/s.

The monthly means per year present that for significant wave height it is virtually certain that during April there is an increase and likely to have an increase in June. Mean wave period is very likely to virtually certain to present increasing trends for the period of February to October. It is also likely to have decreasing trend in December. In the annual values, significant wave height is likely to have an increasing trend of 0.001 m, while mean wave period is virtually certain to increase. Additionally, the monthly means of anomalies show that it is likely that there will be an increase of significant wave height, while for mean wave period it is virtually certain that there is an increasing trend. The monthly means show that wind speed is virtually certain to increase in April, very likely to decrease in September and likely to decrease in November. Temperature monthly means show that it is very likely to virtually certain to increase during the period May to September. Finally, as for the annual values, wind speed is likely to decrease while the temperature is virtually certain to increase. The monthly mean anomaly of wind speed is likely to present a decreasing trend, while it is virtually certain that temperature at 2m will increase.

6.2.4 North Ionian

For the North Ionian Sea, a correlation of ERA-Interim with the buoy of Zakynthos was not feasible, due to the location of the buoy, which is between the Ionian Islands and the western mainland of Greece. Therefore, only the long-term analysis of the selected point has been presented for the North Ionian. Mean wave height is of 0.8 m with a maximum of 5.3 m and period is of 4.33 s and max of 10.2 s. Wind speed has a mean of 5.3 m/s and max of 19 m/s whilst temperature has a mean of 19 °C and max of 35 °C. In the North Ionian, waves are primarily propagating from NW and, secondarily, from SW. The most common waves have heights from 0 to 1 m and are related to periods of 2 to 6 s.

For the monthly means per year, significant wave height is likely to virtually certain to show increasing trend for the period February to October. Mean wave period very likely to virtually certain shows increasing trend from February to December. For the annual values, it is virtually certain that significant wave height increases and the same apply for wave period. Finally, the mean monthly anomaly of significant wave height in North Ionian is virtually certain to present an increasing trend. Similarly, mean wave period is virtually certain to present an increasing trend. Winds in North Ionian blow primarily from NW to N and, secondarily, from SE to S with the most frequent having speeds of 2 to 8 m/s. The monthly means per year show that wind speed has likely to virtually certain an increasing trend, during the period May to September. Temperature is virtually certain to increase from April to August. For the annual values, wind speed is virtually certain to show increase and temperature as well. Wind speed monthly mean anomaly is virtually certain to have an increasing trend while it is virtually certain temperature to increase.

6.2.5 South Ionian

The correlation of buoy and ERA-Interim data sets for the South Ionian Sea is shown in Table 6.2.8. The mean wave height ranges from 0.85 m to 0.97 m with the maximum value from 5 m to 8 m, mean wind speed ranges from 4.82 m/s to 5.73 m/s with maximum values from 16.45 to 18.28 m/s and temperature mean is around 19 - 19.5 °C with maximum values in the order of 31.8 -34 °C. The correlation of wave height is around 0.91, wind speed is 0.72 and temperature is 0.92. The RMSE is of 0.33 m, 2.48 m/s and 2.57°C, while the bias is 0.12 m, 0.91 m/s and 0.36 °C, respectively. The mean monthly differences for wave height are from 0.02 m to 0.24 m (buoy higher than ERA-Interim), for wind speed they range from 0.16 m/s to 1.34 m/s (buoy higher than ERA-Interim) and for temperature from 0.18 °C to 2.24 °C (ERA-Interim higher than buoy). For the annual values, the difference for wave height is from 0.10 m to 0.2 m, for wind speed is from 0.64 m/s to 1.12 m/s and for temperature is from 0.03 °C to 1.67 °C.

Table 6.2.8 Statistics of Wave and Atmospheric Parameters Mykonos - ERA-Interim for South Ionian

| Location | N | Corr | RMSE | Bias | Mean | Max | St. Dev. | Min Monthly Dif. | Max Monthly Dif. | Min Annual Dif. | Max Annual Dif. |
|---------------------------|------|------|------|------|-------|-------|----------|-------------------------|-------------------------|-------------------------|-------------------------|
| Pylos Hm ₀ (m) | 5548 | 0.91 | 0.33 | 0.12 | 0.97 | 7.58 | 0.75 | Buoy higher 0.02 (JUL) | Buoy higher 0.24 (DEC) | Buoy higher 0.10 (2010) | Buoy higher 0.2 (2007) |
| Pylos SWH - WA (m) | | | | | 0.85 | 4.96 | 0.59 | | | | |
| Pylos Wind Speed (m/s) | 5767 | 0.72 | 2.48 | 0.91 | 5.73 | 18.28 | 3.3 | Buoy higher 0.16 (MAY) | Buoy higher 1.34 (AUG) | Buoy higher 0.64 (2007) | Buoy higher 1.12 (2011) |
| Pylos W10 SP 1-2 (m/s) | | | | | 4.82 | 16.45 | 2.59 | | | | |
| Pylos Temp. (°C) | 5548 | 0.92 | 2.57 | 0.36 | 19.51 | 31.82 | 5548 | ERA-I higher 0.18 (APR) | ERA-I higher 2.24 (NOV) | Buoy higher 0.03 (2010) | Buoy higher 1.67 (2007) |
| Pylos T2M WA (°C) | | | | | 19.15 | 34.23 | | | | | |

Synopsis

In the area of South Ionian, the most common waves are propagating from W to NW. Mean wave height is of 0.9 m with maximum value of 5.96 m, while period is of 4.72 s and maximum period of 11.04 s. The most frequent waves have heights of 0 to 1m and are related to periods of 2 to 6s. Waves that have heights < 1 m are rather common being associated with periods of 2-6 s. Mean wind speed is of 5.68 m/s with a maximum of 20.84 m/s, while mean temperature is of 19 °C and maximum of 35°C. Most frequent winds have speeds from 2 to 8 m/s. In the South Ionian, winds have as main directionality the NW.

In the case of South Ionian, the mean monthly values for the period 1979-2013 show that it is likely to virtually certain to show increasing trends in significant wave height for the period February to October. It is also very likely to virtually certain to have an increase in mean wave period during the period February to December. In the case of the annual values, it is virtually certain to have a minimal increase of 0.0054 m for wave height and 0.0177 s for wave period. Finally, the mean monthly anomaly is virtually certain to present an increasing trend for both significant wave height and for mean wave period. In the case of the monthly values, wind speed is likely to virtually certain to increase during the period July to October. Temperature is very likely to virtually certain to increase during the period April to September. The annual values, it is virtually certain to have increasing trends for both wind speed and temperature. The monthly mean anomalies show that it is virtually certain for wind speed and temperature to have increasing trends.

6.2.6 Remarks for ERA-Interim analysis

The emphasis given in this chapter is the correlation of reanalysis (i.e. ERA Interim) and *in-situ* (Buoy) data. It is suggested by many researches that reanalysis data can be used for a variety of scientific purposes, where *in-situ* observations are either absent or sparse and when gridded information is needed (Mooney et al., 2011; Shanas and Sanil Kumar, 2013). Temperature is evaluated due to its importance to tourism industries, ecosystems etc. and wind speed and wave height mostly due to their applications in nearshore processes and coastal engineering issues (coastal, maritime, civil etc.). Three methods are proposed and discussed in order to achieve the best correlation factor and the smallest root mean square error. It is shown that there is not a specific method for correlation either for a parameter or for a location. If possible, these methods should be used, evaluated, and then selected, accordingly to their performance and per study needed. It should be noted that variability among locations could be originated from the different temporal scales covered by the buoys data set (e.g. different time recording periods of the atmospheric parameters at Pylos and Athos buoys).

In the case of wave height variability, the methods of measurement of the spectra, and the tilt of the buoy in extreme atmospheric conditions and even the definition of wave heights (downcrossing or upcrossing) might be involved. Uncertainty can also be found in wind speed measurements; using the neutral - stable conditions of the atmosphere method to estimate wind speed at 10 m above sea surface without taking into account the different characteristics of the marine boundary layer. Temperature variability might be attributed to the different reflection of sea surface during the recording time period, or to cloudiness that might not be included accurately in the reanalysis data.

For the correlation of wind speed, it is proven that it is around 0.7 to 0.8 and for wave height around 0.6 to 0.9, at the Greek Seas, which in general agrees with results produced by other scientists as in the case of Red Sea and along the US Coastline (Shanas and Sanil Kumar, 2013; Stopa and Cheung, 2014). The correlation for temperature is also in agreement with the results from Mooney et al. (2011), presenting a correlation of 0.8 to 0.96 at the Irish coastline. The RMSE and Bias also are in accordance with those presented by the aforementioned studies.

For the Aegean, the monthly trends showed that wave height presented an increase during April, mean wave period an increase in April and June, while in South Aegean it decreased in December and increased from February to October. Wind speed increased during April and decreased in September, while temperature increased during the period May to September. The annual values for the North Aegean, showed that wave height did not change, wave period increased, wind speed remained stable and temperature increased. In Central Aegean, wave height decreased, wave period increased, wind speed decreased and temperature increased. In South Aegean, wave height, wave period and temperature increased while wind speed decreased. The anomalies, for the North Aegean, showed that wave height and wind speed remained unchanged, wave period and temperature increased. For the Central Aegean, wave height and wind speed decreased, while wave period and temperature increased. For the South Aegean wave height, wave period and temperature increased, while wind speed decreased. The monthly trends of the Ionian showed that wave height increased during the period February to October and wave period increased during February to December. Temperature increased during April to August (September for South Ionian), wind speed increased from May to September (North Ionian) and from July to October (South Ionian). All parameters increased in the annual and the monthly anomalies trends in the Ionian (North and South).

6.3 Pinios

6.3.1 Wind and Wave Characteristics from ERA-Interim

The results of the analysis of the chosen point considered representative for Pinios River area from ERA-Interim for the period 1979-2013 are presented conclusively in Table 6.1.

Table 6.3.1: Characteristics of Pinios Area from ERA-Interim

| Parameter | Mean | Max | St.Dev. |
|-----------|-------|-------|---------|
| SWH (m) | 0.41 | 3.34 | 0.34 |
| MWP (s) | 3.84 | 8.53 | 1.11 |
| W10 (m/s) | 3.61 | 17.59 | 1.97 |
| T2M (°C) | 17.01 | 40.48 | 7.6 |

The primary sector of wave direction is that of NE-E and the secondary of SE-S; this applies for wind direction as well. Maxima wave heights and wind speed have directions of NE. The most frequent wave heights are < 0.5 m and wind speeds of <6 m/s. The means per month for the period 1979-2013 present that it is likely to very likely to have had an increase for wave height during the periods from June to September. Mean wave period is very likely to virtually certain to have had an increase during June and July, respectively. The annual means show that it is very likely to have had an increase in significant wave height and virtually certain to have had an increase in mean wave period. In the case of the monthly mean anomalies of significant wave height it is shown that it is very likely to have increased, while it is about as likely as not to have had an increase in mean wave period. For the monthly means, wind speed is very likely to virtually certain to have increased during the months July to September. In the case of temperature, it is virtually certain to have had an increase during the months May to September. As for the annual values, it is likely for wind speed to have had an increase and virtually certain for temperature as well. Monthly mean anomalies for the period 1979-2013 show that there is virtually certain to have had an increase for wind speed and for temperature.

6.3.2 MIKE 21 PMS

For the simulation of wave propagation from offshore to nearshore, the module of MIKE 21 PMS is used. Additionally, as suggested in a variety of studies, in cases with mild slopes and with no need of analysing the backscatter (that the PMS does not simulate), PMS can be preferred and ultimately provide similar results with the Boussinesq model (Pandian et al., 2004; Makris and Memos, 2007; Makris et al., 2007; Savioli, 2007). Additionally, in the case of the Greek coastline, PMS has been applied in several beaches in order to be used as an input (the output of radiative stresses) for sediment transport and

hydrodynamic simulations (to gather information about currents etc.) providing adequate results as compared with in situ data (Alexandrakis et al., 2013; Afentoylis, 2013; Mavrantoukakis, 2013). Moreover, the application of ERA-Interim as input data for wave modelling (wave characteristics or renewable energy) is presented and compared as input along with ERA-40 and NCEP data in several studies (Martin et al., 2012; Appendini et al., 2013; Portilla et al., 2013). It has been already established in Chapter 6.2 that ERA-Interim can be used in offshore conditions for the Greek Seas, as the correlation has been proven adequate for such use.

In the case of Pinios River area, all scenarios present a change in the directionality of the waves at both areas, one close to the mouth of the river (north) and one at the settlement of Stomio (south); the latter used to be the active mouth of the river until the 1930's (Stournaras and Galani, 1995; Foutrakis et al., 2007). Furthermore, the northern area of Pinios, especially for the Scenarios 2, 3 and 4 for all wave directionality, presents changes in wave height from depths of close to 30 m, leading to the confirmation of the appearance of the transitional zone ; in the cases of 2% can be from 25 to 37 m depth; from offshore to nearshore conditions, as estimated from the empirical equations of CERC (1984) 1984). These changes are not evident in the southern area, being attributed to the smoother bathymetry

Additionally, for the sea level rise scenarios (3 and 4), there are more areas generated with changes in wave directions and the ones already evident, even from the mean conditions, are becoming wider, simulating in a way the impact of sea level rise to the under-examination area. By comparing all scenarios for all wave directionalities, it is clear that the NE waves are those with more apparent changes in wave propagation, followed by SE waves and finally, the E waves that arrive perpendicularly to the shore, i.e. do not refract that much in contradiction to the others.

In Table 6.3.2, the results of the CERC (1984) empirical equations and those estimated from MIKE21 PMS for profiles A and B for the NE waves under the different scenarios are shown. As presented, there are no data for the CERC equations for the Scenarios 3 and 4 as these equations do not include the potential sea level rise in wave height / breaking depth estimation. Profile A seems to present more similar results to those provided by CERC (1984) equations than profile B, except in the case of the breaking depth for the mean wave conditions. It seems that CERC (1984) estimates are considered adequate only for cases with very small variations in bottom topography, such as in the southern area of Pinios (Profile A). Thus, due to a higher variability in bathymetry in Profile B, the results of MIKE21 PMS are not in agreement with the results of the empirical equations; this may be explained by the difference between the models in simulating the process of shoaling. For Scenario 4, it is shown that in both profiles the breaking depths are smaller than in other scenarios, showing a landward movement of the breaking zone, whilst for Scenario 3 the waves seem to break in larger depths. Analytically, in Scenario 3 for Profile A, the breaking zone is located 144 m from the shore, while for scenario 4 it is 141 m from the shore. For Profile B, the breaking zone is 96 m from the coastline for scenario 3 while 72 m for scenario 4.

Table 6.3.2: Wave characteristics for NE waves as estimated by CERC (1984) and MIKE21 PMS

| NE Scenarios / Parameters | Offshore | | (CERC, 1984) | | PROFILE 3 MIKE 21 PMS | | PROFILE 6 MIKE 21 PMS | |
|---------------------------------|-----------|-----------|--------------|-----------|--------------------------|-----------|--------------------------|-----------|
| | H_o (m) | T_o (s) | H_b (m) | d_b (m) | H_b (m) | d_b (m) | H_b (m) | d_b (m) |
| Mean Condition (Scenario 1) | 0.53 | 4.39 | 0.67 | 0.86 | 0.57 | 3.86 | 0.52 | 0.86 |
| 2% (Scenario 2) | 2.06 | 6.93 | 2.38 | 3.05 | 2.25 | 3.67 | 1.76 | 4.07 |
| 2% & 0.3 SLR (Scenario 3) | - | - | - | - | 2.31 | 3.86 | 2.31 | 1.8 |
| 2% & 0.63 SLR (Scenario 4) | - | - | - | - | 2.32 | 3.62 | 2.32 | 1.75 |

For the E Waves, the characteristics are shown in Table 6.3.3. As in the case of the NE waves, wave characteristics at profile A seem to be closer to the results given by the empirical equations, but with high variations at the breaking depths (this occurs for profile B as well). Wave height at the breaking zone for profile B seems to be lower than what is estimated by the equations of CERC (1984). As it has been mentioned, profile B is characterized by a more variable bathymetry. Once more, it is shown that it is most likely that the equations do not include bathymetry characteristics (i.e. shoaling effect) leading to these discrepancies as in this case there is no evident refraction as the waves approach in perpendicular direction to the shore. In Profile B, for the Scenarios 3 and 4, the breaking zone moves landwards to smaller depths, at 72 m from the coastline in contradiction to the 2% wave conditions, where it was at 105 m from the shore. For profile A, for the 3rd scenario the breaking zone is at 159 m from the shore and 144 m from the coastline for scenario 4.

Table 6.3.3: Wave characteristics for E waves as estimated by (CERC, 1984) and MIKE21 PMS

| E Scenarios / Parameters | Offshore | | (CERC, 1984) | | PROFILE 3 MIKE 21 PMS | | PROFILE 6 MIKE 21 PMS | |
|--------------------------------|-----------|-----------|--------------|-----------|--------------------------|-----------|--------------------------|-----------|
| | H_o (m) | T_o (s) | H_b (m) | d_b (m) | H_b (m) | d_b (m) | H_b (m) | d_b (m) |
| Mean Condition (Scenario 1) | 0.32 | 3.55 | 0.41 | 0.53 | 0.34 | 3.51 | 0.41 | 0.86 |
| 2% (Scenario 2) | 1.48 | 5.68 | 1.69 | 2.16 | 1.59 | 3.86 | 1.35 | 4.89 |
| 2% & 0.3 SLR (Scenario 3) | - | - | - | - | 1.55 | 2.77 | 1.36 | 1.9 |
| 2% & 0.63 SLR (Scenario 4) | - | - | - | - | 1.56 | 3.86 | 1.36 | 1.9 |

In the case of the SE waves (Table 6.3.4), the results of PMS for profile A, show the same breaking depth of 2.77 m (159 m from the coastline) in all cases that differs from the depth estimated by (CERC, 1984) equations. On the other hand, the breaking depth of SE waves in profile B is closer in Scenarios 2, 3 and 4, with what is predicted from the CERC's equations. Furthermore, the landward movement of the breaking zone is shown for profile B, with 72m from the shore at Scenario 3 and 63 m for Scenario 4. It is

also evident that wave height at the breaking zone does not differ substantially at the profiles A and B for all four scenarios.

Table 6.3.4: Wave characteristics for SE waves as estimated by (CERC, 1984) and MIKE21 PMS

| SE Scenarios / Parameters | Offshore | | (CERC, 1984) | | PROFILE 3 MIKE 21 PMS | | PROFILE 6 MIKE 21 PMS | |
|---------------------------------|-----------|-----------|--------------|-----------|--------------------------|-----------|--------------------------|-----------|
| | H_o (m) | T_o (s) | H_b (m) | d_b (m) | H_b (m) | d_b (m) | H_b (m) | d_b (m) |
| Mean Condition (Scenario 1) | 0.28 | 3.36 | 0.41 | 0.53 | 0.27 | 2.77 | 0.28 | 1.12 |
| 2% (Scenario 2) | 1.24 | 5.65 | 1.69 | 2.16 | 1.11 | 2.77 | 1.25 | 1.91 |
| 2% & 0.3 SLR (Scenario 3) | - | - | - | - | 1.11 | 2.77 | 1.25 | 1.91 |
| 2% & 0.63 SLR (Scenario 4) | - | - | - | - | 1.08 | 2.77 | 1.28 | 1.29 |

According to the above scenarios, the breaking zone changes position (water depth) from 2.8 m to 3.9 m for profile A and from 0.7 m to 4.9 m, for profile B. It is also shown that by increasing the sea level rise will likely move the breaking zone closer to the shore; this indicates that incoming high waves come more close to the shore. Additionally, the sea level rise scenarios have shown different parts of the nearshore zone (wider or new ones) where onshore propagating waves are changing directionality and are becoming more perpendicular to the shoreline (especially in the case of NE and SE waves).

The NE waves are those who appear to have a larger effect to the west shore of Pinios delta, even in the case of the mean wave conditions. They show also higher variability in wave characteristics in association with bathymetry differences.

Finally, the importance of a detailed bathymetry has been revealed in the case of the transformation of wave characteristics in the nearshore zone, whose simulations by numerical models (e.g. MIKE21 PMS) provide better results from those provided by the empirical and semi-empirical equations (e.g. CERC, 1984) as the latter do not include the processes of the nearshore zone and estimate parameters only in specific depths (such as breaking depth).

Chapter 7 - Synopsis, Conclusions & Future Work

7 Synopsis, Conclusions & Future Work

A synopsis of the results that have been presented and discussed in the previous chapters is given along with suggestions of future work.

7.1 Synopsis of the Results

A synopsis of the wind and wave regional characteristics of the Greek Seas is shown in Table 7.1.1; thus, the means of wave height parameters, as provided by the buoy data and ERA-Interim dataset.

Table 7.1.1: Mean values of wave heights for the Greek Seas. H_{m0} : spectral significant wave height (buoy and SSE analysis); $H_{1/3}$: statistical significant wave height; H_{max} : maximum wave height (buoy and SSE analysis); H_{m0a} : swell wave height (buoy); H_{m0b} : wind induced wave height (buoy); and, SWH: significant wave height (ERA-Interim)

| | Mean Wave Height | | | | | | | |
|-----------|---------------------|---------------------|---------------------|---------------------|---------------------|---------------------|---------------------|--------------------|
| | H_{m0} (m) | | $H_{1/3}$ (m) | H_{max} (m) | | H_{m0a} (m) | H_{m0b} (m) | SWH (m) |
| | <i>Buoy Records</i> | <i>SSE Analysis</i> | <i>SSE Analysis</i> | <i>Buoy Records</i> | <i>SSE Analysis</i> | <i>Buoy Records</i> | <i>Buoy Records</i> | <i>ERA-Interim</i> |
| N. Aegean | 0.4-0.9 | 1.0 | 0.9-1.0 | 1.2-1.5 | 1.6-1.7 | 0.02-0.05 | 0.4-0.9 | 0.8 |
| C. Aegean | 0.5-1.00 | 1.1 | 1.00 | 0.5-1.6 | 1.7 | 0.02-0.06 | 0.5-1 | 1.0 |
| S. Aegean | 0.9-1.00 | 1.0 | 0.9 | 1.3-1.4 | 1.5 | 0.06-0.13 | 0.6-1 | 1.1 |
| N. Ionian | 0.8 | 1.0 | 0.9 | 3.9 | 1.51 | 0.11 | 0.8 | 0.8 |
| S. Ionian | 0.3-1.0 | 0.7-1.0 | 0.6-1.0 | 0.3-1.4 | 1.0-1.8 | 0.02-0.12 | 0.3-1.0 | 0.9 |

The ranges are similar for all sub-regions with the relatively higher wave heights formed in the North Aegean and the Ionian Sea. Swell heights are higher being associated with, as expected, larger fetches. The mean heights of ERA-Interim are quite similar to the spectral significant wave height given by the buoys. It has to be mentioned that these ranges are given by the mean of more than one buoy that are considered representatives of their surrounding areas.

The mean values of the wave periods of the different regions of the Greek Seas are shown in Table 7.1.2. It is proven that most of the regions are characterized by wind-induced waves, whilst swells have longer periods in areas with longer fetches, i.e. North and South Aegean and the Ionian. Mean wave periods provided by ERA-Interim also support that the Greek Seas are mostly wind-wave dominated.

Table 7.1.2: Mean values of wave periods for the Greek Seas. T_{m02} : spectral wave period (buoy and SSE analysis); $T_{1/3}$: statistical significant wave period; T_p : peak period (buoy and SSE analysis); T_{m02a} : swell wave period (buoy); T_{m02b} : wind induced wave period (buoy); and MWP: mean wave periods (ERA-Interim)

| | Mean Wave Period | | | | | | | |
|-----------|---------------------|---------------------|---------------------|---------------------|---------------------|---------------------|---------------------|--------------------|
| | T_{m02} (s) | | $T_{1/3}$ (s) | T_p (s) | | T_{m02a} (s) | T_{m02b} (s) | MWP (s) |
| | <i>Buoy Records</i> | <i>SSE Analysis</i> | <i>SSE Analysis</i> | <i>Buoy Records</i> | <i>SSE Analysis</i> | <i>Buoy Records</i> | <i>Buoy Records</i> | <i>ERA-Interim</i> |
| N. Aegean | 2.9-3.6 | 3.8-4.0 | 5.2-5.4 | 3.5-4.6 | 4.9-5.1 | 13.4-14.1 | 2.9-6.7 | 4.1 |
| C. Aegean | 3.2-3.7 | 3.8 | 5.4 | 4.2-4.9 | 5.2 | 11.4-13.4 | 3.2-3.6 | 4.56 |
| S. Aegean | 3.7-4.0 | 3.84 | 5.5 | 5.0-5.2 | 5.2 | 12.1-15.0 | 3.7-7.1 | 4.9 |
| N. Ionian | 3.9 | 4.1 | 6.1 | 5.3 | 5.8 | 13.1 | 3.8 | 4.3 |
| S. Ionian | 3.4-4.3 | 3.9-4.5 | 5.7-6.4 | 4.4-5.8 | 5.3-6.1 | 11.8-12.4 | 3.4-4.4 | 4.72 |

From the monthly means of wave heights (Table 7.1.3), it is evident that the higher values, as given by the buoys and ERA-Interim, are observed in winter months, whilst there is no specific pattern for the minimum values.

Table 7.1.3: Months with the minimum and maximum mean values of wave heights for the Greek Seas. H_{m0} : spectral significant wave height (buoy and SSE analysis); $H_{1/3}$: statistical significant wave height; and SWH: significant wave height (ERA-Interim)

| Mean Monthly Wave Height | H_{m0} (m) | | | | $H_{1/3}$ (m) | | SWH (m) | |
|--------------------------|--------------|------------|------------|------------|---------------|------------|-------------|------------|
| | Buoy | | SSE | | ERA-Interim | | ERA-Interim | |
| | <u>Min</u> | <u>Max</u> | <u>Min</u> | <u>Min</u> | <u>Min</u> | <u>Min</u> | <u>Min</u> | <u>Max</u> |
| N. Aegean | APR | FEB | JUN | JAN | JUN | JAN | JUN | JAN |
| C. Aegean | MAY | DEC | MAY | FEB | MAY | FEB | JUN | FEB |
| S. Aegean | SEPT | FEB | AUG | DEC | AUG | DEC | MAY | FEB |
| N. Ionian | MAY | FEB | JUN | FEB | JUN | DEC | JUN | DEC |
| S. Ionian | AUG | DEC | AUG | JAN | AUG | JAN | AUG | DEC |

In Table 7.1.4, it is shown that the maximum values of the monthly means of wave period occur also during winter, as in the case of wave height while the smaller values of wave period are during the summer period (May to September).

Table 7.1.4: Months with the minimum and maximum mean values of wave periods for the Greek Seas. T_{m02} : spectral wave period (buoy and SSE analysis); $T_{1/3}$: statistical significant wave period; MWP mean wave periods (ERA-Interim)

| Mean Monthly Wave Period | T_{m02} (s) | | | | $T_{1/3}$ (s) | | MWP (m) | |
|--------------------------|---------------|-----|-----|-----|---------------|-----|-------------|-----|
| | Buoy | | SSE | | SSE | | ERA-Interim | |
| | Min | Max | Min | Max | Min | Max | Min | Max |
| N. Aegean | SEPT | DEC | JUN | FEB | JUN | FEB | JUN | JAN |
| C. Aegean | SEPT | DEC | MAY | FEB | MAY | FEB | JUN | FEB |
| S. Aegean | AUG | FEB | AUG | DEC | AUG | DEC | JUN | FEB |
| N. Ionian | JUL | FEB | MAY | FEB | MAY | FEB | AUG | DEC |
| S. Ionian | AUG | DEC | JUL | JAN | JUL | JAN | AUG | DEC |

The mean values of atmospheric parameters are given in Table 7.1.5, where it is shown that atmospheric pressure presents an overall decreasing pattern from north to south, with the lowest ranges to be observed in the Central Aegean. On the contrary, temperature is increasing southwards, as it is expected; this applies to the ERA-Interim and the buoy datasets. The opposite pattern is shown by the values of wind speed and of wind gusts.

Table 7.1.5: Means of Atmospheric Parameters for the Greek Seas from buoys and ERA-Interim (ERA-I)

| Mean Atmospheric Parameters | Atmospheric Pressure (hPa) | Air Temperature (°C) | | Wind Speed (m/s) | | Wind Gust (m/s) |
|-----------------------------|----------------------------|----------------------|--------------|------------------|--------------|-----------------|
| | <i>Buoy</i> | <i>Buoy</i> | <i>ERA-I</i> | <i>Buoy</i> | <i>ERA-I</i> | <i>Buoy</i> |
| N. Aegean | 1014.7-1017.1 | 14.9-17.6 | 18.3 | 4.5-6.0 | 5.7 | 6.2-7.8 |
| C. Aegean | 1012.8-1013.23 | 18.6-19.5 | 18.8 | 4.73-6.81 | 6.8 | 6.2-8.8 |
| S. Aegean | 1014.2-1014.7 | 19.6-19.7 | 19.6 | 5.31-5.51 | 6.5 | 7.1-7.5 |
| N. Ionian | 1015.5 | 17.6 | 19.0 | 5.0 | 5.3 | 6.7 |
| S. Ionian | 1013.1-1015.0 | 18.89-19.52 | 20.0 | 3.7-4.9 | 5.7 | 4.9-6.6 |

The seasonal (monthly) variability (Table 7.1.6) is evident, as expected, in the case of temperature as provided by both datasets, i.e. the buoys and ERA-Interim; wind speed is lower during late spring - early summer and in autumn, while the maximum values are during winter. Atmospheric pressure is lower during summer and higher during late autumn and winter. Wind gusts are lower in spring and higher in winter (**Error! Reference source not found.**). The aforementioned characteristics and results are in accordance to earlier studies (e.g. (Poulos et al., 1997; Kouroutzoglou et al., 2011; Bagiorgas et al., 2012)

Table 7.1.6: Months with minimum and maximum means of atmospheric parameters from buoys and ERA-Interim (ERA-I)

| Mean Monthly Atmospheric Parameters | Atmospheric Pressure (hPa) | | Air Temperature (°C) | | | | Wind Speed (m/s) | | | | Wind Gust (m/s) | |
|-------------------------------------|----------------------------|------------|----------------------|------------|-------------|-------------|------------------|------------|-------------|-------------|-----------------|------------|
| | Min (Buoy) | Max (Buoy) | Min (Buoy) | Max (Buoy) | Min (ERA-I) | Max (ERA-I) | Min (Buoy) | Max (Buoy) | Min (ERA-I) | Max (ERA-I) | Min (Buoy) | Max (Buoy) |
| N. Aegean | JUL | NOV | DEC | JUL | JAN | AUG | MAY | DEC | JUN | FEB | MAY | DEC |
| C. Aegean | JUL | JAN | FEB | AUG | FEB | AUG | MAY | FEB | JUN | FEB | MAY | FEB |
| S. Aegean | JUL | JAN | FEB | AUG | FEB | AUG | MAY | FEB | MAY | FEB | MAY | FEB |
| N. Ionian | AUG | JAN | FEB | AUG | FEB | AUG | MAY | JAN | JUN | DEC | MAY | DEC |
| S. Ionian | AUG | JAN | FEB | AUG | FEB | AUG | OCT | DEC | SEP | DEC | APR | DEC |

7.2 Wave and Weather State of the Greek Seas

Throughout the process of this research, the following concluding remarks should be made, **in relation to the methodology** used:

- Sea surface elevation data analysis provides more information about the wave state than that of the buoy direct measurements, i.e. statistical and spectral wave parameters, such as the spectral moments, spectrum broadness - width parameters, apparent wave height and period can be obtained (not usually provided from direct buoy records).
- For the collocation of the ERA-Interim with the buoy data, it is proven that there is not a specific method suggested for all parameters and locations. It should be noted that the method of the Weighted Distance Average of the Grid Boxes is rejected due to the locality of some of the grid boxes on land.

The concluding remarks concerning the **conditions of the wave and wind state** of the different regions of the Greek Seas, as provided by the analysis of the buoys and the ERA-Interim dataset, are:

- In the **North Aegean**, frequent wave heights are up to 0.5 m are related to periods of 2 to 4 sec and propagating, primarily, from North and, secondarily, from the South. Most frequent wind speeds are from 3 to 8 m/s blowing from N, whilst wind speeds more than 15 m/s are from the NE-E. Wave heights up to 1 m are related to wind speeds of up to 8 m/s, whilst those of more than 3 m are induced by wind speeds of more than 12 m/s.
- For the **Central Aegean**, frequent wave heights are up to 0.8 m and are related to periods ranging from 2 to 4 sec, propagating from N to NE directions. The most frequent winds blow from NW – NE, with speeds of 2-8 m/s; the same applies for higher wind speeds. The aforementioned most frequent wave heights (<0.8 m) are related to wind speeds that range from 3 to 6 m/s whilst those with heights of more than 4 m are related to wind speeds of more than 12 m/s.

- In the **South Aegean**, frequent wave heights are from 0.5 to 1 m and are related to periods of up to 4 sec, propagating from westerly directions. The associated westerly winds have speeds of 3 to 6 m/s. Even though Santorini is located in the South Aegean, its characteristics are similar to those of the Central Aegean with wind speeds of 6 to 9 m/s and blowing from the North. Maximum wind speeds are from W - NW. Frequent waves of 0.5 to 1 m are related to winds with speeds of 3 to 6 m/s while the higher waves (>3 m) are related to wind speeds of more than 15 m/s.
- For the **North Ionian**, frequent waves have heights <0.5 m with periods of around 3 s and propagate from the SW. Most frequent winds have speeds of 2 to 4 m/s and are blowing from the NW to NE while maximum wind speeds >14 m/s have NE directions. Frequent wave heights of up to 0.8 m are related to wind speeds of 2 to 4 m/s, while waves with heights >3 m are related to wind speeds of >10 m/s.
- For the **South Ionian**, frequent waves have heights also up to 0.8 m with periods of 3-4 sec and propagate from the SW to NW (Pylos) and from SE to S (Kalamata). Most frequent winds range from 1 to 3 m/s and blow from NW, E and SE (Pylos) and NW and SE (Kalamata). Higher winds (>12 m/s) in Pylos blow from the SE and in Kalamata from the SE. Frequent waves with heights <0.8 m are related to wind speeds of 2 - 4 m/s, while waves with heights of more than 2.4 m are related to speeds of more than 8 m/s.
- It is evident in both datasets that the complex coastal topography and the presence of the islands have a profound impact on the directionality and through fetch on wave height and period.
- It should be noted that the analysis of wind and wave state based on data from one buoy or a selected point of ERA-Interim should be considered as representative only for its surrounding area.
- Wave parameters should be examined not only with the wind dominant, but should be carefully analyzed with previous temporal and non-local data, as propagation might have caused alterations.
- The common empirical equation that relates maximum wave height with significant wave height ($H_{\max} = 2 * H_s$) should be carefully applied in the Greek Seas, as the ratio had ranges from 1.5 to 1.7. The statistical and the spectral significant wave height have a ratio of approximately 1. The ratio of $H_{1/3} = 4 * \sqrt{m_0}$ is also shown to be closer to the range of 3.5 to 3.7 (as noted in (Vandever et al., 2001)).
- It is proven that in comparison to the Rayleigh and Weibull probability distributions, Kumaraswamy distribution describes better the apparent wave height in the Greek Seas, but underestimates the higher values; all Goodness of Fit Tests supports this: Chi-square, Anderson - Darling and Kolmogorov - Smirnov.

7.3 Concluding remarks on the correlation of ERA-I and buoys

A synopsis of the statistical relationship amongst the Poseidon Buoys and the ERA-Interim dataset is given in Table 7.3.1. It is revealed that the ERA-Interim have generally a sufficient correlation with the *in-situ* data and can be, therefore, used to describe the wind and wave characteristics of the Greek Seas.

The region of North Ionian cannot be correlated to the buoy of Zakynthos, as the latter is located nearshore and among two islands (Zakynthos and Kefallinia) and the coast of Western Greece.

Table 7.3.1: Correlation, RMSE and Absolute Bias per region between the buoy and ERA-Interim dataset for the parameters of Significant Wave Height (SWH), Wind Speed at 10 m (W10) and Temperature at 2 m (T2M)

| Region / Parameter | Correlation | | | RMSE | | | BIAS | | |
|--------------------|-------------|---------|---------|---------|-----------|----------|-----------|-----------|-----------|
| | SWH | W10 | T2M | SWH (m) | W10 (m/s) | T2M (°C) | SWH (m) | W10 (m/s) | T2M (°C) |
| N. Aegean | 0.6-0.9 | 0.7-0.8 | 0.9-1.0 | 0.2-0.6 | 2-2.6 | 2.1-2.4 | <0.17 | 0.01-0.33 | 0.28-0.52 |
| C. Aegean | 0.9 | 0.8 | 0.9 | 0.3 | 2.3 | 2.4 | 0.04 | 1.21 | 0.47 |
| S. Aegean | 0.7-0.9 | 0.7 | 0.8-1.0 | 0.3-0.5 | 2.2-2.6 | 1.7-1.8 | 0.10-0.16 | 0.01-0.38 | 0.64-0.82 |
| N. Ionian | – | – | – | – | – | – | – | – | – |
| S. Ionian | 0.9 | 0.7 | 0.9 | 0.3 | 2.5 | 2.6 | 0.12 | 0.91 | 0.36 |

7.4 Trends of wave and atmospheric parameters from ERA-Interim long-term analysis

The likelihood of having a changing trend, or not, for the monthly means of the significant wave height, mean wave period, wind speed at 10m and temperature at 2m, expressed as percentages are presented in Table 7.4.1 for the five regions of the Greek Seas as given by the ERA-Interim database.

Table 7.4.1: Percentages of likelihood of having a trend in the mean monthly values for the parameters of Significant Wave Height (SWH), Wind Speed at 10 m (W10) and Temperature at 2 m (T2M)

| | Likelihood of Trends (%) | | | |
|-----------|--------------------------|--------------------------------|---------------------------------------|--------------------|
| | SWH | MWP | W10 | T2M |
| N. Aegean | >99% ↓Feb & >90% ↑ Apr | >99% ↑ Apr & >90% ↑Jun | >66%↑ | >90% ↑ May to Sept |
| C. Aegean | >90% ↑ Apr & >66% ↓ Sept | >99% ↑ Apr & >90% ↑Jun | >66% ↑ Apr & >90% ↓ Sept | >66% ↑ May to Sept |
| S. Aegean | >99% ↑ Apr & >66% ↑ Jun | >90% ↑ Feb to Oct & >66% ↓ Dec | >99% ↑ Apr & >90% ↑ Sept & >66% ↓ Nov | >90% ↑ May to Sept |
| N. Ionian | >66% ↑ Feb to Oct | >90% ↑ Feb to Dec | >66% ↑ May to Sept | >99% ↑ Apr to Aug |
| S. Ionian | >66% ↑ Feb to Oct | >90% ↑ Feb to Dec | >66% ↑ July to Oct | >90% ↑ Apr to Sept |

There is >90% likelihood to have an increase in the Aegean of significant wave height during April, while in the Ionian there is >66% likelihood to increase during the period of February to October. Only in the case of the North and Central Aegean, the wave height might decrease (99% likelihood in February and 66% in September, respectively).

It is evident that in the case of mean wave period, there is the same pattern for the Ionian and the Southern Aegean, with >90% likelihood to increase during the period of February to December. It is possible that this increase can be due to the increase of the storm events that have been identified in the Adriatic from a variety of studies, leading to an increase of wave periods (i.e. higher period waves such as swells) in the Ionian that can propagate possible to the Southern Aegean. The North and Central Aegean is characterized by 90% and 99% likelihood, respectively, to have an increasing trend during April and June. Wind speed does not present similar trends at the Greek Seas. Moreover, the North Aegean has a 66% likelihood of increasing trend whilst the Central Aegean, 66% in April and the South Aegean shows 99% in April and > 90% in September. Additionally, Central and South Aegean show decreasing trends in September (90%) and November (66%), respectively. In the Ionian, the likelihood of having increasing trends is > 66% but differs temporally, i.e. May to September (in the North) and July to October (in the South). Finally, the temperature presents increasing trends of more than 90% likelihood in North and South Aegean, 66% in the Central Aegean for the period of May to September, while in the North Ionian there is >99% for April to August and 90% for the South Ionian from April to September.

With respect to the trends of the annual means (Table 7.4.2), the significant wave height is <33% likely to present a trend in the case of North Aegean, whilst it is >66% likely to decrease in Central Aegean. For the South Aegean (>66%) and the Ionian (>99%), it is shown that there will be increasing trends; thus, for mean wave period, there is >99% probability of having an increasing trend in the Greek Seas (asides Central Aegean with >90%). Wind speed annual means present a 33% to 66% likelihood to change in North Aegean, >90% increase in Central Aegean and 66% decrease in the South Aegean. The Ionian presents more than 99% increase in wind speed. Temperature annual values present more than 99% likelihood to have an increasing trend for the Greek Seas.

Table 7.4.2: Percentages of likelihood of having a trend in the values of annual means for the parameters of Significant Wave Height (SWH), Wind Speed at 10 m (W10) and Temperature at 2 m (T2M)

| | Likelihood of Trends (%) | | | |
|-----------|--------------------------|--------|------------------|--------|
| | SWH | MWP | W10 | T2M |
| N. Aegean | <33% to change | >99% ↑ | 33-66% to change | >99% ↑ |
| C. Aegean | >66% ↓ | >90% ↑ | >90% ↓ | >99% ↑ |
| S. Aegean | >66% ↑ | >99% ↑ | >66% ↓ | >99% ↑ |
| N. Ionian | >99% ↑ | >99% ↑ | >99% ↑ | >99% ↑ |
| S. Ionian | >99% ↑ | >99% ↑ | >99% ↑ | >99% ↑ |

In the case of the mean monthly anomalies, in the case of the Ionian it is >99% likely to have had an increase in significant wave height, while it is <33% for the North Aegean, between 33% and 66% for South Aegean to change and >66% to have a decrease in Central Aegean. Annual means of wave period show generally increasing trends in the Greek Seas. Wind speed will >66% (South Aegean) and 99% (Central Aegean) decrease, while the likelihood to change in the North Aegean ranges from 33% to 66%. The Ionian presents > 99% likelihood to have an increasing trend in wind speed. Temperature as in the case of the annual trends, presents >99% likelihood to increase in all sub regions of the Greek Seas (Table 7.4.3).

Table 7.4.3: Percentages of likelihood of having a trend in the values of monthly mean anomalies for the parameters of Significant Wave Height (SWH), Wind Speed at 10 m (W10) and Temperature at 2 m (T2M)

| | Likelihood of Trends (%) | | | |
|-----------|--------------------------|--------|------------------|--------|
| | SWH | MWP | W10 | T2M |
| N. Aegean | <33% to change | >99% ↑ | 33-66% to change | >99% ↑ |
| C. Aegean | >66% ↓ | >99% ↑ | >99% ↓ | >99% ↑ |
| S. Aegean | 33-66% to change | >99% ↑ | >66% ↓ | >99% ↑ |
| N. Ionian | >99% ↑ | >99% ↑ | >99% ↑ | >99% ↑ |
| S. Ionian | >99% ↑ | >99% ↑ | >99% ↑ | >99% ↑ |

7.5 Wave propagation of offshore generated waves to the nearshore zone: present characteristics and the effect of potential SLR

The main conclusions considering different wave scenarios (mean, mean average of 2%) and sea level rise of 0.3 m and 0.6 m, according to RCP 8.5 and AR5 scenarios of climate change) on the wave propagation in intermediate (water depth <math>< \text{wave length (L) / 2}</math>) and shallow water (>math>> L/20</math>) are:

- The east deltaic coast of Pinios River, especially for the Scenarios 2, 3 and 4 for all wave directionality, presents changes in wave height from water of approximately the 30 m, leading to the confirmation of the appearance of the transitional zone that in the case of the average of the upper 2% wave heights is identified between the depths of 25 - 37 m.
- It is clear that the most common NE waves are those inducing the most apparent changes in wave propagation, followed by SE waves and, finally, the E waves; the latter due to their perpendicular arrival relatively to the shore do not refract that much in contradiction to the other directions.
- In terms of wave breaking, for Scenario 4 (mean upper 2% of wave conditions with a sea level rise of 0.6 m), it is shown that in nearshore profiles the breaking depths are smaller than in other scenarios. According to the above scenarios, the breaking zone changes position (water depth) from 2.8 m to 3.9 m for profile A and from 0.7 m to 4.9 m, for profile B, relatively to the present shoreline position.
- The NE waves are those who appear to have a larger effect to the northern sector of the east deltaic shore of Pinios River, even in the case of the mean wave conditions (as the reflection of the waves is more evident than in other directions).

7.6 Future Work

On the basis of the outcome of this research, in terms of methodology, results and discussion, further analyses are suggested related to:

- The correlation between statistical and spectral wave periods (as done for significant wave height). This analysis can provide more information about the relationships of wave periods given from spectral and from time series analysis and how these ratios differ from what is given from empirical equations.
- The improvement of the accuracy on the difference of the ratios of wave height as provided by this research and the ratios given by literature and empirical equations, the spectral width - broadness parameters should be also examined.
- Mean conditions of monthly anomalies and annual trends of the extreme values (i.e. upper 2%, 5% and 10%) of the ERA-Interim datasets could be examined in order to identify how likely could be having changing trends in the case of extreme conditions.
- A further investigation concerning the correlation of the results of the analysis of the *in-situ* (this research) with other data sets (e.g. altimetry data) could be applied.
- The relationship of the ERA-Interim trends and peaks in annual values and teleconnection patterns that appear in the Eastern Mediterranean (MOI, NAO etc.) can be investigated to explain if changes in these patterns are related to the aforementioned peaks and trends.
- A comparison of the outcome of MIKE 21 PMS with other existing models (e.g. XBEACH, WaveWatch III) and with the products of empirical or semi-empirical equations in cases with more complex nearshore bathymetry can be done.
- The coupling of the MIKE 21 PMS results with the module of Sediment Transport (ST) might provide information about any morphological changes related to different sea level rise scenarios.

Bibliography

Bibliography

1. Abdalla, S., and Hersbach, H., 2004, The technical support for global validation of ERS wind and wave products at ECMWF, in Final Report for ESA contract 15988/02/I-LG, Reading, U. K.
2. Afentoylis, V.C., 2013, Numerical investigation of the intensification of wave action in the downstream of a harbor: National and Technical University of Athens, Greece.
3. Airy, G.B., 1845, Tides and Waves: *Encyclopedia Metropolitana*, v. 192, p. 241–396.
4. Alexandrakis, G., Ghionis, G., and Poulos, S., 2013, The effect of beach rock formation on the morphological evolution of a beach. The case study of an Eastern Mediterranean beach: Ammoudara, Greece: *Journal of Coastal Research*, v. 69, p. 47–59.
5. Alexandrakis, G., Poulos, S., Petrakis, S., and Collins, M., 2011, The development of a Beach Vulnerability Index (BVI) for the assessment of erosion in the case of the North Cretan Coast (Aegean Sea): *Hellenic Journal of Geosciences*, v. 45, p. 11–22.
6. Anagnostopoulou, C., Zanis, P., Katragkou, E., Tegoulas, I., and Tolika, K., 2014, Recent past and future patterns of the Etesian winds based on regional scale climate model simulations: *Climate Dynamics*, v. 42, no. 7-8, p. 1819–1836.
7. Andrae, U., Sokka, N., and Onogi, K., 2004, The radiosonde temperature bias correction in ERA-40, in ERA-40 Project Report Series, ECMWF, Reading, U. K.
8. Appendini, C.M., Torres-Freyermuth, A., Oropeza, F., Salles, P., López, J., and Mendoza, E.T., 2013, Wave modeling performance in the Gulf of Mexico and Western Caribbean: Wind reanalyses assessment: *Applied Ocean Research*, v. 39, p. 20–30.
9. Athanasoulis, G.A., and Skarsoulis, E.K., 1992, Wind and wave atlas of the Mediterranean Sea: Athens, Greece.
10. Bagiorgas, H.S., Mihalakakou, G., Rehman, S., and Al-Hadhrami, L.M., 2012, Offshore wind speed and wind power characteristics for ten locations in Aegean and Ionian Seas: *Journal of Earth System Science*, v. 121, no. 4, p. 975–987.
11. Battjes, J.A., 1974, Surf similarity, in 14th International Conference on Coastal Engineering, ASCE, Reston, VA, p. 466–480.
12. Battjes, J.A.A., and Janssen, J.P.F.M.P.F.M., 1978, Energy loss and set-up due to breaking of random waves, in Proceedings of the 16th international conference on coastal engineering, p. 569–587.
13. Berkhoff, J.C.W., 1972, Computation of Combined Refraction - Diffraction, in Proceedings of the 13th International Conference on Coastal Engineering, ASCE, p. 471 – 490.
14. Berrisford, P., Dee, D., Poli, P., Brugge, R., Fielding, K., Fuentes, M., Kallberg, P., Kobayashi, S., Uppala, S., and Simmons, A., 2009, The ERA-Interim Archive:.
15. Berrisford, P., Dee, D., Poli, P., Brugge, R., Fielding, K., Fuentes, M., Kallberg, P., Kobayashi, S., Uppala, S., Simmons, A., and Brugger, R., 2011, ERA report: The ERA-Interim archive:.
16. Bidlot, J.R., Holmes, D.J., Wittmann, P.A., Lalbeharry, R., and Chen, H.S., 2002, Intercomparison of the performance of operational ocean wave forecasting systems with buoy data: *Weather and Forecasting*, v. 17, p. 287–310.
17. Bidlot, J.-R., Janssen, P., and Abdalla, S., 2007, Impact of the revised formulation for ocean wave dissipation on the ECMWF operational wave model:.
18. Booij, N., Ris, R.C., and Holthuijsen, L.H., 1999, A third-generation wave model for coastal regions: 1. Model description and validation: *Journal of Geophysical Research*, v. 104, no. C4, p. 7649.
19. Brodtkorb, P.A., Johannesson, P., Lindgren, G., Rychlik, I., RydÅn, J., and SjöÅ, E., 2000, WAFO—a Matlab toolbox for analysis of random waves and loads: Seattle, USA.
20. Cartwright, D.E., and Longuet-Higgins, M.S., 1956, The statistical distribution of the maxima of a random function: *Proceedings of the Royal Society of London. Series A, Mathematical and Physical Sciences*, v. 237, no. 1209, p. 212–232.
21. Carvalho, D., Rocha, A., and Gómez-Gesteira, M., 2012, Ocean surface wind simulation forced by different reanalyses: Comparison with observed data along the Iberian Peninsula coast: *Ocean Modelling*, v. 56, p. 31–42.
22. Casas-Prat, M., and Holthuijsen, L.H., 2010, Short-term statistics of waves observed in deep water: *Journal of Geophysical Research*, v. 115, no. C9, p. C09024.
23. CERC, 1984, Shore protection manual:.
24. Chawla, A., Spindler, D.M., and Tolman, H.L., 2013, Validation of a thirty year wave hindcast using the Climate Forecast System Reanalysis winds: *Ocean Modelling*, v. 70, p. 189–206.
25. Christopoulos, S., and Koutitas, C.G., 1991, Wave modeling in the North Aegean Sea: *Annales Geophysicae*, v. 9, p. 91–101.
26. Church, J.A., and White, N.J., 2011, Sea-Level Rise from the Late 19th to the Early 21st Century: *Surveys in Geophysics*, v. 32, no. 4-5, p. 585–602.
27. Clarke, L., Edmonds, J., Jacoby, H., Pitcher, H., Reilly, J., and Richels, R., 2007, Scenarios of greenhouse gas emissions and atmospheric concentrations: *US Department of Energy Publications*, no. July, p. 6.
28. Courtier, P., Thépaut, J.-N., and Hollingsworth, A., 1994, A strategy for operational implementation of 4D-Var, using an incremental approach: *Quarterly Journal of the Royal Meteorological Society*, v. 120, no. 519, p. 1367–1387.
29. Dean, R.G., and Dalrymple, R.A., 1984, Water Wave Mechanics for Engineers and Scientists: Prentice Hall, Inc., New Jersey, USA.

30. Dee, D.P., Uppala, S.M., Simmons, a. J., Berrisford, P., Poli, P., Kobayashi, S., Andrae, U., Balmaseda, M. a., Balsamo, G., Bauer, P., Bechtold, P., Beljaars, a. C.M., van de Berg, L., Bidlot, J., Bormann, N., et al., 2011, The ERA-Interim reanalysis: configuration and performance of the data assimilation system: *Quarterly Journal of the Royal Meteorological Society*, v. 137, no. 656, p. 553–597.
31. DHI, 2014, MIKE 21, Parabolic Mild - Slope Wave Module.
32. Dingemans, M.W., 1983, Verification of numerical wave equation models with field measurements.
33. European Environmental Agency, 2014, Global and European sea-level rise:.
34. Flocas, H.A., and Karacostas, T.S., 1994, Synoptic and dynamic characteristics of cyclogenesis over the Aegean Sea, *in* International Symposium on the Life Cycles of Extratropical Cyclones, Bergen, Norway, p. 186–191.
35. Flocas, H.A., Simmonds, I., Kouroutzoglou, J., Keay, K., Hatzaki, M., Bricolas, V., and Asimakopoulos, D., 2010, On Cyclonic Tracks over the Eastern Mediterranean: *Journal of Climate*, v. 23, no. 19, p. 5243–5257.
36. Forristall, G.Z., 1978, On the statistical distribution of wave heights in a storm: *Journal of Geophysical Research: Oceans*, v. 83, no. C5, p. 2353–2358.
37. Foutrakis, P., Poulos, S., Maroukian, X., Livaditis, G., and Maroukian, H., 2007, A study of the Deltaic coast morphometry of river Pinios in relation to its hydro- & sediment dynamics: *Bulletin of the Geological Society of Greece*, p. 1522–1528.
38. Fujino, J., Nair, R., Kainuma, M., Masui, T., and Matsuoka, Y., 2006, Multi-gas mitigation analysis on stabilization scenarios using aim global model: *Energy Journal*, v. 27, no. SPEC. ISS. NOV., p. 343–353.
39. Galiatsatou, P., and Prinos, P., 2014, Analysing the Effects of Climate Change on Wave Height Extremes in the Greek Seas, *in* Kopmann, L.& ed., ICHE 2014, Hamburg, p. 773–781.
40. Galvin, C.J., 1968, Breaker type classification on three laboratory beaches: *Journal of Geophysical Research*, v. 73, no. 12, p. 3651.
41. Goda, Y., 1978, The observed joint distribution of periods and heights of sea waves, *in* Proceedings of the 16th Conference of Coastal Engineering, ASCE, New York, Hamburg, p. 277–246.
42. Hansen, S.E., and Stel, J.H., 1997, Seawatch: Performance and future, *in* Behrens, H. and Borst, J. eds., Operational Oceanography: The Challenge for European Co-operation, Elsevier.
43. Hasselmann, K., 1968, Weak-interaction theory of ocean waves: *Basic Developments in Fluid Dynamics*, v. 2, p. 117–182.
44. Hasselmann, K., Barnett, T.P., and Bouws, E., 1973, Measurements of wind-wave growth and swell decay during the Joint North Sea Wave Project (JONSWAP): *Deutsche Hydrographische Zeitschrift*, v. A12, no. 80, p. 1–95.
45. Hijioka, Y., Matsuoka, Y., Nishimoto, H., Masui, T., and Kainuma, M., 2008, Global GHG emission scenarios under GHG concentration stabilization targets: *Journal of Global Environment Engineering*, v. 13, p. 97–108.
46. Holgate, S.J., Matthews, A., Woodworth, P.L., Rickards, L.J., Tamisiea, M.E., Bradshaw, E., Foden, P.R., Gordon, K.M., Jevrejeva, S., and Pugh, J., 2013, New Data Systems and Products at the Permanent Service for Mean Sea Level: *Journal of Coastal Research*, v. 288, no. 3, p. 493–504.
47. Holthuijsen, L.H., 2007, Waves in oceanic and coastal waters: Cambridge University Press, New York, USA.
48. IPCC, 2013, Climate Change 2013: The Physical Science Basis. Contribution of Working Group I to the Fifth Assessment Report of the Intergovernmental Panel on Climate Change (T. F. Stocker, D. Qin, G.-K. Plattner, M. Tignor, S. K. Allen, J. Boschung, A. Nauels, Y. Xia, V. Bex, & P. M. Midgley, Eds.): Cambridge University Press, Cambridge, UK and New York, NY, USA.
49. IPCC Expert Meeting Report, 2008, Towards New Scenarios for Analysis of Emissions, Climate Change, Impacts and Response Strategies:.
50. Iribarren, C.R., and Nogales, C., 1949, Protection des ports, *in* XVIIth Int. Naval Congress, Lisbon, p. 31–80.
51. Janssen PAEM, 2004, The Interaction of Ocean Waves and Wind: Cambridge University Press, Cambridge, United Kingdom, United Kingdom.
52. Jonsson, I.G., 1966, Wave boundary layers and friction factors: *Proceedings of the 10th International Conference on Coastal Engineering, Tokyo 1966*, v. 1, no. 10, p. 127–148.
53. Kallos G., Kotroni, V., Lagouvardos, K., Varinou, M., Uliasz, M., Papadopoulos, A., Luria, M., Peleg, M., Sharf, G., Matveev, V., Alper-Simanov, D., Wanger, A., Tuncel, G., Tuncel, S., Aras, N.K., et al., 1996, Transport and Transformation of Air Pollutants from Europe to the East Mediterranean Region (T-TRAPEM). Project AVICENNE. Final Report for the EC, DG-XII.
54. Kallos, G., Kotroni, V., and Lagouvardos, K., 1997, The regional weather forecasting system SKIRON: an overview, *in* Symposium on regional weather prediction on parallel computer environments, p. 109–122.
55. Kamphuis, J.W., 2000, Introduction to Coastal Engineering & Management: World Scientific Publishing Co. Pte. Ltd, Singapore.
56. Kamphuis, J.W., 1991, Wave Transformation: *Co. Eng.*, v. 15, p. 173–184.
57. Karympalis, E., and Gaki-Papanastasiou, K., 2008, Geomorphological study of the rivers: Pinios, Kalamas, Evinos and Mornos., *in* 4th Panhellenic Geographical Conference, Athens, Greece, p. 86–94.
58. Kechris, C., and Soukissian, T., 2004, Inter-comparison of Topex/Poseidon, wave buoy and WAM model results in North Aegean Sea, *in* The Fourteenth International Offshore and Polar Engineering Conference - ISOPE 2004, p. 163–168.

59. Kirby, J.T., 1986, Rational approximations in the parabolic equation method for water waves: *Coastal Engineering*, v. 10, no. 4, p. 355–378.
60. Klaic, Z.B., Pasarić, Z., and Tudor, M., 2009, On the interplay between sea-land breezes and Etesian winds over the Adriatic: *Journal of Marine Systems*, v. 78, p. S101–S118.
61. Koletsis, I., Lagouvardos, K., Kotroni, V., and Bartzokas, a., 2009, The interaction of northern wind flow with the complex topography of Crete Island – Part 1: Observational study: *Natural Hazards and Earth System Science*, v. 9, no. 6, p. 1845–1855.
62. Komar, P.D., 2009, Beach processes and sedimentation: Prentice Hall PTR, 1998.
63. Komen, G.J., Cavaleri, L., Donelan, M., Hasselmann, K., Hasselmann, S., and PAEM, J., 1994, Dynamics and Modelling of Ocean Waves: Cambridge University Press, UK.
64. Kotroni, V., Lagouvardos, K., and Lalas, D., 2001, The effect of the island of Crete on the Etesian winds over the Aegean Sea: *Quarterly Journal of the Royal Meteorological Society*, v. 127, no. 576, p. 1917–1937.
65. Kouroutzoglou, J., Flocas, H.A., Keay, K., Simmonds, I., and Hatzaki, M., 2011, Climatological aspects of explosive cyclones in the Mediterranean: *International Journal of Climatology*, v. 31, no. 12, p. 1785–1802.
66. Krestenitis, Y., Androulidakis, Y., Makris, C., Kobiadou, K., Baltikas, V., and Diamanti, P., 2015, Evolution of storm surge extreme events in Greek Seas under climate change scenario, in 11th Panhellenic Symposium of Oceanography & Fisheries2, HCMR, Lesvos, p. 849–852.
67. Kumaraswamy, P., 1980, A generalized probability density function for double-bounded random processes: *Journal of Hydrology*, v. 46, no. 1-2, p. 79–88.
68. LeBlond, P.H., and Mysak, L.A., 1978, Waves in the Ocean: Elsevier Scientific Publishing Company, Amsterdam, The Netherlands.
69. Lelieveld, J., Hadjinicolaou, P., Kostopoulou, E., Chenoweth, J., El Maayar, M., Giannakopoulos, C., Hannides, C., Lange, M. a., Tanarhte, M., Tyrlis, E., and Xoplaki, E., 2012, Climate change and impacts in the Eastern Mediterranean and the Middle East: *Climatic Change*, v. 114, no. 3-4, p. 667–687.
70. Lionello, P., Bhand, J., Buzzi, A., Della-Marta, P.M., Krichak, S.O., Jansà, A., Maheras, P., Sanna, A., Trigo, I.F., and Trigo, R., 2006, Cyclones in the Mediterranean region: Climatology and effects on the environment, in Lionello, P., Malanotte-Rizzoli, P., and Boscolo, R. eds., *Developments in Earth and Environmental Sciences*, Elsevier, Amsterdam, The Netherlands, p. 325–372.
71. Lionello, P., Günther, H., and Janssen, P.A.E.M., 1992, Assimilation of altimeter data in a global third-generation wave model: *Journal of Geophysical Research*, v. 97, no. C9, p. 14453.
72. Lionello, P., Malanotte-Rizzoli, P., Boscolo, R., Alpert, P., Artale, V., Li, L., Luterbacher, J., May, W., Trigo, R., Tsimplis, M., Ulbrich, U., and Xoplaki, E., 2006, The Mediterranean climate: An overview of the main characteristics and issues (P. Lionello, P. Malanotte-Rizzoli, & R. Boscolo, Eds.): *Developments in Earth and Environmental Sciences*, v. 4, p. 1–26.
73. Lionello, P., Malanotte-Rizzoli, P., Boscolo, R., Tsimplis, M.N., Zervakis, V., Josey, S.A., Peneva, E.L., Struglia, M.V., Stanev, E. V., Theocharis, A., Lionello, P., Malanotte-Rizzoli, P., Artale, V., Tragou, E., and Oguz, T., 2006, Changes in the oceanography of the Mediterranean Sea and their link to climate variability, in Lionello, P., Malanotte-Rizzoli, P., and Boscolo, R. eds., *Developments in Earth and Environmental Sciences*, Amsterdam, The Netherlands, p. 227–282.
74. Lionello, P., and Sanna, A., 2005, Mediterranean wave climate variability and its links with NAO and Indian Monsoon: *Climate Dynamics*, v. 25, no. 6, p. 611–623.
75. Longuet-Higgins, M., 1975, On the joint distribution of the periods and amplitudes of sea waves: *Journal of Geophysical Research*, v. 80, no. 18, p. 2688–2694.
76. Longuet-Higgins, M.S., 1952, On the statistical distribution of the heights of sea waves: *Journal of Marine Research*, v. 11, p. 245–266.
77. Maheras, P., 1980, Le probleme des Etesiens: *Mediterranee*, v. 40, p. 57–66.
78. Maheras, P., Flocas, H.A., Patrikas, I., and Anagnostopoulou, C., 2001, A 40 year objective climatology of surface cyclones in the Mediterranean region: spatial and temporal distribution: *International Journal of Climatology*, v. 21, no. 1, p. 109–130.
79. Makris, C. V., Avgeris, I., and Memos, C.D., 2007, Hydraulic behaviour of submerged breakwaters: a case study, in Proceedings of the 4th International Conference Port Development and Coastal Environment, Varna, Bulgaria, p. 10.
80. Makris, C. V., and Memos, C.D., 2007, Wave Transmission over Submerged Breakwaters: Performance of Formulae and Models, in Proceedings of the 17th International Offshore and Polar Engineering Conference, ISOPE, Lisbon, Portugal, p. 2613–2620.
81. Martin, P., Dragani, W., Cerne, B., Alonso, G., Pescio, A., and Prario, B., 2012, Numerical simulation of wind waves on the Río de la Plata: evaluation of four global atmospheric databases: *Brazilian Journal of Oceanography*, v. 60, no. 4, p. 501–511.
82. Masters, D., Nerem, R.S., Choe, C., Leuliette, E., Beckley, B., White, N., and Ablain, M., 2012, Comparison of Global Mean Sea Level Time Series from TOPEX/Poseidon, Jason-1, and Jason-2: *Marine Geodesy*, p. 120830133821002.
83. Mastrandrea, M.D., Field, C.B., Stocker, T.F., Edenhofer, O., Ebi, K.L., Frame, D.J., Held, H., Kriegler, E., Mach, K.J., Matschoss, P.R., Plattner, G.-K., Yohe, G.W., and Zwiers, F.W., 2010, Guidance note for lead authors of the IPCC fifth assessment report on consistent treatment of uncertainties: *Intergovernmental Panel on Climate Change (IPCC)*, v. 9, no. October, p. 11–14.
84. Mavrantonakis, A.I., 2013, Design of marina structures in relation with sediment transport in the entrance and suggestions for improvement: National and Technical University of Athens, Greece.
85. McCowan, J., 1894, On the highest wave of permanent type: *Phil. Mag.*, v. 5, no. 38, p. 351–357.

86. Le Mehaute, B., 1976, An introduction to hydrodynamics and water waves: Springer-Verlag, New York, USA.
87. Mertens, L.P., 2006, Biological Oceanography Research Trends: Nova Science Publishers, Inc., New York, USA.
88. Metaxas, D.A., 1977, The interannual variability of the Etesian frequency as a response of atmospheric circulation anomalies: *Bulletin of the Hellenic Meteorological Society*, v. 2, no. 5, p. 30–40.
89. Miche, R., 1944, Mouvements ondulatoires des mers en profondeur constante on décroissante.: *Ann. Des Ponts et Chaussées*, p. 25–78.
90. Miles, J.W., 1957, On the generation of surface waves by shear flows: *Journal of Fluid Mechanics*, v. 3, p. 185–204.
91. Monioudi, I.N., Karditsa, A., Chatzipavlis, A., Alexandrakis, G., Andreadis, O.P., Velegrakis, A.F., Poulos, S.E., Ghionis, G., Petrakis, S., Sifnioti, D., Hasiotis, T., Lipakis, M., Kampanis, N., Karambas, T., and Marinos, E., 2014, Assessment of vulnerability of the eastern Cretan beaches (Greece) to sea level rise: *Regional Environmental Change*,.
92. Mooney, P.A., Mulligan, F.J., and Fealy, R., 2011, Comparison of ERA-40, ERA-Interim and NCEP/NCAR reanalysis data with observed surface air temperatures over Ireland: *International Journal of Climatology*, v. 31, no. 4, p. 545–557.
93. Moss, R.H., Edmonds, J.A., Hibbard, K.A., Manning, M.R., Rose, S.K., van Vuuren, D.P., Carter, T.R., Emori, S., Kainuma, M., Kram, T., Meehl, G.A., Mitchell, J.F.B., Nakicenovic, N., Riahi, K., Smith, S.J., et al., 2010, The next generation of scenarios for climate change research and assessment.: *Nature*, v. 463, no. 7282, p. 747–756.
94. Munk, W.H., 1949, The solitary wave theory and its application to surf problems: *Annals New York Academy of Sciences*, v. 51, p. 376–424.
95. Nastos, P.T., and Sifnioti, D.E., 2012, Synoptic composite means and anomalies of meteorological parameters associated with high sea waves in the Eastern Mediterranean., in *MedCLIVAR 2012*, Madrid, Spain.
96. Nastos, P.T., Sifnioti, D.E., Poulos, S.E., and Soukissian, T.H., 2013, Seasonal synoptic composite means of the surface vector wind speed associated with sea waves in the Aegean and the Ionian Seas (Eastern Mediterranean), in *13th International Conference on Environmental Science and Technology*, Athens, Greece, p. 8.
97. Nittis, K., Zervakis, V., and Perivoliotis, L., 2001, Operational monitoring and forecasting in the Aegean Sea: system limitations and forecasting skill evaluation: *Marine pollution bulletin*, v. 43, no. 7-12, p. 154–163.
98. NOAA, 2012, MetEd Comet:.
99. Panagopoulos, A., Karyotis, T., Kalfoutzos, D., Alexiou, J., and Kotsopoulos, S., 2001, Influence of land and water use to groundwater resources of the sensitive hydrogeological environment of the river Pinios estuary, central Greece: *Proc. 3rd Int. Conference Future Groundwater Resources at Risk'*, p. 391–398.
100. Pandian, P.K., Ramesh, S., Murthy, M.V.R., Ramachandran, S., and Thayumanavan, S., 2004, Shoreline Changes and Near Shore Processes Along Ennore Coast, East Coast of South India: *Journal of Coastal Research*, v. 203, p. 828–845.
101. Phillips, O.M., 1957, On the generation of waves by turbulent wind: *Journal of Fluid Mechanics*, v. 2, p. 417–455.
102. Pierson, W., 1952, A Unified Mathematical Theory for the Analysis, Propagation, and Refraction of Storm Generated Ocean Surface Waves: Research Division, College of Engr., Dept. of Meteorology, New York University.
103. Pierson, J.W.J., and Moskowitz, L., 1964, A proposed spectral form for fully developed wind seas based on the similarity theory of SA Kitaigorodskii: *Journal of geophysical research*, v. 69, no. 24, p. 5181–5190.
104. Portilla, J., Sosa, J., and Cavaleri, L., 2013, Wave energy resources: Wave climate and exploitation: *Renewable Energy*, v. 57, p. 594–605.
105. Poulos, S.E., 1989, Deltaic sedimentation in the microtidal waves of Greece: *Waves*, Cardiff UK.
106. Poulos, S.E., Collins, M.B., and Evans, G., 1996, Water-sediment fluxes of Greek rivers, Southeastern Alpine Europe: annual yields, seasonal variability, delta formation and human impact: *Z. Geomorph. N.R.*, v. 40, p. 243–261.
107. Poulos, S.E., Drakopoulos, P.G., and Collins, M.B., 1997, Seasonal variability in sea surface oceanographic conditions in the Aegean Sea (Eastern Mediterranean): an overview: *Journal of Marine Systems*, v. 13, p. 225–244.
108. Poulos, S.E., Ghionis, G., Verykiou, E., Roussakis, G., Sakellariou, D., Karditsa, A., Alexandrakis, G., Petrakis, S., Sifnioti, D., Panagiotopoulos, I.P., Andris, P., and Georgiou, P., 2014, Hydrodynamic, neotectonic and climatic control of the evolution of a barrier beach in the microtidal environment of the NE Ionian Sea (eastern Mediterranean): *Geo-Marine Letters*,.
109. Poupkou, A., Zanis, P., Nastos, P., Papanastasiou, D., Melas, D., Tourpali, K., and Zerefos, C., 2011, Present climate trend analysis of the Etesian winds in the Aegean Sea: *Theoretical and Applied Climatology*, v. 106, no. 3-4, p. 459–472.
110. Reiter, E., 1975, Handbook for Forecasters in the Mediterranean; Weather Phenomena of the Mediterranean Basin; Part 1. General Description of the Meteorological Processes.
111. Riahi, K., Grübler, A., and Nakicenovic, N., 2007, Scenarios of long-term socio-economic and environmental development under climate stabilization: *Technological Forecasting and Social Change*, v. 74, no. 7, p. 887–935.

112. Saaroni, H., Ziv, B., Bitan, A., and Alpert, P., 1998, Easterly Wind Storms over Israel: *Theoretical and Applied Climatology*, v. 59, p. 61–77.
113. Savioli, J., 2007, Stockton Beach Coastal Protection Study, Stage 1- Sediment Transport Analysis and Description of On-going Processes.
114. Shanas, P.R., and Sanil Kumar, V., 2013, Temporal variations in the wind and wave climate at a location in the eastern Arabian Sea based on ERA-Interim reanalysis data: *Natural Hazards and Earth System Sciences Discussions*, v. 14, no. 5, p. 7239–7269.
115. Shanas, P.R., and Sanil Kumar, V., 2014, Trends in surface wind speed and significant wave height as revealed by ERA-Interim wind wave hindcast in the Central Bay of Bengal: *International Journal of Climatology*.
116. Shepard, F., 1956, Marginal sediments of Mississippi delta: *AAPG Bulletin*, v. 40, p. 2537–2623.
117. Short, A.D., 2012, Coastal Processes and Beaches: *Nature Education Knowledge*, v. 3, no. 10, p. 15.
118. Sifnioti, D.E., Soukissian, T.H., and Poulos, S.E., 2014, Short term spectral and statistical analysis of sea surface elevation data from buoys located in the Greek Seas, in 10th International Conference of the Hellenic Geomorphological Society, Thessaloniki, Greece, p. 20.
119. Sifnioti, D.E., Soukissian, T.H., Poulos, S.E., and Nastos, P.T., 2013, Study of the relationship of wave and wind data, from offshore buoys in the Aegean and Ionian Seas., in EMS 2013 Annual Meeting Abstracts, p. 2013.
120. Smith, S.J., and Wigley, T.M.L., 2006, Multi-gas forcing stabilization with minicam: *Energy Journal*, v. 27, no. SPEC. ISS. NOV., p. 373–391.
121. Soukissian, T., 2008, Assessment of the wind and wave climate of the Hellenic Seas using 10-year hindcast results: *Open Ocean Engineering Journal*, v. 1, p. 1–12.
122. Soukissian, T., and Chronis, G., 2000, Poseidon: A marine environmental monitoring, forecasting and information system for the Greek seas: *Mediterranean Marine Science*, v. 1, p. 71–78.
123. Soukissian, T.H., Chronis, G.T., and Nittis, K., 1999, POSEIDON: Operational Marine Monitoring System for Greek Seas: *Sea Technology*, v. 40, no. 7, p. 31–37.
124. Soukissian, T., Gizari, N., Fytilis, D., Papadopoulos, A., Korres, G., and Prospathopoulos, A., 2012, Wind and wave potential in offshore locations of the Greek seas, in Proceedings of the 12th international conference on coastal engineering, ISOPE, Rhodes, Greece, p. 525–532.
125. Soukissian, T., Hatzinaki, M., Korres, G., Papadopoulos, A., Kalos, G., and Anandranistakis, N., 2007, Wind and wave atlas of the Hellenic seas: HCMR.
126. Soukissian, T., Perivoliotis, L., and Prospathopoulos, A.M., 2001, Performance of Three Wave Models on Aegean Sea: First Results, in ISOPE ed., Proceedings of the Eleventh International Offshore and Polar Engineering Conference, Stavanger, Norway, p. 40–45.
127. Soukissian, T.H., Sifnioti, D.E., Prospathopoulos, A., and Kastriti, D., 2012, Short - Term Wave Statistics in the Greek Seas: *Proceedings of the Twenty-second (2012) International Offshore and Polar Engineering Conference*, v. 4, p. 784–791.
128. Stocker, T., Dahe, Q., and Plattner, G., 2013, Working Group I Contribution to the IPCC Fifth Assessment Report Climate Change 2013, The Physical Science Basis.
129. Stocker, T.F., Qin, D., Plattner, G.-K., Tignor, M., Allen, S.K., Boschung, J., Nauels, A., Xia, Y., Bex, V., and Midgley, P.M., 2013, The Physical Science Basis. Contribution of Working Group I to the Fifth Assessment Report of the Intergovernmental Panel on Climate Change:.
130. Stopa, J.E., and Cheung, K.F., 2014, Intercomparison of wind and wave data from the ECMWF Reanalysis Interim and the NCEP Climate Forecast System Reanalysis: *Ocean Modelling*, v. 75, p. 65–83.
131. Stopa, J.E., Cheung, K.F., Tolman, H.L., and Chawla, A., 2013, Patterns and cycles in the Climate Forecast System Reanalysis wind and wave data: *Ocean Modelling*, v. 70, p. 207–220.
132. Stournaras, G., and Galani, X., 1995, Morphometric Analysis of the Pinios Delta (Thessaly), in 4th Panhellenic Geographical Conference, Hellenic Geographical Society, Athens, Greece, p. 333–347.
133. Stournaras, G., Nastos, P., Gioxas, G., Evelpidou, N., Vassilakis, E., Partsinevelou, S.A., and Eliopoulos, V., 2011, Impacts of climate change on the surficial and below surface water masses of Greece:.
134. Sverdrup, H.V.H., and Munk, W.H., 1947, Wind, sea, and swell: theory of relations for forecasting.
135. Swart, D.H., 1974, Offshore sediment transport and equilibrium beach profiles: , p. 302.
136. Sylaios, G., 2011, Meteorological influences on the surface hydrographic patterns of the north Aegean Sea: *Oceanologia*, v. 53, no. 1, p. 57–80.
137. Tavolato, C., and Isaksen, L., 2010, ERA report series: Data usage and quality control for ERA-40, ERA-Interim and the operational ECMWF data assimilation system:.
138. Tayfun, M.A., and Fedele, F., 2007, Wave-height distributions and nonlinear effects: *Ocean Engineering*, v. 34, no. 11-12, p. 1631–1649.
139. Trémolet, Y., 2004, Diagnostics of linear and incremental approximations in 4D-Var: *Quarterly Journal of the Royal Meteorological Society*, v. 130, no. 601, p. 2233–2251.
140. Trigo, I., Bigg, G., and Davies, T., 2002, Climatology of cyclogenesis mechanisms in the Mediterranean: *Monthly weather review*, v. 130, p. 549–569.
141. Trigo, I.F., Davies, T.D., and Bigg, G.R., 1999, Objective climatology of cyclones in the Mediterranean region: *Journal of Climate*, v. 12, p. 1685–1696.
142. Tsimplis, M.N., 1994, Tidal Oscillations in the Aegean and Ionian Seas: *Estuarine, Coastal and Shelf Science*, v. 39, no. 2, p. 201–208.
143. Tsimplis, M.N., and Spencer, N.E., 1997, Collection and analysis of monthly mean sea level data in the Mediterranean and the Black Sea: *Journal of Coastal Research*, v. 13, p. 534–544.

144. Tyrlis, E., and Lelieveld, J., 2013, Climatology and Dynamics of the Summer Etesian Winds over the Eastern Mediterranean*: *Journal of the Atmospheric Sciences*, v. 70, no. 11, p. 3374–3396.
145. Tyrlis, E., Lelieveld, J., and Steil, B., 2013, The summer circulation over the eastern Mediterranean and the Middle East: Influence of the South Asian monsoon: *Climate Dynamics*, v. 40, no. 5-6, p. 1103–1123.
146. Uppala, S.M., Kållberg, P.W., Simmons, A.J., Andrae, U., Bechtold, V.D.C., Fiorino, M., Gibson, J.K., Haseler, J., Hernandez, A., Kelly, G.A., Li, X., Onogi, K., Saarinen, S., Sokka, N., Allan, R.P., et al., 2005, The ERA-40 re-analysis: *Quarterly Journal of the Royal Meteorological Society*, v. 131, no. 612, p. 2961–3012.
147. Vandever, J.P., Siegel, E.M., Brubaker, J.M., and Friedrichs, C.T., 2001, Evaluation of Wave Parameter Estimates in Coastal Environments, *in* AGU 2006, p. 2048.
148. Vasiljevic, D., 2005, Handling biases in surface pressure (Ps) observations in data assimilation, *in* Proceedings of ECMWF/EUMETSAT NWP-SAF Workshop on bias estimation and correction in data assimilation, ECMWF, Reading, U. K., p. 107–117.
149. Vasiljevic, D., Andersson, E., Isaksen, I., and Garcia-Mendez, A., 2006, Surface pressure bias correction in data assimilation: *ECMWF Newsletter 108*, p. 20–27.
150. Veerse, F., and Thepaut, J.-N., 1998, Multiple-truncation incremental approach for four-dimensional variational data assimilation: *Quarterly Journal of the Royal Meteorological Society*, v. 124, no. 550, p. 1889–1908.
151. van Vuuren, D.P., Edmonds, J., Kainuma, M., Riahi, K., Thomson, A., Hibbard, K., Hurtt, G.C., Kram, T., Krey, V., Lamarque, J.F., Masui, T., Meinshausen, M., Nakicenovic, N., Smith, S.J., and Rose, S.K., 2011, The representative concentration pathways: An overview: *Climatic Change*, v. 109, no. 1, p. 5–31.
152. van Vuuren, D.P., Eickhout, B., Lucas, P.L., and den Elzen, M.G.P., 2006, Long term multi-gas scenarios to stabilise radiative forcing-exploring costs and benefits within an integrated assessment framework: *The Energy Journal*, v. 27, no. 201-233.
153. Van Vuuren, D.P., Den Elzen, M.G.J., Lucas, P.L., Eickhout, B., Strengers, B.J., Van Ruijven, B., Wonink, S., and Van Houdt, R., 2007, Stabilizing greenhouse gas concentrations at low levels: An assessment of reduction strategies and costs: *Climatic Change*, v. 81, no. 2, p. 119–159.
154. Wise, M., Calvin, K., Thomson, A., Clarke, L., Bond-Lamberty, B., Sands, R., Smith, S.J., Janetos, A., and Edmonds, J., 2009, Implications of limiting CO₂ concentrations for land use and energy.: *Science (New York, N.Y.)*, v. 324, no. 5931, p. 1183–1186.
155. WMO, 1998, Guide to Wave Analysis and Forecasting.: World Meteorological Organization.
156. Woodworth, P.L., and Blackman, D.L., 2004, Evidence for systematic changes in extreme high waters since the mid-1970s: *Journal of Climate*, v. 17, no. 6, p. 1190–1197.
157. Zampakas, G.D., 1981, General Climatology:.
158. Zecchetto, S., and De Biasio, F., 2007, Sea surface winds over the Mediterranean basin from satellite data (2000-04): Meso- and local-scale features on annual and seasonal time scales: *Journal of Applied Meteorology and Climatology*, v. 46, no. 6, p. 814–827.
159. Zenetos, A., 2005, State of the Hellenic Marine Environment: *SoHelME, EPHCMR Publ.*, p. 362.

APPENDIX

ACRONYMS

| | |
|-----------------------|----------------------------------------------------------------------------------------------------------------------------------------------------------------------------------|
| AMV | ATMOSPHERIC MOTION VECTOR |
| AR5 | INTERGOVERNMENTAL PANEL ON CLIMATE CHANGE ASSESSMENT REPORT 5 |
| AVISO | HTTP://WWW.AVISO.ALTIMETRY.FR/EN/HOME.HTML |
| DAUT | 2 ND GENERATION AUT MODEL |
| DHI | DANISH HYDRAULIC INSTITUTE |
| DHI MIKE 21 HD | MIKE 21 HYDRODYNAMIC MODULE |
| DHI MIKE 21 OSW | OFFSHORE SPECTRAL WIND-WAVE MODULE |
| DHI MIKE 21 SW | MIKE 21 SPECTRAL WAVE MODULE |
| ECMWF | EUROPEAN CENTRE FOR MEDIUM-RANGE WEATHER FORECASTS |
| ENSEMBLES | ENSEMBLES PROJECT (HTTP://WWW.ENSEMBLES-EU.ORG/) |
| ENVISAT | ENVIRONMENTAL SATELLITE OF ESA |
| ERA-40 | ERA- 40 REANALYSIS DATASET HTTP://APPS.ECMWF.INT/DATASETS/DATA/ERA40-DAILY/ |
| ERA-INTERIM | ERA- INTERIM REANALYSIS DATASET HTTP://WWW.ECMWF.INT/EN/RESEARCH/CLIMATE-REANALYSIS/ERA-INTERIM |
| ERS-1, -2 | EUROPEAN REMOTE SENSING SATELLITES |
| ESA | EUROPEAN SATELLITE AGENCY |
| EUMETSAT | EUROPEAN ORGANISATION FOR THE EXPLOITATION OF METEOROLOGICAL SATELLITES |
| FGGE | FIRST GARP (GLOBAL ATMOSPHERIC RESEARCH PROGRAM) GLOBAL EXPERIMENT |
| GCM | GENERAL CIRCULATION MODEL |
| GEOSAT-FOLLOWON (GFO) | RADAR ALTIMETRY SATELLITE OF NASA |
| GHG | GREENHOUSE GASES |
| GMSL | GLOBAL MEAN SEA LEVEL |
| HCMR | HELLENIC CENTRE OF MARINE RESEARCH (WWW.HCMR.GR) |

| | |
|----------------------|---------------------------------------------------------------------------------------------------------------------------------------------|
| HNHS | HELLENIC NAVY HYDROGRAPHIC SERVICE (WWW.HNHS.GR) |
| IFS | INTEGRATED FORECAST SYSTEM (IFS) |
| IPCC | INTERGOVERNMENTAL PANEL ON CLIMATE CHANGE |
| METEOSAT 3, 4 , 5 ,6 | SERIES OF GEOSTATIONARY METEOROLOGICAL SATELLITES OPERATED BY EUMETSAT |
| NAO | NORTH ATLANTIC OSCILLATION |
| NASA | NATIONAL AERONAUTICS AND SPACE ADMINISTRATION |
| NCEP | NATIONAL CENTRE FOR ENVIRONMENTAL PREDICTION, |
| NETCDF | NETWORK COMMON DATA FORM (HTTP://WWW.UNIDATA.UCAR.EDU/SOFTWARE/NETCDF/) |
| OI | OPTIMAL INTERPOLATION |
| OISST | OPTIMAL INTERPOLATION SEA SURFACE TEMPERATURE |
| OSTIA | OPERATIONAL SEA SURFACE TEMPERATURE AND SEA ICE ANALYSIS |
| QUICKSCAT | NASA QUIKSCAT EARTH OBSERVATION SATELLITE |
| RCM | REGIONAL CLIMATE MODEL |
| RCP | REPRESENTATIVE CONCENTRATION PATHWAY |
| RTG | REAL TIME GLOBAL |
| SIC | SEA ICE COVER |
| SKIRON | HTTP://FORECAST.UOA.GR/FORECASTNEWINFO.PHP |
| SLR | SEA LEVEL RISE |
| SRES | SPECIAL REPORT EMISSION SCENARIOS |
| SST | SEA SURFACE TEMPERATURE |
| TOPEX/POSEIDON | HTTPS://SEALEVEL.JPL.NASA.GOV/MISSIONS/TOPEX/ |
| V.O.S. | VOLUNTARY OBSERVING SHIPS |
| WAFO | WAVE ANALYSIS FOR FATIGUE AND OCEANOGRAPHY (HTTP://WWW.MATHS.LTH.SE/MATSTAT/WAFO/) |
| WAM- WAMDI | WAVE MODEL DEVELOPMENT AND IMPLEMENTATION |

List of Figures

| | |
|----------------------------------------------------------------------------------------------------------------------------------------------------------------------------------------------------------------------------------------------------------------------------------------------------------------------------------------------------------------------------------------------------------------------------------------------------------------------------------------------------------------------------------------------------------------------------------------------------------------------------------------------------------------------------------------------------------------------------------------------------|----|
| Figure 2.1.1: A coastal subsystem and controlling processes (from (Kamphuis, 2000))..... | 8 |
| Figure 2.1.2: Shore zone physiographic characteristics (Short, 2012) | 9 |
| Figure 2.2.1: Basic Wave Parameters (Holthuijsen, 2007) | 9 |
| Figure 2.2.2: Classifying waves according to their period and height (Holthuijsen, 2007)..... | 10 |
| Figure 2.3.1: Wave theories applications in relation to water depth (from Le Mehaute, 1976)..... | 12 |
| Figure 2.3.2: Definition of surface elevation and wave, a) zero-down crossing waves and b) zero-up crossing waves. (Holthuijsen, 2007)..... | 14 |
| Figure 2.3.3: Wave spectrums and how they describe ocean waves. (Holthuijsen, 2007)..... | 17 |
| Figure 2.4.1: Equivalent fetch (F_{eq}) for the generation of a wind wave (Holthuijsen, 2007)..... | 20 |
| Figure 2.4.2 Comparison of a PM and a Jonswap Spectrum (Kamphuis, 2000)..... | 21 |
| Figure 2.4.3: Wave Spectra according to fetch as given by JONSWAP (Hasselmann et al., 1973; Holthuijsen, 2007) | 22 |
| Figure 2.5.1: Wave Shoaling (NOAA, 2012)..... | 23 |
| Figure 2.5.2: Wave Refraction (1) (NOAA, 2012) | 24 |
| Figure 2.5.3: Wave Refraction (2) (Kamphuis, 2000) | 25 |
| Figure 2.5.4: Wave diffraction in the lee of the barrier (Holthuijsen, 2007) | 26 |
| Figure 2.5.5: Wave Breaking Parameters (Kamphuis, 2000)..... | 27 |
| Figure 2.5.6:Types of Breaking Waves (Galvin, 1968)..... | 28 |
| Figure 2.7.1: Global mean sea level from 1880 to 2013 relative to the level of 1990 according to tide gauge and satellite altimetry data. Uncertainty level is shown in grey and dark blue line is time series of satellite altimetry data for the period 1993-2013(Church and White, 2011; Masters et al., 2012)..... | 31 |
| Figure 2.7.2: Sea level trends as estimated by several European tide gauges (from EEA, 2014; Woodworth and Blackman, 2004) | 31 |
| Figure 2.7.3: Trend of absolute sea level in Europe from satellite altimetry data for the period 1992-2013 (Holgate et al., 2013; European Environmental Agency, 2014) | 32 |
| Figure 2.7.4: Projections of GMSLR and its contributors (IPCC, 2013)..... | 35 |
| Figure 2.7.5: Projections for relative sea level (Church and White, 2011; IPCC, 2013) | 35 |
| Figure 3.1.1: The sub-basins of the Mediterranean: 1) Alboran Sea, 2) Algerian, 3) Balearic, 4) Liguro-Provençal, 5) Tyrrhenian, 6) Ionian Sea, 7) Adriatic Sea, 8) Levantine and 9) Aegean Sea. SG: Strait of Gibraltar, BC: Balearic Channels, CC: Corsica Channel, SC: Sardinia Channel, SS: Strait of Sicily, OS: Otranto Strait, CAS: Cretan Arc Straits, DC: Dardanelles Channel, GL: Gulf of Lions; BS: Black Sea. (Mertens, 2006)..... | 38 |
| Figure 3.1.2: Major morphological features of the Greek Seas. Adopted by (Zenetos, 2005) | 39 |
| Figure 3.1.3: Sedimentary Classification of the Greek Coastline (Zenetos, 2005) | 40 |
| Figure 3.1.4: Main local winds of the Mediterranean (Lionello, Bhend, et al., 2006) | 41 |
| Figure 3.1.5: Regions of similar wave characteristics (Athanasoulis and Skarsoulis, 1992) | 43 |
| Figure 3.1.6: Grid of the WAM model for the Mediterranean (upper) and b) of the Greek Seas (lower) . | 44 |
| Figure 3.1.7: Annual wind speed (a), Annual wind direction (b) (Soukissian et al., 2007)..... | 46 |
| Figure 3.1.8: Annual Significant Wave Height (a), Annual Peak Period (b) and Annual Wave Direction (c) (Soukissian et al., 2007)..... | 47 |
| Figure 3.1.9: Buoys locations (Soukissian et al., 2007)..... | 48 |
| Figure 3.1.10: Distribution of maximum significant wave height (contours in m) and direction (arrows) (Lionello and Sanna, 2005) | 50 |
| Figure 3.1.11: Synoptic charts of surface pressure related with maximum significant wave height, a) Ionian, b) Levantine basin (from Lionello and Sanna 2005)..... | 51 |
| Figure 3.1.12: Variation of significant wave height as given from linear trends of ERA40 reanalysis (Lionello and Sanna, 2005) | 52 |
| Figure 3.1.13: M2 tidal component from the models (contours) and the HNMS tide gauges (points) (a), sum of the four tidal components for the Hellenic Seas (b) (Tsimplis, 1994; Zenetos, 2005) | 53 |
| Figure 3.1.14: Evolution of annual maxima of SLH (m) for 6 Areas of the Eastern Mediterranean. The Solid lines represent past and future 2 nd degree polynomials ((Krestenitis et al., 2015) | 53 |
| Figure 3.2.1: Geomorphological map of the Pinios Delta on a 1:5000 scale, 1: Alluvial deposits, 2: Alluvial cones, 3: Deposits of the deltaic plain, 4: Neogene formations, 5: Flysch, 6: Schists, gneiss, Amphibolite, 7:Marbles, Limestone , 8: Fault, 9: Possible fault, 9: Lower river terrace, 11: Upper river terrace, 12: Coastal slate, 13: Existing riverbed (since 1955), 14: River bed prior to 1955, 15: Riverbed during 1910-1924, 16: Abandoned beds, 17: Abandoned meanders, 18: Point ridges - bars, 19: Fragmented overflow fine-grained deposits, 20: flinch coastline, 21: Advancing coastline, 22: Currents, 23: Sandy seashore zone, 24: Active sand dunes, 25: Coastal ridges (Karympalis and Gaki-Papanastasiou, 2008)..... | 55 |
| Figure 3.2.2: Annual wave directionality of the Greek Seas (from Athanasoulis and Skarsoulis, 1992).... | 57 |
| Figure 3.2.3: Annual Contours of significant wave height (a), wave period (b), wave steepness (c) and wave direction (d) (from Soukissian et al., 2007)..... | 59 |

| | |
|-------------------------------------------------------------------------------------------------------------------------------------------------------------------------------------------------------------------------------------------------------------------------------------------------------------------------------------------------------------------|-----|
| Figure 3.2.4: Monthly variation of sea level in Thessaloniki (http://www.psmsl.org/data/obtaining/stations/373.php) | 60 |
| Figure 3.2.5: Relative sea level of the tide gauge of Thessaloniki (http://www.psmsl.org/data/obtaining/rlr.diagrams/373.php)..... | 60 |
| Figure 3.2.6: Monthly variation of sea level in Skopelos (http://www.psmsl.org/data/obtaining/stations/1907.php) | 61 |
| Figure 3.2.7: Relative sea level of the tide gauge of Skopelos (http://www.psmsl.org/data/obtaining/rlr.diagrams/1907.php)..... | 61 |
| Figure 3.2.8: Co-tidal (--) and co-range (-) contours for the M2 tidal component of the Greek Seas (Tsimplis, 1994; Zenetos, 2005)..... | 62 |
| Figure 3.2.9: Pinios mouth: sand reposition (a), silt (b) and clay (c) in percent of total weight (*station positions) (originally from Poulos, 1989) | 63 |
| Figure 3.2.10: Pinios mouth: types of sediment according to Shepard, of the bottom of the basin (originally from Poulos, 1989) | 63 |
| Figure 4.1.1: Photos of Seawatch Buoy (left), Wavescan (middle), Wavescan-Deep Sea Module (right) (http://www.oceanor.com)..... | 67 |
| Figure 4.1.2: Initial locations of HCMR buoys (http://poseidon.hcmr.gr/article_view_no_news.php?id=117) | 68 |
| Figure 4.1.3: Buoys Locations | 69 |
| Figure 4.1.4: SSE Records | 72 |
| Figure 4.1.5: Basic structure of the algorithm used | 72 |
| Figure 4.2.1: Daily observations assimilated by ERA-Interim atmospheric model, (after Dee et al., 2011) | 78 |
| Figure 4.2.2: Timeline of conventional data included in ERA-Interim (Dee et al., 2011) | 79 |
| Figure 4.2.3: Scatterometer data sources included in ERA-Interim (Dee et al., 2011) | 80 |
| Figure 4.2.4: Normalized standard deviations of significant wave height (a), peak period (c), zero-crossing mean wave period (e) and wind speed in 10m (g) and biases of model and observations of wave parameters respectively (b, d, f, h) (Dee et al., 2011)..... | 81 |
| Figure 4.2.5: Website of ERA-Interim, ECMWF | 82 |
| Figure 4.2.6: Choosing area and grid spacing..... | 83 |
| Figure 4.2.7: Methods of collocation (7-point star is the buoy)..... | 85 |
| Figure 4.2.8: Correlation coefficients and root mean square error for the 8 stations between the buoy data and the ERA-Interim according to the 3 different collocation methods for wave height (a, b), wind speed (c, d) and temperature at 2 m (e,f). Stations are: 1: Athos, 2: Avgo, 3: E1M3A, 4: Lesvos, 5: Mykonos, 6: Pylos, 7: Santorini, 8: Skyros | 87 |
| Figure 4.2.9: Locations of the 5 selected points of ERA-Interim | 88 |
| Figure 4.3.1: Location of selected point of ERA-Interim (23°E, 39.875°N)..... | 89 |
| Figure 4.3.2: Locations of the Southern topographic surveys (yellow marks) and digital survey of the coastline (red line)..... | 90 |
| Figure 4.3.3: Photographs of location 3, landwards (a), seawards (b), northwards (c) and southwards (d) - Survey Conducted in October 2013..... | 91 |
| Figure 4.3.4: Photographs of location 6, landwards (a), seawards (b), northwards (c) and southwards (d) Survey Conducted in October 2013..... | 91 |
| Figure 4.3.5: Isobaths from the bathymetric survey (Akti Engineering - THALIS- DAPHNE) | 92 |
| Figure 5.1.1: Rose Diagrams for Significant Wave Height and Wave period for all wave directions (a,b), swells (c,d) and wind waves (e,f) from Athos buoy..... | 103 |
| Figure 5.1.2: Box and Whiskers plots for Monthly Wave Height and Wave Period for Athos Buoy..... | 104 |
| Figure 5.1.3: Random SSE record and it's spectral definition for Athos Buoy | 105 |
| Figure 5.1.4: Scatterplots of statistical and spectral wave parameters for Athos Buoy | 106 |
| Figure 5.1.5: Spectral and Statistical Monthly Values per Wave Parameter for Athos Buoy | 106 |
| Figure 5.1.6: Probability Distributions and QQ plots for Athos Buoy for random wave heights | 107 |
| Figure 5.1.7: Wind Chart for Athos Buoy..... | 109 |
| Figure 5.1.8: Monthly Box and Whiskers Plots for Atmospheric Parameters for Athos Buoy | 109 |
| Figure 5.1.9: Charts of Wind Direction and Wave Height - periodfor Athos Buoy..... | 111 |
| Figure 5.1.10: Rose Diagrams for Significant Wave Height and Wave period for all waves (a,b), swells (c,d) and wind waves (e,f) for Avgo Buoy..... | 113 |
| Figure 5.1.11: Box and Whiskers plots for Monthly Wave Height and Wave Period for Avgo Buoy | 114 |
| Figure 5.1.12: Wind Chart for Avgo Buoy | 115 |
| Figure 5.1.13: Monthly Box and Whiskers Plots for Atmospheric Parameters for Avgo Buoy | 116 |
| Figure 5.1.14: Charts of Wind Direction and Wave Height - periodfor the Avgo Buoy..... | 118 |
| Figure 5.1.15: Rose Diagrams for Significant Wave Height and Wave period for all waves (a,b), swells (c,d) and wind waves (e,f) for Dia Buoy..... | 120 |
| Figure 5.1.16: Box and Whiskers plots for Monthly Wave Height and Wave Period for Dia Buoy..... | 121 |
| Figure 5.1.17: Rose Diagrams for Significant Wave Height and Wave period for all waves (a,b), swells (c,d) and wind waves (e,f) for E1M3A Buoy | 123 |

| | |
|-----------------------------------------------------------------------------------------------------------------------------------------------------------|-----|
| Figure 5.1.18: Box and Whiskers plots for Monthly Wave Height and Wave Period for E1M3A Buoy ... | 124 |
| Figure 5.1.19: Wind Chart for E1M3A Buoy | 125 |
| Figure 5.1.20: Monthly Box and Whiskers Plots for Atmospheric Parameters for E1M3A Buoy | 125 |
| Figure 5.1.21: Charts of Wind Direction and Wave Height - Period for E1M3A Buoy | 127 |
| Figure 5.1.22: Rose Diagrams for Significant Wave Height and Wave period for all waves (a,b), swells (c,d) and wind waves (e,f) for Kalamata Buoy..... | 129 |
| Figure 5.1.23: Box and Whiskers plots for Monthly Wave Height and Wave Period for Kalamata Buoy | 130 |
| Figure 5.1.24: Random SSE record and it's spectrum for Kalamata Buoy..... | 131 |
| Figure 5.1.25: Scatterplots of statistical and spectral wave parameters for Kalamata Buoy | 132 |
| Figure 5.1.26: Spectral and Statistical Monthly Values per Wave Parameter for Kalamata Buoy..... | 132 |
| Figure 5.1.27: Probability Distributions and QQ plots for Kalamata Buoy for random wave heights | 133 |
| Figure 5.1.28: Wind Chart for Kalamata Buoy..... | 135 |
| Figure 5.1.29: Monthly Box and Whiskers Plots for Atmospheric Parameters for Kalamata Buoy | 135 |
| Figure 5.1.30: Charts of Wind Direction and Wave Height - Period for Kalamata Buoy..... | 137 |
| Figure 5.1.31: Rose Diagrams for Significant Wave Height and Wave period for all waves (a,b), swells (c,d) and wind waves (e,f) for Katerini Buoy | 139 |
| Figure 5.1.32: Box and Whiskers plots for Monthly Wave Height and Wave Period for Katerini Buoy .. | 140 |
| Figure 5.1.33: Wind Chart for Katerini Buoy | 141 |
| Figure 5.1.34: Monthly Box and Whiskers Plots for Atmospheric Parameters for Katerini Buoy..... | 142 |
| Figure 5.1.35: Charts of Wind Direction and Wave Height - Period for Katerini Buoy | 144 |
| Figure 5.1.36: Rose Diagrams for Significant Wave Height and Wave period for all waves (a,b), swells (c,d) and wind waves (e,f) for Lesvos Buoy | 146 |
| Figure 5.1.37: Box and Whiskers plots for Monthly Wave Height and Wave Period for Lesvos Buoy | 147 |
| Figure 5.1.38: Wind Chart for Lesvos Buoy | 148 |
| Figure 5.1.39: Monthly Box and Whiskers Plots for Atmospheric Parameters for Lesvos Buoy | 149 |
| Figure 5.1.40: Charts of Wind Direction and Wave Height - Period for Lesvos Buoy | 150 |
| Figure 5.1.41: Rose Diagrams for Significant Wave Height and Wave period for all waves (a,b), swells (c,d) and wind waves (e,f) for Mykonos Buoy..... | 152 |
| Figure 5.1.42: Box and Whiskers plots for Monthly Wave Height and Wave Period for Mykonos | 153 |
| Figure 5.1.43: Random SSE record and it's spectrum for Mykonos Buoy..... | 154 |
| Figure 5.1.44: Scatterplots of statistical and spectral wave parameters for Mykonos Buoy | 155 |
| Figure 5.1.45: Spectral and Statistical Monthly Values per Wave Parameter for Mykonos Buoy..... | 156 |
| Figure 5.1.46: Probability Distributions and QQ plots for Mykonos for random wave heights..... | 156 |
| Figure 5.1.47: Wind Chart for Mykonos Buoy | 158 |
| Figure 5.1.48: Monthly Box and Whiskers Plots for Atmospheric Parameters for Mykonos Buoy | 159 |
| Figure 5.1.49: Charts of Wind Direction and Wave Height - Period for Mykonos Buoy | 160 |
| Figure 5.1.50: Rose Diagrams for Significant Wave Height and Wave period for all waves (a,b), swells (c,d) and wind waves (e,f) for Petrokaravo Buoy..... | 162 |
| Figure 5.1.51: Box and Whiskers plots for Monthly Wave Height and Wave Period for Petrokaravo Buoy | 163 |
| Figure 5.1.52: Wind Chart for Petrokaravo Buoy | 164 |
| Figure 5.1.53: Monthly Box and Whiskers Plots for Atmospheric Parameters for Petrokaravo Buoy | 165 |
| Figure 5.1.54: Charts of Wind Direction and Wave Height - Period for Petrokaravo Buoy | 167 |
| Figure 5.1.55: Rose Diagrams for Significant Wave Height and Wave period for all waves (a,b), swells (c,d) and wind waves (e,f) for Pylos Buoy | 169 |
| Figure 5.1.56: Box and Whiskers plots for Monthly Wave Height and Wave Period for Pylos Buoy..... | 170 |
| Figure 5.1.57: Random SSE record and it's spectrum for Pylos Buoy | 171 |
| Figure 5.1.58: Scatterplots of statistical and spectral wave parameters for Pylos Buoy | 172 |
| Figure 5.1.59: Spectral and Statistical Monthly Values per Wave Parameter for Pylos Buoy | 172 |
| Figure 5.1.60: Probability Distributions and QQ plots for Athos for random wave heights | 173 |
| Figure 5.1.61: Wind Chart for Pylos Buoy | 175 |
| Figure 5.1.62: Monthly Box and Whiskers Plots for Atmospheric Parameters for Pylos Buoy..... | 175 |
| Figure 5.1.63: Charts of Wind Direction and Wave Height - Period for Pylos Buoy..... | 177 |
| Figure 5.1.64: Rose Diagrams for Significant Wave Height and Wave period for all waves (a,b), swells (c,d) and wind waves (e,f) for Santorini Buoy | 179 |
| Figure 5.1.65: Box and Whiskers plots for Monthly Wave Height and Wave Period for Santorini Buoy | 180 |
| Figure 5.1.66: Random SSE record and it's spectrum for Santorini Buoy | 181 |
| Figure 5.1.67: Scatterplots of statistical and spectral wave parameters for Santorini Buoy..... | 182 |
| Figure 5.1.68: Spectral and Statistical Monthly Values per Wave Parameter for Santorini Buoy | 182 |
| Figure 5.1.69: Probability Distributions and QQ plots for Santorini Buoy for random wave heights..... | 183 |
| Figure 5.1.70: Wind Chart for Santorini Buoy | 185 |
| Figure 5.1.71: Monthly Box and Whiskers Plots for Atmospheric Parameters for Santorini Buoy..... | 185 |
| Figure 5.1.72: Charts of Wind Direction and Wave Height - Period for Santorini Buoy | 187 |
| Figure 5.1.73: Rose Diagrams for Significant Wave Height and Wave period for all waves (a,b), swells (c,d) and wind waves (e,f) for Skyros Buoy | 189 |

| | |
|-------------------------------------------------------------------------------------------------------------------------------------------------------------------------------------------------|-----|
| Figure 5.1.74: Box and Whiskers plots for Monthly Wave Height and Wave Period for Skyros Buoy..... | 190 |
| Figure 5.1.75: Random SSE record and it's spectrum for Skyros Buoy | 190 |
| Figure 5.1.76: Scatterplots of statistical and spectral wave parameters for Skyros Buoy | 191 |
| Figure 5.1.77: Spectral and Statistical Monthly Values per Wave Parameter for Skyros Buoy | 192 |
| Figure 5.1.78: Probability Distributions and QQ plots for Skyros Buoy for random wave heights | 193 |
| Figure 5.1.79: Wind Chart for Skyros Buoy | 194 |
| Figure 5.1.80: Monthly Box and Whiskers Plots for Atmospheric Parameters for Skyros Buoy | 195 |
| Figure 5.1.81: Charts of Wind Direction and Wave Height - Period for Skyros Buoy..... | 197 |
| Figure 5.1.82: Rose Diagrams for Significant Wave Height and Wave period for all waves (a,b), swells (c,d) and wind waves (e,f) for Zakynthos Buoy | 199 |
| Figure 5.1.83: Box and Whiskers plots for Monthly Wave Height and Wave Period for Zakynthos Buoy | 200 |
| Figure 5.1.84: Random SSE record and it's spectrum for Zakynthos Buoy | 200 |
| Figure 5.1.85: Scatterplots of statistical and spectral wave parameters for Zakynthos Buoy | 201 |
| Figure 5.1.86: Spectral and Statistical Monthly Values per Wave Parameter for Zakynthos Buoy | 202 |
| Figure 5.1.87: Probability Distributions and QQ plots for Zakynthos Buoy for random wave heights ... | 203 |
| Figure 5.1.88: Wind Chart for Zakynthos Buoy | 204 |
| Figure 5.1.89: Monthly Box and Whiskers Plots for Atmospheric Parameters for Zakynthos Buoy..... | 205 |
| Figure 5.1.90: Charts of Wind Direction and Wave Height - Period for Zakynthos Buoy..... | 207 |
| Figure 5.1.91: Seasonal synoptic composite means of the surface vector wind (m/s) associated with the upper 10% of wave height (left graphs) and period (right graphs) for the Aegean Sea | 208 |
| Figure 5.1.92: Seasonal synoptic composite means of the surface vector wind (m/s) associated with the upper 10% of wave height (left graphs) and period (right graphs) for the Ionian Sea | 209 |
| Figure 5.2.1: Athos Buoy and the 4 nearby points of ERA-Interim grid | 210 |
| Figure 5.2.2: Mean monthly (a) and annual (b) significant wave height values (H_{m0}) from the buoy and ERA-Interim, as estimated from the method of WA (swh) | 211 |
| Figure 5.2.3: Mean monthly (a) and annual (b) wind speed values (10 m above sea level) from the buoy and ERA-Interim, as estimated from the method of SP (W10) | 212 |
| Figure 5.2.4 Mean monthly (a) and annual (b) temperature values (at 2 m above sea level) from the buoy and ERA-Interim, as estimated from the method of SP (T2M) | 213 |
| Figure 5.2.5: Avgo Buoy and the 4 nearby points of ERA-Interim grid..... | 213 |
| Figure 5.2.6: Mean monthly (a) and annual (b) significant wave height values from the buoy (H_{m0}) and ERA-Interim as estimated from the method of SP (swh) | 214 |
| Figure 5.2.7: Mean monthly (a) and annual (b) wind speed values from the buoy (Wind speed at 10m) and ERA-Interim as estimated from the method of WA (W10) | 215 |
| Figure 5.2.8: Mean monthly (a) and annual (b) temperature values from the buoy (Temperature at 2m) and ERA-Interim as estimated from the method of SP (T2M) | 216 |
| Figure 5.2.9: E1M3A Buoy and the 4 nearby points of ERA-Interim grid | 216 |
| Figure 5.2.10: Mean monthly (a) and annual (b) significant wave height values from the buoy (H_{m0}) and ERA-Interim as estimated from the method of SP (swh) | 217 |
| Figure 5.2.11: Mean monthly (a) and annual (b) wind speed values from the buoy (Wind speed at 10m) and ERA-Interim as estimated from the method of WA (W10) | 218 |
| Figure 5.2.12: Mean monthly (a) and annual (b) temperature values from the buoy (Temperature at 2m) and ERA-Interim as estimated from the method of SP (T2M) | 219 |
| Figure 5.2.13: Lesvos Buoy and the 4 nearby points of ERA-Interim grid | 219 |
| Figure 5.2.14: Mean monthly (a) and annual (b) significant wave height values from the buoy (H_{m0}) and ERA-Interim as estimated from the method of SP (swh) | 220 |
| Figure 5.2.15: Mean monthly (a) and annual (b) wind speed values from the buoy (Wind speed at 10m) and ERA-Interim as estimated from the method of SP (W10) | 221 |
| Figure 5.2.16: Mean monthly (a) and annual (b) temperature values from the buoy (Temperature at 2m) and ERA-Interim as estimated from the method of SP (T2M) | 222 |
| Figure 5.2.17: Mykonos Buoy and the 4 nearby points of ERA-Interim grid..... | 222 |
| Figure 5.2.18: Mean monthly (a) and annual (b) significant wave height values from the buoy (H_{m0}) and ERA-Interim as estimated from the method of WA (swh) | 223 |
| Figure 5.2.19: Mean monthly (a) and annual (b) wind speed values from the buoy (Wind speed at 10m) and ERA-Interim as estimated from the method of WA (W10). | 224 |
| Figure 5.2.20: Mean monthly (a) and annual (b) temperature values from the buoy (Temperature at 2m) and ERA-Interim as estimated from the method of SP (T2M) | 225 |
| Figure 5.2.21: Pylos Buoy and the 4 nearby points of ERA-Interim grid | 225 |
| Figure 5.2.22: Mean monthly (a) and annual (b) significant wave height values from the buoy (H_{m0}) and ERA-Interim as estimated from the method of SP (swh) | 226 |
| Figure 5.2.23: Mean monthly (a) and annual (b) wind speed values from the buoy (Wind speed at 10m) and ERA-Interim as estimated from the method of SP (W10). | 227 |
| Figure 5.2.24: Mean monthly (a) and annual (b) temperature values from the buoy (Temperature at 2m) and ERA-Interim as estimated from the method of SP (T2M) | 228 |

| | |
|------------------------------------------------------------------------------------------------------------------------------------------------------------------------------------|-----|
| Figure 5.2.25: Santorini Buoy and the 4 nearby points of ERA-Interim grid | 228 |
| Figure 5.2.26: Mean monthly (a) and annual (b) significant wave height values from the buoy (Hm0) and ERA-Interim as estimated from the method of WA (swh) | 229 |
| Figure 5.2.27: Mean monthly (a) and annual (b) wind speed values from the buoy (Wind speed at 10m) and ERA-Interim as estimated from the method of WA (W10)..... | 230 |
| Figure 5.2.28: Mean monthly (a) and annual (b) temperature values from the buoy (Temperature at 2m) and ERA-Interim as estimated from the method of WA (T2M) | 231 |
| Figure 5.2.29: Skyros Buoy and the 4 nearby points of ERA-Interim grid | 231 |
| Figure 5.2.30: Mean monthly (a) and annual (b) significant wave height values from the buoy (Hm0) and ERA-Interim as estimated from the method of WA (swh) | 232 |
| Figure 5.2.31: Mean monthly (a) and annual (b) wind speed values from the buoy (Wind speed at 10m) and ERA-Interim as estimated from the method of WA (W10)..... | 233 |
| Figure 5.2.32: Mean monthly (a) and annual (b) temperature values from the buoy (Temperature at 2m) and ERA-Interim as estimated from the method of SP (T2M) | 234 |
| Figure 5.2.33: Wave Chart of North Aegean from ERA-Interim..... | 235 |
| Figure 5.2.34: Monthly and annual means and monthly anomalies for the period 1979-2013 for significant wave height (a, c, e) and wave period (b, d, f) for North Aegean. | 236 |
| Figure 5.2.35: Wind Chart of North Aegean from ERA-Interim | 237 |
| Figure 5.2.36: Monthly and annual means and monthly anomalies, for the period 1979-2013 for wind speed at 10m (a, c, e) and temperature at 2m (b, d, f) for North Aegean..... | 238 |
| Figure 5.2.37: Wave Chart of Central Aegean from ERA-Interim..... | 240 |
| Figure 5.2.38: Monthly and annual means and monthly anomalies, for the period 1979-2013 for significant wave height (a, c, e) and wave period (b, d, f) for Central Aegean. | 241 |
| Figure 5.2.39: Wind Chart of Central Aegean from ERA-Interim | 242 |
| Figure 5.2.40: Monthly anomalies, monthly and annual means for the period 1979-2013 for wind speed at 10m (a, c, e) and temperature at 2m (b, d, f) for Central Aegean. | 243 |
| Figure 5.2.41: Wave Chart of South Aegean from ERA-Interim..... | 245 |
| Figure 5.2.42: Monthly and annual means and monthly anomalies for the period 1979-2013 for significant wave height (a, c, e) and wave period (b, d, f) for South Aegean..... | 246 |
| Figure 5.2.43: Wind Chart of South Aegean from ERA-Interim | 247 |
| Figure 5.2.44: Monthly and annual means and monthly anomalies, for the period 1979-2013 for wind speed at 10m (a, c, e) and temperature at 2m (b, d, f) for South Aegean..... | 248 |
| Figure 5.2.45: Wave Chart of North Ionian from ERA-Interim..... | 250 |
| Figure 5.2.46: Monthly anomalies, monthly and annual means for the period 1979-2013 for significant wave height (a, c, e) and wave period (b, d, f) for North Ionian. | 251 |
| Figure 5.2.47: Wind Chart of North Ionian from ERA-Interim | 252 |
| Figure 5.2.48: Monthly and annual means and monthly anomalies for the period 1979-2013 for wind speed at 10m (a, c, e) and temperature at 2m (b, d, f) for North Ionian..... | 253 |
| Figure 5.2.49: Wave Chart of South Ionian from ERA-Interim..... | 255 |
| Figure 5.2.50: Monthly and annual means and mean anomalies for the period 1979-2013 for significant wave height (a, b,e) and wave period (c, d,f) for South Ionian..... | 256 |
| Figure 5.2.51: Wind Chart of South Ionian from ERA-Interim..... | 257 |
| Figure 5.2.52: Monthly anomalies, monthly and annual means for the period 1979-2013 for wind speed at 10m (a, c, e) and temperature at 2m (b, d, f) for South Ionian. | 258 |
| Figure 5.3.1: Wave Chart of Pinios from ERA-Interim..... | 260 |
| Figure 5.3.2: Monthly and annual means and monthly anomalies for the period 1979-2013 for significant wave height (a, c, e) and wave period (b, d, f) for Pinios..... | 261 |
| Figure 5.3.3: Wind Chart for Pinios from ERA-Interim | 262 |
| Figure 5.3.4: Monthly and annual means and monthly anomalies, for the period 1979-2013 for wind speed at 10m (a, c, e) and temperature at 2m (b, d, f) for Pinios..... | 263 |
| Figure 5.3.5: a) Bathymetry Data of the area, b) the rotated bathymetry used in MIKE21PMS | 264 |
| Figure 5.3.6: Wave propagation at mean NE conditions | 266 |
| Figure 5.3.7: Wave propagation at the upper 2% of waves propagating from NE | 267 |
| Figure 5.3.8: Wave propagation at the upper 2% of waves propagating from NE with a sea level rise of 0.3 m (RCP 8.5, 2046-2065)..... | 268 |
| Figure 5.3.9: Wave propagation at the upper 2% of waves propagating from NE with a sea level rise of 0.63 m (RCP 8.5, 2081-2100)..... | 269 |
| Figure 5.3.10: Wave Height Profiles for the NE under different scenarios for Location A. (Note: Distance from shore should be multiplied with 3, due to the grid size of 3m). | 270 |
| Figure 5.3.11: Wave Height Profiles for the NE under different scenarios for Location B. Note: Distance from shore should be multiplied with 3, due to the grid size of 3m..... | 271 |
| Figure 5.3.12: Wave propagation at mean E conditions | 272 |
| Figure 5.3.13: Wave propagation at the upper 2% of waves propagating from E..... | 273 |
| Figure 5.3.14: Wave propagation at the upper 2% of waves propagating from E with a sea level rise of 0.3 m (2046-2065)..... | 274 |

| | |
|----------------------------------------------------------------------------------------------------------------------------------------------------------------------------------|-----|
| Figure 5.3.15: Wave propagation at the upper 2% of waves propagating from E with a sea level rise of 0.63 m (2085-2100)..... | 275 |
| Figure 5.3.16: Wave Height Profiles for the E under different scenarios for Location A (Note: Distance from shore should be multiplied with 3, due to the grid size of 3m)..... | 276 |
| Figure 5.3.17: Wave Height Profiles for the E under different scenarios for Location B (Note: Distance from shore should be multiplied with 3, due to the grid size of 3m)..... | 277 |
| Figure 5.3.18: Wave propagation at mean SE conditions | 278 |
| Figure 5.3.19: Wave propagation at the upper 2% of waves propagating from SE | 279 |
| Figure 5.3.20: Wave propagation at the upper 2% of waves propagating from SE for a sea level rise of 0.3 m (RCP 8.5 2046-2065)..... | 280 |
| Figure 5.3.21: Wave propagation at the upper 2% of waves propagating from SE for a sea level rise of 0.63 m (RCP 8.5 2081-2100)..... | 281 |
| Figure 5.3.22: Wave Height Profiles for the SE under different scenarios for Location A (Note: Distance from shore should be multiplied with 3, due to the grid size of 3m)..... | 282 |
| Figure 5.3.23: Wave Height Profiles for the SE under different scenarios for Location B (Note: Distance from shore should be multiplied with 3, due to the grid size of 3m)..... | 283 |
| Figure 6.1.1: Location of the four buoys in the North Aegean Sea | 287 |
| Figure 6.1.2: Location of the 2 buoys in Central Aegean Sea | 291 |
| Figure 6.1.3: Location of the buoys in the South Aegean Sea | 294 |
| Figure 6.1.4: Location of the buoys in the Northeast Ionian Sea | 297 |
| Figure 6.1.5: Location of the buoys in the Southeast Ionian Sea | 300 |

List of Tables

| | |
|-------------------------------------------------------------------------------------------------------------------------------------------------------------|-----|
| Table 2.2.1: Beaufort Wind Scale | 11 |
| Table 2.3.1: Empirical Equations for Wave Parameters (CERC, 1984) | 13 |
| Table 2.5.1: Types of waves according to the surf similarity parameter (Battjes, 1974)..... | 28 |
| Table 2.7.1: Representative Concentration Pathways (RCPs) publications and models (T.F. Stocker et al., 2013)..... | 33 |
| Table 2.7.2: Representative Concentration Pathways (RCPs) (Moss et al., 2010; Riahi et al., 2007) | 34 |
| Table 2.7.3: GMSLR estimates according to the RCPs for the periods 2046-2065 and 20181-2100 in relation to the reference period 1986-2005 (IPCC, 2013)..... | 34 |
| Table 3.2.1: Frequency Table (%) of Wave Height and Periods for the area of Pinios (from Athanasoulis and Skarsoulis, 1992)..... | 57 |
| Table 3.2.2: Frequency (%) of Wind speed and Direction for the area of Pinios (from Athanasoulis and Skarsoulis, 1992)..... | 58 |
| Table 4.1.1 Wave Characteristics as given by the SeaWatch buoys | 70 |
| Table 4.1.2: Basic functions and steps of the WAFO script..... | 73 |
| Table 4.1.3: Rayleigh, Weibull and Kumaraswamy Distributions..... | 74 |
| Table 4.1.4: Atmospheric Characteristics as given by the Poseidon buoys | 76 |
| Table 4.2.1: Datasets of SST and SIC, used in ERA-Interim (Dee et al., 2011)..... | 78 |
| Table 4.2.2: Satellites used for ERA-Interim wave height data (Dee et al., 2011) | 80 |
| Table 4.2.3: Characteristics of data as downloaded from ERA-Interim, ECMWF | 83 |
| Table 4.2.4: Parameters downloaded from ERA-Interim database | 84 |
| Table 4.2.5: Term and Likelihood of the Outcome (Mastrandrea et al., 2010) | 88 |
| Table 4.3.1: Coefficients of the mild slope equation (DHI, 2014) | 95 |
| Table 5.1.1: Location, depth of installation and time periods of recording per database for Athos..... | 102 |
| Table 5.1.2: Descriptive Statistics of Wave Parameters for Athos..... | 102 |
| Table 5.1.3: Pivot Table (%) for Significant Wave Height and Zero-crossing wave period for Athos Buoy | 104 |
| Table 5.1.4: Descriptive Statistics as derived from SSE Analysis for Athos Buoy..... | 105 |
| Table 5.1.5: Statistics of Goodness of Fits according to K-S, A-D and χ^2 test for Athos Buoy | 107 |
| Table 5.1.6: Statistics of various Ratios for Athos Buoy | 108 |
| Table 5.1.7: Descriptive Statistics of Atmospheric Parameters for Athos Buoy | 108 |
| Table 5.1.8: Descriptive Statistics of Wave and Atmospheric Parameters for Athos Buoy | 110 |
| Table 5.1.9: Frequency Table (%) of Wind Speed and Significant Spectral Wave Height for Athos Buoy | 111 |
| Table 5.1.10: Location, depth of installation and time periods of recording per database for Avgo Buoy | 112 |
| Table 5.1.11: Descriptive Statistics of Wave Parameters for Avgo Buoy | 112 |
| Table 5.1.12: Pivot Table for Significant Wave Height and Zero-crossing wave period for Avgo Buoy ... | 114 |
| Table 5.1.13: Descriptive Statistics of Atmospheric Parameters for Avgo Buoy..... | 115 |
| Table 5.1.14: Descriptive Statistics of Wave and Atmospheric Parameters for the Avgo Buoy | 117 |
| Table 5.1.15: Frequency Table (%) of Wind Speed and Significant Spectral Wave Height for Avgo | 117 |
| Table 5.1.16: Location, depth of installation and time periods of recording per database for Dia | 118 |
| Table 5.1.17: Descriptive Statistics of Wave Parameters for Dia Buoy..... | 119 |
| Table 5.1.18 Frequency (%) Table for Significant Wave Height and Zero-crossing wave period for Dia Buoy..... | 120 |
| Table 5.1.19: Location, depth of installation and time periods of recording per database for E1M3A Buoy | 121 |
| Table 5.1.20: Descriptive Statistics of Wave Parameters for E1M3A Buoy | 122 |
| Table 5.1.21: Pivot Table for Significant Wave Height and Zero-crossing wave period for E1M3A Buoy | 123 |
| Table 5.1.22: Descriptive Statistics of Atmospheric Parameters for E1M3A Buoy | 124 |
| Table 5.1.23: Descriptive Statistics of Wave and Atmospheric Parameters for E1M3A..... | 126 |
| Table 5.1.24: Frequency Table (%) of Wind Speed and Significant Spectral Wave Height for E1M3A.... | 127 |
| Table 5.1.25: Location, depth of installation & time periods of recording per database for Kalamata Buoy | 128 |
| Table 5.1.26: Descriptive Statistics of Wave Parameters for Kalamata Buoy..... | 128 |
| Table 5.1.27: Pivot Table (%) for Significant Wave Height and Zero-crossing wave period for Kalamata Buoy..... | 130 |
| Table 5.1.28: Descriptive Statistics as derived from SSE Analysis for Kalamata Buoy | 131 |
| Table 5.1.29: Statistics of Goodness of Fits according to K-S, A-D and χ^2 test for Kalamata Buoy | 133 |
| Table 5.1.30: Statistics of various Ratios for Kalamata Buoy | 134 |
| Table 5.1.31: Descriptive Statistics of Atmospheric Parameters for Kalamata Buoy..... | 134 |
| Table 5.1.32: Descriptive Statistics of Wave and Atmospheric Parameters for Kalamata Buoy | 136 |

| | |
|------------------------------------------------------------------------------------------------------------------|-----|
| Table 5.1.33: Frequency Table (%) of Wind Speed and Significant Spectral Wave Height for Kalamata Buoy..... | 137 |
| Table 5.1.34: Location, depth of installation and time periods of recording per database for Katerini Buoy..... | 137 |
| Table 5.1.35: Descriptive Statistics of Wave Parameters for Katerini Buoy..... | 138 |
| Table 5.1.36: Pivot Table for Significant Wave Height and Zero-crossing wave period for Katerini Buoy..... | 140 |
| Table 5.1.37: Descriptive Statistics of Atmospheric Parameters for Katerini Buoy..... | 141 |
| Table 5.1.38: Descriptive Statistics of Wave and Atmospheric Parameters for Katerini Buoy..... | 142 |
| Table 5.1.39: Frequency Table (%) of Wind Speed and Significant Spectral Wave Height for Katerini Buoy..... | 143 |
| Table 5.1.40: Location, depth of installation and time periods of recording per database for Lesvos Buoy..... | 144 |
| Table 5.1.41: Descriptive Statistics of Wave Parameters for Lesvos Buoy..... | 145 |
| Table 5.1.42: Pivot Table for Significant Wave Height and Zero-crossing wave period for Lesvos Buoy..... | 146 |
| Table 5.1.43: Descriptive Statistics of Atmospheric Parameters for Lesvos Buoy..... | 147 |
| Table 5.1.44: Descriptive Statistics of Wave and Atmospheric Parameters for Lesvos Buoy..... | 149 |
| Table 5.1.45: Frequency Table (%) of Wind Speed and Significant Spectral Wave Height for Lesvos Buoy..... | 150 |
| Table 5.1.46: Location, depth of installation & time periods of recording per database for Mykonos... .. | 151 |
| Table 5.1.47: Descriptive Statistics of Wave Parameters for Mykonos Buoy..... | 151 |
| Table 5.1.48: Pivot Table for Significant Wave Height and Zero-crossing wave period for Mykonos..... | 153 |
| Table 5.1.49: Descriptive Statistics as derived from SSE Analysis for Mykonos Buoy..... | 154 |
| Table 5.1.50: Statistics of Goodness of Fits according to K-S, A-D and χ^2 test for Mykonos Buoy..... | 157 |
| Table 5.1.51: Statistics of various Ratios for Mykonos Buoy..... | 157 |
| Table 5.1.52: Descriptive Statistics of Atmospheric Parameters for Mykonos Buoy..... | 158 |
| Table 5.1.53: Descriptive Statistics of Wave and Atmospheric Parameters for Mykonos Buoy..... | 159 |
| Table 5.1.54: Frequency Table (%) of Wind Speed and Significant Spectral Wave Height for Mykonos Buoy..... | 160 |
| Table 5.1.55: Location, depth of installation & time periods of recording per database for Petrokaravo Buoy..... | 160 |
| Table 5.1.56: Descriptive Statistics of Wave Parameters for Petrokaravo Buoy..... | 161 |
| Table 5.1.57: Pivot Table for Significant Wave Height and Zero-crossing wave period for Petrokaravo Buoy..... | 163 |
| Table 5.1.58: Descriptive Statistics of Atmospheric Parameters for Petrokaravo Buoy..... | 164 |
| Table 5.1.59: Descriptive Statistics of Wave and Atmospheric Parameters for Petrokaravo Buoy..... | 165 |
| Table 5.1.60: Frequency Table (%) of Wind Speed and Significant Spectral Wave Height for Petrokaravo..... | 166 |
| Table 5.1.61: Location, depth of installation and time periods of recording per database for Pylos Buoy..... | 167 |
| Table 5.1.62: Descriptive Statistics of Wave Parameters for Pylos Buoy..... | 168 |
| Table 5.1.63: Pivot Table for Significant Wave Height and Zero-crossing wave period for Pylos Buoy... .. | 169 |
| Table 5.1.64: Descriptive Statistics as derived from SSE Analysis for Pylos Buoy..... | 171 |
| Table 5.1.65: Statistics of Goodness of Fits according to K-S, A-D and χ^2 test for Pylos Buoy..... | 173 |
| Table 5.1.66: Statistics of various Ratios for Pylos Buoy..... | 174 |
| Table 5.1.67: Descriptive Statistics of Atmospheric Parameters for Pylos Buoy..... | 174 |
| Table 5.1.68: Descriptive Statistics of Wave and Atmospheric Parameters for Pylos Buoy..... | 176 |
| Table 5.1.69: Frequency Table (%) of Wind Speed and Significant Spectral Wave Height for Pylos Buoy..... | 177 |
| Table 5.1.70: Location, depth of installation and time periods of recording per database for Santorini Buoy..... | 178 |
| Table 5.1.71: Descriptive Statistics of Wave Parameters for Santorini Buoy..... | 178 |
| Table 5.1.72: Pivot Table for Significant Wave Height and Zero-crossing wave period for Santorini Buoy..... | 180 |
| Table 5.1.73: Descriptive Statistics as derived from SSE Analysis for Santorini Buoy..... | 181 |
| Table 5.1.74: Statistics of Goodness of Fits according to K-S, A-D and χ^2 test for Santorini Buoy..... | 183 |
| Table 5.1.75: Statistics of Various Ratios for Santorini Buoy..... | 184 |
| Table 5.1.76: Descriptive Statistics of Atmospheric Parameters for Santorini Buoy..... | 184 |
| Table 5.1.77: Descriptive Statistics of Wave and Atmospheric Parameters for Santorini Buoy..... | 186 |
| Table 5.1.78: Frequency Table (%) of Wind Speed and Significant Spectral Wave Height for Santorini Buoy..... | 186 |
| Table 5.1.79: Location, depth of installation and time periods of recording per database for Skyros Buoy..... | 187 |
| Table 5.1.80: Descriptive Statistics of Wave Parameters for Skyros Buoy..... | 188 |
| Table 5.1.81: Pivot Table for Significant Wave Height and Zero-crossing wave period for Skyros Buoy..... | 189 |

| | |
|---------------------------------------------------------------------------------------------------------------------------------------------|-----|
| Table 5.1.82: Descriptive Statistics as derived from SSE Analysis for Skyros Buoy..... | 191 |
| Table 5.1.83: Statistics of Goodness of Fits according to K-S, A-D and χ^2 test for Skyros Buoy..... | 193 |
| Table 5.1.84: Statistics of Various Ratios for Skyros Buoy | 193 |
| Table 5.1.85: Descriptive Statistics of Atmospheric Parameters for Skyros Buoy | 194 |
| Table 5.1.86: Descriptive Statistics of Wave and Atmospheric Parameters for Skyros Buoy | 196 |
| Table 5.1.87: Frequency Table (%) of Wind Speed and Significant Spectral Wave Height for Skyros Buoy | 196 |
| Table 5.1.88: Location, depth of installation and time periods of recording per database for Zakynthos Buoy..... | 197 |
| Table 5.1.89: Descriptive Statistics of Wave Parameters for Zakynthos Buoy..... | 198 |
| Table 5.1.90: Pivot Table for Significant Wave Height and Zero-crossing wave period for Zakynthos Buoy | 199 |
| Table 5.1.91: Descriptive Statistics as derived from SSE Analysis for Zakynthos Buoy..... | 201 |
| Table 5.1.92: Statistics of Goodness of Fits according to K-S, A-D and χ^2 test for Zakynthos Buoy..... | 203 |
| Table 5.1.93: Statistics of Various Ratios for Skyros Buoy | 203 |
| Table 5.1.94: Descriptive Statistics of Atmospheric Parameters for Zakynthos Buoy | 204 |
| Table 5.1.95: Descriptive Statistics of Wave and Atmospheric Parameters for Zakynthos Buoy..... | 206 |
| Table 5.1.96: Frequency Table (%) of Wind Speed and Significant Spectral Wave Height for Zakynthos Buoy..... | 206 |
| Table 5.2.1: Statistics of Significant Wave Height of Athos Buoy and ERA-Interim data as estimated by the method WA and their relation..... | 211 |
| Table 5.2.2: Statistics of Wind Speed for Buoy and ERA-Interim Method SP | 211 |
| Table 5.2.3: Statistics of Temperature at 2m for Buoy and ERA-Interim Method SP | 212 |
| Table 5.2.4: Statistics of Significant Wave Height of Avgo Buoy and ERA-Interim Method SP..... | 214 |
| Table 5.2.5: Statistics of Wind Speed for Buoy and ERA-Interim Method WA | 214 |
| Table 5.2.6: Statistics of Temperature at 2m for Buoy and ERA-Interim Method SP | 215 |
| Table 5.2.7: Statistics of Significant Wave Height of E1M3A Buoy and ERA-Interim Method SP | 217 |
| Table 5.2.8: Statistics of Wind Speed for Buoy and ERA-Interim Method WA | 218 |
| Table 5.2.9: Statistics of Temperature at 2m for Buoy and ERA-Interim Method SP | 218 |
| Table 5.2.10: Statistics of Significant Wave Height of Lesvos Buoy and ERA-Interim Method WA..... | 220 |
| Table 5.2.11: Statistics of Wind Speed for Buoy and ERA-Interim Method WA | 221 |
| Table 5.2.12: Statistics of Temperature at 2m for Buoy and ERA-Interim Method SP | 221 |
| Table 5.2.13: Statistics of Significant Wave Height of Mykonos Buoy and ERA-Interim Method WA..... | 223 |
| Table 5.2.14: Statistics of Wind Speed for Buoy and ERA-Interim Method WA | 224 |
| Table 5.2.15: Statistics of Temperature at 2m for Buoy and ERA-Interim Method SP | 224 |
| Table 5.2.16: Statistics of Significant Wave Height of Pylos Buoy and ERA-Interim Method WA | 226 |
| Table 5.2.17: Statistics of Wind Speed for Buoy and ERA-Interim Method SP | 227 |
| Table 5.2.18: Statistics of Temperature at 2m for Buoy and ERA-Interim Method WA | 227 |
| Table 5.2.19: Statistics of Significant Wave Height of Santorini Buoy and ERA-Interim Method WA | 229 |
| Table 5.2.20: Statistics of Wind Speed for Buoy and ERA-Interim Method WA W10..... | 230 |
| Table 5.2.21: Statistics of Temperature at 2m for Buoy and ERA-Interim Method WA | 230 |
| Table 5.2.22: Statistics of Significant Wave Height of Skyros Buoy and ERA-Interim Method WA | 232 |
| Table 5.2.23: Statistics of Wind Speed for Buoy and ERA-Interim Method WA W10..... | 233 |
| Table 5.2.24: Statistics of Temperature at 2m for Buoy and ERA-Interim Method SP | 233 |
| Table 5.2.25: Wave Characteristics of North Aegean as given from ERA-Interim | 234 |
| Table 5.2.26: Frequency (%) table of significant wave height (SWH) and mean wave period (MWP) for North Aegean (ERA-Interim) | 235 |
| Table 5.2.27: Weather Characteristics of North Aegean as given from ERA-Interim | 237 |
| Table 5.2.28: Frequency table (%) of significant wave height (SWH) and wind speed at 10m (W10) for North Aegean (ERA-Interim) | 239 |
| Table 5.2.29: Wave Characteristics of Central Aegean as given from ERA-Interim..... | 239 |
| Table 5.2.30: Frequency (%) table of significant wave height (SWH) and mean wave period (MWP) for Central Aegean..... | 241 |
| Table 5.2.31: Weather Characteristics of Central Aegean as given from ERA-Interim | 242 |
| Table 5.2.32: Frequency table (%) of significant wave height (SWH) and wind speed at 10m (W10) for Central Aegean..... | 244 |
| Table 5.2.33: Wave Characteristics of South Aegean as given from ERA-Interim | 244 |
| Table 5.2.34: Frequency (%) table of significant wave height (SWH) and mean wave period (MWP) for South Aegean (ERA-Interim) | 246 |
| Table 5.2.35: Weather Characteristics of South Aegean as given from ERA-Interim | 247 |
| Table 5.2.36: Frequency table (%) of significant wave height (SWH) and wind speed at 10m (W10) for South Aegean | 249 |
| Table 5.2.37: Wave Characteristics of North Ionian as given from ERA-Interim | 249 |
| Table 5.2.38: Frequency (%) table of significant wave height (SWH) and mean wave period (MWP) for North Ionian (ERA-Interim) | 251 |

| | |
|---------------------------------------------------------------------------------------------------------------------------------|-----|
| Table 5.2.39: Weather Characteristics of North Ionian as given from ERA-Interim | 252 |
| Table 5.2.40: Frequency table (%) of significant wave height (SWH) and wind speed at 10m (W10) for North Ionian | 254 |
| Table 5.2.41: Wave Characteristics of South Ionian as given from ERA-Interim | 254 |
| Table 5.2.42: Frequency (%) table of significant wave height (SWH) and mean wave period (MWP) for South Ionian..... | 256 |
| Table 5.2.43: Weather Characteristics of South Ionian as given from ERA-Interim | 257 |
| Table 5.2.44: Frequency table (%) of significant wave height (SWH) and wind speed at 10m (W10) for South Ionian..... | 259 |
| Table 5.3.1: Wave Characteristics of Pinios as given from ERA-Interim for the period 1979-2013..... | 259 |
| Table 5.3.2: Frequency (%) table of significant wave height (SWH) and mean wave period (MWP) for Pinios | 261 |
| Table 5.3.3: Weather Characteristics of Pinios as given from ERA-Interim for the period 1979-2013.... | 262 |
| Table 5.3.4: Frequency table (%) of significant wave height (SWH) and wind speed at 10m (W10) for Pinios | 264 |
| Table 5.3.5: Frequency (%) of Wave Direction and Wave heights for Pinios River Offshore Area (ERA-Interim)..... | 265 |
| Table 5.3.6: Mean and max 2% of Significant Wave Height (SWH) and Mean Wave Period (MWP) of waves propagating from the NE..... | 265 |
| Table 5.3.7: Wave Characteristics of NE direction as estimated from (CERC, 1984) in offshore and nearshore conditions..... | 270 |
| Table 5.3.8: Mean and max 2% of Significant Wave Height (SWH) and Mean Wave Period (MWP) of waves propagating from the E | 271 |
| Table 5.3.9: Wave Characteristics of E direction as estimated from (CERC, 1984)in offshore and nearshore conditions..... | 276 |
| Table 5.3.10: Mean and max 2% of Significant Wave Height (SWH) and Mean Wave Period (MWP) of waves propagating from the SE..... | 277 |
| Table 5.3.11: Wave Characteristics of SE direction as estimated (CERC, 1984) in offshore and nearshore conditions | 282 |
| Table 6.1.1: Mean values of wave height parameters for the North Aegean Sea | 287 |
| Table 6.1.2: Means of wave period parameters for the North Aegean Sea | 288 |
| Table 6.1.3: Seasonal Description of wave height for the North Aegean Sea..... | 288 |
| Table 6.1.4: Seasonal Description of wave period for the North Aegean Sea | 289 |
| Table 6.1.5: Mean values of Atmospheric Parameters for the North Aegean Sea | 289 |
| Table 6.1.6: Seasonal atmospheric parameters for the North Aegean Sea | 290 |
| Table 6.1.7: Means of wave height parameters for the Central Aegean Sea..... | 291 |
| Table 6.1.8: Means of wave period parameters for the Central Aegean Sea | 292 |
| Table 6.1.9: Seasonal Description of wave height for the Central Aegean Sea | 292 |
| Table 6.1.10: Seasonal Description of wave period for the Central Aegean Sea | 292 |
| Table 6.1.11: Mean of Atmospheric Parameters for the Central Aegean Sea | 293 |
| Table 6.1.12: Seasonal Description of atmospheric parameters for the Central Aegean Sea | 293 |
| Table 6.1.13: Means of wave height parameters for the South Aegean Sea | 294 |
| Table 6.1.14: Means of wave period parameters for the South Aegean Sea..... | 295 |
| Table 6.1.15: Seasonal Description of wave height for South Aegean Sea | 295 |
| Table 6.1.16: Seasonal Description of wave period for the South Aegean Sea | 296 |
| Table 6.1.17: Mean of Atmospheric Parameters for the South Aegean Sea..... | 296 |
| Table 6.1.18: Seasonal Description of atmospheric parameters for the South Aegean Sea..... | 296 |
| Table 6.1.19: Means of wave height and period parameters for the Northeast Ionian Sea..... | 297 |
| Table 6.1.20: Seasonal Description of wave height and period for the Northeast Ionian Sea | 298 |
| Table 6.1.21: Mean of Atmospheric Parameters for the Northeast Ionian Sea..... | 298 |
| Table 6.1.22: Seasonal Description of atmospheric parameters for the Northeast Ionian Sea..... | 299 |
| Table 6.1.23: Means of wave height parameters for the Southeast Ionian Sea | 300 |
| Table 6.1.24: Means of wave period parameters for the Southeast Ionian Sea..... | 300 |
| Table 6.1.25: Seasonal Description of wave height for the Southeast Ionian Sea..... | 301 |
| Table 6.1.26: Seasonal Description of wave period for the Southeast Ionian Sea..... | 301 |
| Table 6.1.27: Mean of Atmospheric Parameters for Southeast Ionian Sea | 301 |
| Table 6.1.28: Seasonal Description of atmospheric parameters for the Southeast Ionian Sea..... | 302 |
| Table 6.2.1: Significant Wave Height Statistics of buoys - ERA-Interim for the North Aegean Sea | 304 |
| Table 6.2.2: Wind Speed at 10 m Statistics of buoys - ERA-Interim for the North Aegean Sea | 305 |
| Table 6.2.3: Temperature at 2m Statistics of buoys - ERA-Interim for the North Aegean..... | 306 |
| Table 6.2.4: Statistics of Wave and Atmospheric Parameters Mykonos - ERA-Interim for the Central Aegean Sea | 307 |
| Table 6.2.5: Significant Wave Height Statistics of buoys - ERA-Interim for the South Aegean..... | 308 |
| Table 6.2.6 Wind Speed at 10 m Statistics of buoys - ERA-Interim for the South Aegean Sea | 309 |
| Table 6.2.7: Temperature at 2 m Statistics of buoys - ERA-Interim for the South Aegean Sea | 310 |

| | |
|--------------------------------------------------------------------------------------------------------------------------------------------------------------------------------------------------------------------------------------------------------------------------------------------------------------------------------------------------------------------------------|-----|
| Table 6.2.8 Statistics of Wave and Atmospheric Parameters Mykonos - ERA-Interim for South Ionian | 312 |
| Table 6.3.1: Characteristics of Pinios Area from ERA-Interim | 314 |
| Table 6.3.2: Wave characteristics for NE waves as estimated by CERC (1984) and MIKE21 PMS | 316 |
| Table 6.3.3: Wave characteristics for E waves as estimated by (CERC, 1984) and MIKE21 PMS | 316 |
| Table 6.3.4: Wave characteristics for SE waves as estimated by (CERC, 1984) and MIKE21 PMS | 317 |
| Table 7.1.1: Mean values of wave heights for the Greek Seas. H_{m0} : spectral significant wave height (buoy and SSE analysis); $H_{1/3}$: statistical significant wave height; H_{max} : maximum wave height (buoy and SSE analysis); H_{m0a} : swell wave height (buoy); H_{m0b} : wind induced wave height (buoy); and, SWH: significant wave height (ERA-Interim) | 320 |
| Table 7.1.2: Mean values of wave periods for the Greek Seas. T_{m02} : spectral wave period (buoy and SSE analysis); $T_{1/3}$: statistical significant wave period; T_p : peak period (buoy and SSE analysis); T_{m02a} : swell wave period (buoy); T_{m02b} : wind induced wave period (buoy); and MWP: mean wave periods (ERA-Interim) | 321 |
| Table 7.1.3: Months with the minimum and maximum mean values of wave heights for the Greek Seas. H_{m0} : spectral significant wave height (buoy and SSE analysis); $H_{1/3}$: statistical significant wave height; and SWH: significant wave height (ERA-Interim) | 321 |
| Table 7.1.4: Months with the minimum and maximum mean values of wave periods for the Greek Seas. T_{m02} : spectral wave period (buoy and SSE analysis); $T_{1/3}$: statistical significant wave period; MWP mean wave periods (ERA-Interim) | 322 |
| Table 7.1.5: Means of Atmospheric Parameters for the Greek Seas from buoys and ERA-Interim (ERA-I) | 322 |
| Table 7.1.6: Months with minimum and maximum means of atmospheric parameters from buoys and ERA-Interim (ERA-I) | 323 |
| Table 7.3.1: Correlation, RMSE and Absolute Bias per region between the buoy and ERA-Interim dataset for the parameters of Significant Wave Height (SWH), Wind Speed at 10 m (W10) and Temperature at 2 m (T2M) | 325 |
| Table 7.4.1: Percentages of likelihood of having a trend in the mean monthly values for the parameters of Significant Wave Height (SWH), Wind Speed at 10 m (W10) and Temperature at 2 m (T2M) | 325 |
| Table 7.4.2: Percentages of likelihood of having a trend in the values of annual means for the parameters of Significant Wave Height (SWH), Wind Speed at 10 m (W10) and Temperature at 2 m (T2M) | 326 |
| Table 7.4.3: Percentages of likelihood of having a trend in the values of monthly mean anomalies for the parameters of Significant Wave Height (SWH), Wind Speed at 10 m (W10) and Temperature at 2 m (T2M) | 327 |

APPENDIX

WAFO Code

% Working with various datapoints of either buoys located in deep ocean waters of the Greek Seas.

% Obtaining statistical and spectral wave parameters from SSE Measurements.

% Created by Dafni Sifnioti in 28/02/2012.

%% Choosing a buoy:

% 'Athos','Kalamata','Mykonos','Pylos','Santorini','Skyros','Zakynthos'

buoy=input('Enter a buoy:','s');

%% Loading data from the chosen buoy:

switch buoy

case 'Athos'

load('Athos_06_11c2_Heave.csv'); % Load file

data=Athos_06_11c2_Heave(:,:); % Choose only the Sea Surface Elevation records

case 'Kalamata'

load('Kalamata_c2.csv');

data=Kalamata_c2(:,21:1044);

case 'Mykonos'

load ('Mykonos_2007_2011.csv');

data=Mykonos_2007_2011(:,21:1044);

case 'Pylos'

load ('Pylos_c2.csv');

data=Pylos_c2(:,21:1044);

case 'Santorini'

```

load ('Santorini_01_02_08_09.csv');

data=Santorini_01_02_08_09(:,20:1043);

case 'Skyros'

load ('Skyros_c2_2007_2011.csv');

data=Skyros_c2_2007_2011(:,21:1044);

case 'Zakynthos'

load ('Zakynthos_c2_2007_2011.csv');

data=Zakynthos_c2_2007_2011(:,21:1044);

end

%% WAFO Toolbox has been previously added to path

initwafo % initialize wafo

pstate='off';

speed='fast';

t=(1:1024)'; % create time variables with 1 to 1023 values

data=detrend(data); % remove any linear trends from SSE

xx=[t data]'; % create xx variables that has at one column time (from 1 to 1023) and in the other the SSE
data

rate=32;

method=3; % Declaring down crossing to downcrossing waves from 0 level

[r,c]=size(xx); % Size of xx variable to be used in the loop

% Check for a record

waveplot(xx(:,2),'r-','bo') % plot sse

%% Declaring arrays

Steep = num2cell(nan(1,c));

H = num2cell(nan(1,c));

```

```

Ac = num2cell(nan(1,c));
At = num2cell(nan(1,c));
Tcf = num2cell(nan(1,c));
Tcb = num2cell(nan(1,c));
S = num2cell(nan(1,c));
m = num2cell(nan(1,c));
mt = num2cell(nan(1,c));
ch = num2cell(nan(1,c));
bw = num2cell(nan(1,c));
skew = num2cell(nan(1,c));
kurt = num2cell(nan(1,c));
mean = num2cell(nan(1,c));
sigma = num2cell(nan(1,c));
T = num2cell(nan(1,c));
R = num2cell(nan(1,c));

%% Start the analysis with WAFO

for i=2:c
    [Steep{i-1},H{i-1},Ac{i-1},At{i-1},Tcf{i-1},Tcb{i-1}]=dat2steep(xx(:,[1 i]),rate,method); % identify
waves
    S{i-1}= dat2spec(xx(:,[1 i])); % estimate spectrum
    [m{i-1}, mt{i-1}]=spec2mom(S{i-1},1); % estimate spectral moments m0,m2,m4
    [ch{i-1}, R,txt]=spec2char(S{i-1},[1 3 6 7 ]); % estimate spectral wave characteristics
    bw {i-1}= spec2bw(S{i-1},[2 3]); % estimate spectrum characteristics
    [skew{i-1}, kurt{i-1}, mean{i-1}, sigma{i-1}] = spec2skew(S{i-1}); % estimate statistical
characteristics from the spectrum
    T{i-1} = dat2wa(xx(:,[1 i]),0,'d2d'); % estimate wave parameters from sse data
end

```

```
%% To find the length of each column of H and T
```

```
length_H_all=cellfun('length',H);
```

```
length_T_all=cellfun('length',T);
```

```
% To find the maximum length
```

```
e=max(length_H_all);
```

```
f=max(length_T_all);
```

```
%% Declaring arrays
```

```
H_all=nan(e,c);
```

```
T_all=nan(f,c);
```

```
Ac_all=nan(e,c);
```

```
At_all=nan(e,c);
```

```
Tcf_all=nan(f,c);
```

```
Tcb_all=nan(f,c);
```

```
Hm0_all=nan(1,c);
```

```
Tm02_all=nan(1,c);
```

```
Tp_all=nan(1,c);
```

```
Ss_all=nan(1,c);
```

```
Na_all=nan(1,c);
```

```
Br_all=nan(1,c);
```

```
Skew_all=nan(1,c);
```

```
Kurt_all=nan(1,c);
```

```
Mean_all=nan(1,c);
```

```
Stdev_all=nan(1,c);
```

```
w=nan(1,c);
```

```
z=nan(1,c);
```

```

HeightsSort=nan(e,c);

TSort=nan(f,c);

num_of_one_third=nan(e,c);

num_of_one_thirdT=nan(f,c);

%% To find the significant wave height H one third

H_One_Third=nan(e,c);

T_One_Third=nan(f,c);

%% Store in one variable all available data

for i=1:c

    w(:,i)=length(H{1,i});

    z(:,i)=length(T{1,i});

    H_all(1:w(:,i),i)=H{1,i}(1:w(:,i),1); % All wave heights

    Ac_all(1:w(:,i),i)=Ac{1,i}(1:w(:,i),1); % All wave crest ampl

    At_all(1:w(:,i),i)=At{1,i}(1:w(:,i),1); % All wave trough ampl

    T_all(1:z(:,i),i)=T{1,i}(1:z(:,i),1); % All wave periods

    Tcf_all(1:w(:,i),i)=Tcf{1,i}(1:w(:,i),1); % All wave crest front periods

    Tcb_all(1:w(:,i),i)=Tcb{1,i}(1:w(:,i),1); % All wave crest rear periods

    Hm0_all(1,i)=ch{1,i}(1,1); % All Hm0

    Tm02_all(1,i)=ch{1,i}(1,2); % All Tm02

    Tp_all(1,i)=ch{1,i}(1,3); % Tpeak

    Ss_all(1,i)=ch{1,i}(1,4); % Significant steepness

    Na_all(1,i)=bw{1,i}(1,1); % Spectrum narrowness factor

    Br_all(1,i)=bw{1,i}(1,2); % Spectrum broadness factor

    Skew_all(1,i)=skew{1,i}(1,1); % Skewness factor

    Kurt_all(1,i)=kurt{1,i}(1,1); % Kurtosis factor

```

```

Mean_all(1,i)=mean{1,i}(1,1); % Mean

Stdev_all(1,i)=sigma{1,i}(1,1); % St. deviation

end

%% Estimating H1/3, T1/3

for i=1:c

    HeightsSort(1:w(i),i)=sort(H_all(1:w(i),i),'descend');

    TSort(1:z(i),i)=sort(T_all(1:z(i),i),'descend');

% To find the number of the highest 1/3 waves in the record

    num_of_one_third(i,1)=round((w(i)/3));

    num_of_one_thirdT(i,1)=round((z(i)/3));

% To find the significant wave height H one third

    H_One_Third(:,i)=nanmean(HeightsSort(1:num_of_one_third(i,1),i));

    T_One_Third(:,i)=nanmean(TSort(1:num_of_one_third(i,1),i));

end

%% Storing variables

H_One_Third=H_One_Third';

T_One_Third=T_One_Third';

Tm02_all=Tm02_all';

H_One_Third=H_One_Third(1:c-1,1);

T_One_Third=T_One_Third(1:c-1,1);

Tm02_all=Tm02_all(1:c-1,1);

Hm0_all=Hm0_all';

Hm0_all=Hm0_all(1:c-1,1);

```

```

%% To estimate main statistics

H_mean=nan(1,c);
T_mean=nan(1,c);
Hmin=nan(1,c);
Tmin=nan(1,c);
H_max=nan(1,c);
T_max=nan(1,c);
H_stdev=nan(1,c);
T_stdev=nan(1,c);
H_coef_var=nan(1,c);
T_coef_var=nan(1,c);

[m{i-1}, mt{i-1}]=spec2mom(S{i-1},1);
for i=2:c
    H_mean(i-1,:)=nanmean(H_all(:,i-1));
    Hmin(i-1,:)=nanmin(H_all(:,i-1));
    H_max(i-1,:)=nanmax(H_all(:,i-1));
    H_stdev(i-1,:)=nanstd(H_all(:,i-1));
    H_coef_var(i-1,:)=nanvar(H_all(:,i-1));
    T_mean(i-1,:)=nanmean(T_all(:,i-1));
    Tmin(i-1,:)=nanmin(T_all(:,i-1));
    T_max(i-1,:)=nanmax(T_all(:,i-1));
    T_stdev(i-1,:)=nanstd(T_all(:,i-1));
    T_coef_var(i-1,:)=nanvar(T_all(:,i-1));
end

```

```
%% To write on xls files
```

```
filename=[buoy 'waveparameters'];
```

```
ds=dataset(H_mean,Hmin,H_max,H_stdev,H_coef_var,T_mean,Tmin,T_max,T_stdev,T_coef_var,Hm0_a  
ll,Tm02_all,H_One_Third,T_One_Third);
```

```
export(ds,'XLSfile',filename2)
```

ERA-Interim Analysis

Chosen Coordinates ERA INTERIM.m

```
%% Chosen coordinates for ERA_INTERIM analysis. Written by Dafni Sifnioti, PhD Candidate,
```

```
% 20/11/2013.
```

```
ATHOS=[39.9635 24.7226];
```

```
AVGO=[35.62193    25.64105];
```

```
DIA=[35.43874 25.14939];
```

```
E1M3A=[35.79102    24.93420];
```

```
KATERINI=[40.24841 22.71717];
```

```
KALAMATA=[36.97266 22.10693];
```

```
LESVOS=[39.1553 25.8081];
```

```
MYKONOS=[37.5113 25.4590];
```

```
PETROKARAVO=[37.60986    23.56445];
```

```
PYLOS=[36.8359 21.6113];
```

```
SANTORINI=[36.2546 25.4956];
```

```
SKYROS=[39.113 24.4653];
```

```
ZAKYNTHOS=[37.9541 20.6104];
```

Code to read ERA Interim 0.125

%% Script to read and unite ECMWF data.

% The database used is that of ERA-Interim with timeperiod 01/01/1979 to 31/08/2013, with resolution analysis 0.125*0.125 and for the domain of the Mediterranean Sea. The files combined have 0 step and

% intervals of 6 hours. Created & Updated by Dafni Sifnioti, 18/12/2013.

%% Choosing a GPS point

run Chosen_Coordinates_ERA_INTERIM.m

Choose_point=input('Enter the name of location:','s');

Point=input('Enter GPS coordinates:');

%% Choose Parameter

Parameter=input('Enter chosen parameter:');

%% Directory of files

switch Parameter

case 'msl' % mean sea level pressure

files=dir('H:\ECMWF_Data\MSLP\0.125X0.125*.nc');

case 'u10' % wind vector at x - axis

files=dir('H:\ECMWF_Data\V10U\0.125X0.125*.nc');

case 'v10' % wind vector at y - axis

files=dir('H:\ECMWF_Data\V10V\0.125X0.125*.nc');

case 'swh' % significant wave height

files=dir('H:\ECMWF_Data\SWH\0.125X0.125*.nc');

case 'mwp' % mean wave period

files=dir('H:\ECMWF_Data\MWP\0.125X0.125*.nc');

```

    case 'mwd' % mean wave direction

    files=dir('H:\ECMWF_Data\MWD\0.125X0.125\*.nc');

    case 'sp' % surface pressure

    files=dir('H:\ECMWF_Data\SP\0.125X0.125\*.nc');

    case 't2m' % temperture at 2m

    files=dir('H:\ECMWF_Data\T2M\0.125X0.125\*.nc');

    case 'sst' % sea surface temperature

    files=dir('H:\ECMWF_Data\SST\0.125X0.125\*.nc');

end

%% The snc tools have been added to path to open the nc files

%% Getting information about the files and the parameters

lat=roundn(nc_varget(files(1,1).name,'latitude'),-3);

lon=roundn(nc_varget(files(1,1).name,'longitude'),-3);

time=cell(1,8);

for i=1:8

    time{1,i}=(datenum(1900,01,01,00,00,00) + nc_varget(files(i,1).name,'time')./24);

end

ui=cell(1,8);

%% Selecting 4 closest points to the chosen and estimating the weighted average according to distance.

x0=roundn(Point(1,1) - mod(Point(1,1)-min(lat),0.125),-3);

y0=roundn(Point(1,2) - mod(Point(1,2)-min(lon),0.125),-3);

point1=[x0 y0]';

point2=[x0+0.125 y0]';

point3=[x0 y0+0.125]';

point4=[x0+0.125 y0+0.125]';

a=[nan;nan];

points=[a point1 point2 point3 point4];

```

```

Distances=[NaN,dist(Point,point1),dist(Point,point2),dist(Point,point3),dist(Point,point4)];

[~,latx1]=ismember(point1(1,1),lat,'rows');
[~,lony1]=ismember(point1(2,1),lon,'rows');
[~,latx2]=ismember(point2(1,1),lat,'rows');
[~,lony2]=ismember(point2(2,1),lon,'rows');
[~,latx3]=ismember(point3(1,1),lat,'rows');
[~,lony3]=ismember(point3(2,1),lon,'rows');
[~,latx4]=ismember(point4(1,1),lat,'rows');
[~,lony4]=ismember(point4(2,1),lon,'rows');

% for 1979-1999
for i=1:4
    ui{1,i}=[time{1,i} nc_varget(files(i,1).name,Parameter,[0 latx1-1 lony1-1],[7670 1 1]),...
    nc_varget(files(i,1).name,Parameter,[0 latx2-1 lony2-1],[7670 1 1]),...
    nc_varget(files(i,1).name,Parameter,[0 latx3-1 lony3-1],[7670 1 1]),...
    nc_varget(files(i,1).name,Parameter,[0 latx4-1 lony4-1],[7670 1 1])];
end

% for 2000-2013
for i=5:8
    ui{1,i}=[time{1,i} nc_varget(files(i,1).name,Parameter,[0 latx1-1 lony1-1],[4992 1 1]),...
    nc_varget(files(i,1).name,Parameter,[0 latx2-1 lony2-1],[4992 1 1]),...
    nc_varget(files(i,1).name,Parameter,[0 latx3-1 lony3-1],[4992 1 1]),...
    nc_varget(files(i,1).name,Parameter,[0 latx4-1 lony4-1],[4992 1 1])];
end

Point_Parameter=double(sortrows([ui{1,1};ui{1,2};ui{1,3};ui{1,4};ui{1,5};ui{1,6};ui{1,7};ui{1,8}],1));

Point_Parameter=[points;Distances;Point_Parameter];

Point_Parameter_WA=((Point_Parameter(4:end,2)./(Distances(1,2)^2))+(Point_Parameter(4:end,3)./(Di
stances(1,3)^2))+(Point_Parameter(4:end,4)./(Distances(1,4)^2))+(Point_Parameter(4:end,5)./(Distances
(1,5)^2)))/(1/(Distances(1,2)^2)+1/(Distances(1,3)^2)+1/(Distances(1,4)^2)+1/(Distances(1,5)^2));

```

```

Point_Parameter_WA=[NaN;NaN;NaN;Point_Parameter_WA];
Point_Parameter=[Point_Parameter,Point_Parameter_WA];
Files_Format='.txt';
fname6Hourly=[Parameter '6HOURLY' Choose_point Files_Format];

% For the 6 Hourly date
Six_Hourly=m2xdate(Point_Parameter(:,1));
Point_Parameter=[Six_Hourly Point_Parameter(:,2:end)];
dlmwrite(fname6Hourly, Point_Parameter, 'delimiter', '\t','precision',10);

```

Code to read ERA Interim 0 125 WA GB

```

%% Script to read and unite ECMWF data and estimate values per grid boxes.
% The database used is that of ERA-Interim with timeperiod
% 01/01/1979 to 31/08/2013, with resolution analysis 0.125*0.125 and for the
% domain of the Mediterranean Sea. The files combined have 0 step and
% intervals of 6 hours. Created & Updated by Dafni Sifnioti, 18/12/2013.

%% Choosing a GPS point
run Chosen_Coordinates_ERA_INTERIM.m
Choose_point=input('Enter the name of location:', 's');
Point=input('Enter GPS coordinates:');

%%

Parameter=input('Enter chosen parameter:');

%% Directory of files

```

switch Parameter

```
case 'u10'  
files=dir('G:\ECMWF_Data\V10U\0.125X0.125\*.nc');  
case 'v10'  
files=dir('G:\ECMWF_Data\V10V\0.125X0.125\*.nc');  
case 'swh'  
files=dir('G:\ECMWF_Data\SWH\0.125X0.125\*.nc');  
case 't2m'  
files=dir('G:\ECMWF_Data\T2M\0.125X0.125\*.nc');
```

end

%% Getting info about the files and the parameters

```
lat=roundn(nc_varget(files(1,1).name,'latitude'),-3);
```

```
lon=roundn(nc_varget(files(1,1).name,'longitude'),-3);
```

```
time=cell(1,9);
```

```
for i=1:9
```

```
time{1,i}=(datenum(1900,01,01,00,00,00) + nc_varget(files(i,1).name,'time')./24);
```

end

```
ui=cell(1,9);
```

%% Selecting 9 closest points to the chosen and estimating the weighted average according to distance.

```
x0=roundn(Point(1,1) - mod(Point(1,1)-min(lat),0.125),-3);
```

```
y0=roundn(Point(1,2) - mod(Point(1,2)-min(lon),0.125),-3);
```

```
point1=[x0 y0]';
```

```
point2=[x0+0.125 y0]';
```

```
point3=[x0 y0+0.125]';
```

```
point4=[x0+0.125 y0+0.125]';
```

```
point5=[x0-0.125 y0]';
```

```

point6=[x0 y0-0.125]';
point7=[x0-0.125 y0-0.125]';
point8=[x0-0.125 y0+0.125]';
point9=[x0+0.125 y0-0.125]';

a=[nan;nan];

points=[a point1 point2 point3 point4 point5 point6 point7 point8 point9];

Distances=[NaN,dist(Point,point1),dist(Point,point2),dist(Point,point3),dist(Point,point4),dist(Point,point
5),dist(Point,point6),dist(Point,point7),dist(Point,point8),dist(Point,point9)];

[~,latx1]=ismember(point1(1,1),lat,'rows');
[~,lony1]=ismember(point1(2,1),lon,'rows');
[~,latx2]=ismember(point2(1,1),lat,'rows');
[~,lony2]=ismember(point2(2,1),lon,'rows');
[~,latx3]=ismember(point3(1,1),lat,'rows');
[~,lony3]=ismember(point3(2,1),lon,'rows');
[~,latx4]=ismember(point4(1,1),lat,'rows');
[~,lony4]=ismember(point4(2,1),lon,'rows');
[~,latx5]=ismember(point5(1,1),lat,'rows');
[~,lony5]=ismember(point5(2,1),lon,'rows');
[~,latx6]=ismember(point6(1,1),lat,'rows');
[~,lony6]=ismember(point6(2,1),lon,'rows');
[~,latx7]=ismember(point7(1,1),lat,'rows');
[~,lony7]=ismember(point7(2,1),lon,'rows');
[~,latx8]=ismember(point8(1,1),lat,'rows');
[~,lony8]=ismember(point8(2,1),lon,'rows');
[~,latx9]=ismember(point9(1,1),lat,'rows');
[~,lony9]=ismember(point9(2,1),lon,'rows');

```

```
% for 1979-1999
```

```
for i=1:4
```

```
    ui{1,i}=[time{1,i} nc_varget(files(i,1).name,Parameter,[0 latx1-1 lony1-1],[7670 1 1]),...  
    nc_varget(files(i,1).name,Parameter,[0 latx2-1 lony2-1],[7670 1 1]),...  
    nc_varget(files(i,1).name,Parameter,[0 latx3-1 lony3-1],[7670 1 1]),...  
    nc_varget(files(i,1).name,Parameter,[0 latx4-1 lony4-1],[7670 1 1]),...  
    nc_varget(files(i,1).name,Parameter,[0 latx5-1 lony5-1],[7670 1 1]),...  
    nc_varget(files(i,1).name,Parameter,[0 latx6-1 lony6-1],[7670 1 1]),...  
    nc_varget(files(i,1).name,Parameter,[0 latx7-1 lony7-1],[7670 1 1]),...  
    nc_varget(files(i,1).name,Parameter,[0 latx8-1 lony8-1],[7670 1 1]),...  
    nc_varget(files(i,1).name,Parameter,[0 latx9-1 lony9-1],[7670 1 1])];
```

```
end
```

```
% for 2000-2013
```

```
for i=5:8
```

```
    ui{1,i}=[time{1,i} nc_varget(files(i,1).name,Parameter,[0 latx1-1 lony1-1],[4992 1 1]),...  
    nc_varget(files(i,1).name,Parameter,[0 latx2-1 lony2-1],[4992 1 1]),...  
    nc_varget(files(i,1).name,Parameter,[0 latx3-1 lony3-1],[4992 1 1]),...  
    nc_varget(files(i,1).name,Parameter,[0 latx4-1 lony4-1],[4992 1 1]),...  
    nc_varget(files(i,1).name,Parameter,[0 latx5-1 lony5-1],[4992 1 1]),...  
    nc_varget(files(i,1).name,Parameter,[0 latx6-1 lony6-1],[4992 1 1]),...  
    nc_varget(files(i,1).name,Parameter,[0 latx7-1 lony7-1],[4992 1 1]),...  
    nc_varget(files(i,1).name,Parameter,[0 latx8-1 lony8-1],[4992 1 1]),...  
    nc_varget(files(i,1).name,Parameter,[0 latx9-1 lony9-1],[4992 1 1])];
```

```
end
```

```
ui{1,9}=[time{1,9} nc_varget(files(9,1).name,Parameter,[0 latx1-1 lony1-1],[488 1 1]),...
```

```
    nc_varget(files(9,1).name,Parameter,[0 latx2-1 lony2-1],[488 1 1]),...
```

```

nc_varget(files(9,1).name,Parameter,[0 latx3-1 lony3-1],[488 1 1]),...
nc_varget(files(9,1).name,Parameter,[0 latx4-1 lony4-1],[488 1 1]),...
nc_varget(files(9,1).name,Parameter,[0 latx5-1 lony5-1],[488 1 1]),...
nc_varget(files(9,1).name,Parameter,[0 latx6-1 lony6-1],[488 1 1]),...
nc_varget(files(9,1).name,Parameter,[0 latx7-1 lony7-1],[488 1 1]),...
nc_varget(files(9,1).name,Parameter,[0 latx8-1 lony8-1],[488 1 1]),...
nc_varget(files(9,1).name,Parameter,[0 latx9-1 lony9-1],[488 1 1]);

```

```
Point_Parameter=double(sortrows([ui{1,1};ui{1,2};ui{1,3};ui{1,4};ui{1,5};ui{1,6};ui{1,7};ui{1,8}],1));
```

```
Point_Parameter=[Point_Parameter;ui{1,9}];
```

```
Point_Parameter=[points;Distances;Point_Parameter];
```

```
Distances_WA=sqrt(2)*0.125/2; % grid boxes diagonal
```

```
% Grid box 1
```

```
Point_Parameter_WA_1=((Point_Parameter(4:end,2)./(Distances(1,2)^2))+(Point_Parameter(4:end,4)./(
Distances(1,4)^2))+(Point_Parameter(4:end,6)./(Distances(1,6)^2))+(Point_Parameter(4:end,8)./(Distanc
es(1,8)^2)))/(1/(Distances(1,2)^2)+1/(Distances(1,4)^2)+1/(Distances(1,6)^2)+1/(Distances(1,8)^2));
```

```
point_wa_1=[x0-0.0625,y0+0.0625];
```

```
Point_Parameter_WA_1=[point_wa_1(1,1);point_wa_1(1,2);Distances_WA;Point_Parameter_WA_1];
```

```
% Grid box 2
```

```
Point_Parameter_WA_2=((Point_Parameter(4:end,2)./(Distances(1,2)^2))+(Point_Parameter(4:end,4)./(
Distances(1,4)^2))+(Point_Parameter(4:end,5)./(Distances(1,5)^2))+(Point_Parameter(4:end,3)./(Distanc
es(1,3)^2)))/(1/(Distances(1,2)^2)+1/(Distances(1,4)^2)+1/(Distances(1,5)^2)+1/(Distances(1,3)^2));
```

```
point_wa_2=[x0+0.0625,y0+0.0625];
```

```
Point_Parameter_WA_2=[point_wa_2(1,1);point_wa_2(1,2);Distances_WA;Point_Parameter_WA_2];
```

```
% Grid box 3
```

```
Point_Parameter_WA_3=((Point_Parameter(4:end,2)./(Distances(1,2)^2))+(Point_Parameter(4:end,3)./(
Distances(1,3)^2))+(Point_Parameter(4:end,7)./(Distances(1,7)^2))+(Point_Parameter(4:end,10)./(Dista
```

```

nces(1,10)^2)))./(1/(Distances(1,2)^2)+1/(Distances(1,3)^2)+1/(Distances(1,7)^2)+1/(Distances(1,10)^2))
;
point_wa_3=[x0+0.0625,y0-0.0625];
Point_Parameter_WA_3=[point_wa_3(1,1);point_wa_3(1,2);Distances_WA;Point_Parameter_WA_3];

% Grid box 4

Point_Parameter_WA_4=((Point_Parameter(4:end,2)./(Distances(1,2)^2)+(Point_Parameter(4:end,6)./(
Distances(1,6)^2)+(Point_Parameter(4:end,8)./(Distances(1,8)^2)+(Point_Parameter(4:end,7)./(Distanc
es(1,7)^2)))./(1/(Distances(1,2)^2)+1/(Distances(1,6)^2)+1/(Distances(1,8)^2)+1/(Distances(1,7)^2));
point_wa_4=[x0-0.0625,y0-0.0625];
Point_Parameter_WA_4=[point_wa_4(1,1);point_wa_4(1,2);Distances_WA;Point_Parameter_WA_4];

%% estimating the wa according to buoy.

points_wa=[a point_wa_1' point_wa_2' point_wa_3' point_wa_4'];

Distances_wa_buoy=[NaN,dist(Point,point_wa_1'),dist(Point,point_wa_2'),dist(Point,point_wa_3'),dist(
Point,point_wa_4')];

Point_Parameter_WA_buoy=((Point_Parameter_WA_1(4:end)./(Distances_wa_buoy(1,2)^2)+(Point_Pa
rameter_WA_2(4:end)./(Distances_wa_buoy(1,3)^2)+(Point_Parameter_WA_3(4:end)./(Distances_wa_
buoy(1,4)^2)+(Point_Parameter_WA_4(4:end)./(Distances_wa_buoy(1,5)^2)))./(1/(Distances_wa_buoy
(1,2)^2)+1/(Distances_wa_buoy(1,3)^2)+1/(Distances_wa_buoy(1,4)^2)+1/(Distances_wa_buoy(1,5)^2))
;

%% Change to excel dates and then save

Dates= m2xdate(Point_Parameter(:,1));

Point_Parameter_WA_buoy=[Dates(4:end),Point_Parameter_WA_buoy];

fname6Hourly=[Parameter '6HOURLY_GB_WA_' Choose_point ];

xlswrite(fname6Hourly, Point_Parameter_WA_buoy)

```